BOEM 2017-34

US-Canada Transboundary Fish and Lower Trophic Communities

Abundance, Distribution, Habitat and Community Analysis

Final report prepared under

BOEM Agreement Number M12AC00011

Principal Investigators

Brenda Norcross
Bodil Bluhm
Sarah Hardy
Russell Hopcroft
Katrin Iken

Institute of Marine Science
College of Fisheries and Ocean Sciences (CFOS)
University of Alaska Fairbanks
PO Box 757220
Fairbanks AK 99775

BOEM
Bureau of Ocean Energy Management

December 2017

Disclaimer

Study concept, oversight, and funding were provided by the US Department of the Interior, Bureau of Ocean Energy Management, Environmental Studies Program, Washington, DC, under Contract Number M12AC00011. This report has been technically reviewed by BOEM and it has been approved for publication. The views and conclusions contained in this document are those of the authors and should not be interpreted as representing the opinions or policies of the US Government, nor does mention of trade names or commercial products constitute endorsement or recommendation for use.

Citation

Norcross, Brenda L., Sarah J. Apsens, Lauren E. Bell, Bodil A. Bluhm, Julia N. Dissen, Lorena E. Edenfield, Alyssa Frothingham, Benjamin P. Gray, Sarah M. Hardy, Brenda A. Holladay, Russell R. Hopcroft, Katrin B. Iken, Caitlin A. Smoot, Kelly L. Walker, and Eric D. Wood. 2017. US-Canada Transboundary Fish and Lower Trophic Communities: Abundance, Distribution, Habitat and Community Analysis. BOEM Final Report Number 2017-034. 463 pp + appendices.

TABLE OF CONTENTS

Table of Contents 3
LIST OF FIGURES 7
LIST OF TABLES 21
LIST OF APPENDICES 27
LIST OF ACRONYMS 29
1.0 OVERALL INTRODUCTION 33
2.0 AT-SEA COLLECTION METHODS 35
2.1 Physical Oceanography, Chemical Oceanography and Chlorophyll-*a* 35
2.2 Benthic Environmental Characteristics 36
2.3 Zooplankton 37
2.4 Infauna 37
2.5 Fish – Midwater Trawls 37
2.6 Epifauna and Fish – Bottom Trawls 38
2.7 Standardizing Effort 39
3.0 HABITAT 41
3.1 Physical Oceanography 41
3.1.1 Introduction 41
3.1.2 Objectives 42
3.1.3 Methods 42
3.1.4 Results and Interpretation 43
3.2 Chemical Oceanography 54
3.2.1 Introduction 54
3.2.2 Objectives 54
3.2.3 Methods 55
3.2.4 Results and Interpretation 55
3.3 Chlorophyll-*a* 71
3.3.1 Introduction 71
3.3.2 Objectives 72
3.3.3 Methods 72
3.3.4 Results and Interpretation 72
3.4 Benthic Environmental Characteristics 73
3.4.1 Introduction 73
3.4.2 Methods 74
3.4.3 Results and Discussion 83
4.0 ZOOPLANKTON 97
4.1 Epipelagic Zooplankton Communities 97
4.1.1 Introduction 97
4.1.2 Methods 98
4.1.3 Results 98
4.1.4 Discussion 131
4.2 Vertical Distribution and Structure of Beaufort Sea Zooplankton during Transboundary 2012–14 136

4.2.1 Introduction 136
4.2.2 Methods 137
4.2.3 Results 138
4.2.4 Discussion 154

5.0 INFAUNA 157
5.1 Introduction 157
5.2 Methods 157
5.3 Results and Discussion 158
5.3.1 General Patterns 158
5.3.2 Habitat Variables 162

6.0 EPIBENTHOS 165
6.1 Introduction 165
6.2 Objectives 165
6.3 Methods 166
6.3.1 Epibenthic Community Sampling 166
6.3.2 Data Analysis 166
6.4 Results 168
6.4.1. Patterns in Taxon Richness and Overall Biomass and Abundance 168
6.4.2 Patterns in Epibenthic Community Structure (Multivariate Patterns) 177
6.5 Discussion 186
6.5.1 Pan-Arctic and Regional Patterns in Taxon Richness 186
6.5.2 Pan-Arctic and Regional Patterns in Total Epibenthic Biomass and Abundance 186
6.5.3 Interannual Variability in Epibenthic Biomass and Abundance 188
6.5.4 Patterns in Epibenthic Community Structure (Multivariate Patterns) 189
6.5.5 Small-Scale Spatial Variability in Community Composition 192
6.6 Summary 193

7.0 Fish Ecolog 195
7.1 Introduction 195
7.1.1 Objectives 195
7.2 Methods 197
7.2.1 Sample Collection 197
7.2.2 Laboratory Processing of Midwater and Demersal Fishes 201
7.2.3 Statistical Analyses of Pelagic and Demersal Fishes 202
7.3 Results 206
7.3.1 Fish Catches 206
7.3.2 Fish Life History Characteristics 223
7.3.3 Midwater Fishes 244
7.3.4 Demersal Fishes – Bottom Assemblages 259
7.4 Discussion 326
7.4.1 Beaufort Large Marine Ecosystem Patterns in Fish Richness, Biomass and Abundance 326
7.4.2 Life History Characteristics of US Beaufort Sea Fishes 327
7.4.3 Pelagic and Demersal Distribution 330
7.4.4 Fish Species Assemblages – Shelf vs. Slope 331
7.4.5. Small-Scale Spatial Variability in Community Composition 333
7.4.6 Interannual Variability in Demersal Biomass and Abundance 333
7.4.7 Fishing Gear and Fish Monitoring 333
7.5 Conclusions 335

8.0 FEEDING ECOLOGY OF ABUNDANT FISHES 337
8.1 Introduction 337
8.2 Fish Diets 337
8.2.1 Introduction 337
8.2.2 Methods 338
8.2.3 Results 339
8.2.4 Discussion 348
8.3 Fish Fatty Acids 350
8.3.1 Introduction 350
8.3.2 Materials and Methods 351
8.3.3 Results 352
8.3.4 Discussion and Conclusions 353
8.4 Benthic Food Web Structure 357
8.4.1 Introduction 357
8.4.2 Objectives 358
8.4.3 Methods 358
8.4.4 Data Analysis 361
8.4.5 Results 363
8.4.6 Discussion 383
8.4.7 Conclusions 387

9.0 CROSS-DISCIPLINARY TROPHIC LEVEL SYNTHESIS 389
9.1 Summary of distribution patterns within the US-Canada Transboundary study area 389
9.2 Depth-related patterns in taxon richness, biomass and abundance 391
9.3 Patterns in the Transboundary area compared with other Arctic regions 392
9.4 Interannual variability in biomass and abundance in the Transboundary region 394
9.5 Community Structure 395
9.5.1 Analytical approach 395
9.5.2 Spatial and temporal variability in community composition 395
9.6 Shelf–Slope, depth and water mass related patterns in community structure 396
9.6.1 Indicator species in the Transboundary area 399
9.7 Taxonomic level of monitoring in the Transboundary area 401
9.8 Interdisciplinary comparisons 403

10.0 UNDER ICE 413
10.1 Introduction 413
10.2 Methods 413
10.2.1 201 Season 413
10.2.3 201 Season 416
10.3 Results–*201 Season* 418
10.3.1 Fish and Amphipod Dive Surveys, Gill Net 418
10.3.2 Bottom Surveys, Grab Samples 419
10.3.3 Zooplankton Communities 420
10.3.4 Hydrography and Water and Sea Ice Chlorophyll 420
10.4 Assessment of Survey Strategies 422
10.4.1 Ice Conditions 422
10.4.2 Under-Ice Surveys 423
10.4.3 Zooplankton Surveys 424
10.4.4 Bottom Sampling 424
10.5 Results–*201 Season* 424
10.6 Discussion 425

11.0 INTERANNUAL VARIATION ASSESSMENT PLAN FOR FISH 429
11.1 Monitoring Recommendations 429
11.2 Lessons Learned 433
LITERATURE CITED 435
TECHNICAL SUMMARY 459

LIST OF FIGURES

Figure 2.1. Transects and stations sampled in the Beaufort Sea 2012–2014. 36

Figure 3.1.1. Oceanographic profile from Transboundary 2012 in the Beaufort Sea. Water masses are noted: PML – Polar Mixed Layer, AHW – Arctic Halocline Water, AW – Atlantic Water. 44

Figure 3.1.2. Oceanographic profile from Transboundary 2013 in the Beaufort Sea. Water masses are noted. PML = Polar Mixed Layer. AHW = Arctic Halocline Water. AW = Atlantic Water. 45

Figure 3.1.3. Oceanographic profile from Transboundary 2014 in the Beaufort Sea. Water masses are noted.PML = Polar Mixed Layer. AHW = Arctic Halocline Water. AW = Atlantic Water. 46

Figure 3.1.4. Temperature and salinity sections along cross-shelf transects in the Beaufort Sea during Transboundary 2012. 47

Figure 3.1.5. Temperature and salinity sections along cross-shelf transects in the Beaufort Sea during Transboundary 2013. 48

Figure 3.1.6. Temperature and salinity sections along cross-shelf transects in the Beaufort Sea during Transboundary 2014. 49

Figure 3.1.7. Surface temperature in the Beaufort Sea during Transboundary 2012–14. 50

Figure 3.1.8. Surface salinity in the Beaufort Sea during Transboundary 2012–14. 51

Figure 3.1.9. Bottom temperature in the Beaufort Sea during Transboundary 2012–14. 52

Figure 3.1.10. Bottom salinity in the Beaufort Sea during Transboundary 2012–14. 53

Figure 3.2.1. Macronutrient and chlorophyll-*a* concentrations across Transboundary 2012 Transect B2, 26–28 Sep. 56

Figure 3.2.2. Macronutrient and chlorophyll-*a* concentrations across Transboundary 2012 Transect B1, 21–29 Sep. 57

Figure 3.2.3. Macronutrient and chlorophyll-*a* concentrations across Transboundary 2013 Transect A6, 13–17 Aug. 58

Figure 3.2.4. Macronutrient and chlorophyll-*a* concentrations across Transboundary 2013 Transect A2, 17–20 Aug. 59

Figure 3.2.5. Macronutrient and chlorophyll-*a* concentrations across Transboundary 2013 Transect A1, 20–23 Aug. 60

Figure 3.2.6. Macronutrient and chlorophyll-*a* concentrations across Transboundary 2013 Transect TBS, 23–26 Aug. 61

Figure 3.2.7. Macronutrient and chlorophyll-*a* concentrations across Transboundary 2013 Transect MAC, 26–31 Aug. 62

Figure 3.2.8. Macronutrient and chlorophyll-*a* concentrations across Transboundary 2013 Transect GRY, 27–29 Aug. 63

Figure 3.2.9. Macronutrient and chlorophyll-*a* concentrations across Transboundary 2014 Transect A6, 19–31 Aug. 64

Figure 3.2.10. Macronutrient and chlorophyll-*a* concentrations across Transboundary 2014 Transect A5, 20–30 Aug. 65

Figure 3.2.11. Macronutrient and chlorophyll-*a* concentrations across Transboundary 2014 Transect A4, 20–21 Aug. 66

Figure 3.2.12. Macronutrient and chlorophyll-*a* concentrations across Transboundary 2014 Transect A2, 21–24 Aug. 67

Figure 3.2.13. Macronutrient and chlorophyll-*a* concentrations across Transboundary 2014 Transect A1, 24–26 Aug. 68

Figure 3.2.14. Macronutrient and chlorophyll-*a* concentrations across Transboundary 2014 Transect TBS, 27–28 Aug. 69

Figure 3.2.15. Macronutrient and chlorophyll-*a* concentrations in the Polar Mixed Layer of the Beaufort Sea during Transboundary 2012–14. 70

Figure 3.2.16. Macronutrient concentrations to 1000 m depth in the Beaufort Sea during Transboundary 2014. 71

Figure 3.3.1. Size fractionated chlorophyll-*a* concentrations in the Beaufort Sea during Transboundary 2013–14. 73

Figure 3.4.1. Map of Transboundary stations where sediments were collected by box core, (2012, B transects: 50–1000 m), van Veen grab (2013–2014, A transects: stations ≤350 m), and bottom trawl (2013). 75

Figure 3.4.2. Map: Gravel percentage in surface sediment. 84

Figure 3.4.3. Map: Sand percentage in surface sediment. 84

Figure 3.4.4. Map: Mud percentage in surface sediment. 85

Figure 3.4.5. Map: Silt percentage in surface sediment. 85

Figure 3.4.6. Map: Clay percentage in surface sediment. 86

Figure 3.4.7. Map: Porosity of surface sediment. 86

Figure 3.4.8. Map: Mean Phi size of surface sediment. 87

Figure 3.4.9. Map of seafloor substrate from the Beaufort Sea (geographic extent reduced from Audubon Alaska 2015). 88

Figure 3.4.10. Trends in sediment chlorophyll-*a* concentration (µg/g dry sediment) with depth along selected transects across the study region. 89

Figure 3.4.11. Principle components analysis (PCA) showing similarity in environmental characteristics among stations. 92

Figure 3.4.12. Canonical discriminant analysis (CDA) comparing benthic habitat characteristics among sampling depths with temperature and salinity included. 93

Figure 3.4.13. Canonical discriminant analysis (CDA) comparing benthic habitat characteristics among sampling depths with temperature and salinity excluded. 94

Figure 3.4.14. Canonical discriminant analysis (CDA) comparing benthic habitat characteristics among transects with temperature and salinity excluded. 95

Figure 4.1.1. The relative contribution of major zooplankton taxonomic groups in terms of abundance and biomass in the Beaufort Sea during Transboundary 2012–14 for the 150- and 505-µm nets. 100

Figure 4.1.2. Abundance of *Pseudocalanus* spp. (ind. m^{-3}) captured in the 150-µm net in the Beaufort Sea during Transboundary 2012–14. 109

Figure 4.1.3. Abundance of *Oithona similis* (ind. m^{-3}) captured in the 150-µm net in the Beaufort Sea during Transboundary 2012–14. 110

Figure 4.1.4. Abundance of *Triconia borealis* (ind. m^{-3}) captured in the 150-µm net in the Beaufort Sea during Transboundary 2012–14. 111

Figure 4.1.5. Abundance of *Microcalanus pygmaeus* (ind. m^{-3}) captured in the 150-µm net in the Beaufort Sea during Transboundary 2012–14. 112

Figure 4.1.6. Abundance of *Heterorhabdus norvegicus* (ind. m^{-3}) captured in the 150-µm net in the Beaufort Sea during Transboundary 2012–14. 113

Figure 4.1.7. Abundance of *Eurytemora* spp. (ind. m^{-3}) captured in the 150-µm net in the Beaufort Sea during Transboundary 2012–14. 114

Figure 4.1.8. Abundance of *Calanus glacialis* (ind. m^{-3}) captured in the 505-µm net in the Beaufort Sea during Transboundary 2012–14. 115

Figure 4.1.9. Abundance of *Calanus hyperboreus* (ind. m^{-3}) captured in the 505-µm net in the Beaufort Sea during Transboundary 2012–14. 116

Figure 4.1.10. Abundance of *Metridia longa* (ind. m^{-3}) captured in the 505-µm net in the Beaufort Sea during Transboundary 2012–14. 117

Figure 4.1.11. Abundance of *Paraeuchaeta glacialis* (ind. m^{-3}) captured in the 505-µm net in the Beaufort Sea during Transboundary 2012–14. 118

Figure 4.1.12. Presence of Pacific expatriate taxa captured in the 150- and 505-µm nets in the Beaufort Sea during Transboundary 2012–14. 119

Figure 4.1.13. Zooplankton community structure for pooled 150-µm net abundance data Transboundary 2012–14. 121

Figure 4.1.14. Zooplankton community structure for pooled 150-µm net biomass data Transboundary 2012–14. 122

Figure 4.1.15. Zooplankton community structure for pooled 505-µm net abundance data Transboundary 2012–14. 123

Figure 4.1.16. Zooplankton community structure for pooled 505-µm net biomass data Transboundary 2012–14. 124

Figure 4.1.17. Abundance and biomass size spectra of copepods from the 150- and 505-µm nets for each survey year in the Beaufort Sea during Transboundary 2012–14..... 133

Figure 4.1.18. Comparison of average abundances (ind. m^{-3}) of select taxa in the Beaufort Sea region over the past 60 years. Trendlines are shown. 135

Figure 4.2.1. Contribution of major taxonomic groups to abundance and biomass of the zooplankton community within each sampling interval in the Beaufort Sea during Transboundary 2012–14. Water masses are noted. 139

Figure 4.2.2a. Vertical zooplankton community structure in the Beaufort Sea during Transboundary 2012–14 based on abundance. 140

Figure 4.2.2.b. Vertical zooplankton community structure in the Beaufort Sea during Transboundary 2012–14 based on biomass. 141

Figure 4.2.3. Abundance (ind. m^{-3}) of indicator species in the Beaufort Sea superimposed on nMDS plots decomposed by water masses for Transboundary 2012–14. 149

Figure 4.2.4. Contribution of holozooplankton trophic guilds to abundance and biomass within each sampling stratum in the Beaufort Sea during Transboundary 2012–14. Water masses are noted. 150

Figure 4.2.5. Contribution of major copepod groups to abundance and biomass within each sampling stratum in the Beaufort Sea during Transboundary 2012–14. Water masses are noted. 151

Figure 4.2.6. Contribution of taxa to dominant guild of Arctic copepods in terms of abundance and biomass in each sampling stratum in the Beaufort Sea during Transboundary 2012–14. Water masses are noted. 152

Figure 4.2.7. Generalized vertical distribution of select copepod species in each sampling stratum in the Beaufort Sea during Transboundary 2012–14. 153

Figure 5.3.1. Total macrofaunal abundance (individuals m^{-2}) by phylum..... 159

Figure 5.3.2. Total polychaete abundance (individuals m^{-2}) by family (including class Oligochaeta), showing only taxa contributing more than 5% of total polychaete abundance. 160

Figure 5.3.3. Photograph of box core surfaces from station B1-350 m (A), showing black, presumably anoxic sediment at the core surface, in contrast to station B1-1000 m (B) which shows no visual evidence of a sharp oxic-anoxic gradient. 160

Figure 5.3.4. nMDS ordination showing relative abundance of polychaete families contributing substantially to within-group similarity based on SIMPER analysis..... 161

Figure 5.3.5. nMDS ordination of overall macrofaunal community structure. 162

Figure 5.3.6. dbRDA ordination showing best-fit DistLM model of annelid assemblage structure (family-level taxonomy). 163

Fig. 6.4.1. Biomass of major epibenthic phyla by depth strata in the Beaufort Sea across years and transects. 170

Fig. 6.4.2. Abundance of major epibenthic phyla by depth strata in the Beaufort Sea across years and transects. 171

Figure 6.4.3. Snow crab (*Chionoecetes opilio*) relationship between body size (carapace width) and body mass (a), and size frequency distribution of snow crab (b), both for collection in 2012 on the central Beaufort Sea shelf and slope. 172

Figure 6.4.4. Absolute biomass (upper panels) and abundance (lower panels) of epibenthic communities in 2013 (left panels) and 2014 (right panels). 174

Figure 6.4.5. Epibenthic biomass (g wet weight 1000 m^{-2}) distribution in 2013 (a and c) and 2014 (b and d) arranged by depth strata (a and b) and by transect lines (c and d). 175

Figure 6.4.6. Epibenthic biomass (g wet weight 1000 m^{-2}) distribution along depth strata at the same transects sampled in 2013 and 2014. 176

Figure 6.4.7. Community structure ordination (nMDS) of epibenthos based on relative biomass for all transects and depths sampled in 2012, 2013, and 2014, based on various transformations. 178

Figure 6.4.8. Community structure ordination (nMDS) of epibenthos based on (a) relative biomass identified to the lowest taxonomic level (species or genus for most taxa, occasionally higher levels for difficult groups), and (b) relative biomass identified to a higher taxonomic level (mostly class level, phylum for some difficult groups). 181

Figure 6.4.9. Community structure of repeat trawls along depth strata of transect A1 (141° W) sampled in 2014 and comparison with transect sampled in 2013..... 183

Figure 6.4.10. Epibenthic community similarity based on biomass grouped by water masses:. 184

Figure 7.1.1. Historical fish surveys in the Beaufort Sea. (a) 1977–2008, (b) 2011 (Norcross et al. in review). 196

Figure 7.2.1. Transects and stations sampled in the Beaufort Sea 2012–2014..... 198

Figure 7.3.1.1. Proportional biomass and abundance for 14 families of fish and unidentified teleosts in the Beaufort Sea 2012–2014, by gear. Isaacs-Kidd midwater trawl (IKMT), otter trawl (OT), beam trawls (BT)..... 210

Figure 7.3.1.2. Proportional biomass for 14 families of fish and unidentified teleosts captured by beam trawl in the Beaufort Sea 2012–2014. 213

Figure 7.3.1.3. Proportional abundance for 14 families of fish and unidentified teleosts captured by beam trawl in the Beaufort Sea 2012–2014. 214

Figure 7.3.1.4. Proportional biomass and abundance for 11 families of fish captured by otter trawl in the Beaufort Sea during 2012. 215

Figure 7.3.1.5. Proportional abundance for 7 families of fish captured by Isaacs-Kidd midwater trawl (IKMT) in the Beaufort Sea 2012–2013..... 216

Figure 7.3.1.6. Curves of cumulative species estimation by pelagic (IKMT, AMT) and bottom (BT and OT) trawl gears, based on presence of most specific level of taxa in successful hauls. 219

Figure 7.3.2.1. Gadidae: *Boreogadus saida*. Length frequency and age estimates from the Beaufort Sea 2012–2014. Length frequency includes fish caught by all gears and is not adjusted for abundance. 228

Figure 7.3.2.2. Distribution of *Boreogadus saida* by age, shelf (≤100 m), slope (≥200 m), and year sampled. 231

Columns indicate percentage of ages 0–5 of *B. saida* in each area, with total number of fish above. N is the number of fish for which each age was estimated. 231

Figure 7.3.2.3. Cottidae: *Gymnocanthus tricuspis*. Length frequency and age estimates from the Beaufort Sea 2012–2014. Length frequency includes fish caught by all gears and is not adjusted for abundance. 232

Figure 7.3.2.4. Agonidae: *Aspidophoroides olrikii*. Length frequency and age estimates from the Beaufort Sea 2012–2014. Length frequency includes fish caught by all gears and is not adjusted for abundance. The largest samples from 2012 and 2013 were not available for aging..... 233

Figure 7.3.2.5. Liparidae: *Liparis fabricii*. Length frequency and age estimates from the Beaufort Sea 2012–2014. Length frequency includes fish caught by all gears and is not adjusted for abundance. 234

Figure 7.3.2.6. Zoarcidae: *Lycodes adolfi*. Length frequency and age frequency estimates from the Beaufort Sea 2012–2014. Length frequency includes fish caught by all gears and is not adjusted for abundance. 235

Figure 7.3.2.7. Zoarcidae: *Lycodes polaris*. Length frequency and age frequency estimates from the Beaufort Sea 2012–2014. Length frequency includes fish caught by all gears and is not adjusted for abundance. Only one fish from 2013 was available for aging. 236

Figure 7.3.2.8. Zoarcidae: *Lycodes sagittarius*. Length frequency and age frequency estimates from the Beaufort Sea 2012–2014. Length frequency includes fish caught by all gears and is not adjusted for abundance. 237

Figure 7.3.2.9. Zoarcidae: *Lycodes seminudus*. Length frequency and age frequency estimates from the Beaufort Sea 2012–2014. Length frequency includes fish caught by all gears and is not adjusted for abundance. 238

Figure 7.3.2.10. Stichaeidae: *Anisarchus medius*. Length frequency and age frequency estimates from the Beaufort Sea 2012–2014. Length frequency includes fish caught by all gears and is not adjusted for abundance. No fish from 2014 were available for aging. 239

Figure 7.3.2.11. Stichaeidae: *Lumpenus fabricii*. Length frequency and age frequency estimates from the Beaufort Sea 2012–2014. Length frequency includes fish caught by all gears and is not adjusted for abundance. No fish from 2014 were available for aging. 240

Figure 7.3.3.1. Total catch per unit effort (# 1000 m^{-3}) of pelagic fish at each station in the Beaufort Sea in 2012 and 2013 for Isaacs-Kidd midwater trawl (IKMT). 247

Figure 7.3.3.2. Numbers of pelagic fish taxa captured at each station in the Beaufort Sea in 2012 and 2013 by Isaacs-Kidd midwater trawl (IKMT). 248

Figure 7.3.3.3. Pelagic fish species richness (Margalef index) at each station in the Beaufort Sea in 2012 and 2013 for Isaacs-Kidd midwater trawl (IKMT). 249

Figure 7.3.3.4. Pelagic fish species evenness (Pielou's index) at each station in the Beaufort Sea in 2012 and 2013 for Isaacs-Kidd midwater trawl (IKMT). 250

Figure 7.3.3.5. Pelagic fish diversity (Simpson's index) at each station in the Beaufort Sea in 2012 and 2013 for Isaacs-Kidd midwater trawl (IKMT). 251

Figure 7.3.3.6. Matrix of community structure of pelagic fishes caught by Isaacs-Kidd midwater trawl (IKMT) in 2012 and 2013 by abundance. 252

Figure 7.3.3.7. Map of pelagic fish communities defined using fourth-root transformed (4RT) abundance data based on clusters in Figure 7.3.3.6. Catches by Isaacs-Kidd midwater trawl (IKMT) in the Beaufort Sea during 2012–2013. 253

Figure 7.3.3.8. nMDS ordination of pelagic fish communities defined using Isaacs-Kidd midwater trawl (IKMT) abundance. Ellipses are significantly different clusters of stations (p <0.005); a) communities and b) year. Stations at which no fish were collected, A2-1000 and A6-750, were not included. 255

Figure 7.3.3.9. Canonical correspondence analysis (CCA) ordination relating pelagic fish abundance during 2012 and 2013 to selected environmental variables. 256

Figure 7.3.4.1. Average number of demersal fishes collected at each station by beam trawl in the Beaufort Sea during 2012–2014. Catch is not adjusted for effort. 260

Figure 7.3.4.2. Number of unique demersal fish taxa captured by beam trawl at each station in the Beaufort Sea during 2012–2014. All quantitative hauls from the station in a single year are combined. 261

Figure 7.3.4.3. Demersal fish species richness (Margalef index) at each station in the Beaufort Sea during 2012–2014 for beam trawl. 262

Figure 7.3.4.4. Demersal fish species evenness (Pielou's index) at each station in the Beaufort Sea during 2012–2014 for beam trawl. 263

Figure 7.3.4.5. Demersal fish diversity (Simpson's index) at each station in the Beaufort Sea during 2012–2014 for beam trawl. 264

Figure 7.3.4.6. Community structure of demersal fishes in replicate beam trawl hauls along depth strata of Transect A1 sampled in 2014 by biomass (upper) and abundance (lower). 266

Figure 7.3.4.7. Biomass (g 1000 m^{-2}) of demersal fishes captured by beam trawl during Transboundary 2013 and 2014, by depth and transect. 269

Figure 7.3.4.8. Abundance (number 1000 m^{-2}) of demersal fishes captured by beam trawl during Transboundary 2013 and 2014, by depth and transect. 270

Figure 7.3.4.9. Demersal fish biomass community structure in 2013 and 2014 at transects A6, A2, A1 and TBS displayed in nMDS. 271

Figure 7.3.4.10. Demersal fish abundance (number fish 1000 m^{-2}) community structure in 2013 and 2014 at transects A6, A2, A1 and TBS displayed in nMDS. 272

Figure 7.3.4.11. Demersal fish biomass (gms fish 1000 m^{-2}) community structure in 2013 and 2014 at transects A6, A2, A1 and TBS displayed in nMDS. Shelf (10–100 m), slope (200–1000 m). 273

Figure 7.3.4.12. Demersal fish abundance (# fish 1000 m^{-2}) community structure on shelf and slope in 2013 and 2014 at transects A6, A2, A1 and TBS displayed in nMDS. Shelf (10–100 m), slope (200–1000 m). 274

Figure 7.3.4.13. Average demersal fish biomass (gms 1000 m^{-2}, upper panel) and abundance (# 1000 m^{-2}, lower panel) of beam trawl samples during 2013–2014. 277

Figure 7.3.4.14. Community structure of demersal fishes in beam trawl hauls in 2013 by biomass (upper) and abundance (lower). 278

Figure 7.3.4.15. Map of demersal fish communities defined using fourth-root transformed (4RT) biomass of species collected by beam trawl in the Beaufort Sea during 2013. 279

Figure 7.3.4.16. Map of demersal fish communities defined using fourth-root transformed (4RT) abundance of species collected by beam trawl in the Beaufort Sea during 2013. 280

Figure 7.3.4.17. Community structure of demersal fishes in beam trawl hauls in 2014 by biomass (upper) and abundance (lower). 286

Figure 7.3.4.18. Map of demersal fish communities defined using fourth-root transformed (4RT) biomass of species collected by beam trawl in the Beaufort Sea during 2014. 287

Figure 7.3.4.19. Map of demersal fish communities defined using fourth-root transformed (4RT) abundance of species collected by beam trawl in the Beaufort Sea during 2014. 288

Figure 7.3.4.20. Matrix of community structure of demersal fishes in beam trawl hauls in 2013 and 2014 by biomass. 292

Figure 7.3.4.21. Matrix of Community structure of demersal fishes in beam trawl hauls in 2013 and 2014 by abundance. Red lines indicate non-significant differences among stations, and black lines indicate differences between clusters of $p < 0.05$ for stations and $p < 0.005$ for taxa. Abundance is # fish 1000 m^{-3} and intensity of the color ramp indicates proportionally higher abundance of the taxon at the station. 293

Figure 7.3.4.22. Demersal fish communities defined using fourth-root transformed (4RT) biomass of species collected by beam trawl in the Beaufort Sea during 2013 and 2014. 294

Figure 7.3.4.23. Demersal fish communities defined using fourth-root transformed (4RT) abundance of species collected by beam trawl in the Beaufort Sea during 2013 and 2014. 295

Figure 7.3.4.24. Demersal fish communities in beam trawls in the Beaufort Sea during 2013 and 2014 based on biomass (upper) and abundance (lower) coded at each station by depth.300

Figure 7.3.4.25. Demersal fish communities in beam trawls in the Beaufort Sea during 2013 and 2014 based on biomass (upper) and abundance (lower) coded at each station by water mass. 301

Figure 7.3.4.26. Canonical correspondence analysis (CCA) ordination relating demersal fish abundance in beam trawls during 2013 and 2014 to selected environmental variables at 89 stations. 303

Figure 7.3.4.27. Community structure of demersal fishes in beam trawl hauls in 2012–2014 by presence/absence. 306

Figure 7.3.4.28. Map of demersal fish communities defined using presence/absence of species collected by beam trawl in the Beaufort Sea during 2012–2014. 307

Figure 7.3.4.29. Number of unique demersal fish taxa captured by otter trawl at each station in the Beaufort Sea during 2012–2013. 310

Figure 7.3.4.30. Community structure of demersal fishes in otter trawl hauls in 2012 and 2013 based by presence/absence. 311

Figure 7.3.4.31. Demersal fish communities defined using presence/absence of species collected by otter trawl in the Beaufort Sea during 2012–2013. 312

Figure 7.3.4.32. Presence/absence (PA) transformation for demersal fish catches from all stations sampled by beam and otter trawls in 2012, 2013, and 2014 in the Beaufort Sea. 315

Figure 7.3.4.33. Demersal fish communities defined using presence/absence of species collected by beam and otter trawls in the Beaufort Sea during 2012–2014. 316

Figure 7.3.4.34. nMDS of demersal fish captured by beam and otter trawls in 2012, 2013, and 2014 in the Beaufort Sea based on presence/absence. 321

Figure 7.3.4.35. nMDS of demersal fish captured by beam and otter trawls in 2012, 2013, and 2014 based on presence/absence. PML – Polar Mixed Layer, AHW – Arctic Halocline Water, AW – Atlantic Water. 322

Figure 7.3.4.36. nMDS of demersal fish captured by beam and otter trawls in 2012, 2013, and 2014 based on presence/absence. BT – beam trawl, OT – otter trawl. 323

Figure 8.2.1. Transects and stations sampled in the Beaufort Sea. 338

Figure 8.2.3.1. The percent contribution by number of small (<5 mm), medium (5–9.5 mm), large (10–19.5 mm) and extra-large (≥20 mm) prey eaten by demersal *Boreogadus saida,* summarized by six size classes of fish: (≤39 mm, 40–49 mm, 50–59 mm, 60–79 mm, 80–169 mm, and 170–240 mm). 341

Figure 8.2.3.2. The percent contribution by number of small (<5 mm), medium (5–9.5 mm), and large (10–19.5 mm) prey summarized by three size classes of pelagic *Boreogadus saida*: (≤39 mm, 40–59 mm, ≥60 mm). Error bars signify the standard error of the mean percent number of prey sizes in pelagic *B. saida* diet. 342

Figure 8.2.3.3. Pooled diet compositions of all *Aspidophoroides olrikii*, *Artediellus scaber*, *Gymnocanthus tricuspis*, *Icelus spatula*, *Triglops pingelii*, *Anisarchus medius*, and *Lumpenus fabricii*, based on mean weight of prey and including stomachs with unidentifiable prey. Stomach sample sizes are listed above each species column. 343

Figure 8.2.3.4. Non-metric multidimensional scaling (nMDS; 3D Stress: <0.01) of %MW of prey to determine diet similarities and differences among seven fish species. 344

Figure 8.2.3.5. Percent mean weight (%MW) values for coarse prey groups found in stomachs of four eelpout species of the genus *Lycodes*. 346

Figure 8.2.3.6. Average stable nitrogen and carbon isotope signatures for four eelpout species. Dots indicate mean values and error bars indicate standard deviations. 346

Figure 8.3.2.1. Stations in the Beaufort and Chukchi seas from which *Lycodes* spp. were collected for this report section. 352

Figure 8.3.3.1. Multivariate representation of fatty acid profiles of species, regions, and years. 354

Figure 8.3.3.2. Variation in major fatty acid classes among *Boreogadus saida,* and Eelpout Species. 355

Figure 8.3.3.3. Regional variation in major fatty acid classes for *Boreogadus saida*. 355

Figure 8.3.3.4. Temporal variation in major fatty acid classes for Beaufort Sea *Boreogadus saida*. 356

Figure 8.4.3.1.1. Map of sampling stations during 2012 and 2013 Transboundary cruises, grouped into four regions (from west to east: Colville Plume (CP, including transects B1, B2 and BX), Camden Bay (CB, including transect A1), Outer Mackenzie Plume (OMP, including transects A2, A1, and TBS), and Inner Mackenzie Plume (IMP, including transects MAC and GRY). 359

Figure 8.4.5.1.1. $\delta^{18}O$ values (‰) of water samples taken from the surface (A) and 10 m depth (B) in the 2013 sampling area (CB, OMP, and IMP regions). 365

Figure 8.4.5.2.1. Biplot of $\delta^{13}C$ and $\delta^{15}N$ values for pelagic particulate organic matter (pPOM) and sediment POM (sPOM) compared alongside potential POM endmembers in the eastern Beaufort Sea. 366

Figure 8.4.5.2.2. Carbon to nitrogen ratios, $\delta^{13}C$ and $\delta^{15}N$ values of pPOM and sPOM against station bottom depth, averaged by region. 367

Figure 8.4.5.3.1. Mean (±SD) $\delta^{13}C$ values (‰) of possible food sources (pPOM and sPOM; shaded background) and consumer feeding guilds (white background), by region and depth group (shelf or slope) for 2012 and 2013. 369

Figure 8.4.5.3.2. $\delta^{15}N$ values (‰) of select benthic consumer by bottom depth (on log-scale) across the 2013–2014 study area. 370

Figure 8.4.5.4.1. Contribution of benthic taxa (percent) to tropic levels (TL), calculated from three different baselines: pPOM (top panel) and the primary consumer *Ophiocten sericeum* (lower panel). 371

Figure 8.4.5.4.2. Trophic positions (TP) of individual consumers by shelf and slope regions in 2012 and 2013. 373

Figure 8.4.5.4.3. Relative distribution of epibenthic consumer biomass to trophic levels (TL) in shelf and slope communities at transect A6 (146° W) in 2014. 374

Figure 8.4.5.4.4. Relative distribution of epibenthic consumer biomass to trophic levels (TL) in shelf and slope communities at transect A2 (142° W) in 2014. 374

Figure 8.4.5.4.5. Relative distribution of epibenthic consumer biomass to trophic levels (TL) in shelf and slope communities at transect A1 (141° W) in 2014. 375

Figure 8.4.5.4.6. Relative distribution of epibenthic consumer biomass to trophic levels (TL) in shelf and slope communities at transect TBS (140° W) in 2014. 375

Figure 8.4.5.5.1. Trophic position of individual taxa sampled in both 2013 and 2014 on the transect A6 shelf, calculated from two different baselines: pelagic POM (TP POM) and the brittle star *Ophiocten sericeum* (TP Os) (upper panel). Proportional contribution of taxa to trophic levels (lower panel)..... 377

Figure 8.4.5.5.2. Trophic position of individual taxa sampled in both 2013 and 2014 on the transect A6 slope, calculated from two different baselines: pelagic POM (TP POM) and the brittle star *Ophiocten sericeum* (TP Os) (upper panel). Proportional contribution of taxa to trophic levels (lower panel)..... 378

Figure 8.4.5.5.3. Trophic position of individual taxa sampled in both 2013 and 2014 on the transect A1 shelf, calculated from two different baselines: pelagic POM (TP POM) and the brittle star *Ophiocten sericeum* (TP Os) (upper panel). Proportional contribution of taxa to trophic levels (lower panel)..... 379

Figure 8.4.5.5.4. Trophic position of individual taxa sampled in both 2013 and 2014 on the transect A1 slope, calculated from two different baselines: pelagic POM (TP POM) and the brittle star *Ophiocten sericeum* (TP Os) (upper panel). Proportional contribution of taxa to trophic levels (lower panel)..... 380

Figure 8.4.5.5.5. Trophic position of individual taxa sampled in both 2013 and 2014 on the transect TBS shelf, calculated from two different baselines: pelagic POM (TP POM) and the brittle star *Ophiocten sericeum* (TP Os) (upper panel). Proportional contribution of taxa to trophic levels (lower panel)..... 381

Figure 8.4.5.5.6. Trophic position of individual taxa sampled in both 2013 and 2014 on the transect TBS slope, calculated from two different baselines: pelagic POM (TP POM) and the brittle star *Ophiocten sericeum* (TP Os) (upper panel). Proportional contribution of taxa to trophic levels (lower panel)..... 382

Figure 9.1. Community patterns for zooplankton and epifauna based on biomass, and fish presence/absence (PA) for B transects (150°–151° W, Colville Region) in the Beaufort Sea in 2012..... 405

Figure 9.2. Community patterns for zooplankton, epifauna, and fish based on biomass for A and Canadian transects (146°–136° W, Camden Bay, US–Canada border, and Mackenzie regions) in the Beaufort Sea in 2013..... 406

Figure 9.3. Community patterns for zooplankton, epifauna, and fish based on biomass for A and TBS transects (146°–140° W, Camden Bay and US–Canada border regions) in the Beaufort Sea in 2014..... 407

Figure 9.4. Community patterns for zooplankton and epifauna based on abundance, and fish presence/absence for B transects (150°–151° W, Colville region) in the Beaufort Sea in 2012..... 408

Figure 9.5. Community patterns for zooplankton, epifauna, and fish based on abundance for A and Canadian transects (146°–136° W, Camden Bay US–Canada border, and Mackenzie regions) in the Beaufort Sea in 2013..... 409

Figure 9.6. Community patterns for zooplankton, epifauna, and fish based on abundance for A and TBS transects (146°–140° W, Camden Bay and US–Canada border regions) in the Beaufort Sea in 2014..... 410

Figure 10.1. Under-Ice study location in the vicinity of Barter Island, eastern Beaufort Sea, 2014. 414

Figure 10.2. Photographic summary of ice removal procedure to create holes for dive access. 415

Figure 10.3. Map of stations sampled during 2015 RV *Sikuliaq* ice trials. Ice concentration from AMSR2 (Advanced Microwave Scanning Radiometer 2) satellite for 22 March 2015, where purple in complete ice cover. (Map courtesy of Steve Roberts)..... 417

Figure 10.4. Midwater trawl stations were divided into two different fishing environments during ice-associated trawling, 2015..... 418

Figure 10.5. Relative abundance of benthic taxa in grab samples at the three study sites in 2014. 420

Figure 10.6. Temperature (left) and salinity (right) vertical profiles at the three study sites. 421

Figure 10.7. Water column (a) and sea ice (b) chlorophyll and phaeophytin concentrations and their respective ratio at the three dive sites..... 422

Figure 11.1. Recommended transect design for a Beaufort Sea interannual assessment plan. .. 431

LIST OF TABLES

Table 3.4.1. Range of grain sizes that make up each descriptive category with equivalents in phi notation. 78

Table 3.4.2 Eigenvalues and eigenvectors for principle components analysis (PCA) shown in Figure 3.4.10. Variables contributing the most to variation along each axis are in bold (defined by values > ±3.5). 80

Table 3.4.3 Loading values for canonical discriminant analysis (CDA) examining variation in habitat parameters among depths with *temperature and salinity included*. Variables contributing the most to each canonical variables (CV) are in bold (defined by values > ±0.4). 80

Table 3.4.4. Loading values for canonical discriminant analysis (CDA) examining variation in habitat parameters among depths with *temperature and salinity excluded*. Variables contributing the most to each canonical variables (CV) are in bold (defined by values > ±0.4). 81

Table 3.4.5 Loading values for canonical discriminant analysis (CDA) examining variation in habitat parameters among transects with *temperature and salinity included*. Variables contributing the most to each canonical variables (CV) are in bold (defined by values > ±0.4). 81

Table 3.4.6 Loading values for canonical discriminant analysis (CDA) examining variation in habitat parameters among transects with *temperature and salinity excluded*. Variables contributing the most to each canonical variables (CV) are in bold (defined by values > ±0.4). 82

Table 4.1. Average abundance and biomass of Beaufort Sea zooplankton taxa captured by the 150-µm net during Transboundary 2012–14. 101

Table 4.2. Average abundance and biomass of Beaufort Sea zooplankton taxa captured by the 505-µm net during Transboundary 2012–14. 104

Table 4.3. Mean zooplankton abundance (ind. m^{-3}) and biomass (mg DW m^{-3}) ±SE for the 150- and 505-µm during Transboundary 2012-14. Upper portion of table is displayed by year; lower portion of table is displayed by isobath and depth interval, when applicable. 107

Table 4.4. Key taxa and their contribution to the first 90% of community similarity for community groupings for the 150-µm net abundance data from Transboundary 2012–14. Outliers not included. 125

Table 4.5. Relationship between pooled 150-µm zooplankton and abiotic factors over different depth intervals during Transboundary 2012–14. 126

Table 4.6. Key taxa and their contribution to the first 90% of community similarity for community groupings for the 505-µm net abundance data from Transboundary 2012–14. Outliers not included. 128

Table 4.7. Relationship between pooled 505-µm zooplankton and abiotic factors over different depth intervals during Transboundary 2012–14. 129

Table 4.8. Mean abundance and biomass over the entire water column for taxa observed during Transboundary 2012–14. 142

Table 4.9. Mean abundance, biomass and species richness of the zooplankton community in each sampling stratum for the Beaufort Sea during Transboundary 2012–14. Water masses are noted. 146

Table 4.10. Relationship between vertical zooplankton community structure and environmental variables during Transboundary 2012–14, as revealed by BEST analysis for Temperature (*T*), Salinity (*S*), and Depth (*D*). 147

Table 4.11. Comparison of average biomass (mg DW m^{-3}) in zooplankton sampling intervals from the Beaufort slope and the Arctic's basins. 155

Table 5.3.1. Results of DistLM model of annelid assemblage structure (family-level taxonomy), showing multiple partial correlations between predictor variables and dbRDA axes (see Figure 5.3.5). 163

Table 6.4.1. Number of taxa within phyla encountered in different sampling years. 168

Table 6.4.2. Effects of factors year, depth and longitude on community composition in 2013 and 2014, based on absolute biomass and abundance data. "Year" was tested with 1-way ANOSIM; ordered factors "depth" and "longitude" were tested in a 2-way crossed ANOSIM design. 179

Table 6.4.3. Percent similarity along transect A1 (141° W) on repeat trawls within 2014 (first column) and between trawls taken in 2013 and 2014 at the same station (second column). 184

Table 6.4.4. Effects of depth and longitude on community composition in 2012, 2013, and 2014, based on relative biomass and abundance data. 185

Table 6.4.5. Correlation of environmental variables with epibenthic communities, based on Spearman rank correlation coefficient (rho, BEST analysis). 185

Table 7.2.1. Successful pelagic and demersal gear deployments at stations occupied 2012–2014. 199

Table 7.3.1.1. Fishes captured in all hauls of pelagic (Isaacs-Kidd midwater trawl, IKMT; Aluette midwater trawl, AMT) and demersal (beam trawl, BT; otter trawl, OT) in Beaufort Sea 2012–2014. 211

Table 7.3.1.2. List of fishes captured in successful hauls during TB-2012-US, TB-2013-US and TB-2014-US with bottom and pelagic trawls, in phylogenetic order by family. 217

Table 7.3.1.3. Abundance of fishes captured in pelagic and demersal habitats in the Beaufort Sea 2012–2014..... 220

Table 7.3.2.1. Weight at length relationships for fish species. 224

Table 7.3.2.3. 95% confidence intervals (CI) for length (mm) at age for each of 12 fish species captured during the Transboundary project, 2012–2014. 241

Table 7.3.3.1. Pelagic fish community composition as defined by abundance (fourth-root transformed) in 2012–2013 Isaacs-Kidd midwater trawl (IKMT) hauls. 254

Table 7.3.3.2. Mean abundance (± standard deviation) (per 1000 m^{-3}) of pelagic fishes caught by Isaacs-Kidd midwater trawl (IKMT) in the Central region (2012) and on the Eastern Shelf (≤100 m) and Eastern Slope (≥200 m) in 2013. 257

Table 7.3.3.3. Effects of year, depth and longitude on pelagic fish abundance (4RT) community composition in 2012–2013 Isaacs-Kidd midwater trawl (IKMT) hauls in the Beaufort Sea..... 258

Table 7.3.3.4. Canonical correspondence analysis abundance (4RT) of pelagic fishes captured by Isaacs-Kidd midwater trawl (IKMT) and environmental (normalized) variables in the Beaufort Sea in 2012 and 2013. 258

Table 7.3.3.5. BEST (stepwise) relationship of pelagic fishes caught by Isaacs-Kidd midwater trawl (IKMT) and environmental variables in the Beaufort Sea in 2012 and 2013. 258

Table 7.3.4.1. Percent similarity of demersal fish community composition within stations along transect A1 from replicate trawls within 2014 and between replicate trawls in 2013 and 2014 at the same station, based on biomass and abundance. Data were fourth-root transformed (4RT). 267

Table 7.3.4.2. PERMANOVA comparisons of relative abundance of demersal fish species and size classes among beam trawl gears (PSBT-A and CBT), depths (20–1000 m), and transects (A2, A1, TBS, GRY). 267

Table 7.3.4.3. Effects of year, depth and transect/longitude on demersal fish biomass and abundance community composition in 2013 and 2014..... 275

Table 7.3.4.4. Mean abundance (± standard deviation) (# 1000 m^{-2}) of demersal fishes caught by beam trawl on the shelf (≤100 m) and slope (≥200 m) in 2013 and 2014. 281

Table 7.3.4.5. Demersal fish community composition as defined by biomass (fourth-root transformed) in 2013 beam trawl hauls. 283

Table 7.3.4.6. Demersal fish community composition as defined by abundance (fourth-root transformed) in 2013 beam trawl hauls. 284

Table 7.3.4.7. Demersal fish community composition as defined by biomass (fourth-root transformed) in 2014 beam trawl hauls. 289

Table 7.3.4.8. Demersal fish community composition as defined by abundance (fourth-root transformed) in 2014 beam trawl hauls. 290

Table 7.3.4.9. Demersal fish community composition as defined by biomass (fourth-root transformed) in combined 2013 and 2014 beam trawl hauls. 296

Table 7.3.4.10. Demersal fish community composition as defined by abundance (fourth-root transformed) in combined 2013 and 2014 beam trawl hauls. 297

Table 7.3.4.11. Effects of depth and longitude on fish biomass and abundance (fourth root transformed) community composition in combined 2013 and 2014 beam trawl hauls in the Beaufort Sea. 299

Table 7.3.4.12. Effect of water mass on community composition as defined by fish biomass (upper half matrix) and abundance (lower half matrix, fourth-root transformed) in combined 2013 and 2014 beam trawl hauls in the Beaufort Sea. 299

Table 7.3.4.13. BEST (stepwise) relationship of demersal fishes captured by beam trawls and environmental variables in the Beaufort Sea in 2013 and 2014 combined. 302

Table 7.3.4.14. Canonical correspondence analysis abundance (4RT) of demersal fishes captured by beam trawls and environmental (normalized) variables in the Beaufort Sea at 89 stations in 2013 and 2014 combined. 304

Table 7.3.4.15. Canonical correspondence analysis abundance (4RT) of demersal fishes captured by beam trawls and environmental (normalized) variables in the Beaufort Sea at 54 stations in 2013 and 2014 combined. The reduced dataset allowed percent mud to be included. 305

Table 7.3.4.16. Presence/absence (PA) of demersal fishes 2012, 2013, and 2014 combined in the Beaufort Sea captured by beam trawl. 308

Table 7.3.4.17. Demersal fish community composition as defined by presence/absence in 2012–2013 combined otter trawl hauls. 313

Table 7.3.4.18. Demersal fishes, by family and species, captured by two different bottom trawls. Beam trawls had 4-mm mesh in codend. Otter trawl had 19-mm mesh codend. N is total number caught. Size range minimum, maximum, mean and standard deviation of fishes by gear. 317

Table 7.3.4.19. Demersal fish community composition as defined by presence/absence in 2012–2014 beam and otter trawl hauls. 319

Table 7.3.4.20. Effects of water mass on community composition of demersal fish based on presence/absence in 2012–2014 beam and otter trawl stations in the Beaufort Sea. 324

Table 7.3.4.21. Effects of year on community composition of demersal fish based on presence/absence at 2012–2014 beam and otter trawl stations in the Beaufort Sea. 324

Table 7.3.4.22. Effects of year and longitude on community composition of demersal fish based on presence/absence at 2012–2014 beam and otter trawl stations in the Beaufort Sea.. 324

Table 7.3.4.23. BEST (stepwise) relationship of presence/absence of demersal fishes and environmental variables at 124 stations in the Beaufort Sea in 2012, 2013 and 2014. .. 325

Table 7.3.4.24. BEST (stepwise) relationship of presence/absence of demersal fishes and environmental variables at 70 stations in the Beaufort Sea in 2012, 2013 and 2014. 326

Table 7.4.1. Life history characteristic summary. 329

Table 8.2.3.1. Size class recommendations for fish families Gadidae, Cottidae, Agonidae, Zoarcidae, and Stichaeidae. 348

Table 9.1. Similarity in distribution of communities of demersal fishes and zooplankton, and demersal fishes and epibenthos in 2013–2014 in the Beaufort Sea. Communities are based on abundance. 411

Table 10.1. Observations of under-ice fauna during dive transects and from gill nets. 419

Table 10.2. Relative abundance (%) of various taxa found in zooplankton net samples at the three study sites. 421

Table 11.1. Sample collections in the Beaufort Sea by year and longitude..... 430

Table 11.2. Sampling alternatives for Beaufort Sea fish and lower trophic level monitoring. .. 434

LIST OF APPENDICES

Appendix A. Details of Field Sampling Plan

Appendix B. UAF Fisheries Oceanography Beaufort Sea US-Canada Transboundary Field Manual

Appendix C. Environmental Data–CTD and Substrate Tables

Appendix D. Epibenthic Fauna

Appendix E1. Fish Counts by Gear

Appendix E2. Maps of Pelagic and Demersal Fish Presence

Appendix E3. Maps of Pelagic and Demersal Fish Abundance and Biomass

Appendix E4. Age Composition and Growth Rates of Arctic Cod in the Chukchi and Beaufort Seas

Appendix E5. CCA Ordination Relating Demersal Fish Abundance in Beam Trawls During 2013 and 2014

Appendix F. Diet of Arctic Cod in the US Beaufort Sea

Appendix G. Diets of Three Families of Demersal Fishes in the Beaufort Sea: Agonidae, Cottidae and Stichaeidae

Appendix H. Diets of Four Eelpout Species (Genus Lycodes) in the US Beaufort Sea Based on Analyses of Stomach Contents and Stable Isotopes of Nitrogen and Carbon

Appendix I. Food Web Tables

Appendix J. Monitoring Plan Design

Appendix K. Database Description

LIST OF ACRONYMS

Acronym	Description
AFS	American Fisheries Society
AHW	Arctic Halocline Water
AKMAP	Alaska Monitoring and Assessment Program; https://dec.alaska.gov/water/wqsar/monitoring/AKMAP.htm
AMT	Aluette midwater trawl
ANOSIM	Analysis of similarity
ANOVA	Analysis of variance
ASIF	Alaska Stable Isotope Facility, University of Alaska Fairbanks; http://ine.uaf.edu/werc/asif
AW	Atlantic Water
BEST	Biota-environment stepwise matching test
BOEM	Bureau of Ocean Energy Management
BPUE	Biomass per unit effort
BREA	Beaufort Regional Environmental Assessment
BT	Beam trawl
CAA	Conflict Avoidance Agreement
CASES	Canadian Arctic Shelf Exchange Study
CB	Camden Bay
CBT	Canadian beam trawl
CCA	Canonical correspondence analysis
CDA	Canonical discriminant analysis
CP	Colville Plume
CPUE	Catch per unit effort
CTD	Conductivity, temperature, density
CV	Canonical variables
CW	Carapace width
DBO	Distributed Biological Observatory

Acronym	Description
dbRDA	Distance-based redundancy analysis
DFO	Fisheries and Oceans Canada
DHA	Docosahexaenoic acid
DistLM	Distance-based linear models
DVM	Diel vertical migration
DW	Dry-weight
EEZ	Exclusive economic zone
EPA	Eicosapentaenoic acid
FAME	Fatty acid methyl esters
FID	Flame ionization detector
FMP	Fishery management plan
FOL	Fisheries Oceanography Laboratory at the University of Alaska Fairbanks
GC	Gas chromatogram
IKMT	Isaacs-Kidd midwater trawl
IMP	Inner Mackenzie Plume
IndVal	Indicator value
IRMS	Isotope ratio mass spectrometer
IPCC	Intergovernmental Panel on Climate Change
MDS	Metric multidimensional scaling
MUFA	Monounsaturated fatty acids
MW; %MW	Mean weight of prey taxon, expressed as percentage
nMDS	Non-metric multidimensional scaling
nmi	Nautical mile
NOAA	National Oceanic and Atmospheric Administration; http://www.noaa.gov/
NP MANOVA	Non-parametric multivariate analysis of variance
NPFMC	North Pacific Fishery Management Council
NT	Not transformed

Acronym	Description
OCS	Outer Continental Shelf
OCSEAP	Outer Continental Shelf Environmental Assessment Program
OM_{terr}	Terrestial organic matter
OMP	Outer Mackenzie Plume
OT	Otter trawl
PCA	Principle components analysis
PERMANOVA	Permutational analysis of variance
PML	Polar Mixed Layer
POC	Particulate organic carbon
POM	Particulate organic matter
PA	Presence/absence
PSBT-A	Modified plumb staff beam trawl
PUFA	Polyunsaturated fatty acids
RUSALCA	Russian-American Long-Term Census of the Arctic
RO	Reverse osmosis
ROV	Remotely operated vehicle
SCUBA	Self-contained underwater breathing apparatus
SFA	Saturated fatty acids
SIAR	Stable Isotope Analysis in R
SIMPER	Similarity percentage analysis
SIMPROF	Similarity profile analysis
SUIT	Surface and under ice trawl
TDR	Time-depth recorder
TL	Trophic level
TOC	Total organic carbon
TP	Trophic position
UAF	University of Alaska Fairbanks; http://www.uaf.edu/

Acronym	Description
VPDB	Vienna Pee Dee Belemnite
VSMOW	Vienna Standard Mean Ocean Water
WEBSEC	Western Beaufort Sea Ecological Cruise

1.0 OVERALL INTRODUCTION

Increasing interest in oil and gas development in the outer continental shelf (OCS) in the eastern Beaufort Sea has elevated the need to collect ecological baseline data for fish and lower trophic organisms in the Beaufort Sea waters of the United States and Canada. This study, "US-Canada Transboundary Fish and Lower Trophic Communities," (BOEM Report 2017-034), offered an interdisciplinary approach to examine resources in the Beaufort Sea OCS.

The purpose of this study was to provide the Bureau of Ocean Energy Management (BOEM) Alaska Outer Continental Shelf Region, the State of Alaska, Alaska and North Slope Borough residents, and other interested stakeholders information regarding presence, abundance, distribution, and habitat of fish and invertebrate (benthic and zooplankton) in the eastern Beaufort Sea OCS lease area during the open water season. This project is the first time that US Beaufort Sea continental slope at 200–1000 m was extensively sampled by bottom trawl. The information gained increases knowledge of the Beaufort Sea ecosystem and may be used to inform decision making by federal and state resource managers. Historical data are limited, especially in the eastern Beaufort Sea, where information about marine fish and lower trophic communities is often extrapolated from data in the western Beaufort Sea. This research identified fish species inhabiting the eastern Beaufort Sea study area and provided baseline information about abundance, distribution, habitat, and seasonal/interannual variability of both fish and invertebrates in this understudied lower trophic food web.

The US and Canada share the Beaufort Sea continental shelf and slope ecosystem. The Beaufort Sea continental shelf extends from the Barrow Canyon in western Alaska eastward across the US-Canada border and the Canadian Mackenzie River Canyon to the Canadian Arctic Archipelago. In Barrow Canyon, the Alaska Coastal Current forms a coastal jet that sweeps along the Beaufort Sea continental slope west to east in the absence of an easterly wind. However, under the influence of a strong easterly wind (>6 m/s), the jet at the edge of the Beaufort shelf reverses and flows westward (Pickart et al. 2011). US Beaufort Sea waters are also influenced by the dynamics of the Mackenzie River, the 12th largest river in the world and the fourth largest river in the Arctic. The Mackenzie River outflow plays a major role in the ecology of the Beaufort Sea shelf, including the habitat and ecology of the fish species that range across the US and Canada border. Therefore, we collaborated with Canada's Department of Fisheries and Oceans to sample the Mackenzie Canyon and westward to examine its influence on the biology and ecosystem on the shelf and slope of our shared Beaufort Sea, particularly with respect to fish and lower trophic levels. Our sample area was in central and east US Beaufort Sea waters and within and east of the Mackenzie River Canyon in the western Canadian Beaufort Sea waters, extending from 151.0º–136.7º W. The entire area was not sampled in every year.

The overall goal of this study was to implement and conduct marine fish surveys in the Beaufort Sea OCS Planning Area in 2012, 2013, and 2014. General objectives are listed here and specific objectives are addressed in each chapter of this report.

Objectives:

1. Collaborate with Fisheries and Oceans Canada (DFO) Central Arctic Region to coordinate cruise times and sample collections (Chapter 2) and to share methods, data formats, and results. There was an exchange of US and Canadian fish scientists on the 2013 cruises.

2. Document and correlate baseline fish (Chapter 7) and invertebrate species (Chapters 4–zooplankton, 5–infauna, 6–epibenthos) presence, abundance, distribution, and habitat in the eastern Beaufort Sea OCS lease area during the open water season (Chapter 9).
3. Contribute samples and data to support Canadian development of a Beaufort shelf fish and marine mammal food web model.
4. Test under-ice methods to provide baseline information for the ice-covered season (Chapter 10).
5. Based on survey results, recommend a nested sampling design and refinements of survey methods for future monitoring studies (Chapter 11).
6. Document the physical and chemical water characteristics that will contribute to a collaborative effort to establish oceanographic boundary conditions in the eastern US Beaufort Sea (Chapter 3).

2.0 AT-SEA COLLECTION METHODS

Brenda Norcross, Bodil Bluhm, Lorena Edenfield, Sarah Hardy, Brenda Holladay, Russell Hopcroft, and Katrin Iken

Open water shipboard surveys to collect zooplankton, infauna, epifauna, fish and associated physical data were conducted during 2012, 2013, and 2014 from the central US Beaufort Sea north of Harrison Bay into the eastern Canadian Beaufort Sea just east of the Mackenzie Canyon (Figure 2.1). Spatial comparisons were made across the whole sample area from 151º–135º W. The central (B) transects 151º–150º W were sampled 20 September–1 October 2012 and the eastern transects 146º–135º W were sampled in 12 August–2 September 2013 and 17 August–2 September 2014. The groups of B and A transects and the TBS transect (in US waters) were placed along lines of longitude. In Canadian waters, the MAC and GRY transects radiated to the northwest from near the mouth of the Mackenzie River. Depths from 20–1000 m were sampled across the study area. Sampling in US Arctic is marked by challenges such as minimizing impact to subsistence hunting, securing research vessel access, and working with variable weather conditions (Appendix A). Over the course of the project, field sample and analysis plans were improved and refined by incorporating knowledge gained on the prior cruises. Protocols for gear deployment and field processing of samples are found in Appendix B.

2.1 Physical Oceanography, Chemical Oceanography and Chlorophyll-*a*

Oceanographic data were sampled along cross-shelf transects at stations ranging from 20–1000 meters in depth from the Colville River to the Mackenzie River (Figure 2.1). Physical oceanographic data were collected with a Seabird SBE25 CTD (2012 and 2013) or SBE911+ CTD (2014) and averaged into 1 m vertical intervals. Chlorophyll-*a* and macronutrient samples were collected with a 6 Niskin bottle SBE55 (2012 and 2013) or 14 bottle SBE32SC (2014) rosette attached to the CTD. Water samples for chlorophyll-*a* and macronutrient analysis were taken at the surface, 10, 20, 30, 40, and 50 m; when stations were shallower than 50 m, the deepest water sample was collected approximately three meters from the seafloor. During 2014, the eight extra bottles available on the SBE32SC allowed additional nutrient sampling at 75, 100, 125, 150, 200, 300, 500, and 1000 m. Water for chlorophyll-*a* analysis was filtered under low pressure onto Whatman GF/F filters and then frozen at -40 °C for post-cruise analysis following Parsons et al. (1984). In 2013 and 2014, 20 µm polycarbonate filters and Whatman GF/F filters were used to size-fractionate cells. Nutrient samples were filtered with 0.45 µm cellulose-acetate filters and frozen immediately at -40 °C for post-cruise analysis following the methods of Gordon et al. (1993).

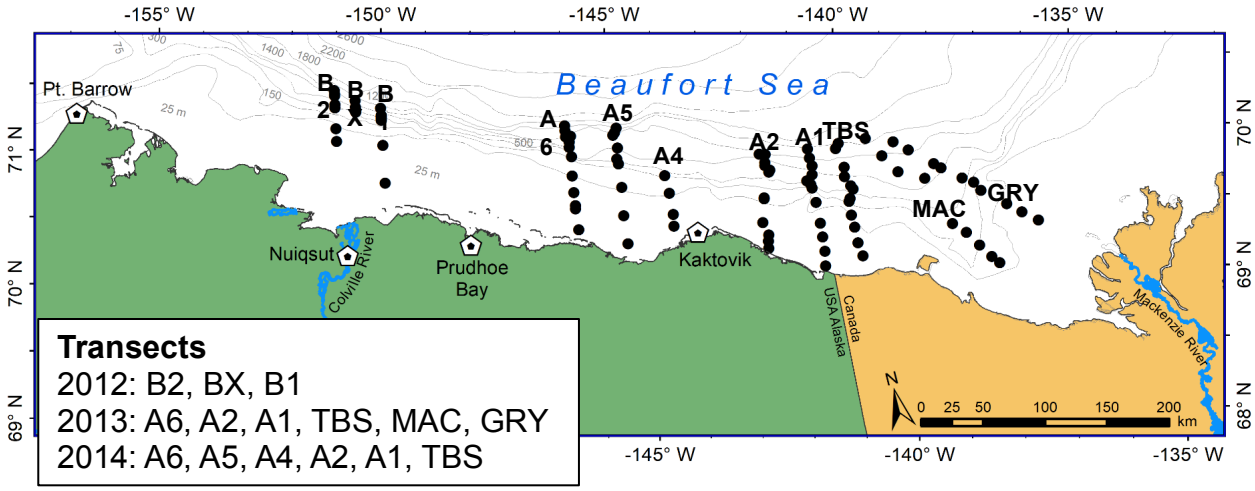

Figure 2.1. Transects and stations sampled in the Beaufort Sea 2012–2014.
2012: B2, BX, B1
2013: A6, A2, A1, TBS, MAC, GRY
2014: A6, A5, A4, A2, A1, TBS

2.2 Benthic Environmental Characteristics

Benthic environmental characteristics were sampled using either a BX-650 Ocean Instruments 0.25 m^2 box corer (2012) or a 0.1 m^2 double (2012) or single (2013, 2014) Van Veen grab. Samples were collected at all sites where sampling was logistically feasible. One core or grab per station was used for environmental sampling. In 2012, shallow stations on transect B1 (20 and 100 m) were sampled using a double Van Veen grab in an effort to save time. Due to weather delays, the nature of the substrate in some areas, and extensive troubleshooting required to develop a successful deployment protocol, box core samples were only collected at a subset of the planned stations. In 2013, grab samples were collected at stations ≤200 m depth, and, in 2014, most stations ≤350 m depth were successfully sampled.

The box corer and grab were deployed on a 9/16" cable from the aft deck. The corer or grab was lowered to the bottom at a rate of ~30 m/min. Once the sampler was approximately 10 m from the bottom, the winch was stopped to allow for any slack in the wire to settle. The instrument was then lowered into the bottom at ~15 m/min, allowed to settle for a few minutes, retrieved to ~10 m above the bottom, and subsequently hauled back at 30 m/min.

Each core or grab was evaluated upon retrieval through the top doors to ensure that the sample was of good quality. Samples were rejected if the surface had been badly disturbed, sediment was seen oozing out the doors, obstructions prevented complete closing of the jaws or spade, or penetration was insufficient (i.e., filled mostly with water). When good cores were obtained, the surface area was divided in half between infauna sampling (see below) and assessment of environmental characteristics. The top water was siphoned off of each sample using a piece of surgical tubing and/or a turkey baster. The core or grab surface was then subsampled for multiple environmental parameters, as described in Section 3.4. The sampler was thoroughly rinsed with seawater after sampling to remove any remaining sediment in preparation for the next deployment.

2.3 Zooplankton

In all years, smaller zooplankton were collected with a vertically-hauled paired 60-cm diameter twin net fitted with 150-µm mesh at shallow stations. A Hydrobios Midi-Multinet (150-µm mesh nets; aperture: 0.25 m^2) was used at stations greater than 50 meters depth to collect vertically-stratified samples. Trigger depths for the Multinet were 50, 100, 200, 300, 500, and 1000 m. Larger, more mobile zooplankton were targeted with a 60-cm Bongo net fitted with 505-µm mesh MARMAP nets hauled obliquely at approximately two knots. All simple nets were outfitted with annually-calibrated General Oceanics flowmeters to estimate volume of water filtered, while the Multinet employed integrated electronic flowmeters. Samples were preserved in 5% buffered formalin and returned to the laboratory for processing.

2.4 Infauna

Infauna samples were collected from box cores (2012) and Van Veen grabs (2014) using the same deployment protocols as described above for sediment sampling (Section 2.2). No infaunal samples were collected in 2013. In 2014, up to three replicate grab samples were collected for infaunal analysis at most stations ≤350 m. In 2012, half of each box core sample was allocated to infaunal analysis and half for environmental sampling. A ruler was used to quantitatively split the surface of the core and then a layer of sediment (5 cm deep) was removed using a spatula.

The top water was siphoned off each infauna sample and passed through a 500-µm sieve to collect any organisms that had been suspended from the sediment surface. Material retained on the sieve was transferred to the same jar as the rest of the sample. All infaunal samples were then processed on board the vessel using a 500-µm sieve. Each sample was emptied into a bucket or large tub and immediately filled with filtered seawater. The sample was gently stirred using a gloved hand or long spoon in order to break up large clumps of sediment. The water was then slowly poured over the sieve to collect organisms and remove as much sediment as possible prior to preservation. The sieved sample was then transferred to a jar and preserved in 10% buffered formalin for later laboratory processing.

2.5 Fish – Midwater Trawls

Pelagic fishes were collected during 2012 and 2013 using an IKMT with 3-mm mesh throughout body and 1-mm mesh codend. The IKMT mouth was 1.5 m wide by 1.8 m high with an effective fishing area of 2.137 m^2 when fished at 45º angle. A rigid diving vane kept the mouth of the net open during towing and exerted a depressing force to stabilize the net vertically. A time-depth recorder (TDR) was attached to the top of the IKMT frame and provided a post-haul record of fishing depth. The IKMT was deployed from the stern and towed with the current at a speed of 4 kts over ground in a double oblique tow. During the haul, the towing cable was continuously released or retrieved at the rate of approximately 30 m/min (modified to maintain the target 45º wire angle). The fishing goal was to examine the water column from the surface to 10 m above the seafloor or to 200 m at deeper sites. IKMT catches were quantifiable as volume of water filtered. Catch per unit effort (CPUE) of IKMT hauls was calculated as (# fish x 1000) / (haul distance in m x 2.137 m^2 net opening) and reported as # fish 1000 m^{-3}. Fishes were typically large larvae or small juveniles; their numbers and weights were so small that biomass per unit effort (BPUE) analysis was not conducted as it would not have been meaningful. We did not fish the IKMT in 2014 because (1) the IKMT collected a limited number of species, (2) the same station locations were to be sampled in eastern Alaska in 2014 as in 2013, (3) time

limitations (needed to leave Alaska waters by 25 August 2014), and (4) the need for additional wire time in 2014 to sample replicate hauls with the same beam trawl gear.

As our objectives were to sample pelagic fishes larger than those collected by the IKMT and to obtain more Arctic Cod (*Boreogadus saida*) for a BOEM-funded genetics project, in 2014, we deployed a single-warp Aluette net (AMT) that had a history of successfully capturing pelagic fishes in the Gulf of Mexico and in the Chukchi Sea (DeSousa, North Slope Borough, pers. comm.) near Utqiaġvik (formerly known as Barrow). The mouth of this net was 8 m wide and 7 m high; net length was 18 m. The mesh was 42 mm at the mouth, 35 mm at the intermediary, with a 12-mm codend liner, 25 m bridles and 41 x 91 cm (32 kg) doors. The width and height of the mouth opening is variable while fishing. A SIMRAD depth sensor was attached above the connection of the bridle and tow line to record real-time depth of the bridle. A TDR was attached to the footrope to provide a post-haul record of maximum fishing depth. The AMT was deployed and retrieved from the stern while the vessel was under way. It was towed with the current at a speed of 3.5–4 kts over ground; the vessel speed was reduced if the width between the doors varied notably or the net appeared to be dropping too slowly. During the haul, the towing cable was continuously released or retrieved at the rate of approximately 30 m/min until the target depth was reached, at which time, the net depth was adjusted by slowing or speeding the vessel. Decreasing vessel speed caused the net to drop and increasing speed lifted the net. A winch was used to haul the doors to the surface and the bridles and net were retrieved by hand. Throughout deployment, water current, vessel direction, vessel speed, vessel position, and net depth were recorded at least every 1–2 minutes. We reported the actual numbers of fishes captured. Unfortunately, though the AMT net could be fished, without associated hydroacoustics to allow it to target a patch of fish at a specific depth it captured very few fish.

2.6 Epifauna and Fish – Bottom Trawls

Three types of bottom trawls were used to capture fishes and epibenthic invertebrates: one plumb staff beam trawl (PSBT-A), one Canadian beam trawl (CBT), and one otter trawl (OT). OT was only used the first two years and PSBT-A and CBT were used in 2012, 2013, and 2014. The OT had a 9.1-m headrope, 38-mm mesh in the body, 19-mm mesh in the codend, 27.5-m bridles and 61 x 122 cm (23 kg) doors. The PSBT-A had a 4.7-m headrope and 4.6-m footrope, 7-mm mesh in body and 4-mm mesh as codend liner, and a rigid 3.05-m pipe forward of the mouth, holding it open for an effective swath of 2.26 m, thereby allowing for accurate quantifications of trawl effort by area swept (Gunderson and Ellis 1986). The PSBT-A was modified according to Abookire and Rose (2005) by adding rollers to the footrope to exclude boulders and rocky substrate and by securing the headrope to the beam in several places in order to prevent fish escapement. Similarly, the CBT had a 4.2-m headrope and 4.2-m footrope, 10-mm mesh in body and 6-mm mesh as codend liner, rigid 3-m beam forward of the net to hold the mouth open and roller gear on the footrope to exclude boulders; its effective swath was 3 m. Use of the two beam trawls will facilitate comparisons with other research in the Beaufort Sea. The PSBT-A was used extensively during an August 2011 expedition in the central Beaufort Sea (cruise BOEM-2011), and the CBT was used during cruises by Canada's Department of Fisheries and Oceans in the Canadian Beaufort Sea during 2012 and 2013.

All bottom trawls were deployed from the stern of the vessel at 30 m/min wire speed with a ratio of 2–3 m of towing cable to 1 m of water depth. These nets were towed with the current at approximately 1–2 kts speed. During 2013 and 2014, a SIMRAD depth sensor was attached above the connection of the net bridle and tow line for real-time depth feedback; the SIMRAD

was not available during 2012. A Star-Oddi TDR was attached near the footrope to provide a post-haul record of maximum fishing depth. Haul duration was approximately 3–15 minutes depending on the substrate and the real-time display on the SIMRAD depth sensor. Haul distance was calculated using a known linear distance with paired timestamps, taken from the linear distance between the positions of the vessel when towing cable was not being deployed or retrieved, and the total time that the net was on the bottom based on TDR records; positions were reported by the vessel's Global Positioning System.

Some bottom hauls were considered to be solely qualitative if (1) the net was damaged during the tow sufficiently to lead to loss of catch or to alter the net dimensions, (2) overfull codend occurred, (3) a high proportion of pelagic rather than demersal animals was collected, or (4) problems occurred with launching and retrieving the net such that the catch was compromised. Qualitative hauls were included in biodiversity analysis but not for quantitative analyses.

Generally 100% of the catch was sorted for fishes. If the catch was large enough that subsampling of fishes or invertebrates was required, the total catch was mixed to provide an unbiased, representative, volumetric subsample. We used area swept CPUE for catches by PSBT-A and CBT, which were quantifiable by area during 2013 and 2014 because towing swath, distance fished, and bottom contact duration were known. CPUE of PSBT-A and CBT catches was calculated as (# fish x 1000) / (haul distance in m x 2.26 m net swath) and reported as # fish 1000 m^{-2}. BPUE was reported as grams fish 1000 m^{-2}. OT doors do not maintain a static distance apart during a haul, but instead move together and apart with changes in vessel speed and substrate. Thus, the CPUE for OT hauls was linear distance towed and reported as # fish 1000 m^{-1}.

Trawling conducted in 2012 was affected by logistical issues that made CPUE and BPUE calculations unreliable. First, the trawling wire was heavier than previously used for bottom trawls, resulting in the net settling on the bottom faster than expected. Second, SIMRADs did not function for the duration of the 2012 cruise, so a real-time display of the net behavior was unavailable. Finally, the TDR sensors had multiple malfunctions that resulted in an inability to record the trawl duration with any confidence. As a result, many hauls were designated as qualitative only and cannot be used for CPUE and BPUE calculations. However, to allow comparisons among all three years, proportional catch was calculated for each haul for all three years by expressing each species and length class as a percentage of all fish captured in each haul.

2.7 Standardizing Effort

For comparison among samples, catches were standardized to a unit of effort specific to the sampling gear used. Zooplankton was expressed as individuals m^{-3} and mg dry-weight (DW) m^{-3}. Infauna was standardized to individuals m^{-2}. Fish and epibenthos BPUE and CPUE were calculated, where possible, for each of the five types of nets that were used: PSBT-A, CBT, and OT for bottom sampling, and IKMT and AMT for midwater sampling. The units of effort were not the same among gears; therefore, values of CPUE and BPUE could not be compared among gears. Beam trawl effective sample width of net and length of tow were known, so the measure of effort was swath of tow for both CPUE (# 1000 m^{-2}) and BPUE (gm 1000 m^{-2}). Since effective sample width is not constant when towing the OT and AMT, measure of effort is limited to length of tow for both CPUE (# 1000 m^{-1}) and BPUE (gm 1000 m^{-1}) for these gear types. IKMT catches were quantifiable as volume of water filtered for CPUE (# 1000 m^{-3}).

3.0 HABITAT

3.1 Physical Oceanography

Russell Hopcroft

3.1.1 Introduction

The physical oceanography of the Beaufort Sea has a major influence on all life forms living in this region (Hopcroft et al. 2008). Through its influence on circulation and nutrient supply, it determines the primary productivity of the sea ice and pelagic algal communities (Gradinger 2009) and the habitat suitability for invertebrates and fish populations that support higher trophic levels such as seabirds and marine mammals.

Physical measurements in the Beaufort Sea can be traced back nearly a century, though access to the region was severely limited by the ice cover. Focused oceanography studies in the Beaufort began after the construction of US icebreakers in the early 1940s. Initially, these Wind-class (and later Glacier-class) icebreakers measured physical oceanography primarily to inform the US Navy. From the Transboundary perspective, the studies of greatest relevance are those that studied the physical, chemical and biological components of this system simultaneously. Notable examples include studies from the USS *Burton Island* in 1950–1953 (Johnson 1956) and by the Western Beaufort Sea Ecological Cruise (WEBSEC) program in 1971–1972 (Hufford et al. 1974). The Outer Continental Shelf Environmental Assessment Program (OCSEAP) sampled the region in the late 1970s and early 1980s (Barnes et al. 1984) and was followed by additional studies (Aagaard et al. 1989). Beginning this century, research activity has expanded considerably with the NSF-ONR sponsored Shelf-Basin Interaction (SBI, 2001–2004) program examining shelf break processes in the western Beaufort Sea and a focus on the Mackenzie Shelf River by the Canadian Arctic Shelf Exchange Study (CASES-2002–2004). Most recently, BOEM's Central Beaufort, Transboundary, and COMIDA programs have addressed the region between those study areas.

The physical oceanography of the Beaufort has been recently reviewed and summarized (Hopcroft et al. 2008, Grebmeier and Maslowski 2014). In brief, the Alaskan Beaufort Sea shelf is ~80 km wide and extends ~500 km from Point Barrow to the Convention Line along the Mackenzie Beaufort Sea shelf in the Canadian Exclusive Economic Zone (EEZ). Bottom depths increase gradually from the coast to approximately the 80-m isobath and then plunge rapidly toward the abyssal plain of the Canada Basin. Although the continental slope is highly corrugated, the shelf is relatively smooth with little along-shelf variability in depth, except for western and eastern boundaries formed by Barrow Canyon and Mackenzie Valley, respectively.

Historically, sea ice has covered much of the shelf throughout the year, although in recent years most of the shelf has become ice-free from late July through early October. Beaufort ice cover consists of two distinct components; freely-drifting pack ice over the middle and outer shelf and the immobile landfast ice on the inner shelf. Landfast ice forms in October anchoring to the coast, and then grows rapidly northward to eventually cover ~25% of the shelf area where it remains through June (Barnes et al. 1984). Landfast ice becomes deformed offshore with ridging that increases throughout winter (Tucker et al. 1979). Ice keels can gouge the seafloor along the seaward edge of the landfast ice and form piles of grounded ice that disturb seafloor habitats (Barnes et al. 1984).

Beaufort shelf water properties are controlled by this annual sea-ice cycle and inflows from its oceanic and coastal boundaries (Weingartner et al. 2005). During winter, temperatures are at or near freezing throughout the shelf's water column. While these near-freezing waters remain on the shelf year-round, highly stratified plume temperatures can be 5–10 ºC during late summer. Seasonal variation in salitinity is even greater. Shelf salinities are typically between 32 and 33 during winter, but during the spring freshet, river waters can spread offshore beneath the landfast ice in meter-thick layers where salinities can be less than 5. As the landfast ice detaches, plume and ambient waters begin to mix, meltwater increases, and all are advected along the shelf and across-shelf by instabilities or upwelling.

At broader scales, Beaufort waters reflect the influence of three distinct oceanic regimes plus the coastal boundary. The coast includes the Colville River and numerous small arctic rivers that enter the central and eastern portions of the Alaskan Beaufort Sea (Weingartner et al. 1998). The first regime consists of Pacific Ocean waters that exit the Chukchi shelf through Barrow Canyon. Depending on the time of year and regional winds, some of this outflow continues eastward in the surface layer or as a subsurface current along the Beaufort shelf break (contributing to the upper halocline of the Canada Basin), spreads westward or offshore in the Polar Mixed Layer (PML), or rounds Pt. Barrow and moves onto the inner Beaufort shelf. The second oceanic regime is the offshore boundary that includes the outer shelf and continental slope. Within the upper 50 m, flow is westward as part of the wind-driven Beaufort Gyre carrying the cold, dilute waters of the PML. Below this layer, flow is eastward over most of the slope but concentrated in a narrow (~20 km wide) jet centered at ~170 m (Pickart 2004) with a mean core speed of 8 cm s^{-1}. This jet carries dense winter water from the Chukchi shelf and warmer, saltier Atlantic Water (AW) upwelled from deeper regions. In offshore waters of approximately 200 m depth, eastward flowing water of Atlantic origin predominates before transitioning slowly into Arctic Bottom Waters. The third oceanic regime occurs over the Mackenzie shelf where year-round discharge from the Mackenzie River dominates hydrographic properties. During the ice-free season, winds can enhance upwelling at the shelf break, push offshore waters and jets far inshore, or push Mackenzie shelf waters far westward.

3.1.2 Objectives

Given the observed complexity and variability in the Beaufort Sea and the lack of contemporary measurements of physical oceanography through much of the central shelf, efforts to understand its ecosystems require contemporaneous documentation of the physical oceanographic state. Specifically, we proposed to:

- Define the physical structure (temperature and salinity) of the Beaufort shelf during Transboundary surveys.
- Determine the relative importance of sea ice and riverine contributions to the Transboundary survey locations.

3.1.3 Methods

Oceanographic profiles were conducted along cross-shelf transects at stations ranging from 20–1000 meters in depth from the Colville River to the Mackenzie River (Figure 2.1). Physical oceanographic data were collected with a Seabird SBE25 CTD (2012 and 2013) or SBE911+ CTD (2014) that was calibrated both pre- and post-season. Instrumentation employed on the SBE25 was rated to 600 m depth, while no relevant limitations existed for the SBE911+. The pre-cast soak, any anomalous spikes, and the upcast were removed after data conversion and observations were

averaged into 1 m vertical intervals as per manufacturer's guidelines. Data were visualized using Ocean Dataview. Water mass characterizations follow those of McLaughlin et al. (2005).

3.1.4 Results and Interpretation

We observed three primary vertically-layered water masses across the entire sampling domain (Figures 3.1.1–3.1.3). The Polar Mixed Layer (PML) extended from the surface to approximately 50 m and exhibited the widest range of temperatures and salinities both within and across years when compared to other water masses. During summer, the PML typically stratifies into an upper layer, freshened by sea melting ice that traps most of the solar energy, overlying a saline sub-zero layer. Arctic Halocline Water (AHW) extended from 50 m to approximately 200 m and was characterized by temperatures <0 °C. Atlantic Water (AW) began between 200–300 m and was characterized by high salinities (~34) and temperatures >0 °C. AW reaches thermal maximum at 350–400 m (Figures 3.1.4–3.1.6). Although the abruptness of transition between AHW and AW varies somewhat, we focused the subsequent presentation on the upper 200 m where the greatest changes occur. In 2012, the surface waters in the PML exhibited temperatures of ~4 °C, averaging 2.46 °C in the upper 50 m (Figures 3.1.4, 3.1.7). In the 2013 survey year, we observed extremely freshened conditions in the upper 10 m of the PML (Figures 3.1.5, 3.1.8) with salinity reaching ~10 and temperatures ranging from -1–10 °C, averaging 0.30 °C in the upper 50 m (Figures 3.1.5, 3.1.7). The 2014 survey year was noticeably less freshened than 2013 (Figures 3.1.6, 3.1.8) with lowest surface salinities reaching ~20. In 2014, surface temperatures in the PML ranged from -1 to 9 °C averaging 0.48 °C in the upper 50 m (Figure 3.1.6, 3.1.7). Surface salinities were highest in 2014 (~30 on the shelf, averaging 30.54 in the upper 50 m), lowest in 2013 (~10, averaging 27.5 in the upper 50 m), and intermediate in 2012 (averaging 29.34 in the upper 50 m) (Figure 3.1.8). Bottom temperatures were generally ≤ 0 °C on the shelf, with the exception of the 2012 field year when temperatures on the shelf were above 0 °C (Figure 3.1.4, 3.1.9). Bottom salinity was generally lower on the shelf and higher on the slope in all survey years (Figure 3.1.20). A data table reports surface and deepest values of temperature, salinity and Sigma-t (Appendix C Table 1).

It is notable that the surface water heat in 2012 extends deeper than in subsequent years suggesting stronger wind-induced mixing than in other years. The later sampling period during 2012 (nearly one month), when day-length and air temperatures were declining, should have resulted in a net loss of surface heat compared to other years. This suggests either an overall warmer year or, perhaps, a greater advection contribution of warmer waters from the Chukchi due to the more western location of the stations sampled during 2012. In contrast, the similarity of upper water column temperatures observed between 2013 and 2014 suggests similar seasonal heating; however, the strong difference in salinity suggest a much greater and more westward influence of the Mackenzie River discharge to our sampling domain in 2013 compared to 2014. This remains true even when comparisons are limited to the same set of stations resampled in those two years.

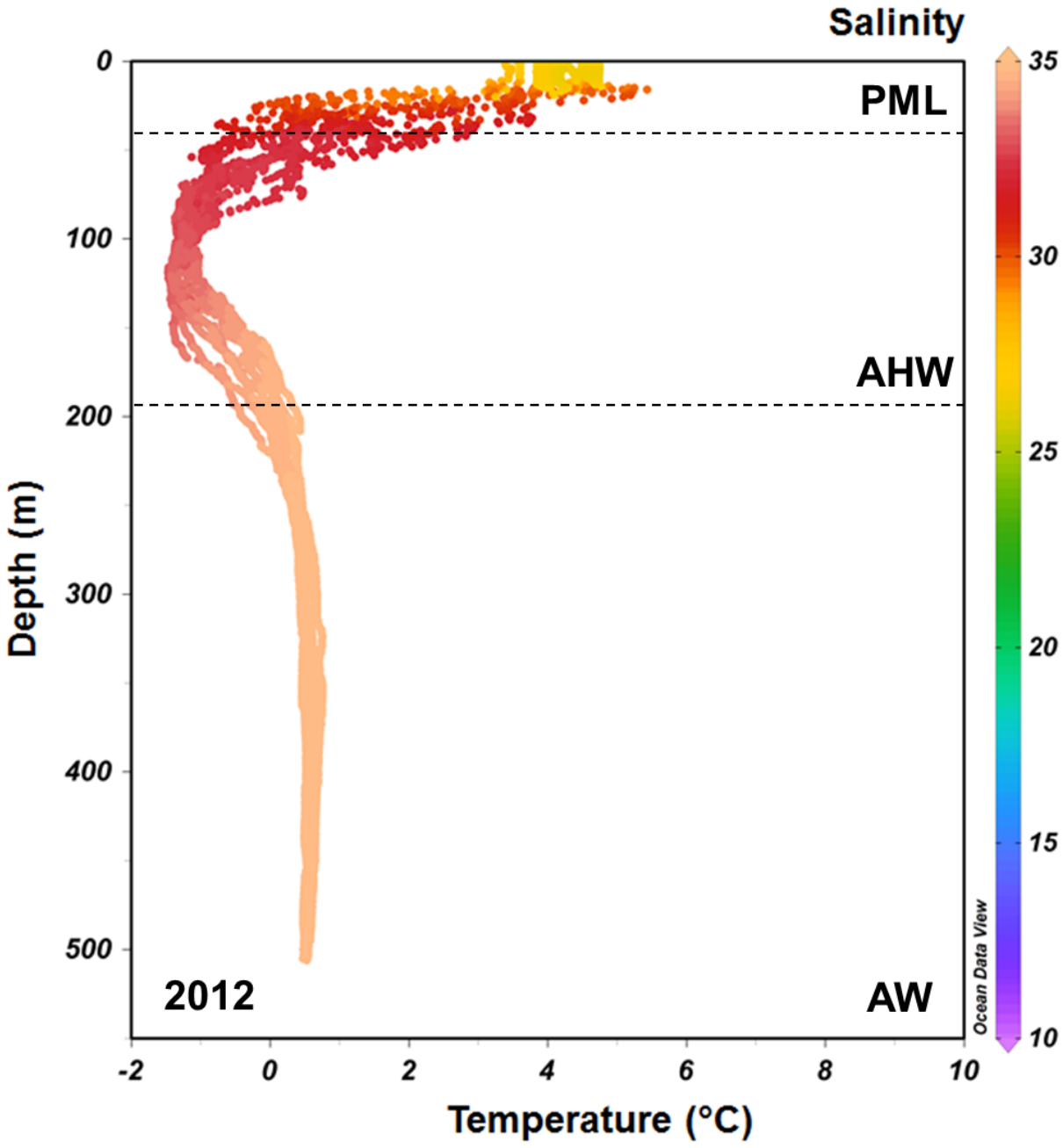

Figure 3.1.1. Oceanographic profile from Transboundary 2012 in the Beaufort Sea. Water masses are noted: PML – Polar Mixed Layer, AHW – Arctic Halocline Water, AW – Atlantic Water.

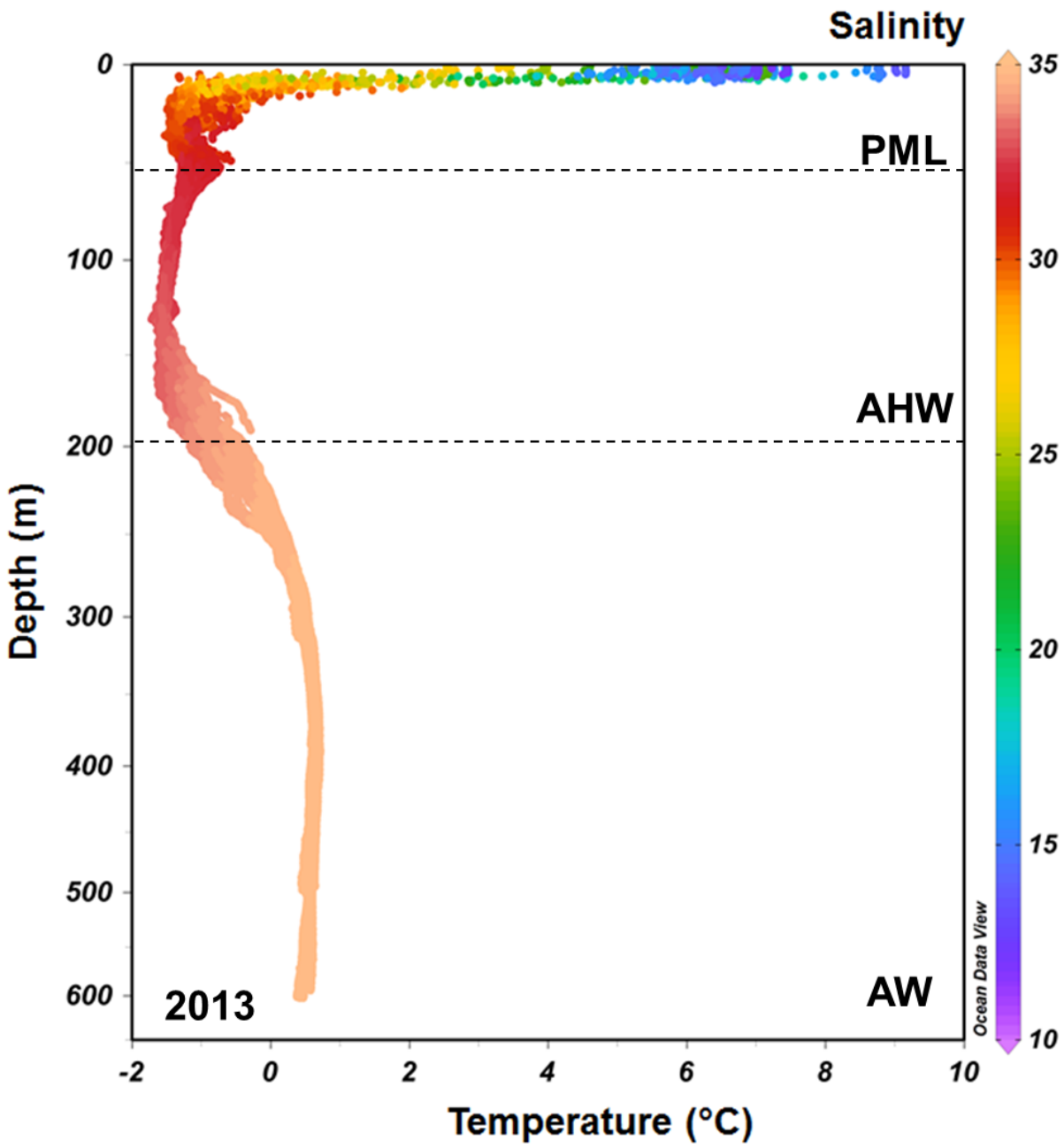

Figure 3.1.2. Oceanographic profile from Transboundary 2013 in the Beaufort Sea. Water masses are noted. PML = Polar Mixed Layer. AHW = Arctic Halocline Water. AW = Atlantic Water.

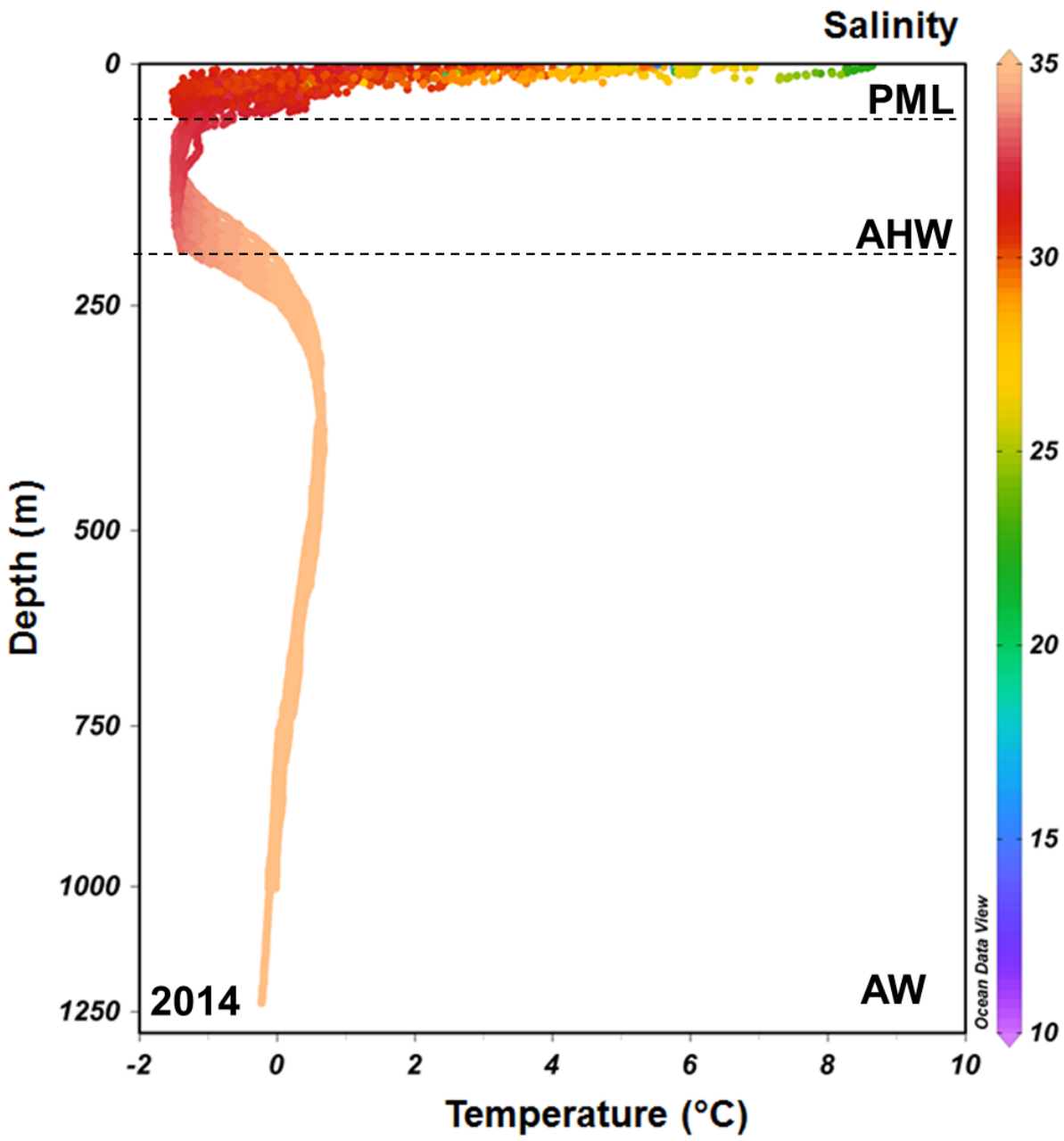

Figure 3.1.3. Oceanographic profile from Transboundary 2014 in the Beaufort Sea. Water masses are noted.PML = Polar Mixed Layer. AHW = Arctic Halocline Water. AW = Atlantic Water.

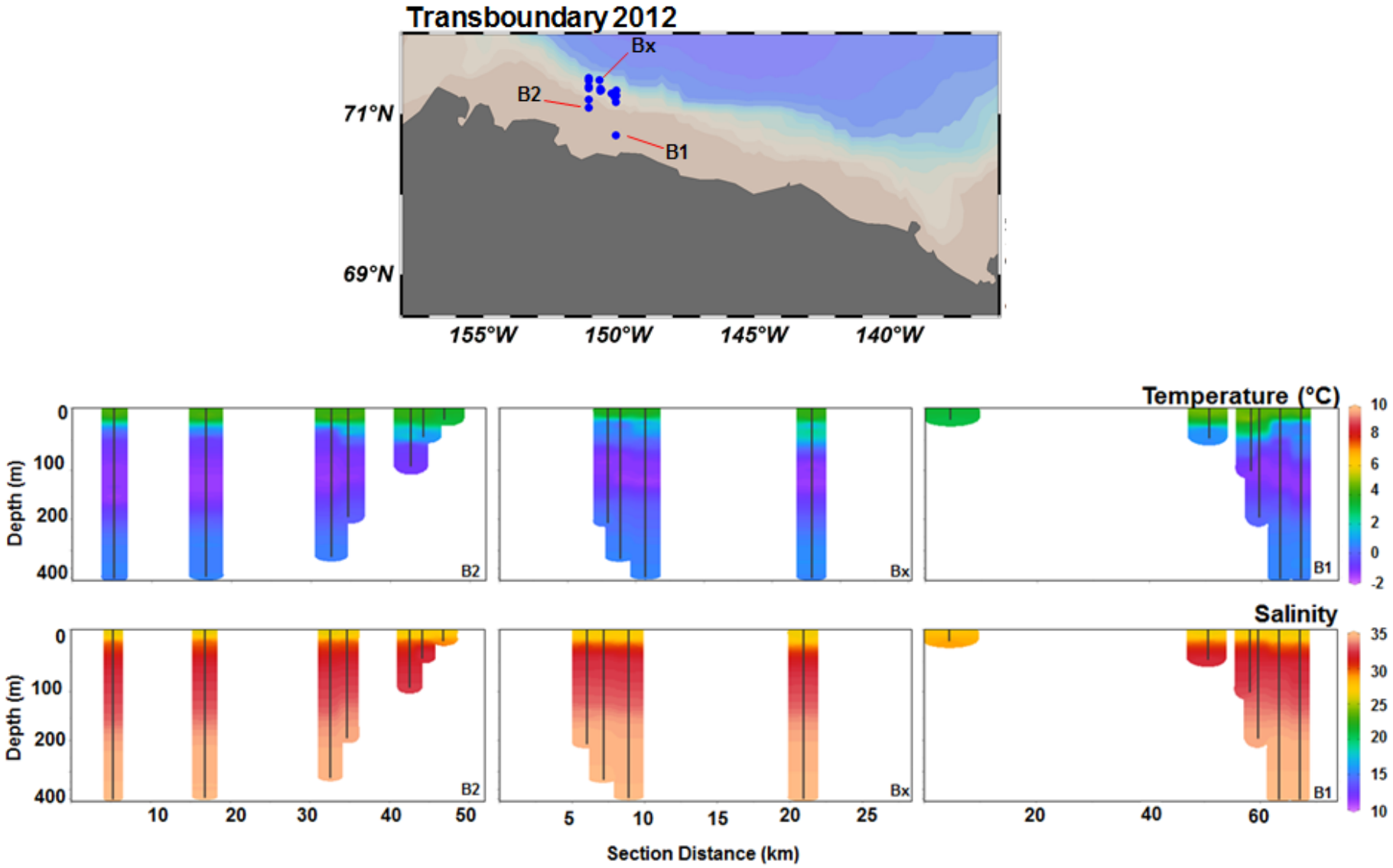

Figure 3.1.4. Temperature and salinity sections along cross-shelf transects in the Beaufort Sea during Transboundary 2012. Dates at each station: B2 26–28 Sep, BX 29–30 Sep, B1 21–29 Sep.

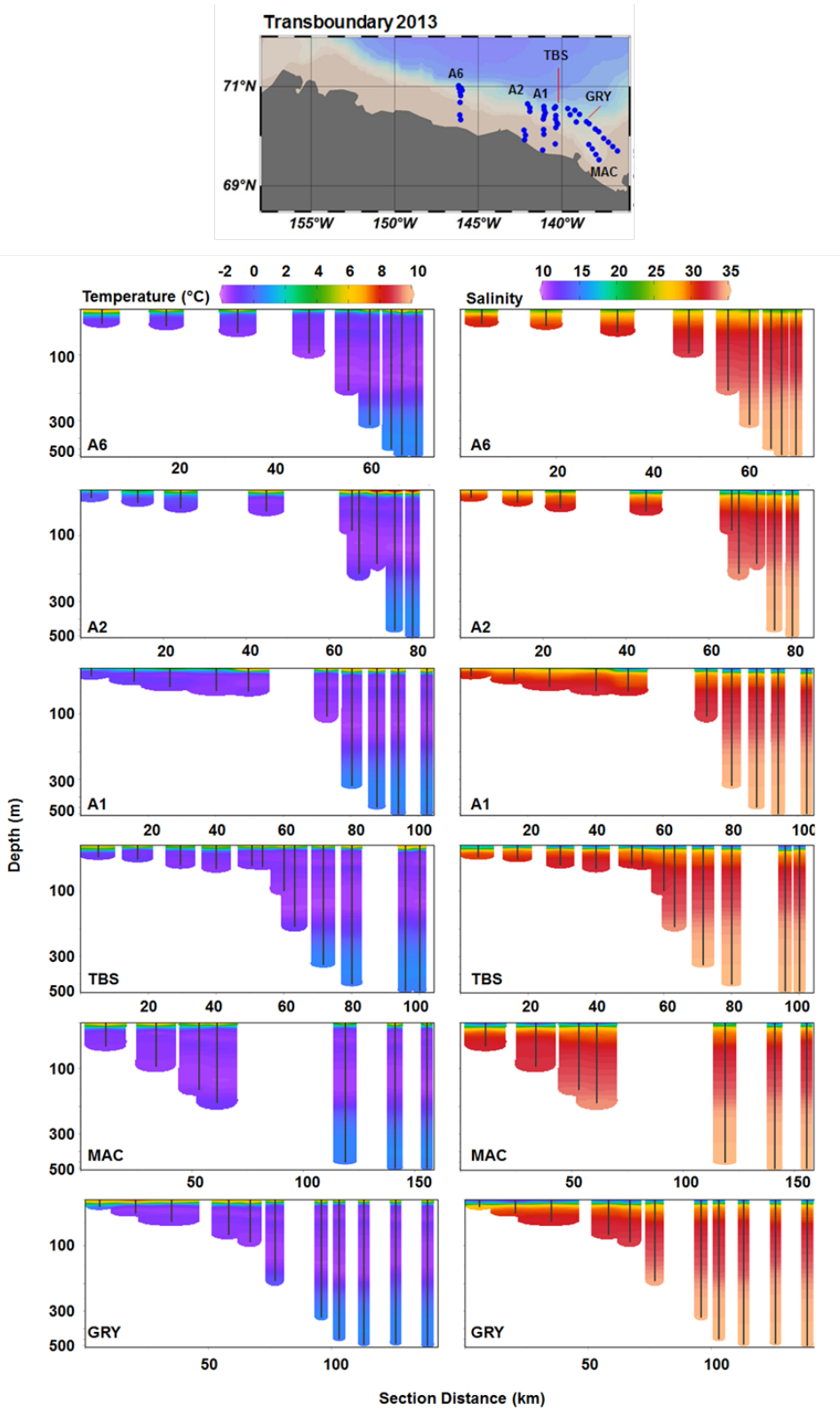

Figure 3.1.5. Temperature and salinity sections along cross-shelf transects in the Beaufort Sea during Transboundary 2013.
Dates at each station: A6 13–17 Aug, A2 17–20 Aug, A1 20–23 Aug, TBS 23–26 Aug, MAC 26–31 Aug, GRY 27–29 Aug.

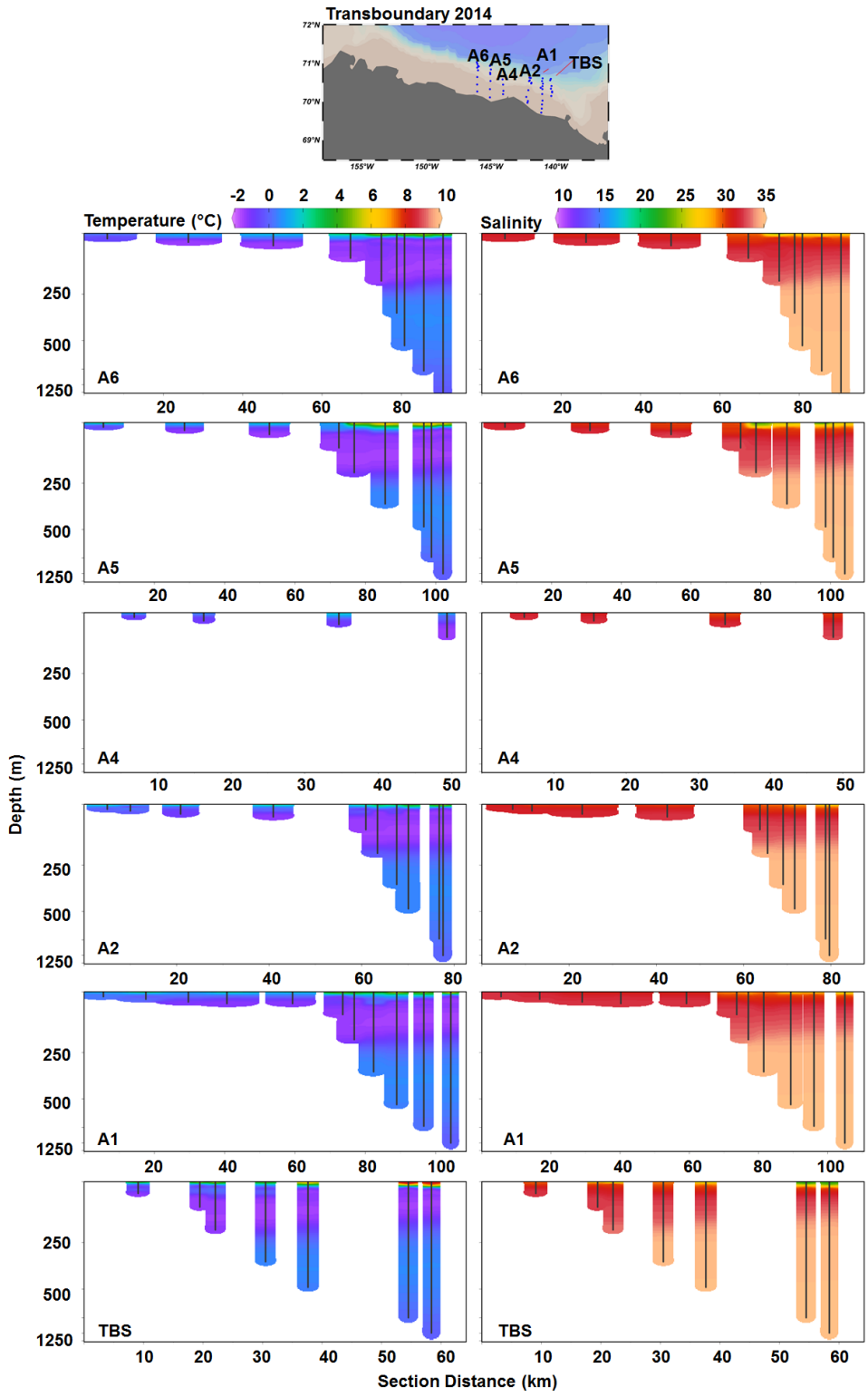

Figure 3.1.6. Temperature and salinity sections along cross-shelf transects in the Beaufort Sea during Transboundary 2014.
Dates at each station: A6 19–31 Aug, A5 20–30 Aug, A4 20–21 Aug, A2 21–24 Aug, A1 24–26 Aug, TBS 27–28 Aug.

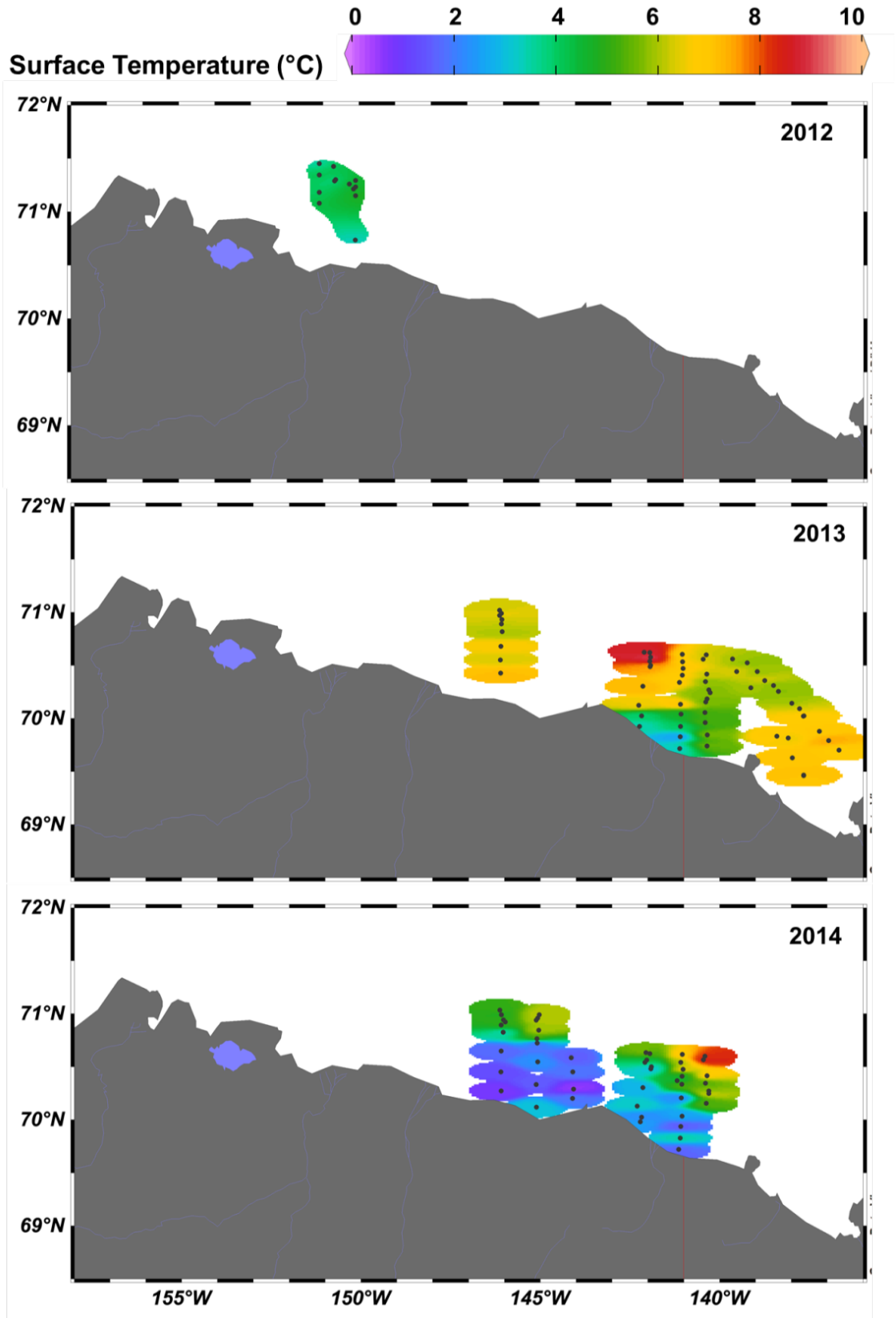

Figure 3.1.7. Surface temperature in the Beaufort Sea during Transboundary 2012–14. Dates: 21–30 September 2012, 13–31 August 2013, 19–31 August 2014.

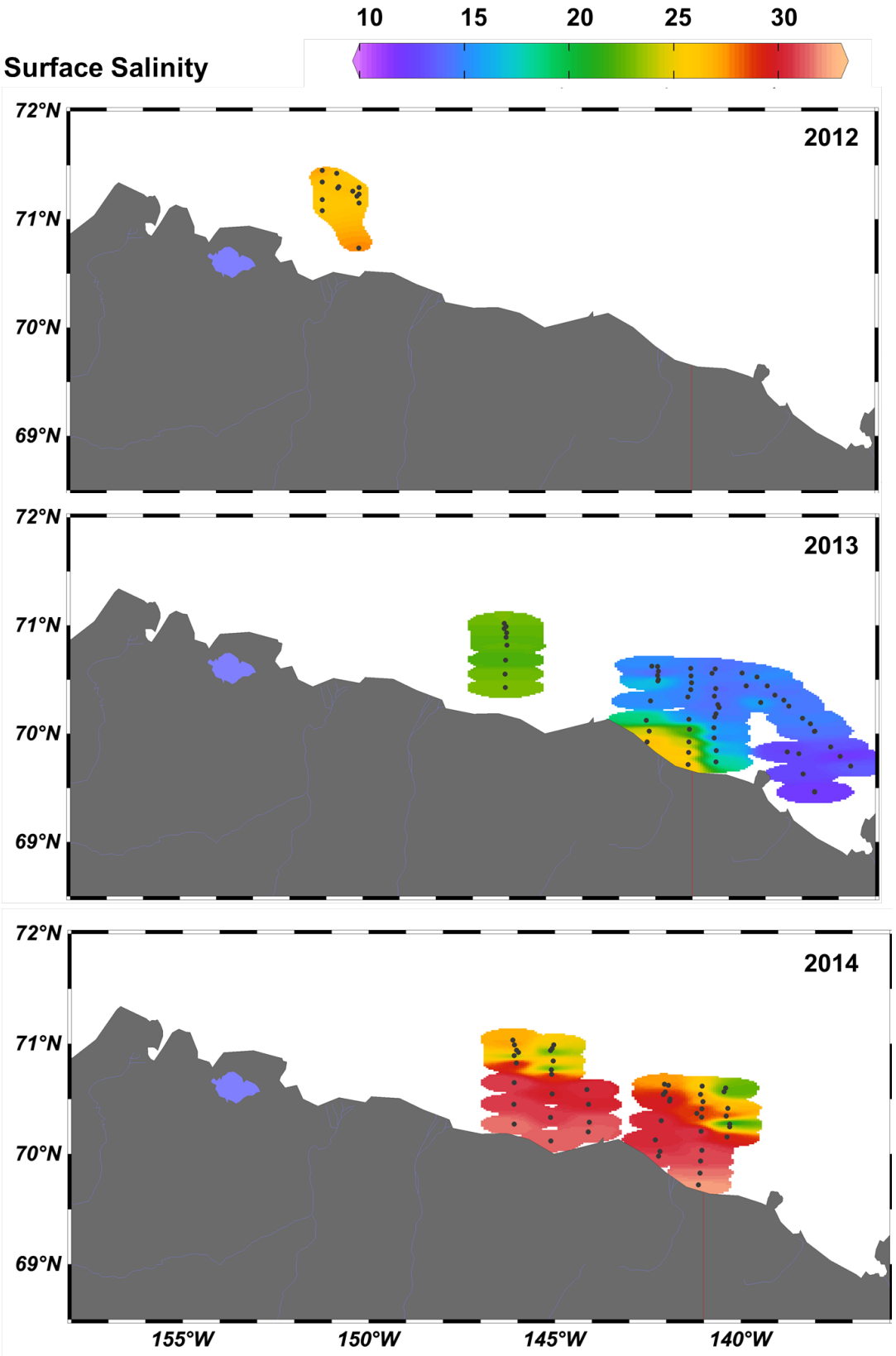

Figure 3.1.8. Surface salinity in the Beaufort Sea during Transboundary 2012–14.
Dates: 21–30 September 2012, 13–31 August 2013, 19–31 August 2014.

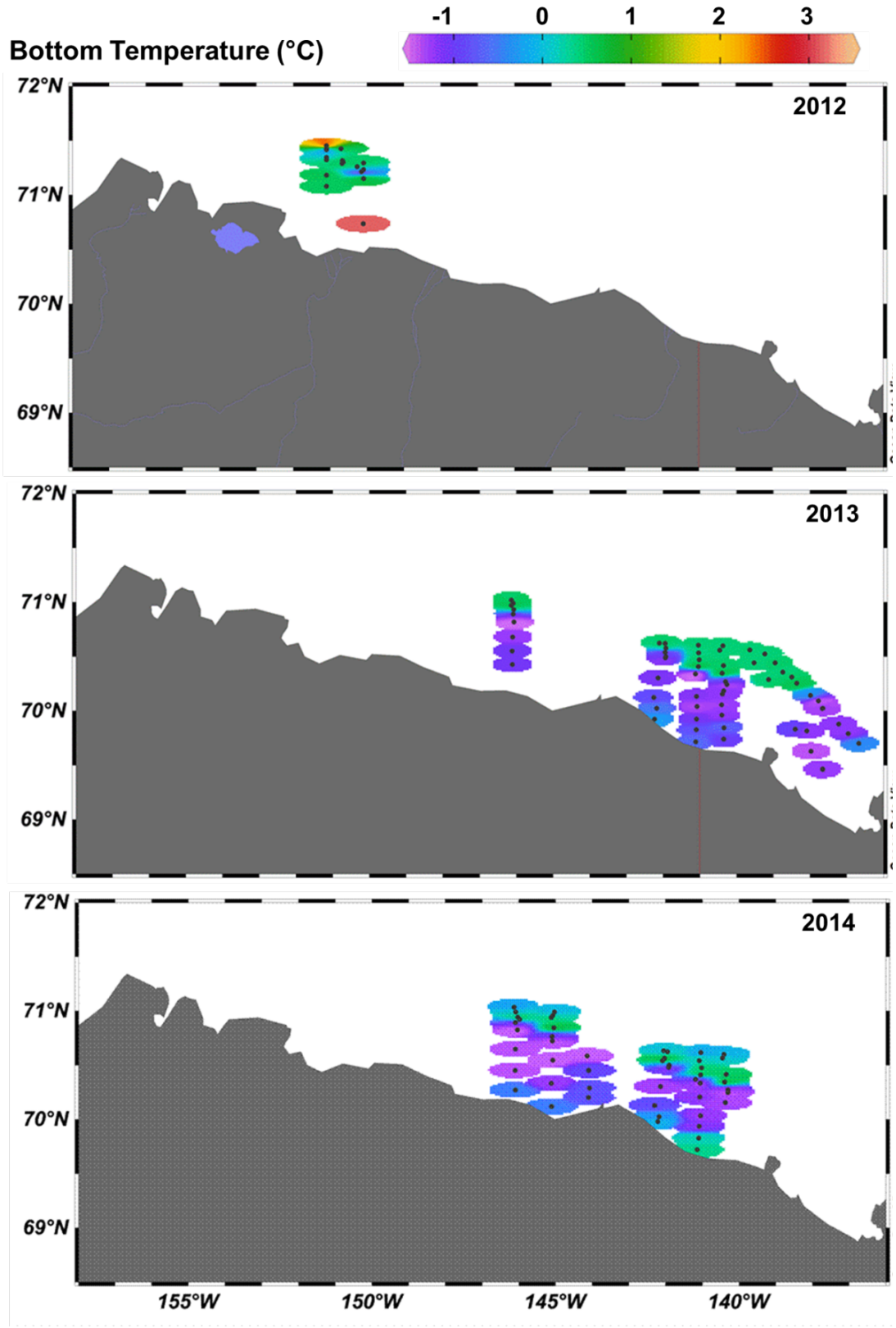

Figure 3.1.9. Bottom temperature in the Beaufort Sea during Transboundary 2012–14. Dates: 21–30 September 2012, 13–31 August 2013, 19–31 August 2014.

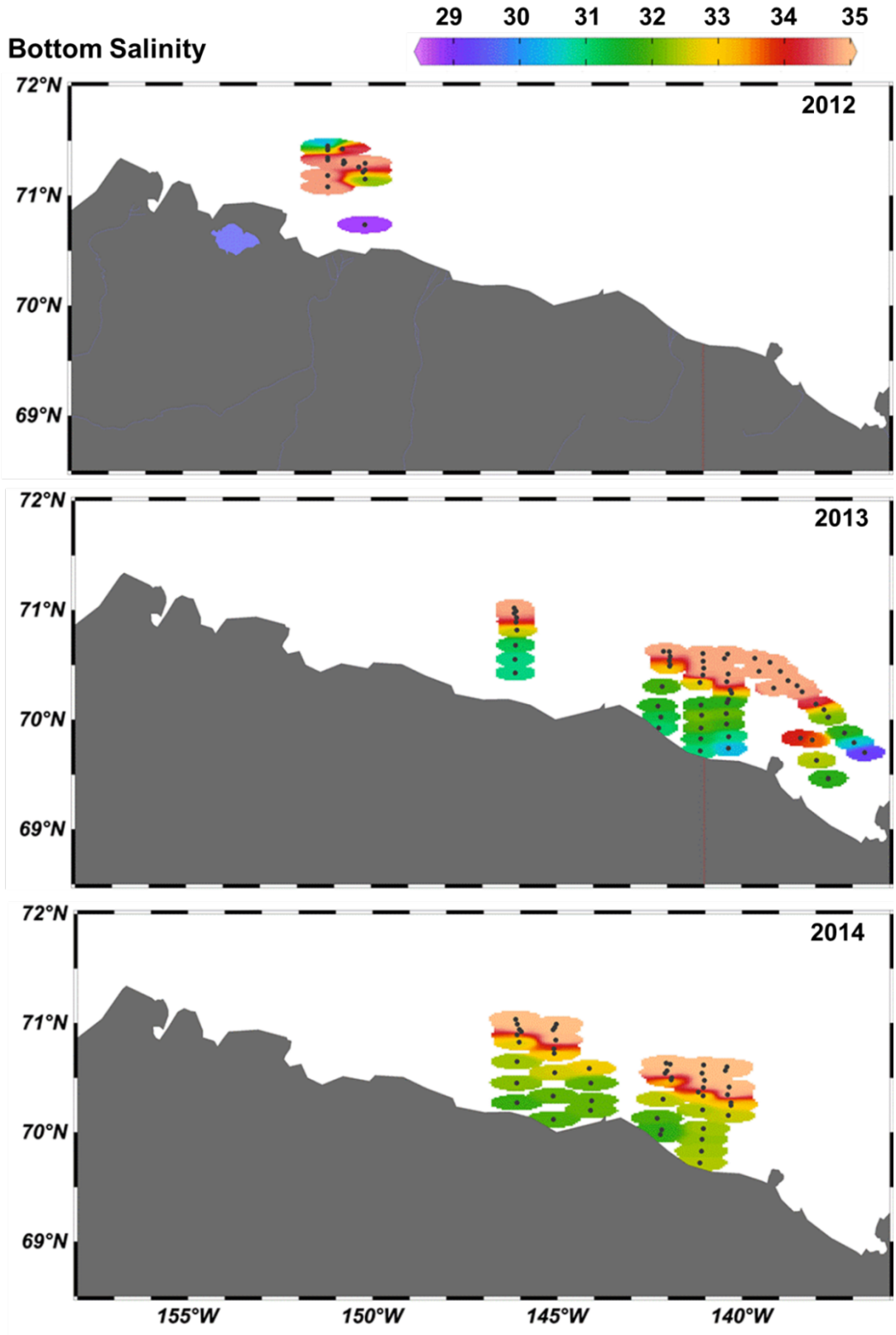

Figure 3.1.10. Bottom salinity in the Beaufort Sea during Transboundary 2012–14.
Dates: 21–30 September 2012, 13–31 August 2013, 19–31 August 2014.

3.2 Chemical Oceanography

Russell Hopcroft

3.2.1 Introduction

Chemical oceanography within the Transboundary program was focused almost exclusively on the macronutrients essential for phytoplankton growth (i.e., nitrate, phosphate, and silicate). The distribution of nutrients is intricately tied to physical processes in the environment and the microbial processes that recycle them after update by phytoplankton. In this sense, macronutrients are the essential connection between physical, biological, and geological processes in the environment.

In most marine environments, surface water nutrient concentrations are depleted during spring/summer due to phytoplankton photosynthesis and are renewed during fall/winter when photosynthesis declines and surface waters are mixed downward with nutrient rich deep waters (Tremblay et al. 2008, Simpson et al. 2008). On the shelves, this seasonal mixing reaches bottom waters where nutrients have been regenerated from the seafloor. Nutrient patterns can also be modified by river input, particularly so by Mackenzie River in the Eastern Beaufort Sea (Emmerton et al. 2008). However, in offshore waters, the strong density stratification typical of Arctic waters greatly limits the depth to which mixing can occur and, therefore, the size of the nutrient reservoir available. Lateral transport of dense nutrient-rich water formed on the shelves during the fall freeze up period may be an important source of the nutrients to the basins (Macdonald et al. 1987, 1989, Rudels et al. 1991).

As with previous physical oceanography surveys, access to the region for chemical oceanography research has long been limited by ice cover – an impediment greatly reduced during the past decade. In 1971–72, considerable research was conducted during the WEBSEC cruises by the US Coast Guard (Hufford et al. 1974) and later under the auspices of OCSEAP. The OCSEAP research is summarized in numerous technical reports, the most relevant of which is Horner (1981), and much of this information is available online at National Centers for Environmental Information (NCEI). Additional measurements of shelf break processes have been made in the western Beaufort Sea with support from the NSF-ONR sponsored Shelf-Basin Interaction (SBI: 2001–2004). Similarly, the area around the Mackenzie River inside the Canadian EEZ has received significant attention by the Canadian Arctic Shelf Exchange Study (CASES: 2002–2004). Much of the existing nutrient data throughout the Arctic has been aggregated and synthesized (Codispoti et al. 2013), and an updated synthesis is underway; however the central Beaufort remains a poorly covered region.

3.2.2 Objectives

Recent syntheses indicate that the distribution of macronutrients on the US Beaufort Shelf has been poorly characterized (Codispoti et al. 2013). Improving such knowledge will provide insights into the controls of primary production in this region. Specifically, we proposed to:

- Define the distribution of macronutrients concentrations of the Beaufort shelf during Transboundary surveys.

3.2.3 Methods

Nutrient samples were collected along cross-shelf transects at stations ranging from 20 to 1000 meters in depth from the Colville River to the Mackenzie River (Figure 2.1). Macronutrient samples were collected with a 6 Niskin bottle SBE55 (2012 and 2013) or a 14 bottle SBE32SC (2014) rosette attached to the CTD. Water samples for macronutrient analysis were taken at the surface, 10, 20, 30, 40, and 50 m; when stations were shallower than 50 m, the deepest water sample was collected approximately three meters from the seafloor. During 2014, the eight extra bottles available on the SBE32SC allowed nutrient sampling at 75, 100, 125, 150, 200, 300, 500, and 1000 m. Nutrient samples were filtered with 0.45-µm cellulose-acetate filters and frozen immediately at -40 °C for post-cruise analysis. The analyses were conducted at NOAA's Pacific Marine Environmental Laboratory using continuous flow autoanalyzers with segmented flow and colorimetric detection following the methods of Gordon et al. (1993). Data were screened for anomalous values and nutrient ratios, and then visualized using Ocean Dataview.

3.2.4 Results and Interpretation

Surface nitrate was generally depleted (and thus limiting to phytoplankton growth) throughout the study region during all surveys, while phosphate and silicate were typically low but non-limiting (Figures 3.2.1–3.2.14). During 2012 and 2013, when nutrient collection was limited to 50 m, higher nitrate, phosphate, and silicate concentrations increased with depth (Figure 3.2.15). Elevated surface nitrate in the freshened off-shelf waters of 2012 represents a notable exception (Figures 3.2.1, 3.2.2). During 2013, we observed elevated silicate levels in surface waters (Figures 3.2.3–3.2.8) with highest concentrations (~20 µm) at stations closest to the mouth of the Mackenzie River (Figures 3.2.7, 3.2.8), showing it is important source for this diatom nutrient. In contrast, phosphate levels were very low in this freshened surface layer. During 2013, there was indication of elevated nutrients near the sea bottom, a pattern made more distinct by the addition of deeper nutrient sampling in 2014 (Figures 3.2.9–3.2.14). Elevated nutrients near the bottom in conjunction with increases in ammonium are consistent with active nutrient regeneration through bacterial activity.

The full water-column sampling in 2014 revealed that nitrate, phosphate, and silicate concentrations reached peaks at depths of 150–200 m (Figure 3.2.16), indicating an AHW deep nutrient pool. The deeper sampling also revealed that AW was noticeably more depleted for phosphate and silicate than AHW. While phosphate:silicate ratios appear relatively stable across depth, the distinctness of AW nitrate:phosphate and nitrate:silicate ratios are a clear indication of different nutrient utilization and regeneration processes in the AW compared to the PML and AHW layers.

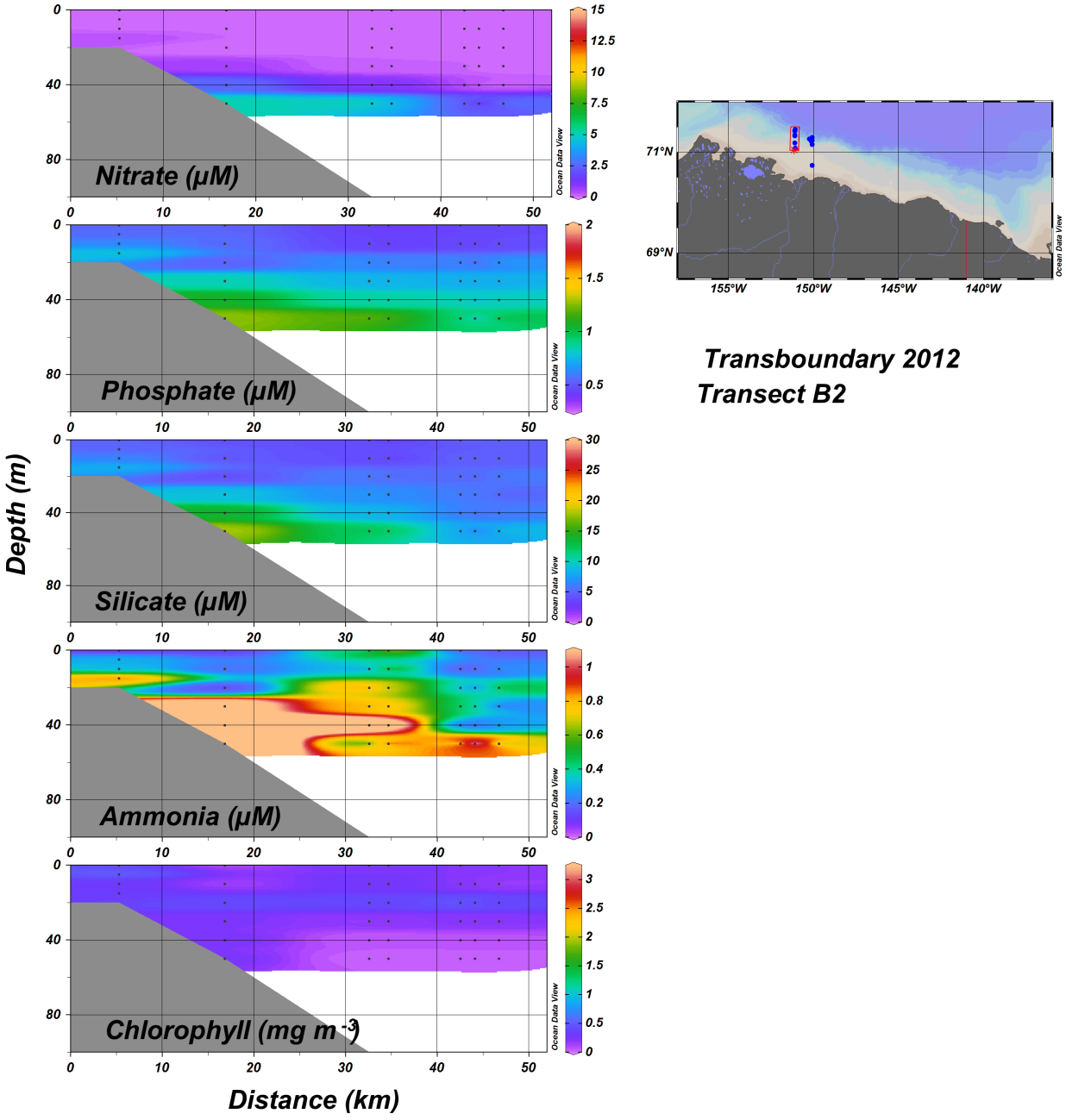

Figure 3.2.1. Macronutrient and chlorophyll-*a* concentrations across Transboundary 2012 Transect B2, 26–28 Sep.

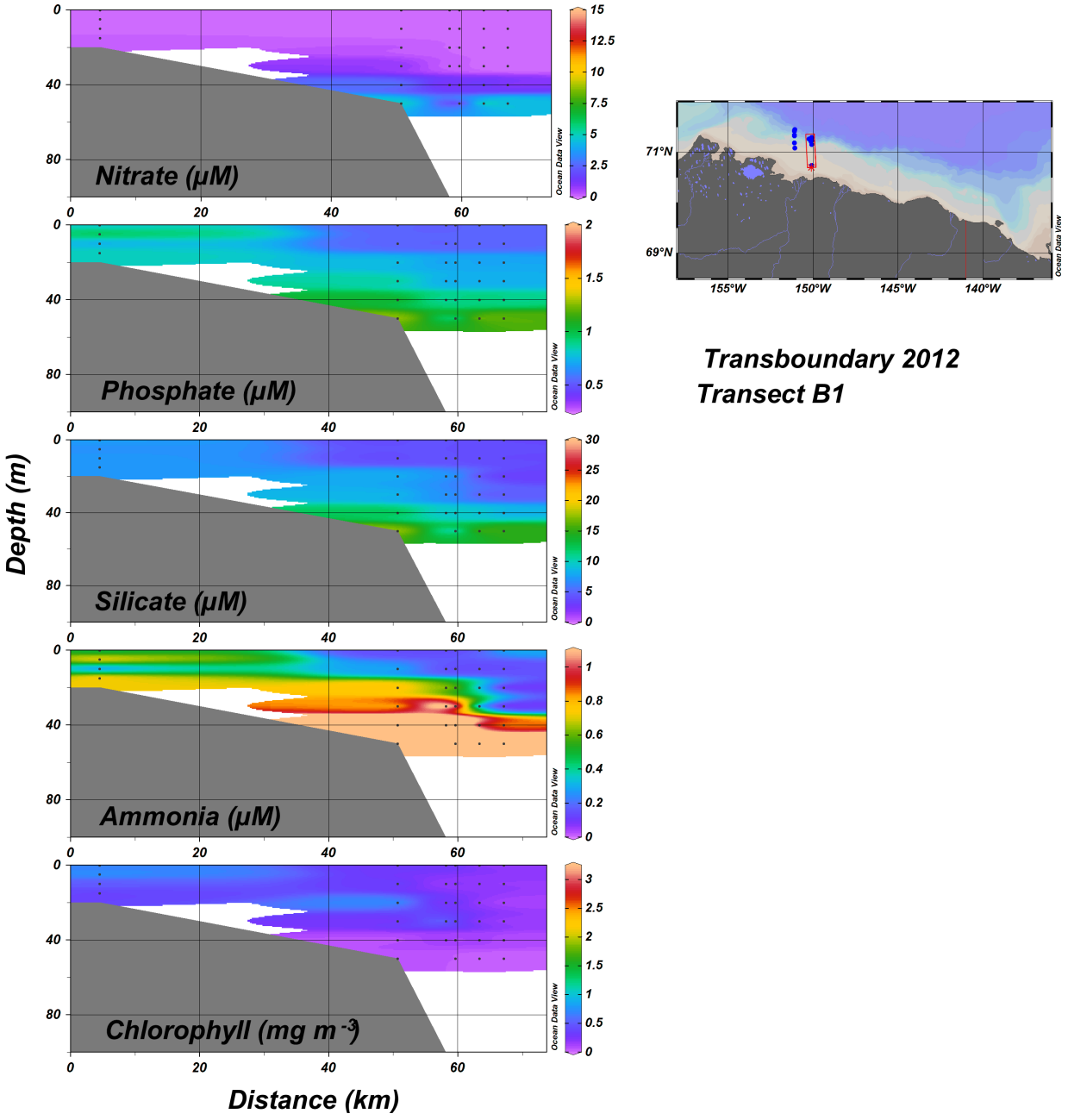

Figure 3.2.2. Macronutrient and chlorophyll-*a* concentrations across Transboundary 2012 Transect B1, 21–29 Sep.

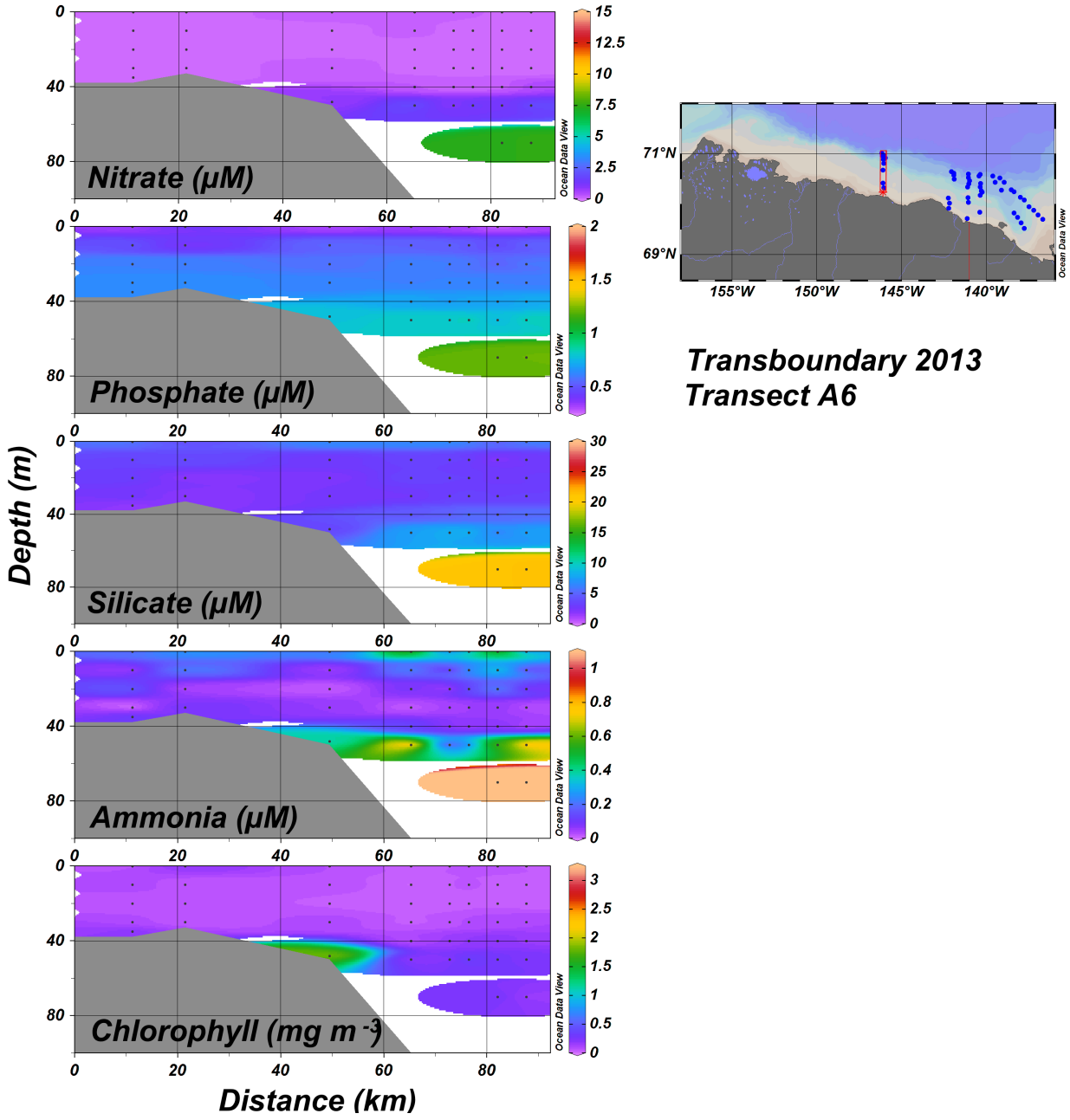

Figure 3.2.3. Macronutrient and chlorophyll-*a* concentrations across Transboundary 2013 Transect A6, 13–17 Aug.

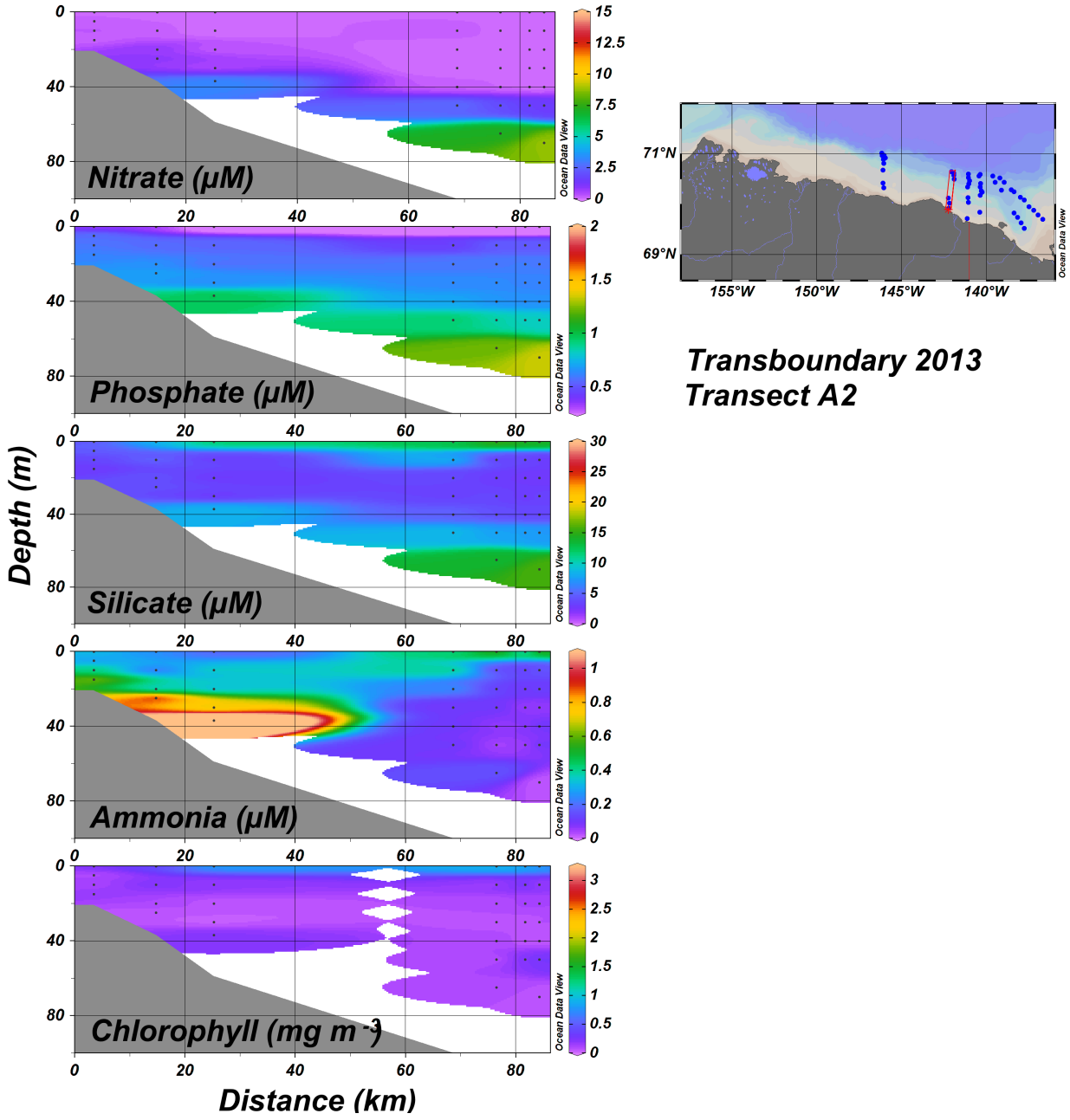

Figure 3.2.4. Macronutrient and chlorophyll-*a* concentrations across Transboundary 2013 Transect A2, 17–20 Aug.

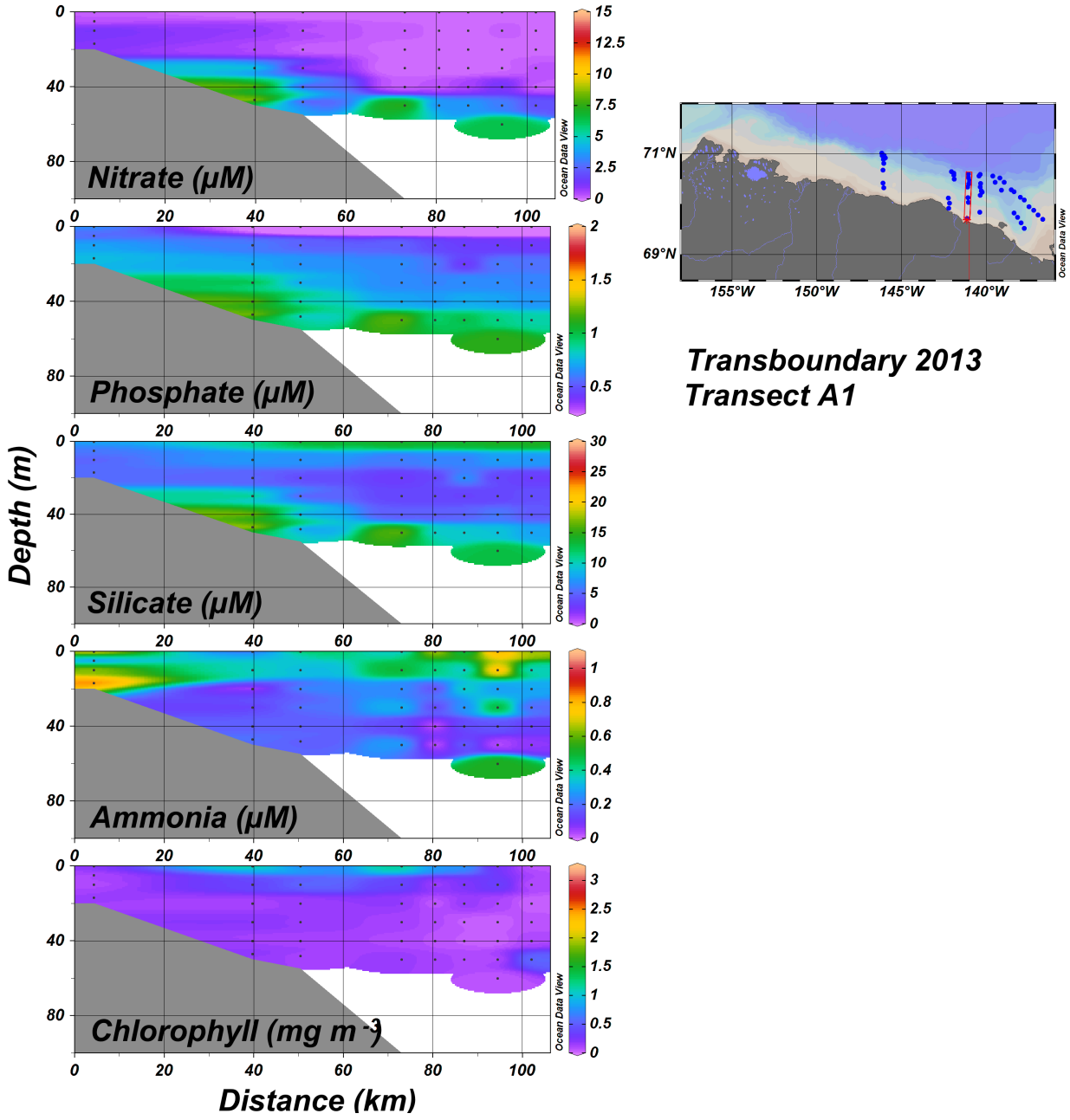

Figure 3.2.5. Macronutrient and chlorophyll-*a* concentrations across Transboundary 2013 Transect A1, 20–23 Aug.

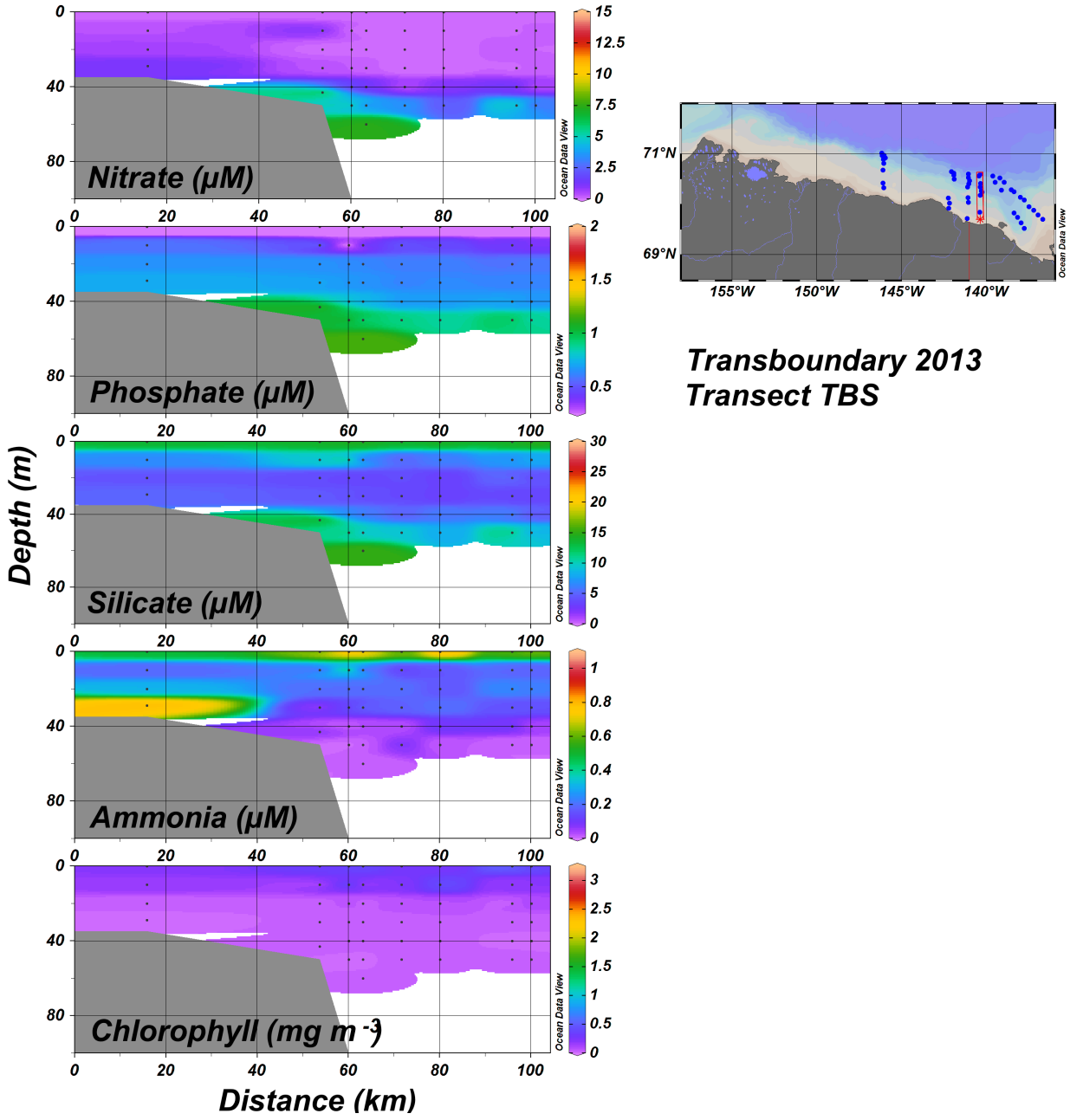

Figure 3.2.6. Macronutrient and chlorophyll-*a* concentrations across Transboundary 2013 Transect TBS, 23–26 Aug.

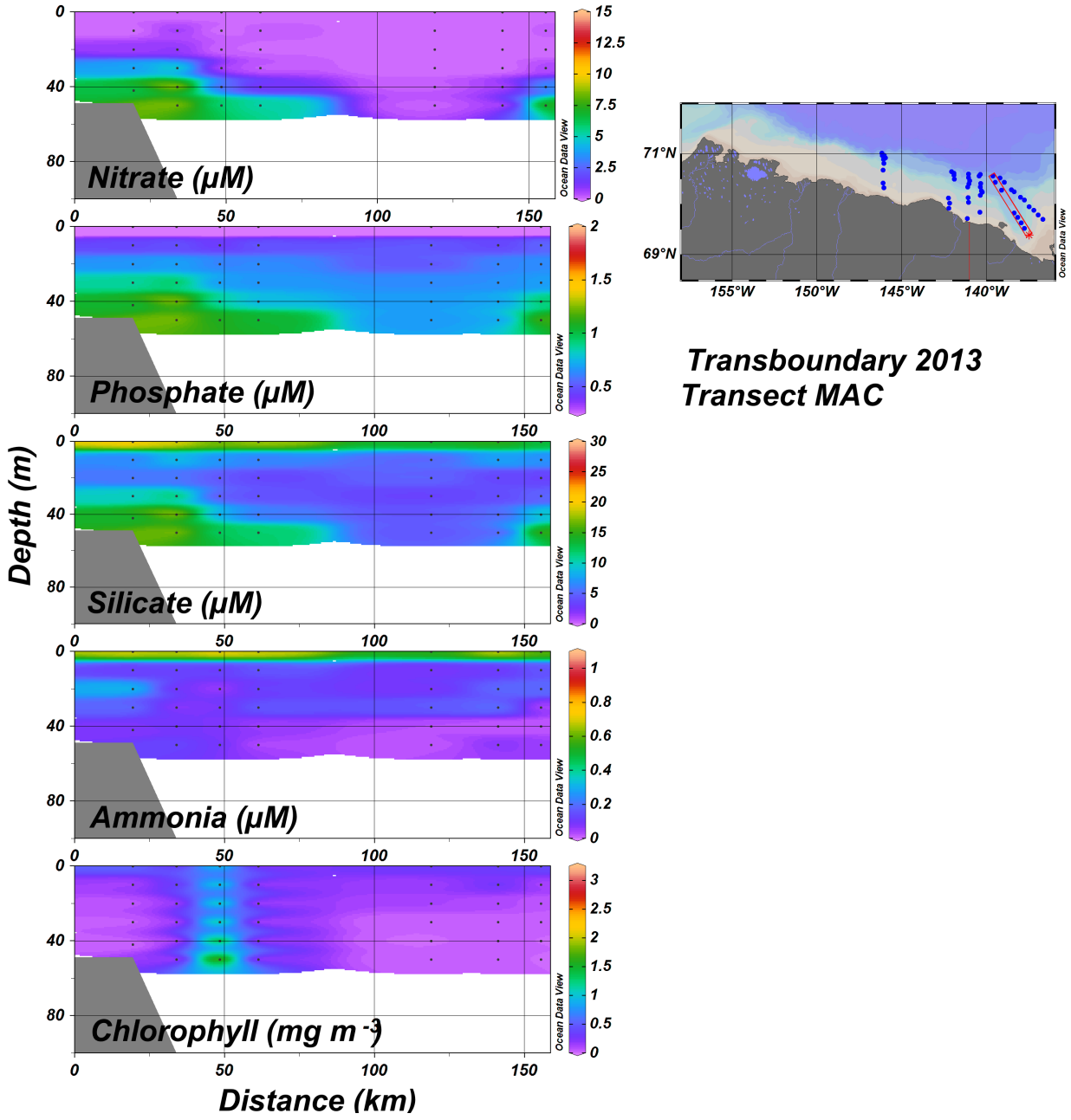

Figure 3.2.7. Macronutrient and chlorophyll-*a* concentrations across Transboundary 2013 Transect MAC, 26–31 Aug.

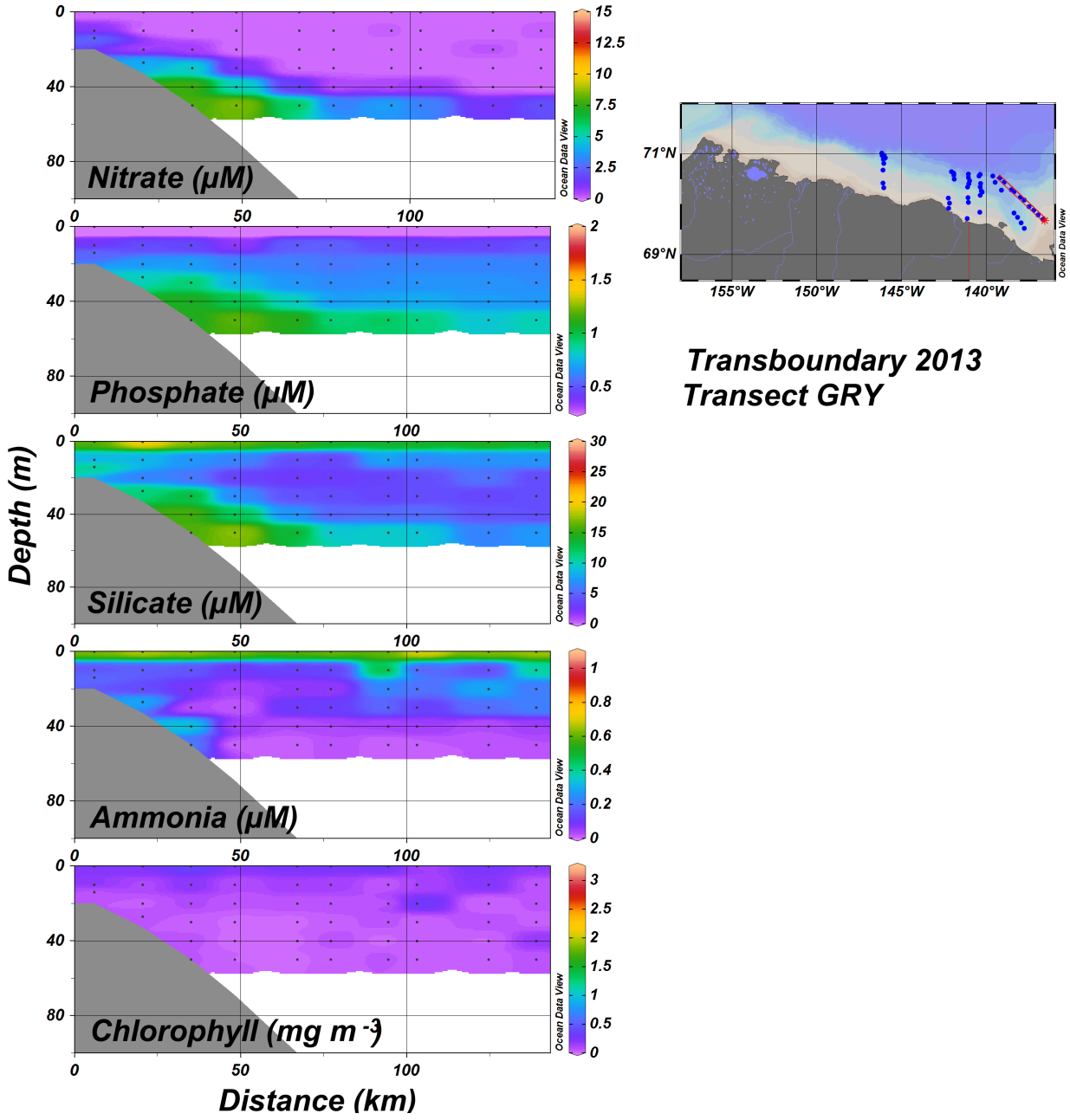

Figure 3.2.8. Macronutrient and chlorophyll-*a* concentrations across Transboundary 2013 Transect GRY, 27–29 Aug.

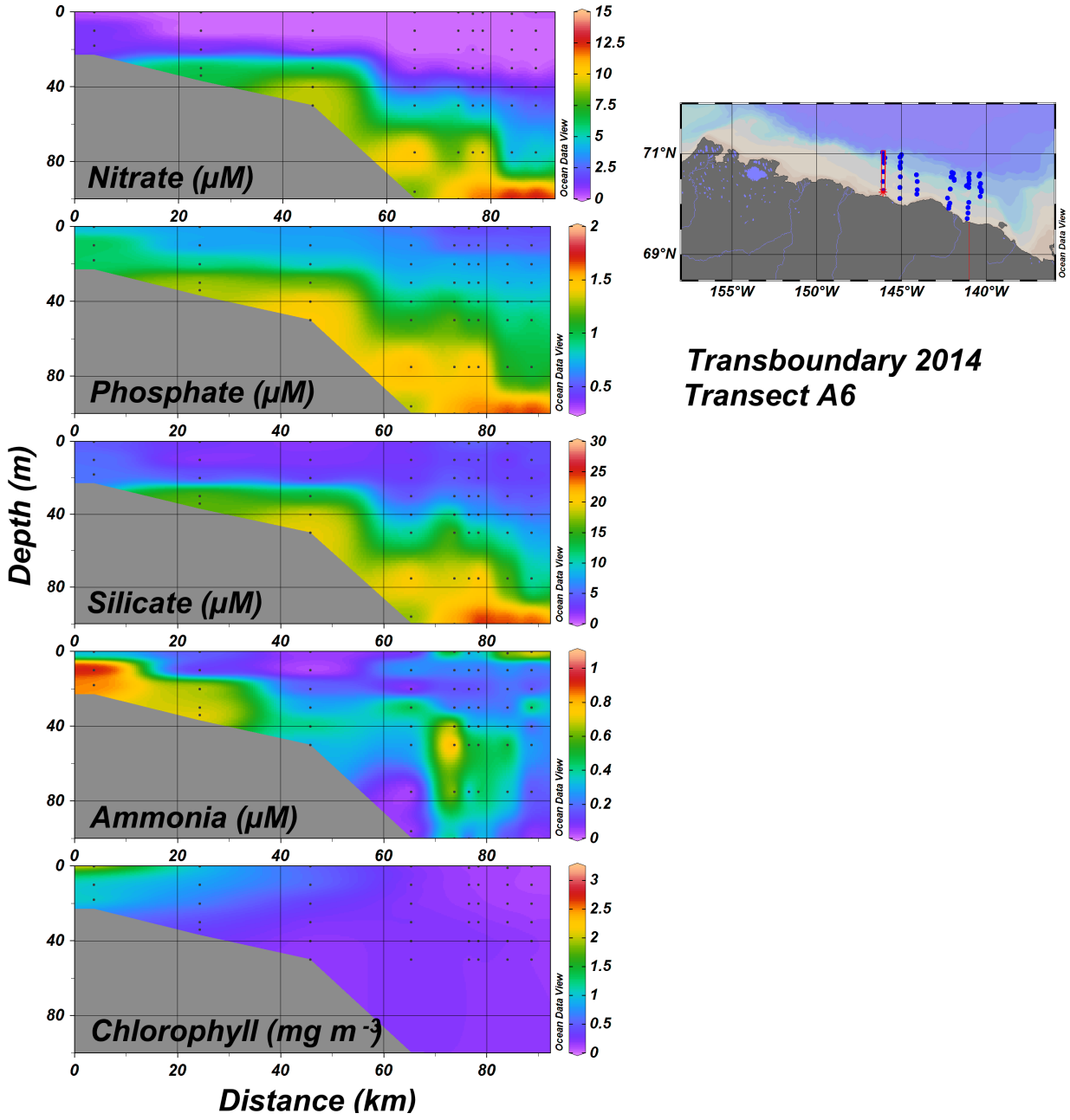

Figure 3.2.9. Macronutrient and chlorophyll-*a* concentrations across Transboundary 2014 Transect A6, 19–31 Aug.

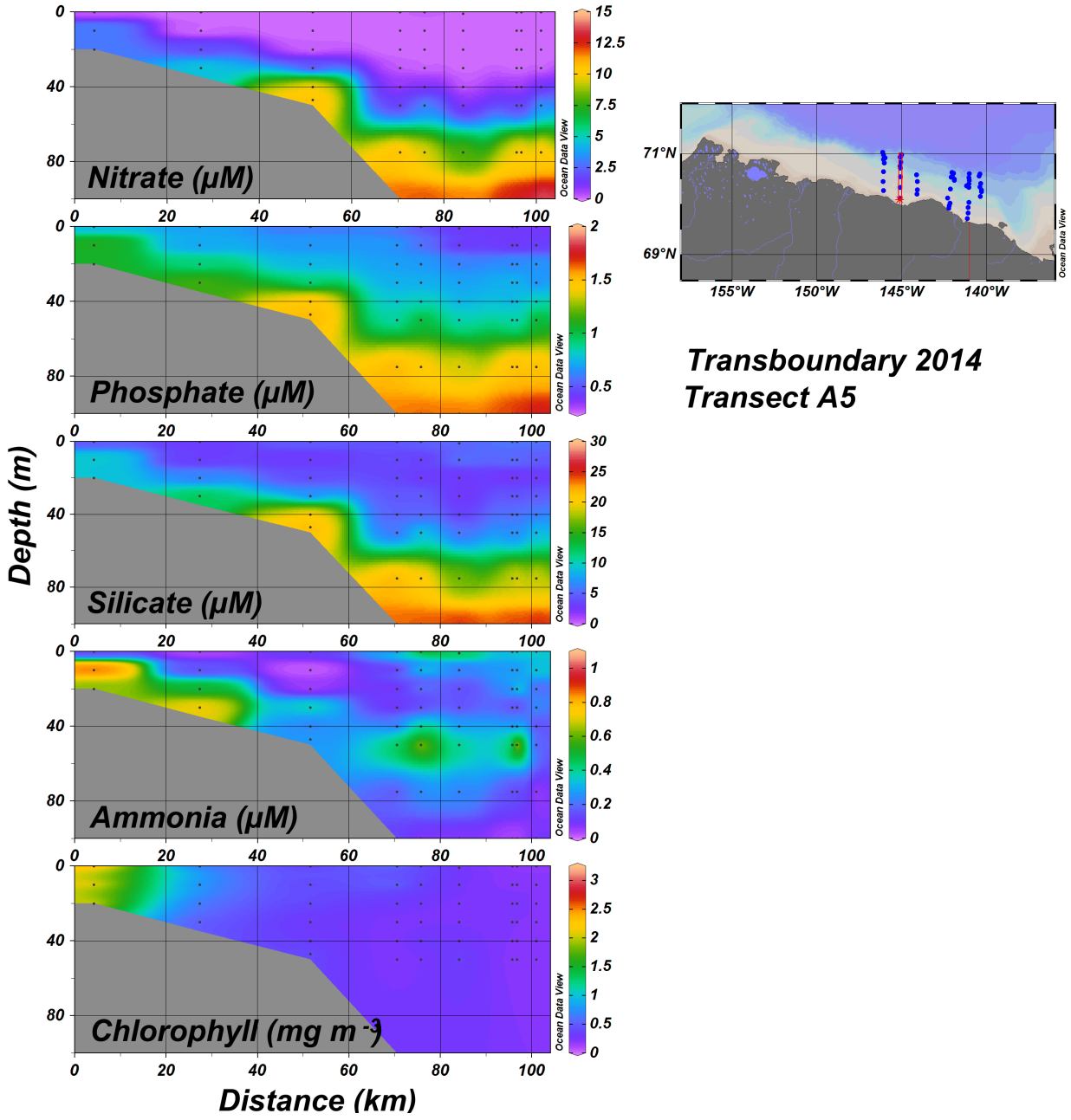

Figure 3.2.10. Macronutrient and chlorophyll-*a* concentrations across Transboundary 2014 Transect A5, 20–30 Aug.

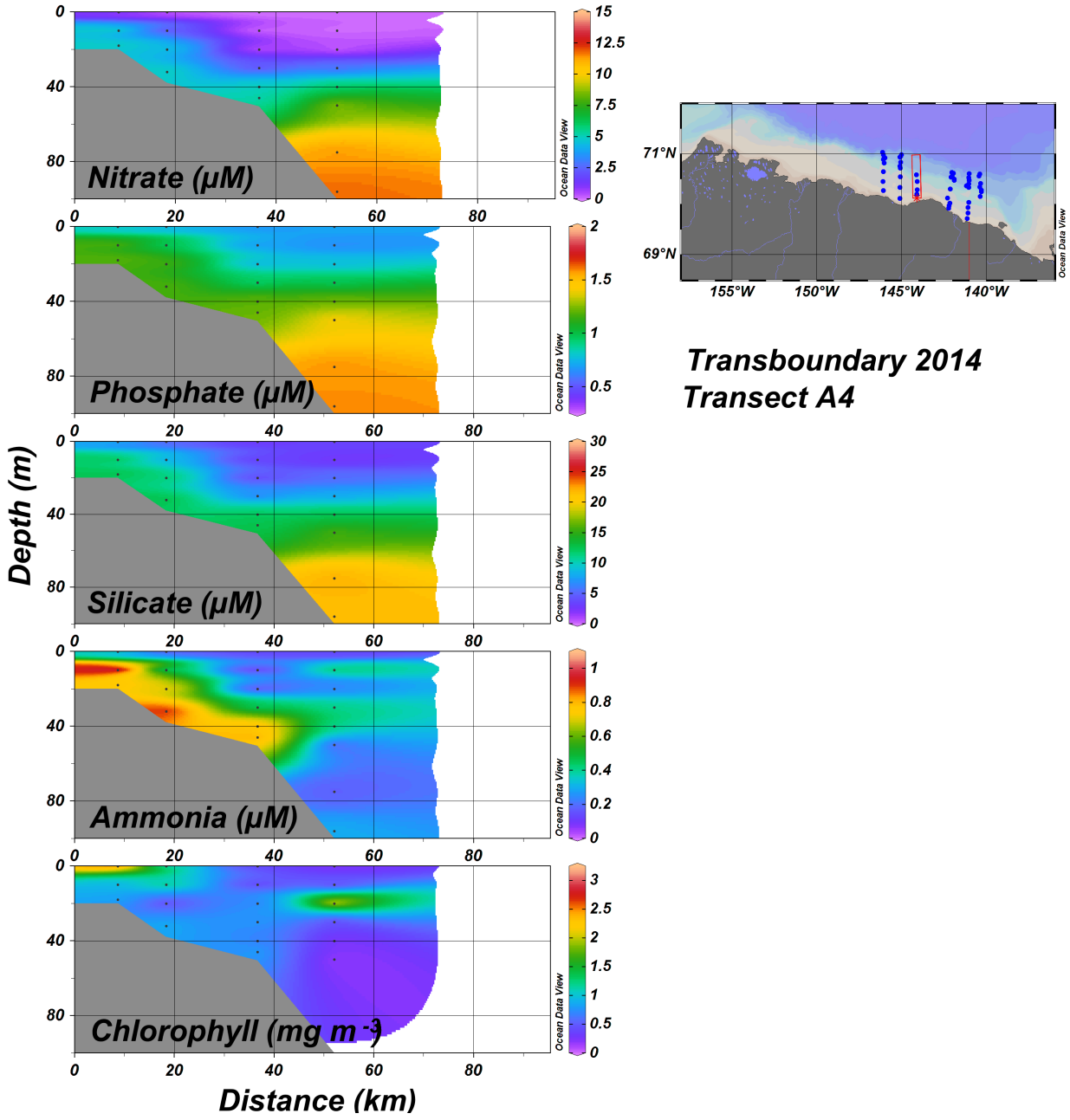

Figure 3.2.11. Macronutrient and chlorophyll-*a* concentrations across Transboundary 2014 Transect A4, 20–21 Aug.

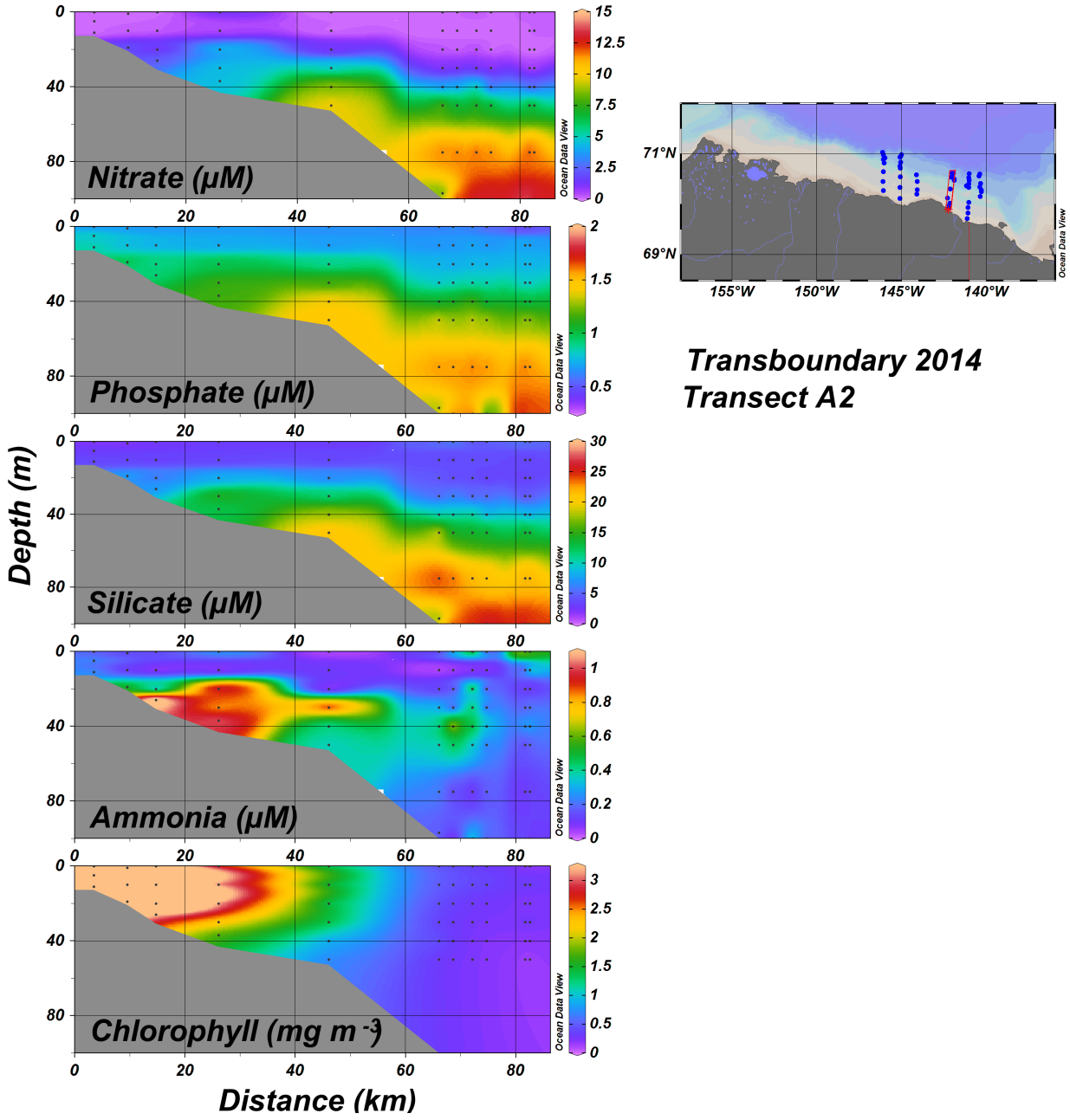

Figure 3.2.12. Macronutrient and chlorophyll-*a* concentrations across Transboundary 2014 Transect A2, 21–24 Aug.

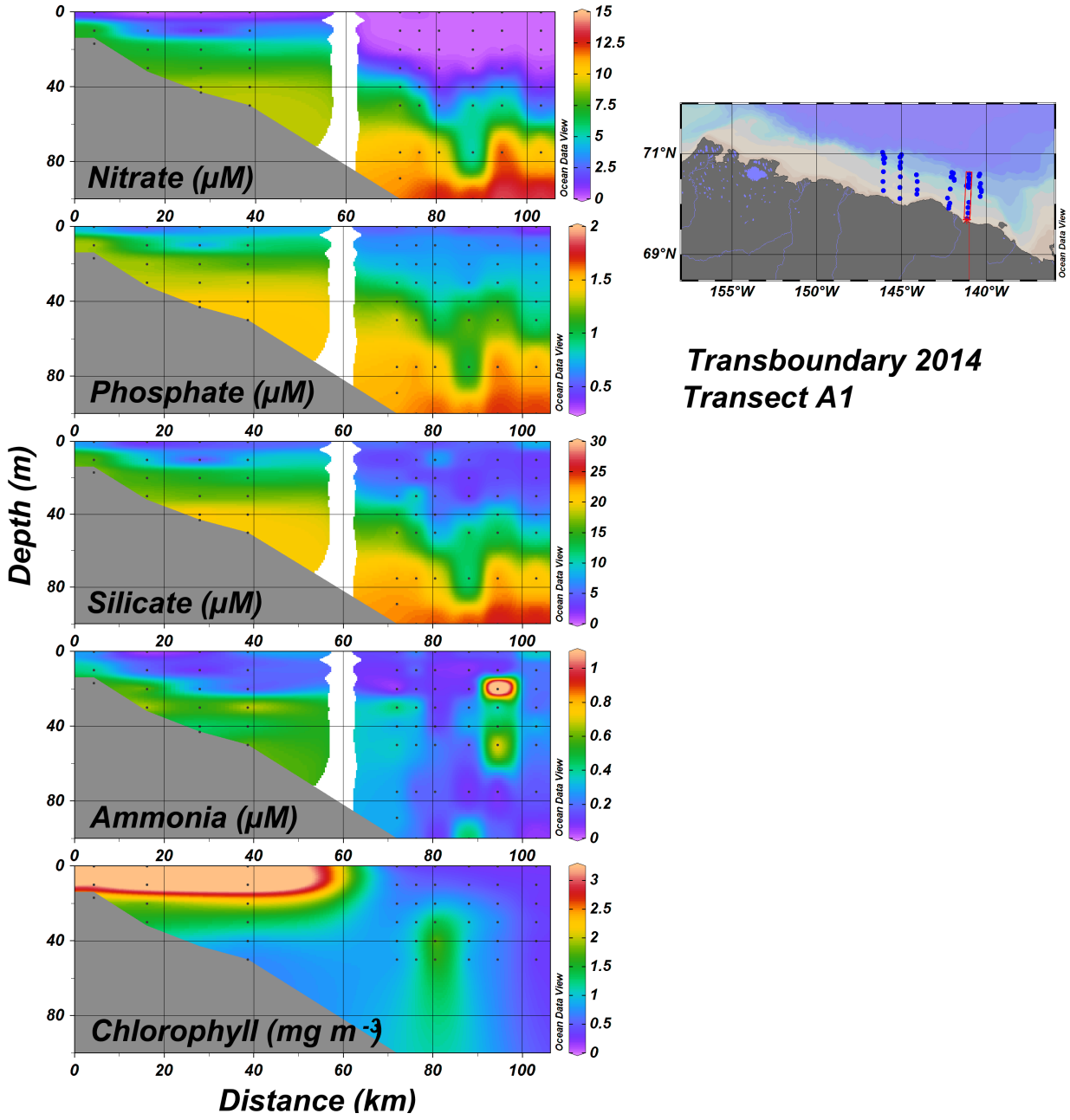

Figure 3.2.13. Macronutrient and chlorophyll-*a* concentrations across Transboundary 2014 Transect A1, 24–26 Aug.

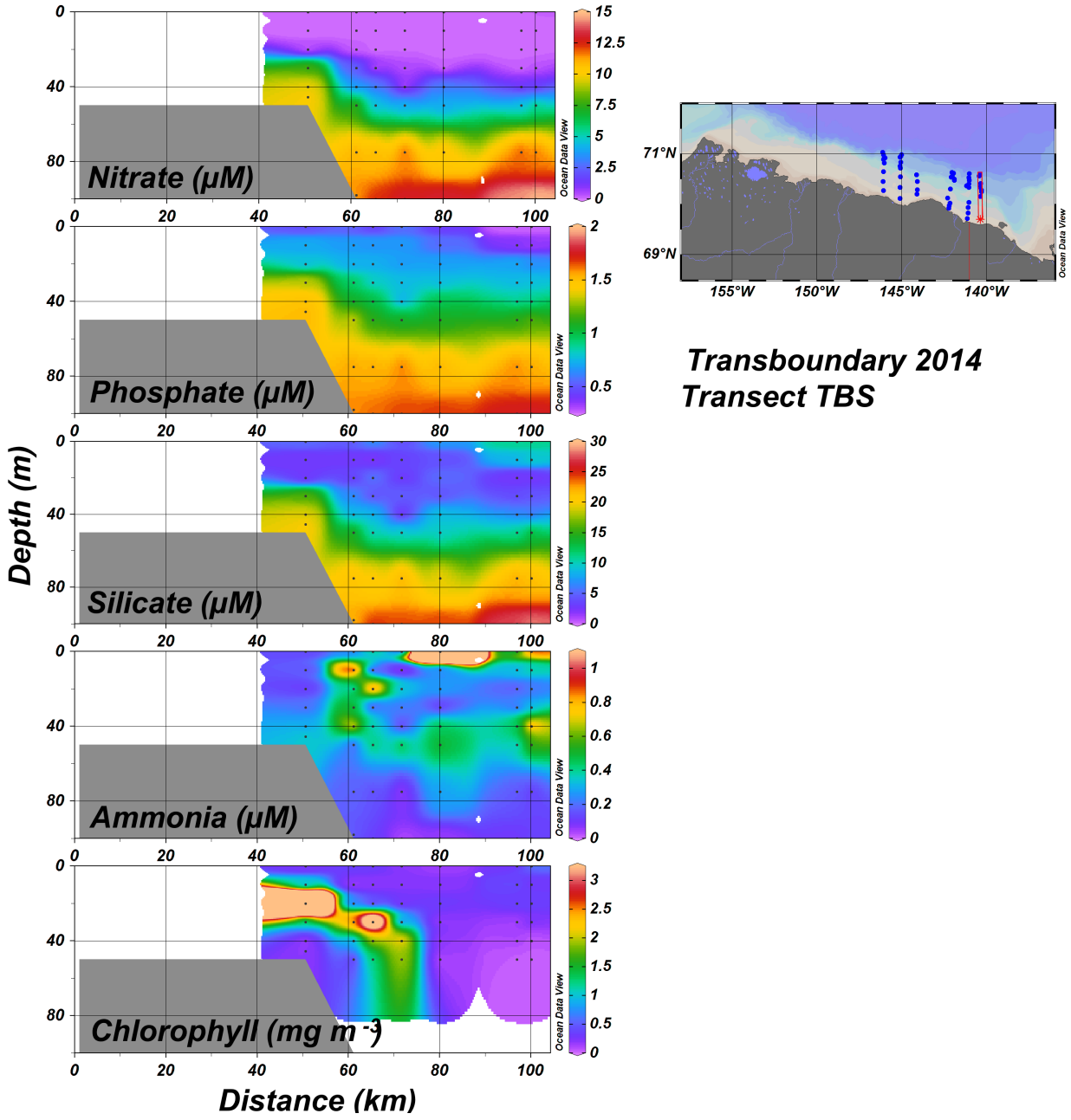

Figure 3.2.14. Macronutrient and chlorophyll-*a* concentrations across Transboundary 2014 Transect TBS, 27–28 Aug.

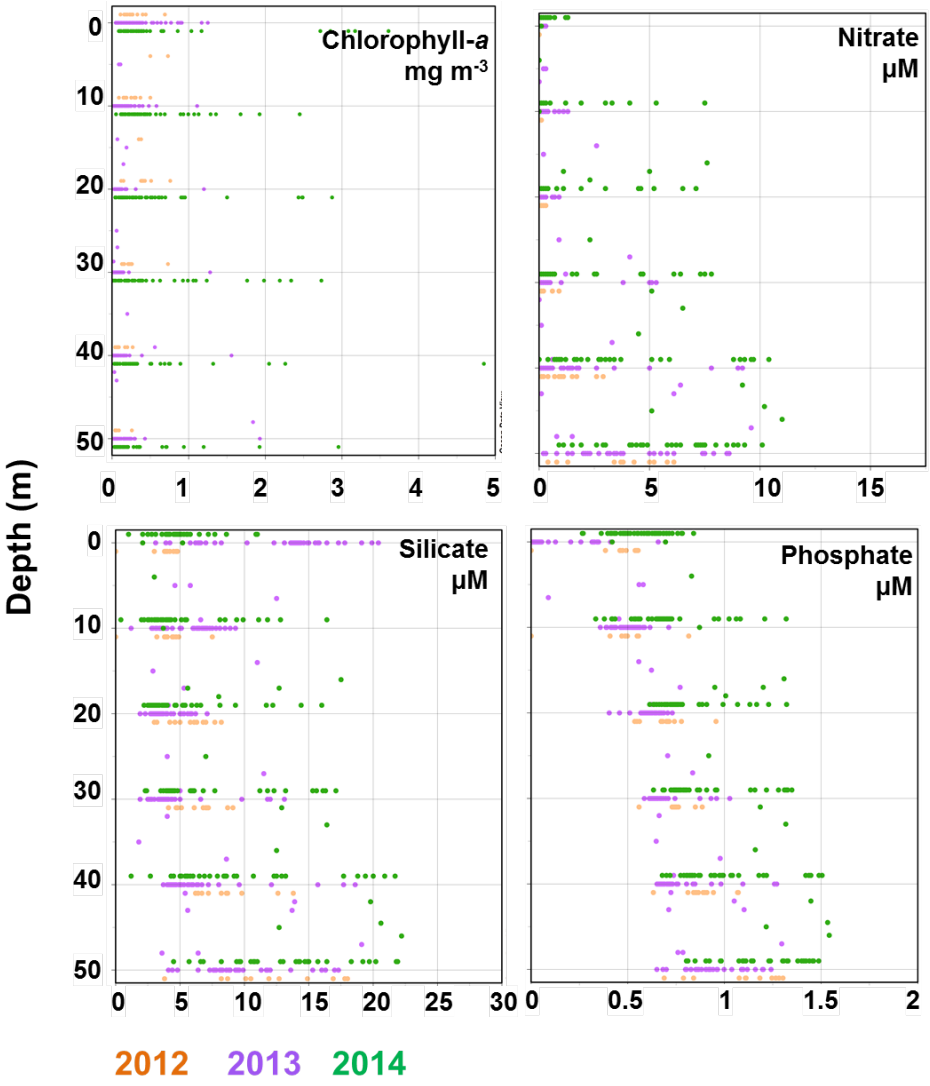

Figure 3.2.15. Macronutrient and chlorophyll-*a* concentrations in the Polar Mixed Layer of the Beaufort Sea during Transboundary 2012–14.
Data at target depths offset slightly to facilitate comparison.

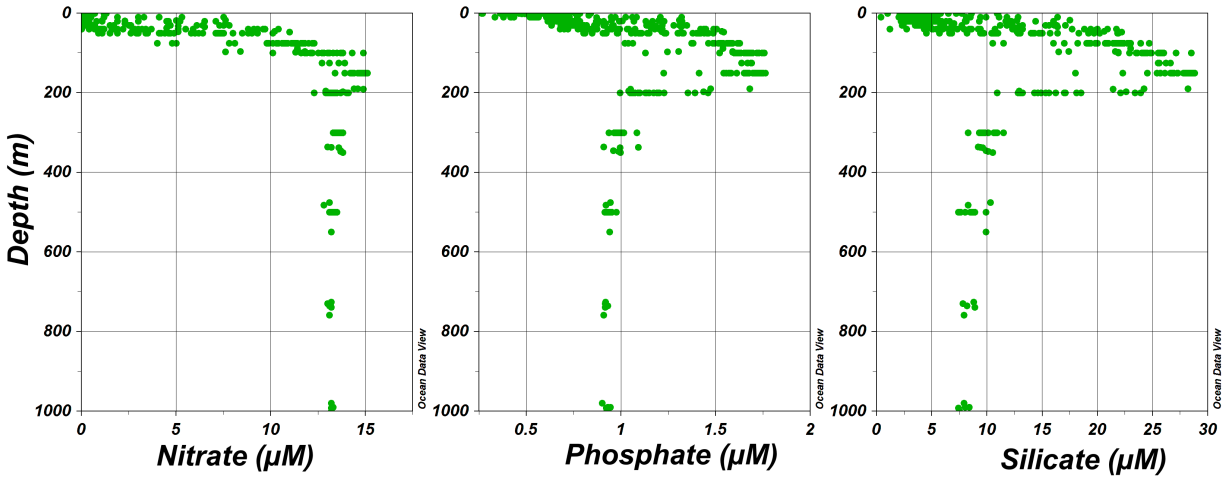

Figure 3.2.16. Macronutrient concentrations to 1000 m depth in the Beaufort Sea during Transboundary 2014.

3.3 Chlorophyll-*a*

Russell Hopcroft

3.3.1 Introduction

Using sunlight, carbon dioxide, and nutrients as fuel, phytoplankton create the biological production at the base of the food chain that feeds various invertebrate consumers. In most oceanographic studies, phytoplankton biomass is assessed by measuring the dominant photosynthetic pigment, chlorophyll-*a*. Patterns of chlorophyll concentration provide an index of food availability and productivity, both in time and space, for the food-web dependent upon this production.

In the Arctic, phytoplankton biomass undergoes stronger seasonal cycles than observed in other oceans. Phytoplankton growth begins in spring, in close association with the ice–water interface, and accelerates within increasing solar irradiance and increasing transparency of the sea-ice (Gradinger 2009). As the cycle progresses, algae is sluffed off in melting sea ice, seeding and enhancing the rising water column production, although much of the sea ice biomass ultimately falls to the seafloor as large mats. The contributions of ice algae to total primary production range from a few percent in coastal regions (Hill et al. 2005) to 60% in the central Arctic Ocean (Gosselin et al. 1997). Intense water-column blooms typically form within and track the poleward progression of the marginal ice zone, giving way to lower biomass in open water and during the summer (Carmack and Wassmann 2006). Thus, the duration of the production period for chlorophyll is sensitive to the extent, thickness, and seasonal melt dynamics of sea ice and the extent to which high chlorophyll can occur under sea-ice is still unresolved (Arrigo et al. 2012). Not surprisingly, estimates of phytoplankton biomass also vary widely depending on location, and it is generally believed that local nutrient re-mineralization on the shelves sustain much higher biomass and primary production than over the basins (see Bates et al. 2005). A pan-arctic synthesis of directly measured (i.e., extracted) and broad-scale satellite-based chlorophyll measurements indicated that productivity in the Pacific Arctic has been

increasing over the past 60 years, largely due to sea ice reduction (Matrai et al. 2013, Hill et al. 2017).

3.3.2 Objectives

Recent syntheses indicate that in situ estimates of chlorophyll on the US Beaufort Shelf are sparse (Matrai et al. 2013, Hill et al. 2013). This presents challenges in understanding how to scale up satellite observations that only integrate the upper several meters of the ocean. Specifically, we proposed to:

- Define the chlorophyll concentrations in the upper 50 m of the Beaufort shelf during Trans-boundary surveys.

3.3.3 Methods

Chlorophyll samples were collected along cross-shelf transects at stations ranging from 20 to 1000 meters in depth from the Colville River to the Mackenzie River (Figure 2.1). Water samples were collected with a 6 Niskin bottle SBE55 (2012 and 2013) or a 14 bottle SBE32SC (2014) rosette attached to the CTD concurrent with nutrient collection. Water samples for chlorophyll analysis were taken at the surface, 10, 20, 30, 40, and 50 m; when stations were shallower than 50 m, the deepest water sample was collected approximately three meters from the seafloor. Nutrient samples were filtered with 0.45-µm cellulose-acetate filters and frozen immediately at -40 °C for post-cruise analysis. Water for chlorophyll-*a* analysis was filtered under low pressure onto Whatman GF/F filters and then frozen at -40 °C for post-cruise analysis. In 2013 and 2014, 20-µm polycarbonate filters and Whatman GF/F filters were used to size-fractionate cells. Post-cruise analysis used acetone extraction and the fluorometric acidification method as described in Parsons et al. (1984). Data were screened for anomalous values and aberrant phaeopigment concentration and visualized using Ocean Dataview.

3.3.4 Results and Interpretation

Seawater chlorophyll-*a* concentration was generally low (rarely >5 and typically <1 mg m^3) throughout the region in all surveys (Figure 3.2.15). During 2012, chlorophyll was slightly elevated over the shelf (Figures 3.2.1, 3.2.2), while, in 2013, it was most elevated in the freshened surface layer (Figures 3.2.4–3.2.8). Concentrations were greatest during 2014 in the most inshore waters (Figures 3.2.9–3.2.13), with a subsurface peak also occurring along the incomplete TBS transect (Figure 3.2.14). Considered in conjunction with nutrient concentration, these observations suggest that sampling occurred well after the seasonal phytoplankton bloom and that phytoplankton productivity during our cruises would be relatively low.

Size-fractionated chlorophyll-*a* analysis in 2013 and 2014 revealed similar average contributions between each size fraction. Chlorophyll-*a* values in 2014 were generally higher than those of the same depth and size fraction in 2013 (Figure 3.3.1) and, on average, both fractions contributed equally. Nonetheless, as total chlorophyll concentration increased, the proportion of chlorophyll in the >20-µm size fraction typically increased (Figure 3.3.1), as did the proportion of chlorophyll-*a* in the total pigments (not shown). These size-related patterns in relative contribution are consistent with expectations (Chisholm 1992), though relatively noisy compared to other ecosystems. The low chlorophyll concentrations, particular within the large cells preferred by suspension-feeding zooplankton, suggest a generally food-limited environment for zooplankton. This likely compensated for the extremely low metabolic demands that can be expected for zooplankton (Ikeda et al. 2001).

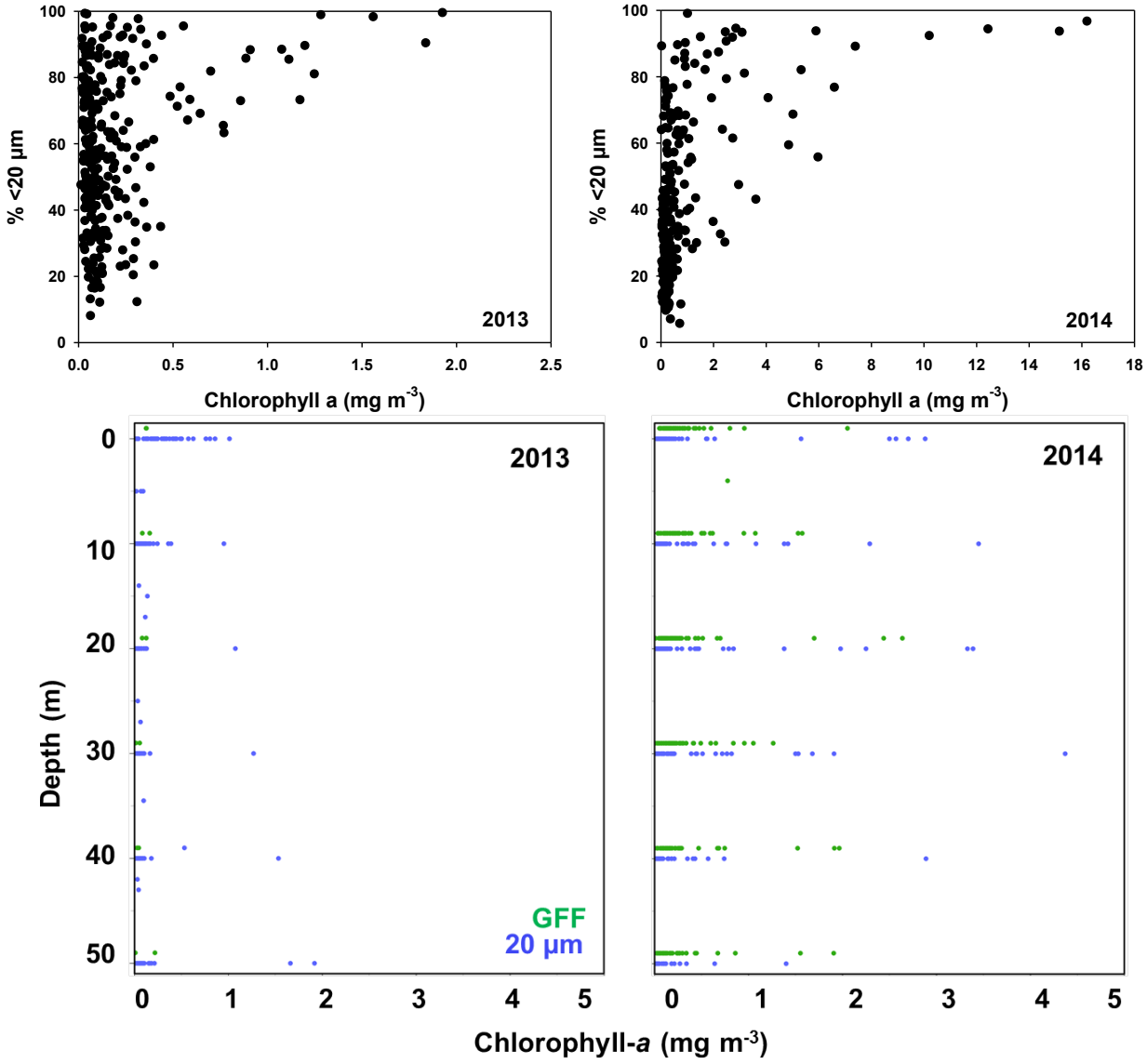

Figure 3.3.1. Size fractionated chlorophyll-*a* concentrations in the Beaufort Sea during Transboundary 2013–14.
Data at target depths offset slightly to facilitate comparison.

3.4 Benthic Environmental Characteristics

Sarah Hardy

3.4.1 Introduction

The data presented in this section support other major components of the program that address the primary objective of correlating epibenthic and infaunal community structure, abundance, and biomass with hydrographic characteristics and benthic habitat information.

These data are integrated into other sections of this report where community structure analyses of various faunal components are presented. Here, we present an independent analysis of the benthic environmental variables as a stand-alone dataset. The parameters measured are all known to be potential drivers of benthic community structure in other geographic areas. Our goals were to describe how these parameters vary across the study region and to identify any key variables that can be used as proxies for benthic habitat type at a given location (i.e., variables that explain a majority of the variance among stations). We included various parameters that described the distribution of sediment grain sizes, porosity, and measures of organic matter content including total organic carbon (TOC), carbon-to-nitrogen ratio (C:N), and chloropigment concentrations (chl-*a* and phaeopigment concentrations). Carbon and nitrogen stable-isotope values for surface sediments are also presented. Lastly, our statistical analyses included bottom water temperature and salinity values taken from CTD profiles (see Oceanography Section 3.2).

Grain size is well known to influence benthic community structure, with finer, muddier sediments occupied by different consortia of species than more coarse-grained sandy sediments. For example, suspension-feeding taxa tend to be relatively more abundant in coarser-grained sediments because finer particles, which are more easily resuspended in bottom currents, can clog the feeding apparatus of suspension feeders. In addition, many deposit-feeders tend to target the smaller (silt) size-class of particles (Roberts et al. 2000, Ward and Shumway 2004). Small grain size is correlated with food availability for deposit-feeders because organic-rich particles settle to the bottom more readily under the same hydrographic conditions that allow for sedimentation of finer sediments. Deposit-feeders also vary in their strategies for particle collection, providing a basis for niche separation among benthic organisms (Levin et al. 2001).

Various measures of organic matter content were quantified to estimate the availability of food for deposit-feeders. Chl-*a* is a commonly used tracer of labile food particles targeted by deposit-feeding species in soft-sediment habitats because it degrades fairly quickly upon cell death and, therefore, is associated with "fresh" phytoplankton detritus and actively photosynthetic microphytobenthos (Stephens et al. 1997). Phaeopigments are degradation products of chlorophyll (Mantoura et al. 1997), and their concentration relative to that of chlorophyll can indicate algal material that has been grazed (e.g., material deposited in fecal pellets). TOC also gives a bulk estimate of bioavailable carbon but may include more refractory carbon sources, which are lower quality food sources. The C:N ratio is commonly used to provide a relative measure of the food quality of organic matter (Dorgelo and Leonards 2001). Nitrogen-rich compounds in sediments tend to be used more rapidly by microbes as they process organic matter, such that the ratio of C:N increases with increasing organic matter processing (Henrichs 1993). Thus, a lower C:N can indicate more labile organic matter available for detritivores. We also present stable isotope values of sediment organic matter, which provide information on the source of primary production reaching the sediments (i.e., marine vs. terrestrial organic matter inputs).

3.4.2 Methods

We conducted analysis of sediment parameters at all stations where box cores (2012; 50–1000 m) and van Veen grabs (2013–2014; stations ≤350 m) were collected (Figure 3.4.1). In addition, we analyzed one muddy sediment sample collected ancillarily by bottom trawl and box core samples from the 2012 Beaufort Regional Environmental Assessment (BREA) project, which sampled deeper sites that could not be accessed using the van Veen grab during our cruises.

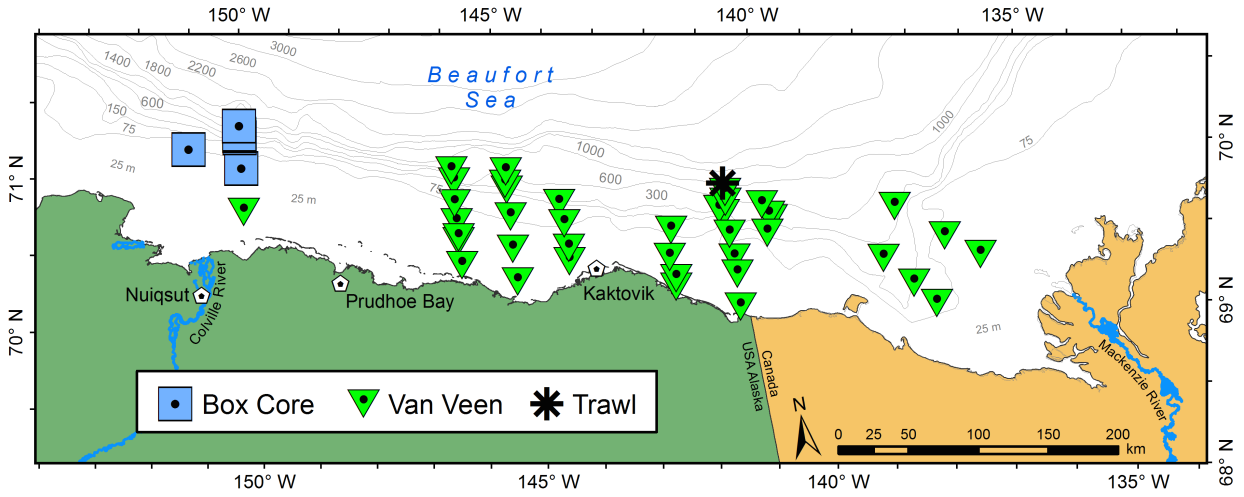

Figure 3.4.1. Map of Transboundary stations where sediments were collected by box core, (2012, B transects: 50–1000 m), van Veen grab (2013–2014, A transects: stations ≤350 m), and bottom trawl (2013).

3.4.2.1 Grain Size and Porosity

Sediments for grain-size analysis were removed from the top 5-cm surface layer of box cores and grabs using a 60-cc syringe. Samples were frozen in Whirl-pak® bags at -20 °C and returned to the home lab for processing.

Grain size samples were processed in accordance with the US EPA protocol (US EPA 2010; see also Kenny and Sotheran 2013 for method description and discussion). Before processing, samples were thawed and homogenized by stirring with a spatula. Subsamples (1 cc) were then analyzed for moisture content (i.e., porosity, wt water/wt dry sediment) by drying in a drying oven at 90 °C for 24 hours or until they showed no further loss of water weight. Porosity data provide additional information about the sediment environment. Water entrapped in sediments contains nutrients and oxygen used by infaunal organisms and higher porosity indicates more water content per unit volume of sediment. Porosity data also provided sediment volume-to-dry weight conversions used to calculate inventories of chl-*a* (mg/m^2) in sediments and to correct dry sediment weights for residual salt left behind by evaporated water in measurements of chl-*a* concentration (µg/g).

After porosity measurements had been made, the remainder of each sample was used for grain size analysis. Samples were transferred to a beaker along with 20 ml of a 2 g/l solution of dispersant (sodium hexametaphosphate) and 30 ml reverse osmosis (RO) water. Samples were stirred to break up large aggregates and then passed through two stainless steel sieves (#10, 2 ml; #230, 63-µm) to separate gravel, sand, and silt/clay fractions. Material that passed through the 63-µm sieve was retained in a large evaporating dish, and material collected on the #10 and #230 sieves was transferred to beakers. All three fractions were dried at 90 °C until completely dry and then re-weighed and recorded as gravel, sand, and silt/clay fractions. The weight of the silt/clay portion was corrected for dispersant weight and set aside for further analysis. The sand fraction was sieved dry through a series of brass sieves for further subdivision into additional size categories (see Table 3.4.1). Each fraction was weighed and recorded as a fraction of the total sample weight.

Some studies refer to the fraction of the sample that is retained on the evaporating dish (i.e., <63 μm) as the "mud" fraction, which is not a recognized grain size category (Table 3.4.1). Here, we present data for %mud for comparison to other similar studies, but we also processed this fraction into its component silt and clay fractions for more detailed analysis. The combined silt/clay portion was treated with 30% hydrogen peroxide to remove organic material, rinsed with RO water, and dried again until completely dry. The organic-free silt/clay was then analyzed to determine %silt and %clay using a Micrometrics SediGraph III, which uses the X-ray gravitational method (full description found in ISO 13317-3: 2001 Determination of particle size distribution by gravitational liquid sedimentation methods–Part 3: X-ray gravitational technique). This method is based on sedimentation and photon absorption. Samples are suspended in a dispersant solution, and Stokes' law is applied to determine particle size by measurement of the terminal settling velocities of particles of various sizes. Relative mass concentration for each size class is determined by applying the Beer-Lambert-Bouguer law to the measured absorption of a low-power X-ray beam projected through the fraction of sample remaining in suspension.

Weights of all size fractions of sediment (Table 3.4.1) were recorded as proportions of the total sample weight and analyzed using Gradistat software (Blott and Pye 2001). The object of grain-size analysis is to characterize the sediment as a frequency distribution of particle diameters. This distribution is defined using an arbitrary set of finite intervals to convert the continuous distribution to a discrete series. The Wentworth scale is a geometric scale that combines numerical intervals with descriptive definitions (e.g., fine sand, coarse sand, etc.; Table 3.4.1). A log transformation of the Wentworth scale gives the phi notation:

$$\text{phi } (\phi) = (-\log_{10} (\text{diameter in mm})) / \log_{10} 2$$

The phi scale is used to graphically represent data in order to derive informative measures that describe the distribution (e.g., median, skewness, standard deviation, and kurtosis). Here, we present the proportional data for each size fraction and the value of mean phi for each sample. Phi is useful for condensing grain size information into a single value that can be easily incorporated into environmental data matrices that analyze environmental drivers of community structure. We also include the sorting and kurtosis values in our statistical analysis. Sorting is the standard deviation of the grain-size distribution and quantifies the "diversity" of grain sizes present, which has been linked to taxonomic diversity (Etter and Grassle 1992).

3.4.2.2 Sediment Pigments

Sediments from cores and grabs were subsampled for chl-*a* and phaeopigment analysis by inserting a 60-cc syringe to 1-cm depth. Samples were stored in Whirl-pak® bags wrapped in aluminum foil and stored at -80 °C prior to laboratory processing.

Pigment analysis was performed according to the protocol outlined in Mincks et al. (2005). Briefly, samples were thawed, homogenized, and weighed prior to analysis. Each sample was suspended in 5 ml 100% acetone, mixed using a vortex mixer, and sonicated in an ice water bath for 10 minutes. Samples were allowed to extract overnight at -20 °C. The following day, each sample was centrifuged to remove sediment, and the supernatant was transferred to a clean test tube. Chl-*a* concentration of the supernatant was then determined using a fluorometer. After recording fluorescence values, samples were acidified with HCl, and fluorescence readings were taken of the acidified samples to produce phaeopigment values. A standard curve produced using

commercially available chl-*a* standard was used to convert fluorescence readings into concentrations.

3.4.2.3 Stable Isotope and Elemental Analysis

Surface sediments from cores and grabs were subsampled for stable isotope and TOC analysis. Sediment was collected to approximately 1 cm depth from the undisturbed surface of each core or grab sample and placed in a sterile plastic bag. Samples were frozen at -20 °C. Before analysis, each sample was thawed and homogenized. Approximately 1 ml of sample was then placed into a centrifuge tube with 5 ml of 1N HCl. Samples were vortexed and checked for bubbling. Caps were loosened and allowed to sit overnight or until bubbling ceased. After adding distilled water, samples were vortexed and centrifuged at 2500 rpm for 5 minutes and the supernatant discarded. This process was repeated several times until pH was determined to be close to neutral. Samples were then freeze-dried and submitted to the Alaska Stable Isotope Facility (ASIF) for analysis on a Thermo Finnigan Delta isotope ratio mass spectrometer (IRMS) with PDB and atmospheric nitrogen as standards for carbon and nitrogen, respectively. Data provided by ASIF included stable isotope values as well as percent carbon and nitrogen content obtained using a Costech Elemental Analyzer. These values were used to calculate the TOC and C:N ratios presented here.

Table 3.4.1. Range of grain sizes that make up each descriptive category with equivalents in phi notation.

Grain Size phi	mm	Descriptive term	
-10	1024	Very Large	Boulder
-9	512	Large	
-8	256	Medium	
-7	128	Small	
-6	64	Very small	
-5	32	Very coarse	Gravel
-4	16	Coarse	
-3	8	Medium	
-2	4	Fine	
-1	2	Very fine	
0	1	Very coarse	Sand
1	500 µm	Coarse	
2	250	Medium	
3	125	Fine	
4	63	Very fine	
5	31	Very coarse	Silt
6	16	Coarse	
7	8	Medium	
8	4	Fine	
9	2	Very fine	
		Clay	

3.4.2.4 Statistical Analysis

Multivariate analysis of all benthic environmental parameters was conducted to identify particular variables or combinations of variables that best characterize "benthic habitat" at each location across the study region. Principle components analysis (PCA), an ordination technique, was used to visualize patterns in environmental characteristics across all stations without imposing any a priori groupings (e.g., by depth or transect). Canonical discriminant analysis (CDA) was then used to examine how habitat parameters change across depth and by transect (as a proxy for longitudinal trends across the study area). CDA is a related technique to PCA but allows for a priori groups to be examined. Both analyses produce a matrix of eigenvectors that indicate which variables are more heavily loaded on each axis. This information can be interpreted in a similar manner for both analyses, with large (positive or negative) values indicating that the variable(s) explain more of the separation of points along that axis. PCA was performed using the software PRIMER-E v.7, and CDA was performed using R.

Depth, longitude, and latitude were excluded from both analyses in order to examine only the patterns in environmental parameters, many of which strongly co-vary with depth in particular. Chl-*a* and phaeopigment concentrations were log-transformed because distributions were strongly left-skewed, which is commonly the case for concentration data (Clarke et al. 2014a). For grain size, %mud (= silt + clay) and %sand were included; other size fractions were excluded because the various size fractions were highly correlated. CDA was first run with sediment and bottom water variables included, but temperature and salinity dominated the outcome of the analysis, so CDA was run again without bottom water variables. The results of both analyses are reported in Tables 3.4.2–3.4.6. For the analysis by depth, plots are shown for the analyses with and without temperature and salinity included, but for the analysis by transect, only the analysis that excludes these variables is plotted. For all the CDA analyses, some depth ranges or transects were grouped to reduce the number of categories, which reduced some of the variation among groups and helped to clarify patterns.

Table 3.4.2 Eigenvalues and eigenvectors for principle components analysis (PCA) shown in Figure 3.4.10. Variables contributing the most to variation along each axis are in bold (defined by values > ±3.5).

Variable	PC1	PC2	PC3	PC4	PC5
Chl-*a*	0.185	**-0.417**	0.128	**-0.423**	0.056
Phaeopigment	0.320	**-0.401**	-0.087	-0.161	0.174
Porosity	**0.372**	0.081	-0.021	0.095	0.114
%Sand	-0.321	-0.095	-0.276	-0.241	-0.014
%Mud	**0.367**	0.291	0.103	0.128	-0.127
Phi	**0.358**	0.304	0.049	0.085	-0.185
Sorting	-0.064	**-0.491**	0.340	0.136	-0.138
Kurtosis	-0.161	0.136	**-0.552**	-0.023	0.229
$\delta^{15}N$	0.056	-0.116	-0.370	-0.160	0.080
$\delta^{13}C$	-0.306	-0.06	0.234	0.374	**0.527**
C:N	-0.256	0.237	**0.454**	-0.176	0.220
TOC	0.333	-0.160	0.088	0.009	0.272
Temperature	0.057	0.338	0.207	**-0.654**	0.301
Salinity	0.230	0.013	-0.136	0.246	**0.578**
Eigenvalues	5.48	2.03	1.77	1.13	0.91
% Variation	39.1	14.5	12.6	8.1	6.5
Cum. % Variation	39.1	53.7	66.3	74.4	80.9

Table 3.4.3 Loading values for canonical discriminant analysis (CDA) examining variation in habitat parameters among depths with *temperature and salinity included*. Variables contributing the most to each canonical variables (CV) are in bold (defined by values > ±0.4).

Variable	CV1	CV2	CV3
Chl-*a*	0.044	0.307	0.293
Phaeopigment	**-0.486**	0.033	0.182
Porosity	**-0.777**	0.051	0.079
%Mud	**-0.525**	0.197	0.082
Phi	**-0.521**	0.155	0.092
Sorting	0.262	-0.377	0.389
Kurtosis	0.084	-0.002	-0.220
$\delta^{15}N$	-0.133	-0.142	0.029
$\delta^{13}C$	0.150	-0.170	0.162
C:N	0.363	0.166	0.019
TOC	-0.399	0.145	**0.446**
Temperature	-0.133	**0.840**	-0.008
Salinity	**-0.924**	0.036	-0.049
% Variation	79	15	6

Table 3.4.4. Loading values for canonical discriminant analysis (CDA) examining variation in habitat parameters among depths with *temperature and salinity excluded*. Variables contributing the most to each canonical variables (CV) are in bold (defined by values > ±0.4).

Variable	**CV1**	**CV2**	**CV3**
Chl-*a*	0.117	0.034	**0.623**
Phaeopigment	**-0.501**	0.066	0.397
Porosity	**-0.800**	0.226	0.251
%Mud	**-0.499**	0.249	0.273
Phi	**-0.507**	0.208	0.229
Sorting	0.156	**-0.633**	-0.119
Kurtosis	0.097	0.133	-0.095
$\delta^{15}N$	-0.177	-0.072	0.037
$\delta^{13}C$	0.102	-0.275	0.018
C:N	**0.422**	0.003	0.124
TOC	-0.397	-0.045	**0.742**
% Variation	69	22	9

Table 3.4.5 Loading values for canonical discriminant analysis (CDA) examining variation in habitat parameters among transects with *temperature and salinity included*. Variables contributing the most to each canonical variables (CV) are in bold (defined by values > ±0.4).

Variable	**CV1**	**CV2**	**CV3**
Chl-*a*	0.085	0.344	0.147
Phaeopigment	0.109	0.306	-0.102
Porosity	0.142	**0.438**	-0.187
%Mud	0.187	**0.520**	-0.214
Phi	0.162	**0.447**	-0.272
Sorting	-0.118	0.252	0.399
Kurtosis	-0.074	**-0.452**	-0.180
$\delta^{15}N$	0.147	-0.088	-0.132
$\delta^{13}C$	-0.266	-0.248	**0.735**
C:N	0.292	-0.039	**0.702**
TOC	0.151	**0.420**	0.081
Temperature	**0.905**	-0.080	0.037
Salinity	0.211	-0.083	-0.104
% Variation	50	32	18

Table 3.4.6 Loading values for canonical discriminant analysis (CDA) examining variation in habitat parameters among transects with *temperature and salinity excluded*. Variables contributing the most to each canonical variables (CV) are in bold (defined by values > ±0.4).

Variable	**CV1**	**CV2**	**CV3**
Chl-*a*	-0.377	-0.027	-0.091
Phaeopigment	-0.306	-0.188	0.101
Porosity	-0.372	-0.110	0.322
%Mud	**-0.479**	-0.213	0.313
Phi	-0.369	-0.153	**0.408**
Sorting	-0.281	-0.101	**-0.607**
Kurtosis	**0.461**	0.030	0.119
$\delta^{15}N$	0.016	0.035	0.260
$\delta^{13}C$	0.178	**0.407**	**-0.809**
C:N	-0.297	**0.718**	-0.164
TOC	**-0.478**	-0.123	-0.033
% Variation	46	30	24

3.4.3 Results and Discussion

The series of maps in Figures 3.4.2–3.4.8 shows the distribution of different grain size fractions across the study region; data are provided in Appendix C Table 2. Note that polygons encompassing areas not sampled represent interpolations between sampling locations. Thus, grain-size maps do not capture the potential variation in grain size distribution that can occur over smaller (meters to 10s of meters) spatial scales. In general, the grain size fractions encountered at Transboundary stations were similar to those indicated by the large-scale seafloor substrate map (Figure 3.4.9) that was synthesized from a variety of sources by Audubon Alaska (2015). Here we describe broader-scale patterns based on data interpolated between our sample collection locations, as these more precisely describe the environment occupied by fauna assessed by our survey. The central 'B' transects (Figure 2.1) were dominated by muddier sediments. The eastern US 'A' transects showed a higher proportion of sand and gravel, particularly at shallower stations. In the eastern Canadian area of the study region, finer sediments were again dominant. The map of phi values (indicating mean grain size on the phi scale) shows higher values of phi, indicating high silt content (Table 3.4.1) particularly in the eastern area influenced by the Mackenzie River plume (Figure 3.4.8). As discussed above, the dominance of fine sediment will influence the composition of the infaunal community. Small-scale (i.e., meters to 10s of meters) topographic depressions on the seafloor may focus fine particles and organic matter in localized areas, but this possibility cannot be evaluated without high-resolution bathymetric mapping of the area. This type of topographic complexity, common in slope and canyon environments, is thought to enhance the diversity of benthic organisms by allowing for niche separation among taxa with specific feeding strategies (see McClain and Barry 2010, Blanchard and Feder 2014).

The concentration of chl-*a* (µg/g dry sediment) in surface sediments was also highly variable across the study region (Figure 3.4.10). Values were more similar among sites in the shallow areas, but transect 'B' sampled in 2012 showed an extremely high value at the 350-m site (about 4x the mean for all samples). A few other transects showed this trend with depth but not with the same magnitude. As mentioned above, topographic features may focus sedimentation of organic particles into depressions where values of chl-*a* may become elevated relative to the surrounding sediments. This chl-*a* peak suggests high food availability below the shelf break and merits further investigation. However, this single high value at one location should not be over-interpreted. Chl-*a* can be highly patchy over small (cm to m) spatial scales for a variety of reasons, and this value was obtained from a single box core sample with no available replicates.

Chl-*a* concentration across all locations sampled ranged from 0.9–79.5 µg/g (mean 6.3 ± 9.7 µg/g). The values of chl-*a* shown here for deeper stations (>350 m) are an order of magnitude higher than Antarctic shelf sediments of comparable depth measured with the same method used here (Fabiano and Danovaro 1998, Mincks et al. 2005). This comparison to Antarctic sediments helps to place our results into a broader context, given that relatively few data are available from comparable depths in our study region. Moreover, this contrast in sediment chlorophyll concentration between Arctic and Antarctic sediments at comparable depths is noteworthy because it suggests Arctic sediments may harbor substantially higher food availability for benthos than similar high-latitude settings on the Antarctic shelf. Another study from the Beaufort Sea reports a similar range of values (Link et al. 2013). For comparable depths in the Barents Sea (79–459 m), Cochrane et al. (2009) report concentrations of total benthic pigments on the order of 2–14 µg/g, which is somewhat lower than in our study region; however, this study applied HPLC analysis, which can yield lower values of chl-*a* than the fluorometric

method used here (Mincks et al. 2005). Chl-*a* inventories for the upper 1 cm of sediment (mg chl-*a*/m^2) were calculated for comparison with other published studies from Arctic waters and ranged from 2.1–1406.8 mg/m^2 (mean 32.4 ± 51.9 mg/m^2). Roughly comparable average values have been reported for the Chukchi Sea (Grebmeier et al. 2015a).

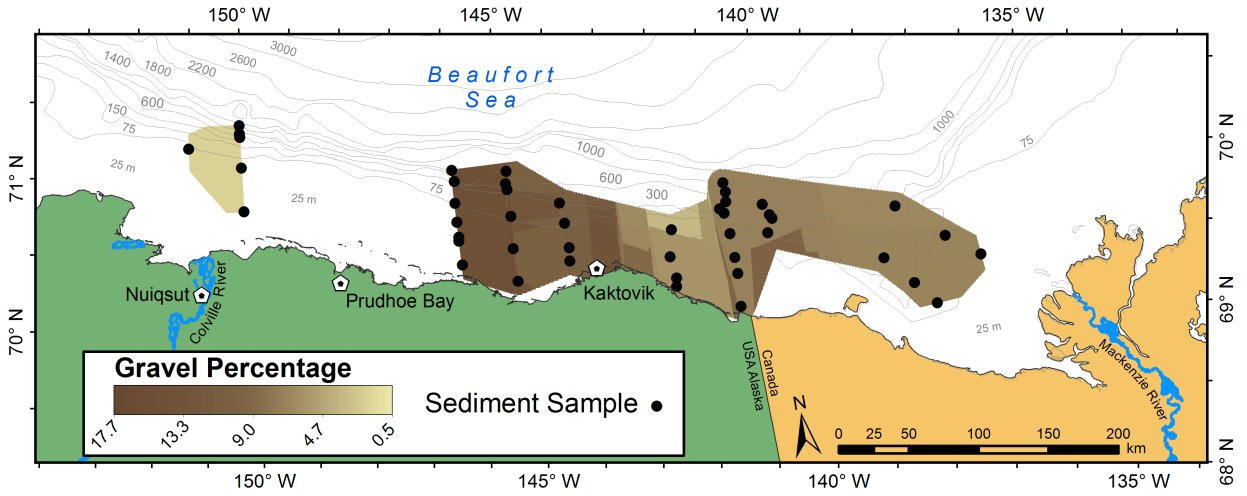

Figure 3.4.2. Map: Gravel percentage in surface sediment.

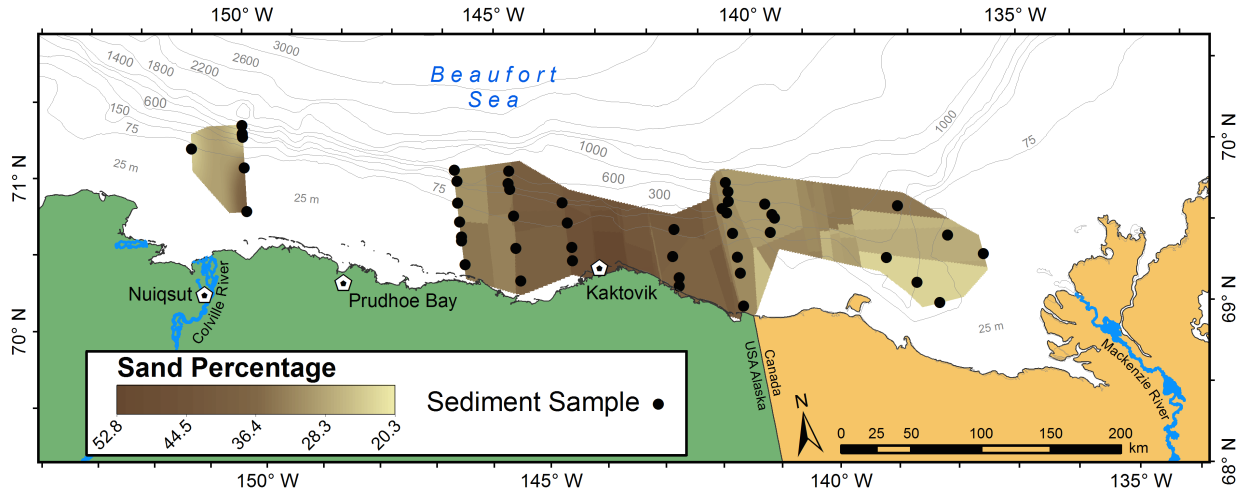

Figure 3.4.3. Map: Sand percentage in surface sediment.

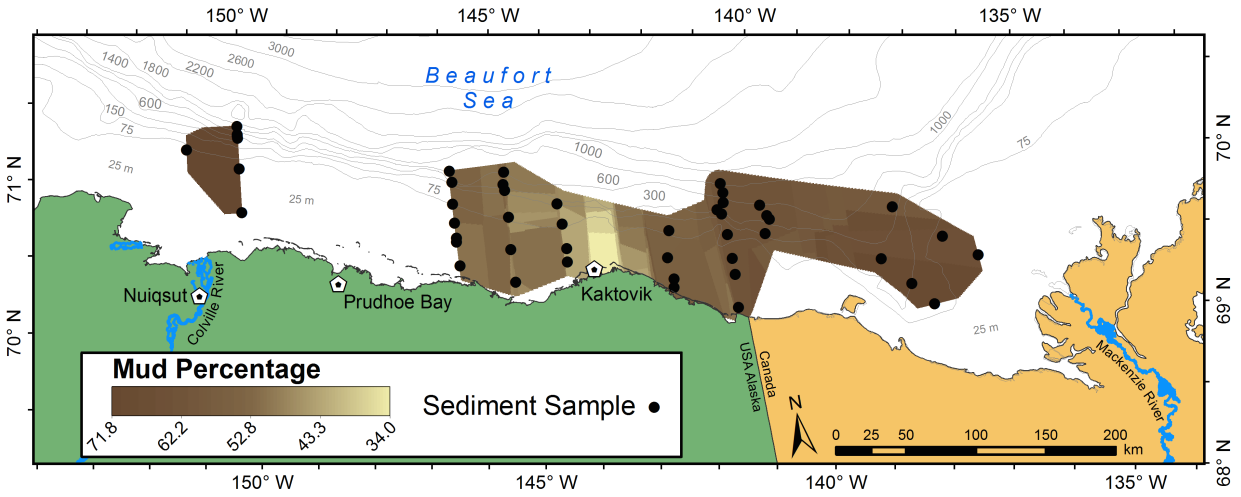

Figure 3.4.4. Map: Mud percentage in surface sediment.

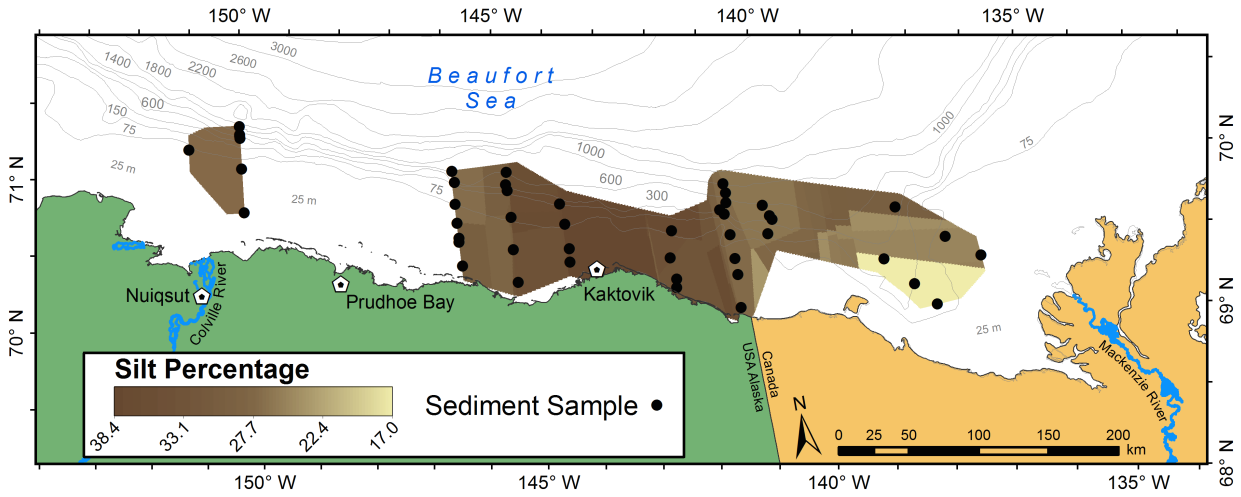

Figure 3.4.5. Map: Silt percentage in surface sediment.

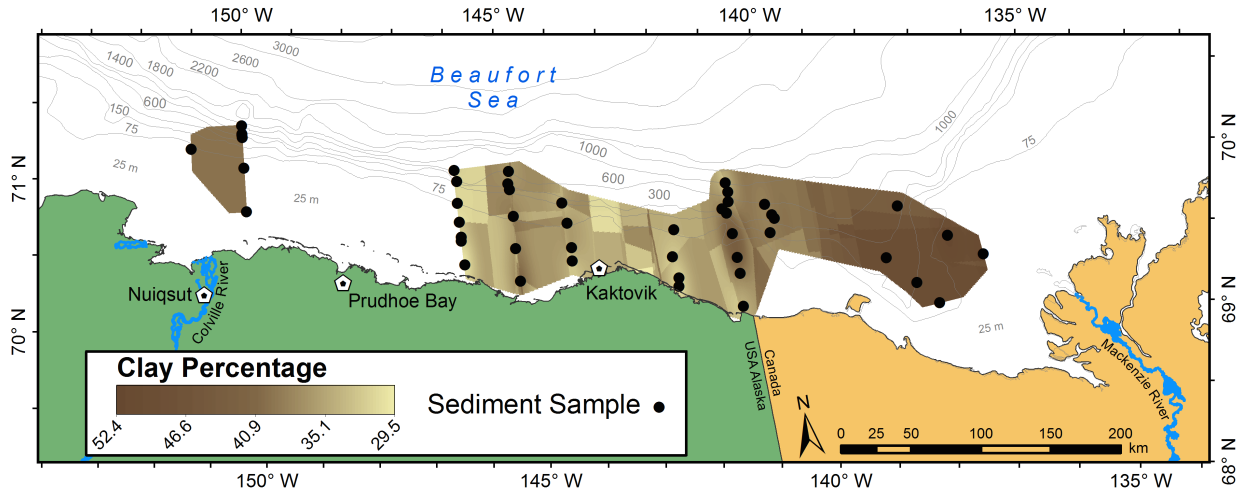

Figure 3.4.6. Map: Clay percentage in surface sediment.

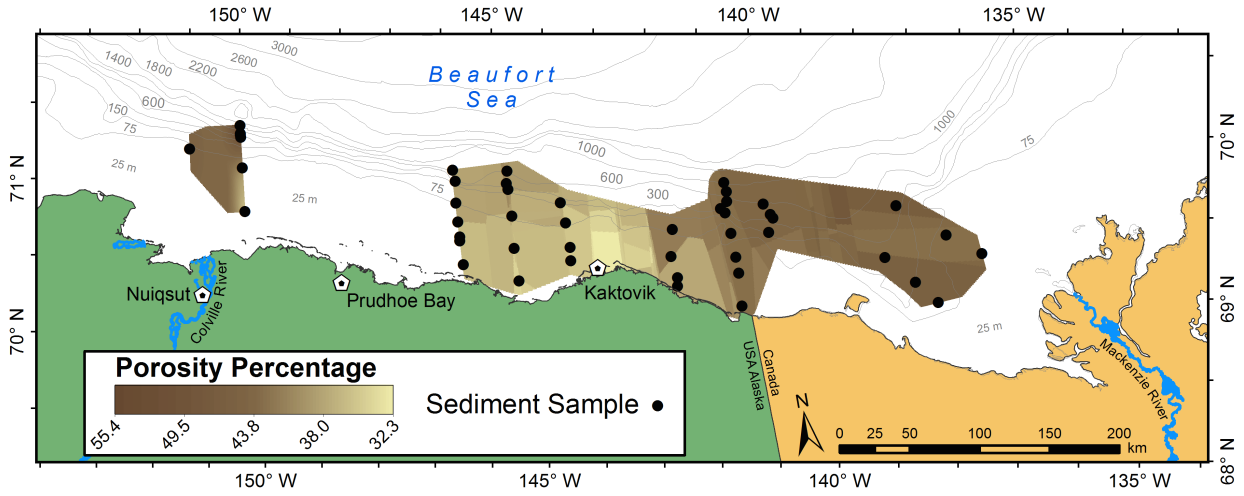

Figure 3.4.7. Map: Porosity of surface sediment.

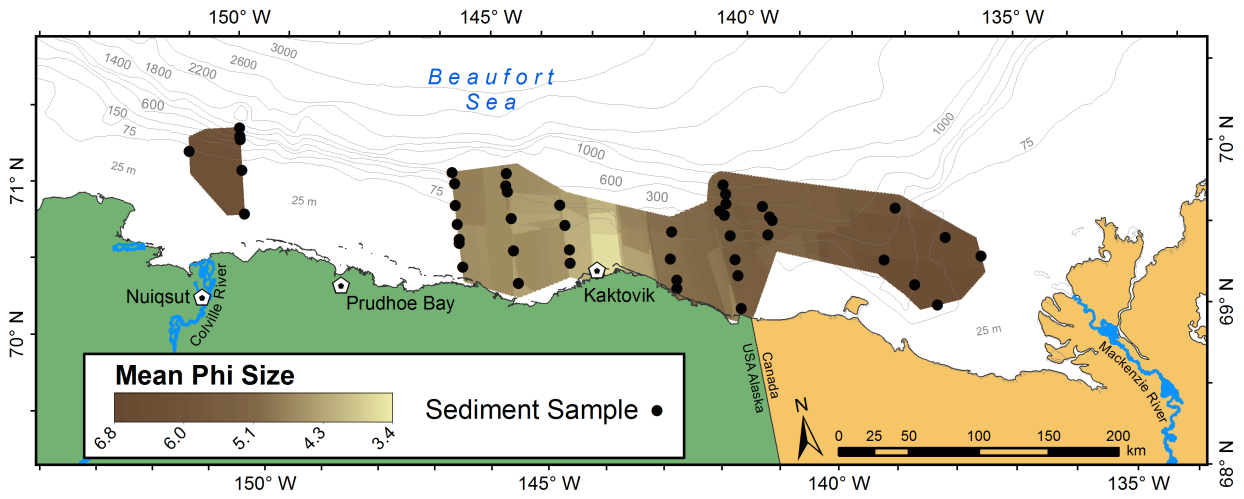

Figure 3.4.8. Map: Mean Phi size of surface sediment.

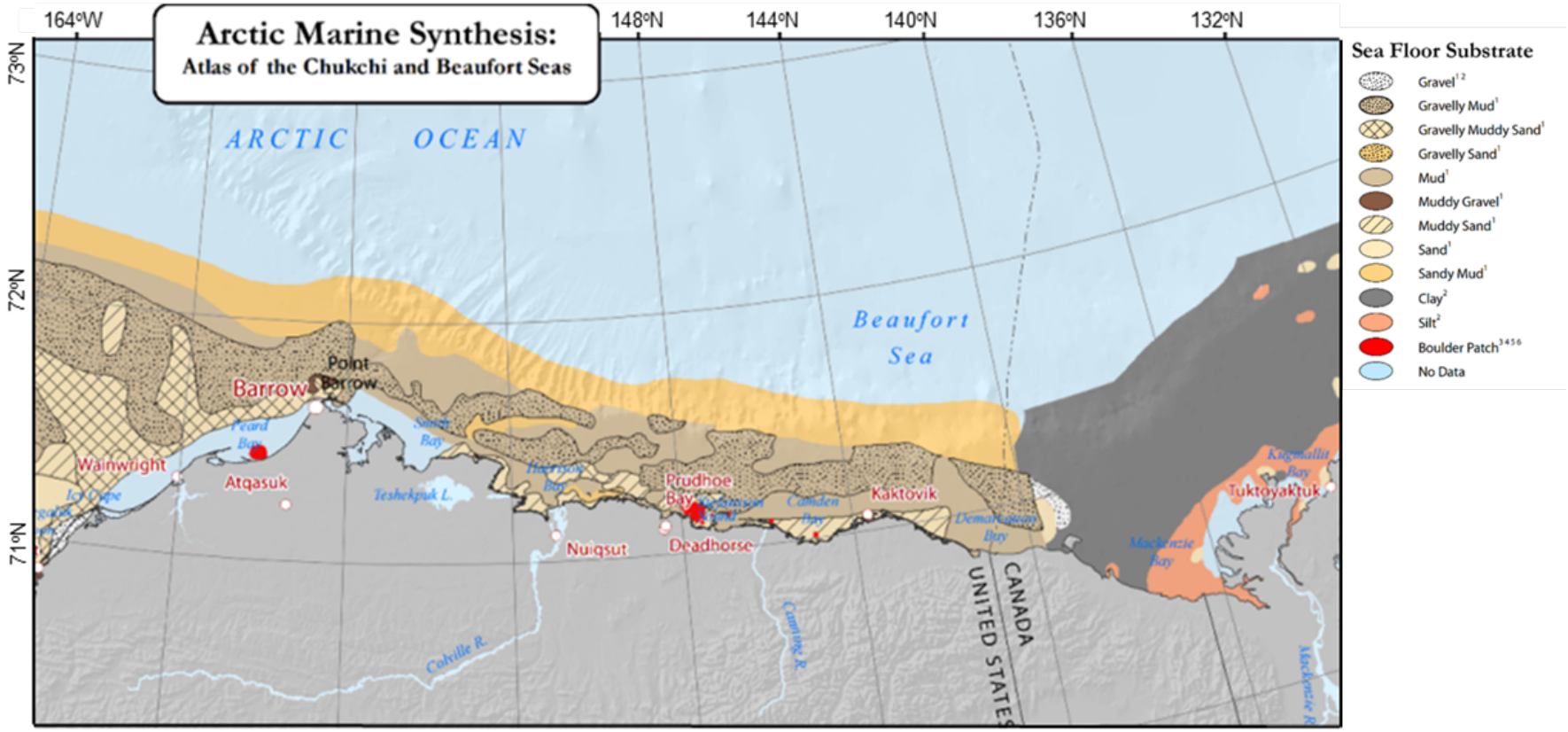

Figure 3.4.9. Map of seafloor substrate from the Beaufort Sea (geographic extent reduced from Audubon Alaska 2015).

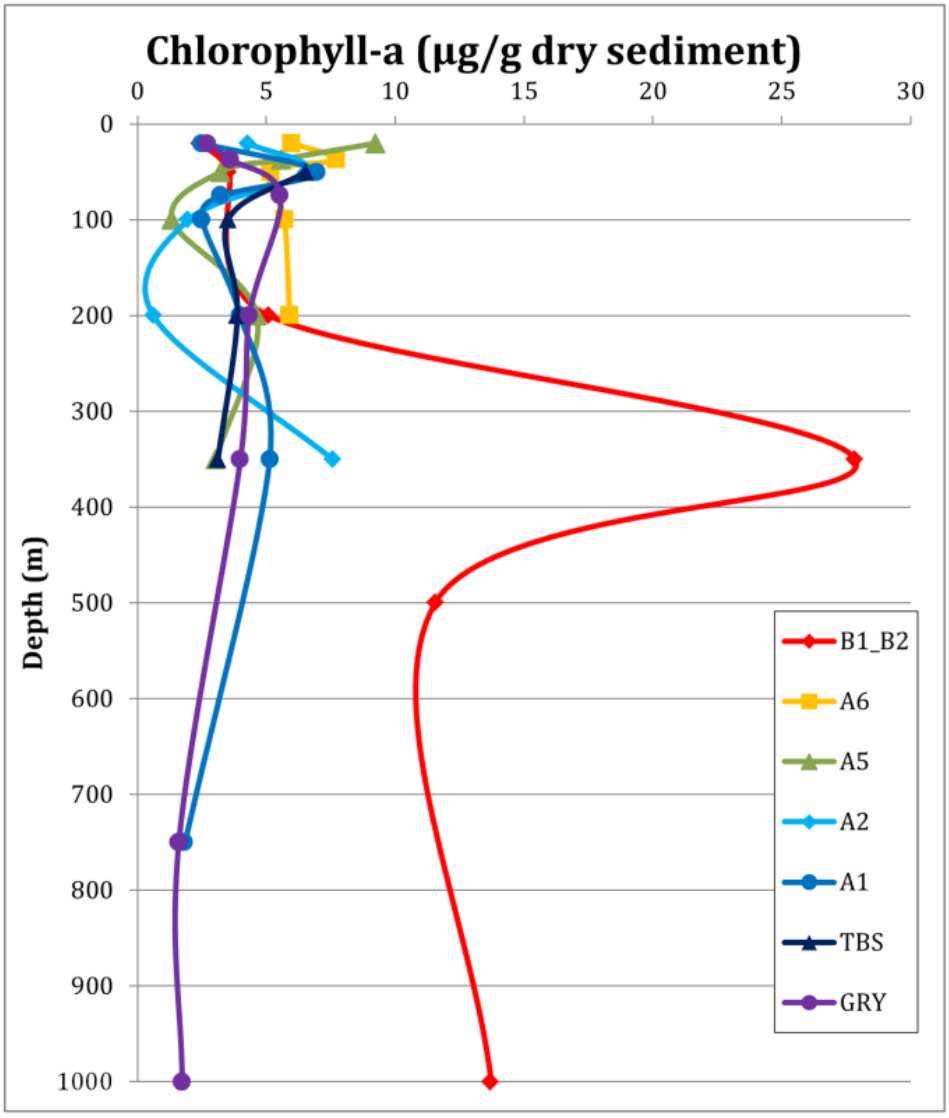

Figure 3.4.10. Trends in sediment chlorophyll-*a* concentration (µg/g dry sediment) with depth along selected transects across the study region.
The legend depicts transects in order as they are located from west to east across the study region. Only one station (50 m) was sampled on transect B2, so data were combined with transect B1, which lies in very close proximity.

3.4.3.1 Multivariate Analysis

Results of PCA of environmental characteristics among stations are shown in Figure 3.4.11, and the eigenvectors for the first five principle components are shown in Table 3.4.2. Stations did not group clearly according to transect, but patterns across depth were more distinct with most of the variation among depths occurring along PC1, which accounted for 39.1% of the total variation. This axis was dominated by grain-size information, including %mud (i.e., proportion of fine sediments), porosity (an indicator of muddier sediments), and phi (high phi indicates small mean grain size). All three variables increased in the positive direction, indicating that deeper stations were characterized by finer-grained, muddier sediments as would be expected for slope habitat. Values for %sand were also relatively high and increased in the negative direction along PC1 toward the shallower sites, which further supports separation of stations by grain size characteristics across depth. PC2 was dominated by sorting and pigment concentrations, which all increased in the negative direction. Much of the spread of points along this axis occurred at the shallower sites (<100 m), suggesting shelf locations may be much more variable in both food availability of fresh detritus and diversity of grain sizes. In addition, high sorting coefficients indicate poorly sorted sediments, which typically indicate highly disturbed sediments. Physical disturbance and/or more energetic currents at shallower sites may be contributing to this pattern. PC3 was dominated by kurtosis and C:N but only a few stations show much variation along this axis. Again, all of these sites are in the shallower depths, with the 20- and 100-m stations along transect A2 appearing to be quite distinct from other locations and exhibiting high kurtosis and low C:N values. High kurtosis indicates a platykurtic grain-size distribution, indicating a more even distribution of sediment mass among grain size categories. These stations also had more gravelly sediments.

The CDA examining variation in benthic habitat characteristics across depth yielded three significant canonical variables (CVs) (Figure 3.4.12, Table 3.4.3). Salinity and temperature were responsible for much of the separation of stations along CV1 and CV2, respectively (Table 3.4.3). TOC and sorting were driving most of the variation along CV3. Although a few other variables related to grain size also had relatively high loading values (porosity, %mud, phi) on CV1, values must be squared to be directly compared, so the salinity value of -0.924 indicates a substantially greater effect than the next most important variable. Due to the heavy influence of temperature and salinity, we re-ran the analysis with these variables excluded to identify important sediment variables (Figure 3.4.13, Table 3.4.4). In this analysis, phaeopigments, porosity, %mud, and phi all increased in the negative direction along CV1, suggesting a transition toward finer-grained sediments and more degraded detritus (or high fecal pellet flux) with depth. Sorting dominates the variation along CV2, such that shallow (20 m) and deeper (>350 m) sites have lower sorting coefficients, indicating less diversity of grain sizes. Examination of the raw data indicates higher sand content at shallower sites and siltier sediments at depth. Chl-*a* and TOC, two measures of food availability, are heavily loaded on CV3, although there is relatively little variation in sites along this axis. Sites >500 m had higher chl-*a* and TOC, and 20-m sites showed relatively high variation along this axis, suggesting higher spatial variability in food availability in the shallowest sampling depths.

Results of the CDA examining variation by transect were less straightforward to interpret. Again, when temperature and salinity were included, temperature dominated the signal (Table 3.4.5), so we ran the analysis again without those variables. Both analyses yielded three

significant CVs. In the second analysis, TOC, %mud, and kurtosis were most heavily loaded on CV1, but most of the spread along this axis represents differences between a few sites on transect A2 and the rest of the stations (Table 3.4.6). These sites appear to be more gravelly locations. C:N is heavily loaded on CV2 and increases in the positive direction, whereas sorting and $\delta^{13}C$ are heavily loaded on CV3 and both increase in the negative direction. Visual inspection of the plots in Figure 3.4.14 essentially shows that the distribution of points is inverted along the vertical axis when the upper and lower panels are compared. B1, B2, A4, A5 and A6 (central and western study region) have higher C:N, lower sorting (sediment grain size diversity), and higher $\delta^{13}C$. Transects A1, TBS, GRY and MAC (eastern study region) showed the opposite trend. These eastern transects are likely influenced by the Mackenzie River outflow.

When results of all these analyses are considered together, it appears that grain size parameters are particularly important in separating sites by depth, whereas source and lability of organic material deposited to sediments may be more important in separating locations from west to east. Previous studies have also documented the strong gradient in carbon stable isotope value across this region, with a clear signal of the Mackenzie River delta in the east (e.g., Dunton et al. 2012). In addition, studies of macrofauna have highlighted the influence of the Mackenzie River on patterns in community structure, which are likely mediated by sediment properties (e.g., Conlan et al. 2008). Our results showed more evidence of disturbance and more variability among locations at shallower sites, whereas deeper sites may have more persistent conditions.

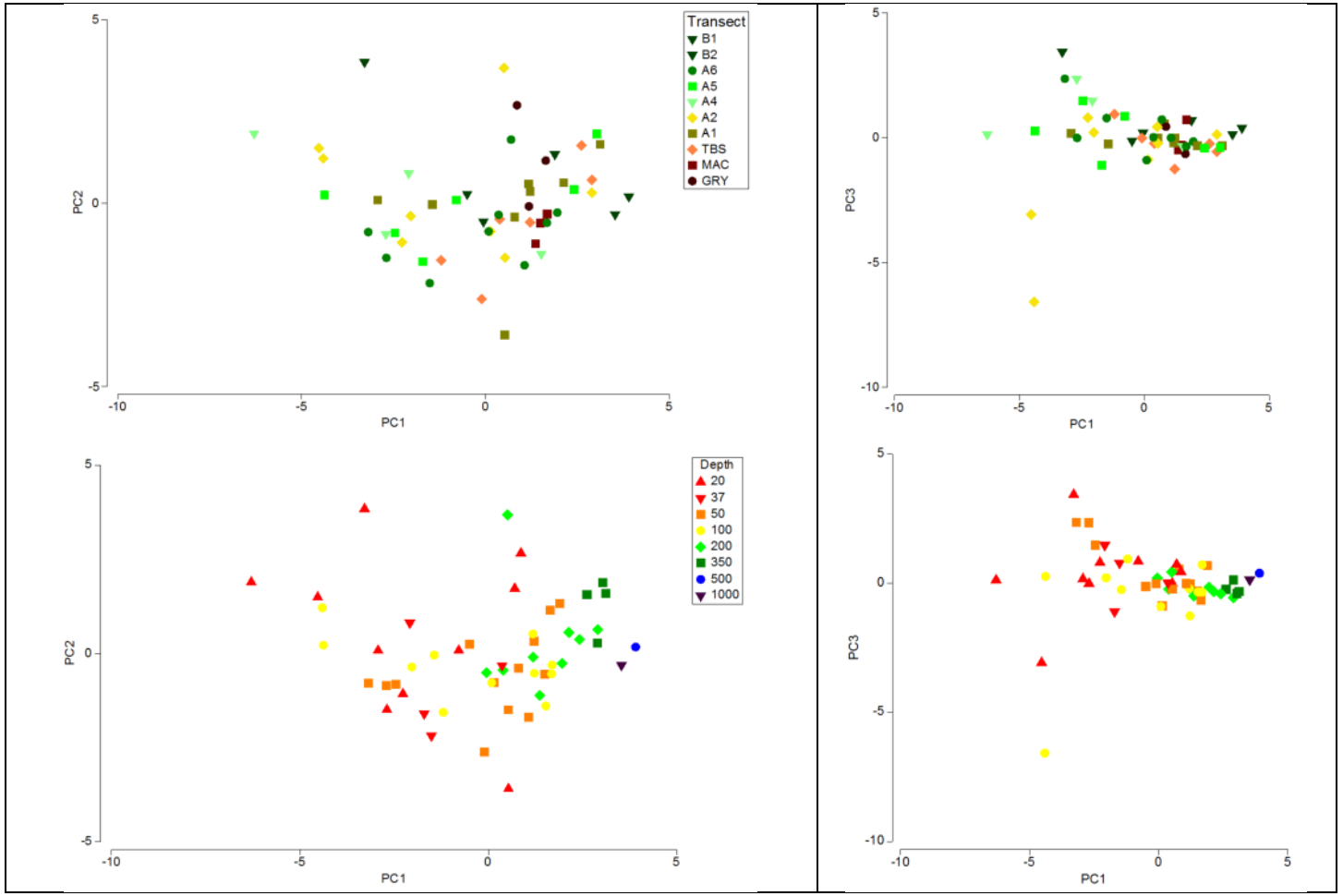

Figure 3.4.11. Principle components analysis (PCA) showing similarity in environmental characteristics among stations.
All panels show results of the same analysis. Top panels are colored to show patterns among transects; bottom panels are colored to show patterns among depths sampled. Left panels both show variation along first two principle components; right panels both show variation along first and third principle components. The first three principle components account for 66.3% of the variation among stations. Eigenvalues and eigenvectors are shown in Table 3.4.2.

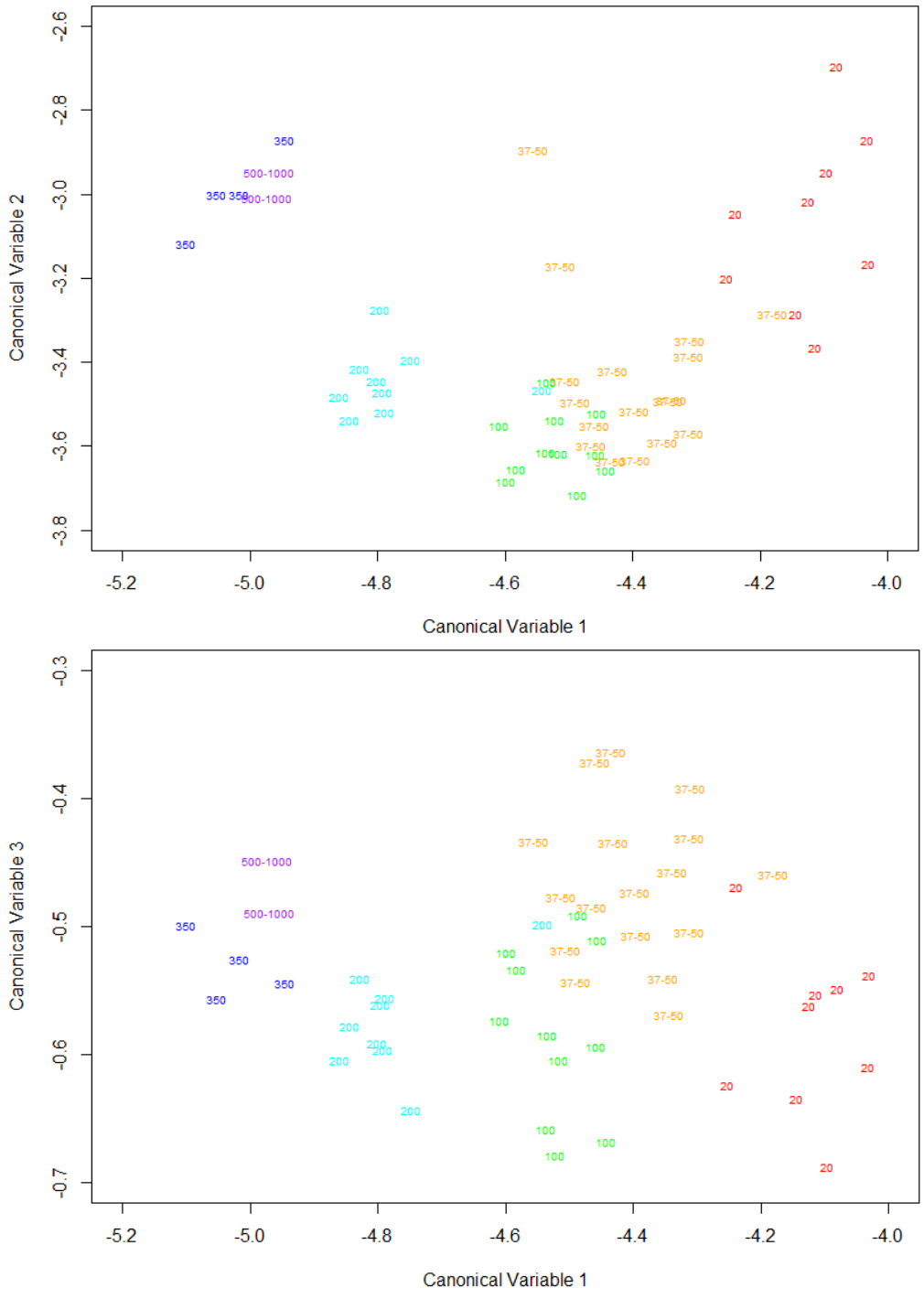

Figure 3.4.12. Canonical discriminant analysis (CDA) comparing benthic habitat characteristics among sampling depths with temperature and salinity included.
Some depth categories (indicated by colored numbers) were combined due to low sample numbers, and to reduce the number of categories and improve analysis. Upper panel shows variation along CV1 and CV2, bottom panel shows variation along CV1 and CV3. The first three CVs were significant. Loading values are shown in Table 3.3.

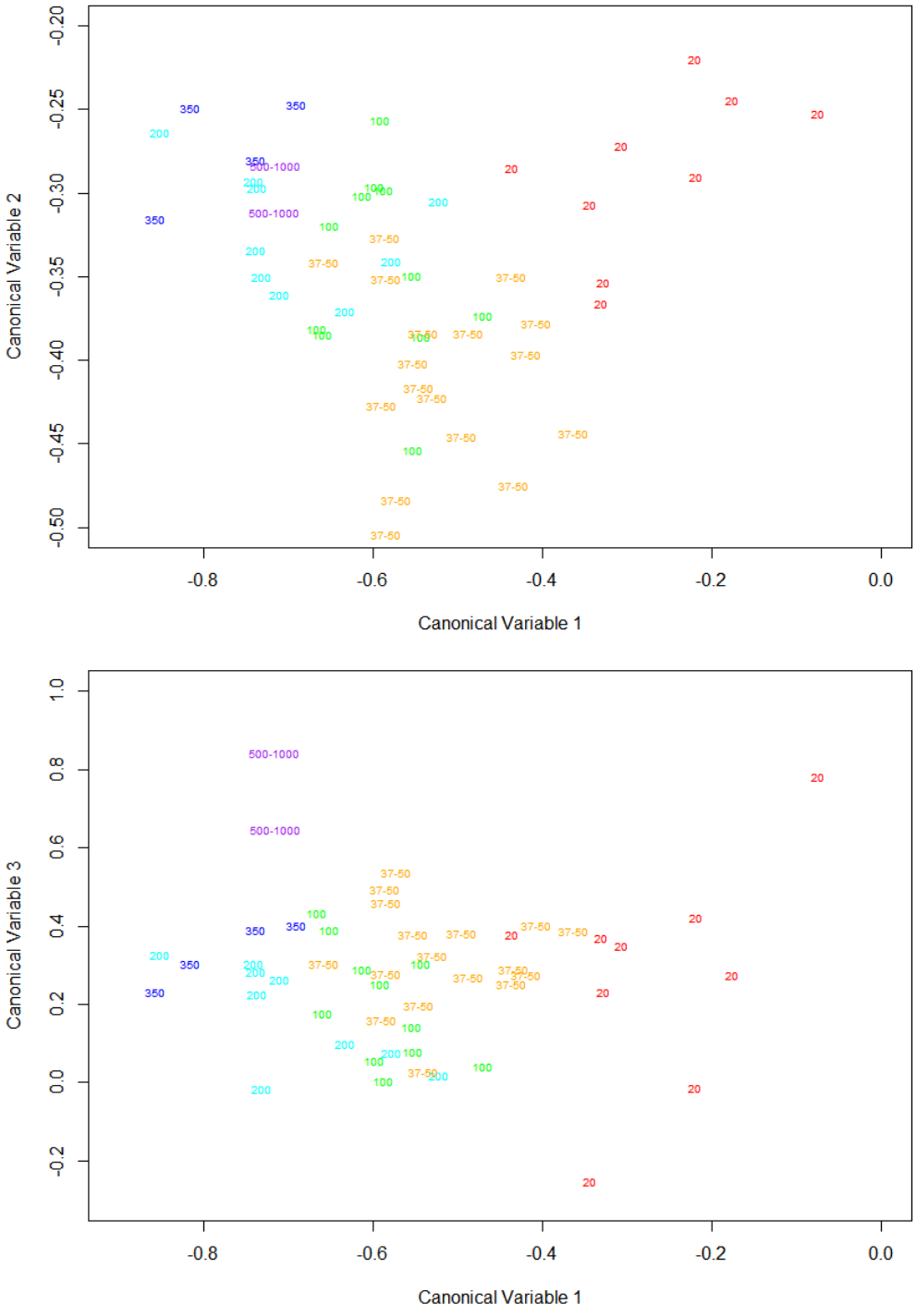

Figure 3.4.13. Canonical discriminant analysis (CDA) comparing benthic habitat characteristics among sampling depths with temperature and salinity excluded.
Some depth categories (indicated by colored numbers) were combined due to low sample numbers, and to reduce the number of categories and improve analysis. Upper panel shows variation along CV1 and CV2, bottom panel shows variation along CV1 and CV3. The first three CVs were significant. Loading values are shown in Table 3.4.

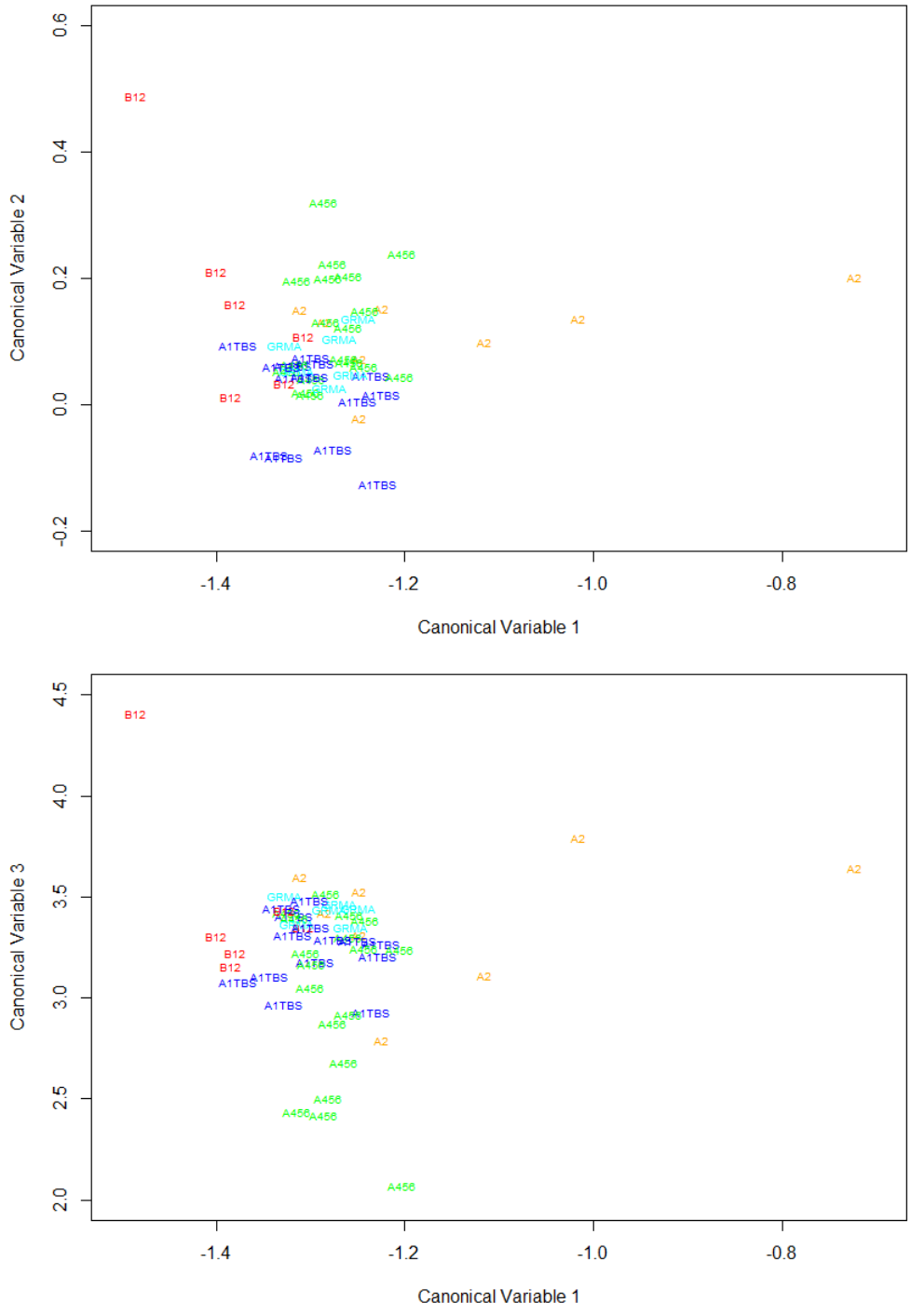

Figure 3.4.14. Canonical discriminant analysis (CDA) comparing benthic habitat characteristics among transects with temperature and salinity excluded.
Points are labelled by transect category. Some adjacent transects were combined into a single category due to low sample numbers, and to reduce the number of categories and improve analysis (B12 = B1 + B2; A1TBS = A1 + TBS; A456 = A4 + A5 + A6; GRMA = GRY + MAC). Upper panel shows variation along CV1 and CV2, bottom panel shows variation along CV1 and CV3. The first three CVs were significant. Loading values are shown in Table 3.6.

4.0 ZOOPLANKTON

Russell Hopcroft and Caitlin Smoot

4.1 Epipelagic Zooplankton Communities

4.1.1 Introduction

Zooplankton are important trophic intermediaries in marine systems; in the Beaufort Sea, zooplankton communities connect the highly seasonal pulse of primary production to upper trophic levels, such as fish and marine mammals, that are of cultural and ecological significance (Lowry et al. 2004; Walkusz et al. 2011). It is well-established that the Arctic Ocean is undergoing changes in sea ice cover, temperature, and carbonate mineral saturation states (Serreze et al. 2007, Bates et al. 2009, Stroeve et al. 2012, Bates et al. 2013); it is less certain how Arctic marine zooplankton communities will respond to these changes. Zooplankton will likely be among the first responders to climate change due to their poikilothermic nature and relatively short lifespans (Hays et al. 2005, Richardson 2008). The paucity of consistent baseline data for many Arctic ecosystems is one of the main challenges of quantifying and documenting zooplankton community response to development and climate change (e.g., Wassmann et al. 2011, Ershova et al. 2015a); therefore, it is critical to monitor its biological communities.

Early efforts to characterize the physical oceanography and zooplankton communities of the Beaufort Sea by the USS *Burton Island* cruises (Johnson 1956) focused mostly from the shelf break into the Canada Basin. The Western Beaufort Sea Ecological Cruise (WEBSEC) program in the 1970s (Hufford et al. 1974, McConnell, 1977, Hopcroft et al. 2012) and the Outer Continental Shelf Environmental Assessment Program (OCSEAP) (Horner 1978, 1979, 1980) provided better spatial coverage of the Alaskan Beaufort shelf; however, the coarse mesh (≥333 μm) used in these programs resulted in a bias toward larger bodied taxa while completely excluding small-bodied and numerically dominant taxa. Most data from OCSEAP do not provide species-level taxonomic resolution; rather, organisms were grouped into broad taxonomic categories, thus rendering its data of limited use. Similary the Canadian Beaufort has been sporadically studied (Grainger 1965, Grainger and Grohe 1975, Mohammed and Grainger, 1974, Hopky et al. 1994a, b, c) with similar issues of gear biases, inadequate taxonomic resolution of key groups, and limited spatial coverage that preclude rigorous comparisons between many data sets, and highlight the paucity of consistent baseline ecological data for zooplankton communities of the Beaufort Sea. More recent efforts in the Alaskan Beaufort Sea have focused on the oceanographically complex area around Barrow Canyon (e.g. Lane et al. 2008, Ashjian et al. 2010), while Canadian efforts include the 2002 R/V *Mirai* cruise in the Chukchi and Beaufort Seas, the CCGS *Nahidik* cruises (Walkusz et al. 2010, Walkusz et al. 2012, Walkusz et al. 2013), the Canadian Arctic Shelf Exchange Study (CASES) (Darnis et al. 2008), and the Beaufort Regional Environmental Assessment (BREA). As a result, a large contemporary data gap exists for much of the central and eastern Alaskan Beaufort Sea.

In the Pacific-Arctic, zooplankton communities are highly associated with water masses and their underlying hydrographic properties (e.g., Darnis et al. 2008, Lane et al. 2008, Hopcroft et al. 2010, Ershova et al. 2015b). Understanding zooplankton assemblages and their hydrographic associations become particularly critical as we study a rapidly changing Arctic. The volume of Pacific water flow through Bering Strait into the Arctic has increased in recent years (Woodgate et al. 2012), upwelling events have increased in frequency and strength in the Beaufort Sea

(Pickart et al. 2013), and modelling efforts suggest that Mackenzie River discharge, along with other Arctic rivers, may increase in a warming climate (Nijssen et al. 2001, Nohara et al. 2006). Changes in these physical parameters likely impact biological communities; therefore, determining faunal associations can document the extent and magnitude resulting from such environmental forcing. Given the trophic position of zooplankton, changes in community structure have the potential to reverberate throughout Arctic food webs. This study contributes to a multi-year and multi-disciplinary effort to characterize both the physical and biological oceanography of the Beaufort Sea, and serves as a spatially comprehensive assessment of contemporary epipelagic zooplankton communities in the Alaskan Beaufort Sea.

4.1.2 Methods

4.1.2.1 Sample Processing and Statistical Analyses

During laboratory processing, zooplankton samples were subsampled using a Folsom splitter until a given aliquot contained approximately 100 individuals of the most abundant taxa. Increasingly larger fractions were examined for less abundant taxa. Organisms were identified, enumerated, measured, and, when appropriate, staged to determine species composition, abundance, and biomass. Measurements were completed using the ZoopBiom program (Roff and Hopcroft 1986). The weight of measured animals was predicted from species-specific length-weight relationships or from relationships of morphologically similar species (Questel et al. 2013). Typically, 400–600 animals were measured within each sample and organisms were identified to lowest taxonomic level possible. For epipelagic analyses, data from stratified samples were integrated to produce a single stratum representative of the epipelagic realm (upper 200 meters).

Analyses were performed separately for both abundance and biomass using fourth-root-transformed (4RT) data pooled across all years for each mesh size. Community similarity was assessed using the Bray-Curtis similarity index (Bray and Curtis 1957), and community structure was explored with cluster analysis and non-metric multidimensional scaling (nMDS) using PRIMER (v6) (Clarke and Warwick 2010). Taxa that contributed to community similarity were identified using PRIMER's similarity percentage (SIMPER) routine. Finally, we related the observed biological community patterns to a suite of explanatory environmental variables using PRIMER's biota-environment stepwise matching test (BEST) routine. The BEST routine relates matrices of multidimensional biological and environmental data using both forward-selection and backward-elimination techniques (Clarke and Warwick 2010).

4.1.3 Results

4.1.3.1 General Patterns

We observed 107 taxonomic categories in the epipelagic realm (0–200 m) over the course of the three Transboundary field seasons in the two mesh sizes (Tables 4.1, 4.2). Copepods exhibited the highest species richness (36 species), followed by the cnidarians (17 species) and amphipods (14 taxa). We also observed five euphausiid, four ctenophore, two chaetognath, two cladoceran, two pteropod, and three mysid species. Numerous meroplanktonic taxa were observed, including ophiuroid, polychaete, and bivalve larvae. In the 150-µm net, average holozooplankton abundance and biomass ranged from 1110–1950 individuals m^{-3} and 40.2–76.9 mg dry-weight (DW) m^{-3}, respectively (Table 4.3). Average holozooplankton abundance and

biomass captured in the 505-µm net ranged from 47–196 individuals m^{-3} and 25.6–57.6 mg DW m^{-3}, respectively (Table 4.3). Mean zooplankton abundance and biomass were generally highest at 20- and 50-m stations and declined offshore until the 500-m isobath. We observed a slight increase in both parameters at the 1000-m isobath. This trend held true for both the 150- and 505-µm nets. With respect to stratified 150-µm samples, the trend was most consistent in the Polar Mixed Layer (PML) (Table 4.3). Copepods dominated community abundance and biomass in all years in both nets (Figure 4.1.1). Larvaceans had their highest relative numerical contribution in 2012. Predators, primarily cnidarians and chaetognaths, made important contributions that varied both between and within years. The community was numerically dominated by the copepods *Calanus glacialis*, *Calanus hyperboreus*, *Metridia longa*, *Oithona similis*, *Triconia borealis*, *Microcalanus pygmaeus*, and the *Pseudocalanus* species-complex in all surveys. These taxa have long been recognized as dominant in Arctic surface waters (see Grainger 1965) and are henceforth referred to as an Arctic guild of taxa, despite the fact that some species also occur outside of the Arctic. Numerically, this group accounted for 69–81% of zooplankton abundance and 64–72% of the biomass in the 150-µm net across all survey years. In the 505-µm net, the guild of Arctic copepods composed 78–92% of community abundance and 63–68% of the biomass.

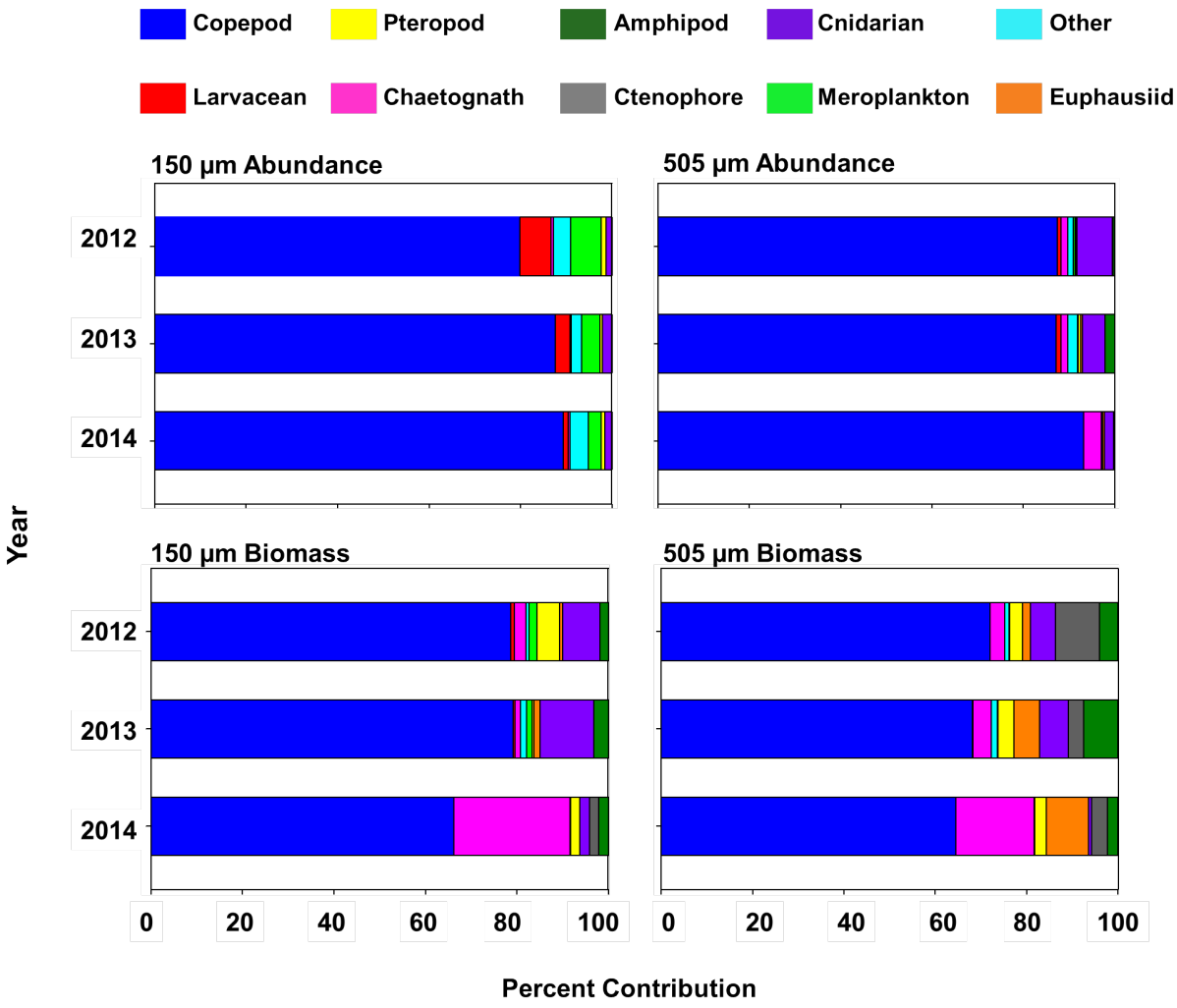

Figure 4.1.1. The relative contribution of major zooplankton taxonomic groups in terms of abundance and biomass in the Beaufort Sea during Transboundary 2012–14 for the 150- and 505-µm nets.

Table 4.1. Average abundance and biomass of Beaufort Sea zooplankton taxa captured by the 150-µm net during Transboundary 2012–14.
* - indicates that a taxon was only observed in abundances <0.01 ind. m^{-3}; biomass <0.01 mg DW m^{-3}.
NC – indicates biomass was not calculated.

Taxon	150 µm					
	Abundance (Ind. m^{-3})			Biomass (mg DW m^{-3})		
	2012	2013	2014	2012	2013	2014
Calanoida						
Aetideopsis minor	-	0.09	-	-	*	-
Acartia longiremis	4.06	6.53	0.25	0.02	0.03	*
Acartia bifilosa	-	1.65	-	-	0.03	-
Acartia spp. (copepodite)	4.85	5.07	1.13	0.01	0.01	*
Augaptilus glacialis	-	*	-	-	*	-
Eurytemora herdmani	-	6.17	0.10	-	0.06	*
Eurytemora richsingi	-	*	-	-	*	-
Eurytemora spp. (copepodite)	-	62.92	0.52	-	0.22	*
Calanus glacialis	137.23	42.49	236.37	43.00	5.70	23.49
Calanus hyperboreus	0.68	15.11	6.99	1.98	15.05	6.532
Centropages abdominalis	-	0.40	-	-	0.01	-
Chiridius obtusifrons	0.36	0.31	0.21	0.07	0.04	0.03
Eucalanus bungii	*	0.50	0.01	0.01	1.82	*
Gaetanus tenuispinus	-	0.02	0.06	-	*	0.03
Heterorhabdus norvegicus	0.22	0.88	0.70	0.04	0.16	0.06
Jashnovia tolli	0.23	*	-	0.01	*	-
Limnocalanus macrurus	-	1.16	-	-	0.03	-
Metridia longa	17.73	7.87	5.42	1.55	1.25	0.69
Metridia pacifica	-	-	0.05	-	-	0.10
Metridia spp. (copepodite)	3.98	1.47	6.49	0.03	0.01	0.03
Microcalanus pygmaeus	13.99	47.52	38.04	0.02	0.06	0.08
Neocalanus cristatus	*	*	*	0.33	1.87	*
Neocalanus flemingeri	0.10	*	0.03	0.05	*	*
Neocalanus plumchrus	-	-	*	-	-	*
Paraeuchaeta glacialis	1.55	2.08	0.93	1.11	1.82	1.29
Paraheterorhabdus compactus	-	0.01	-	-	*	-
Pseudocalanus acuspes	3.06	12.41	1.47	0.03	0.14	0.02
Pseudocalanus mimus	2.84	*	0.01	0.03	*	*
Pseudocalanus minutus	13.28	5.26	1.53	0.21	0.08	0.30
Pseudocalanus newmani	10.67	3.27	0.36	0.07	0.02	0.14
Pseudocalanus spp. (male)	6.40	3.47	0.85	0.03	0.02	0.01
Pseudocalanus spp. (copepodite)	217.91	557.59	524.46	0.60	1.99	1.62
Scaphocalanus antarcticus	-	0.11	0.05	-	0.08	0.03
Scolecithricella minor	0.65	1.07	0.90	0.01	0.01	0.01
Spinocalanus longicornis	-	-	0.37	-	-	0.14
Spinocalanus antarcticus	-	0.47	0.01	-	*	*
Cyclopoida						
Oithona similis	474.08	483.45	590.52	0.59	0.49	2.49

Table 4.1, continued.

Taxon	150 µm					
	Abundance (Ind. m^{-3})			Biomass (mg DW m^{-3})		
	2012	2013	2014	2012	2013	2014
Mormonilloida						
Neomormonilla minor	-	-	0.03	-	-	*
Poecilostomatoida						
Triconia borealis	27.53	88.40	156.70	0.05	0.14	1.58
Harpacticoida						
Harpacticoid unid.	-	0.15	0.27	-	*	*
Microsetella norvegica	1.57	1.82	2.76	0.01	0.01	0.01
Nauplii						
Harpacticoid nauplii	0.03	0.02	0.20	*	*	*
Calanoid nauplii	83.65	245.12	121.24	0.05	0.15	0.50
Cyclopoid nauplii	1.07	5.12	0.06	*	*	*
Appendicularia						
Oikopleura vanhoeffeni	5.67	18.29	32.91	0.02	0.08	0.10
Fritillaria borealis	7.18	48.87	95.17	*	*	0.12
Pteropoda						
Clione limacina	0.18	*	0.05	1.94	0.02	0.41
Limacina helicina	9.20	5.66	17.02	0.01	0.05	4.25
Chaetognatha						
Eukrohnia hamata	-	0.10	0.20	-	0.33	0.31
Parasagitta elegans	31.36	2.39	10.18	1.19	0.16	0.81
Cladocera						
Evadne nordmanni	-	2.88	2.72	-	0.07	*
Podon leuckartii	-	31.82	22.81	-	0.14	*
Ostracoda						
Boroecia maxima	0.14	1.51	1.02	0.01	0.14	0.11
Euphausiacea						
Euphausid nauplii	-	0.01	-	-	*	-
Euphausid calyptopis	-	-	*	-	-	*
Euphausid juvenile	-	-	*	-	-	*
Euphausid furcillia	-	-	*	-	-	*
Thysanoessa inermis	0.19	0.01	0.06	1.84	0.08	0.01
Thysanoessa longipes	-	*	-	-	0.02	-
Thysanoessa raschii	0.06	0.04	0.05	0.46	0.19	0.06
Mysidae						
Mysis spp.	-	0.01	-	-	0.01	-
Mysis oculata	-	*	-	-	0.01	0.01
Decapoda						
Hippolytidae	0.01	*	0.01	0.02	0.02	0.05
Pandalidae	*	0.01	0.01	0.01	-	0.04
Cumacea	-	*	-	-	*	-

Table 4.1, continued.

Taxon	150 µm					
	Abundance (Ind. m^{-3})			Biomass (mg DW m^{-3})		
	2012	2013	2014	2012	2013	2014
Amphipoda						
Amphipod unid.	0.08	0.07	0.02	0.05	0.05	*
Apherusa glacialis	-	0.01	0.01	-	*	*
Gammarus wilkitzkii	0.01	-	*	*	-	*
Cyphocaris challengeri	-	0.01	*	-	0.04	*
Hyperia galba/medusarum	0.03	*	0.01	*	0.01	*
Onisimus sp.	-	0.01	-	-	*	*
Themisto abyssorum	0.17	0.95	0.49	0.57	0.90	0.15
Themisto libellula	0.28	0.27	0.48	0.70	0.37	0.47
Isopoda (parasitic)	0.22	0.22	0.39	*	*	*
Siphonophora						
Dimophyes arctica	-	0.02	0.03	-	3.43	*
Hydrozoa						
Aeginopsis laurentii	*	0.21	0.4614	*	0.09	0.34
Aglantha digitale	24.93	13.07	18.07	0.69	4.68	2.54
Euphysa flammea	-	*	*	-	*	0.01
Halitholus cirratus	-	0.03	0.15	-	0.21	3.11
Obelia longissima	-	0.24	0.06	-	0.09	*
Ptychogena lactea	-	0.07	*	-	*	*
Ctenophora						
Beroe cucumis	-	-	*	-	-	0.01
Mertensia ovum	0.13	0.01	0.04	0.50	0.19	0.34
Polychaeta						
Tomopteris septentrionalis	-	0.01	0.01	-	0.03	0.01
Rotifera	-	73.91	44.58	-	NC	NC
Meroplankton						
Barnacle cyprid	0.23	0.06	0.96	*	*	0.24
Barnacle nauplii	0.05	0.47	0.65	*	*	*
Bipinnaria	0.49	2.35	1.85	*	*	*
Bivalve larvae	32.63	25.00	34.85	0.01	0.04	0.28
Brachyuran zoea	0.01	*	*	0.01	*	*
Cyphonautes	0.57	0.36	0.51	*	0.10	*
Echinoderm larvae	1.38	1.64	1.31	*	*	0.02
Gastropod larvae	3.52	1.02	1.97	*	*	*
Megalops	0.05	*	0.02	0.04	*	0.20
Ophiuroid larvae	-	-	0.06	-	-	*
Pagurid zoea	0.03	0.05	0.06	*	*	*
Polychaete larvae	4.67	99.32	91.48	0.02	0.23	0.17

Table 4.2. Average abundance and biomass of Beaufort Sea zooplankton taxa captured by the 505-µm net during Transboundary 2012–14.
* - indicates that a taxon was only observed in abundances <0.01 ind. m^{-3}; biomass <0.01 mg DW m^{-3}.
NC – indicates biomass was not calculated.

Taxon	505-µm					
	Abundance (Ind. m^{-3})			Biomass (mg DW m^{-3})		
	2012	2013	2014	2012	2013	2014
Calanoida						
Acartia longiremis	0.01	0.01	-	*	*	-
Acartia bifilosa	-	0.04	-	-	*	-
Aetideopsis minor	-	*	-	-	*	-
Calanus glacialis	179.95	21.74	157.58	45.71	4.90	21.06
Calanus hyperboreus	0.42	11.28	6.33	0.83	10.04	6.55
Chiridius obtusifrons	0.07	0.09	0.05	0.01	0.02	0.01
Eucalanus bungii	*	*	*	*	*	*
Gaetanus brevispinus	-	*	*	-	*	*
Gaetanus tenuispinus	*	0.02	0.01	*	*	*
Heterorhabdus norvegicus	0.03	0.23	0.29	*	0.04	0.03
Jashnovia tolli	*	0.01	0.02	*	*	*
Limnocalanus macrurus	-	1.86	-	-	0.05	-
Metridia longa	8.30	4.10	2.64	0.67	0.61	0.35
Metridia pacifica	-	*	0.02	-	*	0.01
Metridia spp.	0.01	0.02	0.03	*	*	*
Neocalanus cristatus	0.04	0.01	0.02	0.22	0.10	0.08
Neocalanus plumchrus	*	*	-	*	0.01	-
Paraeuchaeta glacialis	0.52	1.22	0.65	0.26	0.60	0.53
Paraheterorhabdus compactus	-	0.05	-	-	*	-
Pseudocalanus acuspes	-	*	*	-	*	*
Pseudocalanus minutus	1.39	0.63	0.86	0.03	0.01	0.08
Pseudocalanus spp. (male)	*	0.01	0.04	*	*	*
Pseudocalanus spp. (copepodite)	0.07	0.43	1.63	*	0.01	0.03
Scaphocalanus antarcticus	-	0.05	0.03	-	0.03	0.016
Scolecithricella minor	0.01	0.04	0.05	*	*	*
Spinocalanus antarcticus	-	-	*	-	-	*
Appendicularia						
Oikopleura vanhoeffeni	0.03	0.65	0.7	-	0.02	*
Fritillaria borealis	-	0.05	0.1	-	*	*
Pteropoda						
Clione limacina	0.12	*	*	*	*	0.02
Limacina helicina	0.08	0.28	0.7	0.87	1.75	0.60
Chaetognatha						
Eukrohnia hamata	-	0.09	0.47	4.58	0.11	0.29
Parasagitta elegans	2.93	0.47	0.68	-	0.78	0.56
Cladocera						
Evadne nordmanni	-	*	-	-	*	-
Podon leuckartii	-	0.11	-	*	*	-

Table 4.2, continued.

Taxon	505-µm					
	Abundance (Ind. m^{-3})			Biomass (mg DW m^{-3})		
	2012	2013	2014	2012	2013	2014
Ostracoda						
Boroecia maxima	0.02	0.43	0.34	-	0.08	0.05
Euphausiacea						
Juvenile euphausiids (all stages)	*	*	0.02	0.45	*	*
Meganyctiphanes norvegica	*	-	-	0.15	-	-
Thysanoessa inermis	0.10	0.06	0.00	1.24	0.64	0.02
Thysanoessa longipes	*	*	-	0.87	*	-
Thysanoessa raschii	0.18	0.10	0.04	0.01	0.83	0.29
Thysanoessa spinifera	-	0.02	-	-	0.15	-
Mysidae						
Erythrops sp.	-	-	*	-	-	*
Boreomysis arctica	-	*	-	-	*	-
Mysis oculata	0.01	*	*	*	0.03	0.11
Decapoda						
Hippolytidae	*	0.01	0.01	-	0.01	0.02
Pandalidae	*	0.01	0.05	-	0.03	0.09
Eualus sp.	*	*	-	*	0.04	-
Sabinea septemcarinata	-	*	-	-	0.02	-
Cumacea	*	*	0.01	*	*	*
Amphipoda						
Amphipod unid.	*	0.01	-	*	0.01	-
Argissa hamatipes	-	*	-	-	*	-
Apherusa glacialis	*	0.01	0.0003	-	0.02	*
Gammarus wilkitzkii	*	-	-	*	-	-
Eusirus holmi	-	*	-	-	*	-
Hyperia galba/medusarum	-	*	*	0.02	*	*
Hyperoche medusarum	-	*	-	-	*	-
Monoculoides schneideri	-	*	-	-	*	
Onisimus sp.	*	*	*	-	*	*
Themisto abyssorum	0.05	0.57	0.21	-	1.11	0.14
Themisto libellula	0.01	0.07	0.04	-	0.76	0.52
Pardalisca cuspidata	-	*	-	-	*	-
Phoxocephalidae	-	*	-	-	0.01	-
Syrrhoe spp.	-	*	-	-	*	-
Isopoda						
Munnopsis typica	-	*	*	-	*	*
Siphonophora						
Dimophyes arctica	*	0.01	*	0.20	*	*

Table 4.2, continued

Taxon	505-µm					
	Abundance (Ind. m^{-3})			Biomass (mg DW m^{-3})		
	2012	2013	2014	2012	2013	2014
Scyphozoa						
Chrysaora melanaster	P	P	P	NC	NC	NC
Cyanea capillata	-	-	*	-	-	*
Hydrozoa						
Aeginopsis laurentii	0.01	0.10	2.33	-	0.09	0.20
Aglantha digitale	1.67	2.17	9.14	1.50	1.18	1.25
Bougainvillia superciliaris	-	*	*	-	*	*
Catablema vesicarium	-	0.01	*	-	0.13	0.01
Eumedusa birulai	-	*	0.01	-	*	*
Euphysa flammea	-	*	0.01			0.03
Halitholus cirratus	-	0.05	0.01	-	0.39	0.23
Melicertum octopunctata	-	*	0.01	-	-	0.02
Mitrocomella polydiademata	-	-	0.02			0.29
Obelia longissima	-	0.01	*	-	*	*
Ptychogena lactea	-	*	-	-	*	-
Sarsia princeps	-	*	-	-	0.01	-
Sarsia tubulosa	-	*	*	-	0.01	0.02
Tiaropsis multicirrata	-	*	0.02	-	*	0.15
Ctenophora						
Bolinopsis infundibulum	-	*	0.01	-	0.27	0.17
Beroe cucumis	*	*	0.01	*	0.06	2.92
Beroe abyssicola	-	*	-	-	0.02	-
Mertensia ovum	0.11	0.01	0.13	0.06	0.56	2.10
Polychaeta						
Tomopteris septentrionalis	-	*	0.02	-	*	0.12
Meroplankton						
Barnacle nauplii	-	0.01	0.14	-	*	*
Brachyuran zoea	-	-	*			*
Echinoderm larvae	-	0.02	0.16	-	*	*
Megalops	*	-	-	0.20	-	-
Pagurid zoea	-	*	-	-	*	-
Polychaete larvae	0.01	0.06	0.16	*	*	*

Table 4.3. Mean zooplankton abundance (ind. m^{-3}) and biomass (mg DW m^{-3}) ±SE for the 150- and 505-µm during Transboundary 2012-14. Upper portion of table is displayed by year; lower portion of table is displayed by isobath and depth interval, when applicable.

Year	Dates	No. Stations 150-/505-µm	Abund. 150-µm	Abund. 505-µm	Biomass 150-µm	Biomass 505-µm
2012	09/21-09/30	11/14	1110 ± 124	196 ± 114	76.9 ± 11.7	57.6 ± 28.8
2013	08/13-08/31	39/39	1910 ± 187	47 ± 5	40.2 ± 4.9	25.6 ± 2.4
2014	08/19-09/01	40/40	1950 ± 121	189 ± 39	54.2 ± 7.6	38.9 ± 7.0
Depth Interval (m)	**Isobath (m)**					
Abund. 150-µm	**20 m**	**50 m**	**100 m**	**200 m**	**500 m**	**1000 m**
0-50	2165 ± 654	1905 ± 230	1457 ± 148	1118 ± 144	1106 ±161	1487 ±124
50-100			325 ± 76	257 ± 46	265 ± 86	258 ± 47
100-200				80 ± 15	87 ± 11	133 ± 16
200-300					92 ± 15	120 ± 20
300-500					82 ± 17	94 ± 15
500-1000						26 ± 6
Biomass 150-µm	**20 m**	**50 m**	**100 m**	**200 m**	**500 m**	**1000 m**
0-50	57.5 ± 7.5	59.4 ± 14.7	35.4 ± 14.1	30.5 ± 8.2	18.4 ± 3.9	25.8 ± 5.4
50-100			17.2 ± 5.0	10.9 ± 1.6	14.3 ± 3.7	13.6 ± 4.2
100-200				10.4 ± 5.3	6.3 ± 1.5	9.1 ± 1.4
200-300					11.5 ± 2.2	8.0 ± 1.0
300-500					9.4 ± 2.1	4.0 ± 0.7
500-1000						1.9 ± 0.8
505-µm	**20 m**	**50 m**	**100 m**	**200 m**	**500 m**	**1000 m**
Abund.	303 ± 139	154 ± 43	91 ± 20	53 ±12	38 ± 7	40 ± 9
Biomass	90.9 ± 34.7	36.1 ± 4.2	23.5 ± 3.3	16.6 ± 2.1	13.8 ± 1.4	20.4 ± 3.6

4.1.3.2 Species-Specific Patterns

The 150-µm net provides insight to spatial patterns in the numerically dominant small-bodied taxa, such as *Pseudocalanus* spp., *Oithona similis*, *Triconia borealis*, and *Microcalanus pygmaeus*. *Pseudocalanus* spp. were found across the survey region, with highest abundances typically observed at inshore stations (Figure 4.1.2). *O. similis*, a eurytopic copepod, was distributed across the shelf and slope, with no immediately apparent spatial pattern (Figure 4.1.3). *T. borealis* was also distributed across the shelf and slope, with peak abundances usually observed at slope stations, particularly in the 2012 field season (Figure 4.1.4). *M. pygmaeus* was also common across the study area, and reached peak abundances at offshore stations (Figure 4.1.5). Less dominant taxa also provide insights to habitat associations. For example, the oceanic copepod *Heterorhabdus norvegicus* was largely restricted to stations over the shelf break and slope (Figure 4.1.6). Conversely, euryhaline copepods of the genus *Eurytemora* were found in

highest abundances at freshened stations, mostly in the vicinity of the Mackenzie River sampled in 2013 (Figure 4.1.7).

Distributional patterns in larger-bodied and lipid-rich taxa, such as *Calanus* species, are demonstrated in the 505-µm net. *Calanus glacialis* was present across the shelf in all years. In 2012 and 2013 no immediate spatial pattern was apparent. In 2014, *C. glacialis* was found in highest abundances on the shelf (Figure 4.1.8). *Calanus hyperboreus*, considered an oceanic species, was absent from the shelf in 2012 but present in moderate numbers on the shelf in 2013–14, indicating some degree of shelf-slope exchange (Figure 4.1.9). The same pattern was apparent for the oceanic taxa *Metridia longa* (Figure 4.1.10) and *Paraeuchaeta glacialis* (Figure 4.1.11). Euphausiids were found in low numbers throughout the entire survey area. *Thysanoessa raschii* and *Thysanoessa inermis* were the most common euphausiid species, though *Thysanoessa longipes* was encountered in extremely low abundances (<0.01 ind. m^{-3}) in offshore waters. Two notable expatriate euphausiids were encountered in the study region: one individual of the Atlantic-affinity *Meganyctiphanes norvegica* was observed at an offshore station in 2012 (captured in a midwater trawl) and one individual of the Pacific-affinity *Thysanoessa spinifera* was observed at an inshore station in 2013. Juvenile euphausiid distribution was extremely patchy and abundances were generally low. We also observed one mysid specimen of the genus *Erythrops*, likely of Atlantic origin, in the 2014 survey year. We observed several Pacific expatriate copepod species in all years of the Transboundary project (Figure 4.1.12), albeit in extremely low abundances (<1 ind. m^{-3}). Pacific expatriate copepods included *Neocalanus cristatus*, *Eucalanus bungii*, and *Metridia pacifica*. *Neocalanus flemingeri* and *Neocalanus plumchrus* were observed at only a few stations across all survey years.

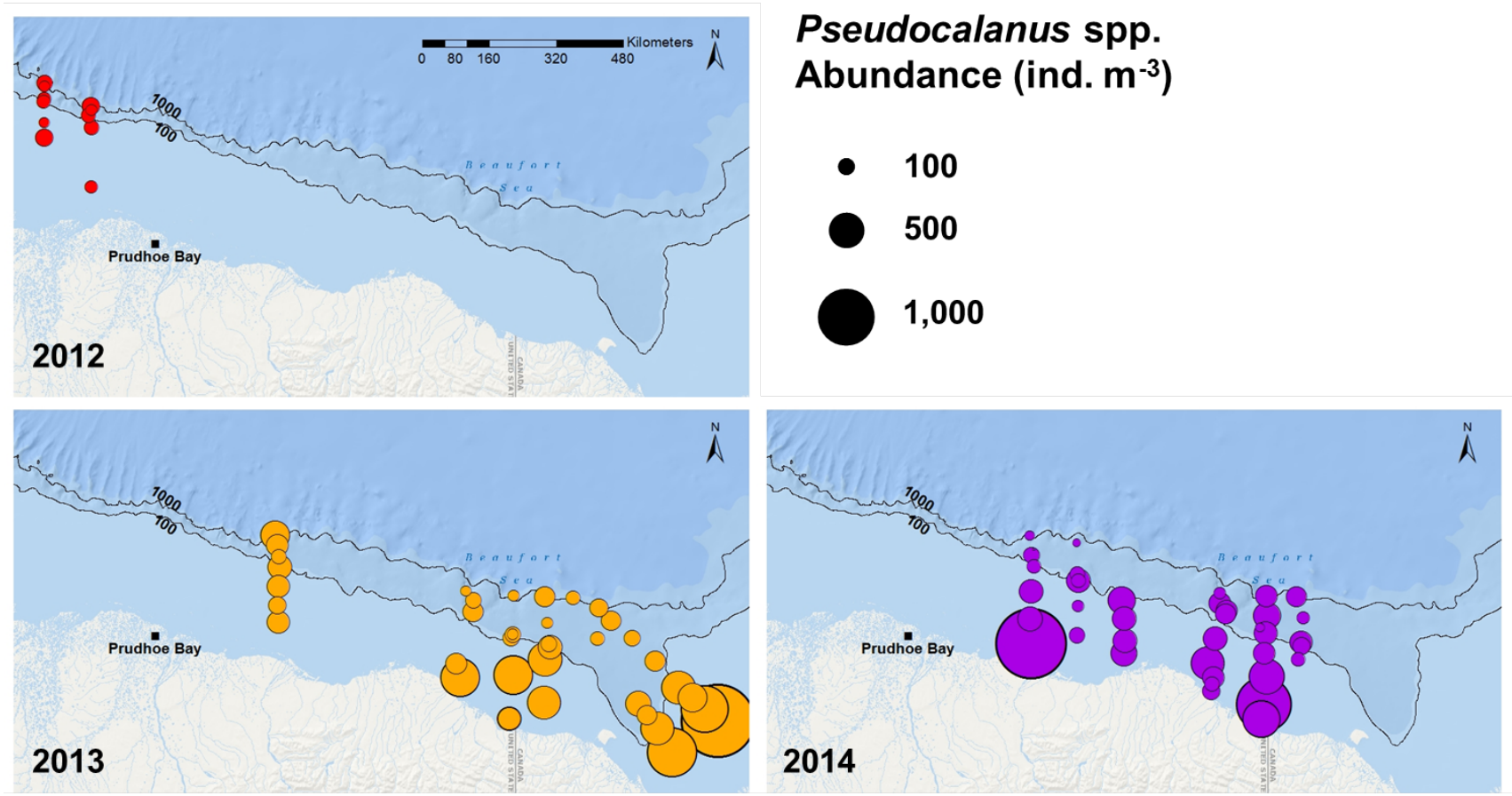

Figure 4.1.2. Abundance of *Pseudocalanus* spp. (ind. m^{-3}) captured in the 150-µm net in the Beaufort Sea during Transboundary 2012–14.

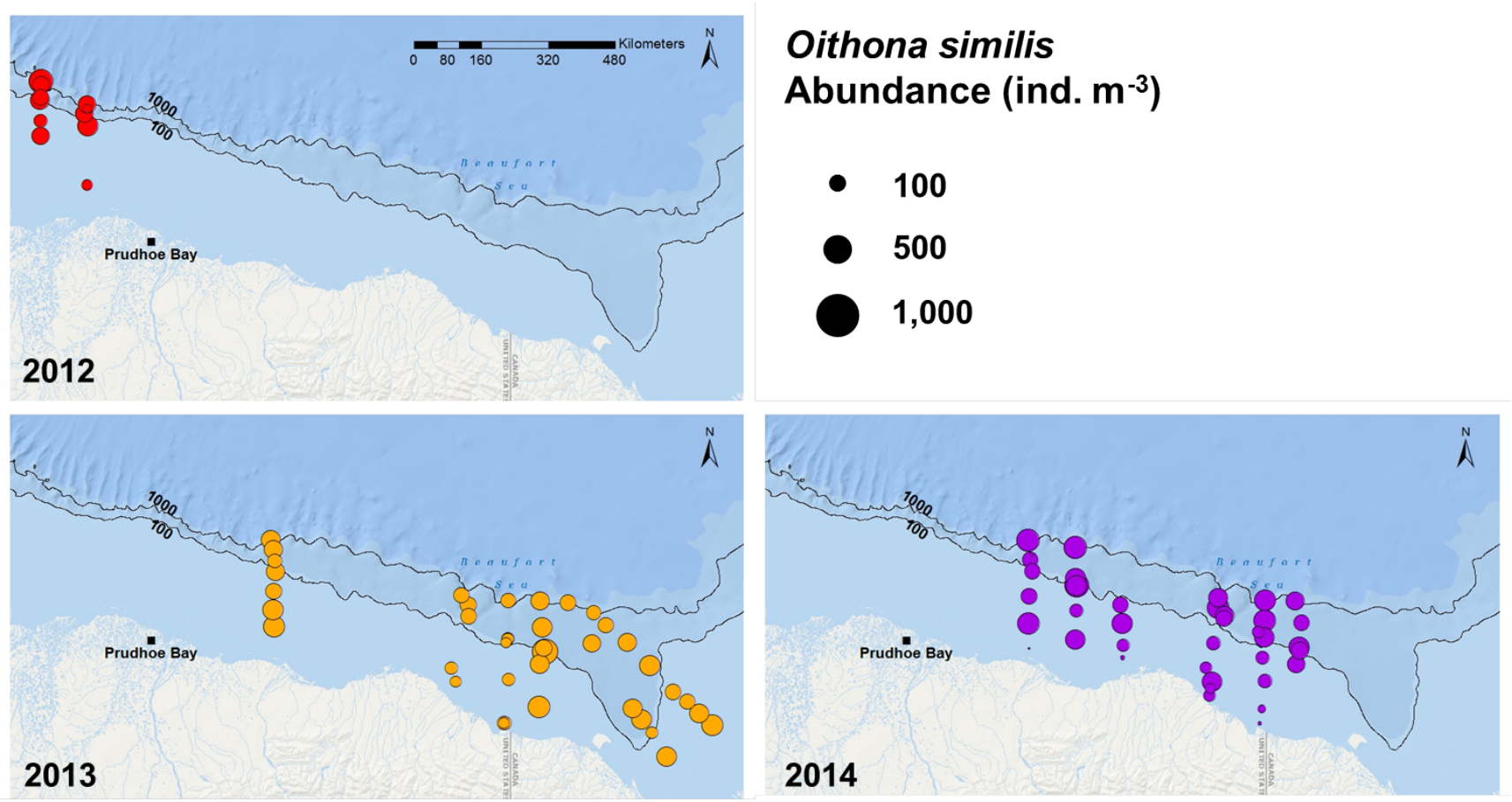

Figure 4.1.3. Abundance of *Oithona similis* (ind. m^{-3}) captured in the 150-µm net in the Beaufort Sea during Transboundary 2012–14.

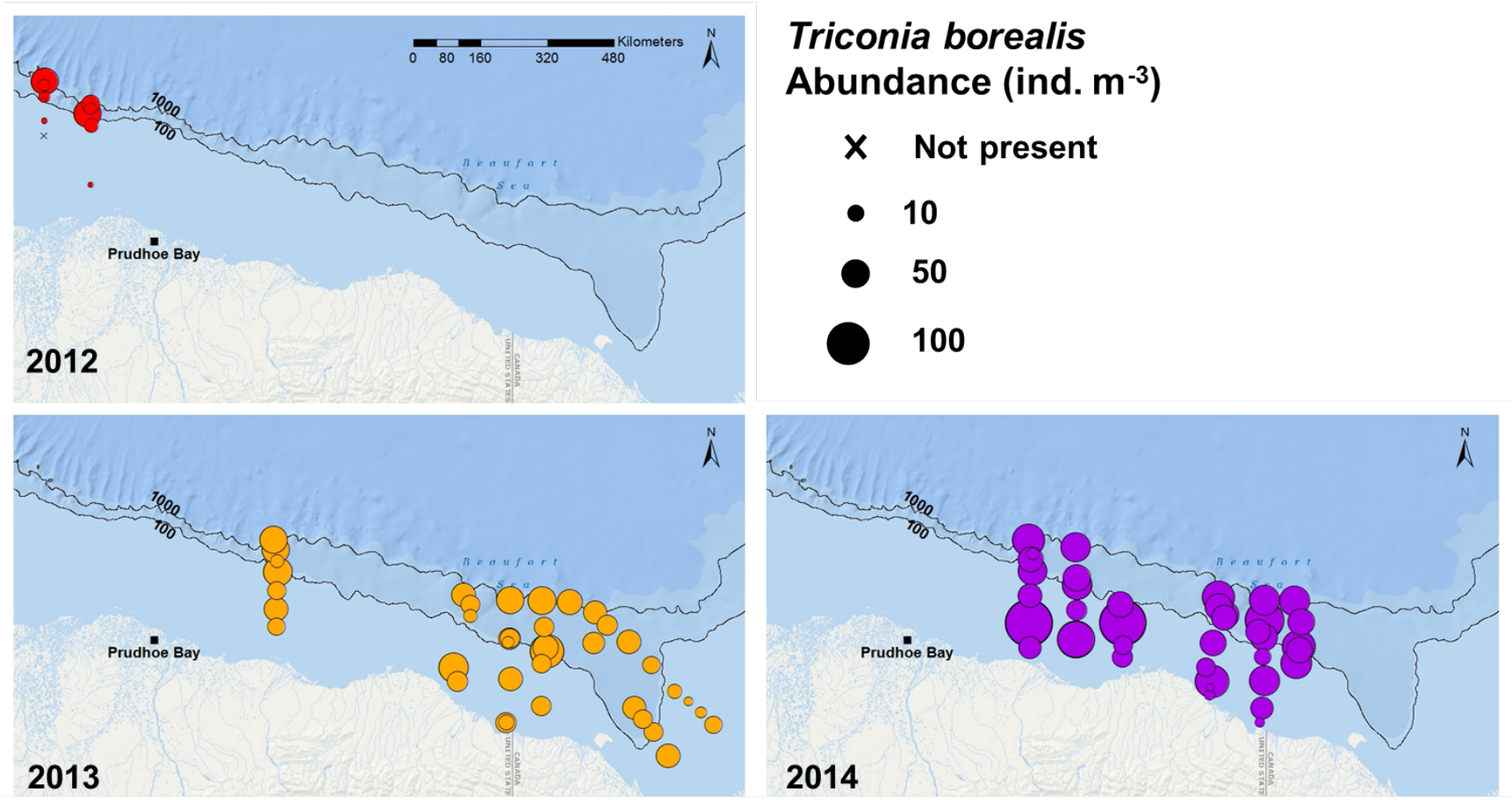

Figure 4.1.4. Abundance of *Triconia borealis* (ind. m^{-3}) captured in the 150-µm net in the Beaufort Sea during Transboundary 2012–14.

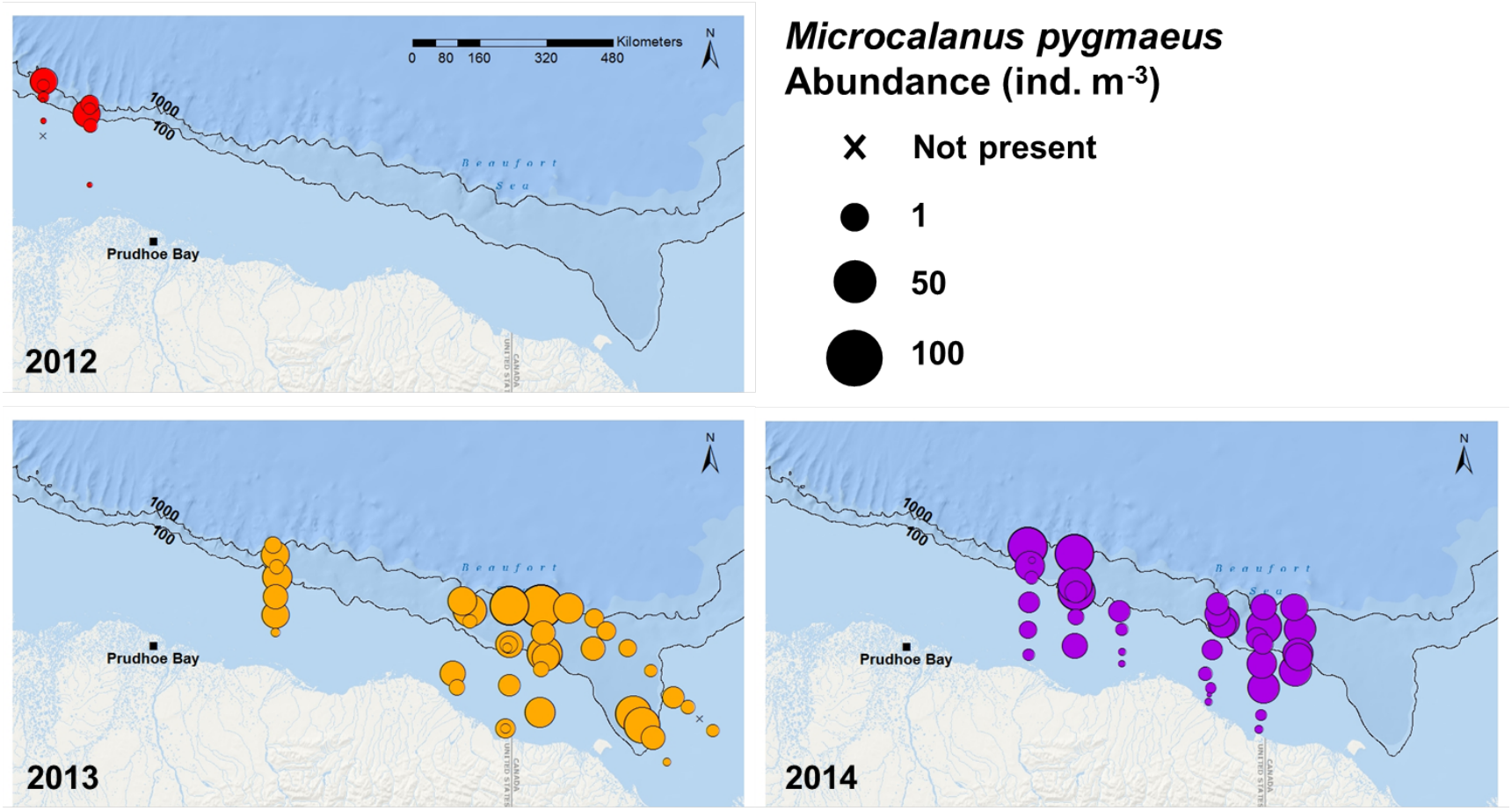

Figure 4.1.5. Abundance of *Microcalanus pygmaeus* (ind. m^{-3}) captured in the 150-µm net in the Beaufort Sea during Transboundary 2012–14.

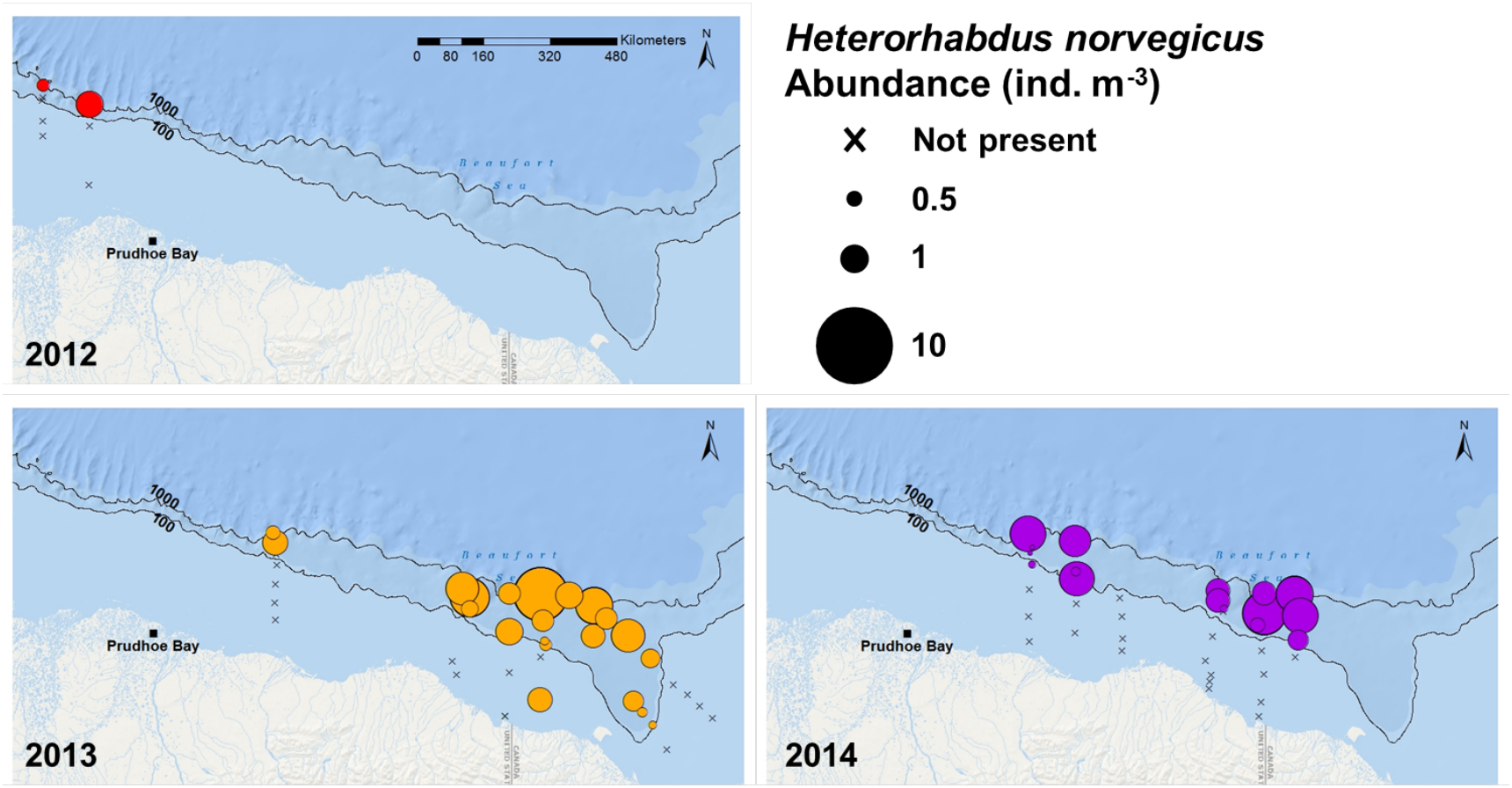

Figure 4.1.6. Abundance of *Heterorhabdus norvegicus* (ind. m^{-3}) captured in the 150-µm net in the Beaufort Sea during Transboundary 2012–14.

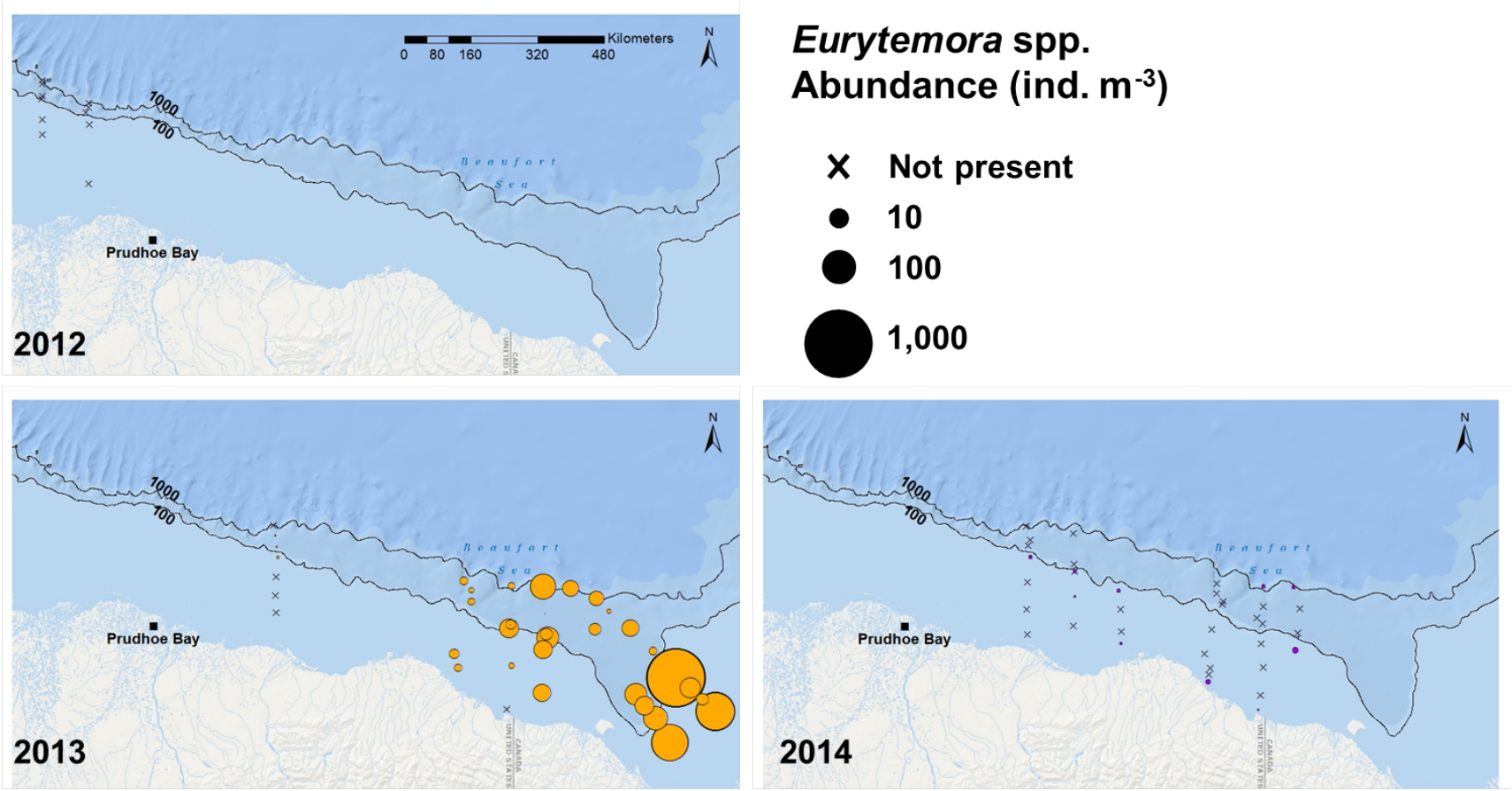

Figure 4.1.7. Abundance of *Eurytemora* spp. (ind. m^{-3}) captured in the 150-µm net in the Beaufort Sea during Transboundary 2012–14.

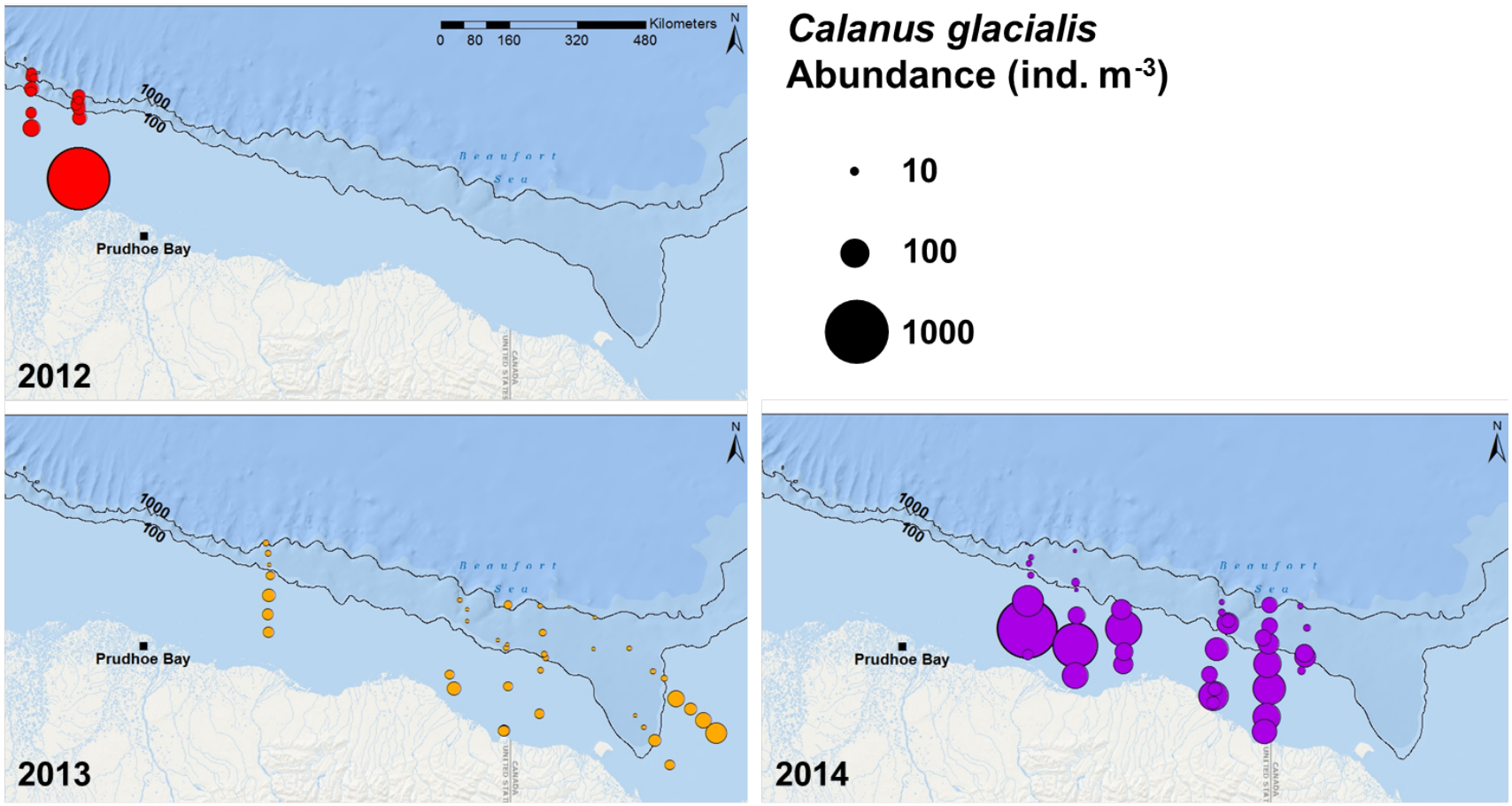

Figure 4.1.8. Abundance of *Calanus glacialis* (ind. m^{-3}) captured in the 505-µm net in the Beaufort Sea during Transboundary 2012–14.

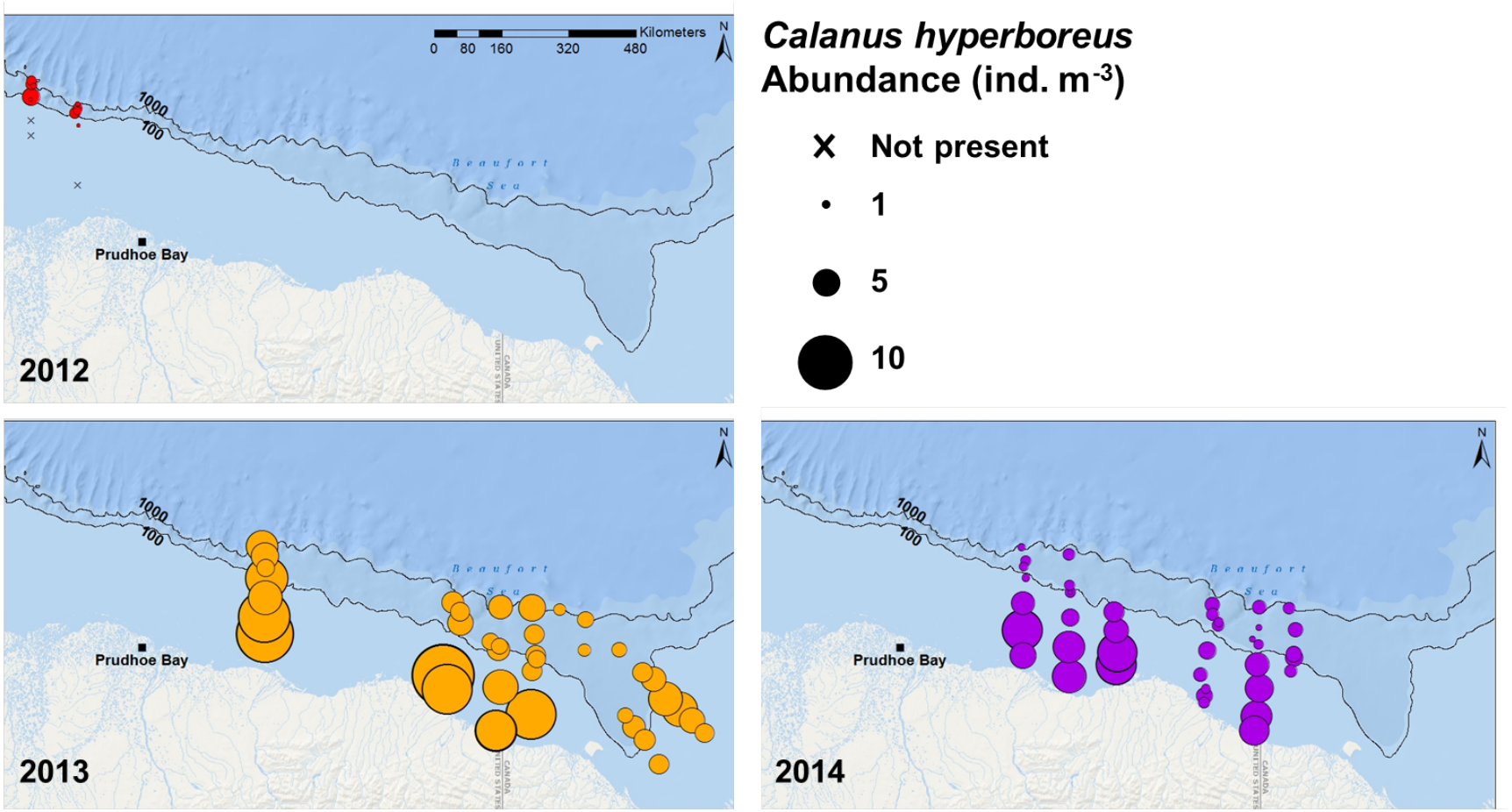

Figure 4.1.9. Abundance of *Calanus hyperboreus* (ind. m^{-3}) captured in the 505-µm net in the Beaufort Sea during Transboundary 2012–14.

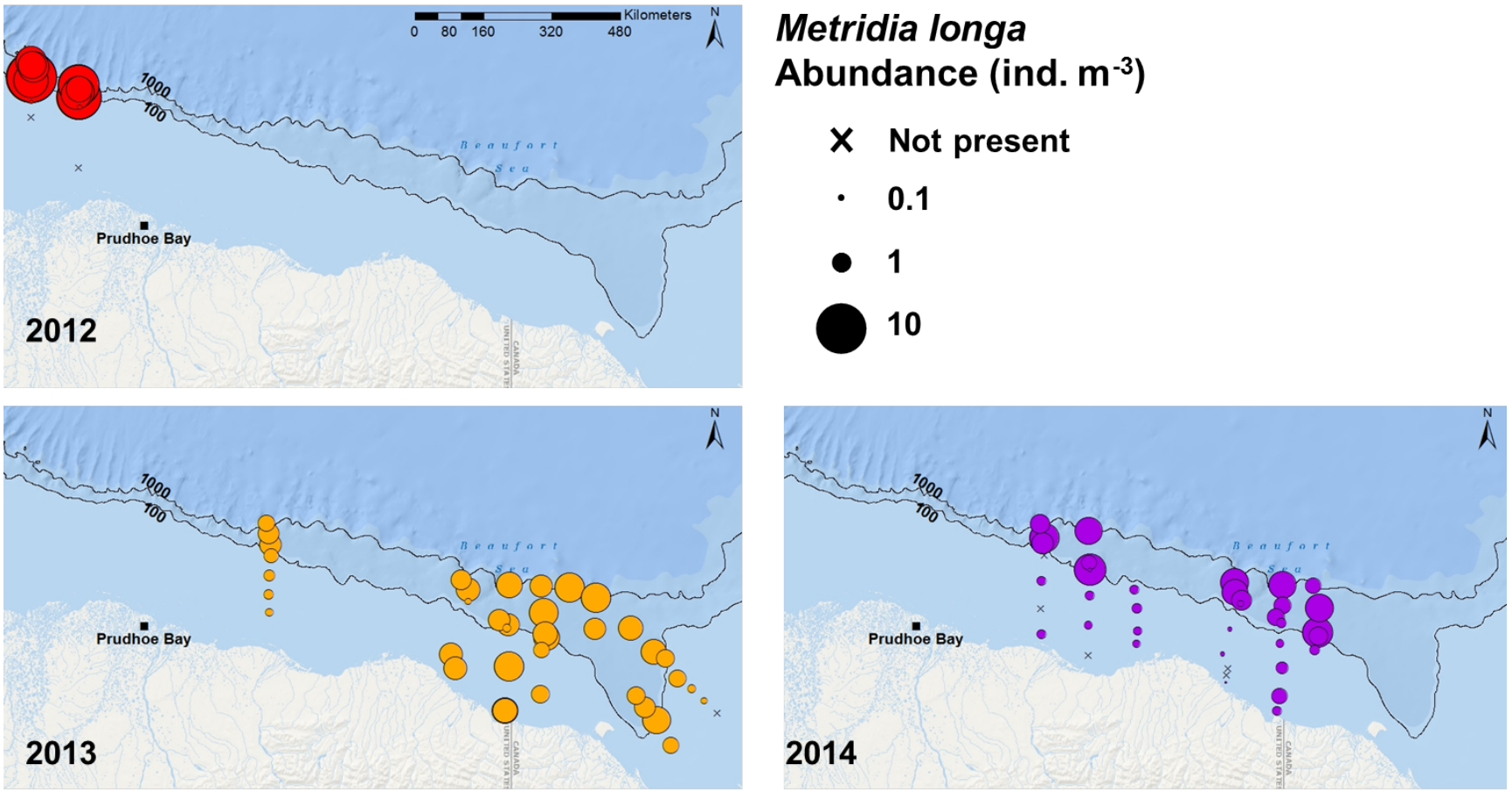

Figure 4.1.10. Abundance of *Metridia longa* (ind. m^{-3}) captured in the 505-µm net in the Beaufort Sea during Transboundary 2012–14.

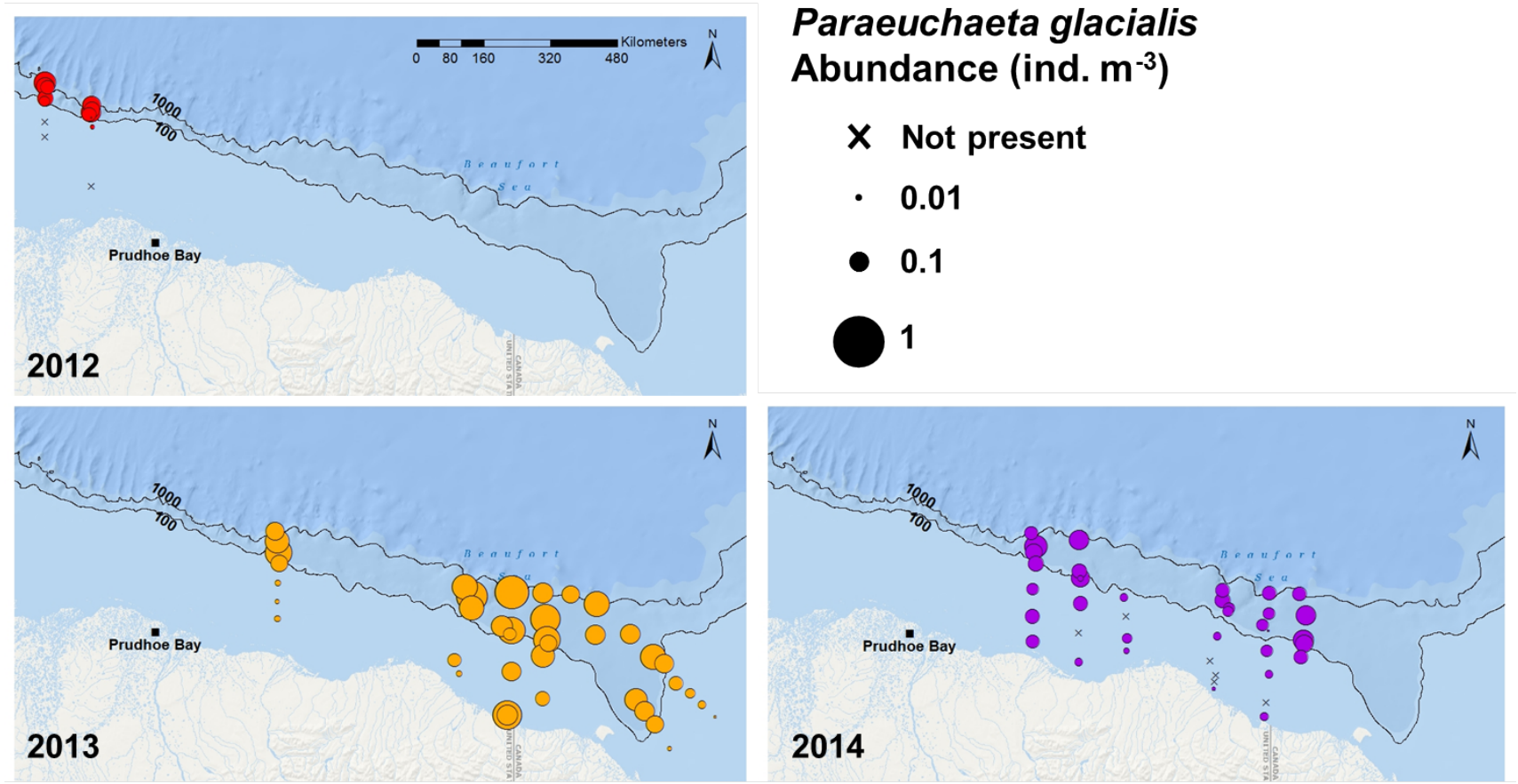

Figure 4.1.11. Abundance of *Paraeuchaeta glacialis* (ind. m^{-3}) captured in the 505-µm net in the Beaufort Sea during Transboundary 2012–14.

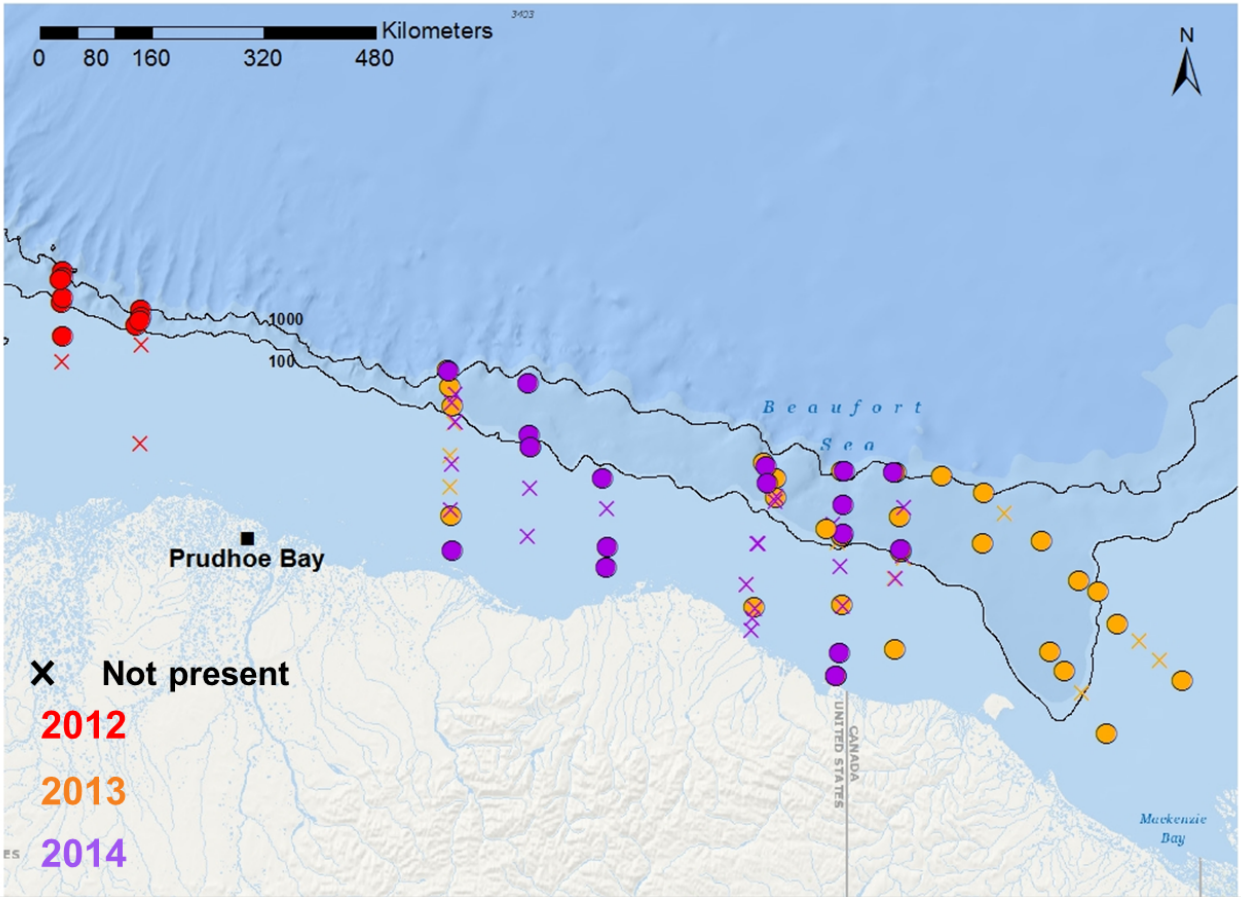

Figure 4.1.12. Presence of Pacific expatriate taxa captured in the 150- and 505-µm nets in the Beaufort Sea during Transboundary 2012–14.

4.1.3.3 Community Structure and Relation to Hydrography

150-µm net

Pooled data from all field seasons revealed strong separation of shelf and slope zooplankton communities by both abundance (Figure 4.1.13) and biomass (Figure 4.1.14). Cluster analysis revealed four major groupings in the pooled Transboundary 150-µm abundance data: slope, central shelf, eastern shelf, and freshwater-influenced. Similarity percentage analysis (SIMPER) of 150-µm abundance data (Table 4.4) showed that the slope group was characterized by high abundances of *Oithona similis*, *Pseudocalanus* spp. copepodites, calanoid nauplii, *Triconia borealis*, *Calanus glacialis*, and *Microcalanus pygmaeus*. The central shelf group was characterized by high abundances of *O. similis*, *Pseudocalanus* spp. copepodites, *C. glacialis*, and calanoid nauplii. In the eastern shelf group, *Pseudocalanus* spp. copepodites were the largest contributors to within-group similarity, followed by *O. similis*, *C. glacialis*, and *T. borealis*. Finally, the freshwater-influenced group was characterized by *Pseudocalanus* spp. copepodites, *O. similis*, calanoid nauplii, *T. borealis*, and *Eurytemora* spp. Cluster analysis of the pooled 150-µm biomass data revealed the same four primary groupings; however, the freshwater-influenced group also split along a shelf-slope axis. The slope stations of the freshwater-influenced group were differentiated from those on the shelf by a higher contribution of the predatory chaetognath

Eukrohnia hamata to biomass on the slope. The structure observed in samples collected by the 150-µm net was most highly correlated with temperature and salinity averaged over the upper 200 m in terms of both abundance (Spearman correlation (ρ) = 0.41, p <0.01) and biomass (ρ = 0.44, p <0.01) (Table 4.5).

505-µm net

Community structure pattern observed in the 505-µm net samples was very similar to that observed in the 150-µm net. The zooplankton community from the 505-µm net generally separated along a shelf-slope axis, whether considered in terms of abundance (Figure 4.1.15) or biomass (Figure 4.1.16). Cluster analysis of abundance data revealed five groupings: central shelf, central slope, eastern slope, eastern shelf, and freshwater-influenced. SIMPER analysis of 505-µm abundance data (Table 4.6) revealed that the central shelf group was characterized by *Calanus glacialis*, *Mertensia ovum*, *Aglantha digitale*, and the predatory pteropod *Clione limacina*. The central slope group was characterized by *C. glacialis*, *Metridia longa*, *Parasagitta elegans*, and the hydrozoan *Aglantha digitale*. *C. glacialis*, *M. longa*, *Calanus hyperboreus*, and *Paraeuchaeta glacialis* were highest contributors to within-group similarity of the eastern slope grouping. The eastern shelf grouping was characterized by *C. glacialis*, *Aglantha digitale*, *C. hyperboreus*, and *P. elegans*. Finally, the Mackenzie-influenced group was characterized by the *Calanus* species mentioned above, as well as the hyperiid amphipod *Themisto abysorrum* and the brackish-water copepod *Limnocalanus macrurus*. Cluster analysis of the 505-µm biomass data resulted in the same groupings as those observed for the abundance data. The structure observed in the 505-µm net was most highly correlated with bottom salinity in terms of both abundance (ρ = 0.46, p <0.01) and biomass (ρ = 0.38, p <0.01) (Table 4.7).

Size based estimates of prey field

The size-spectra of copepods captured in the Beaufort Sea was relatively consistent throughout all Transboundary survey years (Figure 4.1.17). Peaks in abundance and biomass in the spectra between 2000 and 4000 µm prosome length coincide well with the size of later stages *Calanus glacialis*. Beyond about 4000 µm, size spectra from the 150-µm net become noisy due to low underlying counts; however, the two broad nodes at ~5000 and 6700 µm correspond to the later developmental stages of *Calanus hyperboreus.*

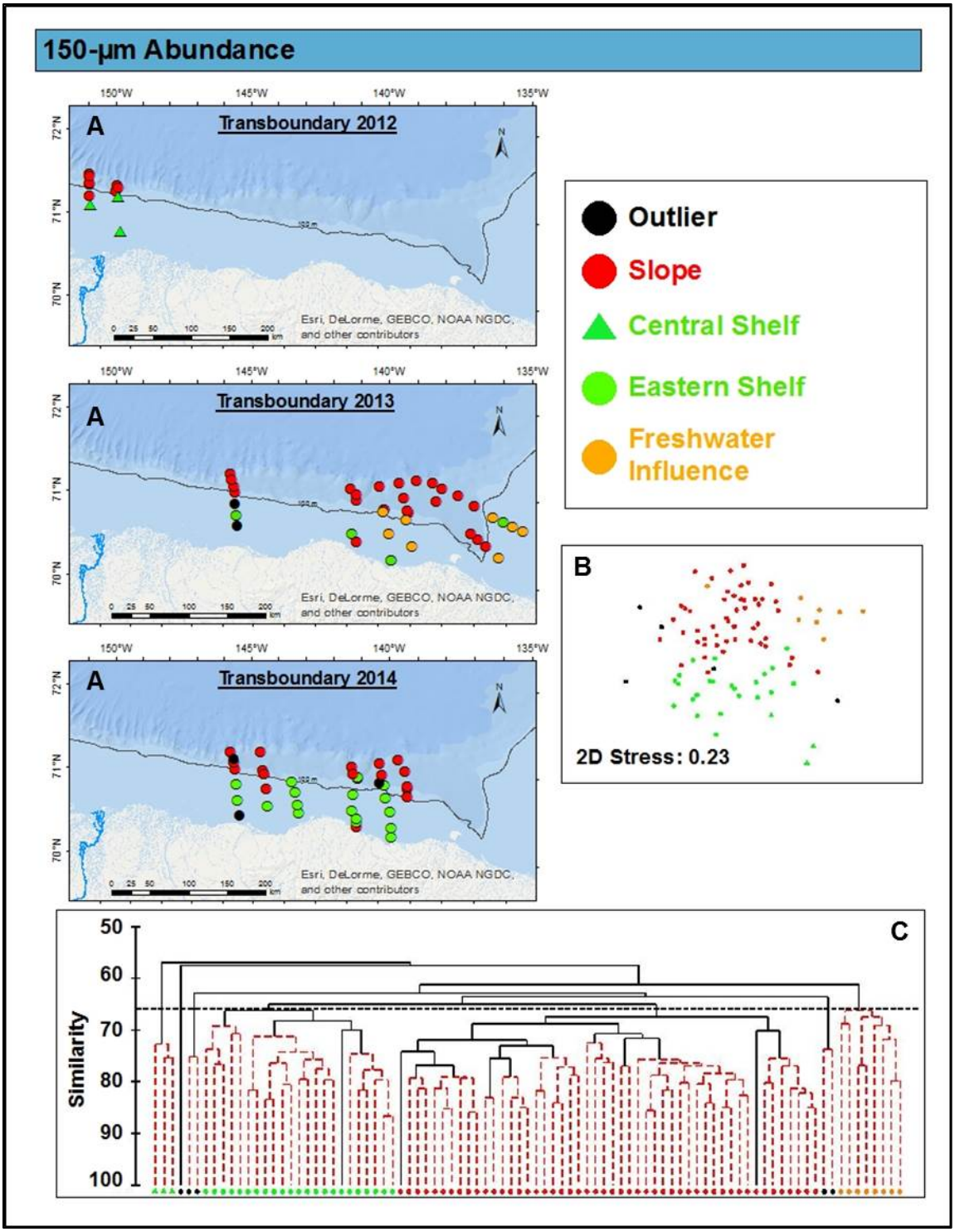

Figure 4.1.13. Zooplankton community structure for pooled 150-µm net abundance data Transboundary 2012–14.
A) Spatial distribution of observed community groups. B) Non-parametric multidimensional scaling (nMDS) of zooplankton community overlain with observed groupings. C) Bray-Curtis sample similarity as determined by hierarchical clustering of species abundance. Dotted red lines connect samples that are not statistically unique (SIMPROF, p <0.05).

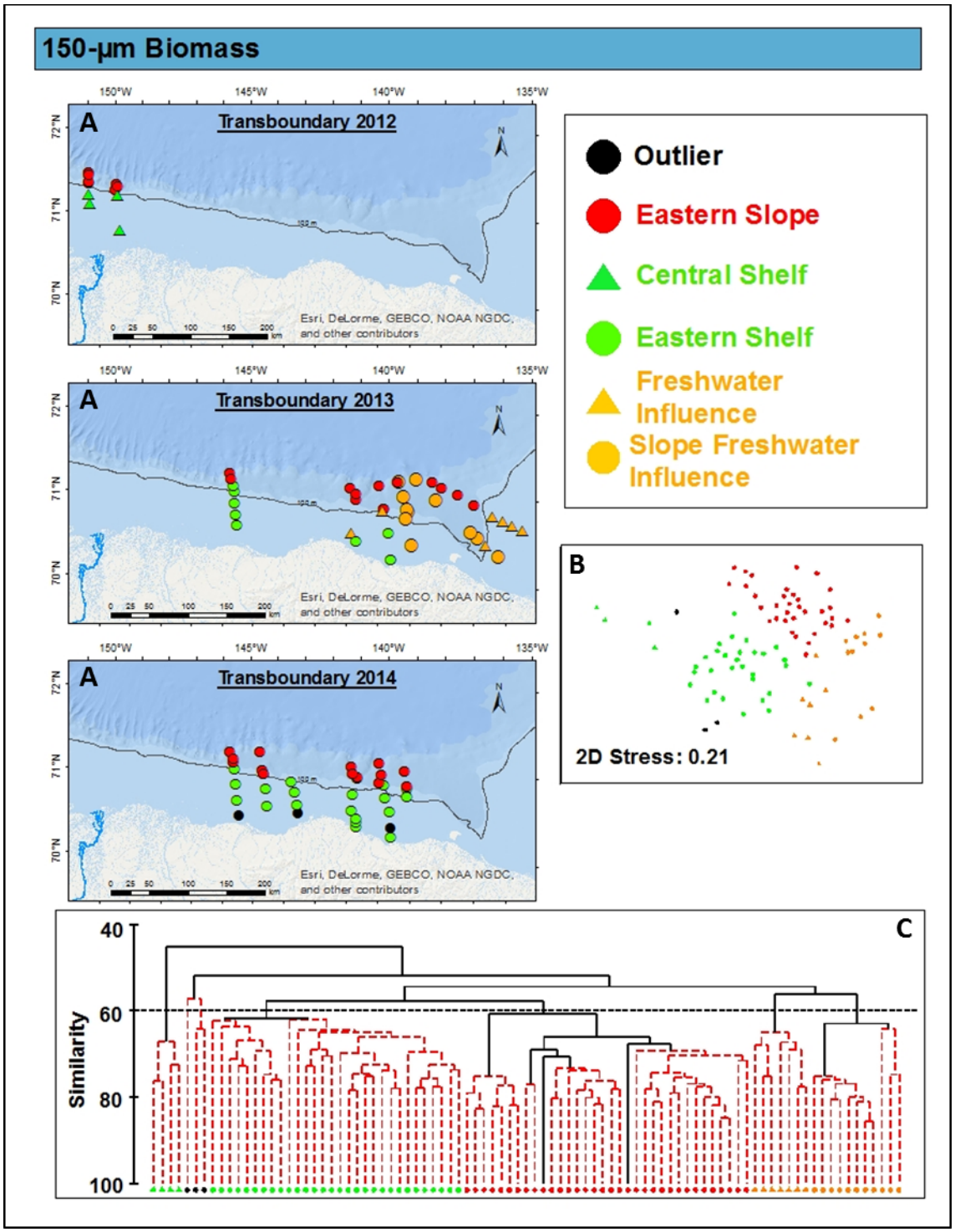

Figure 4.1.14. Zooplankton community structure for pooled 150-µm net biomass data Transboundary 2012–14.
A) Spatial distribution of observed community groups. B) Non-parametric multidimensional scaling (nMDS) of zooplankton community overlain with observed groupings. C) Bray-Curtis sample similarity as determined by hierarchical clustering of species biomass. Dotted red lines connect samples that are not statistically unique (SIMPROF, p <0.05).

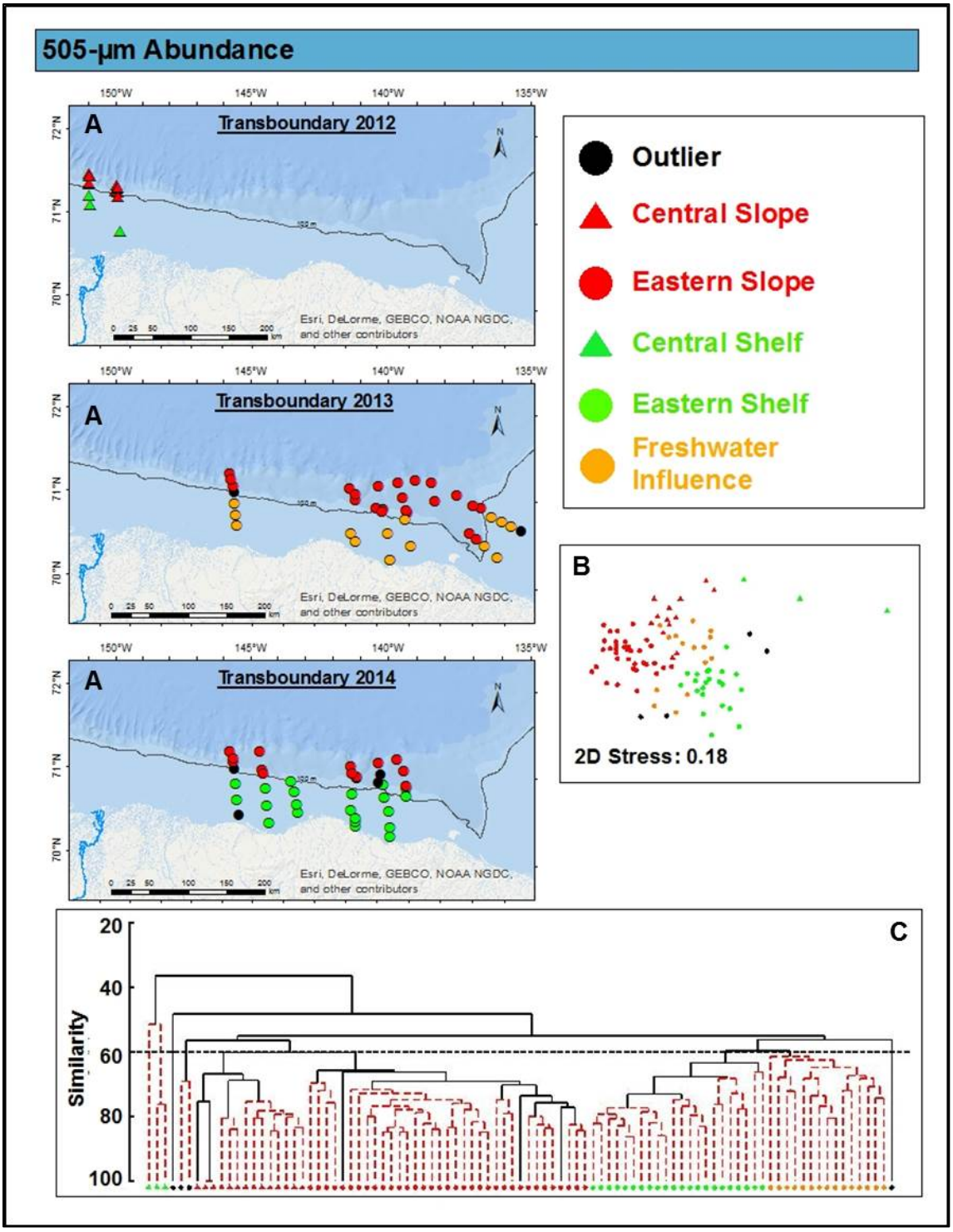

Figure 4.1.15. Zooplankton community structure for pooled 505-µm net abundance data Transboundary 2012–14.
A) Spatial distribution of observed community groups. B) Non-parametric multidimensional scaling (nMDS) of zooplankton community overlain with observed groupings. C) Bray-Curtis sample similarity as determined by hierarchical clustering of species abundance. Dotted red lines connect samples that are not statistically unique (SIMPROF, p <0.05).

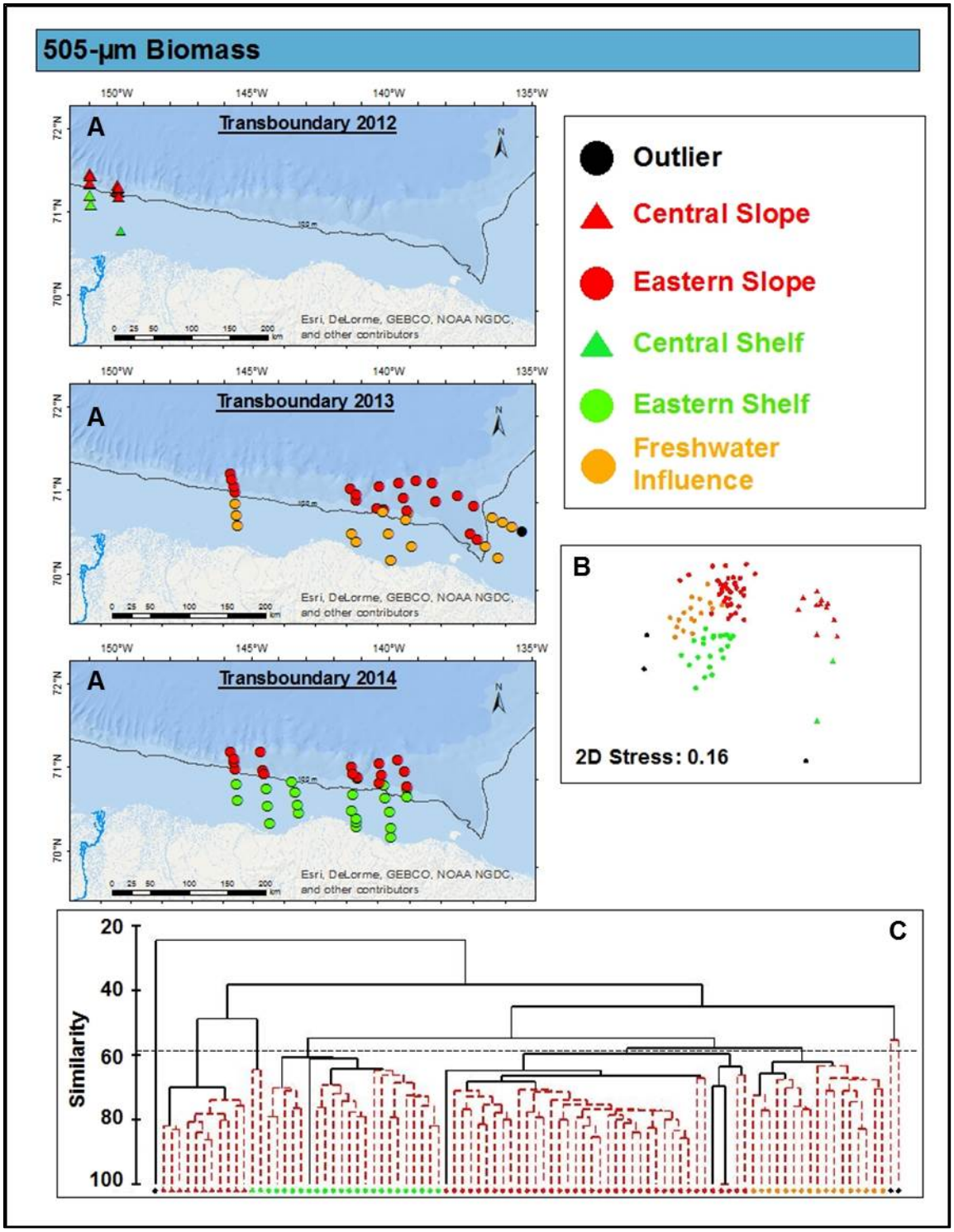

Figure 4.1.16. Zooplankton community structure for pooled 505-µm net biomass data Transboundary 2012–14.
A) Spatial distribution of observed community groups. B) Non-parametric multidimensional scaling (nMDS) of zooplankton community overlain with observed groupings. C) Bray-Curtis sample similarity as determined by hierarchical clustering of species biomass. Dotted red lines connect samples that are not statistically unique (SIMPROF, p <0.05).

Table 4.4. Key taxa and their contribution to the first 90% of community similarity for community groupings for the 150-µm net abundance data from Transboundary 2012–14. Outliers not included.

Group (within group similarity)	Taxon (% Contribution)		
Central Shelf (72.83)	*Oithona similis* (13.62) *Pseudocalanus* spp. (copepodite) (12.66) *Calanus glacialis* (10.74) Calanoid nauplii (7.68) *Podon leuckarti* (6.99) Polychaete larvae (6)	*Pseudocalanus newmani* (4.9) *Acartia longiremis* (4.71) *Aglantha digitale* (4.41) *Pseudocalanus mimus* (3.74) *Parasagitta elegans* (3.62)	*Themisto abyssorum* (3.54) *Boroecia maxima* (2.9) *Pseudocalanus minutus* (2.05) *Themisto libellula* (1.77) *Acartia* spp. (copepodite) (1.71)
Slope (71.06)	*Oithona similis* (10.91) *Pseudocalanus* spp. (copepodite) (8.55) Calanoid nauplii (7.51) *Triconia borealis* (6.82) *Calanus glacialis* (5.84) *Microcalanus pygmaeus* (5.34) *Fritilliaria borealis* (4.6) Polychaete larvae (4.58) *Aglantha digitale* (3.99)	*Metridia longa* (3.39) *Oikopleura vanhoeffeni* (3.14) *Calanus hyperboreus* (3.1) *Limacina helicina* (2.76) Bivalve larvae (2.61) *Parasagitta elegans* (2.53) *Paraeuchaeta glacialis* (2.3) *Metridia* spp. (C1-3) (2.3)	*Pseudocalanus minutus* (1.91) *Scolecithricella minor* (1.6) *Microsetella norvegica* (1.42) *Pseudocalanus acuspes* (1.3) *Themisto abyssorum* (1.19) *Pseudocalanus* spp. (male) (1.15) *Eurytemora* spp. (copepodite) (1.11) *Aeginopsis laurentii* (1.07)
Eastern Shelf (70.18)	*Pseudocalanus* spp. (copepodite) (12.28) *Oithona similis* (11.02) *Calanus glacialis* (8.87) *Triconia borealis* (7.81) Calanoid nauplii (7.5) Polychaete larvae (5.89)	*Microcalanus pygmaeus* (4.95) *Oikopleura vanhoeffeni* (4.91) *Calanus hyperboreus* (4.17) Bivalve larvae (3.61) *Aglantha digitale* (3.59) *Limacina helicina* (3.56)	*Fritilliaria borealis* (3.48) *Microsetella norvegica* (3.31) *Parasagitta elegans* (2.78) *Podon leuckarti* (2.04) *Themisto abyssorum* (1.66)
Mackenzie Influence (68.57)	*Pseudocalanus* spp. (copepodite) (12.66) *Oithona similis* (10.8) Calanoid nauplii (8.3) *Triconia borealis* (6.19) *Eurytemora* spp. (copepodite) (6.16) *Calanus glacialis* (5.32) Polychaete larvae (4.91)	*Pseudocalanus acuspes* (4.64) *Aglantha digitale* (4.36) *Calanus hyperboreus* (3.82) *Microcalanus pygmaeus* (3.36) *Limacina helicina* (3.14) Bivalve larvae (2.67) *Parasagitta elegans* (2.47)	*Pseudocalanus minutus* (2.18) *Aeginopsis laurentii* (2.15) *Acartia* spp. (copepodite) (2.11) *Pseudocalanus newmani* (1.93) Echinoderm larvae (1.77) *Acartia longiremis* (1.49)

Table 4.5. Relationship between pooled 150-µm zooplankton and abiotic factors over different depth intervals during Transboundary 2012–14. Temperature (*T)* and salinity (*S)* averages, Fluorescence (Fl), and station depth (m) (*D)*. * Indicates best variable combination explaining observed zooplankton community structure.

	#Var	Abundance						Biomass					
Bottom	**1**	***S*** 0.36	***T*** 0.15	***D*** 0.03	***Fl*** 0.21			***S*** 0.41	***T*** 0.15	***D*** 0.06	***Fl*** 0.12		
	2	***T,S*** 0.23	***D,T*** 0.17	***D,S*** 0.12	***T,Fl*** 0.13	***S,Fl*** 0.35	***D, Fl*** 0.02	***T,S*** 0.25	***D,T*** 0.19	***D,S*** 0.14	***T,Fl*** 0.12	***S,Fl*** 0.34	***D, Fl*** 0.01
	3	***T,S,Fl*** 0.21	***T,S,D*** 0.18	***S,Fl,D*** 0.10	***T,Fl,D*** 0.13			***T,S,Fl*** 0.20	***T,S,D*** 0.21	***S,Fl,D*** 0.10	***T,Fl,D*** 0.14		
	4	**All** 0.16						**All** 0.17					
200 m avg.	**1**	***S*** 0.34	***T*** 0.26	***D*** 0.03	***Fl*** 0.21			***S*** 0.36	***T*** 0.25	***D*** 0.06	***Fl*** 0.18		
	2	***T,S*** **0.41***	***D,T*** 0.29	***D,S*** 0.25	***T,Fl*** 0.29	***S,Fl*** 0.33	***D, Fl*** 0.06	***T,S*** **0.44***	***D,T*** 0.31	***D,S*** 0.26	***T,Fl*** 0.27	***S,Fl*** 0.32	***D, Fl*** 0.05
	3	***T,S,Fl*** 0.39	***T,S,D*** 0.37	***S,Fl,D*** 0.23	***T,Fl,D*** 0.28			***T,S,Fl*** 0.40	***T,S,D*** 0.40	***S,Fl,D*** 0.22	***T,Fl,D*** 0.28		
	4	**All** 0.35						**All** 0.36					
100 m avg.	**1**	***S*** 0.35	***T*** 0.24	***D*** 0.03	***Fl*** 0.21			***S*** 0.37	***T*** 0.24	***D*** 0.06	***Fl*** 0.19		
	2	***T,S*** 0.40	***D,T*** 0.28	***D,S*** 0.25	***T,Fl*** 0.27	***S,Fl*** 0.33	***D, Fl*** 0.06	***T,S*** 0.44	***D,T*** 0.30	***D,S*** 0.26	***T,Fl*** 0.27	***S,Fl*** 0.34	***D, Fl*** 0.05
	3	***T,S,Fl*** 0.39	***T,S,D*** 0.36	***S,Fl,D*** 0.23	***T,Fl,D*** 0.27			***T,S,Fl*** 0.42	***T,S,D*** 0.40	***S,Fl,D*** 0.23	***T,Fl,D*** 0.28		
	4	**All** 0.35						**All** 0.37					

Table 4.5, continued.

	#Var	Abundance						Biomass					
50 m avg.	1	***S*** 0.34	***T*** 0.27	***D*** 0.03	***Fl*** 0.22			***S*** 0.34	***T*** 0.29	***D*** 0.06	***Fl*** 0.19		
	2	***T,S*** 0.39	***D,T*** 0.29	***D,S*** 0.24	***T,Fl*** 0.29	***S,Fl*** 0.31	***D, Fl*** 0.06	***T,S*** 0.42	***D,T*** 0.31	***D,S*** 0.25	***T,Fl*** 0.27	***S,Fl*** 0.28	***D, Fl*** 0.04
	3	***T,S,Fl*** 0.37	***T,S,D*** 0.35	***S,Fl,D*** 0.21	***T,Fl,D*** 0.27			***T,S,Fl*** 0.37	***T,S,D*** 0.37	***S,Fl,D*** 0.19	***T,Fl,D*** 0.26		
	4	**All** 0.32						**All** 0.33					
10 m avg.	1	***S*** 0.34	***T*** 0.28	***D*** 0.03	***Fl*** 0.22			***S*** 0.35	***T*** 0.30	***D*** 0.06	***Fl*** 0.19		
	2	***T,S*** 0.39	***D,T*** 0.29	***D,S*** 0.24	***T,Fl*** 0.30	***S,Fl*** 0.32	***D, Fl*** 0.06	***T,S*** 0.43	***D,T*** 0.32	***D,S*** 0.25	***T,Fl*** 0.29	***S,Fl*** 0.30	***D, Fl*** 0.05
	3	***T,S,Fl*** 0.38	***T,S,D*** 0.35	***S,Fl,D*** 0.21	***T,Fl,D*** 0.27			***T,S,Fl*** 0.39	***T,S,D*** 0.38	***S,Fl,D*** 0.21	***T,Fl,D*** 0.28		
	4	**All** 0.33						**All** 0.34					

Table 4.6. Key taxa and their contribution to the first 90% of community similarity for community groupings for the 505-µm net abundance data from Transboundary 2012–14. Outliers not included.

Group (within group similarity)	Taxon (% contribution)		
Central Slope (72.07)	*Calanus glacialis* (23.41) *Metridia longa* (12.53) *Parasagitta elegans* (9.19) *Aglantha digitale* (7.71)	*Pseudocalanus minutus* (7.32) *Paraeuchaeta glacialis* (6.65) *Calanus hyperboreus* (6.1) *Thysanoessa raschii* (5.18)	*Thysanoessa inermis* (3.59) *Themisto libellula* (3.1) *Themisto abyssorum* (2.99) *Limacina helicina* (2.96)
Central Shelf (59.66)	*Calanus glacialis* (50.39) *Mertensia ovum* (11.81) *Aglantha digitale* (11.71)	*Clione limacina* (11.06) *Parasagitta elegans* (8.13) *Heterorhabdus norvegicus* (5.38)	*Chiridius obtusifrons* (2.67)
Eastern Slope (70.61)	*Calanus glacialis* (12.29) *Metridia longa* (10.59) *Calanus hyperboreus* (9.79) *Paraeuchaeta glacialis* (7.82) *Aglantha digitale* (6.94) *Boroecia maxima* (5.69)	*Themisto abyssorum* (4.92) *Parasagitta elegans* (4.61) *Eukrohnia hamata* (3.9) *Themisto libellula* (3.1) *Limacina helicina* (2.76)	*Oikopleura vanhoeffeni* (2.65) *Thysanoessa raschii* (2.18) *Pseudocalanus minutus* (1.8) *Scaphocalanus antarcticus* (1.63) *Thysanoessa inermis* (1.36)
Mackenzie Influence (65.16)	*Calanus glacialis* (16.94) *Calanus hyperboreus* (13.58) *Aglantha digitale* (8.26) *Metridia longa* (8.18) *Themisto abyssorum* (5.44) *Paraeuchaeta glacialis* (5.06)	*Limacina helicina* (4.74) *Parasagitta elegans* (4.37) *Pseudocalanus minutus* (4.05) *Aeginopsis laurentii* (3.6) *Oikopleura vanhoeffeni* (3.54) *Limnocalanus macrurus* (3.5)	*Pseudocalanus* spp. (copepodite) (3.28) *Themisto libellula* (2.8) *Thysanoessa raschii* (2.62) *Halitholus cirratus* (2.61)
Eastern Shelf (70.91)	*Calanus glacialis* (23.02) *Aglantha digitale* (10.98) *Calanus hyperboreus* (9.88) *Aeginopsis laurentii* (6.83) *Parasagitta elegans* (5.84)	*Pseudocalanus* spp. (copepodite) (5.64) *Limacina helicina* (5.19) *Oikopleura vanhoeffeni* (4.5) *Pseudocalanus minutus* (4.08) *Metridia longa* (3.79)	*Themisto abyssorum* (3.24) *Mertensia ovum* (3) *Paraeuchaeta glacialis* (2.39) *Eukrohnia hamata* (2.37)

Table 4.7. Relationship between pooled 505-µm zooplankton and abiotic factors over different depth intervals during Transboundary 2012–14. Temperature (*T)* and salinity (*S)* averages, and station depth (m) (*D)*. * Indicates best variable combination explaining observed zooplankton community structure.

	#Var	Abundance						Biomass					
Bottom	**1**	***S*** **0.46***	***T*** 0.21	***D*** 0.12	***Fl*** 0.2			***S*** **0.38***	***T*** 0.3	***D*** 0.08	***Fl*** 0.21		
	2	***T,S*** 0.317	***D,T*** 0.28	***D,S*** 0.21	***T,Fl*** 0.21	***S,Fl*** 0.43	***D, Fl*** 0.11	***T,S*** 0.38	***D,T*** 0.29	***D,S*** 0.16	***T,Fl*** 0.28	***S,Fl*** 0.35	***D, Fl*** 0.07
	3	***T,S,Fl*** 0.3	***T,S,D*** 0.3	***S,Fl,D*** 0.2	***T,Fl,D*** 0.26			***T,S,Fl*** 0.35	***T,S,D*** 0.31	***S,Fl,D*** 0.15	***T,Fl,D*** 0.26		
	4	**All** 0.285						**All** 0.29					
200 m avg.	**1**	***S*** 0.29	***T*** 0.23	***D*** 0.12	***Fl*** 0.23			***S*** 0.2	***T*** 0.26	***D*** 0.08	***Fl*** 0.16		
	2	***T,S*** 0.38	***D,T*** 0.36	***D,S*** 0.24	***T,Fl*** 0.27	***S,Fl*** 0.24	***D, Fl*** 0.12	***T,S*** 0.34	***D,T*** 0.34	***D,S*** 0.15	***T,Fl*** 0.28	***S,Fl*** 0.16	***D, Fl*** 0.06
	3	***T,S,Fl*** 0.35	***T,S,D*** 0.39	***S,Fl,D*** 0.21	***T,Fl,D*** 0.34			***T,S,Fl*** 0.32	***T,S,D*** 0.33	***S,Fl,D*** 0.12	***T,Fl,D*** 0.31		
	4	**All** 0.37						**All** 0.31					
100 m avg.	**1**	***S*** 0.29	***T*** 0.24	***D*** 0.12	***Fl*** 0.23			***S*** 0.2	***T*** 0.27	***D*** 0.08	***Fl*** 0.17		
	2	***T,S*** 0.39	***D,T*** 0.12	***D,S*** 0.25	***T,Fl*** 0.27	***S,Fl*** 0.25	***D, Fl***	***T,S*** 0.35	***D,T*** 0.34	***D,S*** 0.16	***T,Fl*** 0.28	***S,Fl*** 0.16	***D, Fl*** 0.06
	3	***T,S,Fl*** 0.36	***T,S,D*** 0.4	***S,Fl,D*** 0.22	***T,Fl,D*** 0.34			***T,S,Fl*** 0.31	***T,S,D*** 0.31	***S,Fl,D*** 0.13	***T,Fl,D*** 0.33		
	4	**All** 0.38						**All** 0.32					

Table 4.7, continued.

	#Var	Abundance						Biomass					
50 m avg.	1	***S*** 0.27	***T*** 0.28	***D*** 0.12	***Fl*** 0.23			***S*** 0.19	***T*** 0.32	***D*** 0.08	***Fl*** 0.18		
	2	***T,S*** 0.38	***D,T*** 0.36	***D,S*** 0.23	***T,Fl*** 0.31	***S,Fl*** 0.24	***D, Fl*** 0.12	***T,S*** 0.36	***D,T*** 0.35	***D,S*** 0.15	***T,Fl*** 0.32	***S,Fl*** 0.15	***D, Fl*** 0.06
	3	***T,S,Fl*** 0.37	***T,S,D*** 0.39	***S,Fl,D*** 0.22	***T,Fl,D*** 0.35			***T,S,Fl*** 0.33	***T,S,D*** 0.34	***S,Fl,D*** 0.12	***T,Fl,D*** 0.32		
	4	**All** 0.38						**All** 0.32					
10 m avg.	1	***S*** 0.29	***T*** 0.28	***D*** 0.12	***Fl*** 0.21			***S*** 0.22	***T*** 0.29	***D*** 0.08	***Fl*** 0.15		
	2	***T,S*** 0.38	***D,T*** 0.35	***D,S*** 0.24	***T,Fl*** 0.29	***S,Fl*** 0.25	***D, Fl*** 0.11	***T,S*** 0.35	***D,T*** 0.32	***D,S*** 0.17	***T,Fl*** 0.28	***S,Fl*** 0.17	***D, Fl*** 0.05
	3	***T,S,Fl*** 0.35	***T,S,D*** 0.38	***S,Fl,D*** 0.21	***T,Fl,D*** 0.34			***T,S,Fl*** 0.32	***T,S,D*** 0.33	***S,Fl,D*** 0.13	***T,Fl,D*** 0.29		
	4	**All** 0.36						**All** 0.3					

4.1.4 Discussion

4.1.4.1 Community Structure

The zooplankton communities observed during the Transboundary field surveys primarily separated along a shelf-slope axis (see Figures 4.1.13–4.1.16). The across-shelf transition from neritic to more oceanic taxa has long been recognized in the Arctic; Grainger (1965) reported species assemblages associated with Arctic surface waters and coastal surface waters. Similarly, Darnis et al. (2008) report a distinct off-shelf assemblage and a neritic assemblage. In these surveys and the Transboundary project, *Pseudocalanus* species usually typify neritic shelf assemblages, while the oceanic *Calanus hyperboreus* and *Microcalanus pygmaeus* are characteristic of offshore assemblages.

The primary shelf-slope community gradient observed in the Beaufort Sea can be modified by localized hydrographic conditions and processes, as demonstrated by the freshened conditions in the 2013 field season. During 2013, the survey area was heavily influenced by a freshwater lens resulting from a mixture of Mackenzie River water and meltwater. This freshwater influence was reflected in the presence of a distinct faunal grouping consisting of taxa such as *Limnocalanus macrurus*, marine cladocerans, and *Eurytemora* spp. in addition to the typical neritic assemblages. The 2014 survey area overlapped much of the same geographic range; however, prevailing oceanographic conditions in the upper water column were drastically different. Thus, it is not surprising that the zooplankton communities observed on the shelf in 2013 and 2014 were different. The euryhaline taxa that were present in 2013, such as *Eurytemora* spp. (see Figure 4.1.17), *Limnocalanus macrurus*, *Podon leuckartii*, *Evadne nordmanni*, and rotifers, were largely absent in 2014. Across-shelf gradients associated with the Mackenzie River plume have also been recognized in the Canadian Beaufort. Walkusz et al. (2010) report ecological zones associated with intensity of the Mackenzie River plume, noting an "intense plume" assemblage, a "diffuse plume" assemblage, and an "offshore" assemblage. Our findings mirror this description; stations from the 2013 survey year exhibit internal structure associated with location relative to the shelf break and the degree of freshwater influence. In both our work and that of Walkusz et al. (2010), the "intense plume" assemblage is characterized by euryhaline and brackish water taxa, consistent with observations of other marginal Arctic seas influenced by major riverine input (see Abramova and Tuschling 2005).

It is notable that the epipelagic realm exhibited not only along- and across-shelf gradients, but depth-associated structure as well. Often, zooplankton sampling in the epipelagic realm integrates zooplankton from the surface to 200 m. The depth-stratified sampling conducted during the Transboundary project highlights the complexity and structure of the shelf that is missed by traditional integrative sampling methods. The PML (0–50 m) had the highest concentrations of zooplankton abundance and biomass, with mean abundance and biomass 2–4 times higher than the underlying 50–100 m stratum (see Table 4.3). This trend holds true on the shelf and the epipelagic realm overlying the slope. Our analyses highlight the fact that the pelagic realm must be considered in three dimensions (across-shelf, along-shelf, and vertically) to understand patterns in its biological communities. Importantly, this also implies differential impacts of industrial activity on zooplankton communities of the Beaufort Sea depending on the depth interval being considered (i.e., PML vs. AHW).

In the Arctic, zooplankton communities are tied to the underlying hydrographic conditions. This relationship has been observed in the Chukchi Sea (Hopcroft et al. 2010, Questel et al.

2013, Ershova et al. 2015b), the Canadian Beaufort (Walkusz et al. 2010), the Canada Basin (Kosobokova and Hopcroft 2010), and in the Alaskan Beaufort. The community groupings observed during the Transboundary surveys reflect this phenomenon in addition to the traditional shelf-slope community differences. In summary, across-shelf gradients represent a transition from neritic assemblages on the shelf, as typified by *Pseudocalanus* spp. to more oceanic assemblages of the slope as typified by *Calanus hyperboreus* and *Microcalanus pygmaeus*. The region around the Mackenzie River represents an extreme example of across-shelf gradients, as indicated by a "plume" assemblage, characterized by euryhaline copepods such as *Eurytemora* spp., in addition to the traditional neritic and oceanic assemblages. The presence of Pacific expatriate species, including *Neocalanus* spp. and *Metridia pacifica*, demonstrate the hydrographic connectivity between the subarctic Pacific, the Chukchi Sea, and the Beaufort Sea.

Integration of the Transboundary dataset with previous studies in the Beaufort Sea during 2010 and 2011 improves spatial coverage and allows some broad general characterizations of gradients across the Beaufort shelf as a whole (see Smoot 2015). The Beaufort Sea around Barrow Canyon represents a transitional zone between the Pacific-affinity, benthic-rich Chukchi Sea and the Beaufort Sea, as reflected in its relatively high abundances of meroplanktonic larvae and Pacific expatriate taxa when compared to the rest of the Beaufort. In contrast, the central and eastern Beaufort are more traditionally Arctic in faunal character, with the influence of the Chukchi Sea and Pacific-derived waters increasingly weakened toward the Mackenzie River. The eastern Beaufort near the Mackenzie River is generally more estuarine than the rest of the Alaskan Beaufort, although conditions at specific locations likely vary seasonally and from year to year depending on the intensity and extent of the river plume.

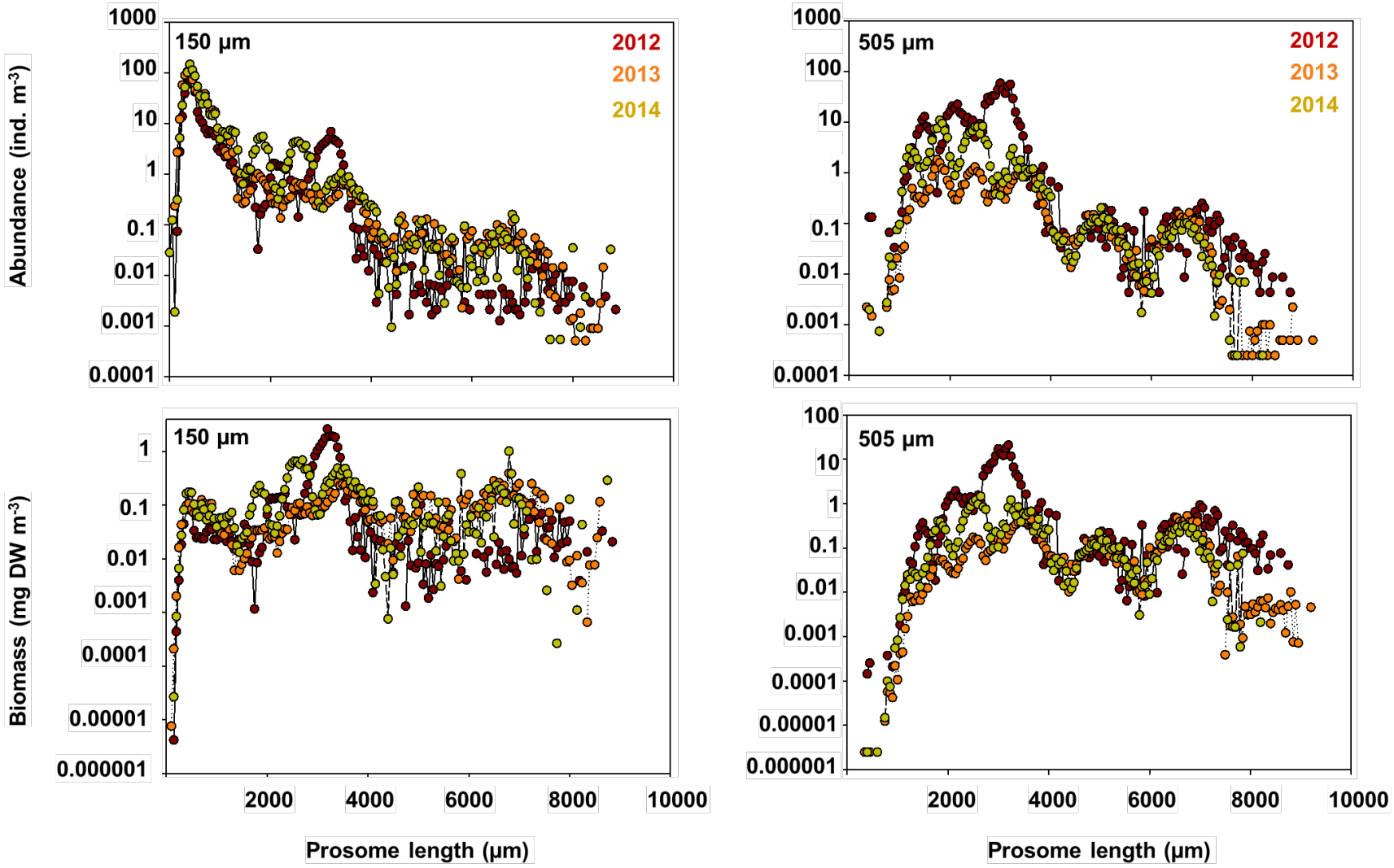

Figure 4.1.17. Abundance and biomass size spectra of copepods from the 150- and 505-µm nets for each survey year in the Beaufort Sea during Transboundary 2012–14.

4.1.4.2 Historical Context and Future Outlook

It is notable that the species composition of the major players of the Beaufort Sea mesozooplankton community appear to have remained relatively stable over the past decades; historical studies (e.g., Johnson 1956, Grainger and Grohe 1975, McConnell 1977, Hopky et al. 1994a, b, c) show a clear dominance of the key Arctic copepods reported in this study, as do other contemporary studies in the western Beaufort (e.g., Lane et al. 2008). Our results, and other studies in the western Arctic (Ashjian et al. 2003, Hopcroft et al. 2005, Lane et al. 2008, Kosobokova and Hopcroft 2010), suggest increased zooplankton standing stock in the modern Arctic when compared to early work, although we note there is quite a large range in abundances. Other caveats include methodological differences that may have resulted in an underestimate of historical abundance and biomass (see Ashjian et al. 2003, Hopcroft et al. 2008). Nonetheless, available data point to an upward trend in abundances of several key copepod species in the Beaufort Sea region. Concomitant with this apparent increase, the Arctic has undergone rapid declines in sea ice extent and thickness (Comiso 2002, Serreze et al. 2007, Kwok and Rothrock 2009). Loss of sea ice increases the area of open water available for phytoplankton production (Arrigo et al. 2008), thereby increasing resources available to herbivorous copepod grazers that dominate the Beaufort Sea ecosystem, and potentially accelerating life cycles due to higher water temperatures (Ringuette et al. 2002). Increased resource availability could result in increased zooplankton abundance. Average abundances of the key herbivore *Calanus glacialis* and the small-bodied omnivore *Oithona similis* seem to have increased over the past decades in the Beaufort Sea region (Figure 4.1.18); however, additional data are needed to rigorously assess this trend. Other groups, such as the microcalanoids (*Microcalanus pygmaeus* and *Pseudocalanus* spp.) and larvaceans, do not show a clear trend (Figure 4.1.18). We note that the difficulties associated with collection and preservation of larvaceans (see Hopcroft 2005) make comparisons particularly challenging because they are very likely underrepresented in all of the above-mentioned collections.

The key Arctic *Calanus* species undergo extensive seasonal vertical migration; the timing of this seasonal migration, diapause, and reproduction are tightly coupled to the timing of the spring/summer phytoplankton bloom and can vary across the Arctic (Daase et al. 2013). While the current and near-future climate environment may favor a prolonged bloom that *Calanus* spp. are still able to exploit (Lavoie et al. 2010), extreme shifts in bloom phenology could result in a mismatch between the timing of *Calanus* spp. reproduction and the highly pulsed food environment that these Arctic copepods are physiologically fine-tuned to exploit (Søreide et al. 2010, Leu et al. 2011). This could result in an environment that is more favorable to smaller-bodied copepod species (e.g., *Pseudocalanus* spp. and *Oithona similis*) (Daufresne et al. 2009) or subarctic species (Falk-Petersen et al. 2006). Such shifts have the potential to profoundly impact Arctic food webs and energy flow (Falardeau et al. 2014). In addition to large-scale changes in sea ice extent and phenology, more localized impacts of climate change may impact Beaufort Sea zooplankton communities on seasonal and annual time scales. For example, changes in relative influence of different water masses on the Beaufort shelf have the potential to actuate changes in zooplankton community structure and magnitude; more frequent upwelling events (Pickart et al. 2013) could bring the large-bodied and lipid-rich copepod *Calanus hyperboreus* onto the shelf more often or in higher abundances, providing high-quality food for upper trophic levels utilizing the shelf environment. Upwelling events can also bring Arctic Halocline Water (AHW) that is under-saturated with respect to aragonite from the slope onto the shelf (Mathis et

al. 2012), resulting in unfavorable conditions for marine calcifiers such as the pteropod *Limacina helicina*. Conversely, increased freshwater input from river systems along the coast may create conditions more beneficial to neritic and euryhaline taxa than to oceanic taxa.

Continued efforts to survey Beaufort Sea zooplankton communities as the region undergoes environmental change will be critical in attempts to quantify community shifts and to inform process-based examinations of the region. Efforts to quantify change associated with a warmer climate [e.g., Intergovernmental Panel on Climate Change (IPCC 2014a)] or anthropogenic activities must necessarily consider the natural variability of the biological system of the Beaufort Sea; therefore, future efforts to quantify inter-annual variability in zooplankton communities of the Beaufort Sea would be particularly valuable. The interplay between climate change and zooplankton communities is complex and likely species-specific; therefore, robust datasets are needed to assess change.

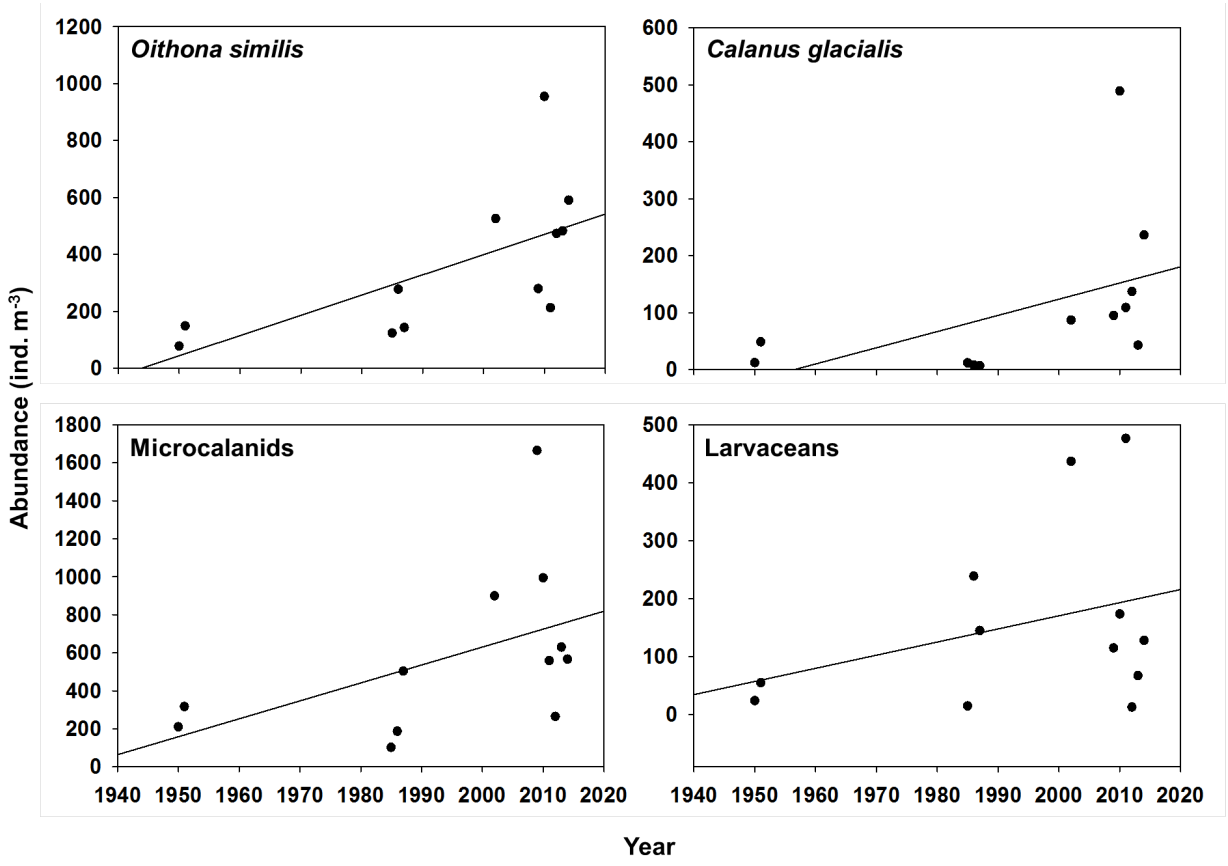

Figure 4.1.18. Comparison of average abundances (ind. m-^{3}) of select taxa in the Beaufort Sea region over the past 60 years. Trendlines are shown.

Data sources:
1950: USS *Burton Island*, 120-µm net, stations 3-11, 32, 33, 57, 58, 60, 62, 64, 66; Johnson 1956
1951: USS *Burton Island*, 120-µm net, stations 1, 5-11, 17, 20, 22, 31, 32, 36, 37, 38, 63, 64; Johnson 1956
1985-1987: NOGAP2, 85-µm net; Hopky et al. 1994a,b,c
2002: SBI, 150-µm net; Lane et al. 2008
2009: *Nahidik*, lower stratum 20–100 m, 150-µm net; Walkusz et al. 2013
2010: Camden Bay, 150-µm net; Smoot 2015
2011: BOEM 2011, 150-µm net; Smoot 2015
2012–14: Transboundary, 150-µm net

4.2 Vertical Distribution and Structure of Beaufort Sea Zooplankton during Transboundary 2012–14

4.2.1 Introduction

In addition to their widely recognized role as tropic intermediaries, zooplankton play an important role in processing and repackaging organic material as it sinks through the water column. Mesopelagic zooplankton fragment and aggregate particles via feeding and fecal pellet production; these modifications can influence remineralization and sinking rates, thereby impacting deeper waters and benthic communities (Dilling et al. 1998, Wilson et al. 2010, Robinson et al. 2010). Omnivory and carnivory generally increase in importance with depth (Auel and Hagen 2002, Yamaguchi et al. 2002, Blachowiak-Samolyk et al. 2007, Darnis et al. 2008, Wilson et al. 2010). Aetideids in the Greenland Sea can consume upwards of 40% of vertical carbon flux (Auel 1999), and although the simplified classical food chain depicts zooplankton as a uniform group, extensive trophic interactions take place between zooplankters. Euchaetidae are known to be voracious carnivores, exerting predation pressure not only on other copepods, but on fish eggs and larvae as well (Yen 1983, Yen 1987, Auel 1999). Therefore, zooplankton interactions may influence the flux and remineralization of organic matter, as well as trophic transfer.

Despite their important ecological and biogeochemical roles, mesopelagic communities are less studied than their epipelagic counterparts due to the inherent logistical demands and costs associated with deep-water sample collection and multi-layer sample processing. Vertical examinations of zooplankton communities have been done in the Arctic's basins (e.g., Hopkins 1969, Mumm 1991, Kosobokova and Hirche 2000, Auel and Hagen 2002, Hopcroft et al. 2005, Kosobokova and Hopcroft 2010), Fram Strait and the Greenland Sea (Blachowiak-Samolyk et al. 2007, Laakmann et al. 2009), and for key copepods in the Amundsen Gulf (Darnis and Fortier 2014). These efforts have inventoried mesopelagic taxa and demonstrated distinct communities associated with different water masses (Auel and Hagen 2002, Kosobokova et al. 2011, Kosobokova 2012), as well as vertical partitioning of the water column by congeners (Auel 1999, Laakmann et al. 2009, Kosobokova and Hopcroft 2010). Depth-stratified examinations of zooplankton communities have been carried out for other marginal Arctic seas (Eilertsen et al. 1989, Kosobokova et al. 1998, Arashkevich et al. 2002) but only with a coarse two-layer resolution of the epipelagic realm for two transects in the Canadian Beaufort Sea (Walkusz et al. 2013).

Historical efforts to document zooplankton in the Beaufort Sea are fragmented and hampered by gear biases (e.g. Johnson 1956, McConnell 1977), and focus on the epipelagic waters of the shelf. More recent efforts in the Alaskan and Canadian Beaufort have documented the influence of physical processes on zooplankton communities (Lane et al. 2008, Darnis et al. 2008, Walkusz et al. 2010, Walkusz et al. 2013, Smoot and Hopcroft 2017), but also focus on the epipelagic realm. This study focuses on the mesopelagic realm of the Beaufort Sea slope.

4.2.2 Methods

4.2.2.1 Sample Processing and Statistical Analyses

Here we present an examination of vertical structure in the zooplankton communities of the Beaufort Sea slope (depth ≥200 m) during Transboundary 2012–14 ranging from the surface to 1000 m in depth.

During laboratory processing, zooplankton samples were subsampled using a Folsom splitter until a given aliquot contained approximately 100 individuals of the most abundant taxa. Increasingly larger fractions were examined for larger and less abundant taxa. Organisms were identified, enumerated, measured, and, when appropriate, staged to determine community composition, abundance, and biomass. Measurements were completed using the ZoopBiom program (Roff and Hopcroft 1986) with the biomass of organisms predicted from species-specific length-dry-weight relationships derived from the literature or from morphologically similar species (Questel et al. 2013). Typically, 400–600 organisms were measured in each sample and organisms were identified to species level when possible; indistinguishable early copepodite stages of congeneric species were grouped together.

Samples were collected primarily during the extended daylight hours of the Arctic summer; however, a minority of stations fell during the short dark period. The literature suggests that synchronized diel vertical migration (DVM) is muted at this time of year (e.g., Cottier et al. 2006, Wallace et al. 2010). We compared day and night species abundances of individual species within each sampling interval (Wilcoxon test, $p < 0.05$). These analyses revealed no significant differences between day and night abundances of dominant species, with the exception of *Metridia longa* in the 0–50 m layer. Therefore, all day and night data were pooled for these analyses.

Data from Transboundary 2012–14 were pooled for these analyses and analyses were performed separately for 4RT abundance and biomass data. Community similarity was assessed using the Bray-Curtis similarity index (Bray and Curtis 1957) and community structure was explored with a hierarchical clustering routine and nMDS conducted in Primer (v6) (Clarke and Warwick 2010). Differences in the zooplankton community between water masses were assessed with a permutational analysis of variance (PERMANOVA) using 10,000 unrestricted permutations of raw data; this method has been shown to be robust to heterogeneous dispersions and unbalanced designs that are often encountered in ecological datasets (Anderson and Walsh 2013). Indicator species were identified for each water mass using the Indicator Value (IndVal) function (Dufrene and Legendre 1997) in R's labdsv software package (http: //cran.r-project.org/web/packages/labdsv/index.html). IndVal analysis identifies indicator species based on both specificity and fidelity to a given grouping; thus, the IndVal for a given species is maximized (1.0) when individuals of a species are observed at all sites of only one grouping. Significance of IndVals was assessed with Monte Carlo randomization using 10,000 permutations. We classified zooplankton taxa into trophic guilds based on published literature (Boxshall 1985, Nishida and Ohtsuka 1996, Mauchline et al. 1998, Matsuura and Nishida 2000, Turner et al. 2001, Haro-Garay 2003, Darnis et al. 2008, Homma and Yamaguchi 2010) to explore broad-scale trophic patterns associated with depth; however, we acknowledge that feeding modes of zooplankters are quite flexible and often vary across developmental stages. Finally, an average value for each physical parameter (T, S) was calculated for each zooplankton sampling interval. Missing physical data for water depths below 600 m in 2012 and 2013 were considered equivalent to data obtained from CTD casts conducted in 2014 with a Seabird

SBE911 CTD. These averages were related to the observed biotic community patterns using PRIMER's BEST routine. The BEST routine relates matrices of multidimensional biological and environmental data using both forward-selection and backward-elimination techniques (Clarke and Warwick 2010).

4.2.3 Results

4.2.3.1 General Patterns

We observed 112 taxonomic categories, including 55 copepod species, 10 hydromedusae, 10 amphipod, three polychaete, three chaetognath, two cladoceran, two euphausiid, two ctenophore, two pteropod, and one siphonophore species (Table 4.8). We also documented various groups of meroplankton, the most common of which were polychaete and bivalve larvae. Average abundance and biomass generally declined with depth, with the exception of a slight increase in both parameters at the transition to Atlantic Water (AW) (200–300 m), driven by stations along the 500 m isobath (see Table 4.3). In contrast, species richness generally increased with depth, with a maximum in the 300–500 m layer (Table 4.9). Species composition was generally characteristic of Arctic waters, with the exception of several Pacific expatriates, such as *Neocalanus cristatus*, *Eucalanus bungii*, *Metridia pacifica*, and *Pseudhaloptilus pacificus*. Although present in extremely low abundances (<1 ind. m^{-3}), these taxa reflect the influence of Pacific-origin waters far into the Arctic. Copepods were dominant in all sampling intervals in terms of both abundance and biomass; however, their relative importance in terms of biomass declined with depth as other groups, such as the amphipods and ostracods, became important contributors (Figure 4.2.1). The zooplankton community separated according to water mass (Figure 4.2.2a, 4.2.2b) with each water mass hosting a significantly different zooplankton community (PERMANOVA; p <0.001), regardless of whether abundance or biomass was used in the analysis. Similarly, community structure was correlated with salinity and depth, whether considered in terms of abundance (Spearman correlation (ρ) = 0.76, p <0.01) or biomass (ρ = 0.67, p <0.01). The addition of temperature did not improve the model (Table 4.10).

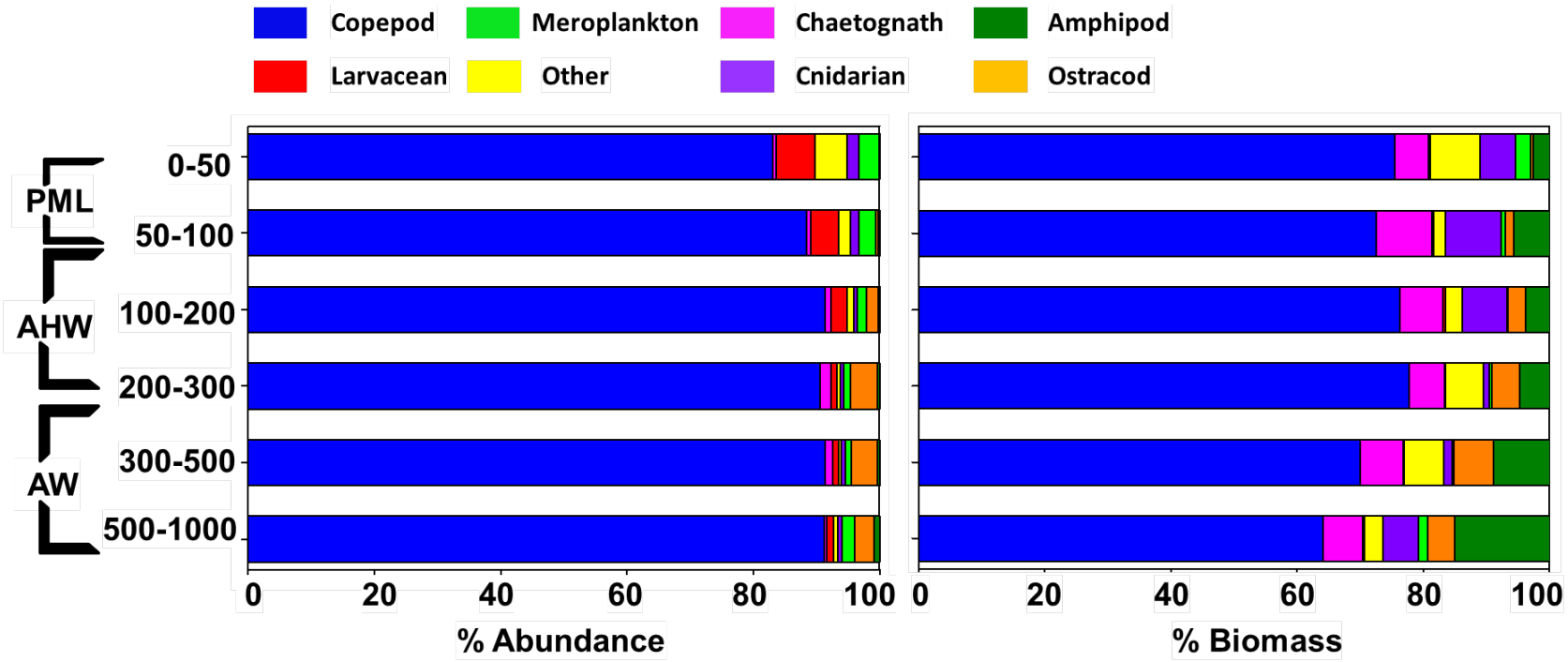

Figure 4.2.1. Contribution of major taxonomic groups to abundance and biomass of the zooplankton community within each sampling interval in the Beaufort Sea during Transboundary 2012–14. Water masses are noted.

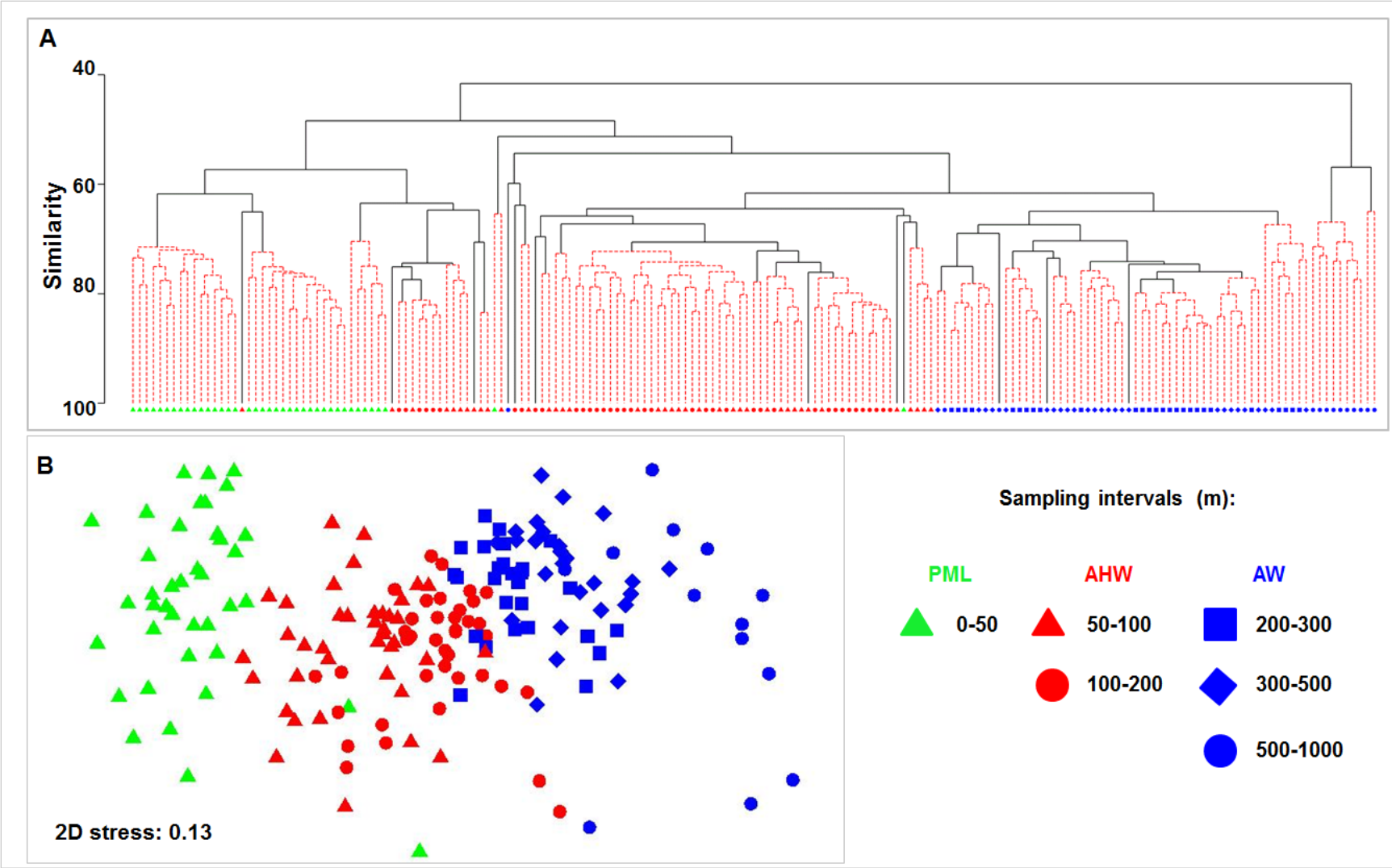

Figure 4.2.2a. Vertical zooplankton community structure in the Beaufort Sea during Transboundary 2012–14 based on abundance. A) Hierarchical clustering of Bray-Curtis sample similarity. Dotted lines connect samples that are not statistically unique (SIMPROF, p <0.05). B) Non-parametric multidimensional scaling (nMDS) of zooplankton community abundance overlain with observed clusters.

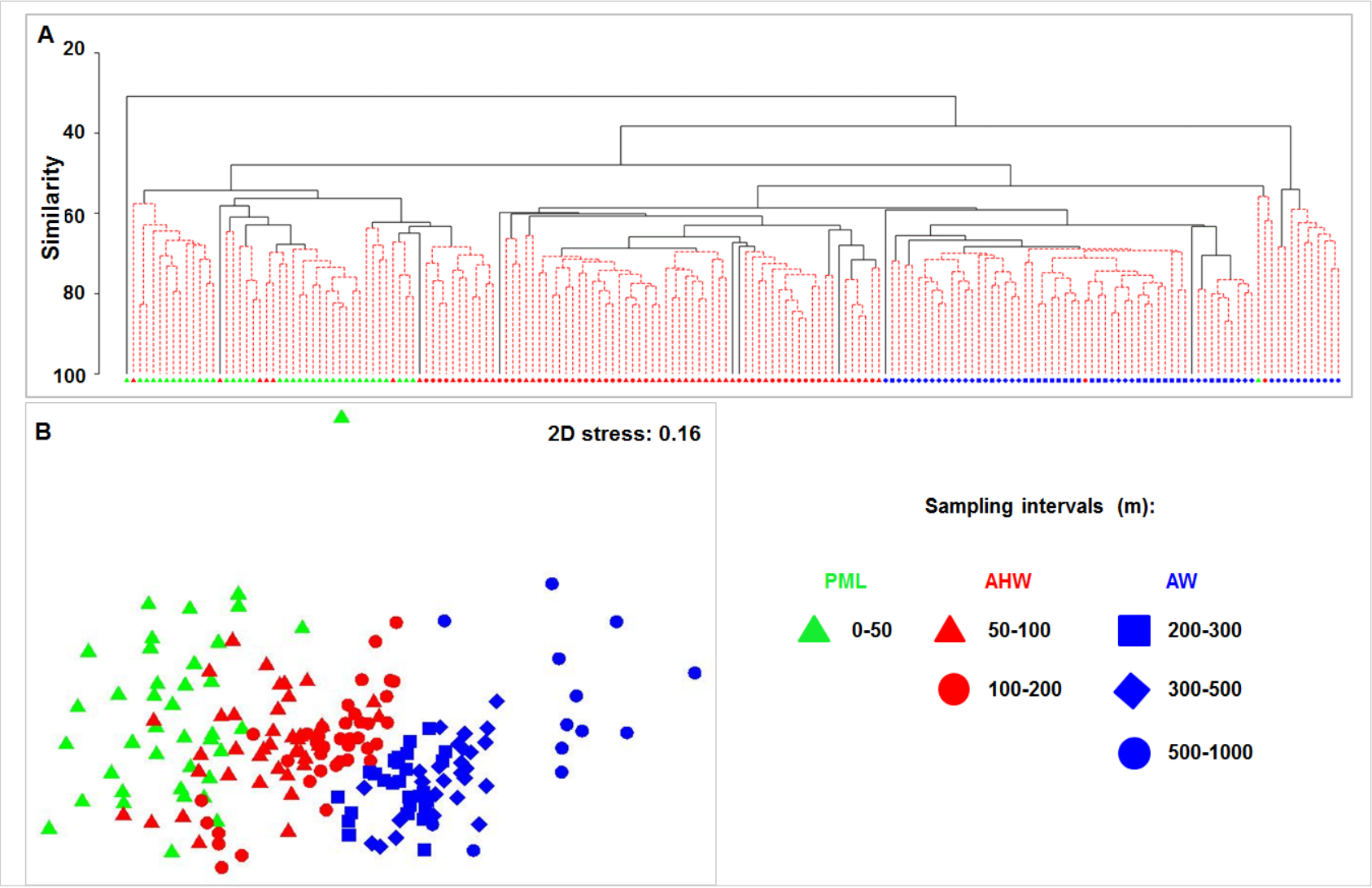

Figure 4.2.2.b. Vertical zooplankton community structure in the Beaufort Sea during Transboundary 2012–14 based on biomass. A) Hierarchical clustering of Bray-Curtis sample similarity. Dotted lines connect samples that are not statistically unique (SIMPROF, p <0.05). B) Non-parametric multidimensional scaling (nMDS) of zooplankton community biomass overlain with observed clusters.

Table 4.8. Mean abundance and biomass over the entire water column for taxa observed during Transboundary 2012–14.
Trophic guilds are indicated. *O* = omnivore, *P* = predator, *H* = herbivore, *Pa* = parasitic, * indicates sampling stratum where taxon was most abundant. Water masses and depth intervals (m) are noted. *Observed* indicates that taxon was encountered only a few times. –indicates average biomass <0.0001. *NC* indicates biomass was not calculated.

				PML	AHW		AW		
Guild	**Taxon**	**Avg. Abund. (Ind. m^{-3})**	**Avg. Biomass (mg DW m^{-3})**	**0–50**	**50–100**	**100–200**	**200–300**	**300–500**	**500–1000**
	Calanoida								
O	*Acartia longiremis*	0.424	0.0024	*					
O	*Acartia bifilosa*	0.012	-	*					
O	*Acartia* spp. (copepodite)	0.465	0.0011	*					
P	*Aetideopsis minor*	0.032	0.0015					*	
P	*Aetideopsis rostrata*	0.002	-				*		
O	*Augaptilus glacialis*	0.004	0.0019						*
P	*Euaugaptilus hyperboreus*	0.007	-						
O	*Eurytemora herdmani*	0.308	0.0028	*					
O	*Eurytemora richsingi*	Observed	-	*					
O	*Eurytemora* spp. (copepodite)	3.174	0.0061	*					
H	*Calanus glacialis*	17.101	3.1935	*					
H	*Calanus hyperboreus*	2.357	3.5441	*					
P	*Chiridiella reductella*	Observed	-						*
O	*Chiridius obtusifrons*	0.320	0.0334					*	
H	*Eucalanus bungii*	0.002	0.0010		*				
P	*Gaetanus brevispinus*	0.004	0.0016						*
P	*Gaetanus tenuispinus*	0.065	0.0134				*		
P	*Gaetanus* spp. (copepodite)	0.025	0.0010					*	
O	*Haloptilus acutifrons*	0.009	0.0017						*
P	*Heterorhabdus norvegicus*	0.883	0.0816				*		
H	*Jashnovia tolli*	0.014	0.0008		*				
H	*Limnocalanus macrurus*	0.049	0.0053	*					
O	*Metridia longa*	3.937	0.4761	*					
O	*Metridia pacifica*	0.013	0.0205		*				
O	*Metridia* spp. (copepodite)	3.247	0.0200				*		
O	*Microcalanus pygmaeus*	15.630	0.0261		*				
H	*Neocalanus cristatus*	0.012	0.0830				*		
H	*Neocalanus flemingeri*	Observed	-		*				
H	*Neocalanus plumchrus*	Observed	-		*				
P	*Paraeuchaeta barbata*	0.002	0.0083						*

Table 4.8, continued

				PML	AHW		AW		
Guild	**Taxon**	**Avg. Abund. (Ind. m^{-3})**	**Avg. Biomass (mg DW m^{-3})**	**0–50**	**50–100**	**100–200**	**200–300**	**300–500**	**500–1000**
P	*Paraeuchaeta glacialis*	0.837	0.6121		*				
P	*Paraeuchaeta polaris*	0.001	0.0019						*
P	*Paraheterorhabdus compactus*	0.010	0.0016					*	
P	*Pseudhaloptilus pacificus*	Observed	-					*	
H	*Pseudocalanus acuspes*	0.487	0.0051	*					
H	*Pseudocalanus mimus*	0.071	0.0007	*					
H	*Pseudocalanus minutus*	1.112	0.0175	*					
H	*Pseudocalanus newmani*	0.551	0.0035	*					
H	*Pseudocalanus* spp. (copepodite)	50.581	0.1526	*					
H	*Pseudocalanus* spp. (male)	0.639	0.0034	*					
O	*Scaphocalanus brevicornis*	0.087	0.0142						*
O	*Scaphocalanus magnus*	0.099	0.0284				*		
O	*Scolecithricella minor*	0.835	0.0056					*	
O	*Spinocalanus antarcticus*	0.260	0.0081					*	
O	*Spinocalanus elongatus*	0.003	-					*	
O	*Spinocalanus horridus*	0.018	0.0006						*
O	*Spinocalanus longicornis*	1.650	0.0416					*	
O	*Spinocalanus* spp. (copepodite)	0.011	0.0019						*
O	*Tharybis groenlandica*	Observed	-						*
O	*Temorites brevis*	0.035	0.0010					*	
P	*Tortanus discaudatus*	Observed	-						
O	*Undinella oblonga*	Observed	-					*	
	Monstrilloida								
Pa	*Monstrilla* spp.	Observed	-					*	
	Cyclopoida								
O	*Oithona similis*	127.095	0.5072	*					
	Poecilostomatoida								
	Atrophia glacialis	0.005	-						*
O	*Oncaea notopus*	0.021	0.0004						*
O	*Triconia borealis*	34.015	0.0577	*					
	Harpacticoida								
	Harpacticoida unid.	0.041	0.0102	*					
O	*Microsetella norvegica*	0.388	0.0012	*					
	Mormonilloida								
P	*Neomormonilla minor*	0.306	0.0019					*	

Table 4.8, continued

				PML	AHW		AW		
Guild	**Taxon**	**Avg. Abund. (Ind. m^{-3})**	**Avg. Biomass (mg DW m^{-3})**	**0–50**	**50–100**	**100–200**	**200–300**	**300–500**	**500–1000**
	Copepod Nauplii								
	Harpacticoid nauplii	3.013	0.0011	*					
	Calanoid nauplii	41.942	0.0979	*					
	Cyclopoid nauplii	0.683	0.0001	*					
	Appendicularia								
H	*Oikopleura vanhoeffeni*	3.209	0.0169	*					
H	*Fritillaria borealis*	15.320	0.0067	*					
	Chaetognatha								
P	*Eukrohnia hamata*	0.424	0.2085				*		
P	*Parasagitta elegans*	1.353	0.9661	*					
P	*Pseudosagitta maxima*	0.028	0.0060					*	
	Pteropoda								
P	*Clione limacina*	0.035	0.0534		*				
H	*Limacina helicina*	2.252	0.1068	*					
	Cladocera								
P	*Evadne nordmanni*	0.071	0.0010	*					
P	*Podon leuckartii*	3.008	0.0137	*					
	Ostracoda								
O	*Boroecia maxima*	1.519	0.1603				*		
	Mysidae								
O	*Boreomysis arctica*	0.006	0.1353					*	
O	*Mysis oculata*	0.001	0.1635				*		
	Euphausiacea								
H	*Thysanoessa inermis*	0.011	0.1044		*				
H	*Thysanoessa raschii*	0.008	0.0299			*			
	Euphausiid nauplii	0.004	-			*			
	Calyptopis	Observed	-			*			
	Furcilia	Observed	-		*				
	Euphausiid juvenile	Observed	-	*					
	Decapoda								
O	*Hymenodora glacialis*	0.001	0.0021						*
	Hippolytidae	Observed	0.0009		*				
	Pandalidae	0.002	0.0040			*			

Table 4.8, continued.

				PML	AHW		AW		
Guild	**Taxon**	**Avg. Abund. (Ind. m^{-3})**	**Avg. Biomass (mg DW m^{-3})**	**0–50**	**50–100**	**100–200**	**200–300**	**300–500**	**500–1000**
	Amphipoda								
O	*Apherusa glacialis*	0.003	0.0123						*
P	*Cyphocaris challengeri*	0.005	0.0059		*				
	Eusirus holmi	0.003	0.0781				*		
P	*Hyperia galba/medusarum*	0.004	0.0049			*			
P	*Hyperoche medusarum*	Observed	0.0039	*					
	Lanceola clausi	Observed	0.0001						*
H	*Onisimus* sp.	0.002	0.0002			*			
H	*Scina* sp.	Observed	-					*	
P	*Themisto abyssorum*	0.212	0.1316		*				
P	*Themisto libellula*	0.050	0.2750	*					
	Amphipod unid.	0.001	0.0004						
	Isopoda								
Pa	Isopoda (parasitic)	0.062	-						
	Siphonophora								
P	*Dimophyes arctica*	0.083	0.0131				*		
	Ctenophora								
P	*Beroe cucumis*	0.001	0.0111			*			
P	*Mertensia ovum*	0.004	0.0208	*					
	Hydrozoa								
P	*Aeginopsis laurentii*	0.094	0.0143	*					
P	*Aglantha digitale*	6.135	0.4571	*					
P	*Botrynema brucei*	0.002	-					*	
P	*Catablema vesicarium*	0.001	0.0070	*					
P	*Halitholus cirratus*	0.001	0.0069	*					
P	*Obelia longissima*	0.046	0.0063	*					
P	*Sarsia tubulosa*	Observed	0.0069					*	
P	*Sminthea arctica*	Observed	0.0004						*
P	*Ptychogena* sp.	0.037	-	*					
P	*Tiariopsis multicirrata*	0.052	-	*					
	Annelida								
O	*Pelagobia longicirrata*	0.024	-					*	
O	*Tomopteris septentrionalis*	0.029	0.0012				*		
O	*Typhoscolex muelleri*	0.002	-						*
H	**Rotifera**	9.119	NC	*					

Table 4.8, continued.

				PML	AHW		AW		
Guild	**Taxon**	**Avg. Abund. (Ind. m^{-3})**	**Avg. Biomass (mg DW m^{-3})**	**0–50**	**50–100**	**100–200**	**200–300**	**300–500**	**500–1000**
O	**Cumacea**	0.001	0.0001						
	Meroplankton								
	Barnacle cyprid	0.102	0.0477	*					
	Barnacle nauplii	0.029	-		*				
	Bipinnaria	0.134	0.0002	*					
	Bivalve larvae	2.252	0.0051	*					
	Cyphonautes	0.046	0.0002	*					
	Decapod larvae	Observed	0.0003	*					
	Echinoderm larvae	0.200	0.0035	*					
	Gastropod larvae	0.158	0.0001	*					
	Megalops	0.004	0.0056		*				
	Ophiuroid larvae	0.128	0.0002	*					
	Pagurid zoea	0.020	0.0002		*				
	Polychaete larvae	7.976	0.0203	*					

Table 4.9. Mean abundance, biomass and species richness of the zooplankton community in each sampling stratum for the Beaufort Sea during Transboundary 2012–14. Water masses are noted.

Water Mass	**Depth Interval (m)**	**Avg. Abundance (ind. m^{-3}) ± SE**	**Avg. Biomass (mg DW m^{-3}) ± SE**	**Species Richness**
PML	0–50	1231± 84	24.3±3.4	56
AHW	50–100	257± 35	12.8± 1.9	59
AHW	100–200	102± 9	8.3± 1.7	68
AW	200–300	104±12	10.0± 1.2	61
AW	300–500	81 ±11	7.1± 1.2	74
AW	500–1000	21± 6	1.9 ±0.8	71

Table 4.10. Relationship between vertical zooplankton community structure and environmental variables during Transboundary 2012–14, as revealed by BEST analysis for Temperature (*T*), Salinity (*S*), and Depth (*D*).
* Indicates best variable combination explaining observed zooplankton community structure.

No. Variables			
Abundance			
2	***S,D***	***S,T***	***T,D***
	0.76*	0.61	0.56
3	***S,D,T***		
	0.73		
Biomass			
2	***S,D***	***S,T***	***T,D***
	0.67*	0.52	0.55
3	***S,D,T***		
	0.66		

4.2.3.2 Water Mass Communities

Average abundance and biomass in the PML (0–50 m) were 1230 ± 84 ind. m^{-3} and 24.3 ± 3.4 mg DW m^{-3}, respectively. The *Pseudocalanus* species complex was identified as an indicator (IndVal: 0.60, p <0.001) of the PML (Figure 4.2.3a). Herbivory and omnivory were the dominant feeding modes of the holozooplankton in the PML (Figure 4.2.4); omnivorous *Oithona similis* dominated numerically, while large-bodied *Calanus* species dominated herbivorous biomass. A total of 56 taxa were observed in the PML.

Arctic Halocline Waters (AHW) (50–100 and 100–200 m) were characterized by marked decreases in average abundance (257 ± 35 and 102 ± 9 ind. m^{-3}) and biomass (12.8 ± 1.9 and 8.3 ± 1.7 mg DW m^{-3}). We observed 59 taxa in the 50–100 m layer and 68 taxa in the 100–200 m layer. The community was characterized by higher abundances of the copepods *Paraeuchaeta glacialis*, *Microcalanus pygmaeus*, and *Metridia longa*. *P. glacialis* was identified as an indicator species (IndVal: 0.39, p <0.001) for AHW (Figure 4.2.3b). Predatory biomass increased in AHW (Figure 4.2.4), driven largely by the chaetognath *Parasagitta elegans*.

Average abundance and biomass were lowest in the Atlantic layer (200–300, 300–500, 500–1000 m), where abundance values ranged from 104 ± 12 ind. m^{-3} in the 200–300 m layer to 21 ± 6 ind. m^{-3} in the 500–1000 m layer. Biomass ranged from 10.0 ± 1.2 mg DW m^{-3} in the 200–300 m layer to1.9 ± 0.8 mg DW m^{-3} in the 500–1000 m layer. The 300–500 m layer of the AW exhibited the highest species richness, at 74 taxa. Several taxa were found exclusively in the Atlantic layer, including *Oncaea notopus*, *Chiridiella reductella*, and the cnidarian *Sminthea arctica*. The copepod *Spinocalanus longicornis* was identified as an indicator species (IndVal: 0.89, p <0.001) for the Atlantic layer (Figure 4.2.3c). Mesopelagic copepods, including the species mentioned above and members of the Aetideidae, were important numerical contributors in this layer. Predatory biomass in the Atlantic layer was dominated by the chaetognath *Eukrohnia hamata* and cnidarians, including both siphonophores and hydrozoan medusae. Additionally, the large decapod *Hymenodora glacialis* contributed to high predatory biomass in AW, and the relative numerical contribution of predators peaked in AW (Figure 4.2.4).

Contributions from omnivores, including copepods such as *Triconia borealis* and *Spinocalanus* spp., which are well adapted to utilize refractory material, were also important in AW.

4.2.3.3 Arctic Guild of Copepods

The copepods, dominant in all depth layers, were primarily composed of the Arctic guild of taxa that included *Calanus glacialis*, *Calanus hyperboreus*, *Metridia longa*, *Oithona similis*, *Triconia borealis*, *Microcalanus pygmaeus*, and the *Pseudocalanus* species complex. This group accounted for upwards of 50% of copepod abundance and biomass in all sampling intervals, although relative contribution declined with depth (Figure 4.2.5). The relative contribution of this guild of taxa to copepod abundance and biomass peaked in the 50–100 and 0–50 m layers, respectively. Within the guild of Arctic taxa, small-bodied *O. similis*, *T. borealis*, *M. pygmaeus*, and *Pseudocalanus* spp. dominated numerically. *O. similis* and *Pseudocalanus* spp. dominated the surface layers, giving way to *T. borealis* and *M. pygmaeus* with increasing depth. In terms of biomass, large-bodied *C. glacialis*, *M. longa*, and *C. hyperboreus* dominated all sampling depths, with the relative contribution of each species peaking in the PML, AHW, and AW, respectively (Figure 4.2.6).

4.2.3.4 Mesopelagic Copepods

Although present in lower abundances than the dominant guild of copepods, mesopelagic genera provide insight into community structure. Mesopelagic copepod families, such as Aetideidae, Heterorhabdidae, Scolecitrichidae, and Spinocalanidae occurred in AHW and became important contributors in the Atlantic layer (Figure 4.2.5). Within these families, congeners displayed different depth preferences, even within water masses (Figure 4.2.7). For example, within the aetideids, *Chiridius obtusifrons* exhibited a wide depth range, occurring in all sampling intervals. *Aetideopsis* species occurred in sampling intervals below 200 m, and *Chiridiella reductella* was only encountered in the deepest sampling interval (500–1000 m). The two Heterorhabdid species observed in the study area exhibited vertical partitioning in the water column, with *Heterorhabdus norvegicus* present in all sampling intervals and peaking at depths between 200 and 500 m. In contrast *Paraheterorhabdus compactus* was only present below 100 m. *Spinocalanus* and *Paraeuchaeta* species exhibited similar patterns within their respective genera.

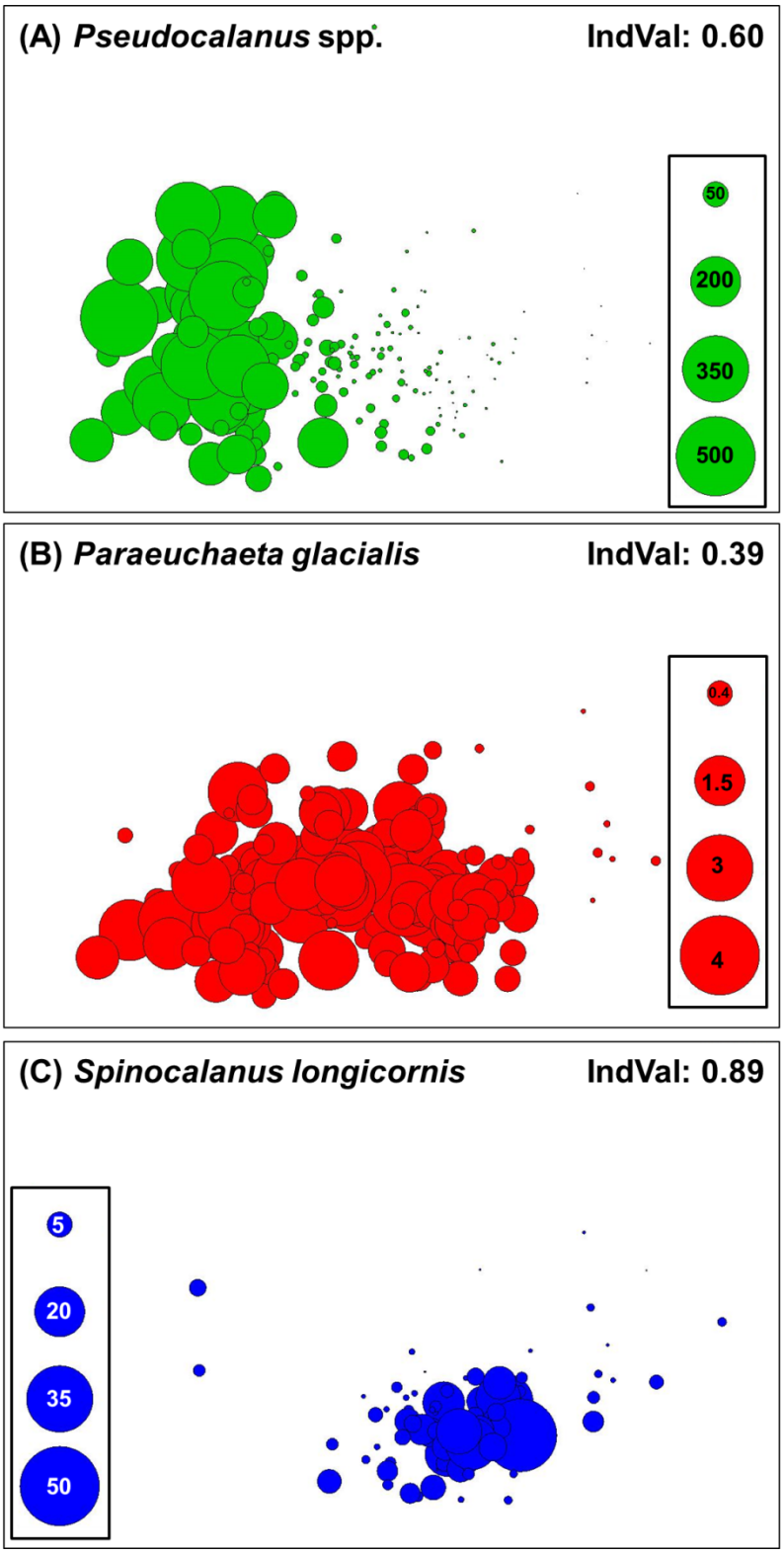

Figure 4.2.3. Abundance (ind. m^{-3}) of indicator species in the Beaufort Sea superimposed on nMDS plots decomposed by water masses for Transboundary 2012–14.
A) PML – Polar Mixed Layer, B) AHW – Arctic Halocline Water, C) AW – Atlantic Water.

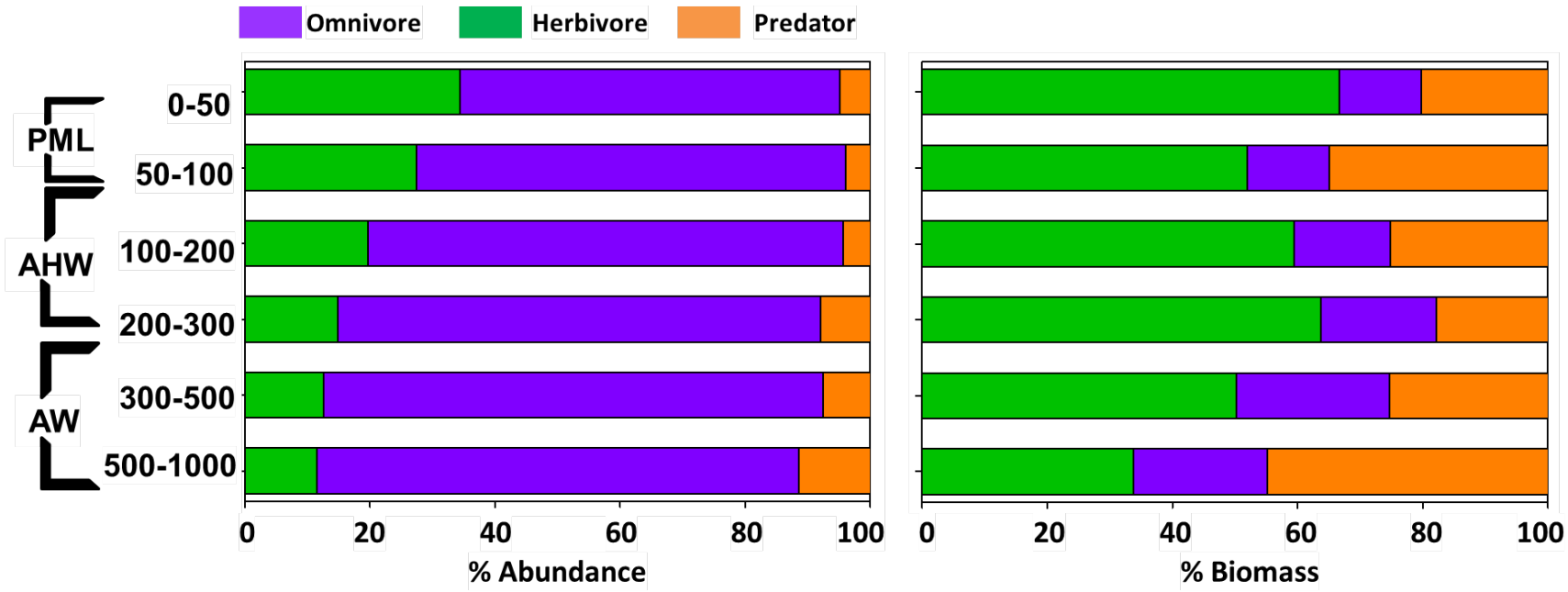

Figure 4.2.4. Contribution of holozooplankton trophic guilds to abundance and biomass within each sampling stratum in the Beaufort Sea during Transboundary 2012–14. Water masses are noted.

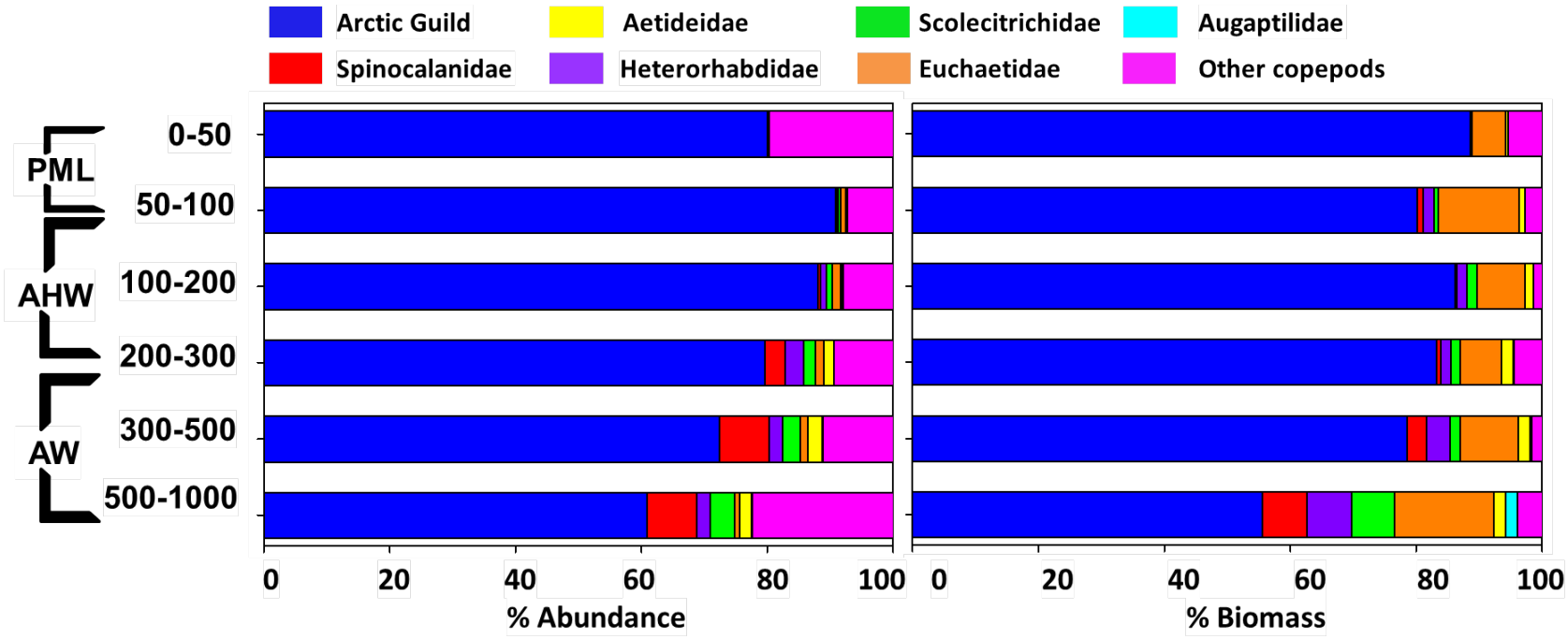

Figure 4.2.5. Contribution of major copepod groups to abundance and biomass within each sampling stratum in the Beaufort Sea during Transboundary 2012–14. Water masses are noted.

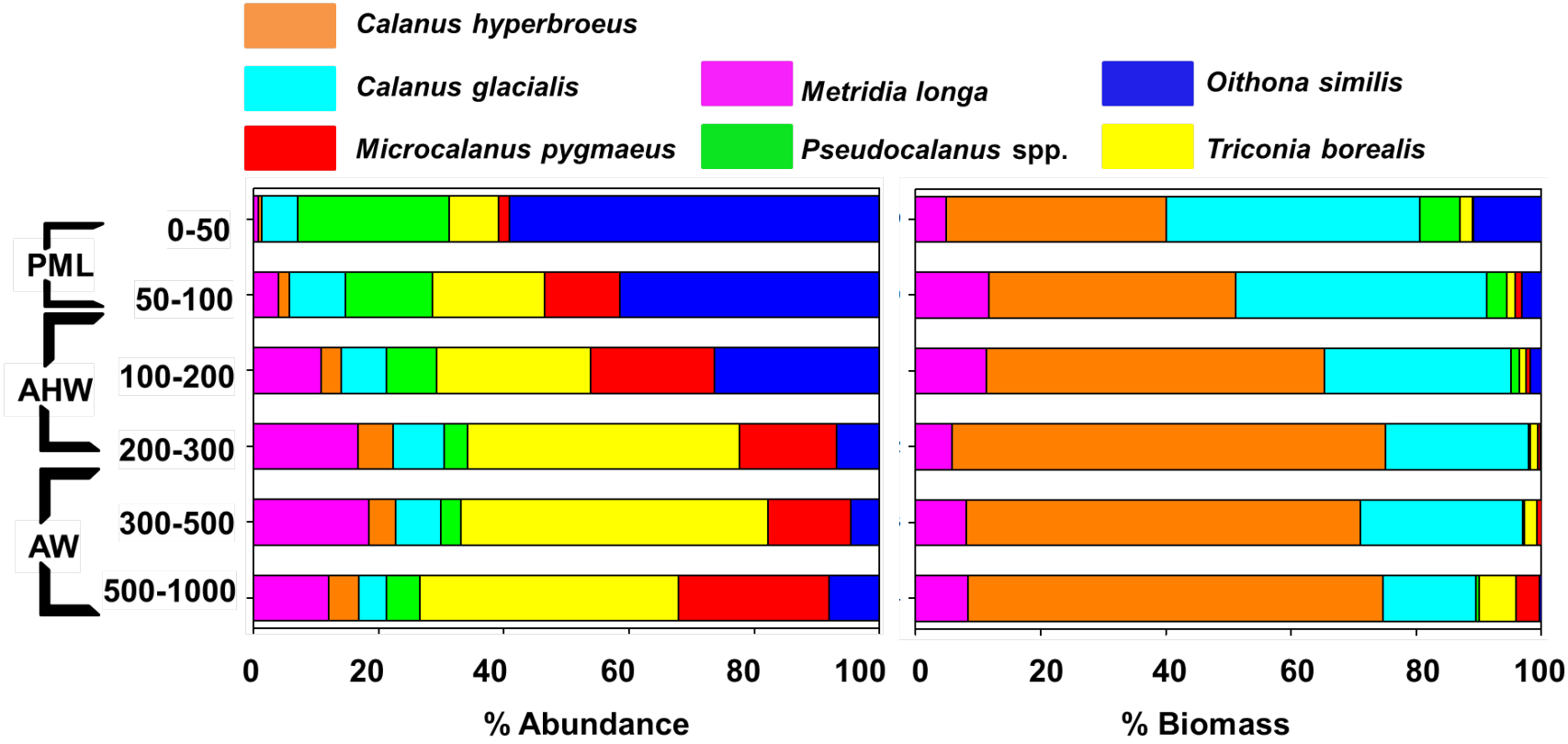

Figure 4.2.6. Contribution of taxa to dominant guild of Arctic copepods in terms of abundance and biomass in each sampling stratum in the Beaufort Sea during Transboundary 2012–14. Water masses are noted.

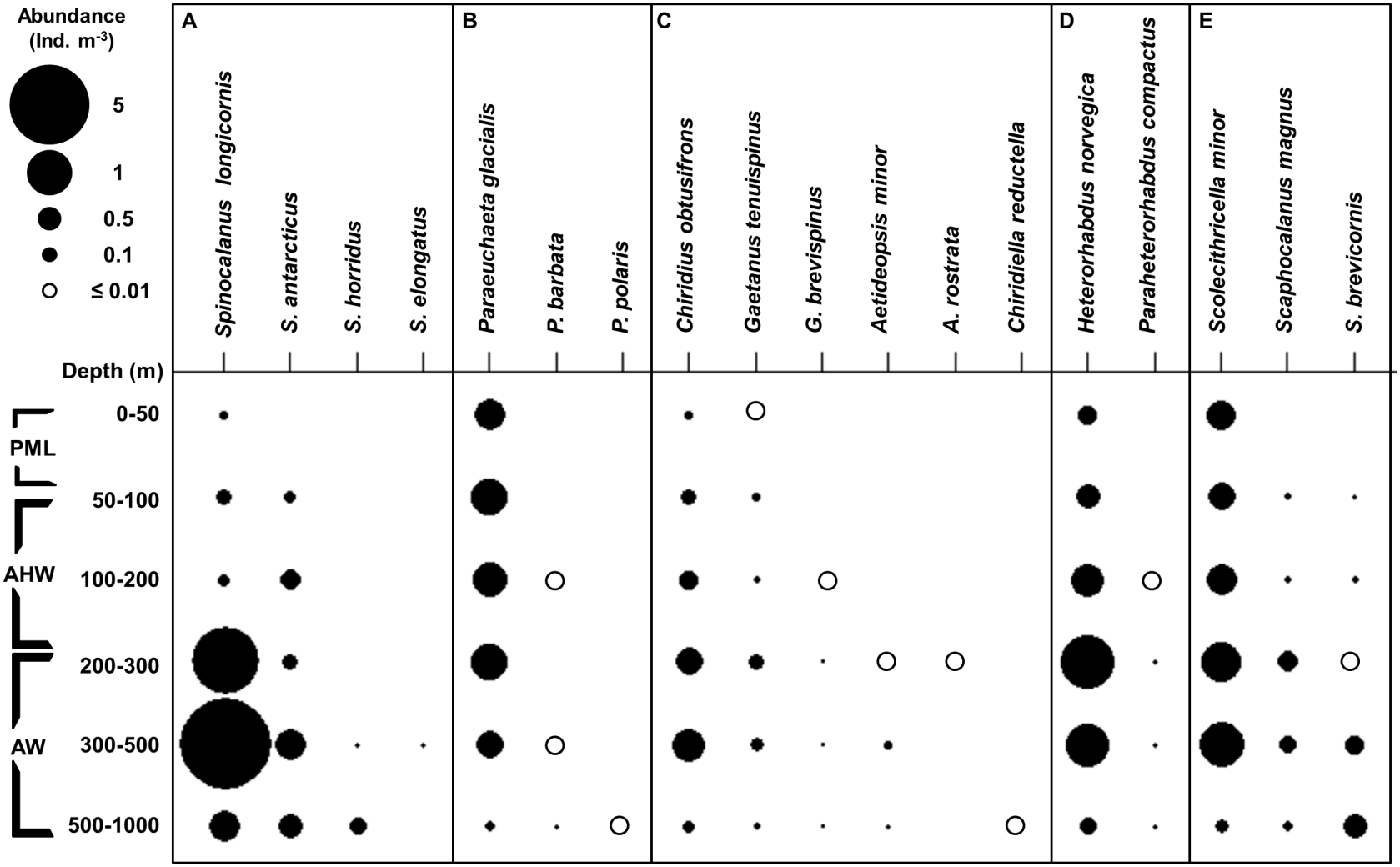

Figure 4.2.7. Generalized vertical distribution of select copepod species in each sampling stratum in the Beaufort Sea during Transboundary 2012–14.
Based on mean of all stations. A) Spinocalanidae B) Euchaetidae C) Aetideidae D) Heterorhabdidae E) Scolecitrichida

4.2.4 Discussion

4.2.4.1 Depth Associated Patterns and Species Inventory

Our results are in accordance with the general depth-associated patterns of abundance, biomass, and species diversity observed in vertical examinations of zooplankton communities in the Arctic's interior basins (Hopkins 1969, Mumm et al. 1998, Auel and Hagen 2002, Kosobokova and Hopcroft 2010, Kosobokova et al. 2011). Abundance and biomass were concentrated in the upper layer of the water column and decreased with depth, while species richness generally increased with depth as mesopelagic genera appeared. We observed a slight increase in abundance and biomass in the transition to Atlantic waters (200–300 m), as did Kosobokova and Hopcroft (2010) in the Canadian Basin. This is likely due to the fact that this layer represents a transitional zone and, therefore, is inhabited by the large-bodied *Calanus* species and also mesopelagic species such as *Spinocalanus longicornis*. We report higher average biomass values for mesopelagic layers between 100 and 1000 meters than reported in Kosobokova and Hopcroft (2010) and Auel and Hagen (2002), which is consistent with the expectation that continental slopes are more productive than the deep basins (Ashjian et al. 2003, Kosobokova and Hirche 2009, Kosobokova and Hopcroft 2010) (Table 4.11).

The species composition of the Beaufort Sea slope observed in this study is in agreement with similar studies from the Canada Basin (e.g., Hunt et al. 2014, Kosobokova and Hopcroft 2010); all confirm the dominance of a low diversity guild of Arctic copepod taxa in the epipelagic realm that gives way to increased contributions from mesopelagic taxa at depth. However, the presence of euryhaline taxa, such as *Eurytemora* spp. and rotifers, in the PML during Transboundary 2013 represents an important departure from similar species inventories from the Arctic's basins. These euryhaline taxa reflect the dynamic nature of the Beaufort Sea shelf environment, which can be profoundly influenced by seasonal freshwater inputs. The presence of rotifers in surface layers is characteristic of major river outflows and is consistent with observations from the Laptev Sea, which is heavily influenced by numerous Siberian rivers (Abramova and Tuschling 2005).

We did not encounter the multiple *Lucicutia* and *Mimocalanus* species documented in Kosobokova and Hopcroft (2010) as being largely restricted to depths below 1000 m. This is likely due to our more limited sampling depth and the use of subsampling rather than processing 100% of every sample. Extremely low abundances of subarctic epipelagic copepods (e.g., *Neocalanus* spp.) have been documented across the Chukchi Plateau and into Central Basin (Hopcroft et al. 2005, Kosobokova and Hopcroft 2010); our results demonstrate the penetration of these taxa into the eastern portion of the Alaskan Beaufort Sea. We also observed *Pseudhaloptilus pacificus*, a mesopelagic subarctic copepod, at one station in our survey in the 300–500 m layer. Kosobokova and Hopcroft (2010) also observed this copepod in low numbers in the Canada Basin, noting that it is likely a Pacific expatriate, despite the lack of a mechanistic explanation for the transport of deep-water copepods through the shallow Bering Strait. In contrast, Atlantic expatriate copepods (e.g., *Calanus finmarchicus*) were not observed in our study region and have rarely been observed past the Lomonosov Ridge (Thibault et al. 1999, Kosobokova and Hirche 2000).

Table 4.11. Comparison of average biomass (mg DW m^{-3}) in zooplankton sampling intervals from the Beaufort slope and the Arctic's basins.

Layer (m)	Transboundary 2012–14	Kosobokova and Hopcroft 2010	Auel and Hagen 2002
0–25	24	21	20.9
25–50		38	
50–100	13	3.8	3.3
100–200	8	2.6	
200–300	10	3.8	0.6
300–500	7	2.2	
500–1000	1.9	0.8	0.5

4.2.4.2 Community Structure

Similar to other depth-stratified examinations in the Arctic, we observed community structure as characterized by gross community separation according to water mass and additional internal structure within water masses (Auel and Hagen 2002, Kosobokova and Hopcroft 2010, Kosobokova et al. 2011). The community in the PML was composed of a fairly low-diversity group of Arctic copepods and, in the case of the 2013 study area, low numerical contributions of euryhaline taxa. Carmack et al. (1989) note that exchange between the shelf environment and the offshore environment occurs primarily in waters above the halocline. Contributions from euryhaline taxa observed in the PML highlight this phenomenon as abundance of euryhaline taxa, such as *Eurytemora* spp., varied across the upper layer of the survey area due to variations in the extent of the freshwater lens. Thus, a given depth interval is not necessarily homogenous, especially when considering the upper layers of the hydrographically-dynamic shelf and slope (see Section 4.1.4.1 and Table 4.3). Despite these nuances, community differences associated with depth were generally more pronounced than differences associated with variation within a given depth interval; this observation also holds true on the basin-level scale (Auel and Hagen 2002).

Below the PML, the traditional guild of Arctic copepods also dominated AHW; however, species richness increased as mesopelagic genera began to appear. The relative contribution of the dominant Arctic group of copepods reached a minimum in AW, where mesopelagic copepods became significant contributors to the community. This general pattern is consistent with previous depth-stratified examinations in the Arctic (Kosobokova and Hirche 2000, Auel and Hagen 2002, Kosobokova and Hopcroft 2010, Kosobokova et al. 2011), as is the pattern of increased omnivory and carnivory with depth. Our results also mirror observations of increased contributions from cnidarians and amphipods with depth and a peak in ostracod contribution at intermediate depths (Kosobokova and Hopcroft 2010, Kosobokova et al. 2011). Kosobokova et al. (2011) report presence of amphipod taxa that are traditionally considered to be ice-associated within the pelagic realm; we also documented several such species within the water column, including *Apherusa glacialis* and *Eusirus holmi*, which supports the previous authors' conclusion that these species may be considered pelagic transients. We also observed vertical partitioning of the water column by congeneric species, contributing to additional community structure within water masses, as reported by Auel (1999), Kosobokova and Hirche (2000), Laakmann et al. (2009), and Kosobokova and Hopcroft (2010). Depth ranges for species were largely consistent

with these studies, with many species exhibiting vertical ranges that overlap multiple water masses. This is not surprising, given that water mass boundary depths are not absolute.

In summary, zooplankton communities of the Beaufort Sea slope are similar in species composition, structure, and diversity to the communities in the Arctic's interior basins, with the exception of increased contributions from euryhaline and neritic taxa in surface waters, which can vary depending on the degree of exchange between the shelf and slope. Additionally, average biomass measures in the depth intervals between 100 and 1000 m were higher than those reported from similar intervals in the basin, likely due to enhanced productivity along the continental shelf margin. Expected increases in pelagic production on continental shelves due to reduced ice cover (Arrigo et al. 2008) may result in increased export production to mesopelagic water layers of the Beaufort Sea. This, in turn, may support higher mesopelagic zooplankton biomass and has implications for trophic interactions, particle flux, and biogeochemical cycles.

5.0 INFAUNA

Sarah Hardy

5.1 Introduction

The objectives of the infauna component were to assess community structure of benthic macro-infaunal invertebrates (>500 μm) and to identify environmental variables that correlate with community structure across the study region. Infauna play a key role in the cycling of organic matter in sediments (Piepenburg et al. 1995) and are prey for higher trophic levels. Moreover, infaunal communities are widely used as ecological indicators in disturbance and pollution monitoring schemes (Patrício et al. 2012) because they tend to integrate processes over longer time spans than pelagic systems. Thus, seasonal and interannual variability ("noise") can be dampened in sediment communities, allowing for observation of longer-term trends in ecosystem function (Smith et al. 2006). The infaunal communities of the US Beaufort shelf have been largely unstudied since the 1970s, and deeper areas on the slope have been ignored. Early studies showed a decreasing influence of advective influx of nutrient-rich Pacific waters toward the east, which was reflected in a gradient of decreasing benthic infaunal biomass from west to east along the Beaufort shelf (e.g., Carey et al. 1984). The Canadian Beaufort shelf benthos was surveyed in the 1960s and 70s (Atkinson and Wacasey 1989), with no additional work until the Canadian Arctic Shelf Exchange program (2002–2004, Conlan et al. 2008).

Due to logistical challenges, a limited number of samples were collected for this project during the 2012 field season. No infaunal sampling was conducted in 2013, and only sites <350 m were sampled in 2014. Here, we present data from the eastern- and western-most regions of the study area (Transects B1/B2 and TBS, Colville Plume (CP) and Outer Mackenzie Plume (OMP), respectively) and from a few stations in the central study area (Transect A5, Camden Bay (CB)) to give a general sense of differences in community structure in these different environmental settings.

5.2 Methods

We conducted quantitative sampling of infauna using a 0.25-m^2 Ocean Instruments spade box core (2012; 50–1000 m) and 0.1-m^2 van Veen grab sampler (2014; stations ≤350 m). Box core samples were primarily collected along transect B1 but one sample (50 m) was collected on B2. Due to their relatively close proximity to one another, samples from these two transects were combined as Transect B1/B2 in the figures below and are referred to as the Colville Plume (CP) region. We also present data from transect A5, referred to as Camden Bay (CB), and TBS, referred to as Outer Mackenzie Plume (OMP). Attempts were made to obtain three replicate box core samples per station, but we only obtained three at one station (B1-200) and two at another station (B1-500). Three replicate grab samples were obtained at most stations. Where available, data from replicate cores or grabs were averaged together, and mean values are used in all data analysis and figures.

Box core samples were divided in half, with one half allocated to environmental sampling and the other half to infauna. For box cores, the top 5-cm layer was removed using a spatula and transferred into a bucket with filtered seawater. For grab samples, the whole grab was emptied into a tub, which was then filled with seawater. Samples were gently agitated by stirring with a gloved hand, and the water/sediment slurry was slowly poured over a 500-μm sieve. Material

retained on the sieve was transferred to jars and preserved in 10% formalin. In the lab, samples were stained with rose bengal and transferred to 70% isopropanol before sorting on a dissecting microscope. All macrofaunal organisms were removed. Some large nematode worms and foraminifera, which are typically considered meiofaunal organisms (<63 μm), were detected in these samples. Nematodes were removed and counted but were not included in the analysis of community structure. Foraminifera were not removed and were returned to sample jars with residual sorted sediments. All macrofaunal organisms were sorted and identified to the lowest possible taxonomic level, and abundance and biomass were recorded. Here we examine the annelid assemblage in more detail as it accounted for the majority of the abundance of macrofauna. We focused on family-level taxonomy for this preliminary analysis because many taxa could not be identified to genus or species due to their small size, need for specialist taxonomic expertise, or damage to specimens. Nonetheless, family-level identifications provide a good indication of the functional role of each taxon in the community.

Analysis of this preliminary dataset was conducted using PRIMER-E v. 7. Abundance data were fourth-root transformed (4RT), and a non-metric multi-dimensional scaling (nMDS) ordination was produced based on the Bray-Curtis resemblance matrix. Similarity profile analysis (SIMPROF) tests were used to determine which stations were statistically similar in terms of community structure. Similarity percentage analysis (SIMPER) analysis was used to examine the Annelida assemblage and determine which families contributed the most to similarity among groups within each cluster identified using the SIMPROF test. Environmental predictors of annelid assemblage structure (based on family-level data) were evaluated using distance-based linear models (DistLM). Predictors of total macrofaunal abundance were evaluated using DistLM conducted on a Euclidean distance matrix, which is equivalent to a univariate linear regression. Results of DistLM for annelid community structure were visualized using distance-based redundancy analysis (dbRDA).

5.3 Results and Discussion

5.3.1 General Patterns

Box core samples collected along transect B1/B2 showed peak macrofaunal abundance at 350 m depth (Figure 5.3.1), coincident with the peak pigment concentration in sediments (see Section 3.4). Approximately 63% of the total macrofaunal abundance at the 350-m station was made up of one family of polychaetes (Cossuridae), indicating low diversity and high dominance (Figure 5.3.2). This pattern can be indicative of high organic enrichment that can lead to anoxia in sediments which excludes many taxa unable to tolerate such conditions (Pearson and Rosenberg 1978). Photographs of the core surface from B1-350 m show black anoxic mud exposed at the surface of the core during recovery, suggesting a very shallow oxygenated sediment layer (Figure 5.3.3).

While stations <350 m were lower in pigment concentration and abundance of total macrofauna, family-level diversity of the Annelida (polychaete worms, the dominant component of the macrofauna; Figure 5.3.1) was higher at these stations (Figure 5.3.2). Eighteen families of polychaetes were represented at the 200-m station while only 11 were present at 350 m. Of the three transects examined here, A5 (Camden Bay) was lowest in total macrofaunal and annelid abundance. The TBS transect (Outer Mackenzie Plume) showed the greatest contribution of crustaceans to total abundance. Molluscs comprised a greater proportion of the total macrofauna at 350 m depth for both A5 and TBS transects, whereas they were not very abundant until 1000

m on transect B1/B2. While A5 and TBS did not show the extreme peaks in abundance at 350 m, they did show a decline with depth down to 200 m and an increase at 350 m, indicating that elevated abundance at 350 m may be a general trend.

Figure 5.3.4 shows a non-metric multidimensional scaling (nMDS) plot of annelid assemblage structure for all the stations analyzed to date; pie slices are proportionately sized to indicate the abundance of that taxon at that station. Four significant groups of stations were identified with SIMPROF tests. Stations B1-350 and B1-500 form one group, characterized by high abundance of Cossuridae and Nephtyidae. The 1000-m site on B1 formed its own group, with a relatively high abundance of Orbiniidae, Spionidae, and Capitellidae. A5-20 and A5-350 also formed their own groups. All of the other stations clustered together at >60% similarity, with high abundance of several families, most notably Cirratulidae, Sigalionidae, and Capitellidae. In comparison, nMDS for whole macrofaunal community structure is plotted in Figure 5.3.5. For both the annelid assemblage and the whole community, Transect B1/B2 appears quite different than the other two transects, with the deepest 1000-m site appearing quite separated from the other locations. The general trend is that shallower stations were more similar in taxonomic composition across the whole sampling region, and stations >200 m showed more variation among transects. Analysis of similarity (ANOSIM) tests for differences in community composition by transect, or between shelf/slope depths (sites pooled across the whole study area), showed no significant difference. These broad-scale comparisons may obscure the variability observed across depths within a given transect.

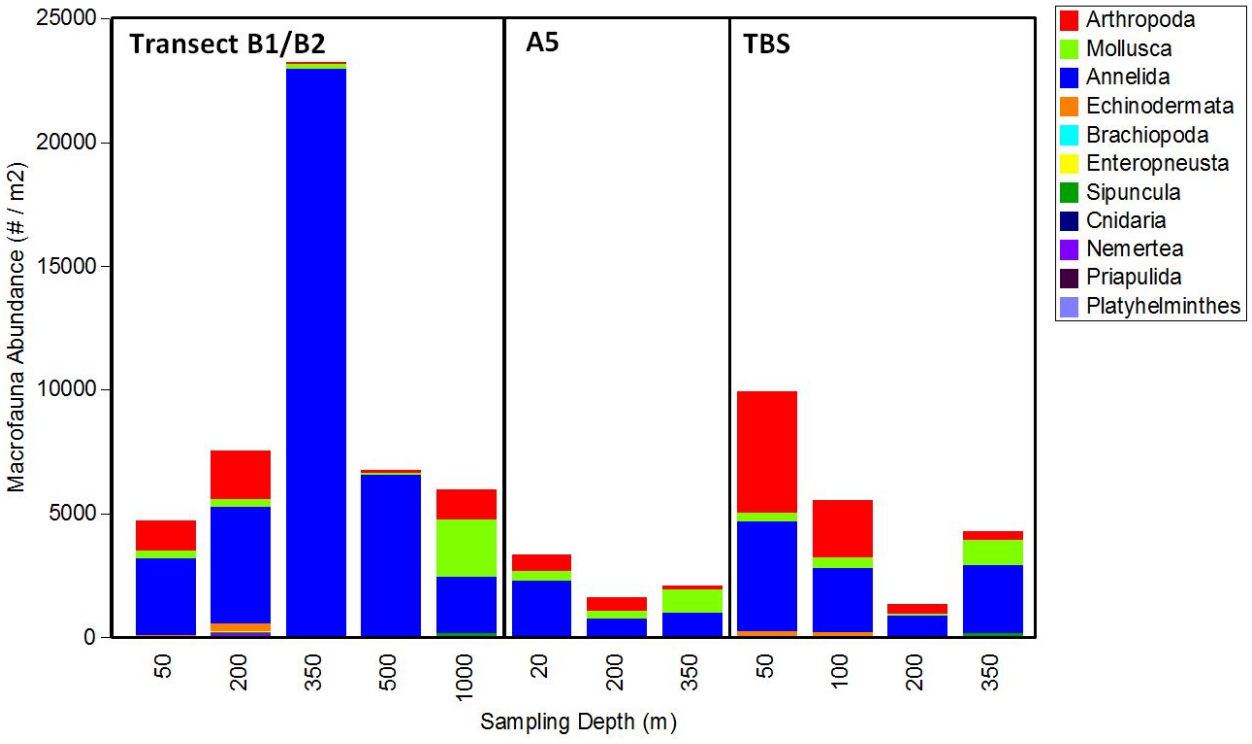

Figure 5.3.1. Total macrofaunal abundance (individuals m^{-2}) by phylum.
Only stations <350 m were sampled at transects A5 (Camden Bay, 2014) and TBS (Outer Mackenzie Plume, 2014). For transects B1/B2 (2012), the 50-m station is located on B-2 and the other stations are located on B1 (both Colville Plume, combined here due to close proximity).

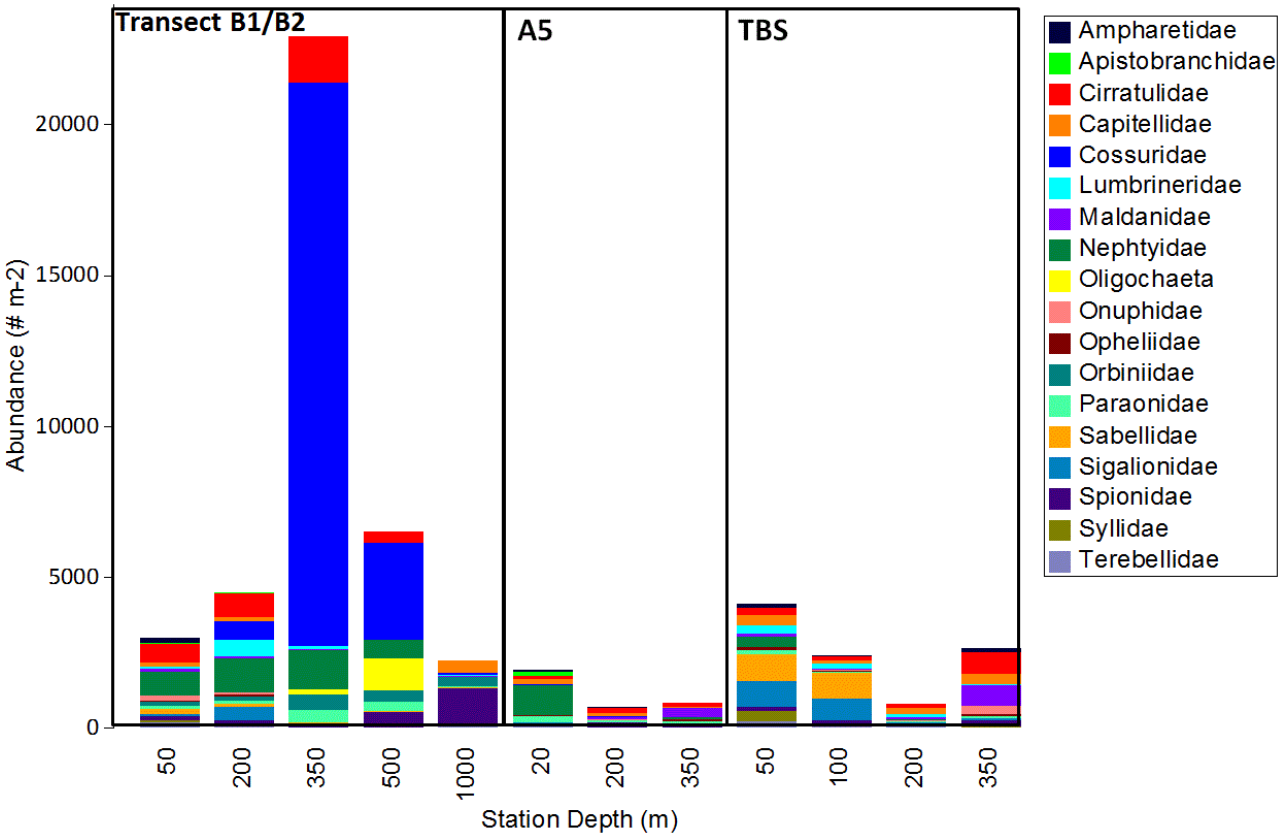

Figure 5.3.2. Total polychaete abundance (individuals m^{-2}) by family (including class Oligochaeta), showing only taxa contributing more than 5% of total polychaete abundance.
Only stations <350 m were sampled at transects A5 (Camden Bay, 2014) and TBS (Outer Mackenzie Plume, 2014). For transects B1/B2 (2012), the 50-m station is located on B-2 and the other stations are located on B1 (both Colville Plume, combined here due to close proximity).

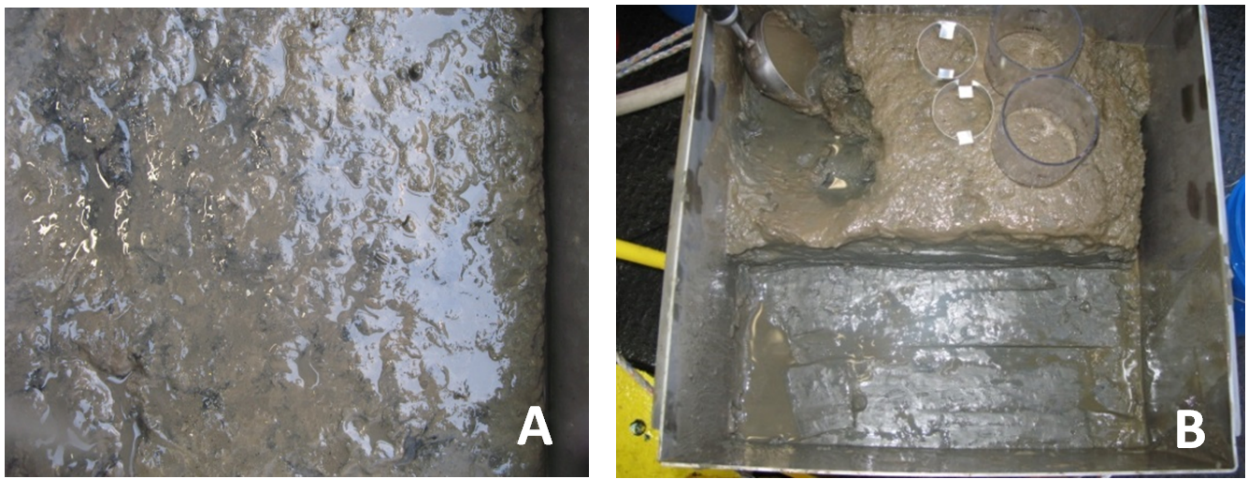

Figure 5.3.3. Photograph of box core surfaces from station B1-350 m (A), showing black, presumably anoxic sediment at the core surface, in contrast to station B1-1000 m (B) which shows no visual evidence of a sharp oxic-anoxic gradient.

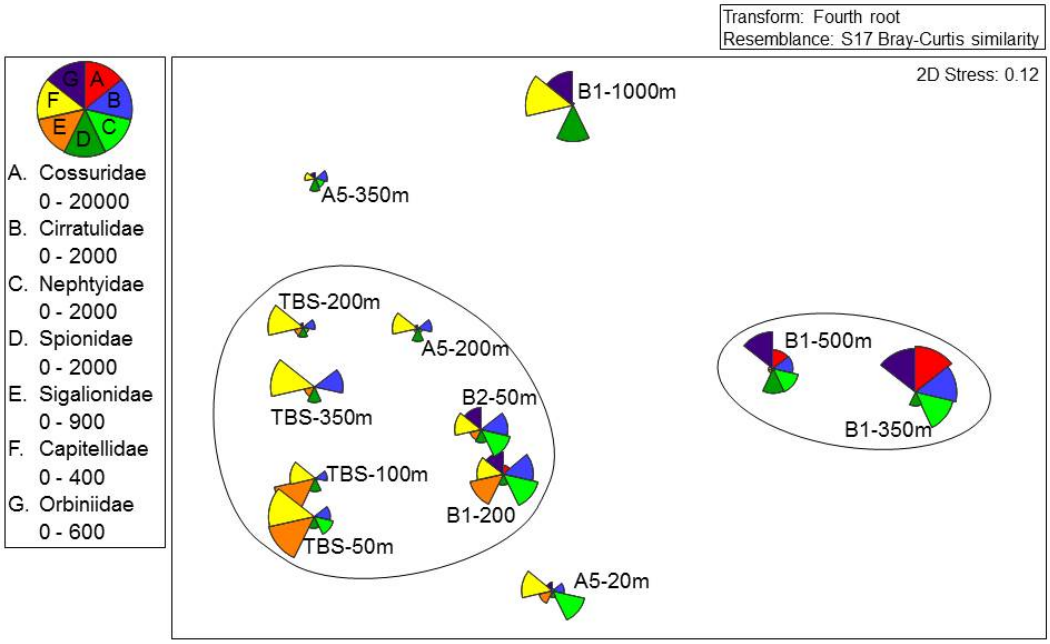

Figure 5.3.4. nMDS ordination showing relative abundance of polychaete families contributing substantially to within-group similarity based on SIMPER analysis.
Ovals indicate significantly different clusters based on SIMPROF test (p <0.05). Labels indicate transect (B = Colville Plume (2012), A5 = Camden Bay (2014), TBS = Outer Mackenzie Plume (2014)) and station depth). 3-D stress = 0.04.

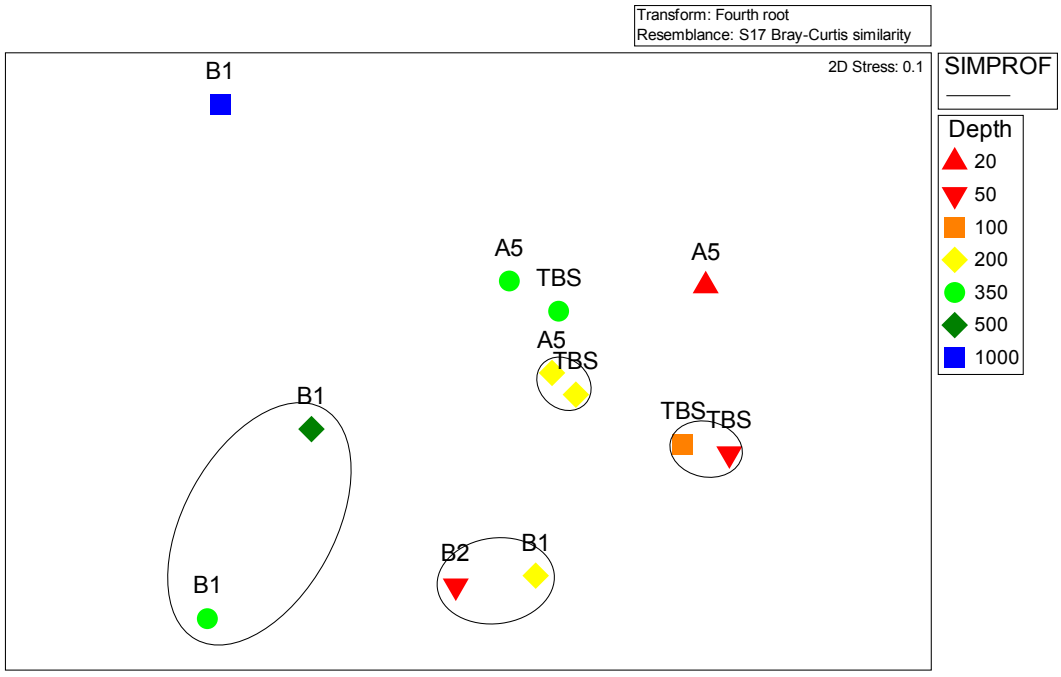

Figure 5.3.5. nMDS ordination of overall macrofaunal community structure.
Ovals indicate significantly different clusters based on SIMPROF test. Labels indicate transect (B = Colville Plume (2012), A5 = Camden Bay (2014), TBS = Outer Mackenzie Plume (2014)) and station depth). 3-D stress = 0.05.

5.3.2 Habitat Variables

DistLM analysis of annelid assemblage structure showed that 59% of the variation could be explained using two dbRDA axes, and 73% could be explained with three axes. The variables most associated with all of the first three axes include chlorophyll-*a* concentration, depth, and sediment sorting (Table 5.3.1; Figure 5.3.6). Stations B1-350 and B1-500 have communities that are distinct from the others; those communities may be supported by high chlorophyll values (see also Figures 5.3.2, 5.3.4, 5.3.5). Also, when predictor variables were examined individually, DistLM analysis of total macrofaunal abundance indicated that only chlorophyll-*a* and phaeopigment concentration were significant predictors of total abundance. Integrating multiple predictor variables into a linear model, chlorophyll-*a* concentration and sediment sorting described most of the variation in total abundance; however, depth, porosity, and phi were also included in the best-fit model. Sorting may provide some indication of the degree of disturbance, which can influence infaunal community structure and diversity. Porosity and phi both provide an indication of the sediment grain-size distribution, a well-known influence on infaunal community structure.

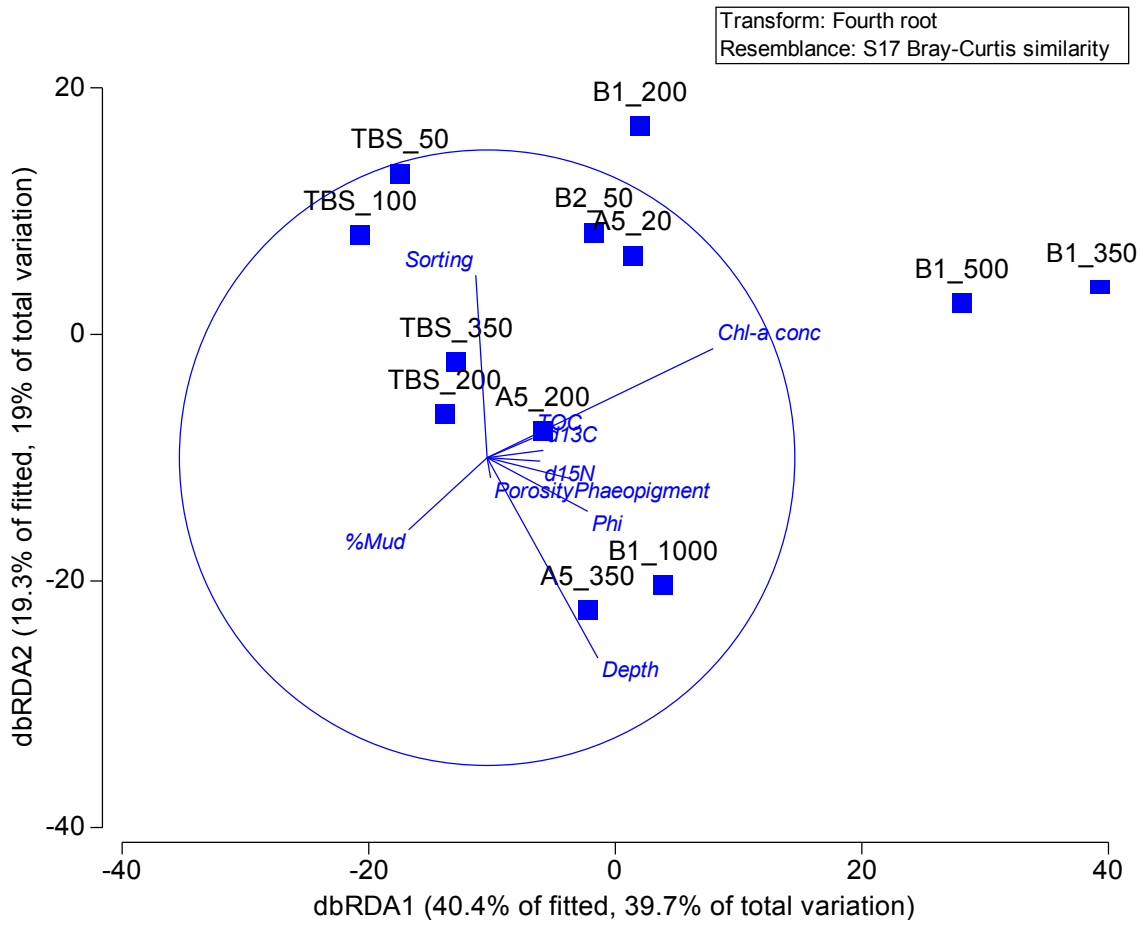

Figure 5.3.6. dbRDA ordination showing best-fit DistLM model of annelid assemblage structure (family-level taxonomy).
Vectors indicate magnitude and direction of change for each predictor variable included in the model. Points are labeled by station (Transect_depth) (B = Colville Plume (2012), A5 = Camden Bay (2014), TBS = Outer Mackenzie Plume (2014)) and station depth.

Table 5.3.1. Results of DistLM model of annelid assemblage structure (family-level taxonomy), showing multiple partial correlations between predictor variables and dbRDA axes (see Figure 5.3.5).

Predictor Variable	dbRDA1	dbRDA2	dbRDA3
Depth	0.360	-0.651	0.533
Chl-*a* concentration	0.735	0.354	0.114
Phaeopigment concentration	0.268	-0.067	-0.136
Porosity	0.011	-0.066	-0.277
%Mud	-0.255	-0.234	0.403
Phi	0.327	-0.174	-0.364
Sorting	-0.037	0.593	0.511
δ15N	0.173	-0.011	0.025
δ13C	0.183	0.024	-0.140
TOC	0.147	0.063	0.176

6.0 EPIBENTHOS

Katrin Iken, Bodil Bluhm, and Lauren Bell

6.1 Introduction

Arctic shelf ecosystems are often dominated by rich benthic communities as a result of tight coupling to primary production in the overlying water column (Grebmeier 2012). These benthic shelf communities play vital roles in remineralization processes (Ambrose et al. 2001). These communities are slow-growing, tend to integrate processes over longer time spans than pelagic systems (Piepenburg et al. 1995), and are prey for higher trophic levels such as bottom-feeding fishes, seals, and diving birds (Coyle et al. 1997, Lovvorn et al. 2003). Moreover, benthic communities are tightly coupled to water-column processes, making them good indicators of the effects of climatic variability (Grebmeier et al. 2006). These organisms are typically long-lived and seasonal. Additionally, interannual variability can be dampened in sediment communities, allowing for observation of longer-term trends in ecosystem function (Dunton et al. 2005, Smith et al. 2006). Among the benthic communities, it is ecologically relevant to differentiate between the macro-infauna living within the sediments and the epifauna living on top of the sediments. These benthic components differ in their mobility, size range of organisms, dominant taxonomic composition, dominant feeding modes, and the mode of collection. This section of the report focuses on epibenthic communities.

Within the Alaskan Arctic, the Chukchi Sea shelf has undergone intense study of epibenthic communities in the past decades, especially in the last ~15 years (e.g., Feder et al. 2005, Bluhm et al. 2009, Blanchard et al. 2013, Ravelo et al. 2014). In contrast, the Beaufort Sea is much less understood. Hydrographically complex, it differs considerably from the Chukchi shelf in water mass characteristics, depth profile, and faunal assemblages. In the US Beaufort Sea, a decreasing influence of advective influx of nutrient-rich Pacific waters toward the east is reflected in a gradient of benthic infaunal and fish biomass, with highest values in the western Beaufort Sea (Rand and Logerwell 2011). A recent assessment of the shelf benthos in the US Beaufort Sea found considerable along-shelf differences in abundance, biomass, and community composition of epibenthos, with an indication that depth may be a factor in structuring these communities (Ravelo et al. 2015). However, little is known about how the steep depth gradients of the Beaufort slope influence epibenthos and whether the observed west to east gradient in community patterns on the shelf is also present at greater depth strata. These environmental conditions, and the potential for oil and gas extraction in the region, warrant an in-depth assessment of the epibenthic community structure, including its food web characteristics.

6.2 Objectives

The specific objectives for the epibenthos component of the Transboundary project were to:

1. Describe epibenthic community structure based on trawl sampling;
2. Correlate epibenthic community structure, abundance, and biomass with hydrographic characteristics (chlorophyll-*a*, salinity, temperature) and benthic habitat information (grain size, sediment chlorophyll, organic carbon content, C:N ratio); and
3. Conduct morphometric and reproductive measurements of snow crab (*Chionoecetes opilio*), if present, as a potential fisheries resource.

6.3 Methods

6.3.1 Epibenthic Community Sampling

Sampling occurred in transects perpendicular to shore from 20 to 1000 m depth. In most cases, target sampling depths were 20 m, 50 m, 100 m, 200 m, 350 m, 500 m, 750 m, and 1000 m. Epibenthic communities were sampled in 2012, 2013, and 2014 using a 3-m plumb-staff beam trawl (7-mm mesh and 4-mm codend liner) that was deployed for fish surveys (see section 7.2.1 for details). A Canadian bottom trawl was also deployed in 2012 and 2013 (6-mm mesh at the codend, width = 3 m). Epibenthic invertebrates (from whole haul catches or defined, well-mixed subsamples) were sorted to the lowest taxonomic level possible. Biomass and abundance per taxon were determined on board the ship. Vouchers and selected samples were preserved in 5% formalin-seawater solution buffered with hexamethylenetetramine for later use by taxonomic specialists in confirming species identifications.

In cases where snow crab (*Chionoecetes opilio*) were encountered, they were sexed based on the shape of the abdominal flap (immature females, females, males), and morphometric measurements were taken including carapace width (CW in mm), left chela height for male crabs (in mm), and body mass (in g).

Environmental context data collected included bottom water temperature and salinity from conductivity, temperature, and depth (CTD) instrument deployments (see Section 2.1 of the report for details). Sediment chl-*a*, sediment phaeopigments, porosity, grain size, and sediment isotope and organic content data were obtained from grab or box core samples as available (see Section 5.0 for details).

6.3.2 Data Analysis

Approximate faunal densities can be calculated from haul size, trawling time on the bottom, and trawling speed (Holme and McIntyre 1984). Comparisons between longitudinal regions and depth strata were made based on the index catch per unit effort (CPUE). CPUE conversions were completed and normalized to 1000 m^{-2} for all trawls except those from 2012, which were deemed non-quantitative. In this report, patterns in epibenthic biomass will be emphasized more than abundance patterns because biomass data include colonial taxa (sponges, hydrozoans, bryozoans, ascidians, and etc.) that cannot be enumerated as individuals, excluding them from abundance assessments. Hence, biomass patterns present a more complete picture of the communities and will be the primary focus, though most analyses will be presented for both metrics. Bulk biomass and abundance measures per station were analyzed for depth trends using Pearson correlations (Systat software).

Epibenthic community structure analysis was completed primarily using multivariate statistics programs within the software package Primer-e V7. Community similarity for transects from 2013 and 2014 (same overall eastern Beaufort Sea region sampled, quantitative trawls) or from all years combined (including central Beaufort Sea region sampled in 2012, non-quantitative trawls) was assessed for year of sampling, depth, and longitudinal patterns using analysis of similarity (ANOSIM). A 1-way ANOSIM was used to compare year and 2-way crossed ANOSIM was used for depth and longitude. ANOSIM yields global R-values, measures of scaled separation between groups that can be directly compared to assess the relative importance of various factors on community composition. R-values range from 0 to 1 with smaller values indicating a factor has less influence, while R-values above ~0.45 are considered biologically relevant (Clarke et al. 2014a). Patterns in community structure were visualized in

non-metric multidimensional scaling (nMDS) plots. A 2D stress level of up to 0.2 was deemed acceptable. Metric multidimensional scaling (MDS) plots were also used to visualize community similarities and groupings by depth strata, by shelf (≤100 m) and slope (200–1000 m) groups, and by water masses (≤50 m Polar Mixed Layer (PML), 60–200 m Arctic Halocline Water (AHW), >250 m Atlantic Water (AW); see Environmental Section 2.2). For the depth strata, the MDS analysis was conducted at the lowest possible taxonomic identification level (lowest level = species or genus for most taxa, occasionally higher levels for difficult groups) and compared with a higher taxonomic level (mostly class level, higher for some difficult groups) to test for taxonomic sufficiency (Ferraro and Cole 1990). Class was chosen as the taxonomic level at which non-taxonomic scientists can most reliably make identifications on board a ship. Therefore, this is a suitable level to investigate the applicability of taxonomic sufficiency for potential future monitoring applications, as they may not involve benthic taxonomic experts. Similarity percentages analysis (SIMPER) was used to identify indicator taxa for communities along the distinct depth strata sampled and for shelf and slope communities. SIMPER also identifies the taxa that are most responsible for the dissimilarity of communities among sample groups (i.e., by depth or by shelf/slope).

In 2014, replicate trawls were taken at stations along transect A1 to assess the variability of epibenthic communities. This variability is typically disregarded when only one trawl per station is taken. Community composition of repeat trawls along transect A1 was analyzed using hierarchical cluster analysis (including similarity profile analysis (SIMPROF) test for significant differences at 95% level) and compared with single trawl data from the same transect in 2013. SIMPER analysis was used to calculate community similarity among repeat trawls from 2014 and between same-station trawls from 2013 and 2014.

We tested the influence of data transformation on similarity relationships in community composition. Community data for biomass and abundance (absolute measures in 2013 and 2014 and relative measures in comparisons with the 2012 trawls, which were not quantitative) underwent the following transformations to examine the influence of rare versus common species on community patterns: no transformation (most emphasis on common species), square root transformation (2RT) (slight downplay of very common species), fourth-root transformation (4RT) (balanced design between common and rare species), Log(x+1) transformation (slightly more severe than 4RT but also considers common and rare species), and presence/absence (PA) transformation (gives equal weight to all species in a sample). Transformed biomass and abundance data were displayed in nMDS plots based on Bray-Curtis similarity matrices. We also used shade plots to visually assess the species distribution after each transformation. All transformations were used to analyze the effects of depth and longitude (by categorizing transects along the longitudinal extent from the central to the eastern Beaufort Sea) using a 2-way crossed ANOSIM design (both factors applied as ordered factors). The factor "year" was disregarded in any analyses that also included 2012 data because the different location of transects in that year confounded the effect of year; hence, year was only considered in a separate 1-way ANOSIM analysis for the combined 2013 and 2014 data.

Epibenthic community structure was matched with environmental variables (based on 4RT biomass data) to assess which variable combination was most influential in determining community composition. Analysis was done using PRIMER's biota-environment stepwise matching test (BEST) routine, which employs Spearman rank correlations. Epibenthic communities were first grouped as shelf communities (20–100 m depth), then as slope communities (mostly 200–350 m and occasional deeper stations where environmental data were

available, see Environmental Section 5.0), and, finally, across the entire depth range (20–1000 m). These groups were matched against the environmental variables of depth, bottom salinity and temperature, sediment chl-*a* (µg/g sediment dry weight, log-transformed), phaeopigments (log-transformed), sediment porosity (%water by weight), %gravel, %sand, %mud, %silt, and %clay. Sediment grain size descriptor phi was excluded because of its high collinearity with %clay and %mud. Additional variables included stable nitrogen and carbon isotope values of sediment (^{15}N and ^{13}C), C:N ratio, and total organic carbon (TOC). In all analyses, environmental variables were normalized to bring them to the same measurement scale. Combinations of up to five variables were considered, and the combination producing the highest correlation coefficient was considered the best match to the biological matrix.

6.4 Results

6.4.1. Patterns in Taxon Richness and Overall Biomass and Abundance

6.4.1.1 Taxon Richness

A total of 153 epibenthic taxa were found in 2012, and 158 and 160 taxa were found in 2013 and 2014, respectively. Real taxon diversity was higher, but we were unable to obtain species identifications for some notoriously difficult groups such as bryozoans, hydroids, and sponges, which were treated on a class or phylum level. The total number of taxa and the distribution of taxa across phyla were highly consistent across years (Table 6.4.1). In all years, the majority of epibenthic taxa were arthropods (mostly amphipods and decapods but also isopods and pycnogonids), mollusks (mostly gastropods), and echinoderms (asteroids and ophiuroids plus several holothurians). Cnidarians (mostly anemones and hydroids) and annelids (polychaetes) were also common phyla present. The group "Other" included miscellaneous groups, mostly nemerteans.

Table 6.4.1. Number of taxa within phyla encountered in different sampling years.

Phylum	2012	2013	2014
Arthropoda	47	48	47
Mollusca	40	41	43
Echinodermata	24	30	30
Cnidaria	6	10	13
Annelida	2	10	11
Ascidiacea	4	5	4
Tentaculata	4	5	5
Porifera	3	2	2
Others	2	6	5

6.4.1.2 Total Biomass and Abundance

Total biomass was dominated by echinoderms at most stations and depth strata (Figure 6.4.1). Abundance patterns were similar to biomass patterns except that many of the deep stations (750 and 1000 m) were dominated by arthropods and occasionally cnidarians (Figure 6.4.2). Arthropod biomass and abundance in the 20-m stratum was primarily amphipod species (mostly *Anonyx* sp., *Arrhis phyllonyx*, *Melita* sp., *Paroediceros lynceus*), the isopod *Saduria*

sabini, cumaceans (*Diastylis* spp.), and the suprabenthic shrimp *Eualus gaimardii*. Echinoderms, primarily the ophiuroid *Ophiocten sericeum* and the holothurian *Myriotrochus rinki,* were occasionally found at high abundance and biomass at shallow stations (20 m). Echinoderm abundance on other shelf depth stations (50–100 m) was typically dominated by the brittle star *O. sericeum* but in biomass by the holothurian *Psolus peronii*, the sea star *Urasterias linkii*, the feather star *Florometra* sp., or the brittle star *Gorgonocephalus* sp. At times, these latter taxa dominated biomass with relatively few individuals because of their large body size. Conversely, *O. sericeum* was numerous, but its contribution to overall biomass was lower due to small body size. Cumacean species of the genus *Diastylis*, the scallop *Similipecten greenlandicus,* and various amphipod taxa were common contributors to shelf abundance, and caridean shrimp, such as *Eualus gaimardii* and *Sabinea septemcarinata,* were common contributors to abundance and weight. Deeper water stations along the slope (≥200 m) were largely dominated in abundance by the brittle star *Ophiopleura borealis,* pycnogonids (especially in the eastern Beaufort Sea), the gastropod *Colus sabini,* the scaphopod *Siphonodentalium lobatum*, the isopod *S. sabini*, and various anemones. Weight contributions at these deeper stations were dominated by large sea stars such as *Icasterias panopla, Pontaster tenuispinus* and *Bathybiaster vexillifer,* the holothuroid *Molpadia borealis*, when present, and the anemone *Allantactis parasitica* (especially in the eastern study region).

Absolute biomass of individual taxa varied between 2013 and 2014 shelf stations and between 2013 and 2014 slope stations (2012 was excluded from this comparison because only relative biomass data were available). Overall, variation around mean biomass was high for individual taxa (Appendix D Table 1). Among the shelf stations, mean biomass for individual taxa was on similar scales between the two years, so most taxa had either high or low biomass values on similar orders of magnitude in both years. For example, among the mollusks, the scallop *Similipecten greenlandicus* and gastropods of the genera *Buccinum*, *Colus,* and *Margarites* were always the highest biomass contributors, while all other mollusk taxa occurred with much lower average biomass in both years. These general patterns were also present on the slope, although some larger between-year differences existed for some taxa (Appendix D Table 1). For example, the snow crab *Chionoecetes opilio* occurred with a mean of 161 g wet weight 1000 m^{-2} in 2013 but did not occur at all on the slope in 2014. Such differences can be related to very patchy distribution of snow crabs, large sea stars (e.g., *Urasterias linckii*), and other large taxa.

The snow crab, *Chionoecetes opilio,* was primarily found during the 2012 collections in the central Beaufort Sea. A total of 48 crabs occurred between 200 and 500 m depth at five stations along the slope with bottom temperatures of -1.27–3.63 °C and salinities of 31.44–32.25. The smallest crab was 62 mm CW, the largest was 144 mm CW, and all were males, except for one female (72 mm CW) found at 350 m depth. Most crabs were in the 90–100 mm CW size group (Figure 6.4.3a) and, as expected, larger crabs were also heavier (Figure 6.4.3b). Crabs occurred at too few stations in the central Beaufort to create meaningful correlations with environmental variables, and only two crabs were found in the eastern Beaufort trawls. One male crab occurred in 2013 at 200 m (transect A6, 119 mm CW) and one in 2014 at 100 m (TBS transect, 117 mm CW).

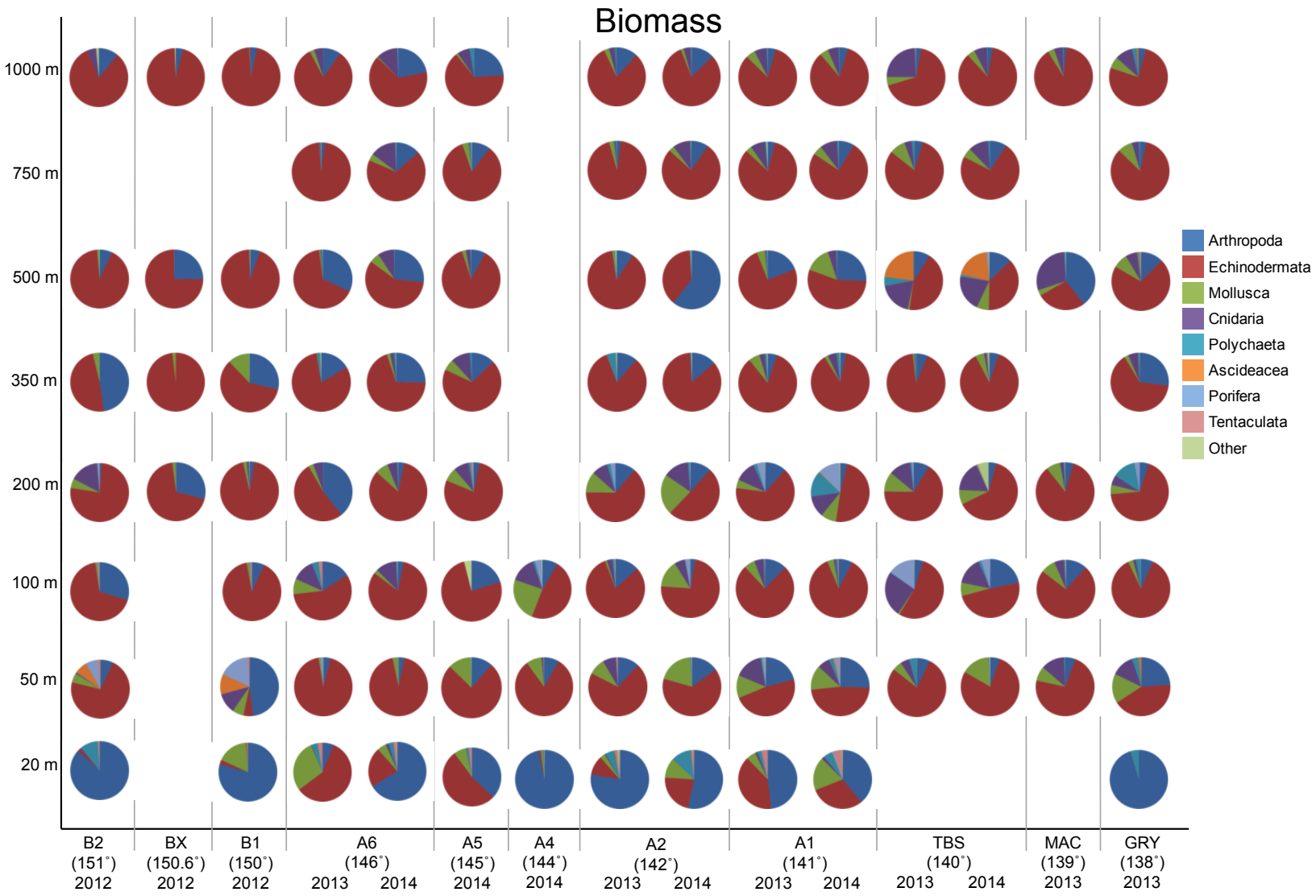

Fig. 6.4.1. Biomass of major epibenthic phyla by depth strata in the Beaufort Sea across years and transects.

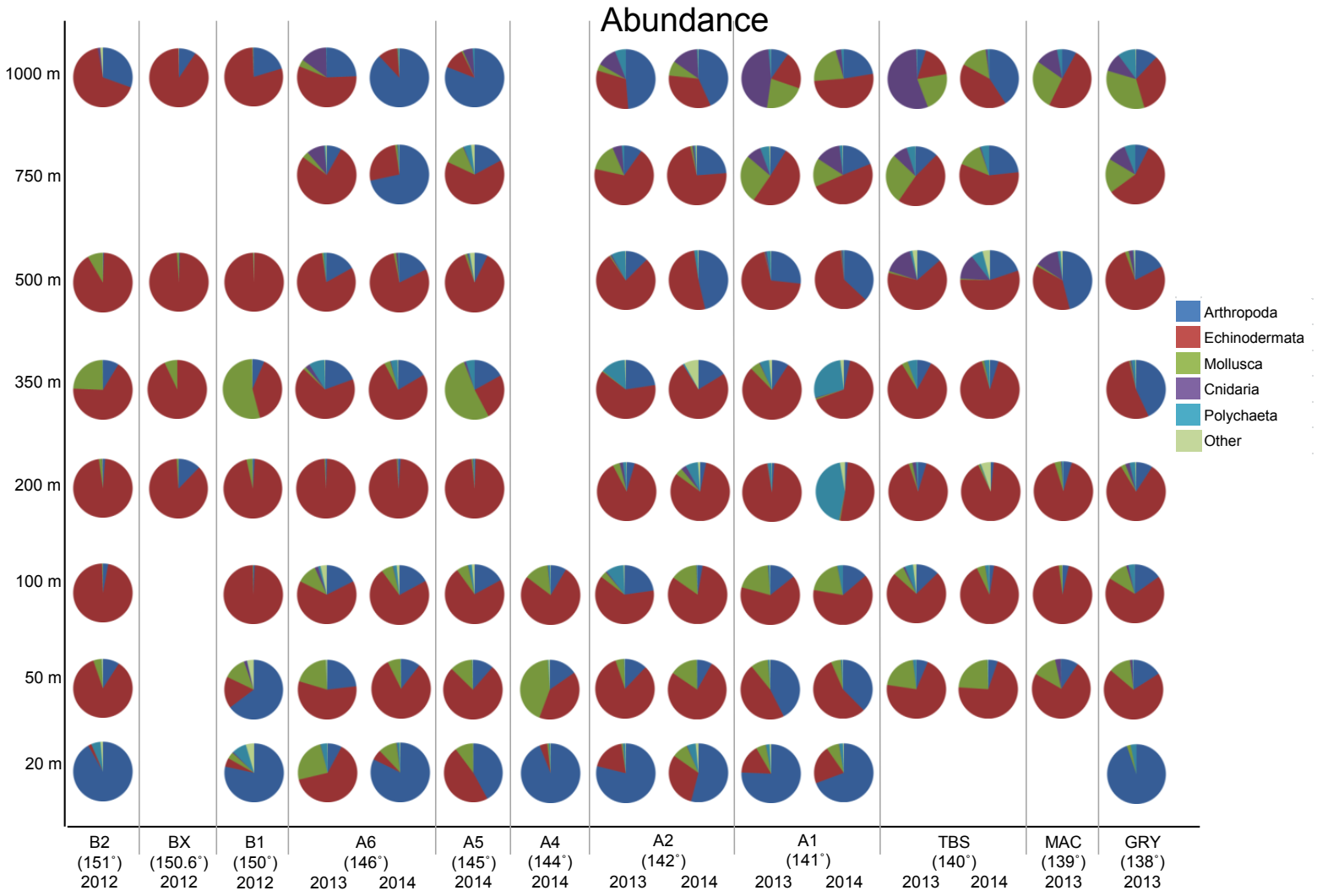

Fig. 6.4.2. Abundance of major epibenthic phyla by depth strata in the Beaufort Sea across years and transects.

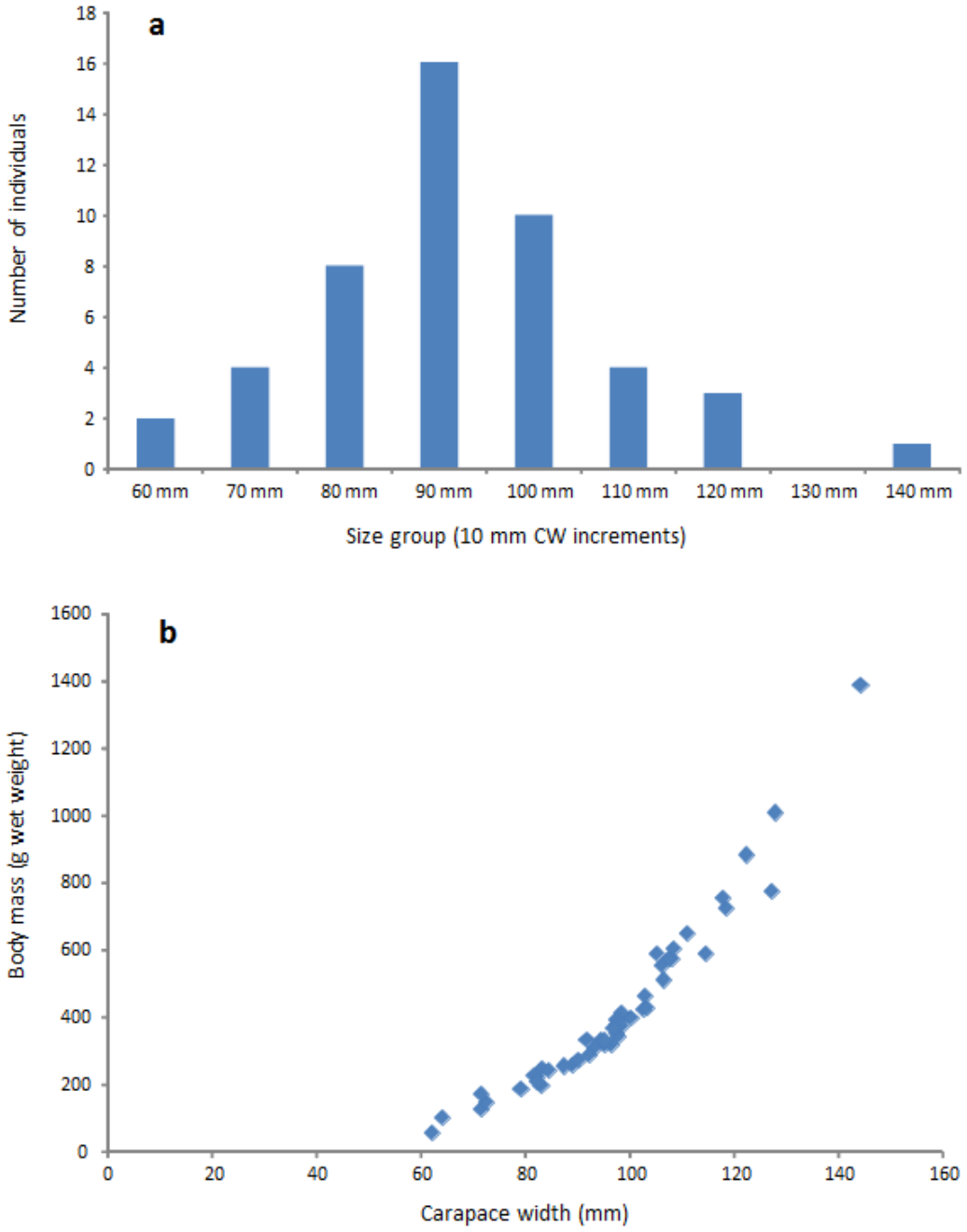

Figure 6.4.3. Snow crab (*Chionoecetes opilio*) relationship between body size (carapace width) and body mass (a), and size frequency distribution of snow crab (b), both for collection in 2012 on the central Beaufort Sea shelf and slope.

6.4.1.3 Depth and Longitudinal Trends in Total Biomass and Abundance

Absolute community biomass and abundance (only available for 2013 and 2014) was overall highest in the 50-m and 100-m depth range, but occasionally the 200-m depth stratum, with decreasing biomass and abundance shallower and deeper (Figure 6.4.4). However, there was variability in this pattern among transects and, on some transects, high biomass was encountered at greater depth (e.g., transect A2, 142° W, in 2013) (Figure 6.4.5). Abundance trends were typically more consistent, although absolute abundance at certain depth strata varied greatly among transects (e.g., 100-m stratum in 2013, Appendix D Figure 1). Despite these variabilities, there were significant negative depth trends in 2013 and 2014 for biomass (Pearson correlation coefficient: -0.359, $p = 0.019$ in 2013 and -0.482, $p = 0.001$ in 2014) and abundance (Pearson correlation coefficient: -0.333, $p = 0.026$ in 2013 and -0.399, $p = 0.005$ in 2014). In both years, both parameters significantly declined with increasing bottom depth.

No clear longitudinal trend could be discerned in total biomass or abundance along transects sampled in 2013 and 2014 (Figures 6.4.4–6.4.5, Appendix D Figure 1). Variability in absolute biomass was also seen in a direct comparison of transects repeatedly sampled in 2013 and 2014 (Figure 6.4.6), although some consistent patterns emerged. For example, in both years, biomass was highest at 50 m along the A1 transect (142° W) and the 100-m stratum on the TBS transect (140° W). Along all repeat transects, biomass drastically decreased at ≥500 m compared with shallower depths.

Epifauna

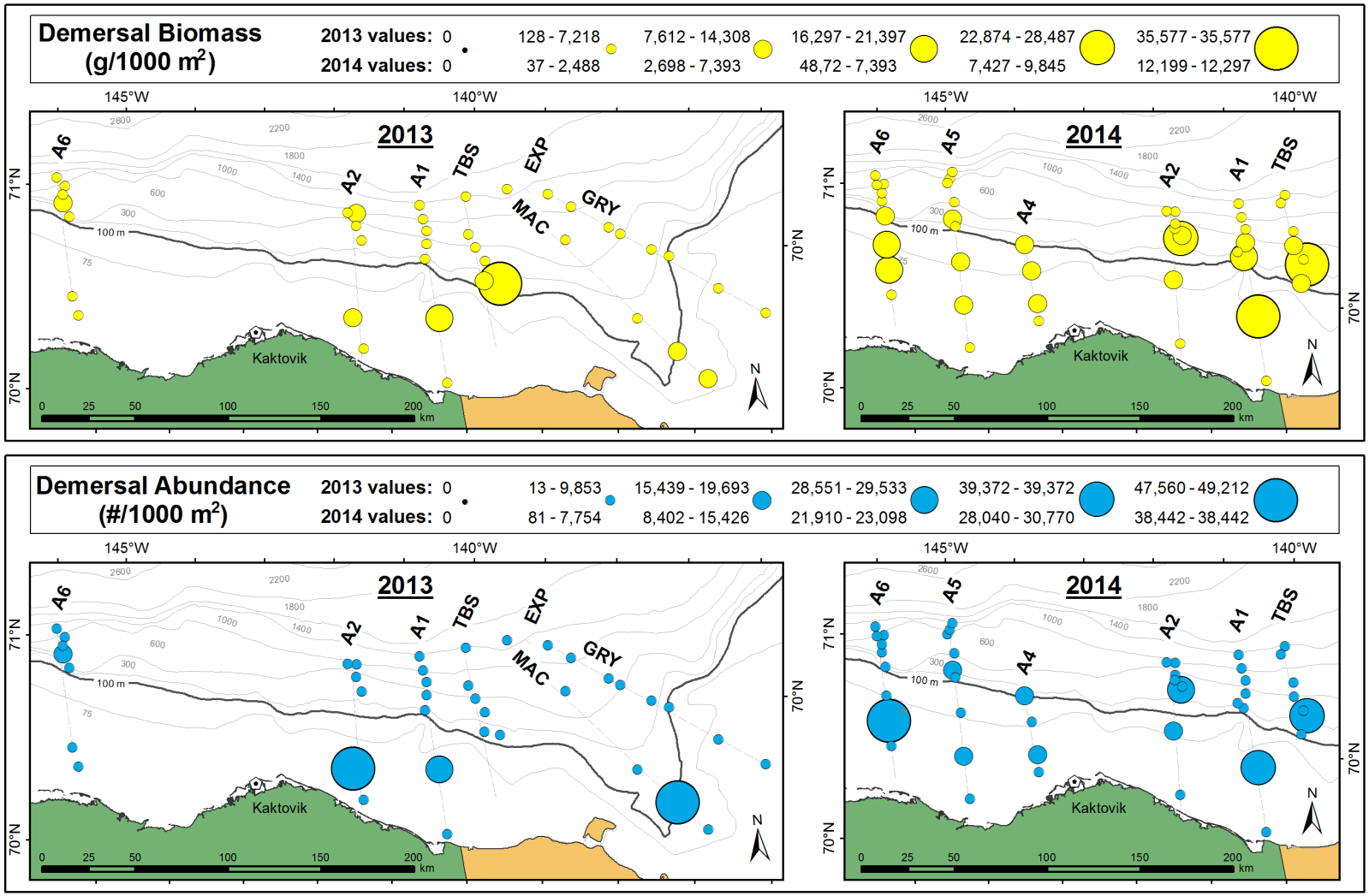

Figure 6.4.4. Absolute biomass (upper panels) and abundance (lower panels) of epibenthic communities in 2013 (left panels) and 2014 (right panels). Data are categorized into five equal intervals over the entire CPUE range for visualization. The 100 m contour is marked as a solid line to distinguish shelf from slope.

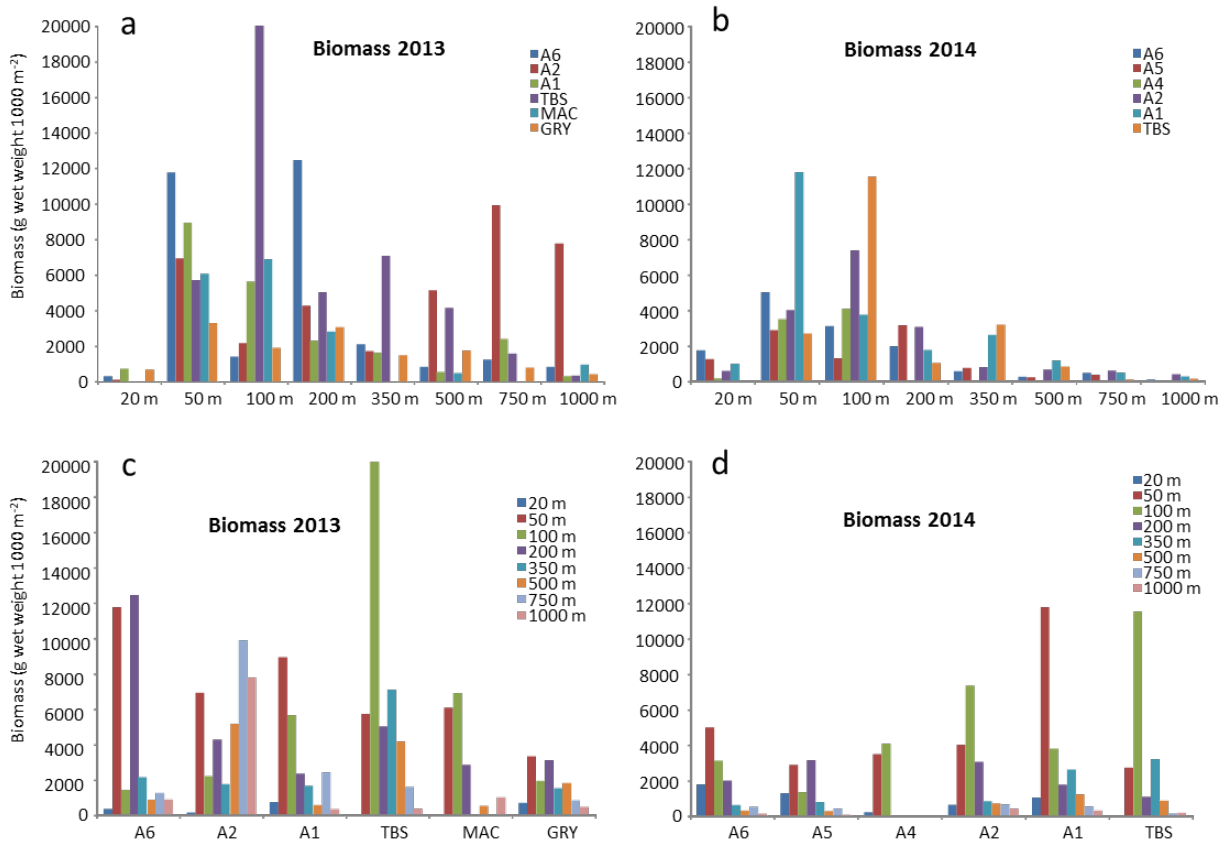

Figure 6.4.5. Epibenthic biomass (g wet weight 1000 m^{-2}) distribution in 2013 (a and c) and 2014 (b and d) arranged by depth strata (a and b) and by transect lines (c and d).
Transects in panels c and d are arranged in longitudinal order from west to east: A6 - 146° W, A5 - 145° W, A4 - 144° W, A2 - 142° W, A1 - 141° W, TBS - 140° W, MAC - 139° W, GRY - 138° W.

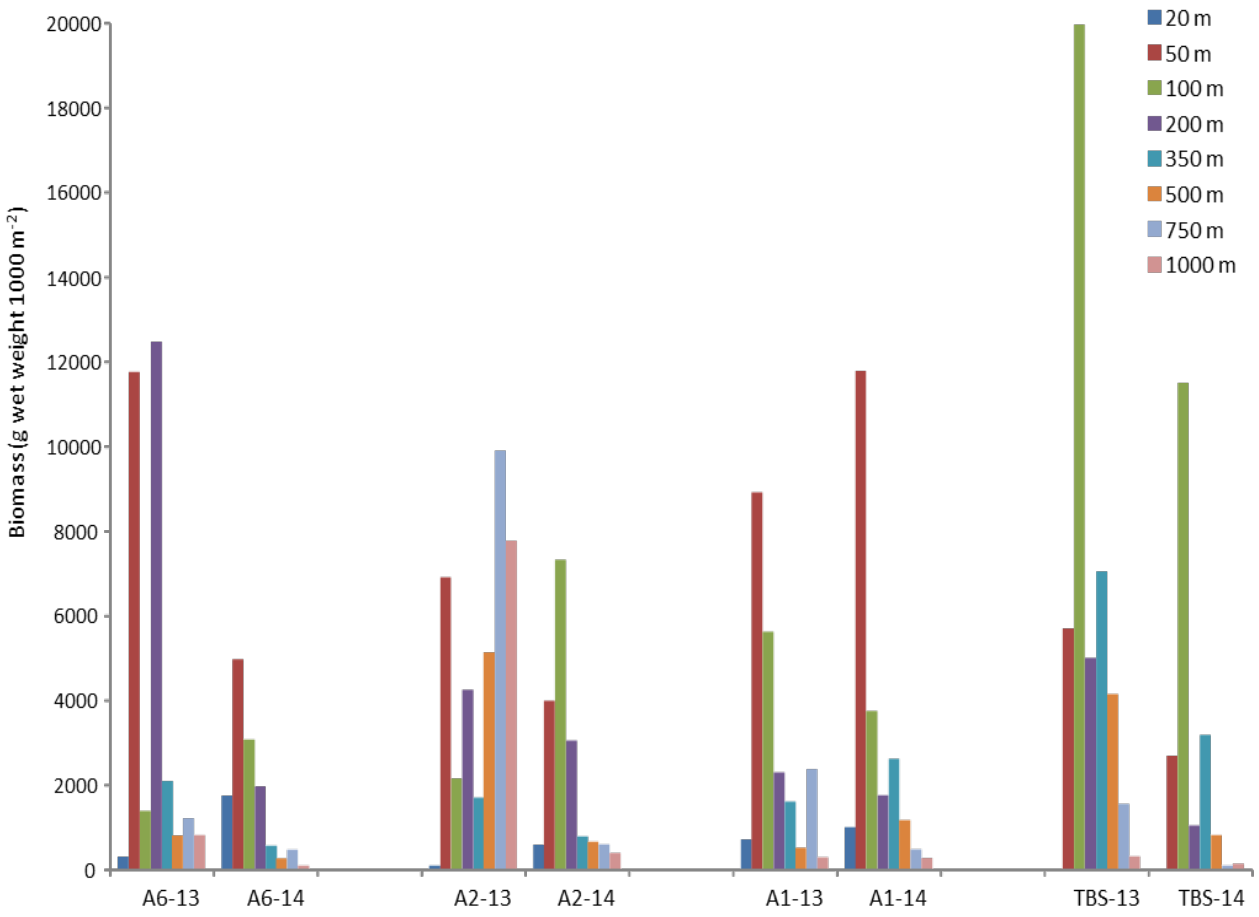

Figure 6.4.6. Epibenthic biomass (g wet weight 1000 m^{-2}) distribution along depth strata at the same transects sampled in 2013 and 2014.
Transects are arranged in longitudinal order from west to east: A6 - 146° W, A5 - 145° W, A4 - 144° W, A2 - 142° W, A1 - 141° W, TBS - 140° W, MAC - 139° W, GRY - 138° W.

6.4.2 Patterns in Epibenthic Community Structure (Multivariate Patterns)

6.4.2.1 Transformation Effects

We first assessed the effects of data transformation as the basis of all subsequent multivariate community analyses. When using the quantitative biomass and abundance data collected in 2013 and 2014, the effect of data transformation was relatively small, although 4RT for both biomass and abundance-based datasets yielded the strongest effects of both depth and longitude (Table 6.4.2). Community ordination was relatively similar regardless of transformation, but 2RT or 4RTs provided the most defined community structure patterns (Figure 6.4.7 for biomass and Appendix D Figure A2 for abundance). In contrast, the ordination based on presence/absence transformation was different from all other transformations and did not show similar community similarity patterns, indicating that the loss of quantitative information with this transformation substantially changes the information to be gleaned from these types of analyses. The 4RT ordination had the least 2D stress for both community metrics (Figure 6.4.7 for biomass and Appendix D Figure A2 for abundance), making it the most suitable transformation for biomass- and abundance-based community analyses of the epifauna.

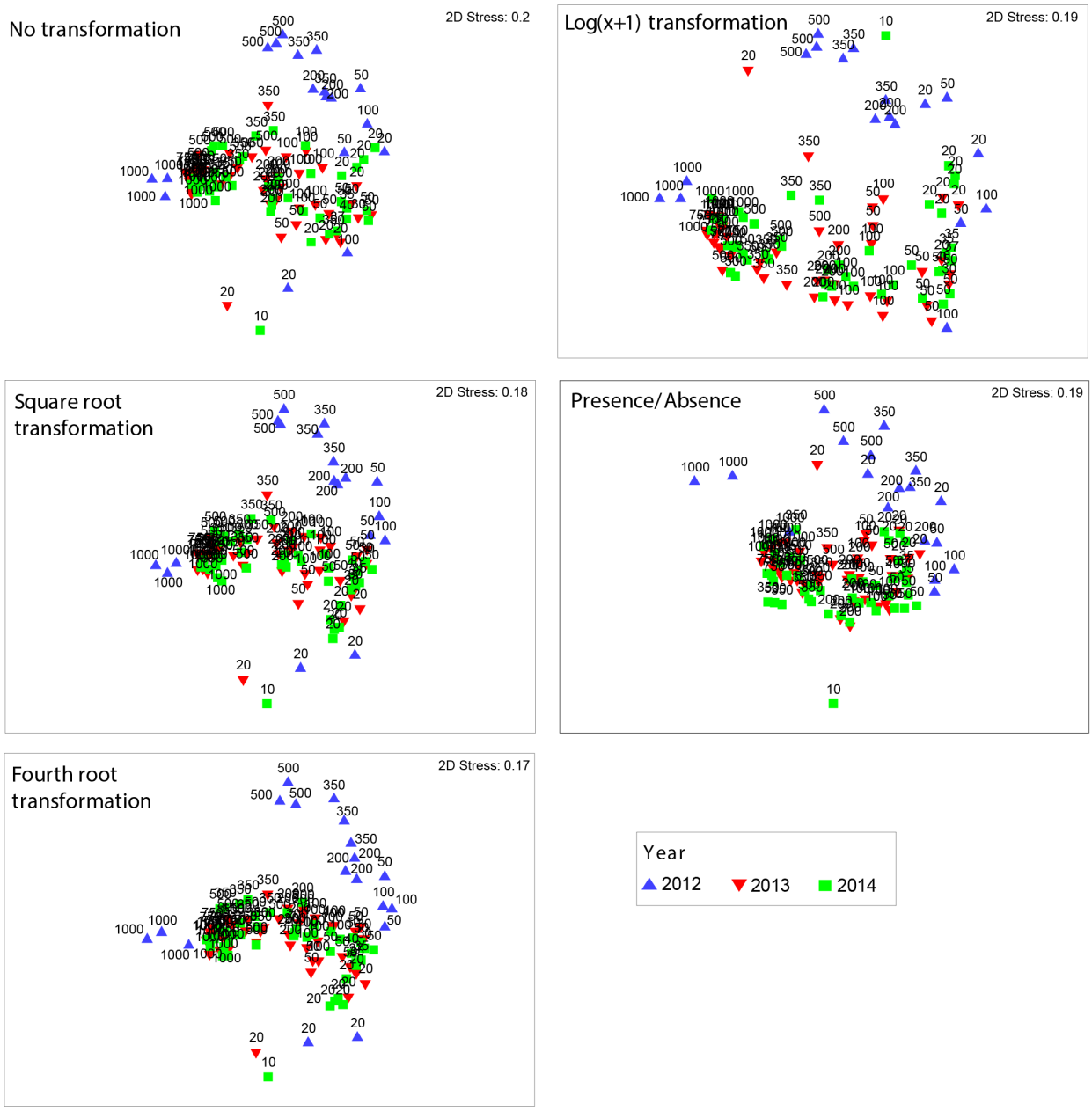

Figure 6.4.7. Community structure ordination (nMDS) of epibenthos based on relative biomass for all transects and depths sampled in 2012, 2013, and 2014, based on various transformations.
All nMDS ordinations are based on Bray-Curtis similarity matrices. Numbers in nMDS plots refer to depth, colored symbols refer to years.

Table 6.4.2. Effects of factors year, depth and longitude on community composition in 2013 and 2014, based on absolute biomass and abundance data. "Year" was tested with 1-way ANOSIM; ordered factors "depth" and "longitude" were tested in a 2-way crossed ANOSIM design.
All data were exposed to a series of transformations before constructing a Bray-Curtis similarity matrix for each transformation.

Biomass-based community structure		
Transformation	**R (depth)**	**R (Long)**
NT	0.727	0.486
SQRT	0.787	0.519
4RT	0.799	0.519
Log(x+1)	0.776	0.503
PA	0.763	0.483
Abundance-based community structure		
Transformation	**R (depth)**	**R (Long)**
NT	0.615	0.401
SQRT	0.728	0.485
4RT	0.776	0.510
Log(x+1)	0.702	0.484
PA	0.779	0.463

6.4.2.2 Epibenthic Community Patterns

Based on relative biomass, epibenthic community composition clearly separated by depth (Figure 6.4.8a). Overall, communities ordinated in a clear progression from right to left (Figure 6.4.8a) according to depth. The 10 m (one station) and 20 m stations diverted from this linear ordination, indicating that these depth strata were quite distinct from other shelf stations. Community composition similarity among the shelf stations (n = 37 for all years) was 36%. Indicative taxa for the shelf group were the brittle star *Ophiocten sericeum*, the scallop *Similipecten greenlandicus*, and caridean shrimp, with 79% dissimilarity, mostly driven by disparate biomass contributions of the primary shrimp *Sabinea septemcarinata*, and the amphipod *Anonyx* sp., which together contributed about 30% of the community similarity of the shelf stations (Appendix D Table 2). Community composition similarity among the slope stations (n = 54 for all years) was 42%. Indicative taxa for the slope stations were the sea stars *Pontaster tenuispinus* and *Bathybiaster vexillifer*, the brittle star *Ophiopleura borealis*, the gastropod *Colus sabini*, and the sea anemone *Allantactis parasitica*, which together contributed more than 40% of the community similarity of the slope stations (Appendix D Table 2). The distinction between shelf and slope community compositions was high, with 79% dissimilarity, mostly driven by disparate biomass contributions of the same taxa (see above) that defined the two depth groupings (Appendix D Table 3).

Based on relative biomass, distinct groupings were found between slope stations in 2012 versus those in 2013 and 2014 (85% dissimilarity, Appendix D Table 4, Figure 6.4.8). It should be noted that regions sampled in 2012 were farther west (151–150° W) than the region sampled in 2013–2014 (146–138° W), so dissimilarities between 2012 and 2013–2014 likely reflect a spatial difference. Indicative of these slope community differences, the sea stars *Pontaster tenuispinus* and *Bathybiaster vexillifer* in the 2013–2014 slope region had much higher biomass than found in the 2012 slope region; in fact, *P. tenuispinus* did not occur at all in the 2012

sampling area but was an indicator species of the slope region sampled in 2013 and 2014. *B. vexillifer* had about twice the average relative biomass in the 2013–2014 slope region than in the 2012 slope region. In contrast, the sea star *Ctenodiscus crispatus* occurred in much higher biomass in the 2012 slope region than in the 2013–2014 slope region (Appendix D Table 4). We also observed a change in brittle star indicator species between the two year/region groups. *Ophiura sarsii* was an indicator of the slope region in 2012 but did not occur in the slope region sampled in 2013–2014; instead, *Ophiopleura borealis* was more indicative in 2013–2014 (Appendix D Table 4). Depth-related changes in epibenthic communities were also noticeable in the MDS ordination when assessed based on abundance (Appendix D Figure 3), although groupings were considerably less tight as with biomass. The distinction of the 2012 stations was also noticeable, especially for 20-m depth stations and 500-m depth stations.

We explored the possibility of taxonomic sufficiency by comparing community composition based on the lowest taxonomic level identified (lowest level = species or genus for most taxa, occasionally higher levels for difficult groups) with composition based on a higher taxonomic identification level (mostly class level, higher for some difficult groups). Much of the clear depth-related progression in community composition visible in the MDS ordination based on the lowest taxonomic level (Figure 6.4.8a) disappeared when taxa were identified on the higher class/phylum level (Figure 6.4.8b). These patterns (loss of community structure with depth when taxa were analyzed at a higher taxonomic level) were also present when analyses were done on relative abundance (Appendix D Figure 3).

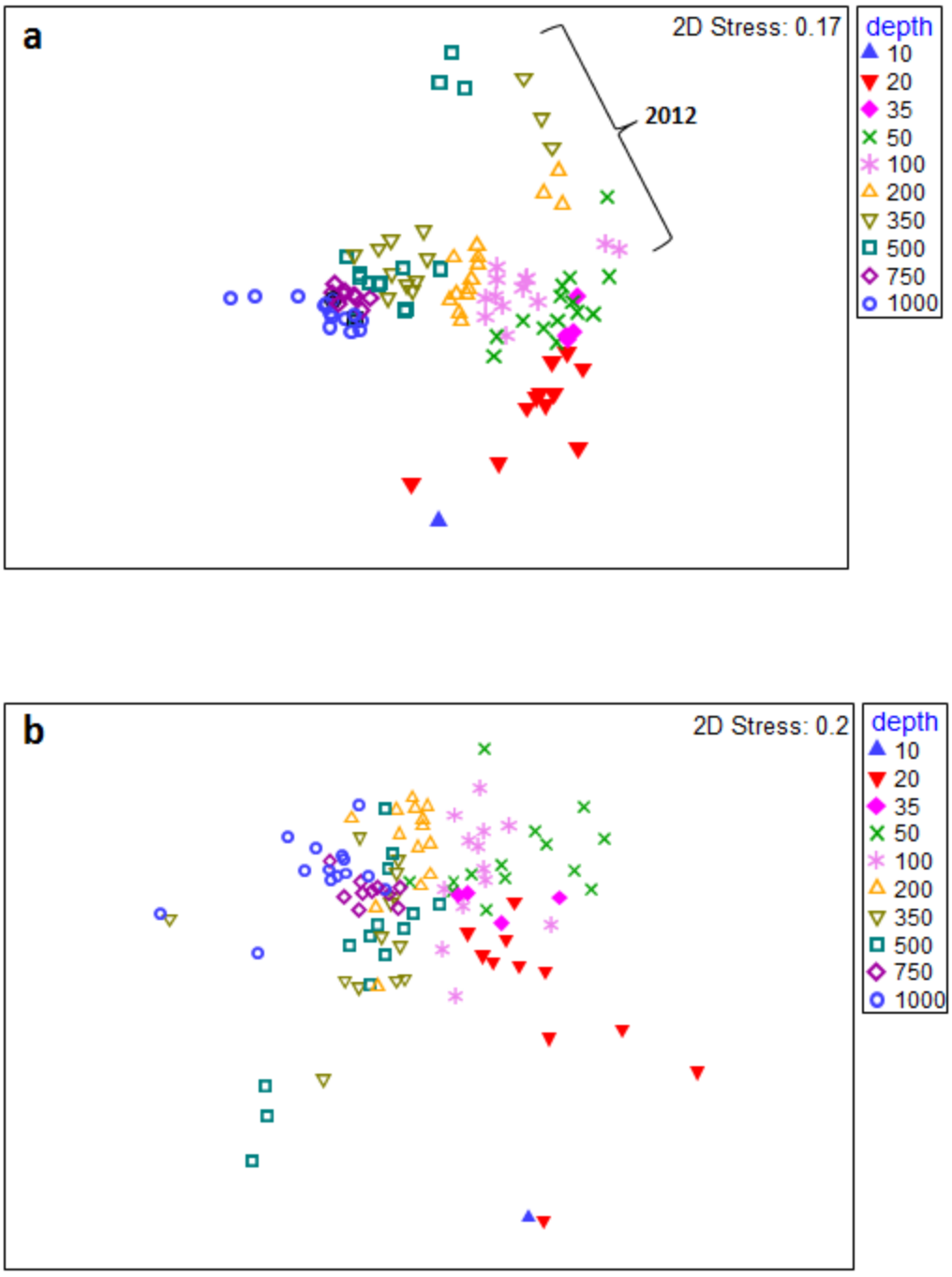

Figure 6.4.8. Community structure ordination (nMDS) of epibenthos based on (a) relative biomass identified to the lowest taxonomic level (species or genus for most taxa, occasionally higher levels for difficult groups), and (b) relative biomass identified to a higher taxonomic level (mostly class level, phylum for some difficult groups).
All nMDS ordinations are based on Bray-Curtis similarity matrices. Colored symbols refer to depth; a distinct station group from 2012 sampling is indicated in panel a.

6.4.2.3 Trawl Replication and Interannual Variability in Community Patterns

The community structures of repeat trawls sampled at transect A1 (142° W) in 2014 were very similar and clustered closely for both biomass and abundance patterns (Figure 6.4.9 and Appendix D Figure 4, respectively). The same stations, sampled with a single trawl in 2013, grouped similarly close to the three repeat trawls from 2014 for both biomass and abundance, showing the high overall consistency of community structure along this transect across these two years. This indicates that variability in community composition between repeat trawls is similar to that among trawls taken in different years. SIMPER analysis confirmed that communities within repeat trawls in 2014 and between trawls taken in 2013 and 2014 were similar (Table 6.4.3). Overall, the factor year had negligible effect on community structure along transect A1 (142° W), and depth had a much higher effect (two-way nested ANOSIM with depth nested within year: R_{year} = 0.025 and R_{depth} = 0.916 for communities based on biomass; R_{year} = -0.028 and R_{depth} = 0.933 for communities based on abundance). Community compositions based on both biomass and abundance grouped strongly by water masses (Figure 6.4.10 and Appendix D Figure 5, respectively), which was similar to the pronounced depth effect because water masses are defined by depth on the Beaufort shelf and slope. Community differences were greatest between upper-most PML and the lower-most AW (R = 0.690 and R = 0.637 for biomass- and abundance-based communities, respectively) and smallest between the PML and the AHW (R = 0.353 and R = 0.267 for biomass- and abundance-based communities, respectively). Separation of AW communities into two distinct groups in the MDS (Figure 6.4.10 and Appendix D Figure 5, green square symbols) was entirely driven by a separation of slope communities at the B-transects compared with all other transects, reflecting a distinct break in community similarity along this longitudinal range. However, community structure across all three sampling years was more strongly affected by depth than by longitude, although both factors were biologically relevant (Table 6.4.2).

Interannual variability was assessed for samples taken in 2013 and 2014 (based on various data transformations for absolute biomass and abundance). Year had no effect on community composition for either biomass or abundance, shown by ANOSIM R-values close to zero (Table 6.4.4). Depth had 2–3 times higher R-values than longitude, reflecting the much stronger depth effects on community structure. R-values for longitude were below the threshold typically considered biologically meaningful. Interannual variability could not be assessed for community comparisons of all three study years (2012, 2013, 2014) because sampling locations in 2012 were different than in the other years, which would confound the time element with location in that comparison.

6.4.2.4 Community Relationships to Environmental Variables

Depth and hydrographic variables provided the best match to patterns in epibenthic shelf (20–100 m, plus latitude) and full depth-range (20–1000 m) communities, and sediment characteristics were more prominent drivers of community structure in slope communities (200–1000 m) (Table 6.4.5). The single-most important variables were temperature for the shelf community and depth for the slope and full depth-range communities.

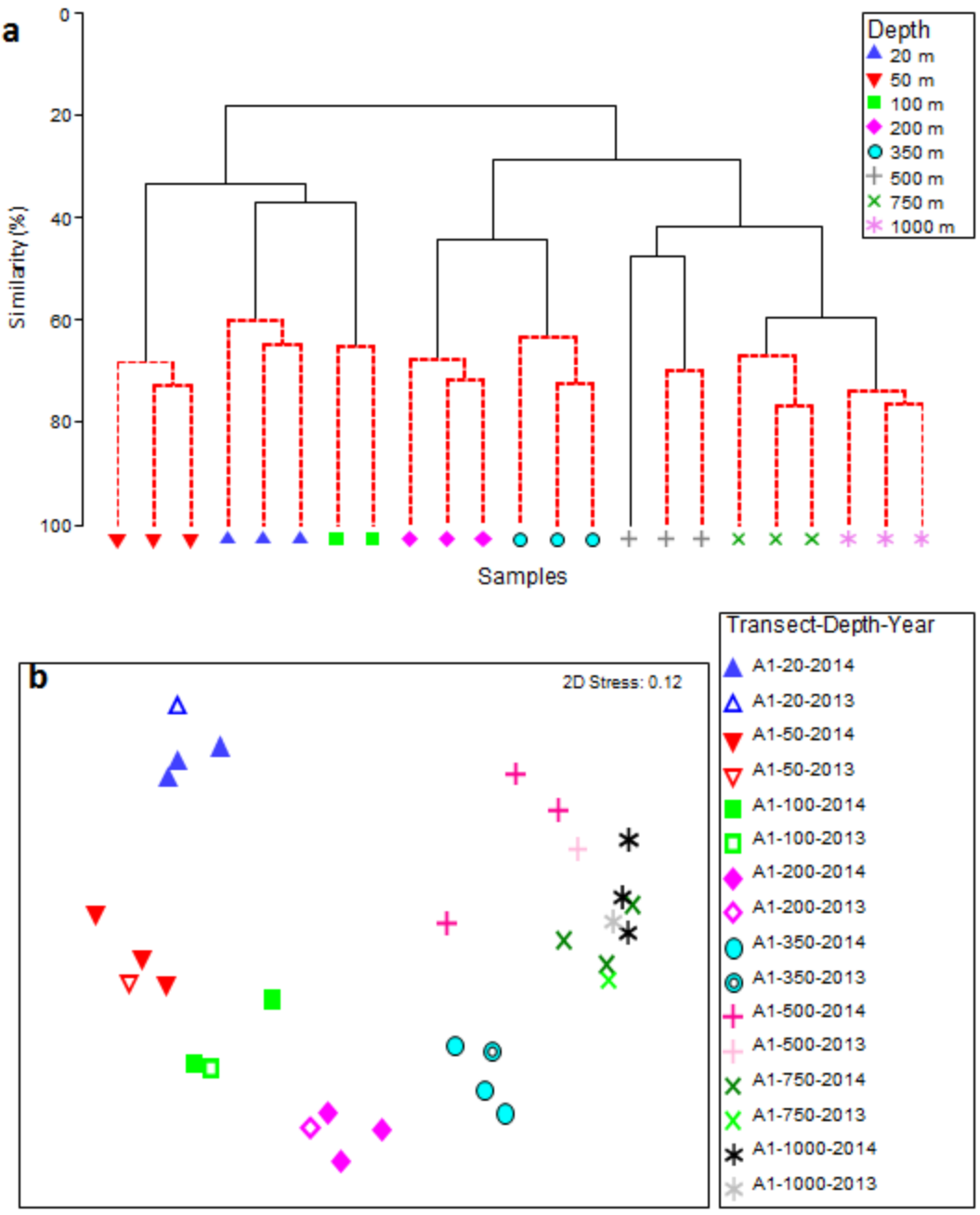

Figure 6.4.9. Community structure of repeat trawls along depth strata of transect A1 (141° W) sampled in 2014 and comparison with transect sampled in 2013.
All analyses based on fourth-root transformed (4RT) community biomass data and use Bray-Curtis similarity matrices.

a) Clusters for 2014 repeat sampling. Red lines indicate non-significant differences among samples based on the SIMPROF test within the hierarchical cluster analysis.
b) Multidimensional scaling plots include 2014 repeat sampling (filled / dark symbols) at depth strata along transect A1 (141° W) as well as the same stations sampled in 2013 (open / light symbols).

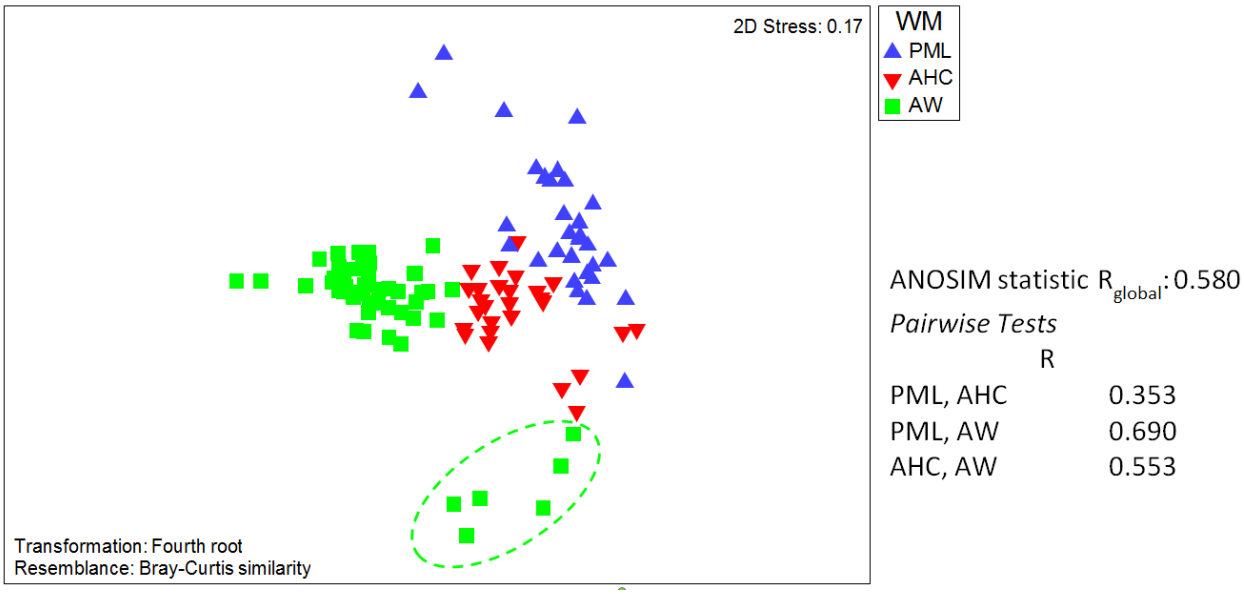

Figure 6.4.10. Epibenthic community similarity based on biomass grouped by water masses: PML – Polar Mixed Layer, AHW – Arctic Halocline Water, AW – Atlantic Water. Dashed ellipse circles stations in the Atlantic Water at 200–500 m along the B-transects sampled in 2012 (151–150° W) that are distinct from all other transect stations within the Atlantic Water. All data were fourth-root transformed (4RT) and MDS plots are based on a Bray-Curtis similarity matrix. ANOSIM test statistics are given for overall test and for pairwise comparisons between water masses.

Table 6.4.3. Percent similarity along transect A1 (141° W) on repeat trawls within 2014 (first column) and between trawls taken in 2013 and 2014 at the same station (second column).
Similarity percentages are based on SIMPER analysis of community composition based on biomass.

transect-depth	repeats within 2014	between 2013–2014
A1-20	61.50	49.72
A1-50	69.74	55.12
A1-100	65.11	57.53
A1-200	69.06	58.27
A1-350	66.34	60.78
A1-500	54.97	46.05
A1-750	70.84	60.55
A1-1000	74.63	69.67

Table 6.4.4. Effects of depth and longitude on community composition in 2012, 2013, and 2014, based on relative biomass and abundance data.
Ordered factors “depth” and “longitude” were tested in a 2-way crossed ANOSIM design. All data were exposed to a series of transformations before a Bray-Curtis similarity matrix was constructed for each transformation.

Biomass-based community structure			
	1-way ANOSIM	2-way crossed ANOSIM	
Transformation	**R (Year)**	**R (depth)**	**R (Long)**
NT	0.080	0.783	0.245
SQRT	0.083	0.809	0.292
4RT	0.088	0.823	0.298
Log(x+1)	0.084	0.822	0.298
PA	0.096	0.792	0.254
Abundance-based community structure			
	1-way ANOSIM	2-way crossed ANOSIM	
Transformation	**R (Year)**	**R (depth)**	**R (Long)**
NT	0.021	0.606	0.211
SQRT	0.031	0.717	0.325
4RT	0.037	0.818	0.332
Log(x+1)	0.039	0.798	0.345
PA	0.042	0.813	0.267

Table 6.4.5. Correlation of environmental variables with epibenthic communities, based on Spearman rank correlation coefficient (rho, BEST analysis).
Environmental variables for shelf/upper slope communities (20–350 m depth) included sediment characteristics. For communities covering the full depth range, only hydrographic variables were available for matching (see text for details). Community structure was based on biomass.

Slope communities (200–1000 m depth)		
# variables	**Rho**	**Variables**
1	0.802	Depth
2	0.816	depth, %gravel
7	0.886	depth, latitude, chl-*a*, porosity, %gravel, TOC, temperature
All-depth communities (20–1000 m depth)		
# variables	**Rho**	**Variables**
1	0.611	depth
2	0.687	depth, salinity
3	0.734	depth, salinity, temperature

6.5 Discussion

6.5.1 Pan-Arctic and Regional Patterns in Taxon Richness

Major taxa contributing to the overall community composition on the Beaufort Sea shelf and slope were very similar to what is known from other Arctic regions. For example, a recent compilation of major taxon richness across the entire Arctic showed that benthic communities in virtually every Arctic region are dominated by arthropods, mollusks, and polychaetes (CAFF 2017). In this same compilation, epibenthic taxon richness on the US Beaufort shelf was similar to the Chukchi Sea shelf. The numerical dominance of ophiuroids is typical for the Arctic epibenthos. In this study, we found the dominant species was *Ophiocten sericeum* in the eastern Beaufort Sea in contrast to the more common *Ophiura sarsii* found in the Chukchi and western Beaufort Seas (Bluhm et al. 2009, Konar 2013, Ravelo et al. 2014, Ravelo et al. 2015). The large abundance and biomass of predatory gastropods (e.g., *Colus* spp.) found in this study is typical for Arctic shelves (Bluhm et al. 2009). Among the arthropods, the Beaufort Sea shelf and slope communities primarily contained a high diversity and abundance of amphipods and decapod shrimp. The numerical abundance of pycnogonids, especially at depth in the eastern Beaufort, was surprising as they are typically a rare group. In a pan-Arctic shelf perspective, pycnogonids present less than 4% of the species richness within the arthropod group (Piepenburg et al. 2011). Very few brachyuran and anomuran crabs occurred in this region, which is different from the adjacent Chukchi Sea shelf where the snow crab *Chionoecetes opilio* and the lyre crab *Hyas coarctatus* can be community dominants (Bluhm et al. 2009, Ravelo et al. 2014). We encountered appreciable numbers of snow crab only during the farther west (central Beaufort Sea) collections in 2012. As has been reported for the western (Logerwell et al. 2010, Rand and Logerwell 2011) and central Beaufort Sea (Bluhm et al. 2015, Ravelo et al. 2015), most snow crab found here are large (Figure 6.4.3) compared with the prominently smaller crab size on the adjacent Chukchi Sea shelf (Konar et al. 2014). Interestingly, with one exception, we only found male crabs, suggesting females are either spatially segregated (see Bluhm et al. 2015 for the western Beaufort Sea) or, perhaps, the Beaufort Sea crabs are a gender-specific extension of the Chukchi shelf crabs. Either way, genetic evidence points to all Pacific Arctic snow crabs being a panmictic population across their distribution range (Albrecht et al. 2014) and strong exchange between the seas is expected.

6.5.2 Pan-Arctic and Regional Patterns in Total Epibenthic Biomass and Abundance

In larger-scale comparisons with other Arctic regions, maximum total epibenthic biomass on the Beaufort shelf was about an order of magnitude lower than maximum epibenthic biomass on the adjacent Chukchi Sea shelf (Bluhm et al. 2009; note: this study used the same trawl setting). In the Chukchi Sea, biomass exceeded 200,000 g wet weight 1000 m^{-2} at some high biomass stations compared with the maximum biomass in this study of ~123,000 g wet weight 1000 m^{-2}. Surveys from 2011 also showed higher maximum biomass on the western Beaufort Sea shelf and upper slope, but biomass on the central and western US Beaufort shelf was similar to results presented here (Konar 2013, Ravelo et al. 2015, note: this study used the same trawl setting). These findings align well with those from the other regions of the Arctic shelf and upper slope, suggesting that high benthic biomass coincides with regions of persistently high food supply (benthic hotspots; Grebmeier and Barry 1991, Piepenburg 2005). Regions, such as the Chukchi

Sea and the Barents Sea in the Atlantic Arctic, are nutrient rich with high levels of primary production. Through tight pelagic-benthic coupling, this primary production settles to the seafloor and supports high benthic biomass (Piepenburg 2005). In contrast, interior shelf systems, such as the Beaufort Sea or the Laptev Sea in the Russian Arctic, are typically less productive and support lower benthic biomass. "Benthic hotspots" are defined as regions with long-term high primary productivity and persistently tight pelagic-benthic coupling. These factors create localized areas of high benthic biomass that persist over time scales of multiple years to decades (Grebmeier et al. 2015a). Thus, the study time of this project was not sufficient to make any inferences on possible benthic hotspots within the Transboundary study region.

Within the Transboundary study region, total biomass and abundance showed distinct depth-related patterns. Total biomass and abundance generally peaked at depths between 50–200 m, which are outer shelf/upper slope (Figures 6.4.4 and 6.4.5). Biomass was often low at shallower depths (20 m), and communities were often dominated by mobile isopods and amphipods, groups that are tolerant to the dynamic shallow-water environment. The shallow shelf (20–50 m) is strongly affected by freshwater discharge from the multiple rivers draining into the Beaufort Sea (Macdonald and Yu 2006), mobile sediments (often sandy bottoms), and strong ice scour, disturbances that limit development of a particularly biomass-rich, stable and diverse epibenthic community. In contrast to biomass, we found some high abundances, especially at the 50-m depth stratum (Figure 6.4.4), which in nearly all cases was dominated by the brittle star *Ophiocten sericeum*. This species can occur in extremely large abundances (e.g., >70,000 individuals 1000 m^{-2} at the 200-m stratum at transect A6 [146° W] in 2013), but with low relative biomass due to the species' small body size (using total abundance and biomass of this taxon per station, we calculated an average body weight of just 0.15 g per individual). High abundances of certain taxa (also found for some isopods and amphipods at the 20-m depth stations) indicate that a select number of species are resilient to the dynamic conditions in this depth range and are able to thrive under these conditions. At greater depth (>200 m), we found less biomass and abundance. The simultaneous decline of both metrics indicates that the decline in biomass and abundance with depth was due to fewer individuals at greater depth and not smaller body size. In fact, some of the most dominant taxa at depth >500 m were large-bodied sea stars (e.g., *Bathybiaster vexillifer*), holothurians (*Molpadia borealis*) and brittle stars (*Ophiopleura borealis*). In a comparison with the above-mentioned individual body weight of the shelf brittle star species *O. sericeum*, the average individual body weight of the deep slope species *O. borealis* was 7 g per individual. This large body size of deeper slope species is contrary to previous observations that Arctic deep-sea fauna is small (Bluhm et al. 2011), but it may be that body size decreases closer to the actual deep-sea plain. The maximum depth stratum sampled in this project (1000 m) was still located on the slope and likely exposed to more dynamic food supply from downward shelf transport or upwelling (Bell et al. 2016) than the deep-sea plain proper where limited food supply is thought to drive epibenthic communities and their food webs (Iken et al. 2005, Bluhm et al. 2011).

There was no clear longitudinal trend in epibenthic biomass within the Transboundary region when considered over the ~9° range in the region covered in 2013 and 2014 (146°–137° W, Table 6.4.2). In contrast, a strong effect of longitude occurred when the region sampled in 2012 (4–5° farther west; 151°–150° W) was included (Table 6.4.4). This indicates the possibility of an abrupt transition zone in epibenthic communities rather than a gradual change. This agrees with significant change previously observed in shelf epibenthic communities between the central and the eastern Beaufort Sea in 2011 (Konar 2013, Ravelo et al. 2015). We show here, however, that

these longitudinal differences are mostly related to slope communities at depths between 200 and 500 m (Figure 6.4.8a and Appendix D Figure 3; note large separation of 2012 data at those depths in MDS plots). The longitudinal community differences on the slope occurred with a switch in the dominant ophiuroid species, from *Ophiura sarsii* in the central Beaufort sampled in 2012 (151°–150° W) to *Ophiocten sericeum* in the eastern Beaufort sampled in 2013 and 2014 (146°–139° W). *O. sericeum* is an Arctic endemic species with general detritus-feeding habits that may allow it to thrive in the more eastern Beaufort shelf region (146°–139° W, sampled in 2013 and 2014), which is farther away from Pacific water influence and subject to more terrestrial organic matter inputs. Snow crabs (see above) were only common in the central region (B-transects at 151°–150° W in 2012) and contributed to the observed longitudinal differences in the 350–500 m depth range. In addition, the mudstar *Ctenodiscus crispatus* played a larger role in the central Beaufort slope communities (151°–150° W in 2012) compared with the more eastern communities sampled at 146°–139° W in 2013 and 2014. Lastly, some of the longitudinal community composition changes we observed were associated with gastropods (e.g., *Cryptonatica affinis*, *Tachyrhynchus erosus*), although none were individually dominant in the communities.

6.5.3 Interannual Variability in Epibenthic Biomass and Abundance

Variability in total biomass and abundance occurred at stations that were sampled in both 2013 and 2014 (Figure 6.4.5, Figure 6.4.6 and Appendix D Figure 1). This is certainly, in part, driven by the spatial patchiness of epibenthic organisms typical for Arctic shelf systems (see Piepenburg and Schmid 1996). Patchiness can be driven by local habitat features (e.g., sediment structure) or food availability, factors to which the mobile epifauna is particularly suited to respond. Some epibenthic taxa can occur in such extremely high abundances or biomass (see example of *Ophiocten sericeum* mentioned above, also: Piepenburg and Schmid 1996, MacDonald et al. 2010) that even a small spatial offset in position can change biomass or abundance patterns quite significantly. In addition, if epibenthic accumulations occur in response to temporally dynamic features such as food deposition, a single location will likely vary in epibenthic biomass and abundance over time. Hence, observing interannual differences in absolute biomass and abundance is not surprising. However, we also showed that many relative patterns of biomass and abundance by depth were consistent over the two sampling years 2013 and 2014 (see Figure 6.4.6). For example, the 50-m depth stratum at transect A1 (141° W) and the 100-m stratum at Transect TBS (140° W) always had the highest biomass, regardless of year sampled. This means that, despite, high variability in absolute biomass, the relative patterns of high or low biomass are quite persistent.

This consistency across years was also evident when looking at the biomass of individual taxa along the shelf and slope station groups for 2013 and 2014 (Appendix D Table 1). It has to be noted that this larger spatial view of "Beaufort shelf" and "Beaufort slope" integrates multiple stations across shelf depth and slope depth strata, and across the longitudinal transects. This averages over the variability of the individual stations, which is evident in the rather high variances associated with the averages (Appendix D Table 1). Though variance was high, absolute biomass values differed between the two years, patterns of species species richness were consistent. Several taxa from various phyla had high biomass on the shelf but not on the slope, e.g., sponges, the scallop *Similipecten greenlandicus*, the gastropod *Margarites* spp., the cumaceans *Diastylis* spp., the isopod *Synidotea bicuspida*, the amphipods *Anonyx* sp. and *Atylus* sp., the holothurian *Psolus peronii*, the sea stars *Crossaster papposus*, *Leptasterias* spp. and

Urasterias linckii, and the bryozoan *Alcyonidium* spp. It is likely that these taxa are stenobathic, meaning they only occur at a specific depth range, in this case, the shelf depth of ≤100 m. Similarly, some taxa, such as octopus, the holothurian *Molpadia borealis*, the brittle star *Ophiopleura borealis*, the sea star *Bathybiaster vexillifer*, and ascidians of the genus *Ascidia* were stenobathic at greater depth along the slope. As such, these taxa can be viewed as indicators of the shelf or the slope environment, respectively (also see discussion of community indicator species below). It is currently unclear whether this stenobathic nature is driven by competitive interactions or physiological factors that prevent species from living at particular depths and may not be the same for all the taxa. Other taxa such as the anemone *Allantactis parasitica*, the gastropods *Buccinum* spp. and *Colus* spp., the isopod *Saduria* spp., decapod shrimp such as *Argis* sp., *Paulus* spp. and *Sabinea septemcarinata*, the sea star *Icasterias panopla*, and others occurred across the entire depth range in appreciable biomass, indicating their eurybathic nature. Some taxa did not show consistent relative patterns of shelf or slope association over the two years. For example, we found the snow crab *Chionoecetes opilio* on the shelf in 2014 but on the slope in 2013. With this particular species, it is likely that its main distribution in the study region is along the shelf edge, thus, can sometimes be found at the edge of the shelf and at other times at the upper slope.

6.5.4 Patterns in Epibenthic Community Structure (Multivariate Patterns)

Analytical considerations of appropriate community data transformations were assessed because benthic communities are generally characterized by the highly unequal distribution of taxa. Often, a few species will make up the majority of the abundance or biomass, and many other species will occur with few individuals or low biomass. Datasets are notorious for having a large number of zeros, indicating non-occurrence of a taxon at a particular location. Such uneven datasets can cause problems in the statistical analysis, although multivariate analyses of community structure are less dependent on the distributional properties of taxa than univariate statistics (Clarke et al. 2014a). However, the specific nature of multivariate datasets with large numbers of zero-values poses a different challenge, specifically, how much "weight" is given to common versus rare species in the analysis. This emphasis can be changed by appropriate data transformations. Unlike univariate analyses, there is no objective criterion that determines the "right" transformation; rather, it depends on the question that is being asked. For example, if the emphasis is on a comparison of common taxa across a region, then a minor transformation should be applied. However, if a rare species is being considered or being treated equivalent with common species, then a strong transformation should be applied (Clarke et al. 2014a). Our current questions targeted the overall community structure, not specific species. As such, we were interested in keeping the main dominance structure within the dataset while accounting for species that occurred irregularly or lower in abundance. We used a variety of transformations to assess the effect on community composition results. Overall patterns in community structure were relatively similar across all transformations, with the exception of the presence/absence transformation, which changed the results considerably and eliminated structure in community patterns seen with other transformations. We decided to employ a 4RT transformation for all our analyses because it yielded the lowest stress level in two-dimensional ordination (stress = 0.17, see Figure 6.4.7 and Appendix D Figure 2) and it best balanced the influence of common and rare species.

Depth was one of the largest drivers of epibenthic community structure, especially on the slope and at full depth-range (Table 6.4.5, Figure 6.4.8, Appendix D Figure 3). Depth is a proxy

for different environmental conditions in the Arctic system (Piepenburg 2005, Roy et al. 2014, 2015). In the Beaufort Sea, depth also coincides with main water masses (Macdonald et al. 1989, Lansard et al. 2012) that correlated strongly with community structure (Figures 6.4.8a, 6.4.10, Appendix D Figures 3 and 5). Very shallow regions (<30 m) are heavily influenced by ice scour, sedimentation, and freshwater influence (Mahoney et al. 2014, Dunton et al. 2006). Shelf communities (to about 100 m depth) are more stable, but are strongly influenced by changing food supply, both seasonally and through variations in water mass characteristics (e.g., nutrient regimes, upwelling; Iken et al. 2010). Generally, food availability decreases with increasing depth (Bluhm et al. 2011, Roy et al. 2014). The slope environment is dynamically impacted by water mass layers with different hydrographic properties and biogeographic affinities. The strong influence of hydrographic conditions on community structure is reflected in our environmental analysis that showed temperature and salinity were driving factors of community composition over the large depth range considered. Vertical water mass layers over the Beaufort shelf and slope include a thin surface freshwater layer (0–10 m) from rivers and a layer from sea icemelt that overlays the Pacific-derived Polar Mixed Layer (PML) (≤50 m; Macdonald et al. 1989). The PML gives way to AHW between ~60–200 m. This AHW transitions into the warmer and more saline Atlantic-derived water below 200 m, which layers over the cold Canada Basin deep water at approximately 800–1000 m depth (Lansard et al. 2012). Each water mass is distinct in temperature, salinity, nutrient concentration, and organic matter composition (Macdonald et al. 1989). Because water masses are so distinctly defined by depth, it is impossible for us to distinguish between depth-driven community patterns, which might indicate community turnover caused by depth related physiological or food limitations, and patterns caused by the influence of other water mass properties.

The continuous change in community composition with depth (Table 6.4.5, Figure 6.4.8, Appendix D Figure 3) was reflected in the distribution of some characteristic taxa. Shallow stations (20 m) were dominated by mobile species such as decapod shrimp (*Eualus gaimardii*, *Sabinea septemcarinata*), *Ophiocten sericeum*, and amphipods (e.g., *Anonyx* sp.). These taxa are either mobile and can avoid larger disturbances, or they have large tolerance windows for environmental conditions such as low salinity. Most also have omnivorous feeding habits, which allows them to capitalize on a large variety of food sources (Bell et al. 2016). At the 50-m depth stratum, the sea cucumber *Psolus peronii* would often dominate the community biomass, but the species was rare at 20 or 100 m (some intermediate depths sampled indicate that *P. peronii* occurs between 35–50 m depth, with highest biomass at 50 m). This species seems to have an extremely patchy distribution, often contributing >50% to biomass at those stations where they occurred. The restricted distribution to around the 50-m depth stratum may indicate specific hydrographic features that favor this filter-feeding taxon (e.g., current regimes) and the reduced level of physical disturbance at that depth may allow this slow-moving species to thrive. Between 20–100 m depth, the brittle star *O. sericeum* was highly abundant; however, with its small size, it contributed less to overall biomass than some less abundant but larger species. This brittle star is common in high densities in many Arctic shelf regions, and it plays important roles in nutrient recycling (Piepenburg et al. 1997). The ophiuroid *Ophiacantha bidentata* was also prominent at 100–200 m depth but was replaced in dominance by *Ophiopleura borealis* at depths >350 m. Together, the distinct depth zonation and the dominant role each species plays within the communities at their specific depth ranges showcase the overall importance of brittle stars in Arctic benthic systems and may indicate resource partitioning among these species (Graeve et al. 1997). The sea star *Pontaster tenuispinus* started to occur regularly at 200 m and occasionally

dominate the community together with *O. borealis* to 750 m depth, which is at the shallower end of the common depth range for this sea star (Smirnov 1994, Howell et al. 2002). At 1000 m, the deep-sea scavenging/predatory sea star *Bathybiaster vexillifer* became co-dominant with the brittle star *O. borealis*. The sea star *B. vexillifer* is known to source carbon from both phyto-detrital and microbial sources (Howell et al. 2003), which supports our hypothesis that microbial processing of organic material is an essential component of the deep-slope food web of the Beaufort Sea (Bell et al. 2016).

SIMPER analysis identified some of these taxa as indicator species for either the shelf or the slope (Appendix D Tables 2, 3). Indicator species are defined by their frequency of occurrence as well as the biomass they contribute overall; this term does not relate to their ecological significance in the system, per se, or their resilience or vulnerability to disturbances in the system. However, given their prominence on shelf or slope, we can certainly assume that they are playing important roles in ecosystem functioning of the shelf or slope. On the shelf, some of the main indicator species were the brittle star *Ophiocten sericeum*, the scallop *Similipecten greenlandicus*, the shrimp *Sabinea septemcarinata*, the amphipod *Anonyx* sp., and cumaceans *Diastylis* spp. (Appendix D Table 2). Some of these taxa are known to be essential in mineralization processes of the organic matter on the Arctic shelf (Piepenburg and Schmid 1996, Blicher and Sejr 2011). We know from food web studies within the Transboundary project (see Chapter 8) and other Arctic food web studies (e.g., Iken et al. 2010) that some taxa such as cumaceans play specific but poorly understood roles in organic matter processing by feeding on particularly low trophic levels. Their status as indicator species on the Beaufort Sea shelf suggests that loss of these species from major disturbances of the system could have significant impacts on energy flow to higher trophic levels. For example, the brittle star *O. sericeum* is known to respond with increased metabolic rates and energy demands to disturbances of temperature increases and ocean acidification (Wood et al. 2011), so it is reasonable to assume that other disturbances, such as from oil and gas development, could also impact the performance of ecosystem functions of this species.

Indicator species of the slope environment were, in particular, the sea stars *Pontaster tenuispinus* and *Bathybiaster vexillifer* and the brittle star *Ophiopleura borealis* (Appendix D Table 2). Again, while their specific ecosystem functions are not entirely known, their frequency and abundance indicate that they must play important roles in the system. The brittle star *O. borealis* is known to contain relatively high total lipid content and high levels of some essential fatty acids (Graeve et al. 1997, Gallagher et al. 1998), which could make them important sources of these lipids to higher trophic levels through predator-prey relationships. While brittle stars are typically not considered high-quality prey because of their high level of inorganic material, this particular species could be an important prey item and lipid/fatty acid source in the deeper slope environment, a system with overall low food availability. There is no information on the vulnerability of this and other slope species to disturbances, but any disruption of such species with important ecosystem functions would likely have cascading effects through the remainder of the system.

We explored the possibility of using higher-level taxonomic identifications for epifauna as a viable tool for cost- and time-efficient monitoring of the Beaufort Sea shelf and slope systems. The premise of taxonomic sufficiency is that identification to a higher taxonomic level is more efficient and can be done by less-trained personnel, but care has to be taken to assure that critical information is not lost in the process. For example, closely related species may exhibit different ecological or biological responses and patterns that could be overlooked by grouping at higher

taxonomic levels. In our analysis, we found that the distinct depth-related gradient in community composition (see discussion above) is considerably weakened when analyzing epibenthic communities at the higher taxonomic level of mostly class or order level (Figure 6.4.8, Appendix D Figure 3). Considering that depth-related trends were most important in both visual community ordinations (Figure 6.4.8, Appendix D Figure 3) and in BioENV analysis of community structure in relation to environmental variables (Table 6.4.5), higher taxonomic grouping could cause loss of this significant information. Using higher taxonomic level identifications would also impact on the level of individual taxa that we identified as ecologically important or as indicator taxa. For example, the separation along a longitudinal trend in the abundance of the brittle star species *Ophiura sarsii* in the more central region (B-transects, 151–150° W) compared with the dominance of *Ophiocten sericeum* in the more eastern study region (146–138° W sampled in 2013 and 2014) was detected based on identification to species level. By grouping on the class level Ophiuroidea, recognition of this separation would disappear. This may be an important consideration for monitoring efforts that focus on changes in community structure over time. Different ophiuroid taxa also were indicator species of the shelf community (*O. sericeum*) versus the slope community (*Ophiopleura borealis*), which could not be distinguished at the class level. Other examples are within the order Isopoda, where we found some taxa to be broadly distributed across all depth strata (*Saduria* spp.) while others were restricted to the shelf (*Synidotea bicuspida*), a distinction only possible with species-level identifications (Appendix D Table 1). Therefore, the value of being able to assess species-specific responses within the benthic community is undeniable. However, ultimately there is no overarching right or wrong approach; use of lower or higher taxonomic identifications depends on the scientific questions being asked or the purpose of the monitoring program to be initiated. If benthic epifauna is being used as indicators of change from climate changes or oil and gas exploration, then species-level information is likely critical, at least for the taxa we identified as indicator species (Appendix D Tables 1–3). A much lower taxonomic identification level is sufficient for purposes of total biomass and abundance. If biodiversity observations are being used as metric that informs managers about ecosystem health and services (Palumbi et al. 2008, Duffy et al. 2013), then an even lower taxonomic level identification than we have done here may need to be implemented (here, some groups were kept at higher levels because of difficulty of field identifications or a global lack of taxonomic experts for verification). This is challenging for some of the taxonomically more difficult groups such as bryozoans, hydroids, sponges, and etc.

6.5.5 Small-Scale Spatial Variability in Community Composition

One logistical constraint common to epibenthic studies is the lack of replication in trawl sampling. Given the highly patchy distribution of epibenthic organisms (see above; Piepenburg and Schmid 1996), lack of replication raises the question: How representative of the actual community is a single trawl haul for a given location? Here, we had the opportunity to take repeat trawl samples along one transect (A1, 141° W) in 2014. Our analysis showed that a single trawl was a good representation of the local community composition, which gives confidence to the information gleaned from the typical single trawl hauls (Figure 6.4.9, Appendix D Figure A). It is important to note that absolute abundance and biomass of individual taxa, or even overall, can still be strongly variable between trawl hauls (data not shown here) while the overall community composition (i.e., the relative composition of taxa and overall structure) remains quite stable. This was also the case in this study when comparing two trawl gear types (see gear

comparison in previous reports) and for repeat trawls completed on shallow shelf stations in the western Beaufort Sea in a previous study (Ravelo et al. 2015). In both cases, there were no significant differences in community composition and community structure among repeat trawls.

We found little evidence of interannual variability in epibenthic communities in the eastern Beaufort Sea, indicating that these communities were quite stable during the two years they were sampled. Community composition at 2013 stations (transect A1, 141° W) that were resampled in 2014 (see above) was very similar among the two years. Separation in the nMDS ordination between repeat trawls within the same year was very similar to the separation between the two years (Figure 6.4.9, Appendix D Figure A), indicating that intra- and inter-annual variability were similar. Further, comparing patterns in total biomass across several transects sampled in both 2013 and 2014 showed that overall patterns were similar (Figure 6.4.6). These results support the idea that the longevity of most benthic invertebrates in the Arctic contributes to the long-term stability of the Arctic benthic communities (Bluhm et al. 1998, Philipp and Abele 2010, Grebmeier et al. 2015b). This longevity allows them to integrate short-term variability in the environment. However, this stability in benthic community structure may be temporally limited, and if environmental conditions were to change over longer time scales, patterns in epibenthic communities would likely also change (Grebmeier et al. 2015b). The time scales for such changes would depend, at a minimum, on the type, severity, and persistence of the changes and the tolerance levels of the taxa involved.

6.6 Summary

Epibenthic communities in the central to eastern Beaufort Sea, including shelf and slope, were diverse with an overall phylum composition typical for Arctic benthic systems. Epibenthic communities had high interannual stability over the study years, especially in community composition, even though the abundance or biomass of some taxa varied greatly. Longitudinal changes in epibenthic communities were particularly noticeable between the central and the eastern study region (150°–146° W) but were less pronounced over the eastern range (146°–137° W). These longitudinal differences may represent a biogeographic break where the Pacific water influence from the Chukchi Sea diminishes and causes a change in the taxa present. They may also reflect the influence of the Mackenzie River delta on the hydrographic environment in the eastern study area, which could impact species composition. Either hypothesis could explain the observed importance of salinity and temperature as environmental variables driving to variability in epibenthic communities. Depth was one of the main factors influencing epibenthic community structure. Depth-related community structure changes coincided with dominance of characteristic taxa according to their typical depth ranges and possibly due to some resource partitioning, especially among the ophiuroid species. Depth as a proxy for environmental conditions and water masses was most likely related to dynamic and stressful environmental conditions in very shallow waters, abundant food supply on shelf depths, and increasing food limitation at greater depth, which may cause greater reliance on microbially altered food sources. It is suggested that the stability of epibenthic communities is related to the longevity of most Arctic benthic species, which creates some resilience to changing conditions caused by climate changes or anthropogenic influences. However, this resilience is necessarily limited and likely depends on severity and persistence of the change and the tolerance levels of the taxa involved.

7.0 FISH ECOLOGY

Brenda Norcross, Brenda Holladay, Lorena Edenfield, Sarah Apsens, Alyssa Frothingham, Ben Gray, and Kelly Walker

7.1 Introduction

Fish resources are important to the coastal communities of Alaska both directly and to upper trophic levels in the Beaufort Sea ecosystem, such as marine mammals and birds which are of great food and cultural importance. The characteristics of marine fishes of the Beaufort Sea are similar to those in other Arctic locations like the Chukchi and Barents Seas, i.e., widely dispersed, small populations, patchy distribution, numerous rare species, and numerous zero counts.

Research to describe fish distribution and abundance in the US Beaufort Sea has been limited to date (Figure 7.1.1). Fish surveys have been conducted sporadically in the US Beaufort Sea from Barrow to the Alaska-Canada border (Figure 7.1.1); however, contemporary data were absent east of 145º W until we sampled 145º–137º W in 2013 and 2014. The only continuous long-term monitoring (1981–present) has been in the very nearshore shallow (<3–20 m) waters in the Prudhoe Bay oil development region (Craig et al. 1985, Fechhelm et al. 2010, LGL 1999, Thorsteinson et al. 1992). Surveying fish on the shelf has been extremely limited to broad but sparse sampling in 1977, depth 40–400 m (Frost and Lowry 1983); dense sampling in the western Beaufort Sea in 2008, depth 30–470 m (Logerwell et al. 2011, Rand and Logerwell 2011), and the broad and dense sampling of 200 km of the Beaufort Sea shelf in 2011, depth 13–223 m (Norcross et al. BOEM 2017-034).

The Arctic environment is warming rapidly, which is likely to have direct and indirect effects on fish individuals and communities (Fossheim et al. 2015). More information is required about the sparsely documented fish species inhabiting the Alaskan Arctic. In 2009 the North Pacific Fishery Management Council (NPFMC) adopted, and the Secretary of Commerce approved, an Arctic Fishery Management Plan (FMP) that prohibits new commercial fishing in Beaufort Sea waters. The FMP closes the Arctic Management Area to commercial fishing so that unregulated fishing does not occur until sufficient information is accrued to allow fishing to be conducted sustainably, and with due concern for other ecosystem components (NPFMC 2009). Also, offshore oil exploration interest in the US Arctic necessitates baseline information. Knowledge of the current status of fish populations in the Beaufort Sea is necessary to identify fish species potentially vulnerable to oil and gas development, their life stages, Essential Fish Habitat, and to inform the new emphasis on food web modeling and Arctic climate change issues.

7.1.1 Objectives

The general objective of the Fish Ecology portion of this project is to document baseline fish species presence, abundance, distribution, and habitat during the open water season. Additionally, we address the objective to analyze age patterns of the most abundant fish species.

This research was designed to address the hypotheses that distribution, relative abundance, and species assemblages are equal across life stage, habitat, central and east US Beaufort Sea waters, east and west sides of the Mackenzie Canyon, and shelf (benthic and pelagic) and slope (benthic and pelagic) waters. These hypotheses are all very complex and will be addressed in several ways through this section.

a.

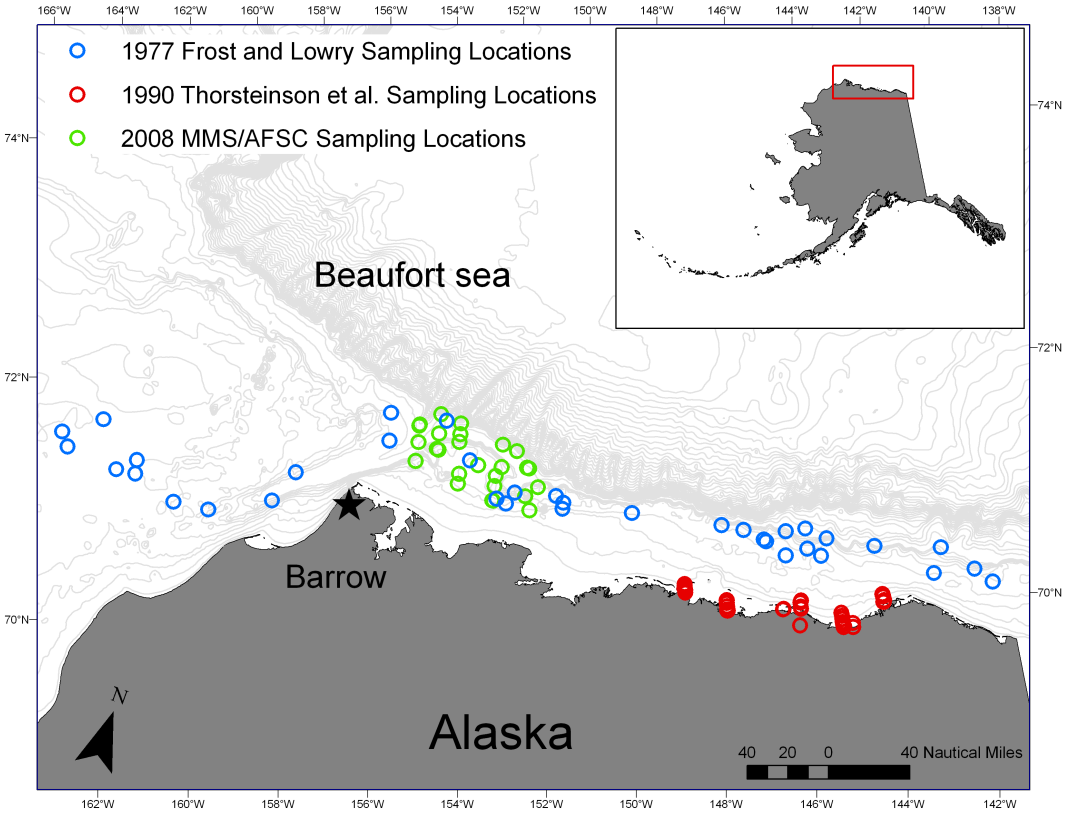

b.

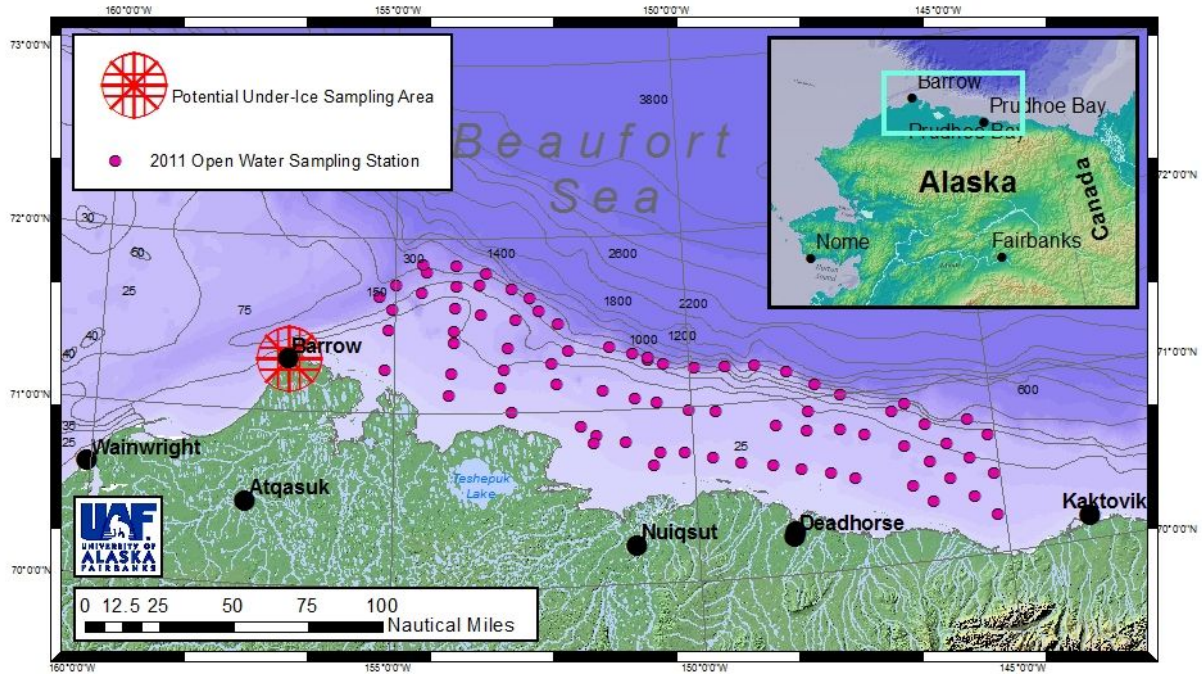

Figure 7.1.1. Historical fish surveys in the Beaufort Sea. (a) 1977–2008, (b) 2011 (Norcross et al. in review).

7.2 Methods

7.2.1 Sample Collection

Open water expeditions were conducted during 2012, 2013, and 2014 from the central US Beaufort Sea into the eastern Canadian Beaufort Sea (Figure 7.2.1). Spatial comparisons were made across the whole sample area from 151º–135º W. The western (B) transects off the Colville River, 151º–150º W, were sampled in 2012 and the eastern transects from Camden Bay (CB) to the Alaska-Canada border, 147º–135º W, were sampled in 2013 and 2014. The groups of B and A transects in US waters, and the TBS transect, were placed along lines of longitude. The MAC and GRY transects radiated to the northwest from near the mouth of the Mackenzie River. Depths from 20 to 1000 m were sampled across the whole study area. We originally intended to sample farther east into the Canadian Beaufort in two years to test the hypothesis that fish distribution was changed by the Mackenzie River. Unfortunately, time constraints only allowed advancing sample in the Canadian Beaufort past the Mackenzie River (MAC and GRY transects) in 2013. However, the Canadian teams sampled in the eastern Beaufort Sea in 2012, 2013, and 2014. We anticipate additional analysis to explore this hypothesis in more detail in conjunction with our Canadian colleagues. As of 2017, we have not yet been able to pursue this because a formal MOU was never signed between the US and Canada, resulting in the requirement that the Canadian information be published before any joint efforts between countries is permitted.

Both pelagic and demersal trawls were deployed (Table 7.2.1, Appendix E1). Gears and deployment methods are described in detail in Sections 2.5 and 2.6. Pelagic fishes were collected in 2012 and 2013 by an Isaacs-Kidd midwater trawl (IKMT) and in 2014 with an Aluette midwater trawl (AMT). Demersal fishes were collected from the seafloor with a plumb staff beam trawl (PSBT-A) in 2012, 2013 and 2014, whereas the Canadian beam trawl (CBT) was only fishes in 2012. Use of the two beam trawls will facilitate comparisons with other research in the Beaufort Sea. Additionally, demersal fishes were collected with a larger otter trawl (OT) in 2012 and on A6 in 2013.

Preliminary identifications were made aboard ship and fishes were returned to and processed at the University of Alaska Fisheries Oceanography Laboratory (FOL) in Fairbanks.

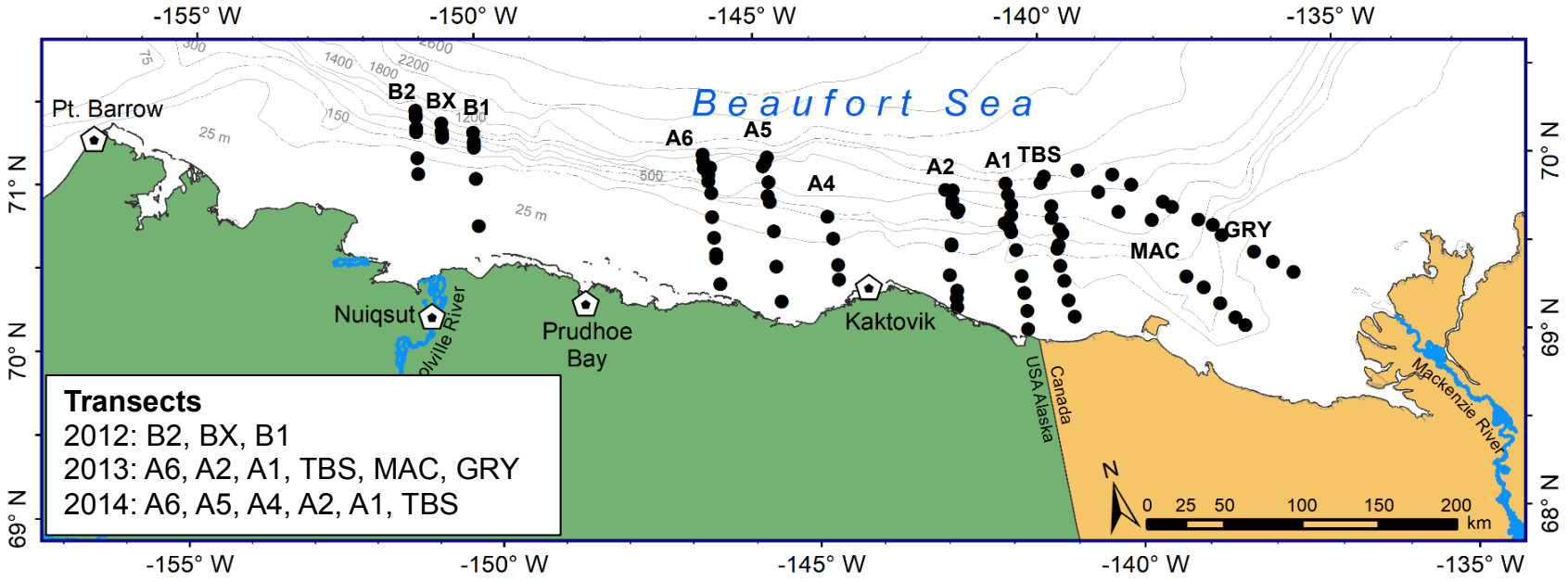

Figure 7.2.1. Transects and stations sampled in the Beaufort Sea 2012–2014.

Table 7.2.1. Successful pelagic and demersal gear deployments at stations occupied 2012–2014.

		2012				2013				2014	
Station	Longitude	IKMT	PSBT-A	CBT	OT	IKMT	PSBT-A	CBT	OT	AMT	PSBT-A
B2-20	151°W	x	x	x	x						
B2-50	151°W	x	x	x	x						
B2-100	151°W	x	x		x						
B2-200	151°W	x	x		x						
B2-350	151°W	x	x	x	x						
B2-500	151°W	x	x	x	x						
B2-1000	151°W	x									
BX-1000	150.5°W	x									
BX-200	150.5°W		x	x	x						
BX-350	150.5°W		x	x	x						
BX-500	150.5°W	x	x	x	x						
B1-20	150°W	x	x	x	x						
B1-50	150°W	x	x	x	x						
B1-100	150°W	x	x	x	x						
B1-200	150°W	x	x	x							
B1-350	150°W	x	x	x	x						
B1-500	150°W	x	x	x	x						
B1-1000	150°W	x	x	x	x						
A6-20-13	146°W					x	x				
A6-20-14	146°W										x
A6-37-13	146°W					x	x	x	x		
A6-37-14	146°W										x
A6-50	146°W					x	x	x	x		x
A6-100	146°W					x	x		x		x
A6-200	146°W					x	x	x		x	x
A6-350	146°W					x	x	x	x		x
A6-500	146°W					x		x	x	x	x
A6-750	146°W					x	x	x	x		x
A6-1000	146°W					x	x	x			x
A6-1500	146°W										x
A5-20	145°W										x
A5-35	145°W										x
A5-50	145°W										x
A5-100	145°W										x
A5-200	145°W										x
A5-350	145°W										x
A5-500	145°W										x
A5-750	145°W										x
A5-1000	145°W										x
A4-20	144°W										x
A4-35	144°W										x
A4-50	144°W										x
A4-100	144°W										x
A2-10	142°W					x	x	x			x
A2-20	142°W										x
A2-30	142°W					x					
A2-40	142°W					x	x	x			x
A2-50	142°W										x
A2-100	142°W					x	x	x			x

Table 7.2.1. continued.

		2012				2013				2014	
Station	Longitude	IKMT	PSBT-A	CBT	OT	IKMT	PSBT-A	CBT	OT	AMT	PSBT-A
A2-200	142°W					x	x	x			x
A2-350	142°W					x	x	x		x	x
A2-500	142°W					x	x	x		x	x
A2-750	142°W					x	x	x			x
A2-1000	142°W					x	x	x			x
A1-20	141°W					x	x	x			x
A1-32	141°W					x					
A1-50	141°W					x	x	x			x
A1-100	141°W					x	x	x			x
A1-200	141°W					x	x	x			x
A1-350	141°W					x	x	x			x
A1-500	141°W					x	x			x	x
A1-750	141°W					x	x	x			x
A1-1000	141°W					x	x	x			x
TBS-35	140°W					x					
TBS-50	140°W					x	x	x			x
TBS-100	140°W					x	x	x			x
TBS-200	140°W					x	x	x			x
TBS-350	140°W					x	x	x			x
TBS-500	140°W					x	x	x			x
TBS-750	140°W					x	x	x			x
TBS-1000	140°W					x	x	x			x
MAC-50	140–138°W					x	x	x			
MAC-100	140–138°W					x	x	x			
MAC-161	140–138°W					x					
MAC-200	140–138°W					x	x	x			
MAC-500	140–138°W					x	x	x			
MAC-1000	140–138°W					x	x	x			
GRY-20	139–137°W					x	x	x			
GRY-50	139–137°W					x	x	x			
GRY-100	139–137°W					x	x	x			
GRY-200	139–137°W					x	x	x			
GRY-350	139–137°W					x	x	x			
GRY-500	139–137°W					x	x	x			
GRY-750	139–137°W					x	x	x			
GRY-1000	139–137°W					x	x	x			

7.2.2 Laboratory Processing of Midwater and Demersal Fishes

At the FOL, each fish was thawed, blotted dry, and field identification was confirmed or revised. Latin names are as accepted in October-2017 by the World Register of Marine Species (WoRMS, http://www.marinespecies.org/). Common names are as in the most recent version of the American Fisheries Society's (AFS) Common and Scientific Names of Fishes from the United States, Canada, and Mexico (Page et al. 2013). Where the fish is not in that source, common names are from WoRMS (2017). The exception is two Osmeridae for which common names are from the Alaska Arctic Marine Fish Ecology Catalog (Thorsteinson and Love 2016): Pacific Capelin – *Mallotus catervarius*, and Arctic Smelt – *Osmerus dentex*. Note that throughout this document the common name of *Lycodes polaris* is referred to as Canadian Eelpout as per the American Fisheries Society, however in Thorsteinson and Love (2016) it is listed as Polar Eelpout. Throughout this report we follow the AFS convention of capitalizing all words in fish common names. Total length was measured to the nearest mm, and wet weight was measured to the nearest 0.01 g for larger fish (≥10 g)) and 0.0001 g for smaller fish (weight <10 g). Sagittal otoliths were removed, cleaned, and stored dry in a centrifuge vial. Stomachs were removed by making an incision on the ventral side of the fish, opening the abdominal cavity, and cutting at the esophagus and the pyloric valve to remove the stomach. Stomachs were placed in Petri dishes, covered with water, and frozen before further processing. During processing of fish for stomachs, two muscle tissue samples were simultaneously collected for stable nitrogen and carbon isotope analysis. Muscle clips (approximately 5 x 5 x 5 mm of muscle, though the all dimensions could be limited by size of fish) were taken from above the lateral line toward the anterior end of the fish, making sure to exclude skin or bone. Muscle samples were freeze-dried for later isotope analysis.

Otoliths were sampled from a subset of the weighed fish and prepared for aging. Ages were estimated from fish species from all three cruises. Fish species were chosen for processing based on the number of individuals available in that year. Species with the most individuals from each family were considered to represent that family for age estimation. Specimens were selected for aging using a size-based selection process. The target quantity of specimens from each species was 20 individuals chosen at random from each 10 mm length increment for each year. However, in many cases an insufficient number of fish was available to reach this target; not all collected fish were able to be aged, e.g., only one *Lycodes polaris* was aged out of 30 individuals captured in 2013 (Figure 7.3.2.7). One sagittal otolith was mounted on the center of a 1 x 3 inch glass slide using Crystalbond™ thermoplastic glue. The otolith was polished (transversely sectioned) using a Buehler rotating wheel with 1200 grit sandpaper while water was continuously sprayed on the sandpaper to lubricate the paper and remove waste. The otolith was polished down to the center and flipped onto its flattened edge and polished to the proper thickness for aging (200–300 μ). Using a compound microscope at 100x magnification, the otolith was checked throughout the polishing process to ensure over-polishing did not occur. If over-polishing or other damage caused the first otolith to be unreadable, the second otolith was processed for aging.

Transverse cross sections of otoliths were photographed under transmitted light using a digital camera mounted on a Leica DM1000 dissecting microscope at 5x magnification. Otoliths were aged initially by two independent readers using the photographed image of each otolith. Ages were assigned by counting each full year of growth on the otolith. One full year or annual mark consists of one opaque zone of faster summer growth and one translucent zone of slower winter growth (Matta and Kimura 2012). Otoliths on which readers disagreed were reread

collaboratively by the same readers and assigned an agreed-upon age. Otolith ages were used for constructing plots for data visualization and quality control.

7.2.3 Statistical Analyses of Pelagic and Demersal Fishes

7.2.3.1 Fish Morphometrics

Statistical and graphic analyses were performed using SigmaPlot 12.5 software (Systat 2013). To exert control over the quality of data, for each species an initial length-weight relationship was estimated by polynomial linear regression using the standard fisheries allometric equation: = $W = a L^b$, where W = total weight (g), L = total length (mm), *a* = the y-intercept, and *b* = the slope (Ricker 1975). The fishes were generally small and lengths were measured in mm instead of cm, with the resulting *a* parameter expressed as 10^{-5}. For each species, scatter plots of weight versus length and age versus length were visually examined (Giacalone et al. 2010). The von Bertalanffy growth function (VBGF) was used to determine growth parameters of Arctic Cod, *Boreogadus saida,* using the following equation (Ricker, 1975): $L(t) = L_\infty[1 - e^{(-K*(t-t_0))}]$, where L(t) is total fish length at age t, L_∞ is the length at which the average fish reaches asymptotic length, t is age of fish in years, and t_0 is the theoretical age when L = 0. The rate of increase in length of the fish is a constant proportion (K) of the difference between the maximum and present length ($L\infty$ -L(t)).

Using the standardized residuals obtained from the initial otolith regressions, we assigned points >3 standard deviations from the mean as "outliers". Otoliths whose initial age observation fell >3 standard deviations outside of the mean were examined again by two readers because repetition of aging could reduce reader error if the originally assigned age was incorrectly estimated. Age observations that still occurred >3 standard deviations outside of the mean were assigned as outliers and eliminated from Tables and Figures. We use the term outliers because few data exist for these arctic species; however, we cannot be certain the data were incorrect. For each species that had been processed for age estimation, a length-frequency histogram was plotted as the percentage of individuals in 10 mm length classes, and age-at-length data were plotted on the same x-axis. Histograms were differentiated by year but not by gear; therefore, the frequencies were based on lengths of all fish measured in the lab and were not adjusted for catch effort. Specimens were plotted by 10 mm length bins (e.g., 41–50 mm, 51–60 mm). Length frequencies were plotted as bars such that all bars were placed between 10-mm tick marks, with 2012 frequency to the left, 2013 frequency centered between the tick marks, and the 2014 frequency was to the right. To better visualize age estimates by year, ages estimated from 2012 were graphed slightly below the age estimate, 2013 was graphed at the age estimate, while 2014 was graphed slightly above the age estimate.

7.2.3.2 Comparisons among Fish Catches

7.2.3.2.1 Biodiversity of Fish Catches

Biodiversity was examined using a suite of standard indices (DIVERSE, PRIMER v. 7) on demersal catches by beam trawls and midwater catches by IKMT. The total number of fish taxa collected at each sample site is dependent upon the sampling effort, i.e., the longer a net is deployed the more likely a different species will be captured. Therefore, in addition to analyzing the number of taxa collected, we used the Margalef richness index that is not biased by the sample size and considers the number of taxa (S) present for a given number (N) of individuals

captured: Margalef index: d = S-1/log(N). Diversity indices provide information in addition to richness as they consider the relative abundance of individual species, i.e., compared to all species captured at a station (Clarke and Gorley 2015). When all taxa are equally abundant, the taxonomic diversity is maximized. Evenness is a measure of how similar in number individual species are within each station. As we wanted to contrast evenness across stations, we used Pielou's J', the most commonly used index of evenness. Pielou's evenness (J') is maximized when all taxa are equally abundant (Clarke et al. 2014a). We did not use the standard Shannon diversity index because our sampling design was not equal, which could affect that index. We used Simpson's diversity index because it corrects for biased sampling design. Simpson's diversity is the probability that two individuals randomly selected from a sample are different species (Clarke et al. 2014a): $1-\lambda' = 1-SUM(N_i*(N_i-1)/(N*N-1))$. The value is always <1 and the higher the value, the more diverse and even the sample. Maps were created to show spatial patterns of biodiversity indices (ArcMap v. 10.2, ESRI 2010). For each index, the Jenk's natural breaks function within ArcMap assigned each station into one of five categories.

7.2.3.2.2 Maps of Presence and Abundance

Maps were prepared of fish presence and abundance (ArcMap v. 10.2, ESRI 2010). Maps of fish presence incorporated data from all hauls, both successful (quantitative) and unsuccessful (non-quantitative) hauls from 2012–2014. Taxon presence in pelagic habitat included data from collections by AMT in 2014 and IKMT in 2012–2013. Presence in demersal habitat included data from collections by PSBT-A, CBT and OT. Maps of pelagic fish relative abundance were prepared for IKMT in 2012–2013, where catch per unit effort (CPUE) was calculated as individuals 1000 m^{-3}. Maps of demersal fish biomass and abundance were prepared for beam trawl (BT) in 2013–2014, where BT included both PSBT-A and CBT. Biomass per unit effort (BPUE) and CPUE were calculated as gm 1000 m^{-2} and individuals 1000 m^{-2}, respectively, and average BPUE and CPUE per station were mapped.

7.2.3.2.3 Comparisons between Beam Trawls – PSBT-A and CBT

Comparisons between the two beam trawls PSBT-A and CBT were conducted for transects A2, A1, TBS and GRY in 2013 using PRIMER 7 and PERMANOVA+. CPUE was calculated for 10-mm size increments within each fish species from this subset of hauls, including 46 fish species captured, representing 10 families and ranging from 17 to 540 mm. CPUE values were fourth-root transformed (4RT) and a Bray-Curtis similarity matrix was calculated. Three factors were used to create a permutational analysis of variance (PERMANOVA) design: transect, depth and gear. A type III sum of squares was used. Significance was set at $p < 0.05$. Catches from multiple types of BT hauls conducted at the same station were averaged to produce one catch value per station for all analyses in this report.

7.2.3.2.4 Replicate PSBT-A Hauls – Same Station

To assess the variability of bottom fish communities and to determine if one haul per station, as is the usual practice due to wire time limits, is representative of a site, three replicate trawls were taken in 2014 with the PSBT-A at stations along transect A1 at the US–Canada border. Community composition of repeat trawls along transect A1 was analyzed using hierarchical cluster analysis. Similarity percentage analysis (SIMPER) was used to quantify percent similarity within stations and clusters. The factor "year" was only considered for the combined 2013 and 2014 data.

7.2.3.2.5 Interannual Analysis BT Hauls – Same Transects and Stations

A rich dataset for interannual comparisons was provided by sampling the same stations along transects A6, A2, A1, and TBS in both 2013 and 2014. Depths from 20 to 1000 m were sampled, providing a large dataset to examine the effects of longitude and depth on fish communities between years. Shade plots (see community analysis below) of each transformation were used to visually assess the species distribution. All transformations were used to analyze the effects of depth and longitude (transect used as proxy) using a 2-way crossed ANOSIM design. Transformed biomass and abundance data were displayed in non-metric multidimensional scaling (nMDS) plots.

To analyze fish assemblages, we examined several transformations to determine which best represented our objectives. Not transformed (NT) data have the most weight on species of high abundance. Square-root transformation (2RT) lessens weight on the species of highest abundance. 4RT further lessens effect of individual high catches as well as increasing effect of zero catches. Log+1 puts even more emphasis on zero catches by adding 1 to each catch. Presence/absence (PA) gives equal weight for all species, so rare species are more strongly emphasized in this transformation. Each set of transformed values was used to construct Bray-Curtis similarity matrices that were used in cluster and similarity analyses. Cluster (PRIMER v. 7) analysis was used to resolve inter-species associations, allowing an examination of community structure (as adapted from Doyle et al. 2002). A hierarchical cluster analysis for 999 permutations identified fish assemblages that grouped stations according to their taxonomic composition. Resulting dendrograms displayed groupings of stations into smaller numbers of groups containing more stations.

We used shade plots in PRIMER v.7 to help visualize geographic concentrations and absences of species; this program standardizes and transforms (at the level specified) data but is not a statistical analysis (Clarke and Gorley 2015). Shade plots are matrices of fish data in which the x-axis contains each station in the order of a dendrogram, and the y-axis contains each taxa in the order of a dendrogram. The matrices in shade plots were produced by transformed (NT, 2RT, 4RT, Log(+1), and PA) CPUE or BPUE data clustered by station on the x-axis and clusters of standardized CPUE or BPUE by species on the y-axis. The y-axis (species clusters) was the same for all transformations because it was not influenced by geographic density patterns. The color intensity in a shade plot visually portrays the influential species and locations, i.e. which species are evenly spread, which show gradations in abundance, which have limited distribution, and can be used to help determine which transformation to use (Clarke et al. 2014b). Shade plots show which transformations capture the “range of view” of the community from solely dominant (NT) to the equal representation of all species PA.

7.2.3.2.6 Community Analysis

Fish communities were evaluated by gear type as the various trawls, i.e., IKMT, BT and OT, have different fishing characteristics and cannot be directly compared as noted in Section 7.2.1. The nets differed in horizontal and vertical mouth opening and mesh size in the body and codend. Based on results of the multiple transformations examined for the interannual analysis, when a measure of effort was available (i.e., 2012/2013 IKMT catches and 2013/2014 BT catches) all further analyses was conducted on 4RT data. PA transformed data were used when no measure of effort was available (i.e., 2012 OT and 2012 BT).

When employing cluster analysis, the biological or environmental conditions being examined must be considered. Cluster analysis may find groups even if they are not relevant in nature

because it is possible for random data to produce groups. We used a similarity profile test (SIMPROF, PRIMER v. 7) to introduce some rigor as an *a posteriori* test of significance of dissimilarities among cluster groups ($p < 0.05$, $p < 0.01$, or $p < 0.005$). The significance level used was chosen to represent fish groups but not to create so many clusters as to render the results meaningless. SIMPROF is a permutation test of the null hypothesis (Clarke and Gorley 2015), i.e., it tests whether distributions of fishes are equal. SIMPROF was used to test the significance of each grouping of fish taxon density that resulted from the cluster analysis. When the statistical test of clusters is not significant, it is inappropriate to consider further differentiation (Clarke et al. 2008). Alternatively, it may be appropriate to group supersets of statistically different clusters when cluster analysis results in only 1 or 2 stations because those might not be valid groups (Clarke et al. 2008).

Species that were good discriminators within designated fish community groups were identified using SIMPER. SIMPER provides a statistical mechanism to show similarities within cluster groups. This test is a breakdown, by taxa, of Bray-Curtis similarities within groups. SIMPER can characterize groups and be used to compare between groups. The objective was to find typicality, i.e., what species typify group A and not group B and vice versa. The result was a list, in decreasing order, of each species' contribution to a fish community group.

As described in Section 7.2.3.2.5, we used shade plots in PRIMER v.7 to help visualize geographic concentrations and absences of species. This program standardizes and transforms data but is not a statistical analysis (Clarke and Gorley 2015). The colors used in the shade plots are relative within each plot, i.e., unitless, and cannot be compared among matrices.

nMDS plots (PRIMER v. 7) were used to examine patterns among sample groups. These ordination plots have no numerical interpretable axes, are based on simple matching coefficients calculated between pairs of species, and describe the precise biotic relationships among samples (Clarke et al. 2008). A stress of <0.1 is considered to be a good fit, while a stress of <0.2 is potentially useful (Clarke et al. 2014a). The nMDS ordinations presented show fish density assemblages for 4RT.

Analysis of similarity (ANOSIM, PRIMER v. 7) was used to estimate differences in fish communities relative to environmental factors. Pelagic fish communities defined based on abundance were tested by ANOSIM relative to year, longitude, bottom depth, maximum gear depth, surface temperature, and surface salinity; because water masses were depth stratified, it was not possible to assign each pelagic station to a single water mass at stations of depths less than 100 m. Therefore, we did not test for pelagic fish communities in relation to water mass. Demersal fish communities based on biomass and abundance were tested by ANOSIM relative to bottom depth, longitude, and water mass. Water masses were strongly associated with water depth and are described in Section 3.1. Generally, water mass could be assigned for each station for demersal fish. Depths 0–50 m were Polar Mixed Layer (PML), 60–200 m were Arctic Halocline Water (AHW), 250 m and deeper were Atlantic Water (AW). The 200 m isobath, where some stations were located, was at the transition from AHW to AW but was typically closer to AHW. ANOSIM is a nonparametric, multivariate permutation test somewhat analogous to the parametric, univariate analysis of variance (ANOVA) (Clarke et al. 2014a). R values range from 0 to 1, with values above ~0.45 considered to be biologically relevant. ANOSIM treatment groups were defined *a priori.* When testing for interannual comparisons, year (2013 vs. 2014) was analyzed as a 1-way ANOSIM, and depth and transect were analyzed interdependently as a 2-way crossed ANOSIM.

Bray-Curtis dissimilarity matrices of transformed CPUE values for each taxon at each station were used for ANOSIM calculations. To provide the best reasonable result, 999 permutations were run for each ANOSIM. An R statistic, defined as a comparison of the average between-group rank similarity to the average within-group rank similarity, was calculated using the following formula:

$$R = \frac{\left(\bar{r}_B - \bar{r}_W\right)}{n(n-1)}$$

where $\bar{r}_B$ and are the average rank similarities for each pair of intervals between and within groups, respectively, and n is the sample size. The R value is between -1 and 1, and the closer R is to 1, the more distinct the groups are (Clarke et al. 2014a).

We used two multivariate methods to examine relationships between measured environmental variables and fish community structure (based on biomass or abundance, 4RT), one to examine whole community patterns and the other to examine patterns in specific multivariate communities. The habitat characteristics considered for pelagic fishes at each station were year, longitude, surface temperature and salinity, and maximum haul depth. We used surface temperature and salinity because pelagic fishes were captured throughout the water column in oblique tows and bottom values were not appropriate as those would react differently to wind and wave conditions at time of collection. Habitat characteristics of demersal fishes considered at each station included year, longitude, bottom temperature, bottom salinity, bottom depth (m), percent gravel, percent sand, and percent mud. In all analyses, biological data for which there was a measure of effort (i.e., BPUE or CPUE) were 4RT and environmental variables were normalized to bring them to the same measurement scale. Canonical correspondence analysis (CCA, R v.3.2.2) was used to relate environmental data to abundance data of all fish species collected pelagically and by BT. CCA treated each station as an individual sampling unit, with fish species representing multivariate response variables (ter Braak 1986). Ordination plots were generated by regressing the environmental variables against axes from a correspondence analysis of the fish abundance data. The resulting ordinations show fish species as weighted averages with overlain vectors indicating the correlation between environmental predictor variables and each axis (Quinn and Keough 2002). Because CCA allows for categorical data, water mass was included. The significance of all predictor variables was determined by a permutation test at a 5% significance level. To match the environmental variables associated with specific multivariate fish communities, we used the biota-environment stepwise matching test (BEST, PRIMER v. 7) (Clarke and Gorley 2015). Both biomass and abundance data were used in BEST analyses. Determination of the best subset of correlated variables, i.e., habitat characteristics, was based on the highest overall Spearman rank correlation. Fewer explanatory parameters are preferable when little improved correlation is to be gained by including additional parameters.

7.3 Results

7.3.1 Fish Catches

Capture gear was used as a proxy for life stage. Fishes captured by midwater trawls (IKMT and AMT) were considered pelagic as those gears only fished in the water column. Fishes collected with bottom trawls (beam and otter) were considered demersal because only those hauls that verifiably contacted the bottom were used. Nets were open while being set and

retrieved as well as while on the bottom so, as with all bottom trawl collections, it is possible that fishes were captured off the seafloor; however, the contribution of midwater taxa was negligible. Fishes generally considered to be demersal may also be caught in midwater while in their pelagic life stage, including larval and early juvenile stages of Gadidae, Cottidae, Agonidae, Liparidae, Stichaeidae and Pleuronectidae, all of which can be present in large numbers in the water column during the same time frame as they are caught near the seafloor. Larval and early juvenile stages of some species of deep-water snailfishes and eelpouts (Mecklenburg et al. 2002) and shallower eelpouts appear to have inhabited the same depths the adults inhabit (Matarese et al. 1989).

We used two pelagic midwater (IKMT and AMT) and two demersal bottom (beam and otter) trawls and captured at least 14 families of fish: Rajidae, Osmeridae, Myctophidae, Gadidae, Cottidae, Hemitripteridae, Agonidae, Psychrolutidae, Cyclopteridae, Liparidae, Zoarcidae, Stichaeidae, Ammodytidae, Pleuronectidae (Table 7.3.1.1, Appendix E1). Two individuals could only be identified to teleost because they were lost at sea or badly damaged; these fishes added to total biomass and abundance, but were excluded from all species-level analyses. Only seven families, all captured by bottom trawls (Figure 7.3.1.1), made appreciable contributions to biomass: Rajidae (skates), Gadidae (cods), Cottidae (sculpins), Liparidae (snailfishes), Psychrolutidae (fathead sculpins), Zoarcidae (eelpouts), and Pleuronectidae (righteye flounders).

Biomass and abundance data for demersal fishes showed different patterns (Figure 7.3.1.1). Gadidae, Cottidae and Agonidae contributed less proportionally to biomass but made up a large percentage of abundance. Liparidae were most notably abundant in the 2012 catches by BT, but contributed little to the overall biomass, meaning that each individual contributed little to overall weight. Conversely, Rajidae, Zoarcidae and Pleuronectidae contributed more to biomass than to abundance, meaning the individuals were larger.

Proportional biomass (Figure 7.3.1.2) and proportional abundance of BT hauls (Figure 7.3.1.3) showed distinct spatial patterns but most likely did not indicate an interannual pattern. Examination of BT catches for all transects and stations for all years showed a similar pattern among shelf (20–100 m) stations; however, the pattern for shelf differed from that seen for slope (200–1000 m) stations (Figures 7.3.1.2–3). Longitudinal patterns were evident but were not as pronounced as the slope/shelf difference. For both biomass and abundance, Cottidae made up a large proportion of catches across the shelf. This family generally was not found deeper than 350 m. Agonidae proportional biomass was less than its proportional abundance, indicating small-size fish. Stichaeidae (pricklebacks) had a similar depth distribution, 20–200 m, but were only heavier or more numerous at two stations on the eastern-most transects and a few to the west. Small Pleuronectidae (flounders) were proportionally numerous at 20 m at the western-most stations (2012), but at A6 in only 2013 and not 2014. Gadidae, which was represented entirely by a single species, *Boreogadus saida*, were found at all depths and transects; there were very few stations at which *B. saida* were not collected. *B. saida* composed a large proportion of biomass and abundance from 200 m to 500 m and especially at 200 m depth at 150º–151º W and at 350–500 m at 145º–146º W. As depths increased, Zoarcidae (eelpouts) dominated both biomass and abundance. A few stations, e.g., A5-750 m, had a high proportion of large snailfishes. At 500 m and 1000 m, an occasional large skate (Rajidae) was captured as evidenced by the large proportion of biomass and small proportion of abundance. Likewise, the biomass at some deep stations was dominated by Pleuronectidae (Figures 7.3.1.2–3).

In comparison to the BT, the less numerous catches with the OT and the IKMT pelagic net showed different patterns at some stations (Figures 7.3.1.4–5). The OT catch at 20 m at the central (B) transects (150º–151º W) in 2012 was almost wholly Gadidae (*Boreogadus saida*),

with a small proportion of Liparidae (Figure 7.3.1.4). Though the proportions were not identical, the catches of the two bottom nets had similar composition at all other depths. In contrast, the smaller mesh of the IKMT captured Stichaeidae at all depths on the central B transects (Figure 7.3.1.5). The IKMT catches at the eastern transects (146º–138º W) are almost entirely Gadidae, except the very shallow stations where some stichaeids, liparids, and cottids were collected.

There were at least 51 unique species from 14 families captured by the four gear types combined from all hauls (Table 7.3.1.1). Most individuals could be identified to the species level, and a much less numerous and less widely distributed subset of individuals could only be identified to genus (e.g., *Careproctus*), subfamily (e.g., Lumpeninae), or family (e.g., Hemitripteridae). As not all individuals were identified to species, it is possible taxa were captured that were not included in the total count of taxa, which would increase the total number. Where not every individual was identified to species, taxa may have been grouped at an "analysis level" for purposes of statistical analyses (Table 7.3.1.2). For example, small (<100 mm) individuals of *Lycodes* spp. are considerably more difficult to identify than larger individuals, and the characteristic scale patterns that allow distinction between *Icelus bicornis* and *I. spatula* are not fully developed in *Icelus* spp. ≤40 mm; a small quantity of larger (41–87 mm) *Icelus* spp. were analyzed at the genus/length level as it was not possible to identify them to species. Specimens ≤50 mm of all species of *Liparis* were combined for statistical analyses as were Cottidae of ≤50 mm that were not identified to species (Table 7.3.1.2).

The bottom trawls caught far more taxa than the midwater trawls. Because individuals identified to levels higher than species may actually belong to species in the list, sums represent a minimum number of taxa that were caught. Successful hauls (i.e., quantitative, in which all gear worked correctly) were included in species accumulation curves by gear (Figure 7.3.1.6), which were calculated at analysis level. Successful IKMT hauls (n = 68) captured at least 15 species; two non-quantitative hauls added no new taxa. In five successful hauls with the AMT, two species were captured; six unsuccessful (non-quantitative) hauls caught another two taxa. The small number of successful AMT hauls made it difficult to compare the number of taxa captured with midwater nets. The 194 successful BT hauls caught at least 49 species; 61 non-quantitative hauls added no new taxa. Successful OT hauls (n = 21) caught 32 taxa; eight non-quantitative hauls added one species (Figure 7.3.1.6). Fishing effort was not equal among gears. BT caught 17 more species than did OT, whereas OT only caught one species, *Aspidophoroides monopterygius*, not caught by BT. Although OT collections were only 11% the number of those by BT, 72% of the species were captured by OT. Additionally, the cumulative catch curve of OT was nearly identical to that of BT (Figure 7.3.1.6). Therefore, presence/absence of species in BT and OT could be compared (see Section 7.3.4.5.3 Combined Bottom Assemblages). At least 50 species were caught with demersal gear (Table 7.3.1.1). There were three times more IKMT hauls than OT hauls, yet only three-fourths the number of taxa were captured. Three times as many BT hauls as IKMT hauls caught three times as many taxa. However, the species accumulation curves showed that the number of taxa captured by IKMT was not increasing at the rate it was for OT and BT, so the taxa available to be captured were not equivalent. There were fewer fish and fewer taxa in the midwater in the size (larvae and juveniles <50 mm) captured by IKMT than there were of bottom fishes >20 mm normally captured by OT and BT. The relatively low abundance and diversity of fishes in the Beaufort Sea midwater compared to demersal collections could be attributed to sampling occurring after juveniles settled to the bottom.

The distribution of fishes at the analysis level revealed details of patterns that could not be seen in proportional plots of families at each station (Figures 7.3.1.2–5). Pelagic-caught fishes were generally larvae or small juveniles representing the first year of life. Demersally caught fishes were generally larger, representing older fishes that have settled out of the water column and have adapted to a demersal habitat. Many taxa like Rajidae (skates) were never collected pelagically, which is expected of taxa that do not have a pelagic life stage. The map of demersal fish presence (see Appendix E2) shows Rajidae at the outer, deeper stations where they made up a large proportion of the biomass station (Figure 7.3.1.2). Thirty-six species of the 50 species that were caught demersally were not caught pelagically. *Limanda proboscidea* (Pleuronectidae) was unique in that it was the only species captured pelagically and not demersally. Small individuals of Cottidae and *Icelus* spp. caught in both pelagic and demersal gears could not be identified to species (Table 7.3.1.3). Several individual pelagic and demersal snailfish could only be identified to the genus *Liparis*, whereas small pelagic Stichaeidae could only be identified to the sub-family Lumpeninae. Pleuronectid larvae could only be identified to family whether captured pelagically or demersally. Distribution maps of presence and absence (Appendix E2) are routinely used to define habitat until knowledge that is more precise is gained.

More insights can be gained by looking at interannual distribution plots for CPUE of the IKMT for the pelagic life stage (2012 and 2013) and BT for the demersal life stage (2013 and 2014). It is readily apparent that presence at a site does not mean that biomass or abundance is equally distributed (Appendix E3). The range in pelagic abundance was zero for many taxa to 51 individuals 1000 m^{-3} for Lumpeninae; most taxa had very low abundance. At stations where a species was present, demersal biomass was as low as <1 g for a few small fish to 1335 g 1000 m^{-3} for one skate (Rajidae) in 2013. This visual approach to analysis clearly demonstrates patterns of distribution of taxa. Very few taxa, such as *B. saida*, were captured both pelagically and demersally at all transects across the shelf and slope. Some genera were captured on both the slope and the shelf, such as *Lycodes*, though the same species were not captured in both locations (Appendix E3). Other taxa were clearly restricted to only the shelf, e.g., *Artediellus scaber* Hamecon, or to only the slope, e.g., *Cottunculus microps* Polar Sculpin (Appendix E3).

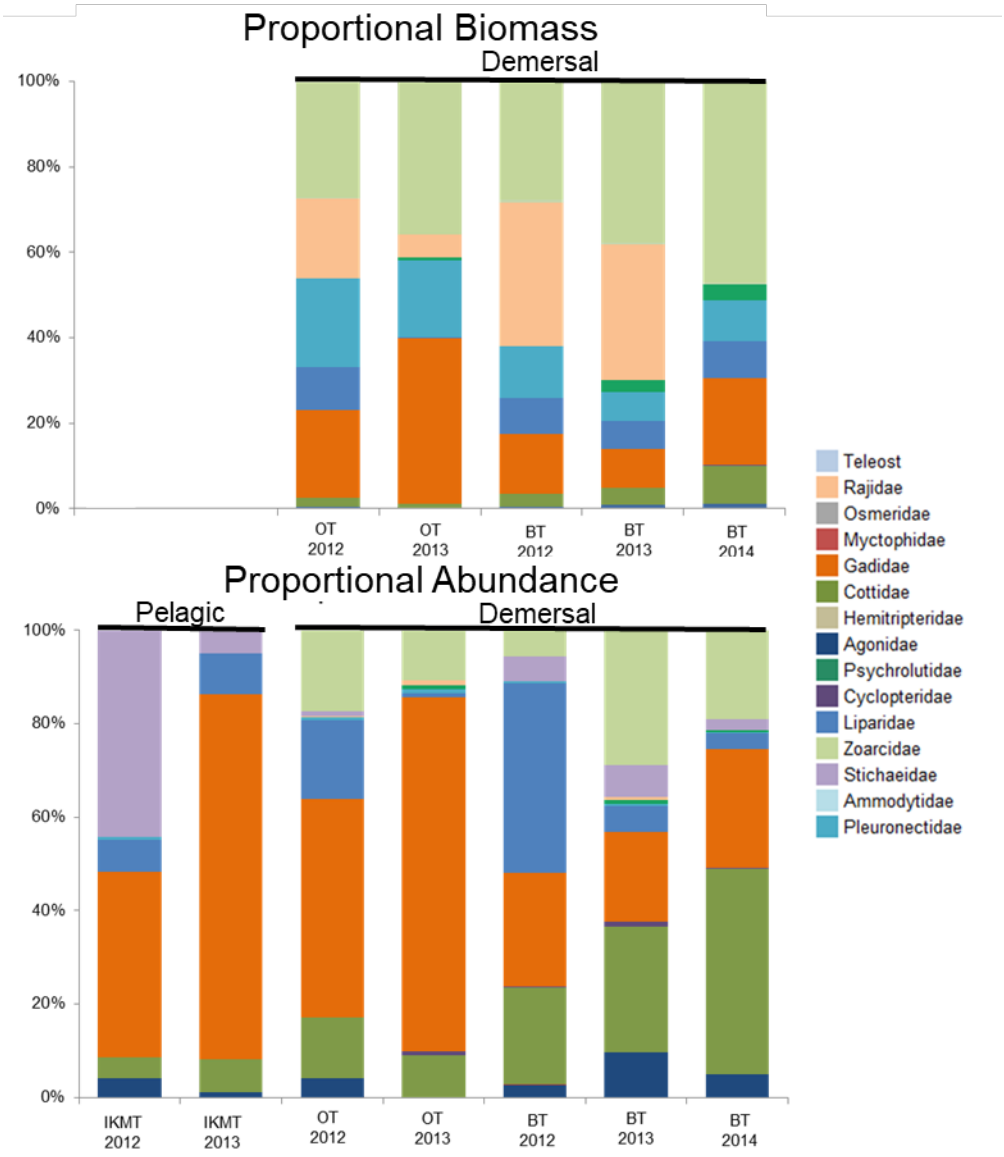

Figure 7.3.1.1. Proportional biomass and abundance for 14 families of fish and unidentified teleosts in the Beaufort Sea 2012–2014, by gear. Isaacs-Kidd midwater trawl (IKMT), otter trawl (OT), beam trawls (BT).

Table 7.3.1.1. Fishes captured in all hauls of pelagic (Isaacs-Kidd midwater trawl, IKMT; Aluette midwater trawl, AMT) and demersal (beam trawl, BT; otter trawl, OT) in Beaufort Sea 2012–2014.
Because individuals identified to levels higher than species may actually belong to species in the list, values of total n species for the gear are of a minimum number of taxa that were caught. Circles indicate taxa captured only unsuccessful hauls.

Survey Year	2012			2013			2014	
	Pelagic	Demersal		Pelagic	Demersal		Pelagic	Demersal
Gear	IKMT	BT	OT	IKMT	BT	OT	AMT	BT
RAJIDAE								
Amblyraja hyperborea		X	X					X
Rajidae unid. 147-185 mm					X	X		X
OSMERIDAE								
Mallotus catervarius	X	X						
Osmerus dentex		X	X					
MYCTOPHIDAE								
Myctophidae unid. 84-144 mm								X
GADIDAE								
Boreogadus saida	X	X	X	X	X	X	X	X
COTTIDAE								
Artediellus scaber		X	X		X			X
Gymnocanthus tricuspis	X	X	X	X	X	X		X
Icelus bicornis					X			X
Icelus spatula		X	X		X	X		X
Icelus spp. unid. ≤40 mm				X	X			X
Icelus spp. unid. 41–87 mm		X	X					
Myoxocephalus scorpius	X	X	X					X
Triglops nybelini		X			X			X
Triglops pingelii	X	X	X	X	X	X		X
Cottidae unid. ≤50 mm	X	X	X	X	X			X
Cottidae unid. 51–81 mm			X					
HEMITRIPTERIDAE								
Hemitripteridae unid.		X						
AGONIDAE								
Aspidophoroides monopterygius			X					
Aspidophoroides olrikii	X	X	X	X	X		ⓧ	X
Leptagonus decagonus		X			X			X
PSYCHROLUTIDAE								
Cottunculus microps					X			X
Psychrolutes sp.						X		
Psychrolutidae unid. 37-120 mm					X			X
CYCLOPTERIDAE								
Eumicrotremus derjugini		X	X		X			X
Cyclopteridae unid. 18-48 mm					X	X		
LIPARIDAE								
Careproctus lerikimae		X	X		X			X
Liparis bathyarcticus		X	X		X			
Liparis fabricii		X	X	X	X	X	X	X
Liparis gibbus	X	X	X		X			X
Liparis spp. unid. ≤50 mm	X	X	X	X	X			X
Liparis spp. unid. 51–110 mm	X	X	X		X		ⓧ	X
Liparis tunicatus		X			X	X		X
Paraliparis bathybius								X
Paraliparis spp.					X			
Rhodichthys regina					X			X

Table 7.3.1.1, continued.

Survey Year	2012			2013			2014	
	Pelagic	Demersal		Pelagic	Demersal		Pelagic	Demersal
Gear	IKMT	BT	OT	IKMT	PSBT-A	OT	AMT	PSBT-A
ZOARCIDAE								
Gymnelus hemifasciatus		X	X		X	X		X
Gymnelus viridis		X	X		X			X
Gymnelus spp. unid. 53-90 mm					X			
Lycenchelys kolthoffi					X			X
Lycodes adolfi		X	X		X	X		X
Lycodes eudipleurostictus		X	X		X			X
Lycodes frigidus		X						X
Lycodes jugoricus		X						
Lycodes mucosus		X	X		X			X
Lycodes pallidus					X			X
Lycodes polaris		X	X		X			X
Lycodes raridens		X	Ⓧ		X			X
Lycodes reticulatus		X	X	X	X			X
Lycodes rossi		X			X			X
Lycodes sagittarius		X	X		X	X		X
Lycodes seminudus		X	X		X	X		X
Lycodes squamiventer		X	X			X		
Lycodes spp. unid. 28-100 mm		X	X		X	X		X
STICHAEIDAE								
Anisarchus medius		X	X		X			X
Eumesogrammus praecisus		X	X					X
Leptoclinus maculatus	X	X	X					X
Lumpenus fabricii	X	X	X	X	X			X
Stichaeus punctatus	X	X						X
Lumpeninae unid. 53-67 mm	X	X						
Lumpeninae unid. ≤51 mm	X	X		X	X			X
AMMODYTIDAE								
Ammodytes hexapterus		X[1]						X
PLEURONECTIDAE								
Hippoglossoides robustus		X	X					
Limanda proboscidea	X							
Reinhardtius hippoglossoides		X	X		X	X		X
Pleuronectidae larva unid. 43-45 mm					X			
Pleuronectidae larvae A 11-20 mm	X							

Total n species IKMT ≥ 15
Total n species AMT = 4
Total n species BT ≥ 49
Total n species OT ≥ 33

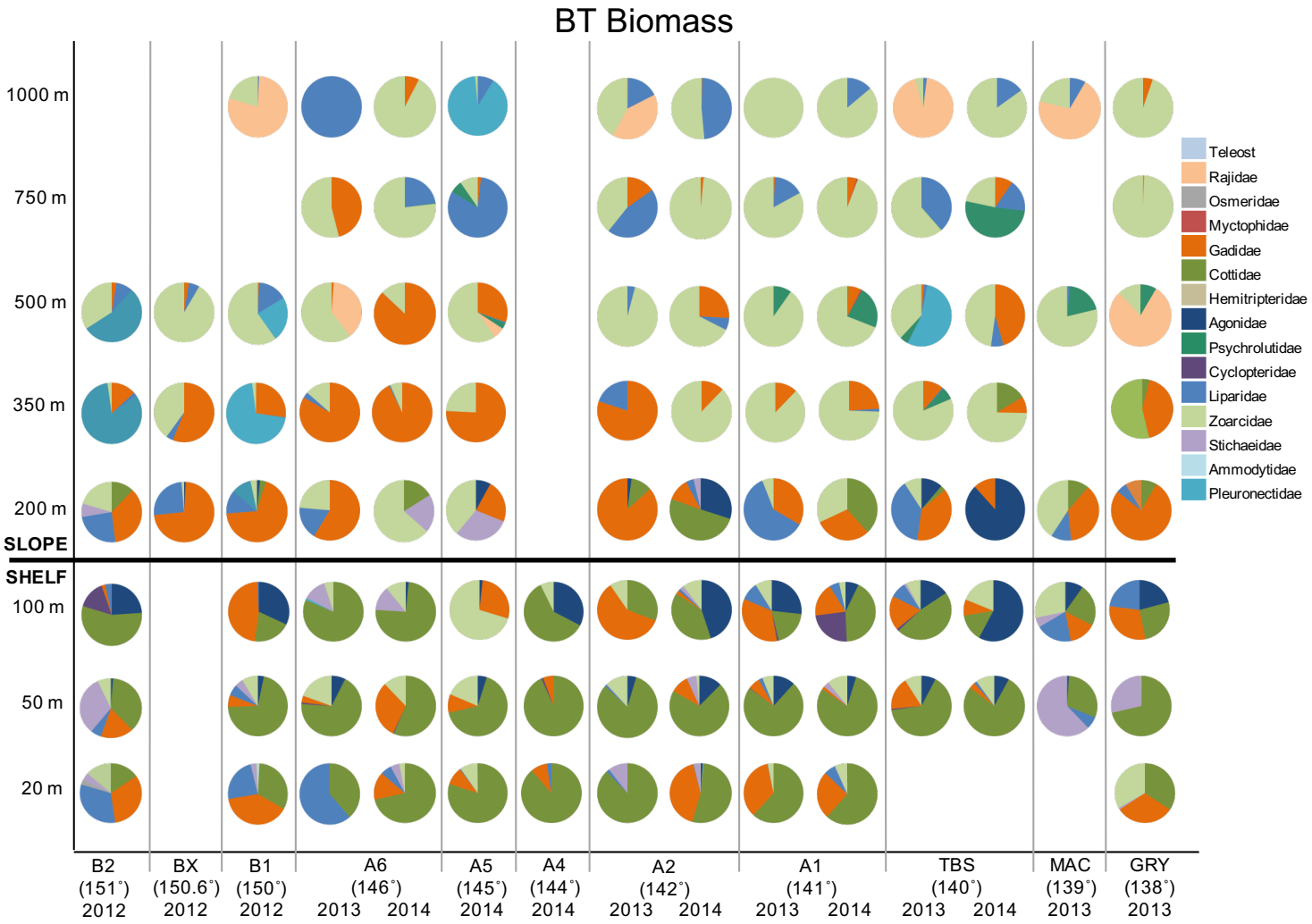

Figure 7.3.1.2. Proportional biomass for 14 families of fish and unidentified teleosts captured by beam trawl in the Beaufort Sea 2012–2014. Transect name, longitude, and year sampled are labeled on the x-axis. Bottom (haul) depth is on the y-axis arranged from nearshore to offshore. Horizontal line between 100 and 200 m signifies the division between the shallower shelf and deeper slope. Each pie is 100% of catch at that station; multiple hauls at the same station were pooled. A blank space indicates no haul was made at that transect and depth.

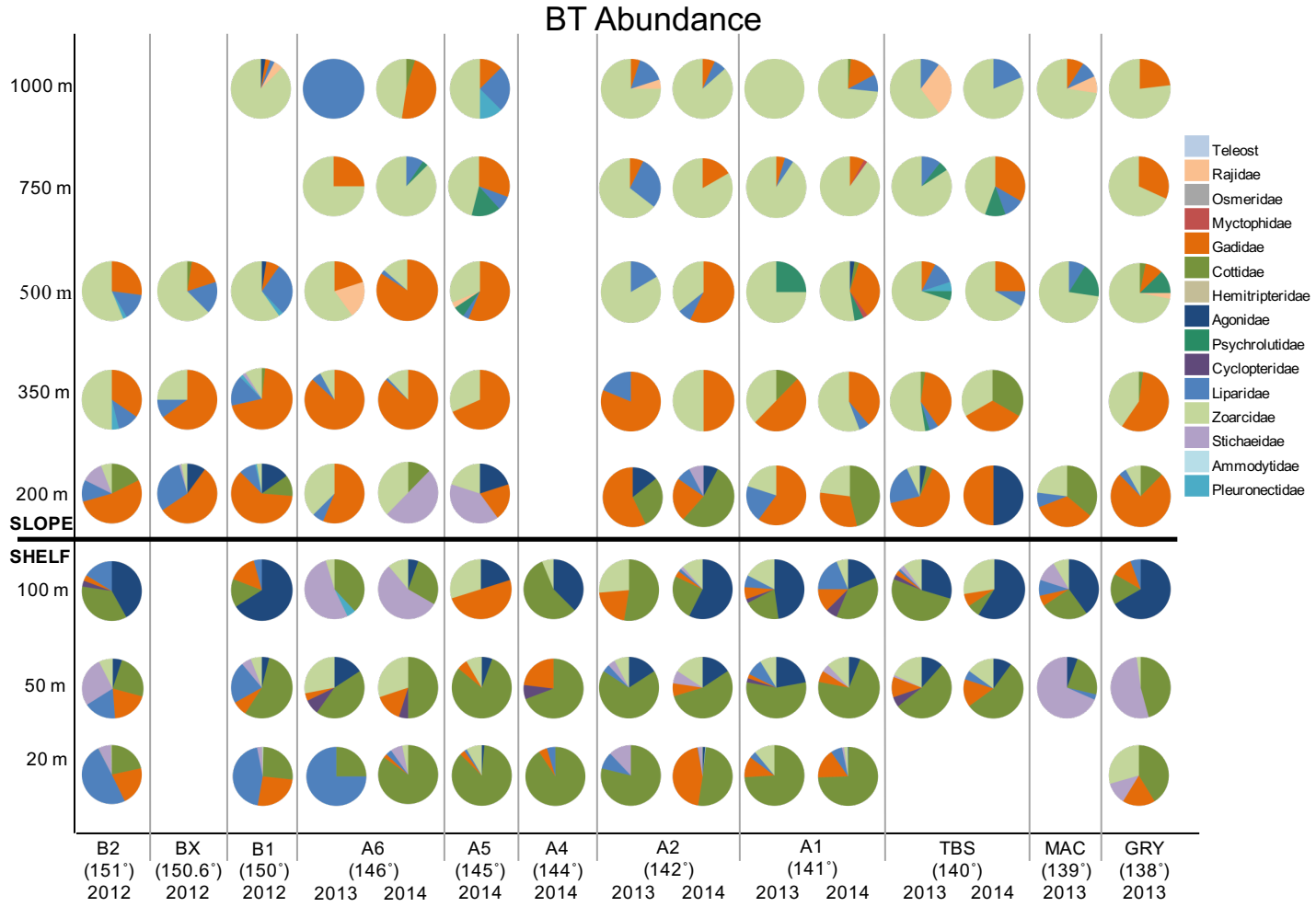

Figure 7.3.1.3. Proportional abundance for 14 families of fish and unidentified teleosts captured by beam trawl in the Beaufort Sea 2012–2014. Transect name, longitude, and year sampled are labeled on the x-axis. Bottom (haul) depth is on the y-axis arranged from nearshore to offshore. Horizontal line between 100 and 200 m signifies the division between the shallower shelf and deeper slope. Each pie is 100% of catch at that station; multiple hauls at the same station were pooled. A blank space indicates no haul was made at that transect and depth.

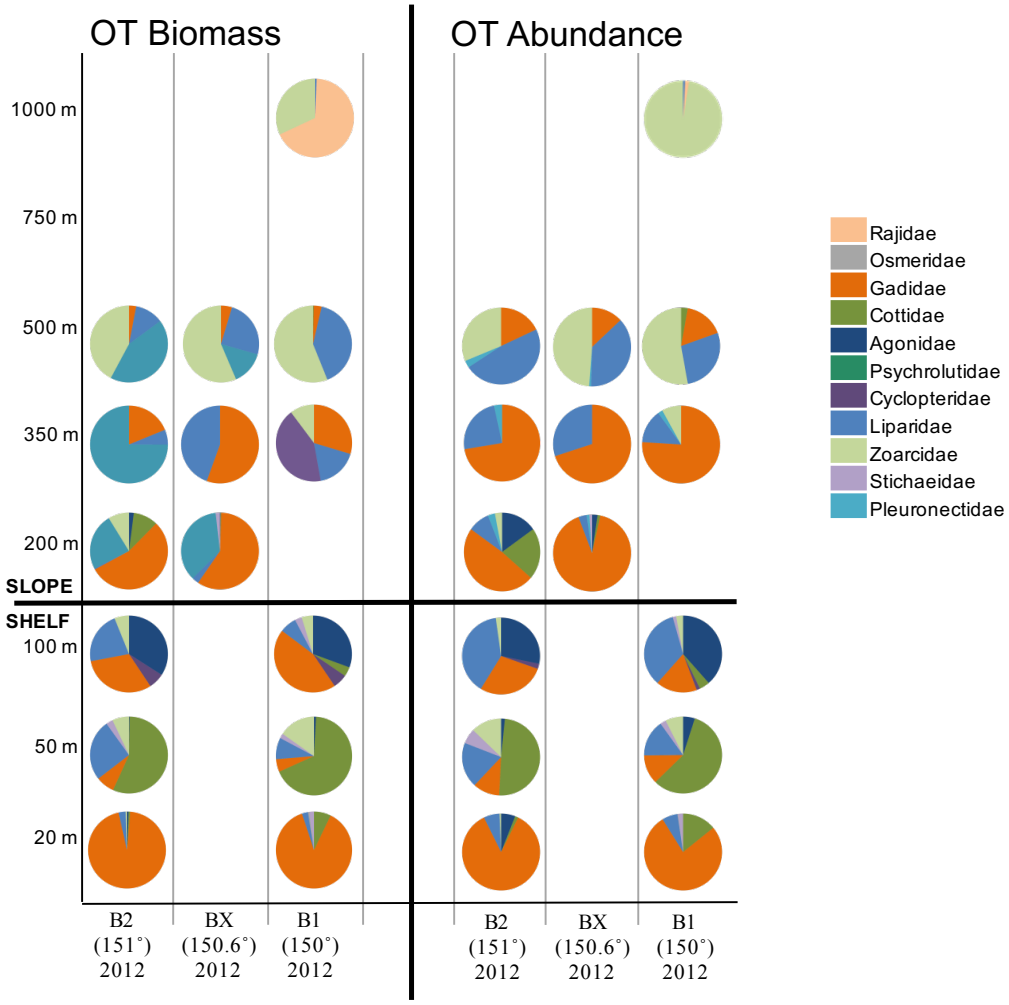

Figure 7.3.1.4. Proportional biomass and abundance for 11 families of fish captured by otter trawl in the Beaufort Sea during 2012.
Transect name, longitude, and year sampled are labeled on the x-axis. Bottom (haul) depth is on the y-axis arranged from nearshore to offshore. Horizontal line between 100 and 200 m signifies the division between the shallower shelf and deeper slope. Each pie is 100% of catch at that station; multiple hauls at the same station were pooled. A blank space indicates no haul was made at that transect and depth.

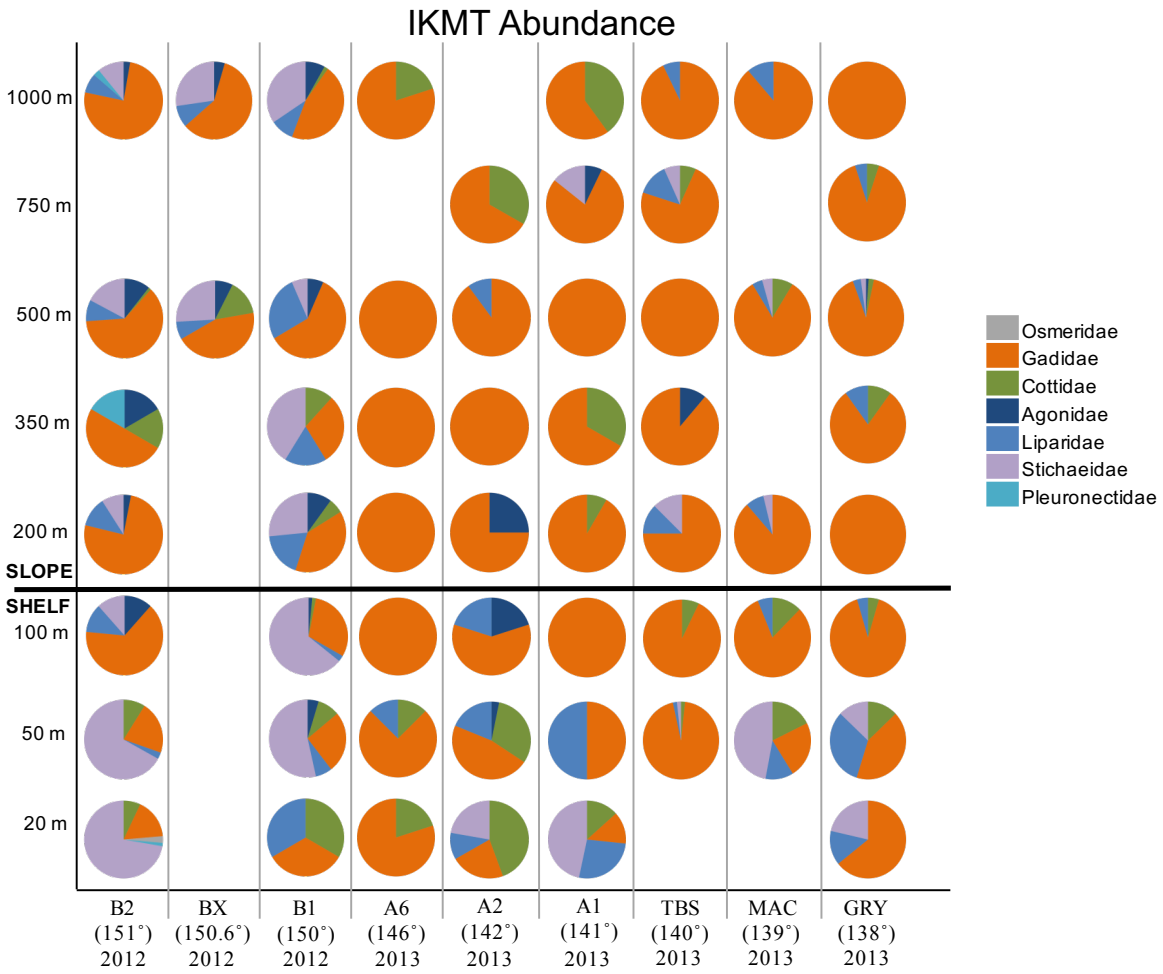

Figure 7.3.1.5. Proportional abundance for 7 families of fish captured by Isaacs-Kidd midwater trawl (IKMT) in the Beaufort Sea 2012–2013.
Transect name, longitude, and year sampled are labeled on the x-axis. Bottom depth is on the y-axis arranged from nearshore to offshore; maximum gear depth was bottom depth minus 10 m to a maximum of 200 m. Horizontal line between 100 and 200 m signifies the division between the shallower shelf and deeper slope. Each pie is 100% of catch at that station; multiple hauls at the same station were pooled. A blank space indicates no haul was made at that transect and depth.

Table 7.3.1.2. List of fishes captured in successful hauls during TB-2012-US, TB-2013-US and TB-2014-US with bottom and pelagic trawls, in phylogenetic order by family.
Taxonomic precision of analyses for community composition and gear comparisons is indicated; note where multiple species are combined for analysis. Species level of analysis is for individuals larger than size range of coarse level taxa. Fishes analyzed at a coarser level than species are indicated here with the maximum or total length range of individuals within the category; "unid." indicates fish were not identified further and "all" indicates all species were combined within the category.

Family	Analysis Level	Scientific Name	Common Name
RAJIDAE skates	Rajidae	*Amblyraja hyperborea*	Arctic Skate
		Rajidae unid.	
OSMERIDAE smelts	*Mallotus catervarius*	*Mallotus catervarius*	Pacific Capelin
	Osmerus dentex	*Osmerus dentex*	Arctic Smelt
MYCTOPHIDAE lanternfishes	Myctophidae	Myctophidae unid.	
GADIDAE cods	*Boreogadus saida*	*Boreogadus saida*	Arctic Cod
COTTIDAE sculpins	*Artediellus scaber*	*Artediellus scaber*	Hamecon
	Gymnocanthus tricuspis	*Gymnocanthus tricuspis*	Arctic Staghorn Sculpin
	Icelus bicornis	*Icelus bicornis*	Twohorn Sculpin
	Icelus spatula	*Icelus spatula*	Spatulate Sculpin
	Icelus spp. all ≤40 mm	*Icelus bicornis*	Twohorn Sculpin
		Icelus spatula	Spatulate Sculpin
		Icelus spp. unid.	
	Icelus spp. unid. 41–87 mm	*Icelus* of the 2 species listed	
	Myoxocephalus scorpius	*Myoxocephalus scorpius*	Shorthorn Sculpin
	Triglops nybelini	*Triglops nybelini*	Bigeye Sculpin
	Triglops pingelii	*Triglops pingelii*	Ribbed Sculpin
	Cottidae unid. ≤50 mm	Cottidae of any species	
	Cottidae unid. 51–81 mm	Cottidae of any species	
HEMITRIPTERIDAE sailfin sculpins	Hemitripteridae all	Hemitripteridae of 1 species	
AGONIDAE poachers	*Aspidophoroides monopterygius*	*Aspidophoroides monopterygius*	Alligatorfish
	Aspidophoroides olrikii	*Aspidophoroides olrikii*	Arctic Alligatorfish
	Leptagonus decagonus	*Leptagonus decagonus*	Atlantic Poacher
PSYCHROLUTIDAE fathead sculpins	*Cottunculus microps*	*Cottunculus microps*	Polar Sculpin
	Psychrolutes sp.	*Psychrolutes* of 1 species	
	Psychrolutidae unid. 37–120 mm	Psychrolutidae of any species	
CYCLOPTERIDAE lumpfishes	*Eumicrotremus derjugini*	*Eumicrotremus derjugini*	Leatherfin Lumpsucker
	Cyclopteridae unid. 18–48 mm	Cyclopteridae of other species	
LIPARIDAE snailfishes	*Careproctus lerikimae*	*Careproctus lerikimae*	Dusty Snailfish
	Liparis bathyarcticus	*Liparis bathyarcticus*	Nebulous Snailfish
	Liparis fabricii	*Liparis fabricii*	Gelatinous Snailfish
	Liparis gibbus	*Liparis gibbus*	Variegated Snailfish
	Liparis tunicatus	*Liparis tunicatus*	Kelp Snailfish
	Liparis spp . all ≤50 mm	*Liparis fabricii*	Gelatinous Snailfish
		Liparis gibbus	Variegated Snailfish
		Liparis tunicatus	Kelp Snailfish
		Liparis spp. unid.	
	Liparis spp. unid. 51–110 mm	*Liparis* of the 3 spp. listed	
	Paraliparis bathybius	*Paraliparis bathybius*	Black Seasnail
	Paraliparis spp.	*Paraliparis* spp.	
	Rhodichthys regina	*Rhodichthys regina*	Threadfin Seasnail

Table 7.3.1.2. continued.

Family	Analysis Level	Scientific Name	Common Name
ZOARCIDAE	*Gymnelus hemifasciatus*	*Gymnelus hemifasciatus*	Halfbarred Pout
	Gymnelus viridis	*Gymnelus viridis*	Fish Doctor
	Gymnelus spp. unid. 53–90 mm	*Gymnelus* of the 2 spp. listed	Halfbarred Pout
	Lycenchelys kolthoffi	*Lycenchelys kolthoffi*	Checkered Wolf Eel
	Lycodes adolfi	*Lycodes adolfi*	Adolf's Eelpout
	Lycodes eudipleurostictus	*Lycodes eudipleurostictus*	Doubleline Eelpout
	Lycodes frigidus	*Lycodes frigidus*	Glacial Eelpout
	Lycodes jugoricus	*Lycodes jugoricus*	Shulupaoluk
	Lycodes mucosus	*Lycodes mucosus*	Saddled Eelpout
	Lycodes pallidus	*Lycodes pallidus*	Pale Eelpout
	Lycodes polaris	*Lycodes polaris*	Canadian Eelpout
	Lycodes raridens	*Lycodes raridens*	Marbled Eelpout
	Lycodes reticulatus	*Lycodes reticulatus*	Arctic Eelpout
	Lycodes rossi	*Lycodes rossi*	Threespot Eelpout
	Lycodes sagittarius	*Lycodes sagittarius*	Archer Eelpout
	Lycodes seminudus	*Lycodes seminudus*	Longear Eelpout
	Lycodes squamiventer	*Lycodes squamiventer*	Scalebelly Eelpout
	Lycodes spp. unid. 28–143 mm	*Lycodes*; likely of the 13 spp. listed	
STICHAEIDAE pricklebacks	*Anisarchus medius*	*Anisarchus medius*	Stout Eelblenny
	Eumesogrammus praecisus	*Eumesogrammus praecisus*	Fourline Snakeblenny
	Leptoclinus maculatus	*Leptoclinus maculatus*	Daubed Shanny
	Lumpenus fabricii	*Lumpenus fabricii*	Slender Eelblenny
	Stichaeus punctatus	*Stichaeus punctatus*	Arctic Shanny
	Lumpeninae all ≤51 mm	*Anisarchus medius*	Stout Eelblenny
		Leptoclinus maculatus	Daubed Shanny
		Lumpenus fabricii	Slender Eelblenny
		Lumpeninae unid.	
	Lumpeninae unid. 53–67 mm	Lumpeninae of the 3 spp. listed	Stout Eelblenny
AMMODYTIDAE sand lances	*Ammodytes hexapterus*	*Ammodytes hexapterus*	Arctic Sand Lance
PLEURONECTIDAE righteye flounders	*Hippoglossoides robustus*	*Hippoglossoides robustus*	Bering Flounder
	Limanda proboscidea	*Limanda proboscidea*	Longhead Dab
	Reinhardtius hippoglossoides	*Reinhardtius hippoglossoides*	Greenland Halibut
	Pleuronectidae larvae	Pleuronectidae larvae unid.	
		Pleuronectidae larva A	likely *Limanda proboscidea* Longhead Dab or *Liopsetta glacialis* Arctic Flounder

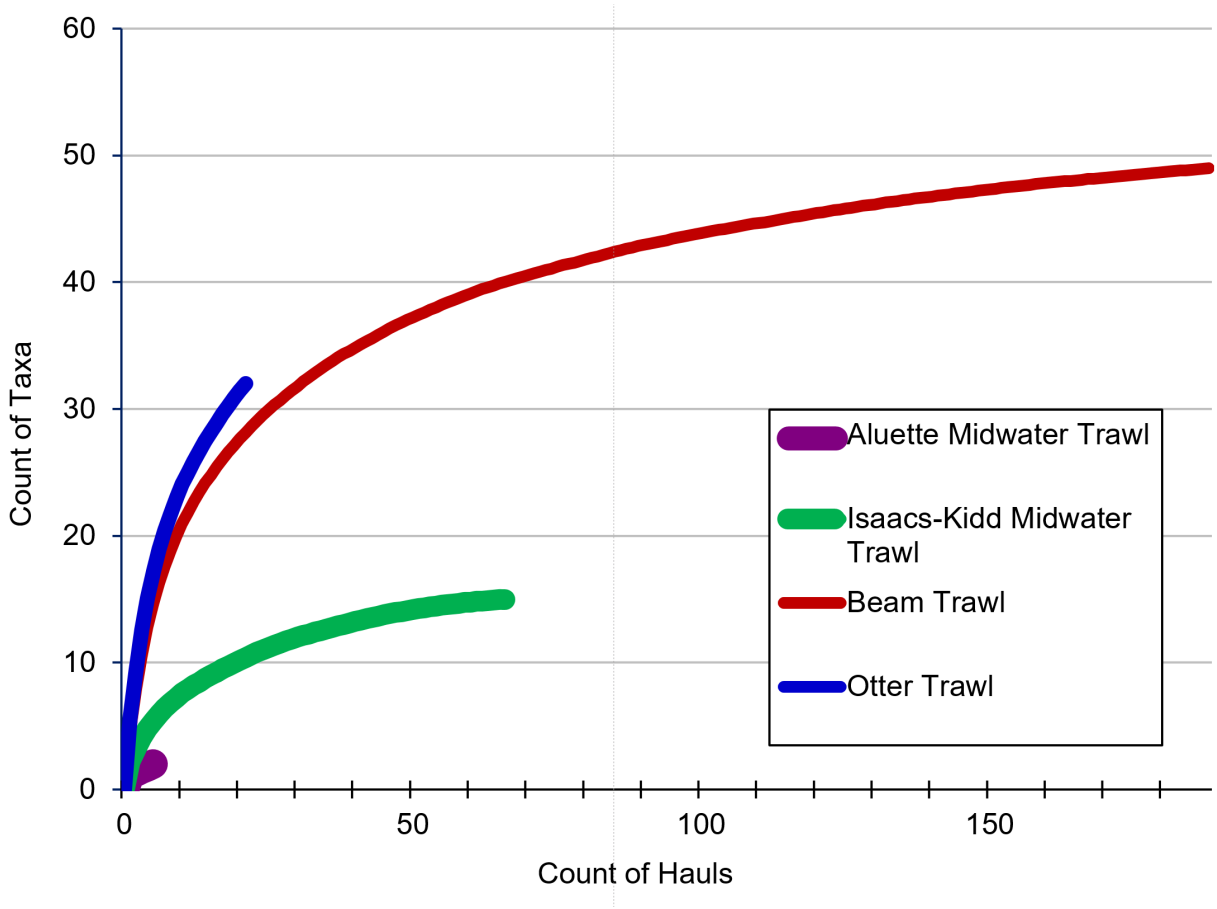

Figure 7.3.1.6. Curves of cumulative species estimation by pelagic (IKMT, AMT) and bottom (BT and OT) trawl gears, based on presence of most specific level of taxa in successful hauls.

Table 7.3.1.3. Abundance of fishes captured in pelagic and demersal habitats in the Beaufort Sea 2012–2014.
Note different years and units of effort. In each collection, the total abundance of fishes was calculated, and the percent each taxon accounted for is the % of total. The ten most abundant fishes in each collection are ranked.

	Pelagic - Isaacs-Kidd Midwater Trawl Abundance (#/1000 m^3)						Demersal - Beam Trawl Abundance (#/1000 m^2)					
	TB-2012-US			TB-2013-US			TB-2013-US			TB-2014-US		
Taxa	Mean	% of Total	Top 10	Mean	% of Total	Top 10	Mean	% of Total	Top 10	Mean	% of Total	Top 10
RAJIDAE	**-**	**-**		**-**	**-**		**0.17**	**0.70%**		**0.01**	**0.03%**	
Rajidae	-	-		-	-		0.17	0.70%		0.01	0.03%	
OSMERIDAE	**0.05**	**0.32%**		**-**	**-**		**-**	**-**		**-**	**-**	
Mallotus catervarius	0.05	0.32%		-	-		-	-		-	-	
MYCTOPHIDAE	**-**	**-**		**-**	**-**		**-**	**-**		**0.01**	**0.02%**	
Myctophidae	-	-		-	-		-	-		0.01	0.02%	
GADIDAE	**5.84**	**36.38%**		**1.65**	**67.74%**		**3.61**	**14.38%**		**7.01**	**19.46%**	
Boreogadus saida	5.84	36.38%	1	1.65	67.74%	1	3.61	14.38%	1	7.01	19.46%	1
COTTIDAE	**0.69**	**4.28%**		**0.24**	**9.77%**		**8.10**	**32.22%**		**19.50**	**54.15%**	
Artediellus scaber	-	-		-	-		0.53	2.11%		2.60	7.22%	7
Cottidae unid. ≤50 mm	0.17	1.08%	7	0.17	7.06%	4	0.66	2.63%		0.09	0.26%	
Gymnocanthus tricuspis	0.48	3.01%	6	0.03	1.10%	7	1.05	4.17%	7	5.67	15.74%	2
Icelus bicornis	-	-		-	-		0.03	0.12%		1.17	3.26%	8
Icelus spatula	-	-		-	-		3.20	12.74%	2	2.97	8.26%	5
Icelus spp. all ≤40 mm	-	-		0.03	1.32%	6	0.70	2.80%		4.16	11.56%	3
Myoxocephalus scorpius	0.01	0.09%		-	-		-	-		0.03	0.08%	
Triglops nybelini	-	-		-	-		0.03	0.14%		0.20	0.55%	
Triglops pingelii	0.02	0.11%		0.01	0.29%	8	1.89	7.51%	4	2.60	7.23%	6
PSYCHROLUTIDAE	**-**	**-**		**-**	**-**		**0.17**	**0.66%**		**0.05**	**0.14%**	
Cottunculus microps	-	-		-	-		0.16	0.63%		0.05	0.13%	
Psychrolutidae unid.	-	-		-	-		0.01	0.03%		<0.01	0.01%	
AGONIDAE	**0.62**	**3.86%**		**0.04**	**1.56%**		**2.70**	**10.73%**		**3.30**	**9.15%**	
Aspidophoroides olrikii	0.62	3.86%	5	0.04	1.56%	5	2.69	10.70%	3	3.28	9.10%	4
Leptagonus decagonus	-	-		-	-		0.01	0.03%		0.02	0.05%	
CYCLOPTERIDAE	**-**	**-**		**-**	**-**		**0.28**	**1.10%**		**0.09**	**0.26%**	
Cyclopteridae unid.	-	-		-	-		0.21	0.83%		-	-	
Eumicrotremus derjugini	-	-		-	-		0.07	0.27%		0.09	0.26%	
LIPARIDAE	**1.02**	**6.36%**		**0.32**	**12.98%**		**1.54**	**6.12%**		**0.79**	**2.18%**	
Careproctus lerikimae	-	-		-	-		0.20	0.81%		0.01	0.04%	
Liparis bathyarcticus	-	-		-	-		0.07	0.26%		-	-	
Liparis fabricii	-	-		<0.01	0.12%	9	0.58	2.32%		0.15	0.42%	
Liparis gibbus	-	-		-	-		0.08	0.32%		0.02	0.05%	

Table 7.3.1.3. continued.

	Pelagic - Isaacs-Kidd Midwater Trawl Abundance (#/1000 m^3)						Demersal - Beam Trawl Abundance (#/1000 m^2)					
	TB-2012-US			TB-2013-US			TB-2013-US			TB-2014-US		
Taxa	Mean	% of Total	Top 10	Mean	% of Total	Top 10	Mean	% of Total	Top 10	Mean	% of Total	Top 10
LIPARIDAE, continued												
Liparis spp. all ≤50 mm	1.01	6.30%	4	0.31	12.86%	2	0.26	1.04%		0.44	1.23%	
Liparis spp. unid. 51–110 mm	0.01	0.06%		-	-		0.26	1.04%		0.10	0.27%	
Liparis tunicatus	-	-		-	-		0.03	0.13%		0.03	0.08%	
Paraliparis spp.	-	-		-	-		0.01	0.04%		0.01	0.02%	
Rhodichthys regina	-	-		-	-		0.04	0.14%		0.03	0.07%	
ZOARCIDAE	**-**	**-**		**-**	**-**		**6.16**	**24.53%**		**4.04**	**11.22%**	
Gymnelus hemifasciatus	-	-		-	-		0.78	3.09%		0.84	2.33%	9
Gymnelus spp. unid.	-	-		-	-		0.21	0.83%		-	-	
Gymnelus viridis	-	-		-	-		0.15	0.60%		0.37	1.04%	
Lycenchelys kolthoffi	-	-		-	-		0.01	0.03%		0.01	0.01%	
Lycodes adolfi	-	-		-	-		1.22	4.86%	6	0.47	1.30%	
Lycodes eudipleurostictus	-	-		-	-		0.20	0.82%		0.09	0.25%	
Lycodes frigidus	-	-		-	-		-	-		0.01	0.03%	
Lycodes mucosus	-	-		-	-		0.02	0.07%		0.16	0.44%	
Lycodes pallidus	-	-		-	-		0.17	0.68%		0.01	0.03%	
Lycodes polaris	-	-		-	-		0.88	3.50%	10	0.59	1.64%	10
Lycodes raridens	-	-		-	-		0.02	0.08%		0.02	0.04%	
Lycodes reticulatus	-	-		-	-		0.07	0.29%		0.03	0.07%	
Lycodes rossi	-	-		-	-		0.04	0.15%		0.40	1.11%	
Lycodes sagittarius	-	-		-	-		0.88	3.50%		0.34	0.96%	
Lycodes seminudus	-	-		-	-		1.22	4.87%	5	0.45	1.25%	
Lycodes spp. unid.	-	-		-	-		0.29	1.16%		0.26	0.73%	
STICHAEIDAE	**7.80**	**48.59%**		**0.20**	**8.05%**		**2.29**	**9.11%**		**1.19**	**3.30%**	
Anisarchus medius	-	-		-	-		0.98	3.92%	8	0.43	1.19%	
Eumesogrammus praecisus	-	-		-	-		-	-		0.09	0.26%	
Leptoclinus maculatus	0.07	0.45%	10	-	-		-	-		0.03	0.08%	
Lumpeninae all ≤51 mm	5.69	35.39%	2	0.20	8.05%		0.33	1.32%		0.13	0.37%	
Lumpeninae unid. 53-67 mm	0.08	0.49%	9	-	-		-	-		-	-	
Lumpenus fabricii	1.87	11.64%	3	-	-		0.97	3.87%	9	0.45	1.26%	
Stichaeus punctatus	0.10	0.62%	8	-	-		-	-		0.05	0.13%	

Table 7.3.1.3. continued.

	Pelagic - Isaacs-Kidd Midwater Trawl Abundance (#/1000 m^3)				Demersal - Beam Trawl Abundance (#/1000 m^2)			
	TB-2012-US		TB-2013-US		TB-2013-US		TB-2014-US	
Taxa	Mean	% of Total Top 10	Mean	% of Total Top 10	Mean	% of Total Top 10	Mean	% of Total Top 10
AMMODYTIDAE	**-**	**-**	**-**	**-**	**-**	**-**	**0.02**	**0.06%**
Ammodytes hexapterus	-	-	-	-	-	-	0.02	0.06%
PLEURONECTIDAE	**0.04**	**0.24%**	**-**	**-**	**0.09**	**0.38%**	**0.01**	**0.02%**
Limanda proboscidea	0.01	0.05%	-	-	-	-	-	-
Pleuronectidae larva unid.	0.03	0.19%	-	-	0.08	0.31%	-	-
Reinhardtius hippoglossoides	-	-	-	-	0.02	0.07%	0.01	0.02%
TELEOST (unid.)	**-**	**-**	**-**	**-**	**0.02**	**0.07%**	**-**	**-**

7.3.2 Fish Life History Characteristics

7.3.2.1 Length-Weight Relationships

There were 16 species for which sufficient numbers of fish were captured in 2012–2014 so that length-weight relationships could be established (Table 7.3.2.1). The 16 species were from seven families: Gadidae (cods) – *Boreogadus saida*, Cottidae (sculpins) – *Gymnocanthus tricuspis, Artediellus scaber, Icelus bicornis, Icelus spatula,* and *Triglops pingelii*, Agonidae (poachers) – *Aspidophoroides olrikii*, Liparidae (snailfishes) – *Careproctus lerikimae* and *Liparis fabricii*, Zoarcidae (eelpouts) – *Lycodes adolfi, Lycodes polaris, Lycodes sagittarius*, and *Lycodes seminudus*, Stichaeidae (pricklebacks) – *Anisarchus medius*, and *Lumpenus fabricii*, and Pleuronectidae (righteye flounders) – *Reinhardtius hippoglossoides.* The number of specimens per species ranged over four orders of magnitude, from 2951 for *B. saida,* to nine *Reinhardtius hippoglossoides*. The minimum lengths varied greatly (14–351 mm), and the maximum size captured ranged from 68 to 525 mm. However, all weight-at-length regressions fit the data closely, with r^2 values of 0.92–0.99, except *I. spatula* that only had an r^2 of 0.90 despite a relationship based on 412 samples. All intercepts (*a*) were near zero. The range of slopes (*b*) was 2.49–3.59. A *b* value close to 3.0 indicates isometric growth, i.e., growth of all body parts occurs at the same rate; values outside of that range indicate allometric growth, i.e., the body changes shape with growth (Andreu-Soler et al. 2005, Froese 2006). The *b* value also indicates body shape; negative allometric growth indicates a decrease, and positive allometric growth indicates an increase, in body thickness or plumpness with increasing fish length (Froese 2006). Three species (e.g., *B. saida*) exhibited isometric growth with *b* values of 3.0 ± 0.03. Three species had *b* values less than 3.0, i.e., negative allometric growth, getting longer and relatively thinner with age. The long, thin prickleback *A. medius* had the most extreme value (*b* = 2.49) (Table 7.3.2.1). Ten of the 16 species exhibited positive allometric growth with the two plump snailfishes, *Careproctus lerikimae* and *Liparis fabricii* being the most extreme (*b* = 3.59, 3.58). Because *C. lerikimae* was only first collected in 2008 (Orr et al. 2015), and this is the first known length-weight relationship, it is important to treat with caution. This is the same value determined for 42 *C. melanurus* (*b* = 3.59) in the western Bering Sea (Orlov and Binohlan 2009). Although there were only nine *Reinhardtius hippoglossoides* (*b* = 3.15), the relationship is within the range (*b* = 2.97–3.57) found in northwest Atlantic for a sample of >10,000 individuals (Román and Paz 1997), though below that for >3,000 individuals (*b* = 3.47) in the western Bering Sea (Orlov and Binohlan 2009).

Table 7.3.2.1. Weight at length relationships for fish species.
$W = a\ L^{b}$, where W = total weight (g), L = total length, (mm), a = y-intercept and b = slope. Ranges of lengths and weights are of fishes where both measurements were recorded. Fishes were captured 2012–2014 in the Beaufort Sea with pelagic and demersal trawls.

Species	n	Weight range (g)	Length range (mm)	$a*10^{-5}$	b	r^2
GADIDAE						
Boreogadus saida	2877	0.03–106.13	15–240	0.587	3.01	0.98
COTTIDAE						
Artediellus scaber	137	0.03–13.63	14–95	1.69	2.98	0.99
Gymnocanthus tricuspis	683	0.08–20.89	19–119	0.315	3.33	0.99
Icelus bicornis	97	0.23–4.45	27–68	0.27	3.37	0.96
Icelus spatula	412	0.09–7.86	24–89	0.488	3.20	0.90
Triglops pingelii	234	0.15–14.3	26–130	0.834	2.97	0.98
AGONIDAE						
Aspidophoroides olrikii	335	0.04–3.69	23–80	0.351	3.17	0.93
LIPARIDAE						
Careproctus lerikimae	41	0.72–42.18	47–145	0.071	3.59	0.98
Liparis fabricii	120	0.07–112.53	19–212	0.05	3.58	0.93
ZOARCIDAE						
Lycodes adolfi	232	0.19–26.62	38–205	0.201	3.09	0.97
Lycodes polaris	64	0.24–26.79	40–164	0.161	3.26	0.99
Lycodes sagittarius	191	0.33–347.6	44–427	0.812	2.88	0.92
Lycodes seminudus	154	0.3–535.99	41–465	1.54	2.82	0.98
STICHAEIDAE						
Anisarchus medius	65	0.23–5.15	49–134	2.79	2.49	0.93
Lumpenus fabricii	157	0.13–5.11	41–124	0.755	2.78	0.97
PLEURONECTIDAE						
Reinhardtius hippoglossoides	9	400.2–1481.23	351–525	0.366	3.15	0.92

7.3.2.2 Length-Age Relationships

A total of 1859 ages were estimated for fishes collected by all gears from the Beaufort Sea over all three years sampled, 2012, 2013, and 2014. Fifteen species from seven families were aged (Table 7.3.2.2). Ten species from six different families had sufficient sample sizes to compare among all three years. They also had high abundance and therefore, are likely important ecologically. These species were examined using length frequency and age frequency graphs (Figures 7.3.2.1–7.3.2.11).

The gadid species, *Boreogadus saida*, arguably the most ecologically significant and thus deserving of more analysis, had lengths that ranged from 15 to 240 mm, with similar length distributions each year (Figure 7.3.2.1). *B. saida* had a length range of 15 mm to 240 mm in 2012, a length range of 17 mm to 230 mm in 2013, and a length range of 25 mm to 191 mm in 2014. *B. saida* were ages 0–5 and had extremely wide ranges of length at age. An age-0 fish could be up to 139 mm, whereas length of an age-1 *B. saida* was 65–203 mm. Ages 2 and 3 lengths overlapped those of every other age. This shows that it is impossible to say with certainty the age of a *B. saida* based solely on a length measurement. The average lengths increased incrementally for each age 1–5 (52, 105, 142, 165, 198, 206 mm; Table 7.3.2.2). Maximum achievable estimated (von Bertalanffy) length for *B. saida* in the central and eastern Beaufort Sea was 271 mm (Appendix E4). Age estimations for 2012 ranged from 0 to 5, in 2013 ages ranged

from 0 to 4, and in 2014 ages ranged from 0 to 3. For all three years combined, approximately 92% of *B. saida* estimated for age were age-2 or younger, and age-0 was the most numerous age class (Figure 7.3.2.1).

There was a pattern of age and size of *Boreogadus saida* with distribution on the shelf (≤100 m) and slope (≥200 m). At least half of the *B. saida* estimated for age collected on the shelf were age-0. The older *B. saida* (age 1+) were more commonly found on the slope than the shelf. Nearly 42.2% of the *B. saida* collected on the slope for 2012 were estimated to be age-1. Similarly, 41% and 36% of the *B. saida* collected on the slope in 2013 and 2014, respectively, were age-1. In 2012, 2013, and 2014, *B. saida* age-3 had higher percentages of capture on the slope (8.8%, 5.1%, and 9%, respectively). In 2012, age-4 *B. saida* captured on the slope comprised 6.7%, compared to only 2.1% of the shelf catch in 2012. In 2013, one age-4 *B. saida* was captured on the slope, comprising 0.5% of the slope catch. No age-4 and age-5 *B. saida* were sampled on the shelf in 2013. Finally, the oldest (age-5) *B. saida* from all 3 years of sampling were collected in 2012 on the slope, comprising 2.2% of the slope catch. As age and length are related, similar trends of older, larger fish on the slope would be expected. For all three years of collection, the average length was greater on the slope than the shelf. In 2012, the average size of *B. saida* collected on the shelf was 66 mm compared to 90 mm on the slope. In 2013, the average size was 40 mm on the shelf compared to 76 mm on the slope. Finally, in 2014, the average size of *B. saida* was 52 mm on the shelf and 100 mm on the slope. *B. saida* were captured at varying depths, though age-0 fish dominated the catch on the shelf in all years (Figure 7.3.2.2). In comparison, a very small percentage of the *B. saida* captured on the slope were age-0. As *B. saida* became larger and older, their prevalence increased in deeper waters. Catches of *B. saida* age-3, age-4, and age-5 were considerably smaller than age-0, age-1, and age-2. Despite the low sample sizes, *B. saida* ages 3–5 were more frequently collected in deeper waters.

Three species of Cottidae were aged. *Gymnocanthus tricuspis* (Figure 7.3.2.3) had narrower length ranges than *Boreogadus saida*, from 24 mm to 110 mm in 2012, 31 mm to 101 mm in 2013, and 19 mm to 147 mm in 2014. Age estimations were 0–3 in 2012, 0–7 in 2013 and 0–7 in 2014. In 2012, in the more western Colville River area, no *G. tricuspis* older than age 3 were captured, whereas some fish ages 4 to 7 were captured in the eastern US Beaufort, which was sampled in 2013 and 2014. The majority of *G. tricuspis* specimens were in the 31–40 mm length class at age 1. *Icelus spatula* were as old as age 6 (Table 7.3.2.2), but at all ages except age 0, they were on average smaller than *G. tricuspis*, whereas there were very few *Microcephalus scorpius* captured and they were on average larger than *G. tricuspis* at ages 0–1 (Table 7.3.2.2).

The agonid *Aspidophoroides olrikii* was as old as age 15, but even at that age it was only 75 mm. The species' total length range was 23–80 mm for 403 individuals (Table 7.3.2.2). The modal size caught was 51–60 mm at ages 1–7 years (Figure 7.3.2.4). Despite the very small individuals, age estimations were 0–10 for 2012, 0–8 for 2013 and 0–15 in 2014. An interesting pattern between the length ranges and age estimates of this species can be seen in this species' length frequency plot. It appeared that older individuals among the long-lived *A. olrikii* were slowing in growth, as 40 mm fish were ages 0–1, while 60 mm fish were ages 3–8. Due to a freezer malfunction no *A. olrikii* >70 mm were available for aging from 2012 or 2013.

The liparid *Liparis fabricii* was only captured to age 5, however, at age 5 it was 2.5 times as long as an age-15 *A. olrikii* (Table 7.3.2.2). It had a length range of 23 mm to 212 mm in 2012, 19 mm to 209 mm in 2013, and 31 mm to 210 mm in 2014. In 2012, age estimations were 0–5 years, 0–3 years in 2013, and 0–5 in 2014 (Figure 7.3.2.5).

All three years of age and length/frequency distributions were available for the four most abundant zoarcid species: *L. adolfi, L. polaris, L. sagittarius*, and *L. seminudus*. The length range of the four *Lycodes* species of the zoarcid family was greater than for any other family: 42 mm to 465 mm in 2012, 32 mm to 410 mm in 2013, and 28 mm to 444 mm in 2014. *L. adolfi* (Figure 7.3.2.6) had a length range of 76 mm to 225 mm in 2012, 49 mm to 185 mm in 2013, and 38 mm to 182 mm in 2014. Ages ranged 0 to 12 years, except for one 16-year old fish collected in 2012. *L. polaris* (Figure 7.3.2.7) had a length range of 42 mm to 205 mm in 2012, 32 mm to 222 mm in 2013, and 40 mm to 109 mm in 2014. Though the length range of *L. polaris* was similar to that of *L. adolfi*, they were much younger (0 to 7 years). Unfortunately, only one *L. polaris* sample was available for aging from 2013 as the others were preserved in formalin. The length range for *L. sagittarius* (Figure 7.3.2.8) was 110 mm to 427 mm in 2012, 51 mm to 292 mm in 2013, and 44 mm to 338 mm in 2014. Age estimations ranged from 6 years to 21 years in 2012, from 2 years to 15 years in 2013, and 0 to 23 years in 2014. Though *L. sagittarius* individuals were longer, but not older, in 2012 than in other years. In 2013 and 2014 smaller and younger individuals of *L. sagittarius* were captured, i.e., <100 mm. These differences in size and age could be due to the different sampling location in 2012. *L. seminudus* (Figure 7.3.2.9) had a length range of 77 mm to 465 mm in 2012, 45 mm to 410 mm in 2013, and 41 mm to 444 mm in 2014. Age estimations for *L. seminudus* ranged 1 to 16 years in 2012, 2 to 24 years in 2013, and 0 to 19 in 2014. These age estimates make *L. seminudus* one of the oldest species that the Norcross Fisheries Oceanography Laboratory has processed for age estimation. In 2013 and 2014, the minimum fish length was less than in 2012. The interannual differences in lengths could be attributed to the difference in sampling times between 2012 (September) and 2013 and 2014 (August) or because collections were in the central Beaufort in 2012 and in the eastern Beaufort in 2013 and 2014. Two additional *Lycodes* species, *L. eudipleurostictus* and *L. reticulatus*, had many fewer individuals captured. These species had large lengths comparable to *L. sagittarius* and *L. seminudus* but were much younger at those lengths (Table 7.3.2.2).

The Stichaeidae family had two species for which the longest lengths were ~130 mm (Table 7.3.2.2). The oldest, *Anisarchus medius,* was age-19 but was only 131 mm (Figure 7.3.2.10). An age-2 *A. medius* was 78 mm, comparable to an age-2 *Lumpenus fabricii* (Figure 7.3.2.11). Unfortunately, due to a freezer malfunction, no *A. medius* or *L. fabricii* were available for aging from 2014.

A unique contribution of this study was estimation of ages of Arctic fish species for which no information has previously been published. Confidence intervals were calculated for lengths at ages for 11 fish species (Table 7.3.2.3). Intervals are not available for all ages due to small sample sizes for some ages. These were often the oldest individuals documented to date for the species. Confidence intervals for 11 of the 12 species overlapped for most of the ages estimated (up to 100% of ages estimated for some species), indicating there is no clear-cut length at age for any species analyzed; no overlap was observed for the four individuals and two ages of *Myoxocephalus scorpius*. Overlap in confidence intervals may be reduced with the addition of more specimens. *Lycodes sagittarius* (0–26 yrs) and *L. seminudus* (0–24 yrs) had the largest age ranges (Table 7.3.2.2) and *L. seminudus* had the widest confidence interval for length at age estimates (age 18, 316.5 mm).

The large age range could explain the overlap in confidence intervals for lengths at ages, when individuals of many different lengths are estimated to be the same age. Other species that were not as long-lived still had overlap in their confidence intervals. This overlap is likely due to the small samples sizes for each age estimated for these species in the Beaufort Sea

(*Gymnocanthus tricuspis*, *Icelus spatula*, *Aspidophoroides olrikii*, *Liparis fabricii* and *Anisarchus medius;* Table 7.3.2.3). *Lumpenus fabricii* only had three ages estimated for the entire sample (84 fish) with confidence intervals only overlapping between age-2 and age-1 fishes (Table 7.3.2.3). Only five individuals were estimated to be age-2, likely contributing to the overlap between the confidence intervals for ages 2 and 1. Confidence intervals for lengths at age-0 did not overlap with intervals for age-1 for seven of the 11 fish species analyzed. It is possible that age-0 for these fish species have a consistent length range, contributing to the narrow confidence intervals for age-0 fishes even at low sample sizes.

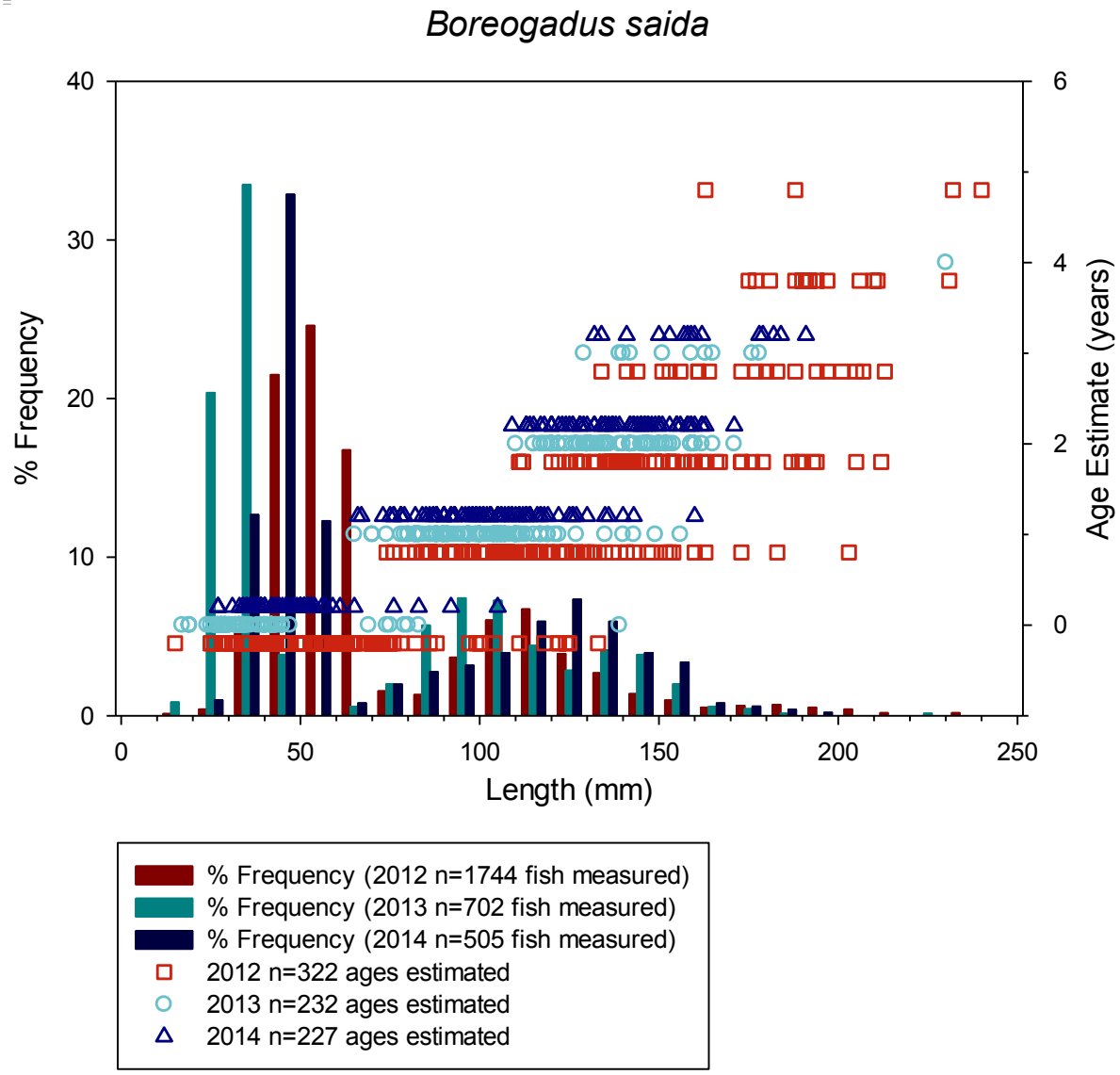

Figure 7.3.2.1. Gadidae: *Boreogadus saida*. Length frequency and age estimates from the Beaufort Sea 2012–2014. Length frequency includes fish caught by all gears and is not adjusted for abundance.

Table 7.3.2.2 Fish from Beaufort Sea 2012–2014. Total number measured, assigned ages, number aged, range of total lengths, mean and standard deviation of total length.
Only fishes with precise measurements (1 mm) are included in this table; additional fishes measured within 10-mm length classes may have been captured. An asterisk (*) indicates each of the ten species for which length frequency and age frequency graphs were prepared.

Taxon	Age	n fish	Min–Max	Mean±StDev
GADIDAE				
**Boreogadus saida*				
	all	2951	15–240	72.7±39.1
	aged	781	15–240	102.1±46
	0	261	15–139	51.8±21.7
	1	262	65–203	105.2±20.9
	2	195	109–212	141.7±18.3
	3	45	129–213	165.4±21.9
	4	14	175–231	198.1±17.6
	5	4	163–240	205.8±36.5
COTTIDAE				
**Gymnocanthus tricuspis*				
	all	831	19–147	42.7±15.2
	aged	203	24–147	54.4±20.6
	0	69	24–47	33.8±4.6
	1	47	41–82	54.1±9
	2	40	41–90	59±10.2
	3	37	61–110	75.2±9.7
	4	3	70–106	89.7±18.2
	5	3	98–106	102.7±4.2
	6	2	89–113	101±17
	7	2	101–147	124±32.5
Icelus spatula				
	all	467	20–111	53.9±12.9
	aged	70	30–83	53.7±12.5
	0	5	30–36	33.4±2.3
	1	8	32–45	40.5±5
	2	26	39–61	49.5±4.9
	3	16	48–70	58.5±6.2
	4	11	52–83	68±11
	5	3	67–80	73.7±6.5
	6	1	75	75
Myoxocephalus scorpius				
	all	8	38–89	63.6±21.6
	aged	5	38–89	67.6±23
	0	2	38–48	43±7.1
	1	2	80–89	84.5±6.4
	2	1	83–83	83–83
AGONIDAE				
**Aspidophoroides olrikii*				
	all	403	23–80	54.1±10.8
	aged	141	34–80	56.3±8.1
	0	5	36–44	39±3.5
	1	13	34–58	44.9±7
	2	14	44–60	48.3±4.2
	3	16	45–62	56.4±4.1
	4	27	48–69	58.3±4.9
	5	34	50–65	58.6±4.2
	6	24	52–71	61.3±5.1
	7	3	58–65	61.3±3.5
	8	1	68	68
	10	1	66	66
	14	2	66–80	73±9.9
	15	1	75	75
LIPARIDAE				
**Liparis fabricii*				
	all	152	18–212	115.4±58.2
	aged	68	19–212	112.2±58.5
	0	14	19–81	35.1±15.3
	1	15	61–167	90.1±27.5
	2	18	31–210	131.1±48.8
	3	13	100–203	153.6±37.9
	4	5	144–212	178.2±27.3
	5	3	176–186	180.7±5
ZOARCIDAE				
**Lycodes adolfi*				
	all	255	38–205	111.5±40.7
	aged	179	38–205	110.9±40.8
	0	19	38–141	75.3±33.4
	1	48	51–160	81.3±28.1
	2	22	60–174	104.9±36.4
	3	19	65–175	121.5±28.3
	4	23	60–170	119.2±31.4
	5	9	100–171	132.8±25.3
	6	8	85–177	133.9±26.3
	7	8	105–194	153.1±27.9
	8	5	90–171	142.8±31.2
	9	8	136–205	172.9±22
	10	6	139–190	159.3±20.5
	11	3	155–160	157.3±2.5
	12	1	145	145
Lycodes eudipleurostictus				
	all	29	55–396	205.5±89.5
	aged	1	310	310
	7	1	310	310
**Lycodes polaris*				
	all	92	32–222	76.8±38.6
	aged	47	44–205	75.2±32.3
	0	8	44–52	45.5±2.7
	1	16	44–74	60.4±10
	2	10	65–97	76.2±9.2
	3	4	72–104	81.8±15
	4	6	78–145	106.2±23
	6	2	164–205	184.5±29
	7	1	109	109
Lycodes reticulatus				
	all	32	105.6	105.6
	aged	2	107–405	256±210.7
	3	1	107	107
	11	1	405	405

Table7.3.2.2. continued.

Taxon	Age	n fish	Min–Max	Mean±StDev
ZOARCIDAE (continued)				
**Lycodes sagittarius*				
	all	217	206.3	206.3
	aged	116	44–427	180±83.9
	0	4	44–132	70.5±41.3
	1	3	45–89	70±22.6
	2	3	69–87	76±9.6
	3	3	57–100	81.3±22.1
	4	2	76–94	85±12.7
	5	5	72–96	83.4±9.8
	6	4	92–143	112.5±22.2
	7	11	78–196	139.4±36.3
	8	3	137–165	150±14.1
	9	13	105–292	155.5±49.9
	10	5	95–306	193±82.7
	11	7	122–235	169.9±42.1
	12	11	126–242	181.4±43.6
	13	8	150–268	202±45.5
	14	3	169–261	227±50.5
	15	9	162–338	267.6±61
	16	4	130–255	186.8±51.8
	17	5	228–373	286.6±61.7
	18	6	225–413	302.8±81.3
	19	2	294–427	360.5±94
	20	1	268	268
	21	1	255	255
	22	2	250–255	252.5±3.5
	26	1	276	276
**Lycodes seminudus*				
	all	204	41–465	176.5±109.2
	aged	115	41–465	206.9±111.4
	0	6	41–65	50±8.3
	1	5	70–97	81.2±10
	2	11	55–122	92.8±22.5
	3	2	123–137	130±9.9
	4	4	90–135	106.3±19.8
	5	4	86–165	121.8±33.5
	6	1	157	157
	7	3	91–144	117±26.5
	8	6	121–253	171±52.6
	9	4	124–191	148.8±29.4
	10	8	159–420	210±87.4
	11	8	132–268	184.8±44.7
	12	6	128–435	266±108.3
	13	9	145–430	283.9±108.2
	14	2	180–248	214±48.1
	15	9	132–404	270.2±101.4
	16	6	225–370	321±59.1
	17	4	190–335	256.3±64.5
	18	3	200–465	358.3±139.9
	19	5	241–385	323±56.1
	20	4	223–401	308.5±82.7
	21	2	343–345	344±1.4
	22	2	353–400	376.5±33.2
	24	1	276	276

Taxon	Age	n fish	Min–Max	Mean±StDev
STICHAEIDAE				
Anisarchus medius				
	all	81	49–134	79.7±20.1
	aged	46	49–134	82.7±21.5
	0	5	49–63	54.6±5.8
	1	3	54–70	59.3±9.2
	2	6	72–85	78±4.5
	3	3	77–97	89.3±10.8
	4	2	91–101	96±7.1
	5	5	60–112	74.6±21.5
	6	3	68–104	81.3±19.7
	7	6	64–86	75.3±9.9
	8	3	73–107	84.3±19.6
	9	3	94–115	103.3±10.7
	10	1	105	105
	11	1	116	116
	12	3	94–134	112±20.3
	17	1	107	107
	19	1	131	131
Lumpenus fabricii				
	all	190	41–124	62±13.5
	aged	84	46–103	62.2±11.7
	0	54	46–75	57.2±6.4
	1	25	51–103	71±12.4
	2	5	47–100	72.4±20.3
PLEURONECTIDAE				
Hippoglossoides robustus				
	all	3	216–314	265±49
	aged	1	216	216
	8	1	216	216

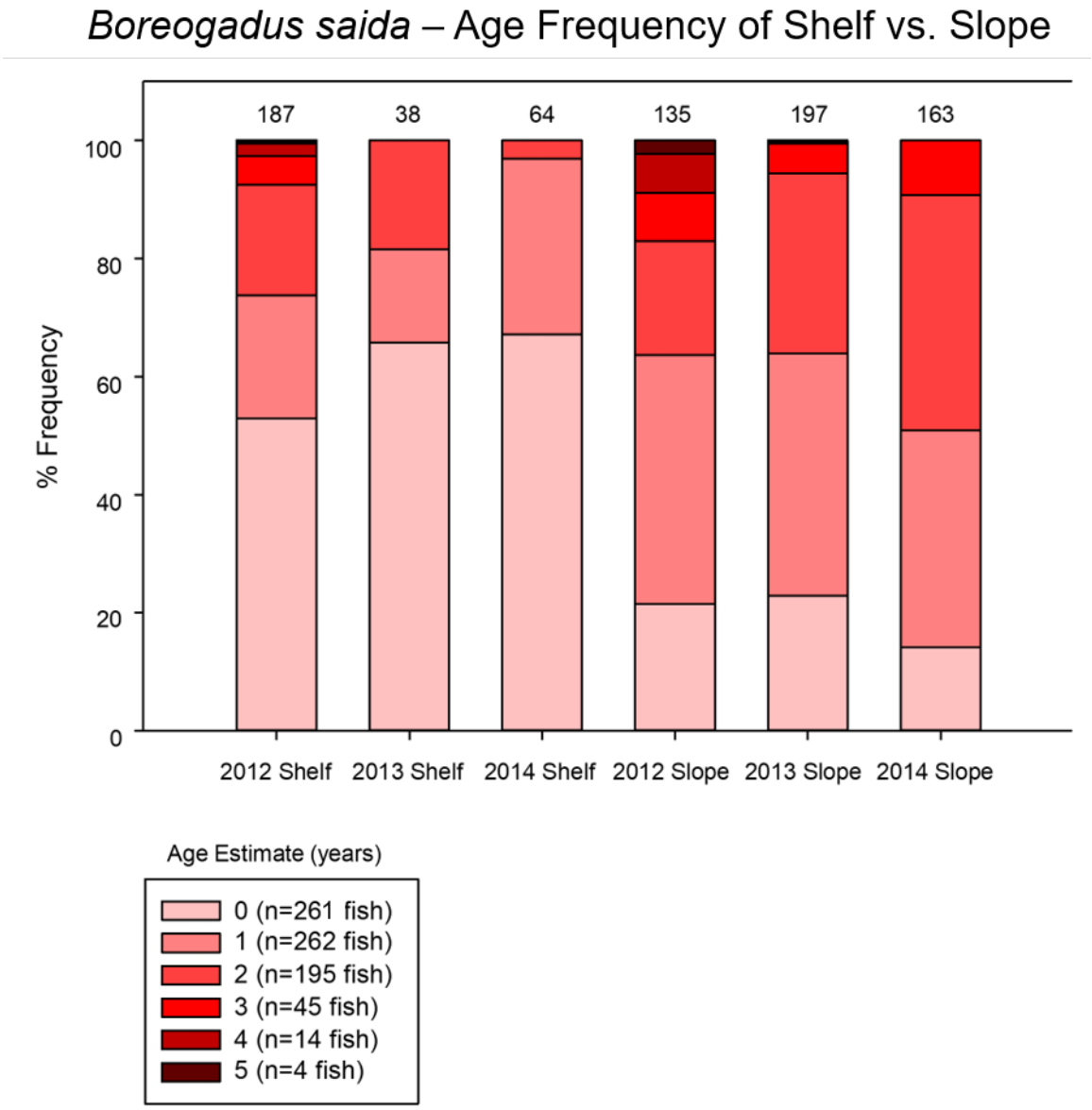

Figure 7.3.2.2. Distribution of *Boreogadus saida* by age, shelf (≤100 m), slope (≥200 m), and year sampled.
Columns indicate percentage of ages 0–5 of *B. saida* in each area, with total number of fish above. N is the number of fish for which each age was estimated.

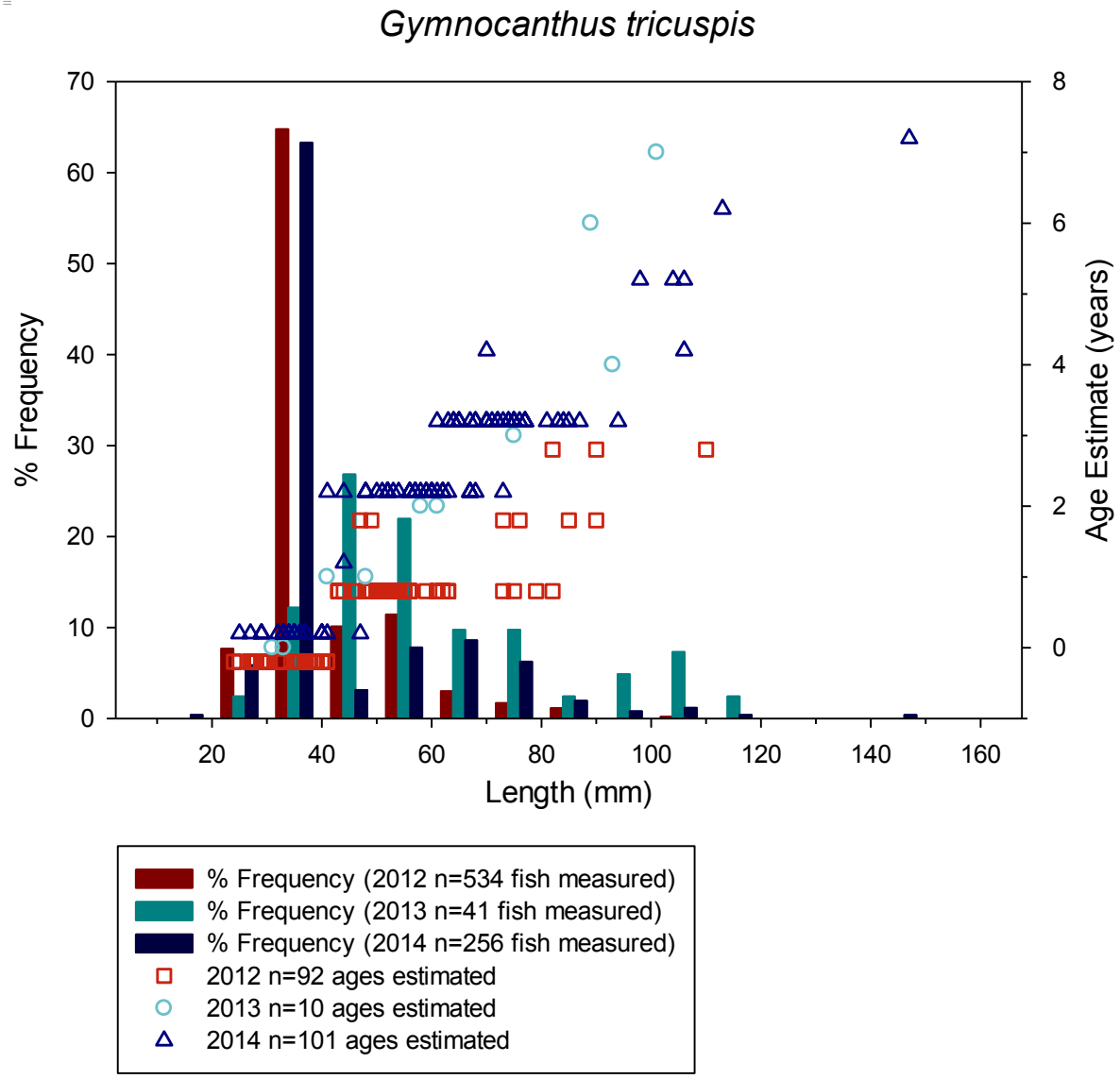

Figure 7.3.2.3. Cottidae: *Gymnocanthus tricuspis*. Length frequency and age estimates from the Beaufort Sea 2012–2014. Length frequency includes fish caught by all gears and is not adjusted for abundance.

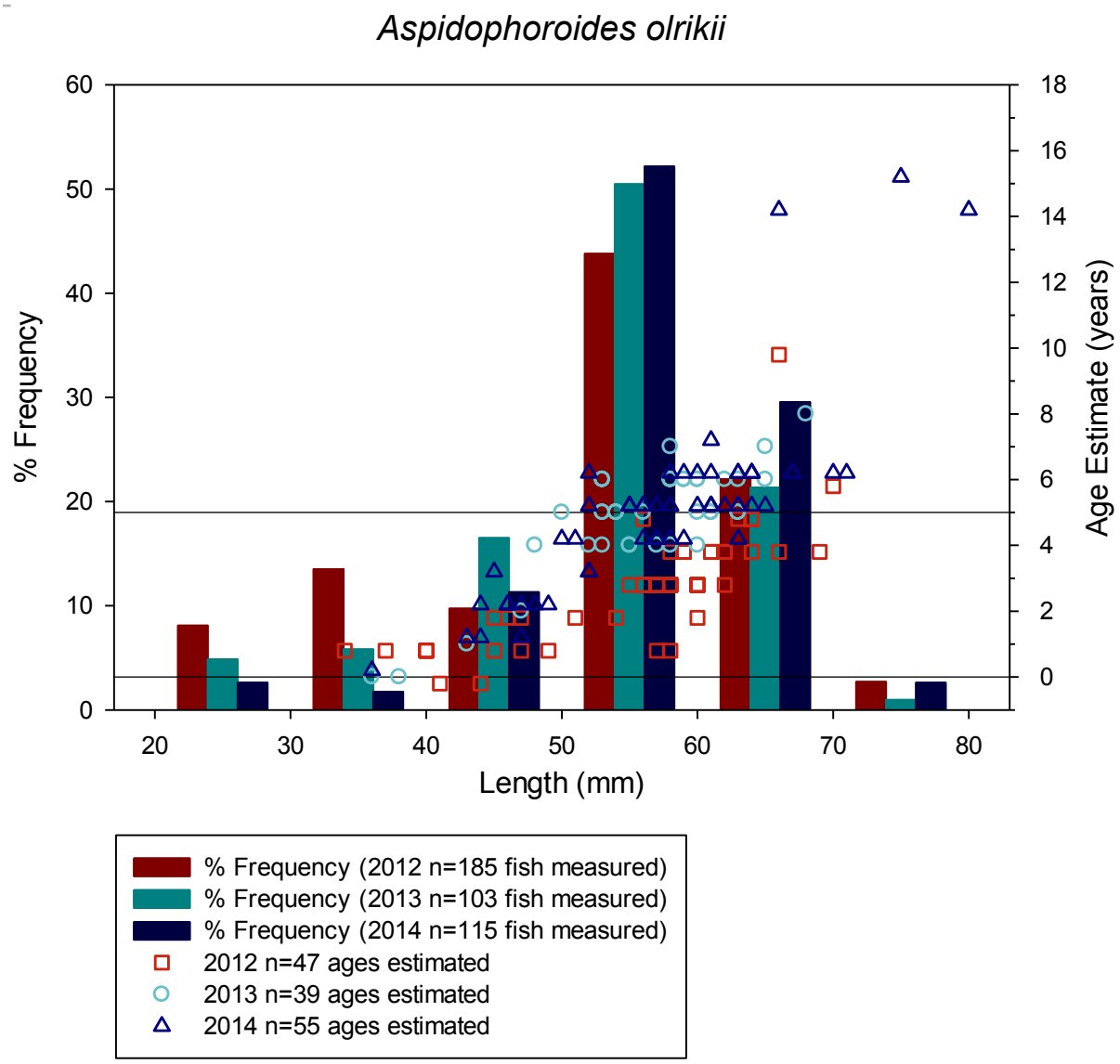

Figure 7.3.2.4. Agonidae: *Aspidophoroides olrikii*. Length frequency and age estimates from the Beaufort Sea 2012–2014. Length frequency includes fish caught by all gears and is not adjusted for abundance. The largest samples from 2012 and 2013 were not available for aging.

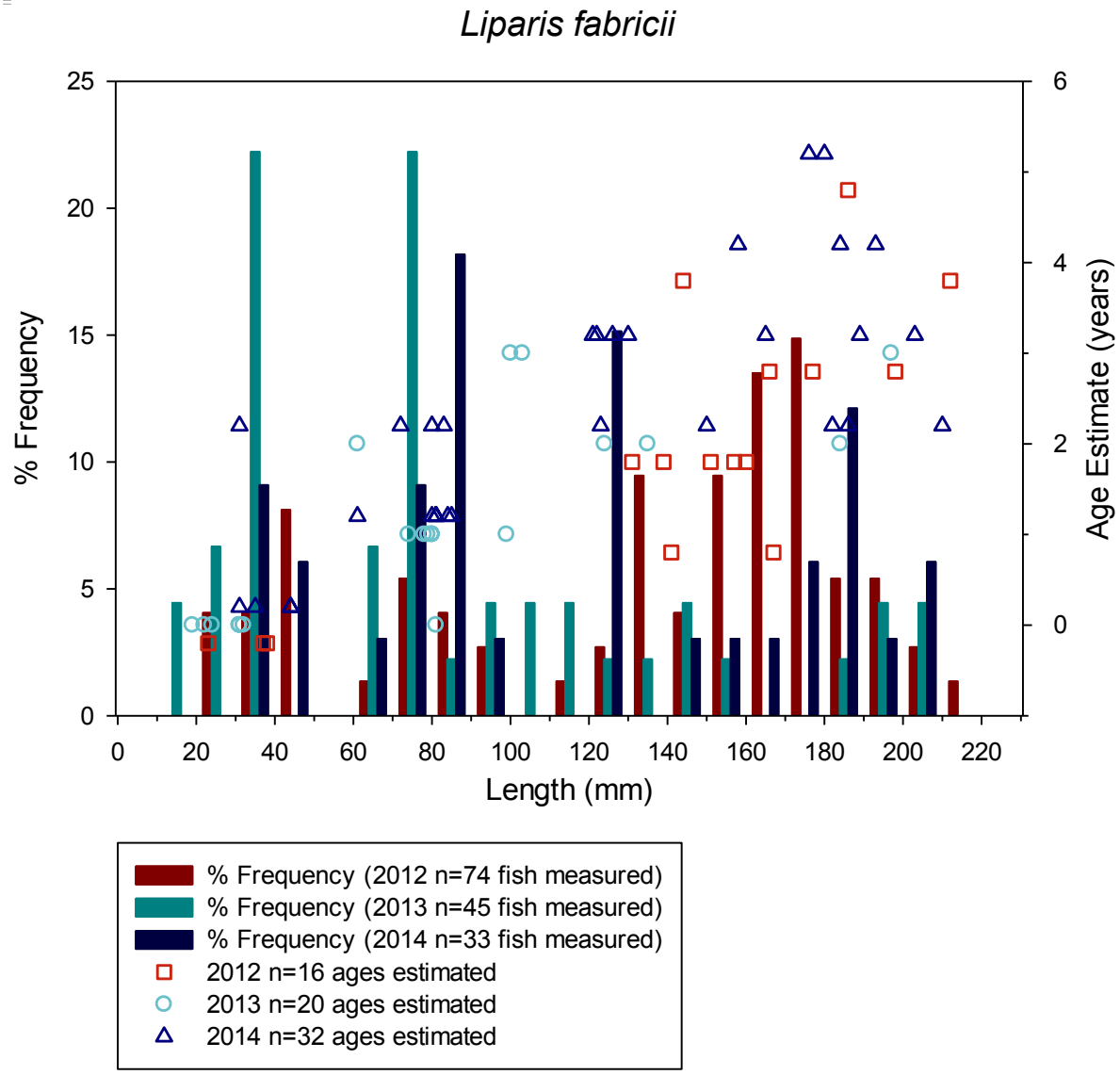

Figure 7.3.2.5. Liparidae: *Liparis fabricii*. Length frequency and age estimates from the Beaufort Sea 2012–2014. Length frequency includes fish caught by all gears and is not adjusted for abundance.

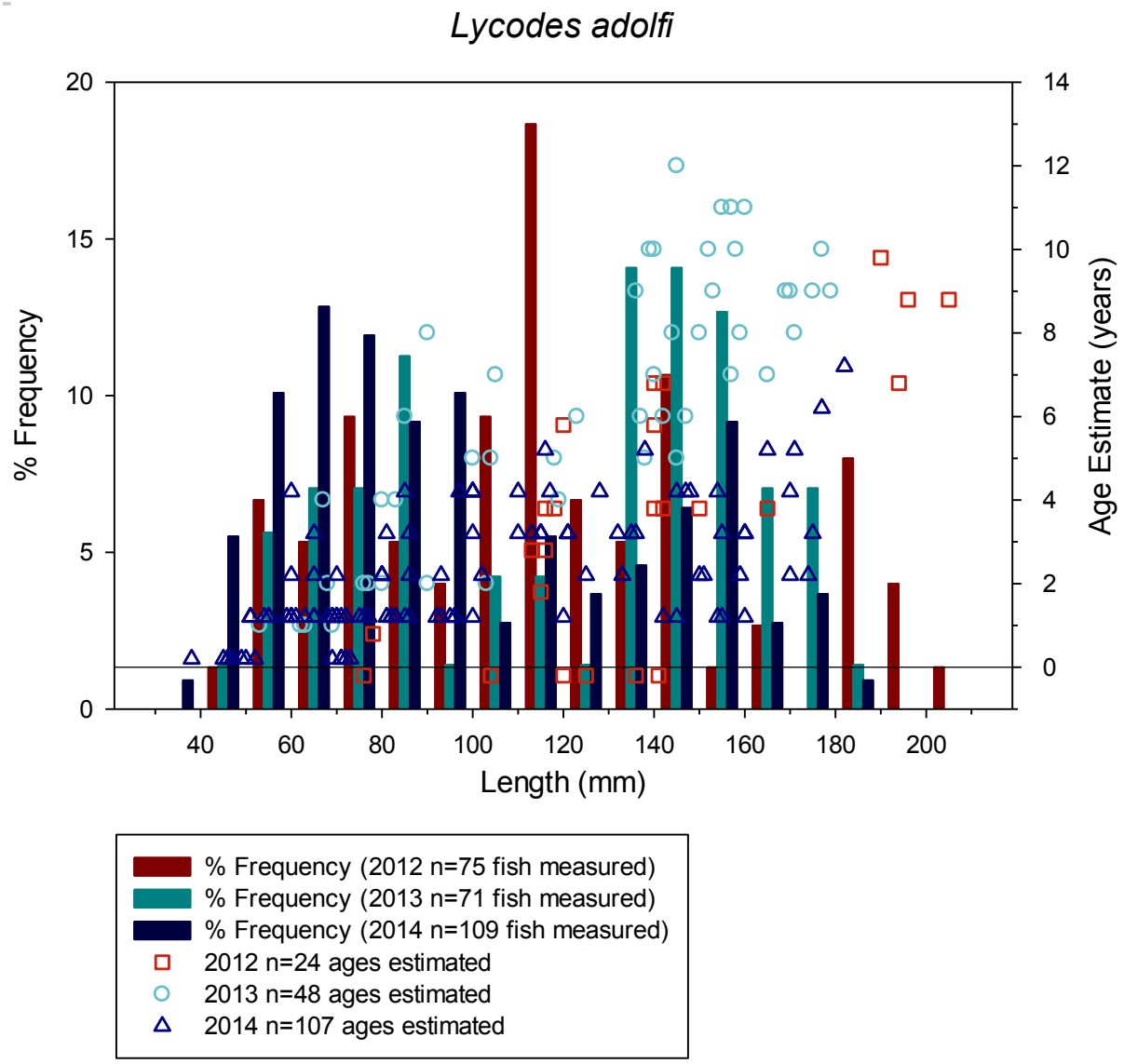

Figure 7.3.2.6. Zoarcidae: *Lycodes adolfi*. Length frequency and age frequency estimates from the Beaufort Sea 2012–2014. Length frequency includes fish caught by all gears and is not adjusted for abundance.

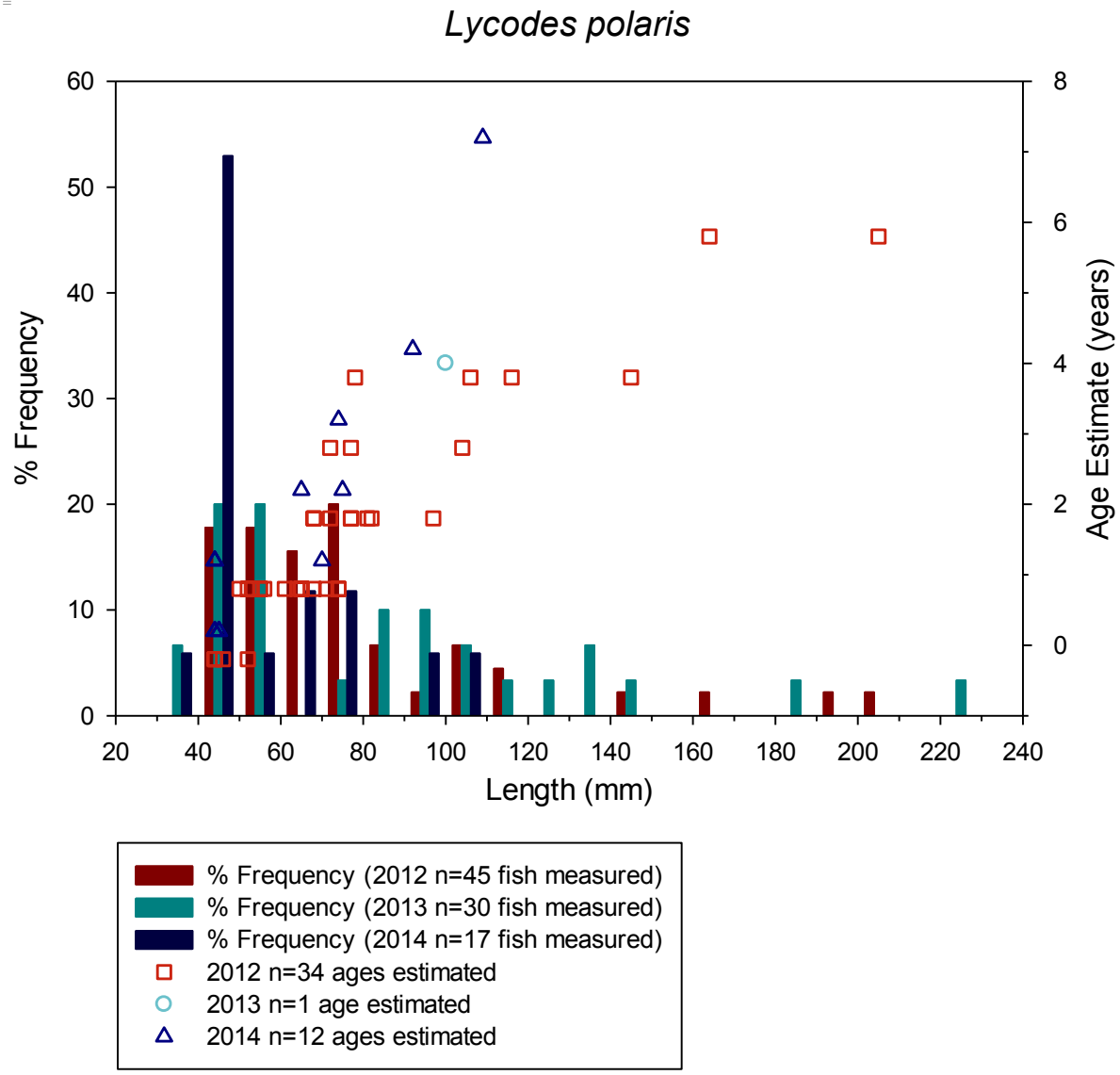

Figure 7.3.2.7. Zoarcidae: *Lycodes polaris*. Length frequency and age frequency estimates from the Beaufort Sea 2012–2014. Length frequency includes fish caught by all gears and is not adjusted for abundance. Only one fish from 2013 was available for aging.

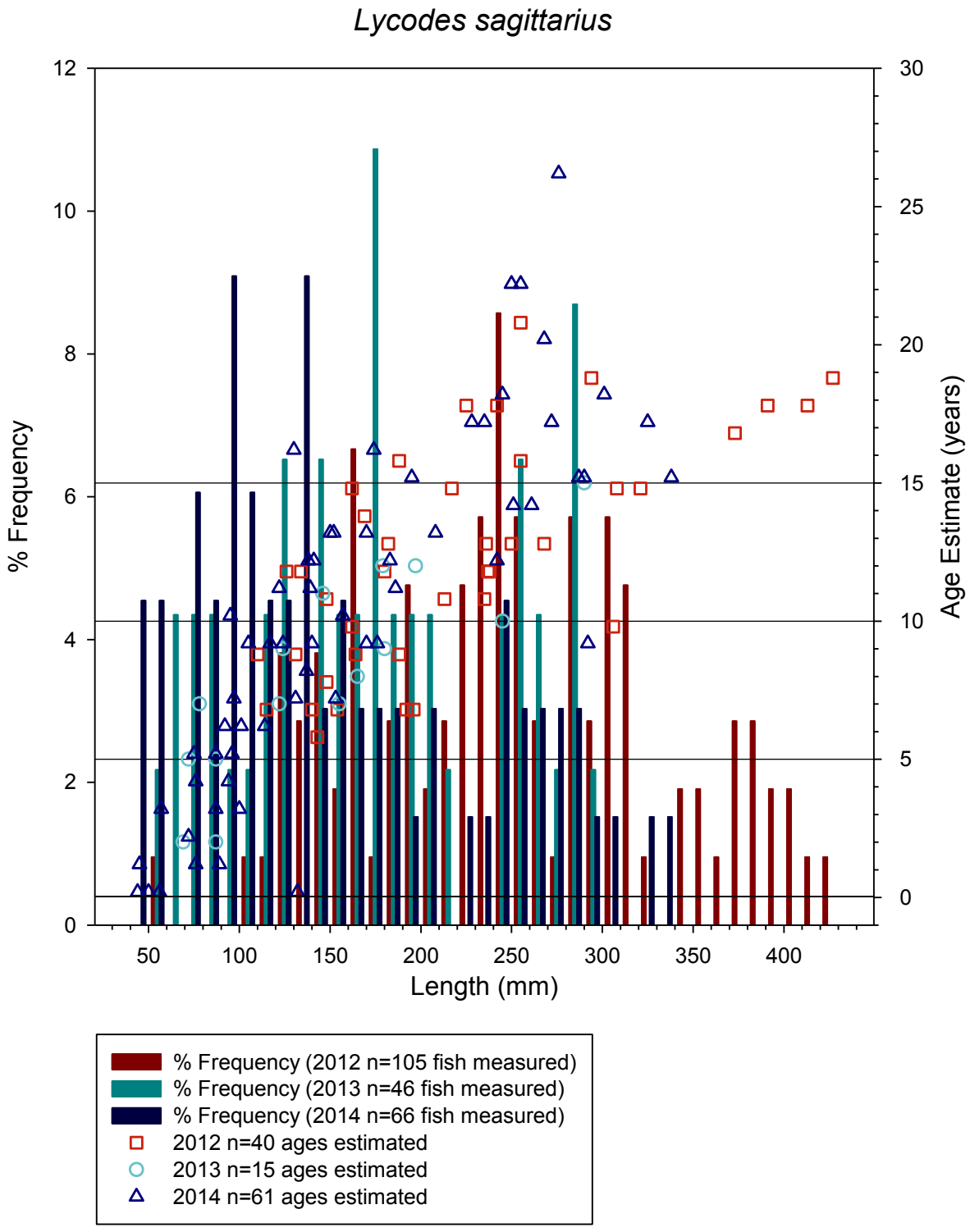

Figure 7.3.2.8. Zoarcidae: *Lycodes sagittarius*. Length frequency and age frequency estimates from the Beaufort Sea 2012–2014. Length frequency includes fish caught by all gears and is not adjusted for abundance.

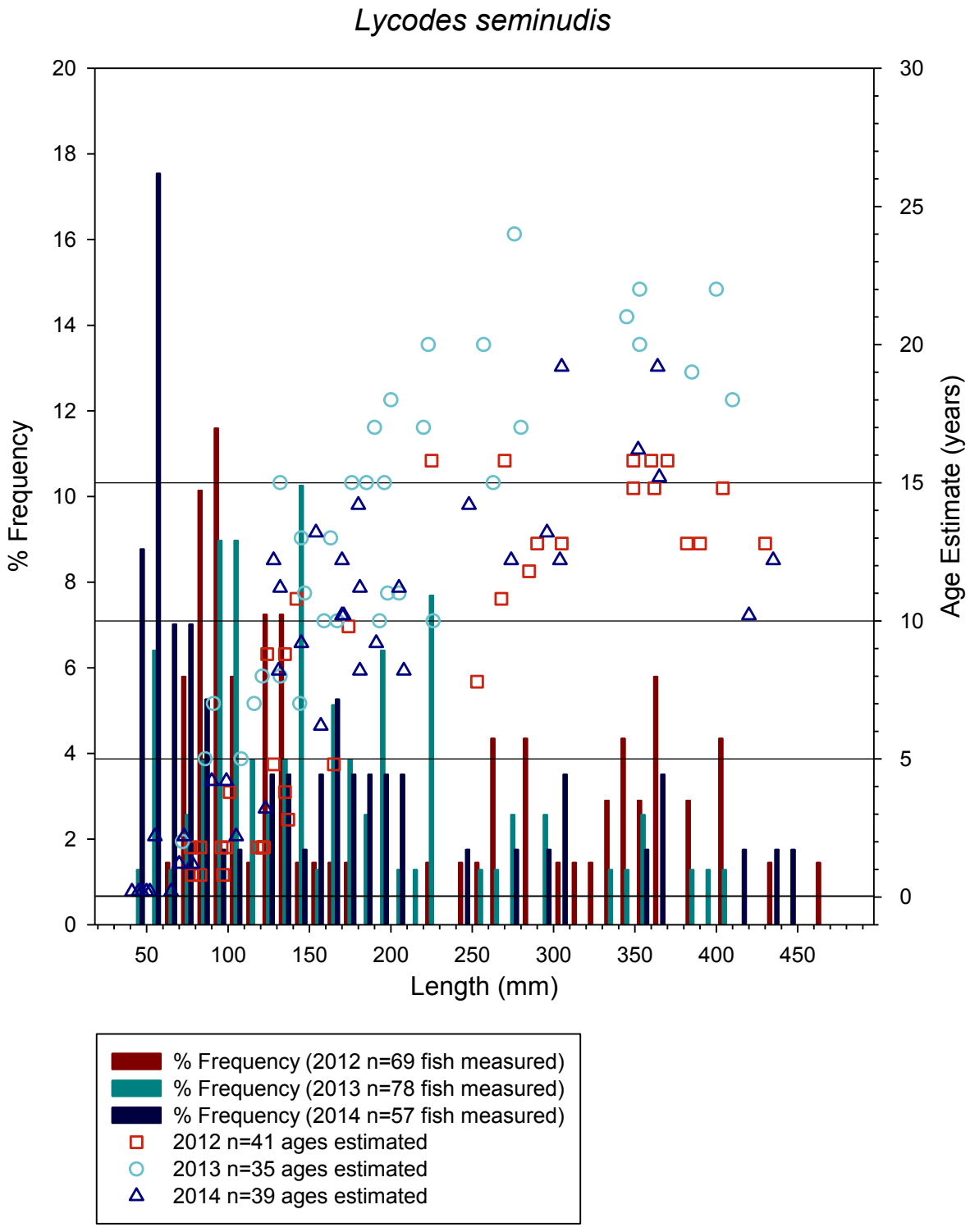

Figure 7.3.2.9. Zoarcidae: *Lycodes seminudus*. Length frequency and age frequency estimates from the Beaufort Sea 2012–2014. Length frequency includes fish caught by all gears and is not adjusted for abundance.

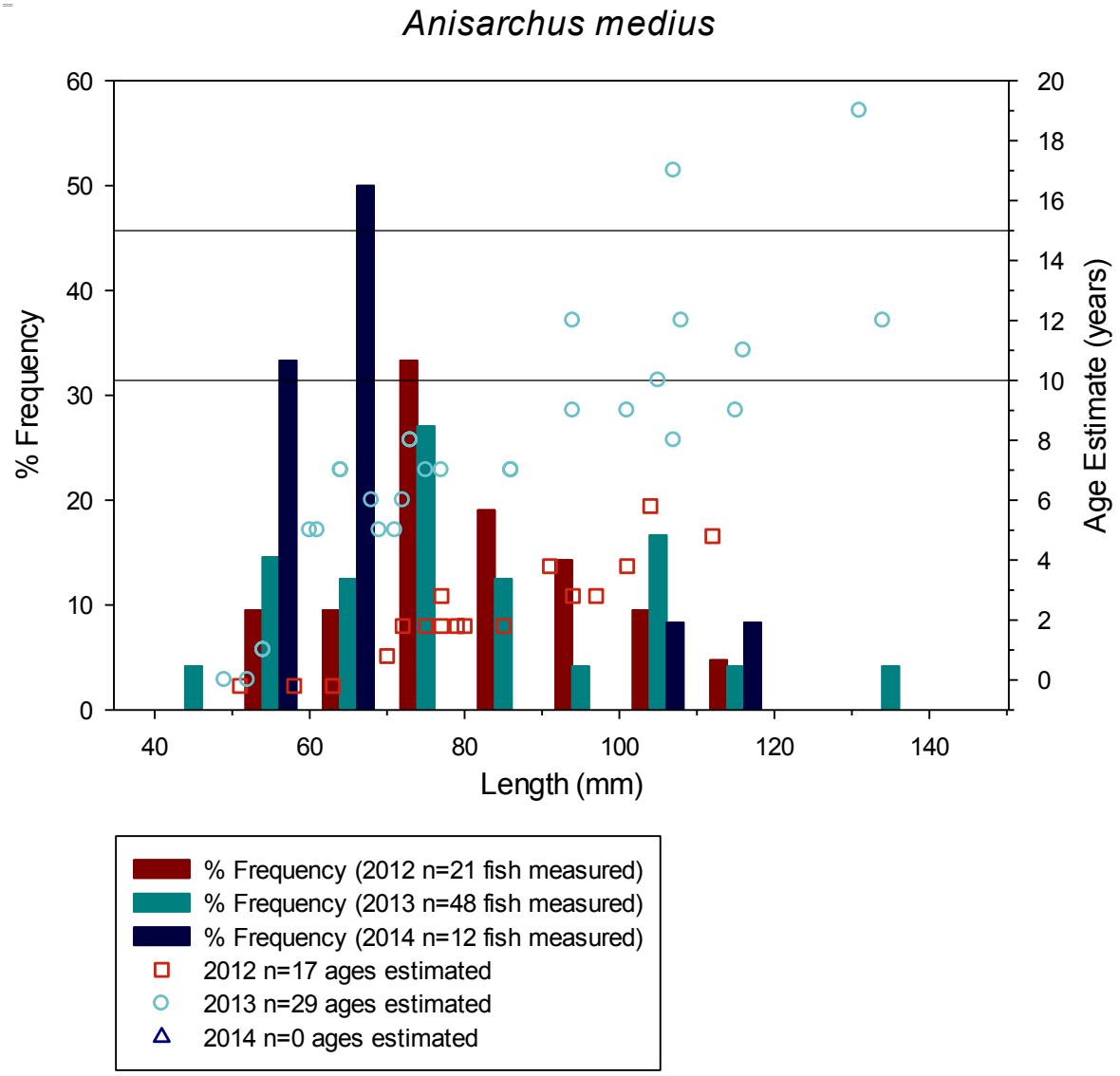

Figure 7.3.2.10. Stichaeidae: *Anisarchus medius*. Length frequency and age frequency estimates from the Beaufort Sea 2012–2014. Length frequency includes fish caught by all gears and is not adjusted for abundance. No fish from 2014 were available for aging.

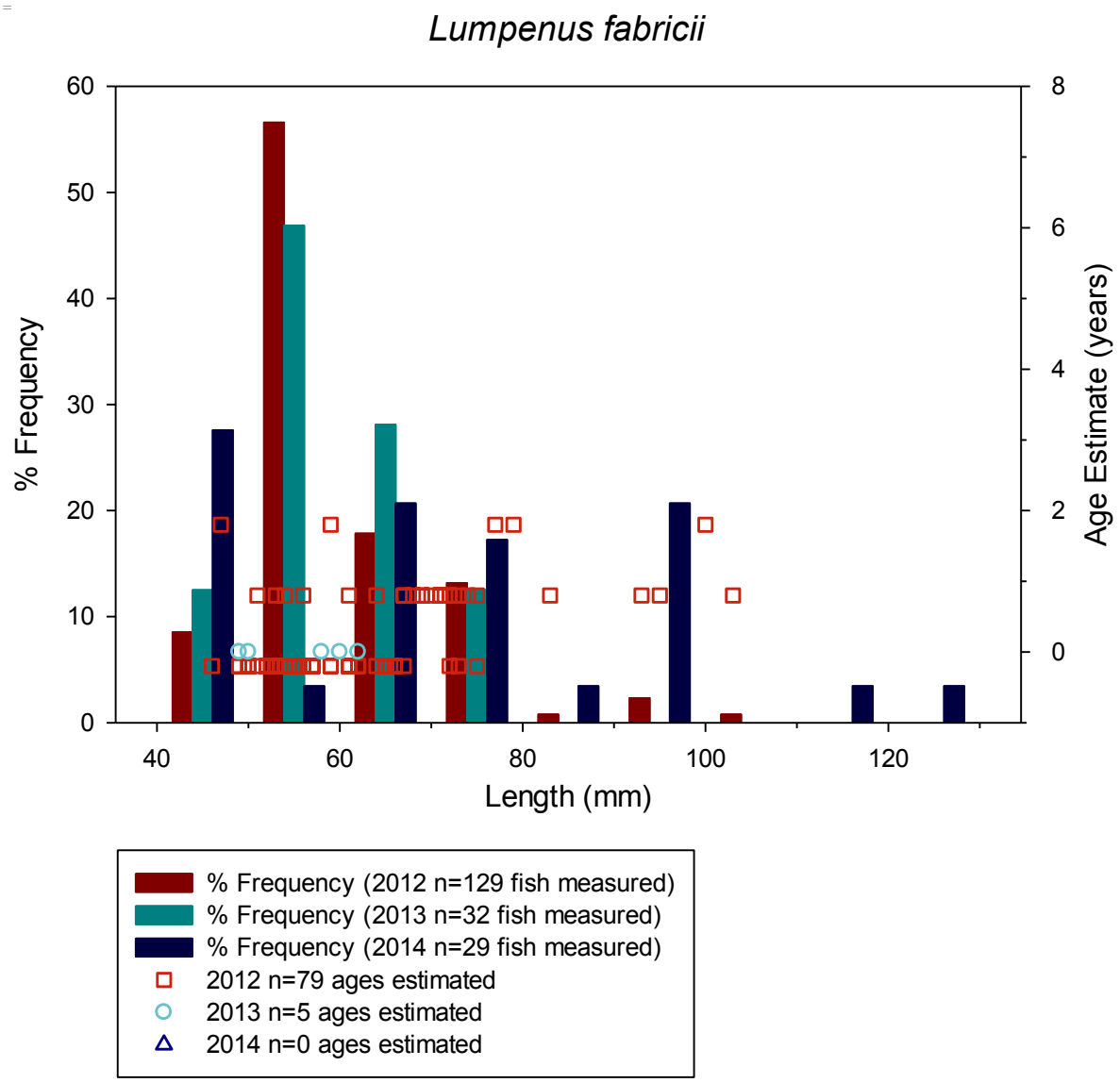

Figure 7.3.2.11. Stichaeidae: *Lumpenus fabricii*. Length frequency and age frequency estimates from the Beaufort Sea 2012–2014. Length frequency includes fish caught by all gears and is not adjusted for abundance. No fish from 2014 were available for aging.

Table 7.3.2.3. 95% confidence intervals (CI) for length (mm) at age for each of 12 fish species captured during the Transboundary project, 2012–2014.

Taxon	Age	n	Length at Age CI (mm)
GADIDAE			
Boreogadus saida	all	781	
	0	261	49.2 – 54.4
	1	262	102.7 – 107.7
	2	195	139.1 – 144.3
	3	45	159.1 – 171.8
	4	14	188.9 – 207.3
	5	4	169.9 – 241.6
COTTIDAE			
Gymnocanthus tricuspis	all	203	
	0	69	32.7 – 34.9
	1	47	51.6 – 56.7
	2	40	55.8 – 62.1
	3	37	72.0 – 78.3
	4	3	69.0 – 110.3
	5	3	98.0 – 107.4
	6	2	77.5 – 124.5
	7	2	78.9 – 169.1
Icelus spatula	all	70	
	0	5	31.4 – 35.4
	1	8	37.0 – 44.0
	2	26	47.6 – 51.4
	3	16	55.5 – 61.5
	4	11	61.5 – 74.5
	5	3	66.3 – 81.0
	6	1	
Myoxocephalus scorpius	all	5	
	0	2	33.2 – 52.8
	1	2	75.7 – 93.3
	2	1	–
AGONIDAE			
Aspidophoroides olrikii	all	141	
	0	5	36.0 – 42.0
	1	13	41.1 – 48.7
	2	14	46.1 – 50.5
	3	16	54.4 – 58.4
	4	27	56.4 – 60.1
	5	34	57.2 – 60.1
	6	24	59.3 – 63.4
	7	3	57.4 – 65.3
	8	1	–
	10	1	–
	14	2	59.3 – 86.7
	15	1	–

Table 7.3.2.3. continued.

Taxon	Age	n	Length at Age CI (mm)
LIPARIDAE			
Liparis fabricii	all	68	
	0	14	27.1 – 43.2
	1	15	76.2 – 104.0
	2	18	108.5 – 153.6
	3	13	133.0 – 174.2
	4	5	154.3 – 202.1
	5	3	175.0 – 186.4
ZOARCIDAE			
Lycodes adolfi	all	179	
	0	19	60.3 – 90.3
	1	48	73.3 – 89.2
	2	22	89.7 – 120.1
	3	19	108.8 – 134.2
	4	23	106.3 – 132.0
	5	9	116.3 – 149.3
	6	8	115.6 – 152.1
	7	8	133.8 – 172.5
	8	5	115.4 – 170.2
	9	8	157.6 – 188.1
	10	6	143.0 – 175.7
	11	3	154.5 – 160.2
	12	1	–
Lycodes polaris		47	
	0	8	43.6 – 47.4
	1	16	55.5 – 65.3
	2	10	70.5 – 81.9
	3	4	67.1 – 96.4
	4	6	87.8 – 124.5
	6	2	144.3 – 224.7
	7	1	–
Lycodes sagittarius	all	116	
	0	4	30.0 – 111.0
	1	3	44.4 – 95.6
	2	3	65.1 – 86.9
	3	3	56.4 – 106.3
	4	2	67.4 – 102.6
	5	5	74.8 – 92.0
	6	4	90.7 – 134.3
	7	11	117.9 – 160.8
	8	3	134.0 – 166.0
	9	13	128.3 – 182.6
	10	5	120.5 – 265.5
	11	7	138.6 – 201.1
	12	11	155.6 – 207.2
	13	8	170.5 – 233.5
	14	3	169.9 – 284.1
	15	9	227.7 – 307.4
	16	4	136.0 – 237.5
	17	5	232.5 – 340.7

Table 7.3.2.3. continued.

Taxon	Age	n	Length at Age CI (mm)
Lycodes sagittarius, continued			
	18	6	237.8 – 367.9
	19	2	230.2 – 490.8
	20	1	–
	21	1	–
	22	2	247.6 – 257.4
	26	1	–
Lycodes seminudus	all	115	
	0	6	43.4 – 56.6
	1	5	72.4 – 90.0
	2	11	79.5 – 106.1
	3	2	116.3 – 143.7
	4	4	86.9 – 125.6
	5	4	88.9 – 154.6
	6	1	–
	7	3	87.0 – 147.0
	8	6	128.9 – 213.1
	9	4	119.9 – 177.6
	10	8	149.4 – 270.6
	11	8	153.8 – 215.7
	12	6	179.3 – 352.7
	13	9	213.2 – 354.6
	14	2	147.4 – 280.6
	15	9	204.0 – 336.5
	16	6	273.7 – 368.3
	17	4	193.1 – 319.4
	18	3	200.1 – 516.6
	19	5	273.8 – 372.2
	20	4	227.5 – 389.5
	21	2	342.0 – 346.0
	22	2	330.4 – 422.6
	24	1	–
STICHAEIDAE			
Anisarchus medius	all	46	
	0	5	49.5 – 59.7
	1	3	48.9 – 69.8
	2	6	74.4 – 81.6
	3	3	77.1 – 101.5
	4	2	86.2 – 105.8
	5	5	55.8 – 93.4
	6	3	59.0 – 103.7
	7	6	67.4 – 83.2
	8	3	62.1 – 106.5
	9	3	91.2 – 115.4
	10	1	–
	11	1	–
	12	3	89.0 – 135.0
	17	1	–
	19	1	–

Table 7.3.2.3. continued.

Taxon	Age	n	Length at Age CI (mm)
Lumpenus fabricii	all	84	
	0	54	55.5 – 58.9
	1	25	66.1 – 75.8
	2	5	54.6 – 90.2

7.3.3 Midwater Fishes

7.3.3.1 Pelagic Assemblages

The IKMT was successfully deployed at 66 stations, which included all stations except BX-200, BX-350, A1-20 and those stations sampled only by CTD and zooplankton net in 2013. During 20 September–1 October 2012, 16 stations were sampled in the central Beaufort Sea along latitudes 150º–151º W (transects B2, BX, and B1). During 12 August–2 September 2013, 50 stations were sampled in the eastern Beaufort Sea along latitudes 146º–140º W (transects A6, A2, A1, and TBS) and the Mackenzie River along latitudes 139º–138º W (transects MAC and GRY).

A total of 1,571 fishes were caught pelagically, of which most were larvae or early juvenile stages of taxa caught at later stages on the seafloor by the beam trawl net. Fishes were captured at all but two of the 66 stations sampled (A6-750 and A2-1000) (Figure 7.3.3.1). *Boreogadus saida* was the most abundant taxon and was the only species captured at all stations that had fishes. *B. saida* larvae and small juveniles captured pelagically were most abundant at the shelf break at about 100 m depth. However, there was an order of magnitude fewer *B. saida* captured in IKMT in 2013 than in 2012, which could be because the sample location in 2012 was farther west or because it was sampled one month later.

In the 2012 central Beaufort Sea stations, the dominant families Gadidae and Stichaeidae were approximately equal in abundance, whereas in the 2013 eastern Beaufort Sea stations, Gadidae was 10 times more abundant than any other family (Appendix E3). At most of the central Beaufort Sea stations sampled in 2012, either Gadidae or Stichaeidae were of proportionally large abundance (Figure 7.3.1.5). At all but five of the 48 stations where fishes were caught by IKMT in the eastern Beaufort Sea, Gadidae provided at least 50% of total fish abundance. In the central Beaufort Sea in 2012, at least 14 fish taxa were collected pelagically (Table 7.3.1.1), and four to seven fish taxa were collected at each station (Figure 7.3.3.2); *Aspidophoroides olrikii*, *Liparis* spp., and Stichaeidae were collected in most hauls in the central Beaufort Sea stations. Half the number of fish taxa were collected pelagically in the eastern Beaufort Sea in 2013 than in the central Beaufort Sea in 2012 (7 vs. 14 taxa). At most eastern stations (east of 146° W), 1–4 fish taxa were collected pelagically, although five taxa were collected at two stations on the easternmost Mackenzie Canyon (GRY) transect (Figure 7.3.3.2). In the eastern Beaufort stations (east of 146° W) *Boreogadus saida*, Cottidae, *Liparis* spp. and Stichaeidae were most often captured.

In the central Beaufort Sea, pelagic species richness was relatively high at all midwater trawl stations on both the shelf and slope (west of 150° W) in 2012 (Figure 7.3.3.3). Richness (Margalef) was relatively low at most stations in the eastern Beaufort Sea in 2013, with the exception of a few stations on the shelf. Some of the highest values of Pielou's Evenness index were at the A2 and A1 transects at the US-Canada border (Figure 7.3.3.4). Species evenness was low at all slope stations offshore of the Mackenzie River canyon and plume (transects MAC and

GRY). Relatively high levels of Simpson's diversity index (the probability that two individuals randomly selected from a sample are different species) were found at the 2012 central Beaufort Sea stations and nearshore at the 2013 eastern Beaufort stations near the Alaska-Canada border (Figure 7.3.3.5). The combination of richness, evenness, and diversity showed that the central Beaufort Sea had more taxa, though not evenly distributed, which resulted in an overall moderate diversity. In contrast, the eastern Beaufort Sea had fewer taxa that were approximately evenly captured at all stations, which resulted in moderate to high diversity. The Mackenzie River stations had very few taxa, which were evenly distributed across the shelf but not on the slope. The result was little to no diversity in Mackenzie River slope stations and low to moderate diversity on the shelf; there was no spatial pattern to the diversity on the shelf.

A shade plot visualizes geographic concentrations and separation of species as well as species communities based on species affiliation (taxa) and geography (stations). There were four clusters of standardized species abundance of pelagic fishes (p <0.01) and three clusters of stations for 4RT abundance data (p <0.005) (Figure 7.3.3.6). *Boreogadus saida* was caught at every station where fish were captured in the IKMT and was part of all three groups of stations (Figure 7.3.3.6). More than half of taxa were observed at only 1–3 stations. Species group "a" included 12 of the 16 taxa; in this group *B. saida* and unidentified *Liparis* spp. were the most prevalent taxa. Species group "b" contained two taxa. The species groups "c" and "d" consisted of one taxon each captured at only one or two stations each. The very limited spatial and numerical occurrence of these taxa makes it highly unlikely that they had any ecological significance. They were considered outliers.

Geographical depiction of the pattern of the three station clusters showed the value of the clustering (Figure 7.3.3.7). The three clusters of stations were assigned according to their primary geographic presence as central Beaufort (n = 19 stations), eastern shelf (n = 21 stations), and eastern slope (n = 23 stations). Stations west of 150° W clustered together and were labelled "central Beaufort"; this cluster included five additional stations east of 150° W: shallow stations on A6, A1, and GRY and one deep GRY station (Figure 7.3.3.7). The central Beaufort station cluster had the most taxa (n = 15), followed by the eastern shelf (N = 8) and eastern slope (n = 7). Three taxa, *Boreogadus saida*, *Liparis* spp. and Lumpeninae, provided 82% of taxa density in the central Beaufort cluster. Most stations east of 146° W and <100 m deep clustered together; therefore, we called this group "eastern shelf". In addition to *B. saida*, most stations in the eastern shelf cluster contained small Cottidae, Lumpeninae, and *Liparis* spp. (Figure 7.3.3.6), although 83% of taxa density in this cluster was provided by the two taxa *B. saida* and *Liparis* spp. (Table 7.3.3.1). All stations ≥100 m on the A6, A2, and A1 transects (141–146° W) were in the eastern slope cluster; four of the six deep TBS stations (140º W) were in this cluster. A single taxon, *B. saida*, provided 95% of taxa density to the eastern slope cluster (Table 7.3.3.1). Farther east on the MAC and GRY transects, only three of 10 deep stations clustered in the eastern slope group (Figure 7.3.3.7). The Mackenzie Canyon stations were a mix of central, eastern shelf, and eastern slope communities. Perhaps the shelf stations that cluster with the central region were influenced by some of the same factors as the Colville River in the Central Beaufort Sea. Note that the diversity pattern does not fit with community patterns in the Mackenzie River (Figure 7.3.3.5). The apparent geographic group in nMDS, with an acceptable stress of 0.13, supports the concept of mixed influences (Figure 7.3.3.8). Note that it is not possible to include the two stations at which no fish were collected (A2-1000 and A6-750) in an nMDS plot because the patterns of stations where fish were collected were obscured. One outlier station, B2-350, fell outside of the central, eastern shelf, and eastern slope clusters, and all four taxa caught there

were required to achieve 70% of taxa density: *B. saida, Myoxocephalus scorpius, A. olrikii*, and Pleuronectid larvae (total = 100% of taxa density; Table 7.3.3.1). The eastern communities were less diverse than the central community. There were no Lumpeninae in the east, and the eastern slope was 95% *B. saida*, while the eastern shelf community was 55% *B. saida* and 29% *Liparis* spp. Not only was the diversity higher in the central, but the abundance of pelagic fish was an order of magnitude greater, mostly composed of *B. saida* and Lumpeninae too small to be identified to species (Table 7.3.3.2).

The effects of year and environment on pelagic fish abundance were assessed by one-way analysis of similarity (ANOSIM), two-way ANOSIM, CCA, and BEST stepwise analysis. ANOSIM indicated a significant effect of year on species abundance (ANOSIM R of 0.524, p <0.01; Table 7.3.3.3), which was clearly demonstrated by the separation seen in nMDS (Figure 7.3.3.8). A two-way crossed ANOSIM indicated that longitude affected species abundance (ANOSIM R = 0.239, p <0.05) but maximum gear depth did not (ANOSIM R = 0.008, p = 0.489). CCA found an overall significant relationship between the environmental data and fish abundance data (F = 2.58, p = 0.001) with the ordination explaining 25.8% of the total variance in pelagic fish abundance (Table 7.3.3.4). The variance inflation factors (VIF) of longitude, year, and surface salinity were 17–34, indicating high correlation between predictors. When year was removed from the CCA, longitude became statistically significant (p = 0.018), though surface salinity did not. Water mass was also significant (p = 0.029). CCA axis 1 (i.e., the axis explaining the most variance in fish abundance) was governed by longitude, year, surface salinity, and surface temperature (Table 7.3.3.4). CCA2 was somewhat influenced by depth, which was related to water mass (Figure 7.3.3.9). Abundance of nearly all fish species was negatively correlated with year (highest abundance in 2012) and positively correlated with surface salinity (highest surface salinity readings in 2012) and longitude (western-most longitudes sampled in 2012). All other environmental variables exerted influence in the ordination but were not significant predictors of pelagic fish abundance. BEST analysis revealed that the single variable of year provided the best correlation with pelagic fish abundance (Rho = 0.439; Table 7.3.3.5). The addition of variables did not improve the correlation.

7.3.3.2 Additional experimental pelagic collections

An AMT was fished in 2014 in an attempt to collect more and larger pelagic *Boreogadus saida*. The AMT was deployed 11 times, resulting in five successful hauls, i.e., collected fishes and appeared to fish with doors apart and mouth of net open (45% success rate). A total of 39 fishes of 3–4 taxa were captured. The catch was primarily composed of *B. saida* (saved for a separate BOEM-funded genetics study), and the second most numerous fish was *Liparis fabricii*.

Single representatives were collected of Arctic Alligatorfish, *Aspidophoroides olrikii*, and an unidentified *Liparis* species. No community analysis was performed on this small set of data.

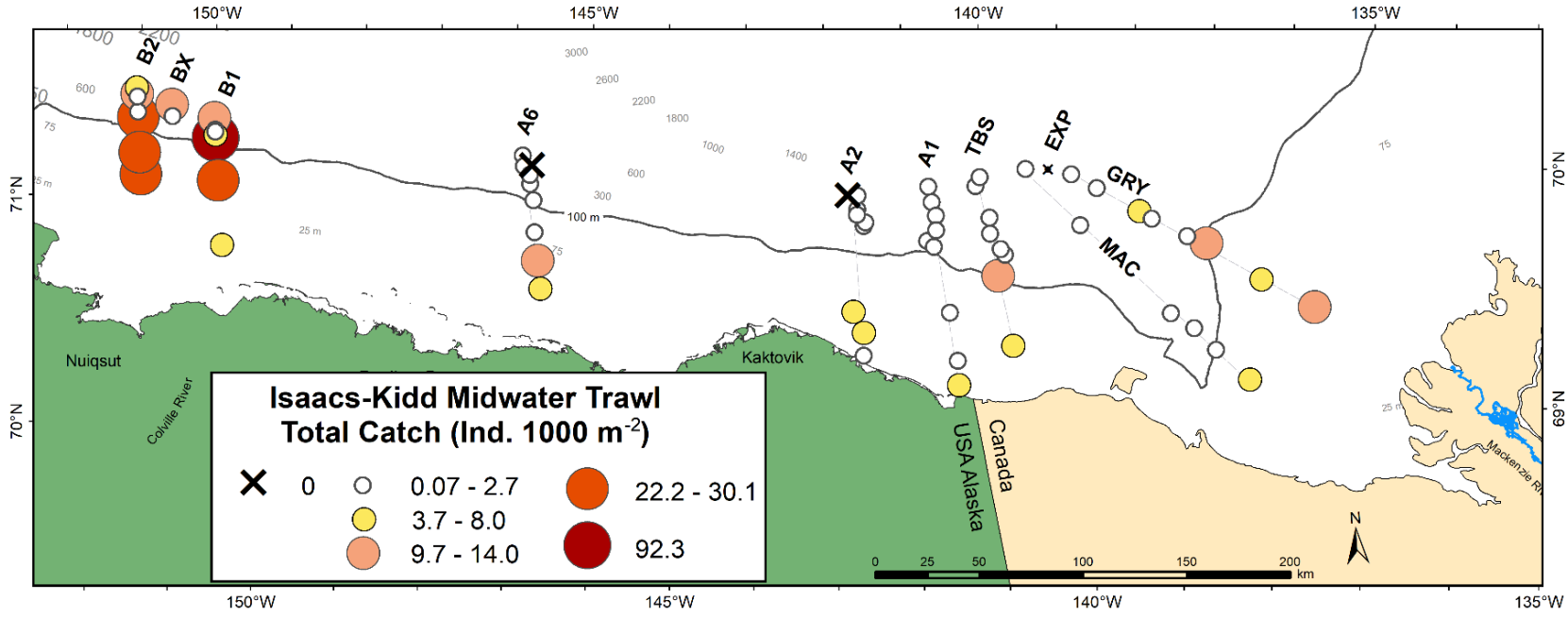

Figure 7.3.3.1. Total catch per unit effort (# 1000 m^{-3}) of pelagic fish at each station in the Beaufort Sea in 2012 and 2013 for Isaacs-Kidd midwater trawl (IKMT).

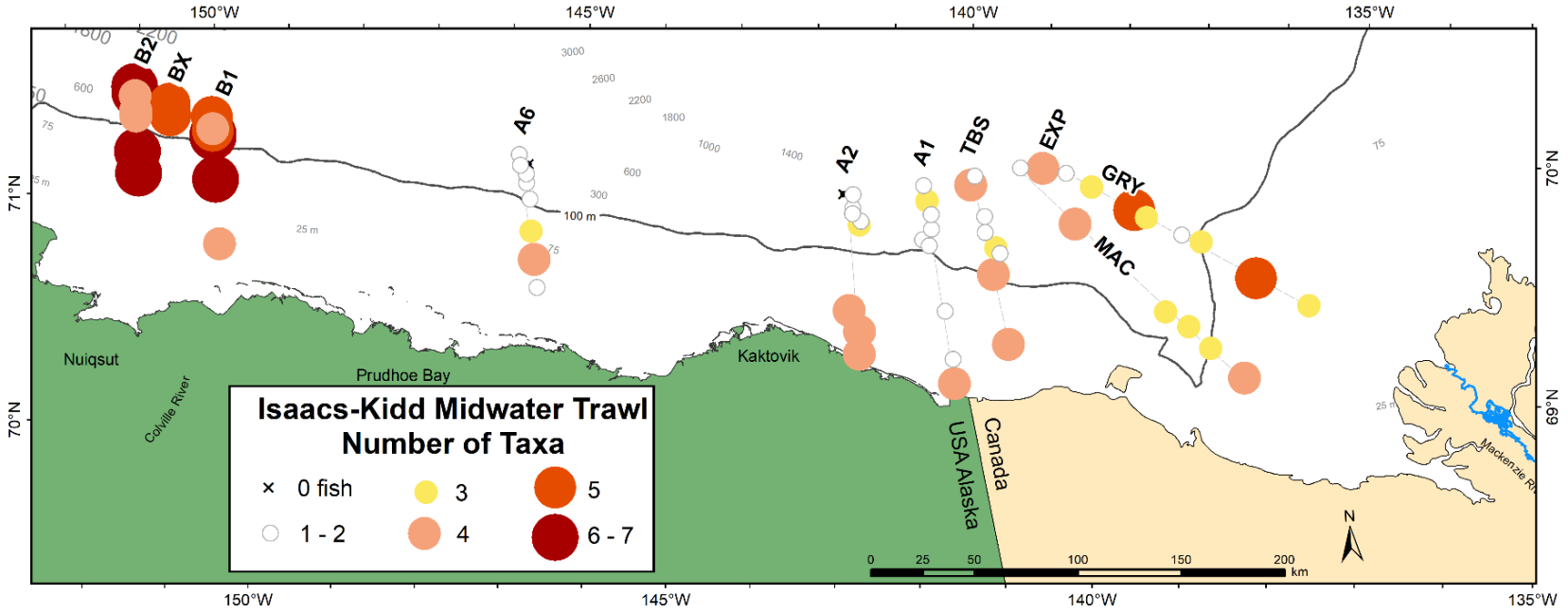

Figure 7.3.3.2. Numbers of pelagic fish taxa captured at each station in the Beaufort Sea in 2012 and 2013 by Isaacs-Kidd midwater trawl (IKMT).

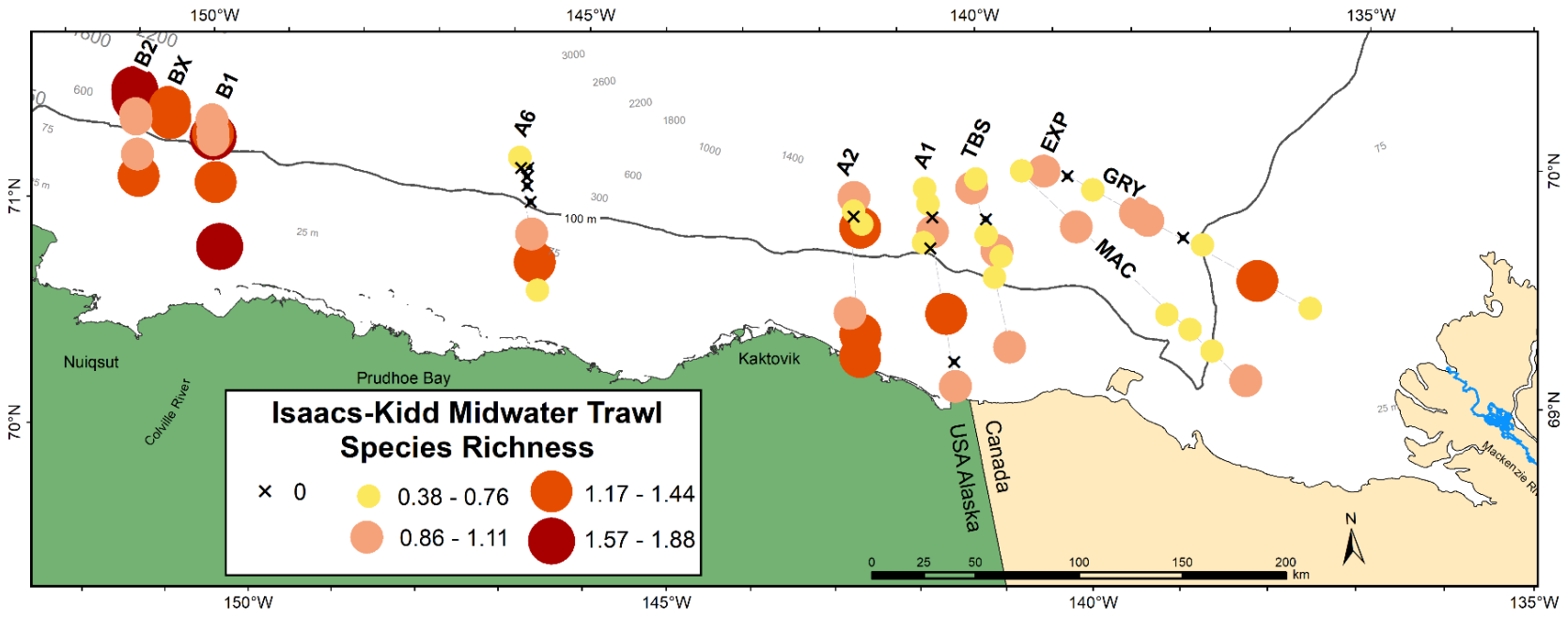

Figure 7.3.3.3. Pelagic fish species richness (Margalef index) at each station in the Beaufort Sea in 2012 and 2013 for Isaacs-Kidd midwater trawl (IKMT).

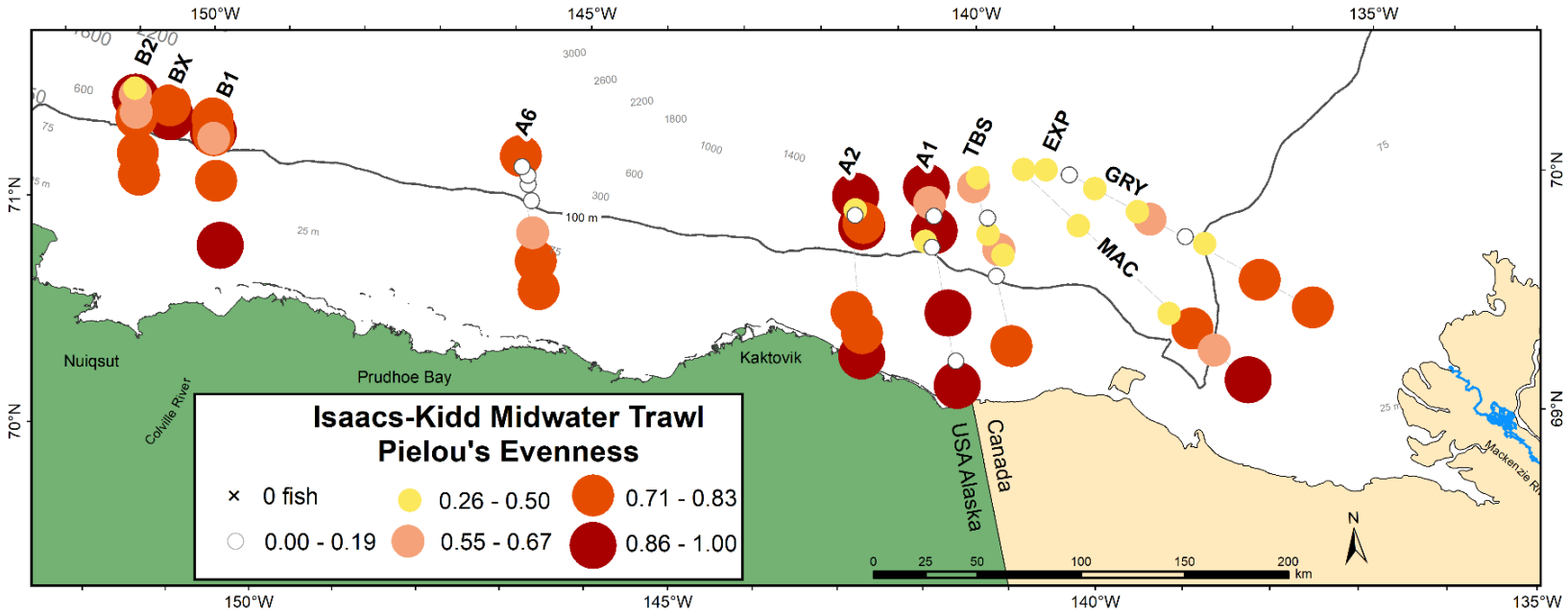

Figure 7.3.3.4. Pelagic fish species evenness (Pielou's index) at each station in the Beaufort Sea in 2012 and 2013 for Isaacs-Kidd midwater trawl (IKMT).

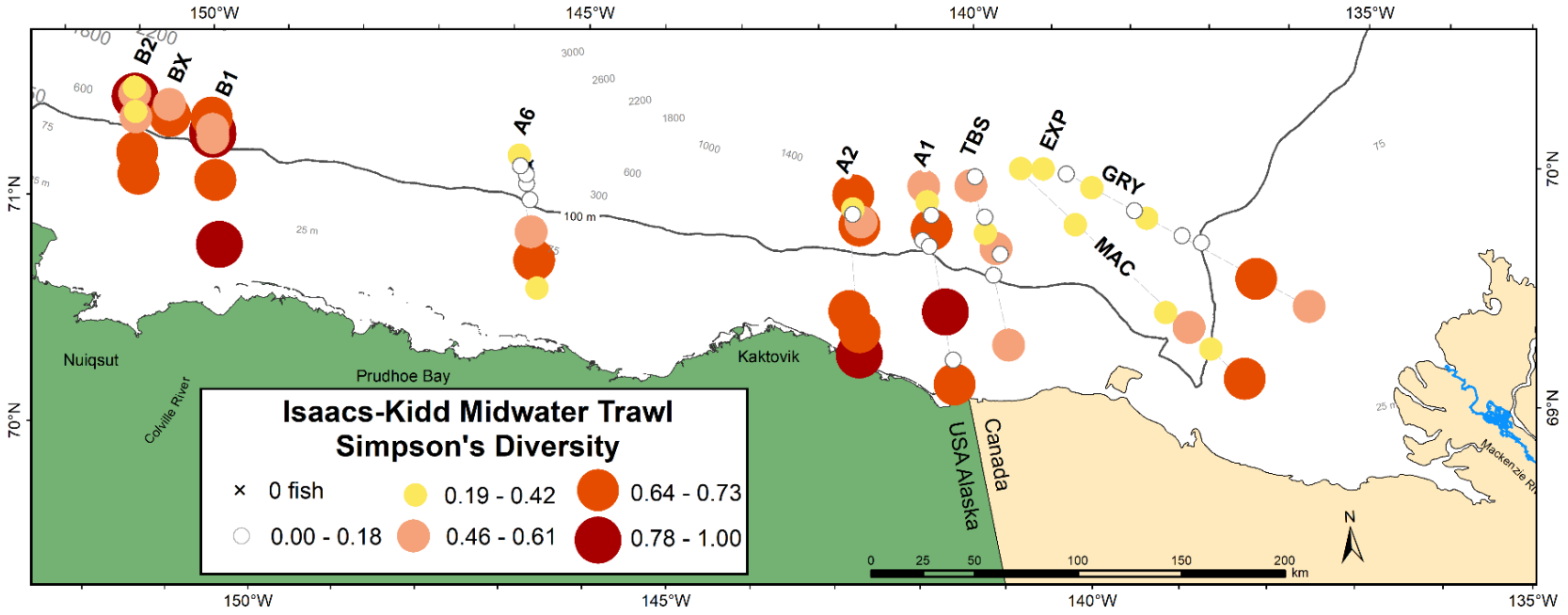

Figure 7.3.3.5. Pelagic fish diversity (Simpson's index) at each station in the Beaufort Sea in 2012 and 2013 for Isaacs-Kidd midwater trawl (IKMT).

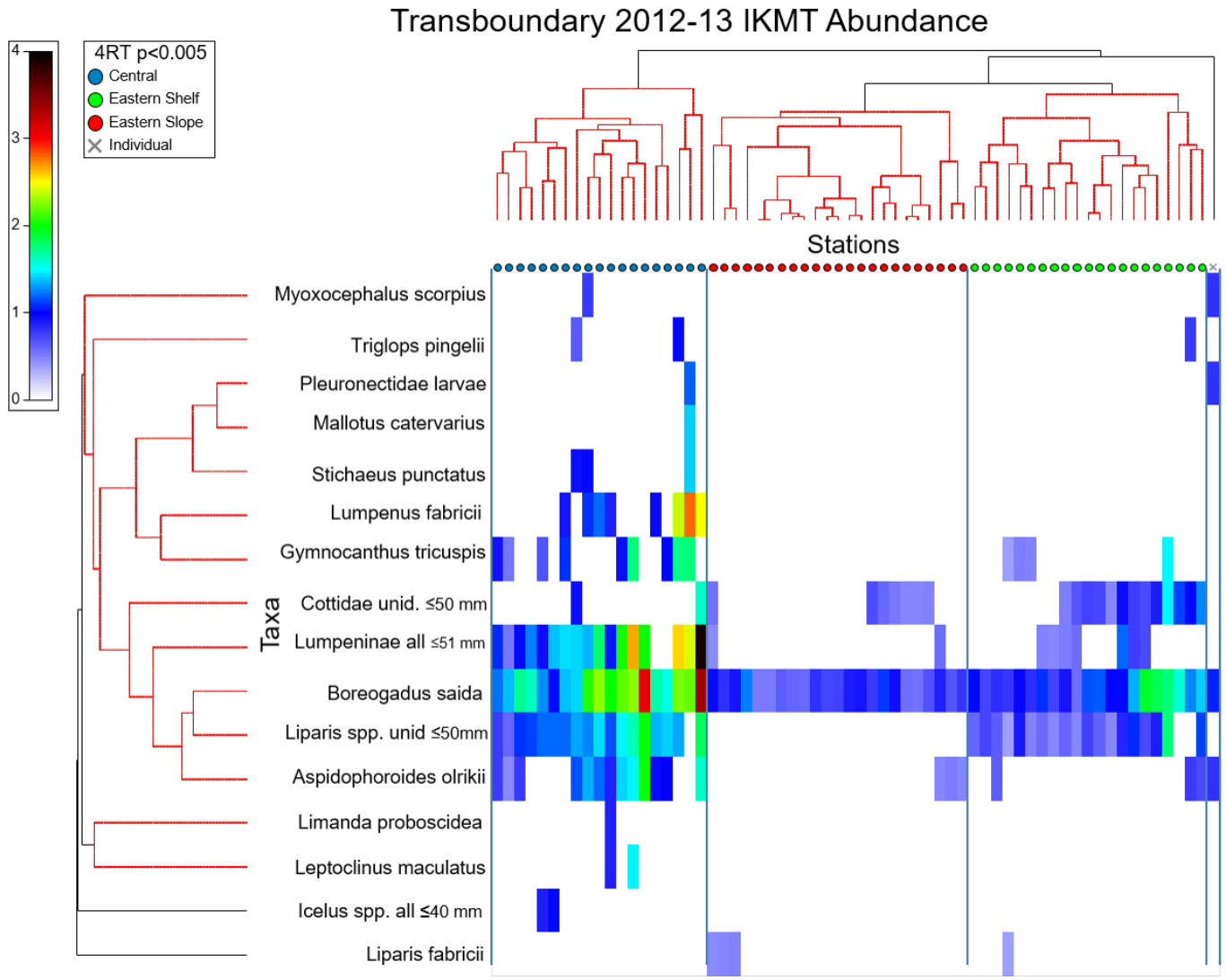

Figure 7.3.3.6. Matrix of community structure of pelagic fishes caught by Isaacs-Kidd midwater trawl (IKMT) in 2012 and 2013 by abundance. Red lines indicate non-significant differences among stations and black lines indicate differences between clusters of p <0.005 for stations and p <0.01 for taxa. Abundance is # fish 1000 m^{-3} and intensity of the color ramp indicates proportionally higher abundance of the taxon at the station.

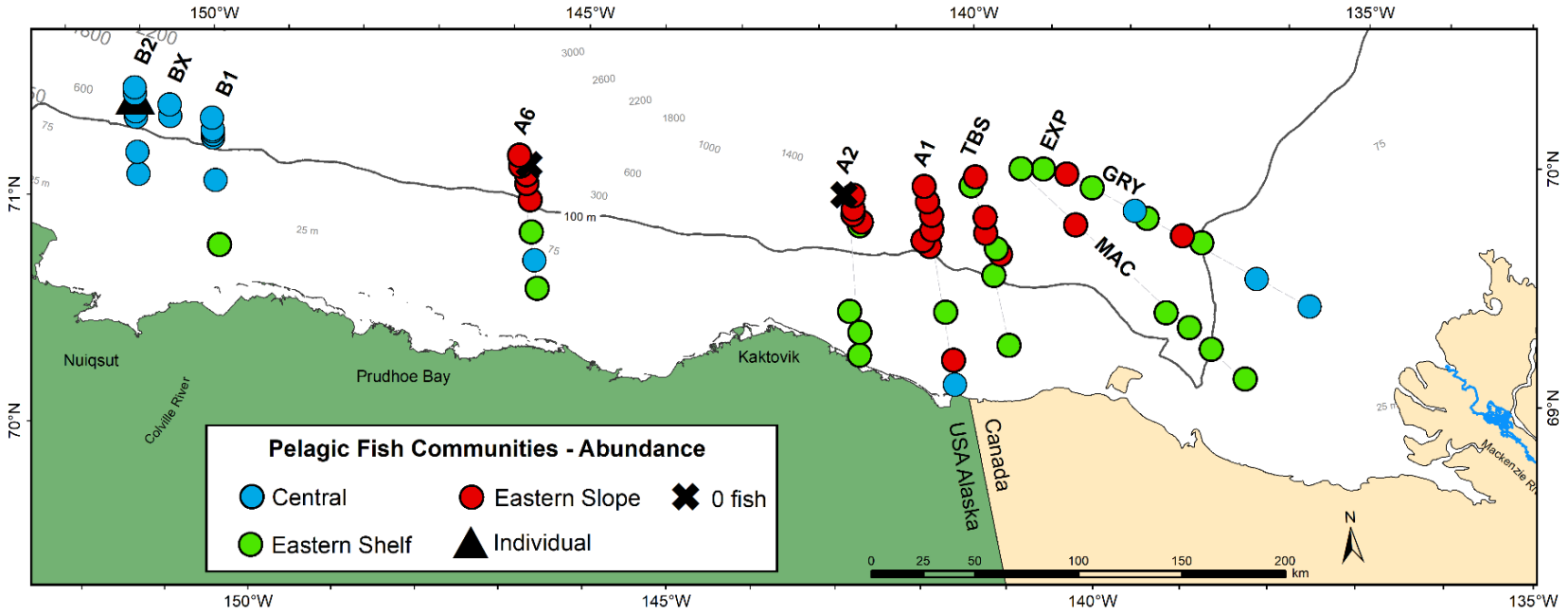

Figure 7.3.3.7. Map of pelagic fish communities defined using fourth-root transformed (4RT) abundance data based on clusters in Figure 7.3.3.6. Catches by Isaacs-Kidd midwater trawl (IKMT) in the Beaufort Sea during 2012–2013.

Table 7.3.3.1. Pelagic fish community composition as defined by abundance (fourth-root transformed) in 2012–2013 Isaacs-Kidd midwater trawl (IKMT) hauls.
Percent contribution of taxa density to each of four fish communities (p <0.005) and mean similarity of taxon density within community. Only taxa selected by SIMPER as descriptive of 70% of the community are included here. The distribution of communities is presented visually in Figure 7.3.3.7.

	Fish Communities			
	Central	Eastern Shelf	Eastern Slope	B2-350
Taxa # Stations	19	21	23	1
Gadidae				
Boreogadus saida	36.27	54.70	94.52	50.00
Cottidae				
Myoxocephalus scorpius				16.67
Agonidae				
Aspidophoroides olrikii				16.67
Liparidae				
Liparis spp. unid	24.48	28.59		
Stichaeidae				
Lumpeninae unid.	21.58			
Pleuronectidae larvae				16.67
Total % Contributed	82.33	83.29	94.52	100.00
Within Community Similarity	59.32	61.13	67.12	100.00

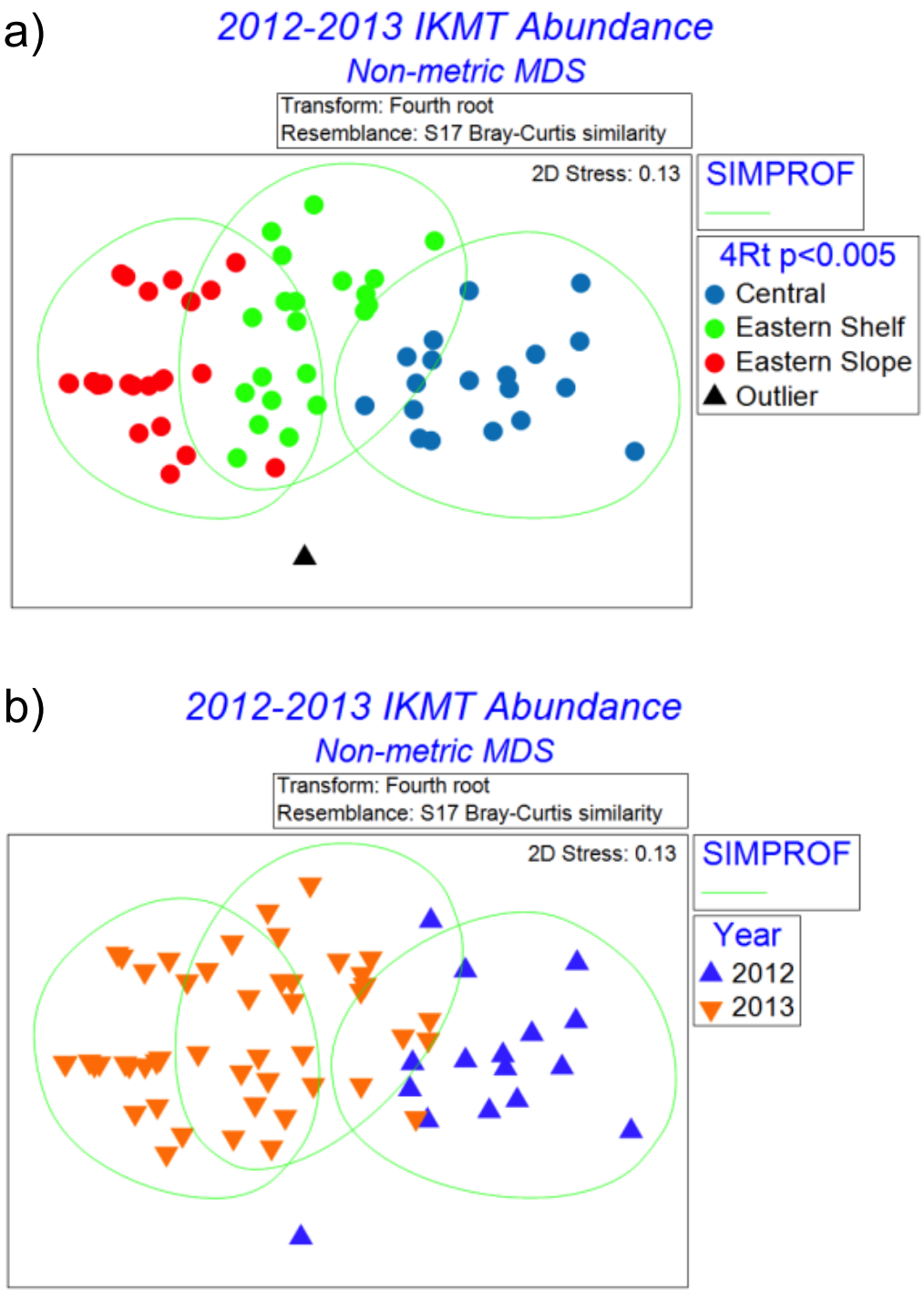

Figure 7.3.3.8. nMDS ordination of pelagic fish communities defined using Isaacs-Kidd midwater trawl (IKMT) abundance. Ellipses are significantly different clusters of stations (p <0.005); a) communities and b) year. Stations at which no fish were collected, A2-1000 and A6-750, were not included.

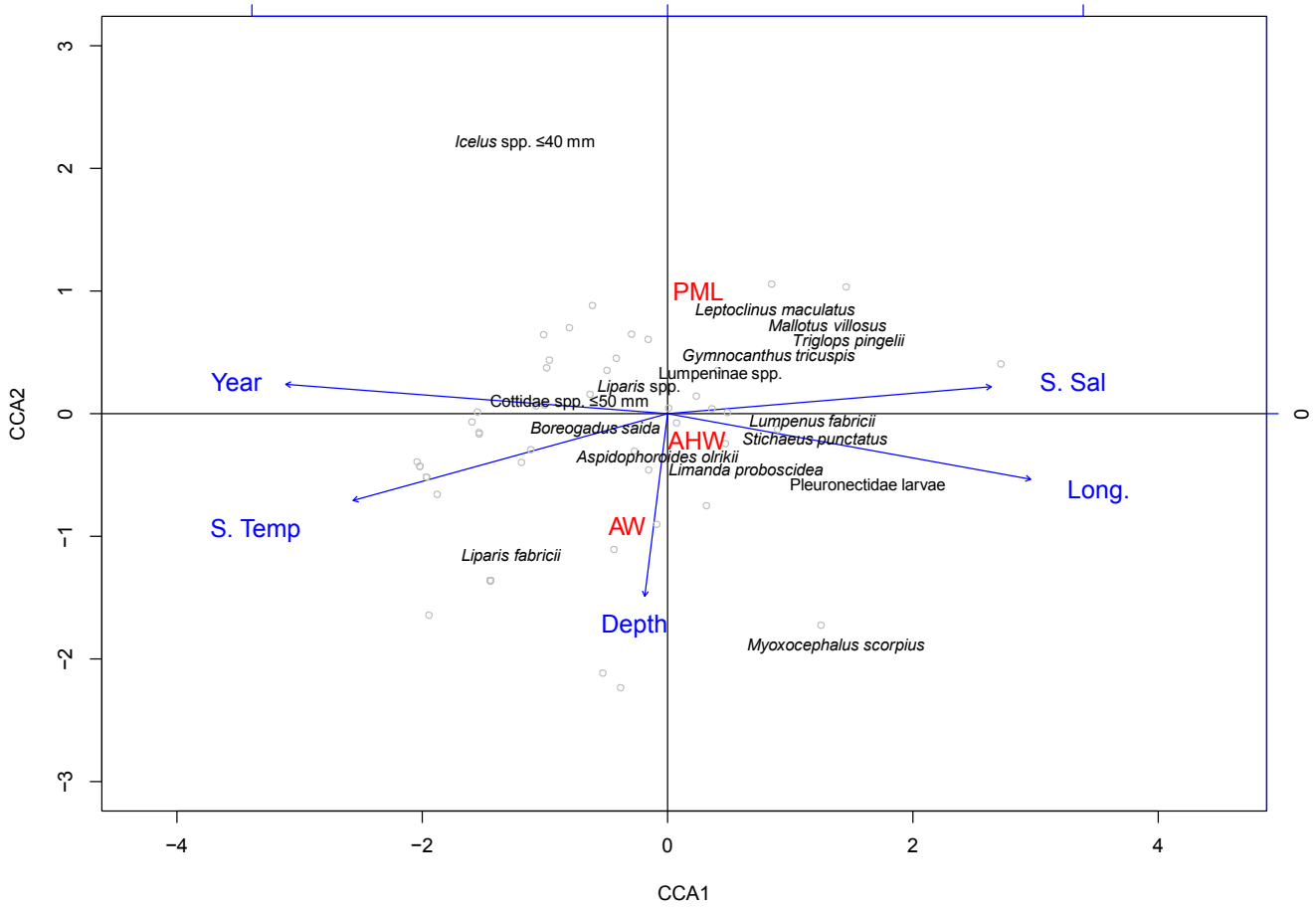

Figure 7.3.3.9. Canonical correspondence analysis (CCA) ordination relating pelagic fish abundance during 2012 and 2013 to selected environmental variables.
Continuous environmental variables (blue) denoted by vectors are haul depth (Depth), surface salinity (S.Sal), surface temperature (S.Temp), and longitude. Categorical variables (red) are water masses): PML – Polar Mixed Layer, AHW – Arctic Halocline Water, AW – Atlantic Water. Grey open circles are stations. Fish taxa (black) are descriptive of 90% of the five communities (Table 7.3.3.1).

Table 7.3.3.2. Mean abundance (± standard deviation) (per 1000 m^{-3}) of pelagic fishes caught by Isaacs-Kidd midwater trawl (IKMT) in the Central region (2012) and on the Eastern Shelf (≤100 m) and Eastern Slope (≥200 m) in 2013.

	2012 Central mean ± SD	2013 Shelf mean ± SD	2013 Slope mean ± SD
OSMERIDAE (smelts)			
Mallotus catervarius	0.1 ± 0.2	0	0
GADIDAE (cods)			
Boreogadus saida	5.6 ± 7.5	3.2 ± 3.7	0.6 ± 0.7
AGONIDAE (poachers)			
Aspidophoroides olrikii	0.6 ± 0.9	0.1 ± 0.2	<0.1 ± <0.1
COTTIDAE (sculpins)			
Gymnocanthus tricuspis	0.5 ± 0.8	0.1 ± 0.2	<0.1 ± <0.1
Icelus spp. ≤40 mm	0	0.1 ± 0.3	0
Myoxocephalus scorpius	<0.1 ± <0.1	0	0
Triglops pingelii	<0.1 ± 0.1	<0.1 ± 0.1	0
Cottidae unid. ≤50 mm	0.2 ± 0.4	0.4 ± 0.6	<0.1 ± <0.1
LIPARIDAE (snailfishes)			
Liparis fabricii	0	0	<0.1 ± <0.1
Liparis spp. unid. ≤50 mm	0.9 ± 1.0	0.7 ± 1.0	<0.1 ± 0.1
Liparis spp. unid. 51-140 mm	<0.1 ± <0.1	0	0
STICHAEIDAE (pricklebacks)			
Leptoclinus maculatus	0.1 ± 0.3	0	0
Lumpeninae unid. ≤51 mm	5.6 ± 12.5	0.5 ± 1.0	<0.1 ± <0.1
Lumpeninae unid. 53-67 mm	0.1 ± 0.2	0	0
Lumpenus fabricii	1.9 ± 4.0	0	0
Stichaeus punctatus	0.1 ± 0.2	0	0
PLEURONECTIDAE (righteye flounders)			
Limanda proboscidea	<0.1 ± <0.1	0	0
Pleuronectidae larvae	<0.1 ± 0.1	0	0
ALL TAXA	15.5 ± 22.9	5.0 ± 4.4	0.7 ± 0.8

Table 7.3.3.3. Effects of year, depth and longitude on pelagic fish abundance (4RT) community composition in 2012–2013 Isaacs-Kidd midwater trawl (IKMT) hauls in the Beaufort Sea.
* denotes p <0.05; ** denotes p <0.01; other test was not significant.

	One-Way ANOSIM	Two-Way Crossed ANOSIM	
	R (Year)	R (Longitude)	R (Maximum Gear Depth)
Pelagic Fish Abundance	**0.524	*0.239	0.008

Table 7.3.3.4. Canonical correspondence analysis abundance (4RT) of pelagic fishes captured by Isaacs-Kidd midwater trawl (IKMT) and environmental (normalized) variables in the Beaufort Sea in 2012 and 2013.
The F statistic, significance (<0.05 is bold), and axis correlation (i.e., CCA1 and CCA2) of each continuous explanatory variable is listed. The cumulative percent variance explained by the first two CCA axes is listed underneath.

	F	*p*	CCA1	CCA2
Depth	2.287	0.119	-0.045	-0.324
Longitude	2.214	0.108	0.719	-0.116
Year	1.599	0.352	-0.755	0.052
Surface Temp	1.261	0.637	-0.622	-0.154
Surface Salinity	1.917	0.195	0.640	0.048
Water Mass	2.396	**0.029**		
Cumulative %			11.37	6.21
Total %	2.575	**0.001**		25.74

Table 7.3.3.5. BEST (stepwise) relationship of pelagic fishes caught by Isaacs-Kidd midwater trawl (IKMT) and environmental variables in the Beaufort Sea in 2012 and 2013.
Measure of effort for fish is abundance, and data were fourth-root transformed (4RT). Variables considered include: year, longitude, bottom depth, maximum gear depth, surface temperature, and surface salinity. N = 62 samples for which Isaacs-Kidd midwater trawl (IKMT) and environmental variables were available.

# Variables	Rho	Variables
1	0.439	Year
2	0.405	Year, Maximum Gear Depth
3	0.430	Year, Maximum Gear Depth, Longitude
4	0.430	Year, Maximum Gear Depth, Longitude, Surface Temperature

7.3.4 Demersal Fishes – Bottom Assemblages

7.3.4.1 Taxonomic Diversity of Bottom Catches

A total of 49 unique fish taxa were captured in 2012–2014 at stations where beam trawl gear was deployed. *Boreogadus saida* was the most abundant taxa and was captured at 87.5% of stations. *B. saida* drove overall patterns in fish abundance throughout the sampling regions, including the one very large catch at the western-most shallow station that overshadowed all other catches (Figure 7.3.4.1). There were as many as eight taxa captured at the 1000 m stations in the central Beaufort Sea west of 150° W (B transects) during 2012, with twice as many taxa at shallower stations (Figure 7.3.4.2). Almost all of the hauls in that area caught 7–15 taxa; a total of 38 unique taxa were captured in the Colville River area (B transects). Arctic Alligatorfish (*Aspidophoroides olrikii*) and Arctic Staghorn Sculpin (*Gymnocanthus tricuspis*) were captured at about half of the 16 central stations. There were fewer taxa captured at the Camden Bay (A6, A5, and A4) and eastern stations (A2, A1, and TBS), with as few as 1 and as many as 10. Similarly, at the Mackenzie River stations (MAC and GRY transects, east of 140° W) there were 3–10 taxa captured. There, *B. saida*, *Anisarchus medius* (Stout Eelblenny), and *A. olrikii* were most abundant, while *B. saida, Lycodes* spp., and *T. pingelii* (Ribbed Sculpin) were present at the most stations. Taxa richness was relatively high throughout much of the study area (Figure 7.3.4.3). Moving west to east, high taxa richness (Margalef) values were found along the B1 transect off the Colville River, along the Camden Bay A6 transect, the eastern A2, A1, and TBS transects, and the Mackenzie River GRY transect (Figure 7.3.4.3). As with pelagic fishes, the highest values of evenness (Pielou's) indices were in the eastern Beaufort Sea at transects east of 150° W. Evenness was high at stations <100 m at transect A6 and >100 m at the eastern and Mackenzie stations (Figure 7.3.4.4). As with the other indices, there was not a distinct east-west or shelf-slope pattern to Simpson's diversity indices (Figure 7.3.4.5). The combination of richness, evenness, and diversity showed that the central Beaufort Sea had more demersal taxa, though not evenly distributed. That resulted in stations ranging in diversity from low through high, without an aggregation pattern. In contrast, transect A6 in Camden Bay was unique with high richness, evenness, and diversity at station <200 m depth. Transect A4 had the lowest richness of any transect and, together with high evenness, resulted in moderate diversity. The eastern Beaufort Sea had richness, evenness, and diversity indices that ranged from low to high, but they did not form any patterns. The Mackenzie River stations had very few taxa, though there was high richness at one GRY station. Evenness and diversity were moderate to high at most stations, except three of the four GRY stations from the shelf break shoreward.

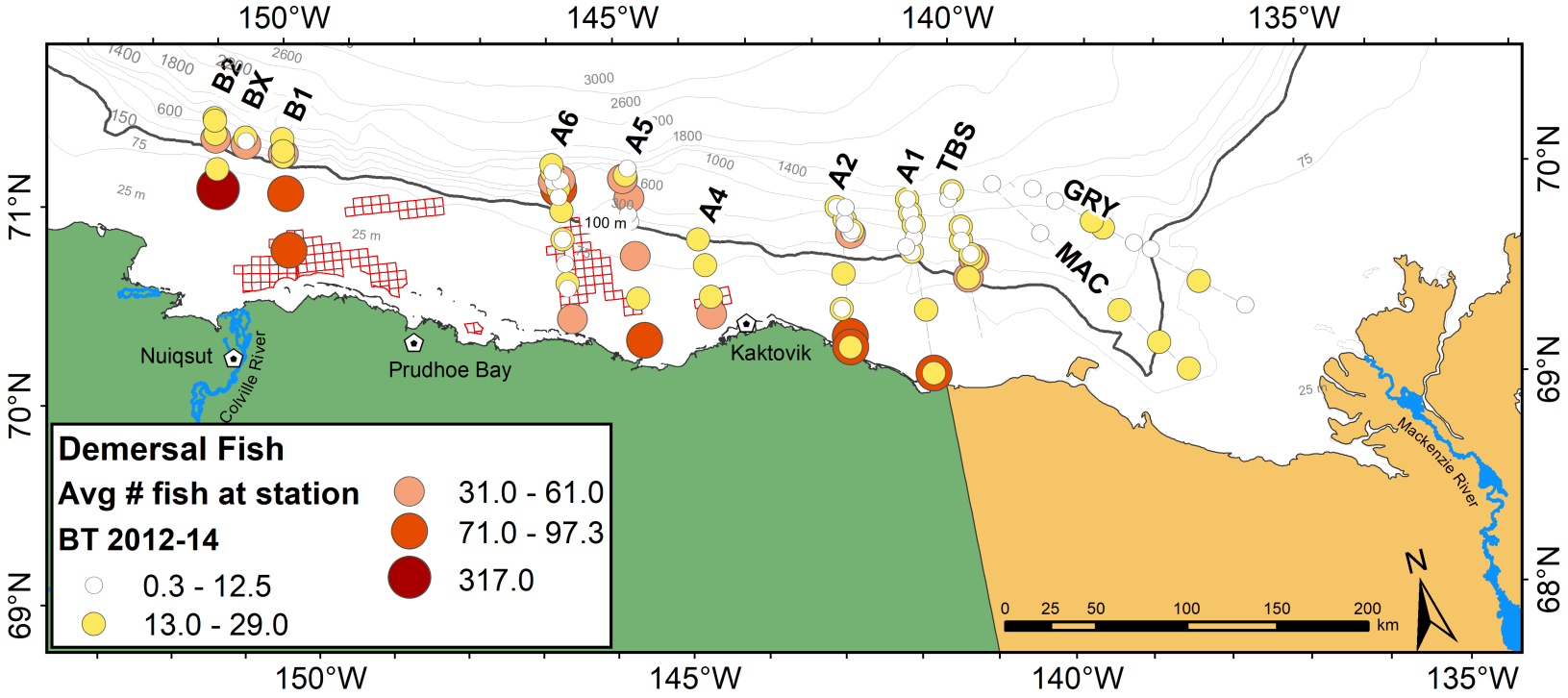

Figure 7.3.4.1. Average number of demersal fishes collected at each station by beam trawl in the Beaufort Sea during 2012–2014. Catch is not adjusted for effort.

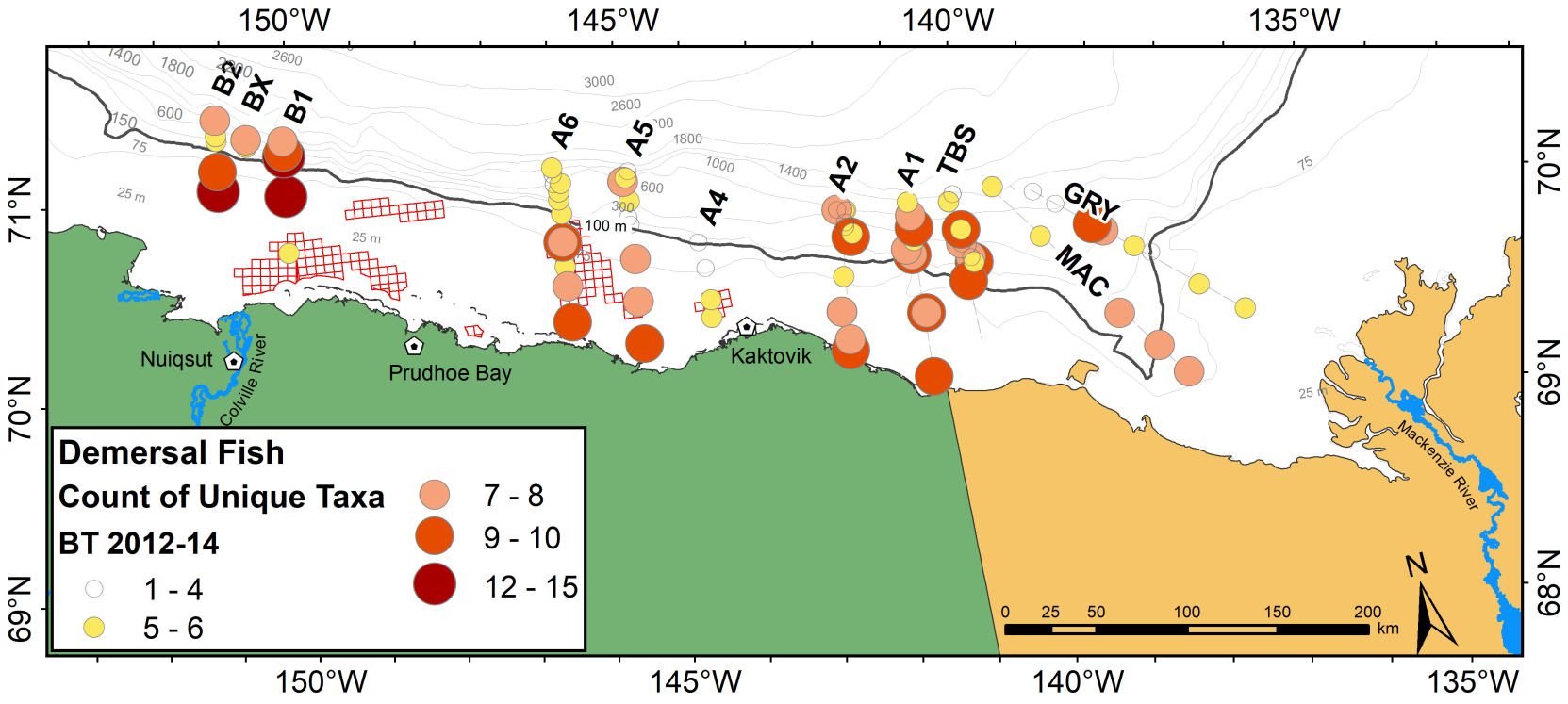

Figure 7.3.4.2. Number of unique demersal fish taxa captured by beam trawl at each station in the Beaufort Sea during 2012–2014. All quantitative hauls from the station in a single year are combined.

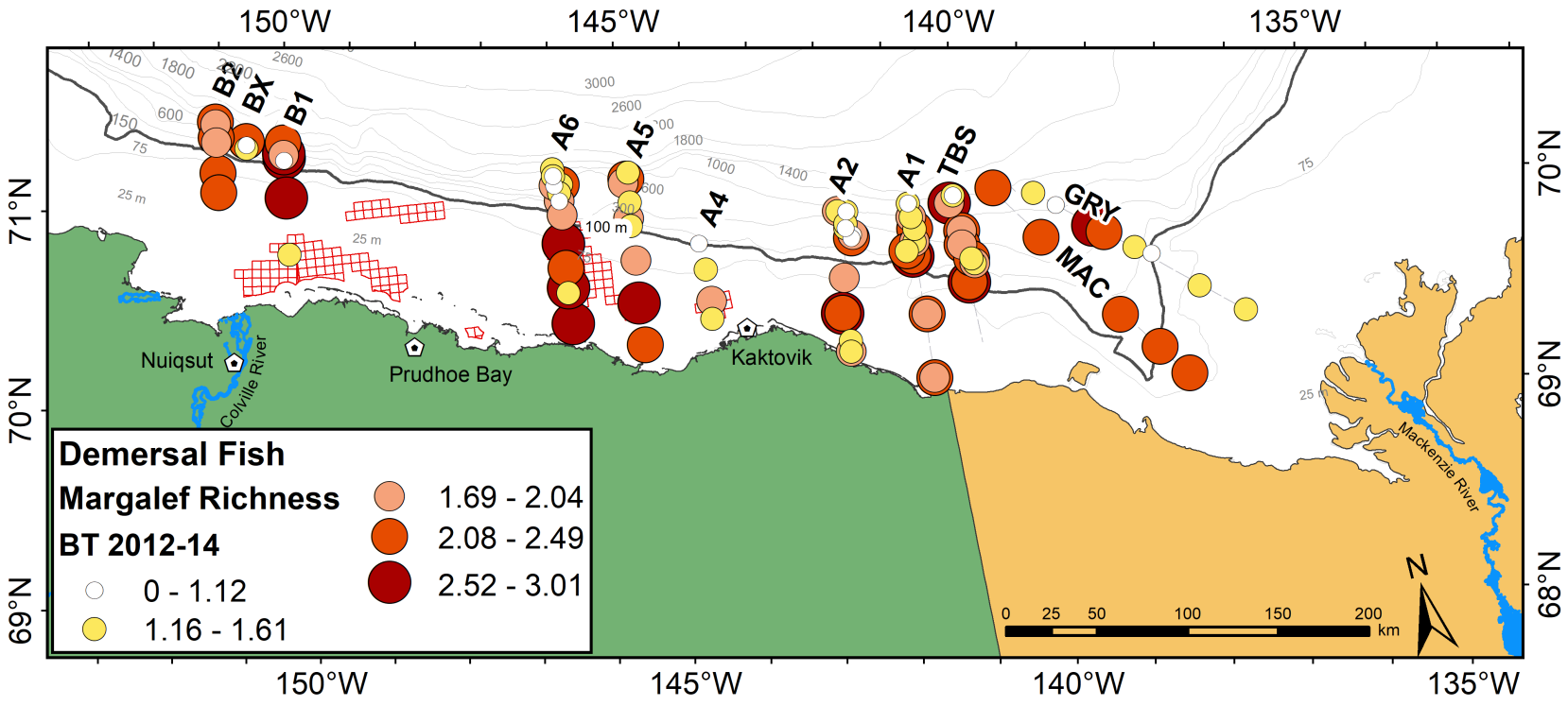

Figure 7.3.4.3. Demersal fish species richness (Margalef index) at each station in the Beaufort Sea during 2012–2014 for beam trawl.

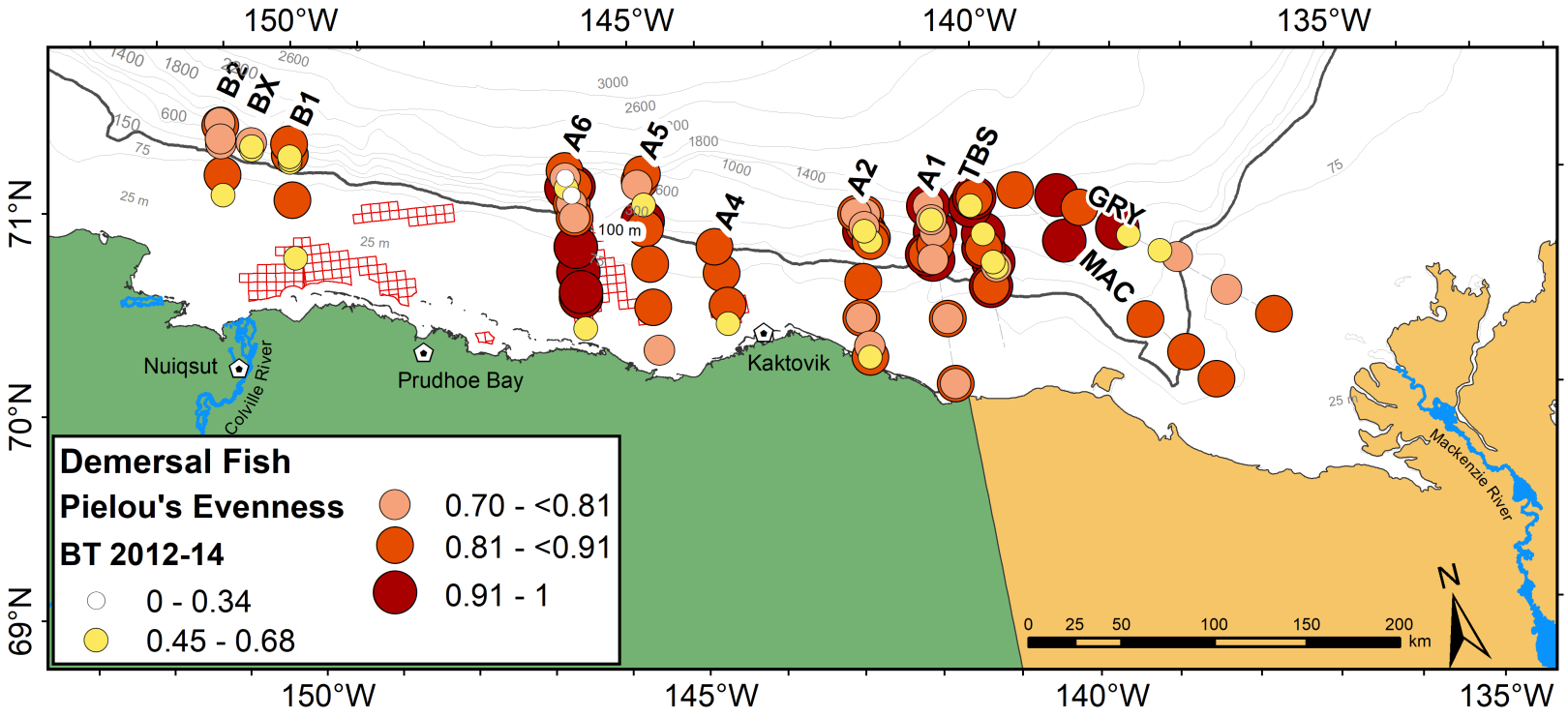

Figure 7.3.4.4. Demersal fish species evenness (Pielou's index) at each station in the Beaufort Sea during 2012–2014 for beam trawl.

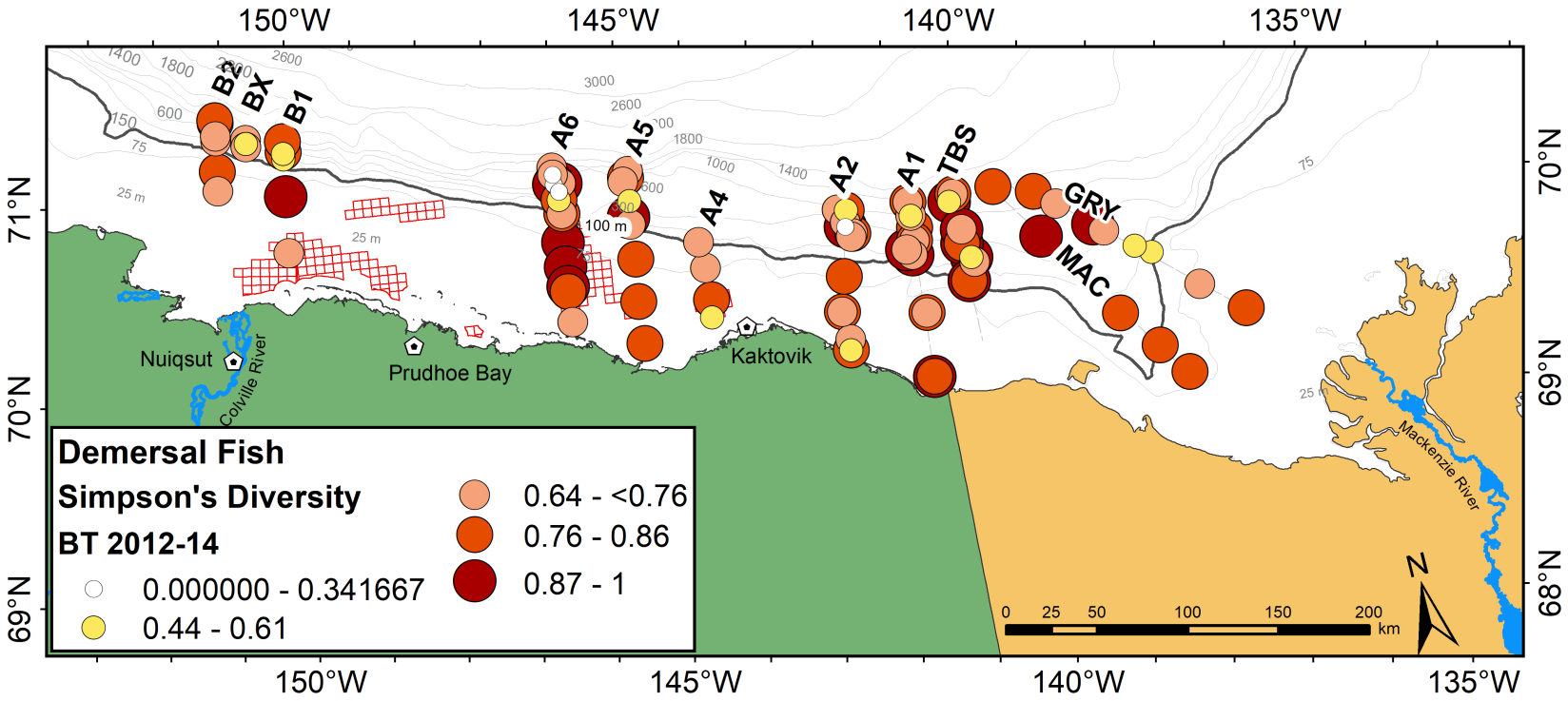

Figure 7.3.4.5. Demersal fish diversity (Simpson's index) at each station in the Beaufort Sea during 2012–2014 for beam trawl.

7.3.4.2 Small Scale Similarities

Repeated sampling at the same stations controlled for day, location, depth, temperature, salinity, and water mass. Fish community structure for replicate PSBT-A hauls taken at transect A1 from 20 to 1000 m in 2014 was similar for both biomass and abundance. Within a station there was no significant difference among replicates for biomass (p <0.05) or abundance (p <0.005). Almost all within-station hauls clustered more closely together than between-station hauls (Figure 7.3.4.6). There was a depth pattern observed; 20–100 m samples on the shelf grouped separately from 200–1000 m samples on the slope. At 20 m, abundance, but not biomass, was significantly higher than at 50–100 m.

Statistical comparisons of replicate hauls within depth stratum showed markedly similar fish communities assessed both as biomass and as abundance. For the three replicate hauls taken at each depth in 2014, biomass similarity ranged from 42.8% at 200 m to 86.8% at 1000 m (Table 7.3.4.1). The lowest similarities were at the shelf break, i.e., 100 m and 200 m. Similarities of abundance were equally impressive with a similar range, again with the lowest value (49.86) at 200 m. Overall patterns were the same for biomass and abundance, i.e., 61–77% similarity of fishes at 20 and 50 m, down to 43–57% similarity at 100 and 200 m, then increasing at 350 to 1000 m to similarities equal to or higher (up to 87%) than at the shallow stations.

PSBT-A and CBT sampling efforts were considered equivalent because the gear dimensions were similar and fishing methods were identical. No significant differences were found between the two beam trawls for catch abundance, species composition, or length of fish. Depth was found to be a significant factor (p <0.05) in the relative abundance of fish species and sizes classes captured (Table 7.3.4.2) There was a difference in depth that was not affected by gear type, which is explored further through additional analyses below.

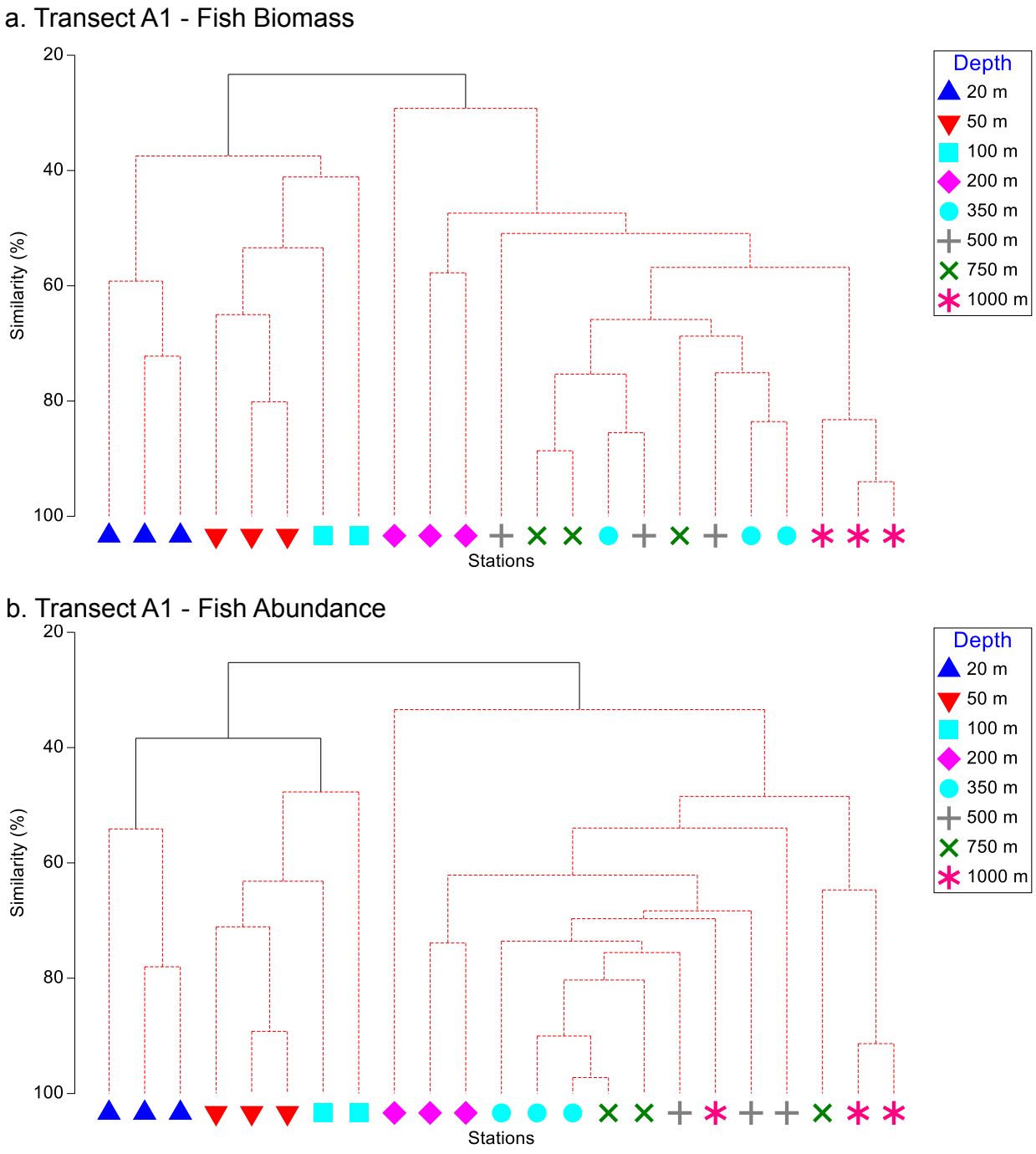

Figure 7.3.4.6. Community structure of demersal fishes in replicate beam trawl hauls along depth strata of Transect A1 sampled in 2014 by biomass (upper) and abundance (lower).
Red lines indicate non-significant differences among hauls, and black lines indicate differences between station groups of p >0.05 for biomass and p >0.005 for abundance.

Table 7.3.4.1. Percent similarity of demersal fish community composition within stations along transect A1 from replicate trawls within 2014 and between replicate trawls in 2013 and 2014 at the same station, based on biomass and abundance. Data were fourth-root transformed (4RT).

	Biomass % Similarity		Abundance % Similarity	
Transect-Depth	Replicates within 2014	Replicates between 2013 and 2014	Replicates within 2014	Replicates between 2013 and 2014
A1-20	63.53	not calc	62.09	not calc
A1-50	70.04	49.71	77.13	48.40
A1-100	45.51	55.60	57.49	59.94
A1-200	42.75	42.20	49.86	51.31
A1-350	78.37	80.02	83.85	75.24
A1-500	60.64	51.56	55.67	47.83
A1-750	65.84	67.07	68.64	69.19
A1-1000	86.83	70.38	72.78	64.37

Table 7.3.4.2. PERMANOVA comparisons of relative abundance of demersal fish species and size classes among beam trawl gears (PSBT-A and CBT), depths (20–1000 m), and transects (A2, A1, TBS, GRY).
Significant results are in bold.

Source	df	Pseudo-F	P(perm)
Gear	1	1.5464	0.463
Transect	5	1.5804	0.262
Depth	**8**	**3.7698**	**0.01**
Gear x Transect	5	1.0088	0.617
Gear x Depth	8	1.0709	0.539
Transect x Depth	31	1.363	0.091
Gear x Transect x Depth	22	1.0509	0.482

7.3.4.3 Interannual Analysis

As we showed PSBT-A and CBT trawls were equivalent (Section 7.3.4.2), the data from the 2013 CBT were combined with the 2014 haul data to examine small-scale interannual differences within transect A1. Combining replicate hauls at the same stations on transect A1 over 2013 and 2014 revealed high similarity of fishes within a station (Table 7.3.4.1) without lowered similarities when 2013 and 2014 data were combined. For biomass, similarities within a station slightly increased or decreased compared to 2014 alone. For abundance, the 2013–2014 similarity value at 200 m was almost the same as for 2014 alone; similarity was similar at other depths. The biggest change when adding the 2013 catches to the 2014 catches was that the similarity of both fish community biomass and abundance decreased at 50 m. The similarities between community compositions defined at a station by fish biomass and abundance were not consistently higher within 2014 than when 2013 and 2014 were combined.

To examine interannual variability across a larger scale, date from transects A6, A2, A1, and TBS were combined for both 2013 and 2014. Biomass was twice as high at deep (>200 m) slope stations in 2013 than in 2014 (Figure 7.3.4.7); whereas, abundance of fishes was approximately the same at replicate deep stations in 2013 than in 2014 (Figure 7.3.4.8). Biomass and abundance were about the same in 2013 and 2014 at 50 and 100 m, but both were up to five times higher at 20 m in 2014. There was no statistical effect of year on total biomass or abundance as all ANOSIM R values were near zero (Table 7.3.4.3). There was clearly no separation between years for biomass (Figure 7.3.4.9) or for abundance (Figure 7.3.4.10) in 4RT nMDS plots. Likewise, transect (as proxy for longitude) did not have an effect on fish biomass or abundance (Table 7.3.4.3). However, depth had an equally significant effect (p <0.01) on both biomass and abundance of fish catches for all transformations (Table 7.3.4.3). The Beaufort Sea shelf break is considered to be at 100 m (Brugler et al. 2014, Thorsteinson and Love 2016); nMDS plots of combined 2013 and 2014 fish biomass (Figure 7.3.4.11) and abundance (Figure 7.3.4.12) show distinct separations between shelf and slope fish communities. There was if there was an effect of type of transformation on interpretation of fish communities and statistical analyses fish for any data transformation showed. Matrices of station clusters (x-axis) by taxa clusters (y-axis) (Shade plots) showed the same patterns and did not support the need for multiple transformations for analyses. Therefore, all subsequent analyses of fish communities in this report are conducted on 4RT data because it offers the best compromise between de-emphasis of abundant taxa (no transformation) and emphasis of non-abundant taxa (presence).

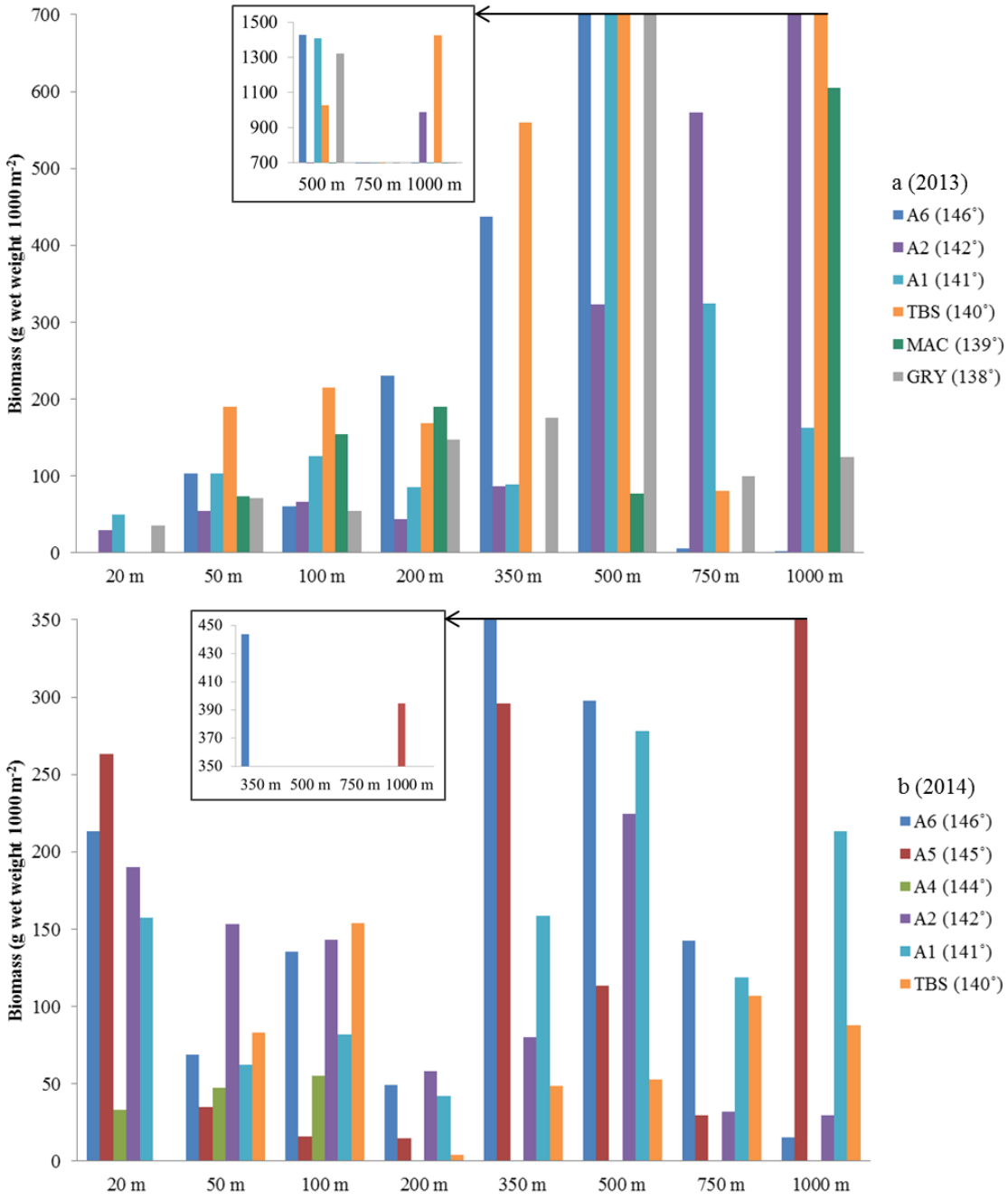

Figure 7.3.4.7. Biomass (g 1000 m^{-2}) of demersal fishes captured by beam trawl during Transboundary 2013 and 2014, by depth and transect.
Note that the scale of the y-axis in (a) 2013 is twice that of (b) 2014, and the inset is four times higher. Identical transects were not sampled each year. Interannual comparisons can be made for transects A6, A2, A1 and TBS.

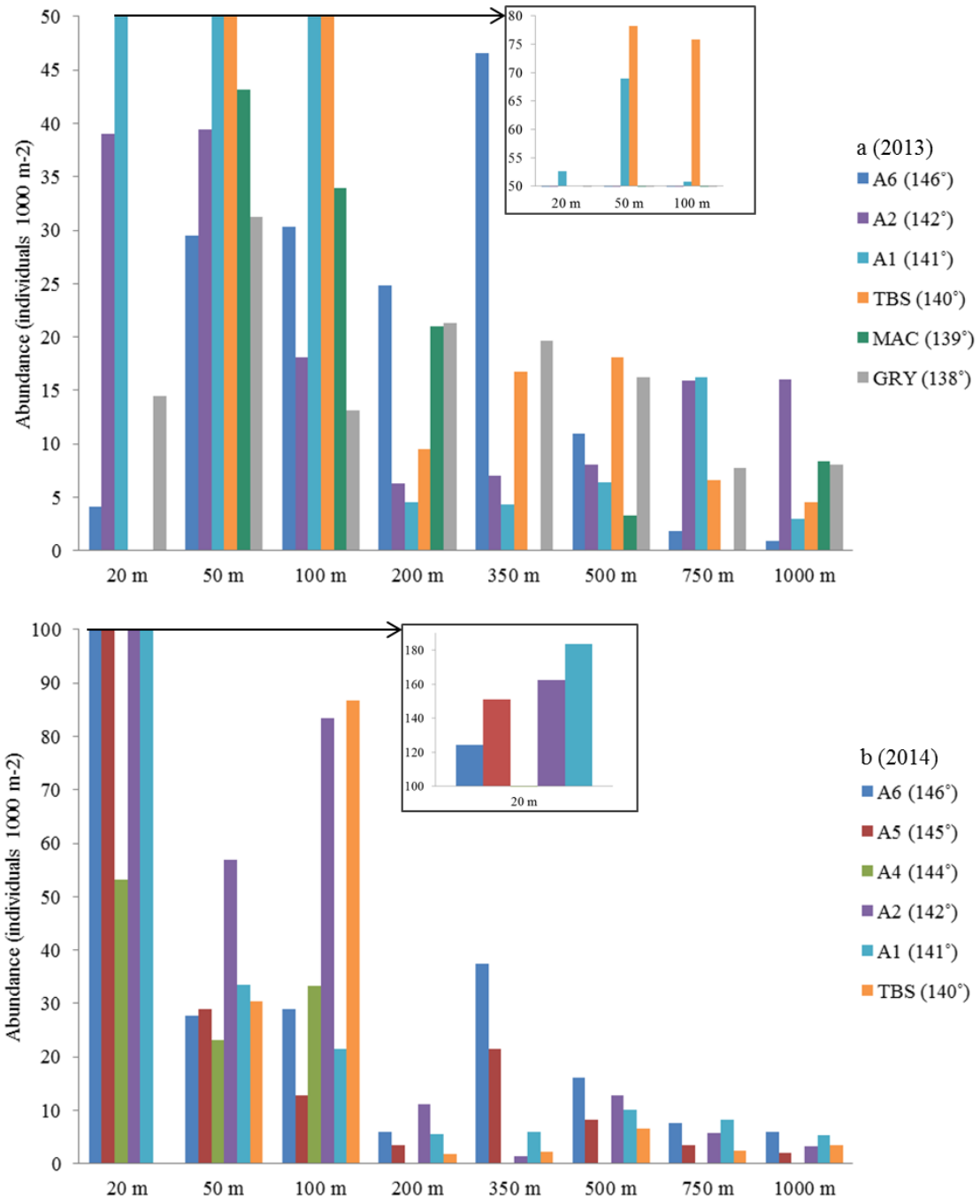

Figure 7.3.4.8. Abundance (number 1000 m^{-2}) of demersal fishes captured by beam trawl during Transboundary 2013 and 2014, by depth and transect.
Note that scale of the y-axis in (a) 2013 is half that of (b) 2014. Identical transects were not sampled each year. Interannual comparisons can be made for transects A6, A2, A1 and TBS.

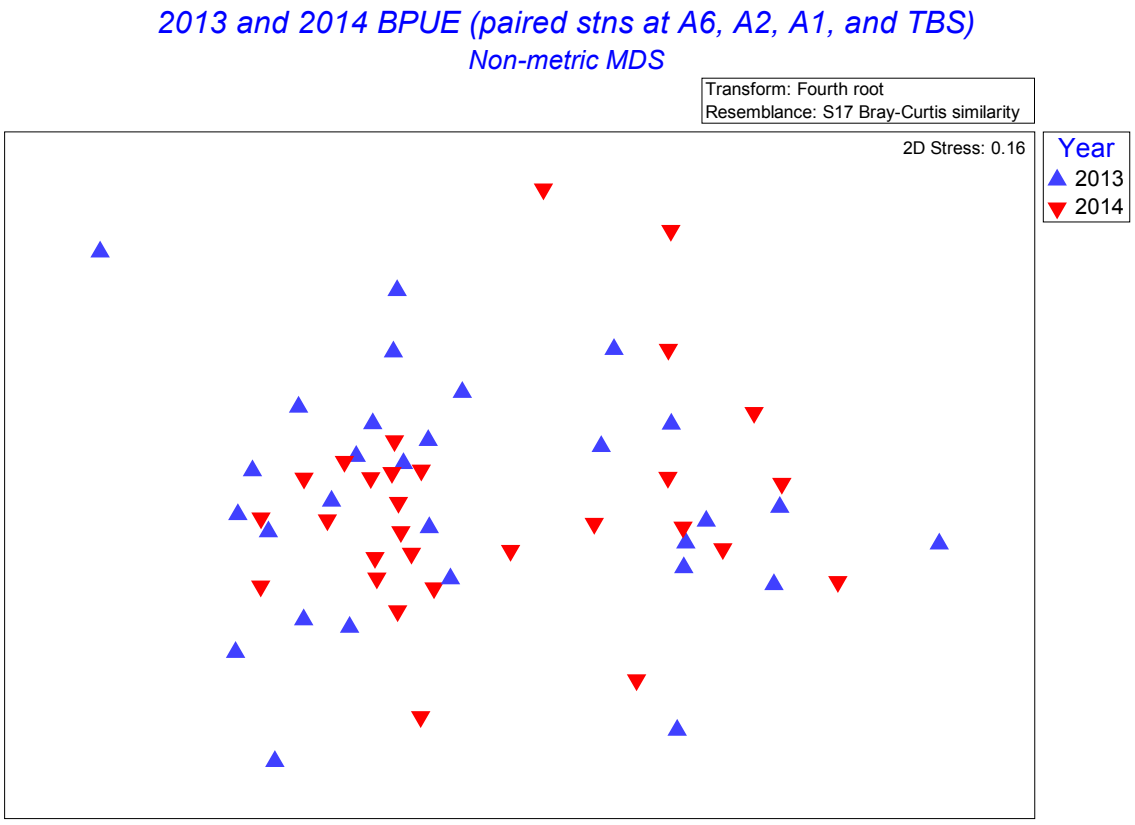

Figure 7.3.4.9. Demersal fish biomass community structure in 2013 and 2014 at transects A6, A2, A1 and TBS displayed in nMDS.

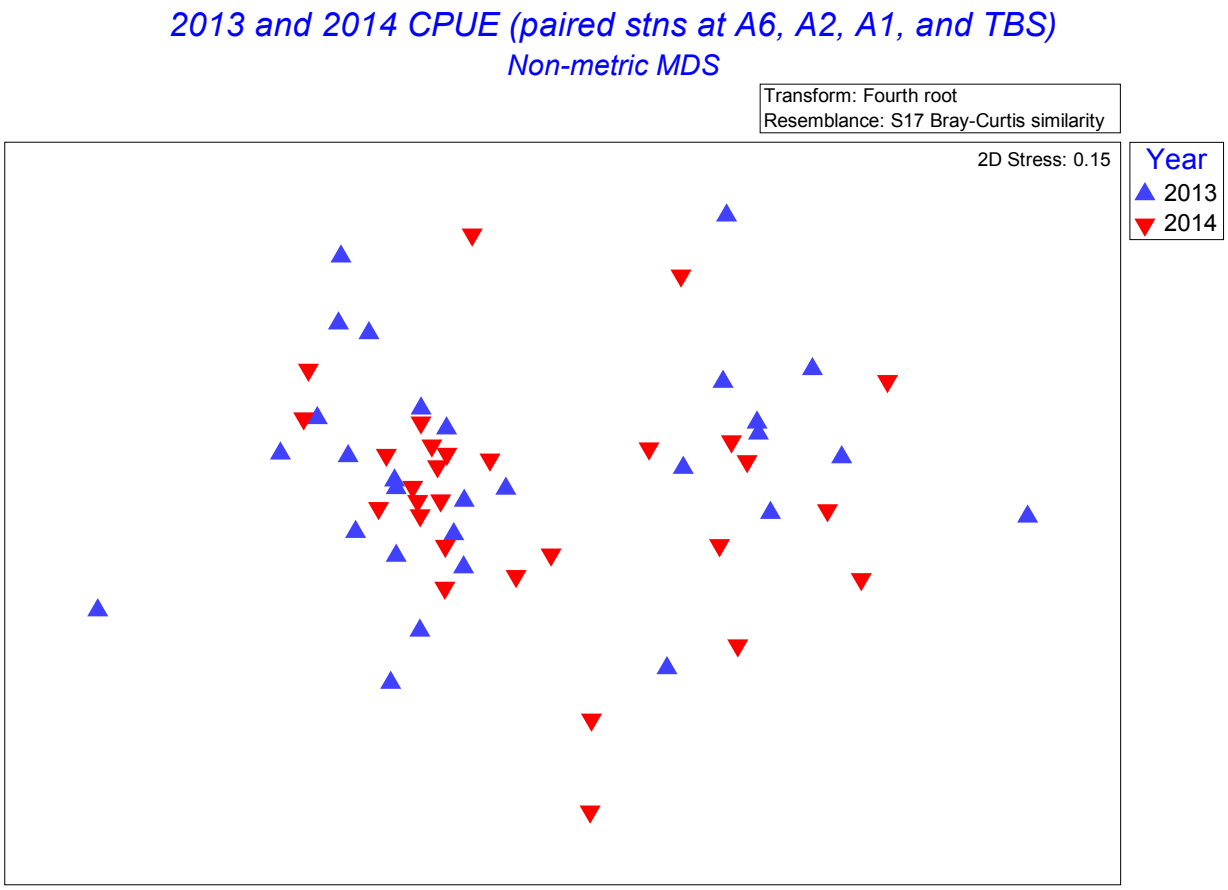

Figure 7.3.4.10. Demersal fish abundance (number fish 1000 m^{-2}) community structure in 2013 and 2014 at transects A6, A2, A1 and TBS displayed in nMDS.

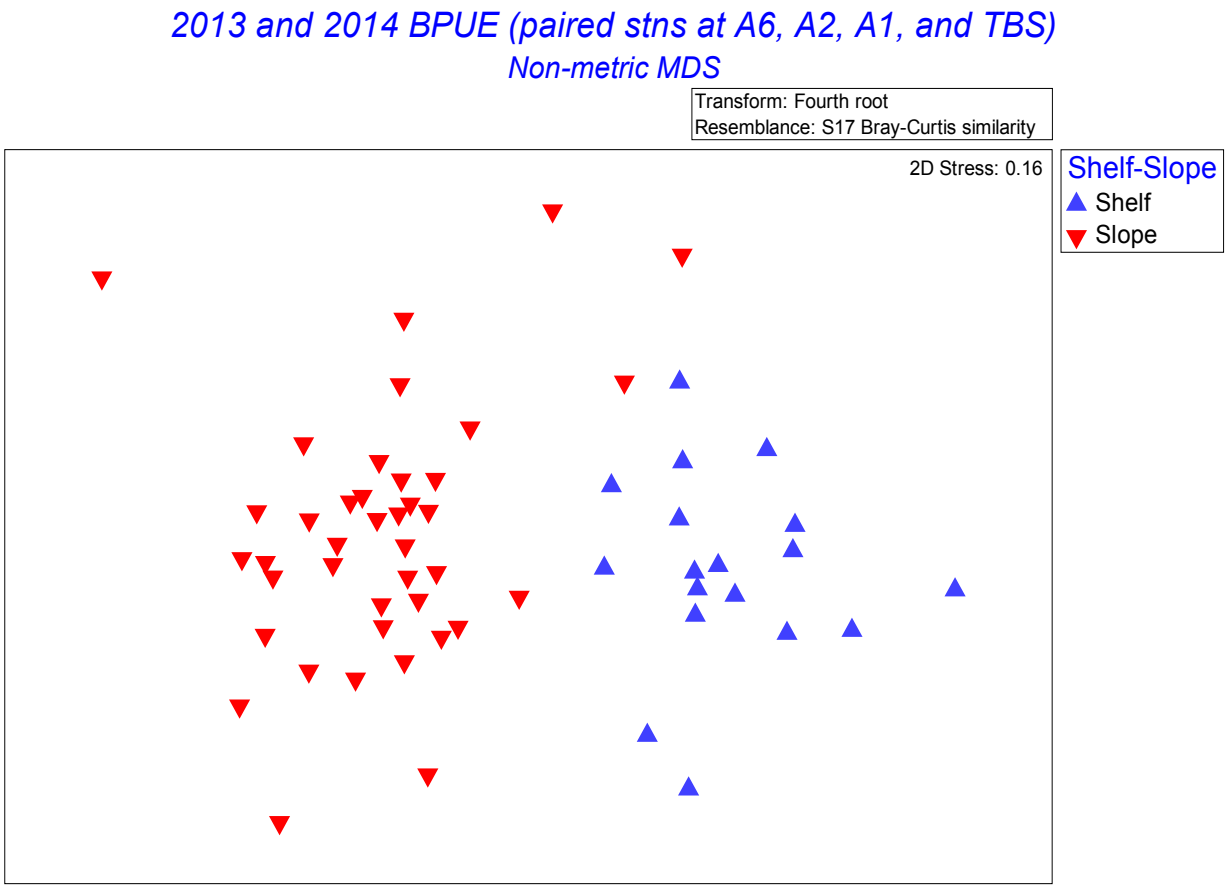

Figure 7.3.4.11. Demersal fish biomass (gms fish 1000 m^{-2}) community structure in 2013 and 2014 at transects A6, A2, A1 and TBS displayed in nMDS. Shelf (10–100 m), slope (200–1000 m).

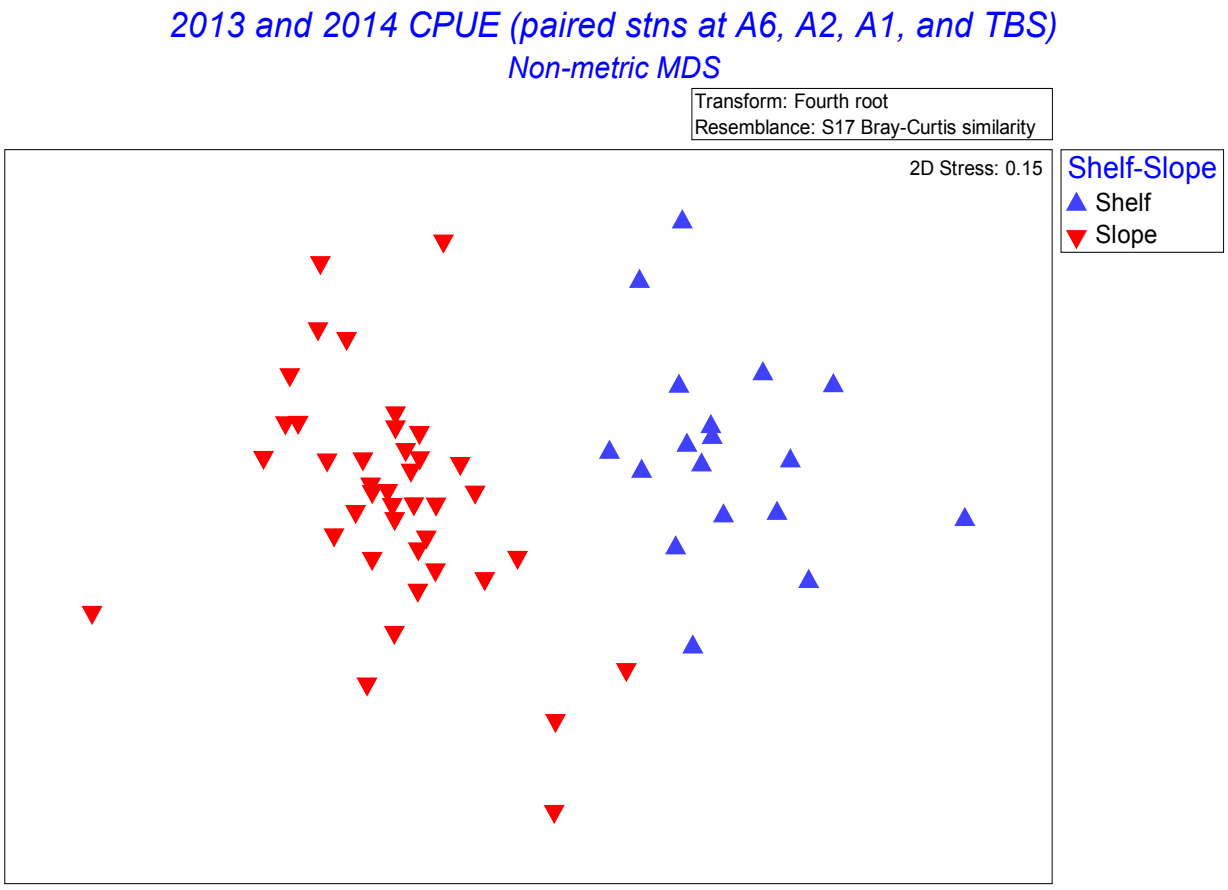

Figure 7.3.4.12. Demersal fish abundance (# fish 1000 m^{-2}) community structure on shelf and slope in 2013 and 2014 at transects A6, A2, A1 and TBS displayed in nMDS. Shelf (10–100 m), slope (200–1000 m).

Table 7.3.4.3. Effects of year, depth and transect/longitude on demersal fish biomass and abundance community composition in 2013 and 2014.
*R denotes p <0.01. All others were not significant.

Biomass			
	1-way ANOSIM	2-way crossed ANOSIM	
Transformation	R (Year)	R (Depth)	R (Transect)
NT	0.049	*0.58	-0.087
2RT	0.031	*0.623	-0.022
4RT	0.012	*0.641	0.044
Log(x+1)	0.012	*0.641	0.049
PA	-0.005	*0.559	0.046

Abundance			
	1-way ANOSIM	2-way crossed ANOSIM	
Transformation	R (Year)	R (Depth)	R (Transect)
NT	-0.005	*0.633	0.048
2RT	-0.004	*0.658	0.072
4RT	-0.004	*0.633	0.113
Log(x+1)	-0.003	*0.657	0.077
PA	-0.005	*0.559	0.046

7.3.4.4 Demersal Assemblages–Catch Per Unit Effort 2013–2014

Beam trawls were successfully deployed at all stations in the Transboundary region along the A and Canadian transects (146.0º–136.7º W) in 2013 and 2014. Interannual analysis of these data was presented in Section 7.3.4.3. Here, we include community analysis for all stations, not just stations sampled in both years and used for interannual comparisons. Analysis was of both PSBT-A and CBT catches averaged at each station. Fishing capabilities were equivalent in both years; therefore, per-unit-effort could be calculated for biomass (BPUE) and abundance (CPUE). Fish biomass and abundance patterns were different from each other (Figure 7.3.4.13) but somewhat similar between years. Biomass was highest at stations ≥500 m in 2013 and 2014 (Figure 7.3.4.7). The average biomass of fish at depth was greater at deep stations in 2013 than in 2014. Average biomass in 2013 was >500 g 1000 m^{-2} at 500 m and 1000 m stations. In 2014, biomass at all stations and depths was much smaller.

In contrast, abundance patterns were similar between years (Figure 7.3.4.8), with abundance was highest at depths ≤100 m both years and higher in 2014 than in 2013. There was a clear pattern of higher abundance of fishes on the shelf (≤100 m) than on the slope (≥200 m). Gadidae, Cottidae, Agonidae, and Stichaeidae were all abundant enough in both 2013 and 2014 to have an average CPUE in single or double digits on the shelf (Table 7.3.4.4). *Boreogadus saida* was the only taxa whose CPUE was higher than 2.0 1000 m^{-2} on the slope. Zoarcidae was the most speciose family, with 14 species (8 on the shelf and 12 on the slope). However, only two species on the shelf (*Gymnelus hemifasciatus* and *Lycodes polaris*) and two on the shelf (*L. sagittarius* and *L. seminudus*) had CPUE values >1.0.

In 2013, the cluster patterns of stations for both biomass and abundance clearly separated at the shelf break (at depths greater than 200 m) to form shelf (≤100 m target depth) and slope (>200 target depth) communities (Figures 7.3.4.14–16). Abundance had one additional three-station coastal community at the 10–20 m stations. Station A6-1000 was significantly distinct from the other shelf and slope clusters, i.e., it did not group with other sites by biomass or abundance (Figure 7.3.4.14). It was also unique because only *Liparis fabricii* was collected at that site. Assemblages of fish had different biomass and abundance patterns on the shelf than on the slope. *Boreogadus saida* contributed to both biomass (Figure 7.3.4.15) and abundance (Figure 7.3.4.16) at almost every station but they were more numerous on the slope than on the shelf. The shelf communities were composed of more (eight) taxa than the slope (seven) communities (Table 7.3.4.5). *B. saida* made up 37% of the biomass at the 24 shelf stations and 11% of the biomass at the 19 slope stations (Table 7.3.4.5) and 36% of the abundance at 23 shelf stations and 13% at the slope stations (Table 7.3.4.6). Four taxa of cottids, *Gymnocanthus tricuspis*, *Icelus spatula*, *Triglops pingelii*, and *Icelus* spp. <40 mm, made up 37% of biomass and 32% of abundance. Four species in the slope community, *Lycodes adolfi, L. eudipleurostictus, L. sagittarius*, and *L. seminudus*, composed 77% of the biomass. Three of those four (not *L. eudipleurostictus)* made up 67% of the abundance in 2013. The biomass and abundance distributions by species were similar in the shelf community but different in the slope community. The differences among species on the slope indicated that *L. adolfi* were relatively small, *L. eudipleurostictus* were few and heavy, and that *L. seminudus* were numerous and large. In terms of abundance, but not biomass, there was a separate coastal community (Station A6-20) composed of numerous very small sculpins and snailfishes, with no *B. saida*. Shelf species were mainly small sculpins (Cottidae), whereas slope species were large eelpouts (Zoarcidae).

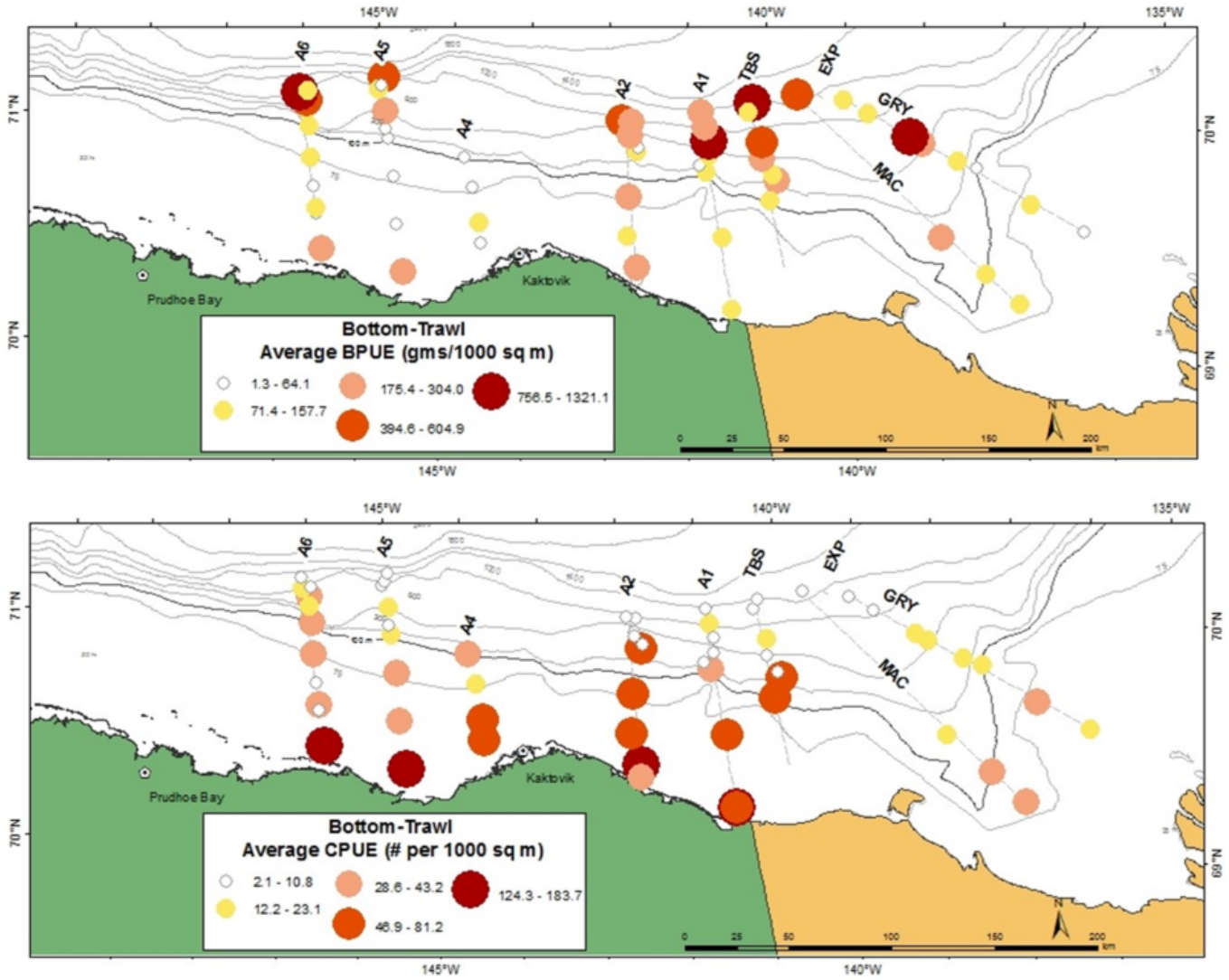

Figure 7.3.4.13. Average demersal fish biomass (gms 1000 m^{-2}, upper panel) and abundance (# 1000 m^{-2}, lower panel) of beam trawl samples during 2013–2014.

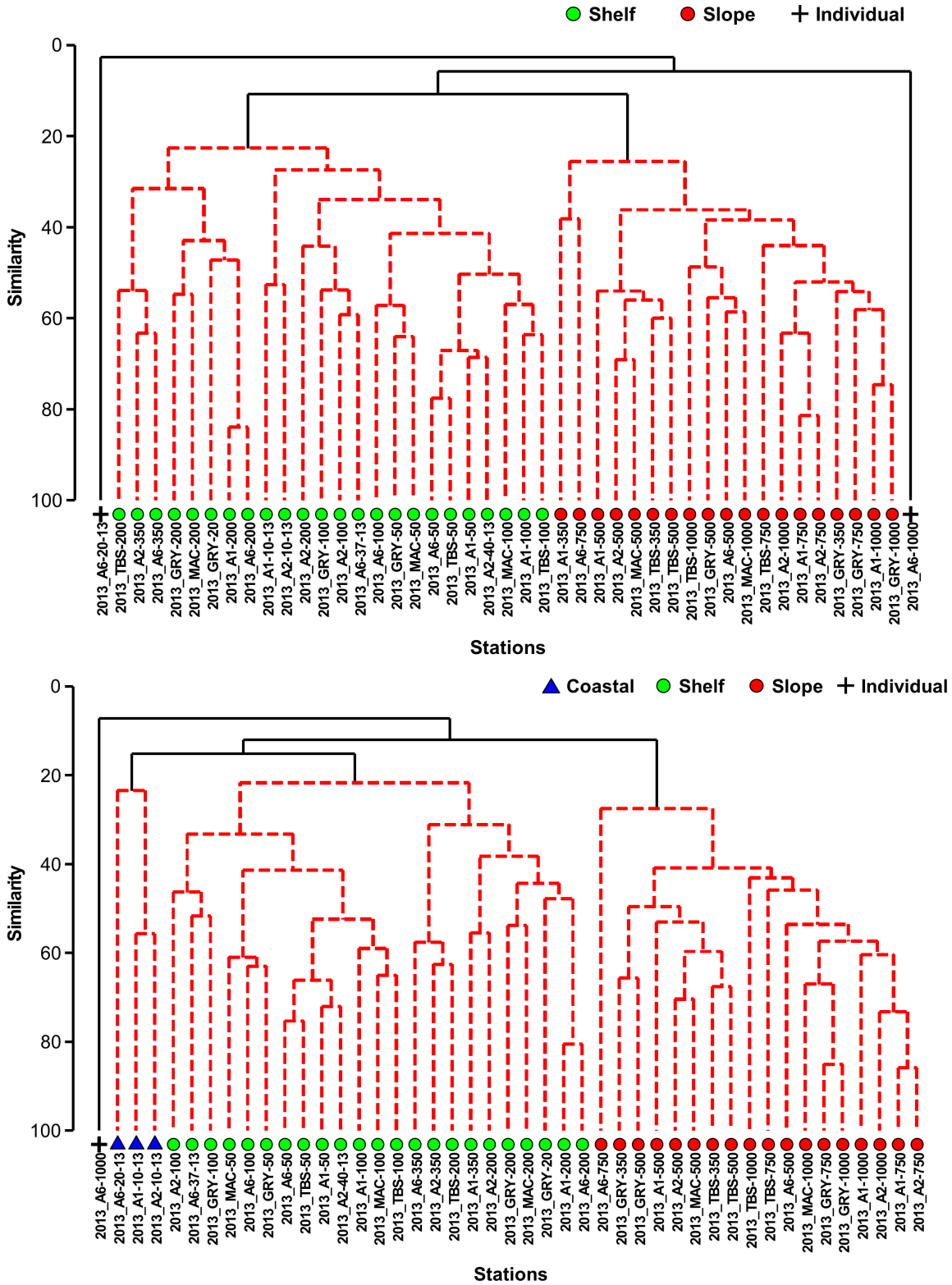

Figure 7.3.4.14. Community structure of demersal fishes in beam trawl hauls in 2013 by biomass (upper) and abundance (lower).
Data were fourth-root transformed (4RT) and cluster is based on Bray-Curtis similarity matrix. Red lines indicate non-significant differences among stations, and black lines indicate differences between station groups of p <0.05 for biomass and p <0.01 for abundance.

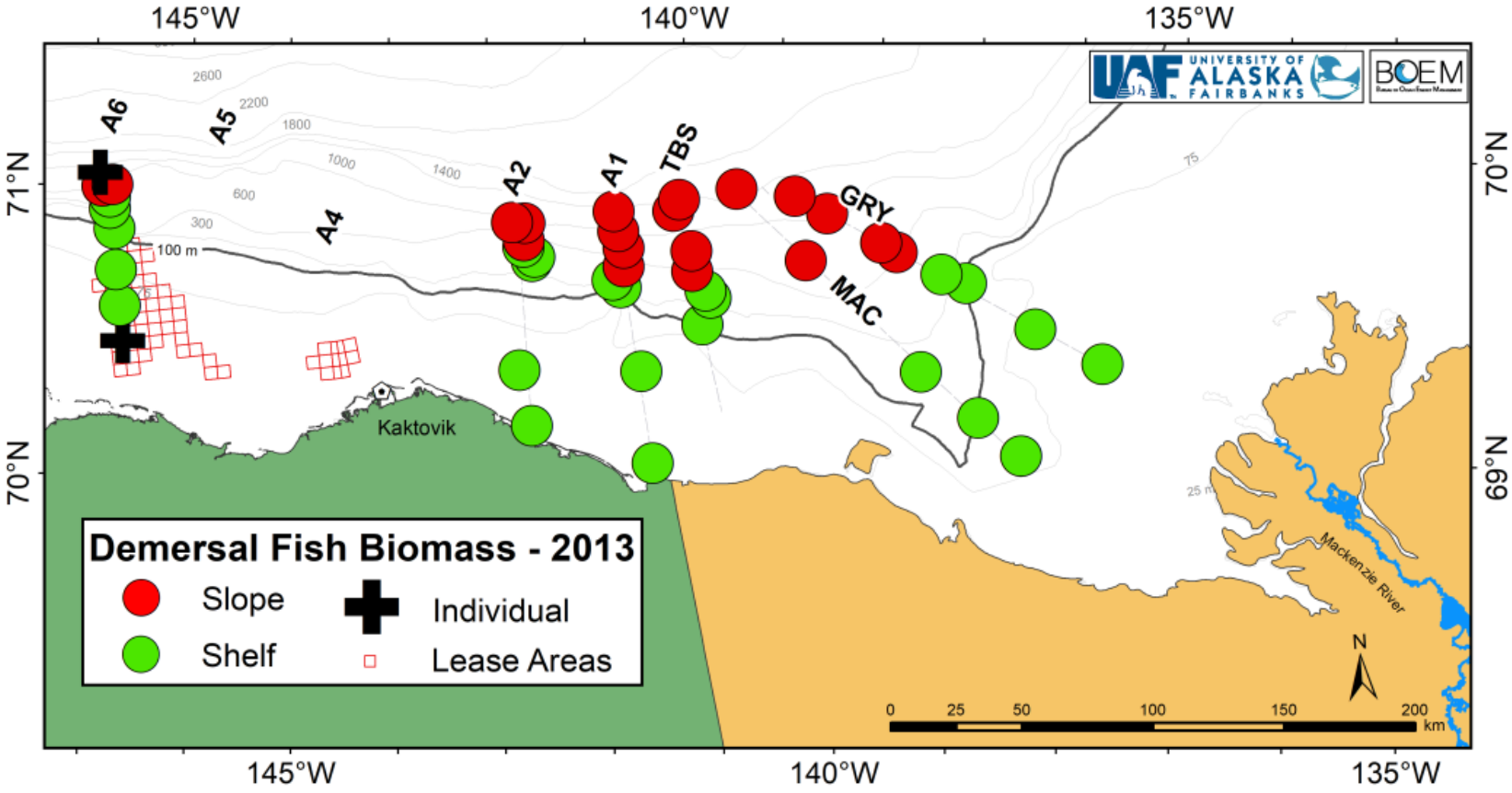

Figure 7.3.4.15. Map of demersal fish communities defined using fourth-root transformed (4RT) biomass of species collected by beam trawl in the Beaufort Sea during 2013.

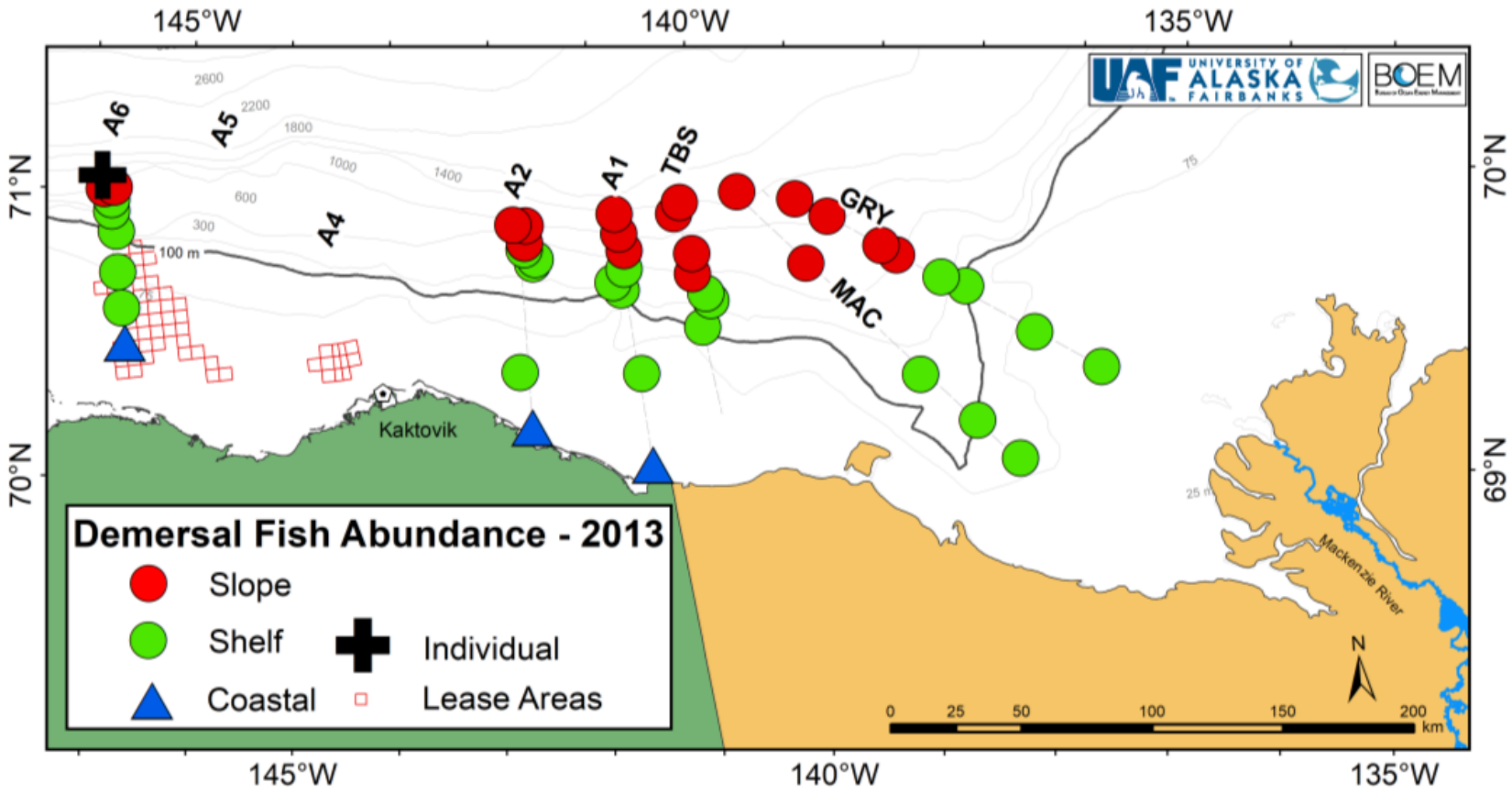

Figure 7.3.4.16. Map of demersal fish communities defined using fourth-root transformed (4RT) abundance of species collected by beam trawl in the Beaufort Sea during 2013.

Table 7.3.4.4. Mean abundance (± standard deviation) (# 1000 m^{-2}) of demersal fishes caught by beam trawl on the shelf (≤100 m) and slope (≥200 m) in 2013 and 2014.

	2013 Shelf mean ± SD	2014 Shelf mean ± SD	2013 Slope mean ± SD	2014 Slope mean ± SD
RAJIDAE	-	-	0.2 ± 0.5	<0.1 ± 0.1
MYCTOPHIDAE	-	-	-	<0.1 ± 0.1
GADIDAE				
Boreogadus saida	1.9 ± 2.4	10.7 ± 21.2	4.5 ± 8.1	3.6 ± 7.0
COTTIDAE				
Artediellus scaber	1.2 ± 3.1	5.6 ± 13.9	-	-
Cottidae unid. ≤50 mm	1.6 ± 4.5	0.2 ± 0.9	-	-
Gymnocanthus tricuspis	2.5 ± 3.3	11.6 ± 17.4	<0.1 ± 0.1	<0.1 ± 0.1
Icelus bicornis	-	2.4 ± 4.4	0.1 ± 0.3	0.1 ± 0.4
Icelus spatula	7.7 ± 9.2	6.5 ± 7.8	<0.1 ± 0.1	<0.1 ± 0.1
Icelus spp. all ≤40 mm	1.6 ± 3.1	9.0 ± 14.3	-	-
Myoxocephalus scorpius	-	0.1 ± 0.3	-	-
Triglops nybelini	-	0.1 ± 0.6	0.1 ± 0.2	0.3 ± 0.9
Triglops pingelii	3.2 ± 3.9	5.3 ± 8.0	0.4 ± 1.1	-
PSYCHROLUTIDAE				
Cottunculus microps	-	-	0.2 ± 0.5	0.1 ± 0.2
Psychrolutidae unid.	-	-	<0.1 ± 0.1	<0.1 ± <0.1
AGONIDAE				
Aspidophoroides olrikii	6.4 ± 8.4	7.0 ± 14.4	<0.1 ± 0.2	0.1 ± 0.2
Leptagonus decagonus	-	-	<0.1 ± 0.1	<0.1 ± 0.2
CYCLOPTERIDAE				
Cyclopteridae unid.	0.5 ± 1.1	-	-	-
Eumicrotremus derjugini	0.2 ± 0.6	0.2 ± 0.5	-	-
LIPARIDAE				
Careproctus lerikimae	-	-	0.2 ± 0.5	<0.1 ± 0.1
Liparis bathyarcticus	0.1 ± 0.4	-	<0.1 ± 0.2	-
Liparis fabricii	0.3 ± 0.6	0.1 ± 0.4	0.5 ± 0.9	0.2 ± 0.3
Liparis gibbus	-	-	0.1 ± 0.4	<0.1 ± 0.2
Liparis tunicatus	0.1 ± 0.3	0.1 ± 0.3	-	-
Liparis spp. all ≤50 mm	0.5 ± 1.2	0.9 ± 2.4	-	<0.1 ± 0.0
Liparis spp. unid. 51–110 mm	0.6 ± 1.5	0.2 ± 0.7	-	<0.1 ± 0.1
Paraliparis spp.	-	-	0.0 ± 0.1	<0.1 ± 0.1
Rhodichthys regina	-	-	0.1 ± 0.3	<0.1 ± 0.2
ZOARCIDAE				
Gymnelus hemifasciatus	1.7 ± 3.1	1.8 ± 2.4	-	-
Gymnelus spp. unid.	0.5 ± 1.4	-	-	-
Gymnelus viridis	0.3 ± 1.0	0.8 ± 1.5	-	-
Lycenchelys kolthoffi	-	-	0.0 ± 0.1	<0.1 ± <0.1
Lycodes adolfi	-	-	1.4 ± 2.3	0.9 ± 1.2
Lycodes eudipleurostictus	-	-	0.2 ± 0.5	0.2 ± 0.4
Lycodes frigidus	-	-	-	<0.1 ± 0.1

Table 7.3.4.4. continued.

	2013 Shelf mean ± SD	2014 Shelf mean ± SD	2013 Slope mean ± SD	2014 Slope mean ± SD
ZOARCIDAE, continued				
Lycodes mucosus	<0.1 ± 0.2	0.3 ± 0.7	-	<0.1 ± 0.2
Lycodes pallidus	-	-	0.2 ± 0.6	<0.1 ± 0.1
Lycodes polaris	1.3 ± 1.6	1.3 ± 1.7	0.4 ± 1.7	<0.1 ± 0.1
Lycodes raridens	-	-	0.0 ± 0.2	<0.1 ± 0.1
Lycodes reticulatus	0.1 ± 0.3	-	0.1 ± 0.2	<0.1 ± 0.2
Lycodes rossi	-	0.7 ± 2.7	0.1 ± 0.3	0.1 ± 0.3
Lycodes sagittarius	-	0.1 ± 0.3	1.0 ± 1.9	0.6 ± 0.6
Lycodes seminudus	<0.1 ± 0.2	0.2 ± 0.9	1.6 ± 2.4	0.7 ± 0.8
Lycodes spp. unid.	-	0.2 ± 0.9	0.5 ± 0.9	0.3 ± 0.5
STICHAEIDAE				
Anisarchus medius	2.4 ± 5.4	1.0 ± 3.5	-	-
Eumesogrammus praecisus	-	0.2 ± 0.5	-	-
Leptoclinus maculatus	-	-	-	0.1 ± 0.3
Lumpeninae all ≤51 mm	0.6 ± 1.0	0.3 ± 0.7	-	-
Lumpenus fabricii	1.5 ± 3.6	0.8 ± 1.8	-	0.1 ± 0.6
Stichaeus punctatus	-	0.1 ± 0.5	-	-
AMMODYTIDAE				
Ammodytes hexapterus	-	<0.1 ± 0.2	-	-
PLEURONECTIDAE				
Reinhardtius hippoglossoides	-	-	<0.1 ± 0.2	<0.1 ± 0.1
Pleuronectidae larvae	0.1 ± 0.3	-	-	-
ALL TAXA	36.9 ± 22.9	67.7 ± 53.5	11.9 ± 9.5	7.7 ± 7.7

Table 7.3.4.5. Demersal fish community composition as defined by biomass (fourth-root transformed) in 2013 beam trawl hauls.
Percent contribution of taxa density to each of four fish communities (p <0.01) and mean similarity of taxon density within community. Only taxa selected by SIMPER as descriptive of 90% of the community are included here. The distribution of communities is presented visually in Figure 7.3.4.15.

		2013 Fish Communities (Biomass)			
		Shelf	Slope	A6-20	A6-1000
Taxa	# Stations	24	19	1	1
Gadidae	*Boreogadus saida*	37.31	11.05		
Cottidae	*Artediellus scaber*			34.70	
	Gymnocanthus tricuspis	6.95			
	Icelus spp. ≤40 mm	2.14			
	Icelus spatula	14.42			
	Triglops pingelii	13.59			
	Cottidae unid. ≤50 mm				
Agonidae	*Aspidophoroides olrikii*	6.20			
Liparidae	*Liparis* spp. ≤50 mm			34.36	
	Liparis spp. 51-110 mm			30.94	
	Liparis fabricii	2.04	4.73		100.00
Zoarcidae	*Gymnelus* spp.				
	Lycodes spp. unid		3.99		
	Lycodes adolfi		15.96		
	Lycodes eudipleurostictus		4.36		
	Lycodes polaris	7.86			
	Lycodes sagittarius		19.43		
	Lycodes seminudus		33.61		
Total % Contributed		90.52	93.13	100.00	100.00
Within Community Similarity		31.75	39.13	100.00	100.00

Table 7.3.4.6. Demersal fish community composition as defined by abundance (fourth-root transformed) in 2013 beam trawl hauls.
Percent contribution of taxa density to each of five fish communities (p <0.01) and mean similarity of taxon density within community. Only taxa selected by SIMPER as descriptive of 90% of the community are included here. The distribution of communities is presented visually in Figure 7.3.4.16.

		2013 Fish Communities (Abundance)			
		Coastal	Shelf	Slope	A6-1000
Taxa	# Stations	3	23	27	1
Gadidae	*Boreogadus saida*		36.34	13.31	
Cottidae	*Artediellus scaber*	12.29			
	Gymnocanthus tricuspis	15.18	3.52		
	Icelus spp. ≤40 mm		2.28		
	Icelus spatula		14.16		
	Triglops pingelii	10.96	11.89		
	Cottidae unid. ≤50 mm	16.84			
Agonidae	*Aspidophoroides olrikii*		8.66		
Liparidae	*Liparis* spp. ≤50 mm	44.74			
	Liparis spp. 51-110 mm				
	Liparis fabricii		1.94	5.13	100.00
Zoarcidae	*Gymnelus* spp.				
	Lycodes spp. unid			6.36	
	Lycodes adolfi			22.03	
	Lycodes eudipleurostictus				
	Lycodes polaris		10.66		
	Lycodes sagittarius			20.49	
	Lycodes seminudus			24.91	
Total % Contributed		100.00	91.22	92.24	100.00
Within Community Similarity		34.25	31.69	45.31	100.00

As in 2013, the 2014 cluster patterns of stations by both biomass and abundance separated at the shelf break, i.e., about 100–200 m, to form shelf (<100 m) and slope (>200 m) communities (Figure 7.3.4.17). In addition to the shelf and slope clusters, both fish biomass and abundance had two other clusters that were more similar in species composition to the shelf than the slope group (Figure 7.3.4.17); each group, designated shelf break A and shelf break B, consisted of three stations (Figures 7.3.4.18 and 7.3.4.19). Assemblage patterns were similar to those seen for 2013, i.e., shelf vs. slope. *Boreogadus saida* contributed to the biomass and abundance at almost every station but contributions were not equal. The shelf communities were composed of more (9) taxa than the slope (5) communities; *B. saida* was the only species in common. *B. saida* made up 17% of the biomass at the 20 shelf stations and 25% at the 21 slope stations (Table 7.3.4.7) and 16% of the abundance at the 21 shelf stations and 31% at the 21 slope stations (Table 7.3.4.8). Shelf species again were mainly small sculpins (Cottidae), with contributions by two small eelpouts. Slope species were large eelpouts (Zoarcidae). There was no separate coastal

community in fish abundance on the shelf as seen in 2013. However, for both biomass and abundance, there were two shelf break stations at depths of 100 and 200 m. *B. saida* was in each of the communities, which otherwise had no species in common. Interestingly, there was no geographic or oceanographic pattern to the shelf break A and shelf break B communities other than they were all at depths of 100–200 m (Figures 7.3.4.18 and 7.3.4.19).

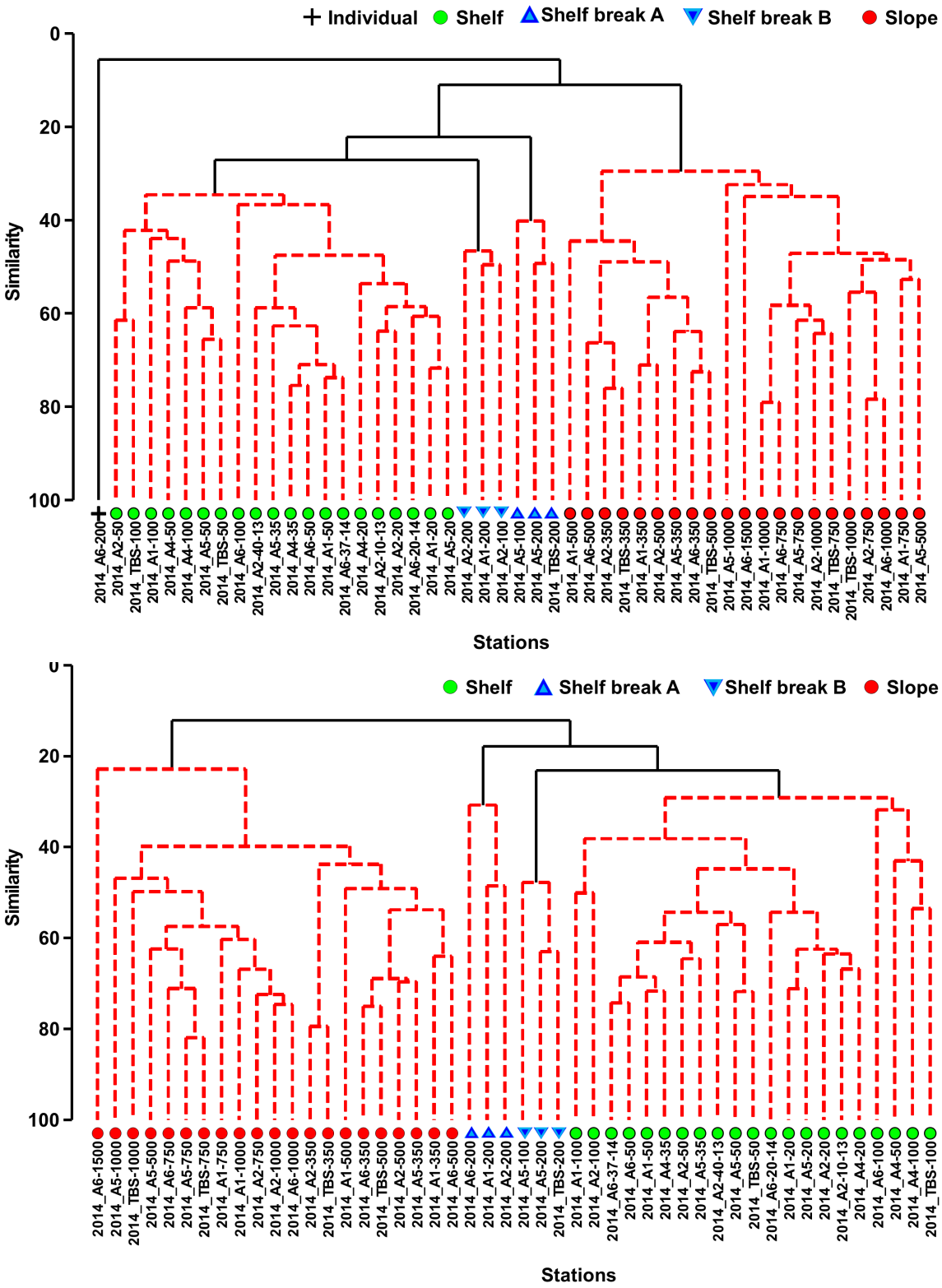

Figure 7.3.4.17. Community structure of demersal fishes in beam trawl hauls in 2014 by biomass (upper) and abundance (lower).
Data were fourth-root transformed (4RT) and cluster is based on Bray-Curtis similarity matrix. Red lines indicate non-significant differences among stations, and black lines indicate differences between station groups of p <0.05 for biomass and p <0.05 for abundance.

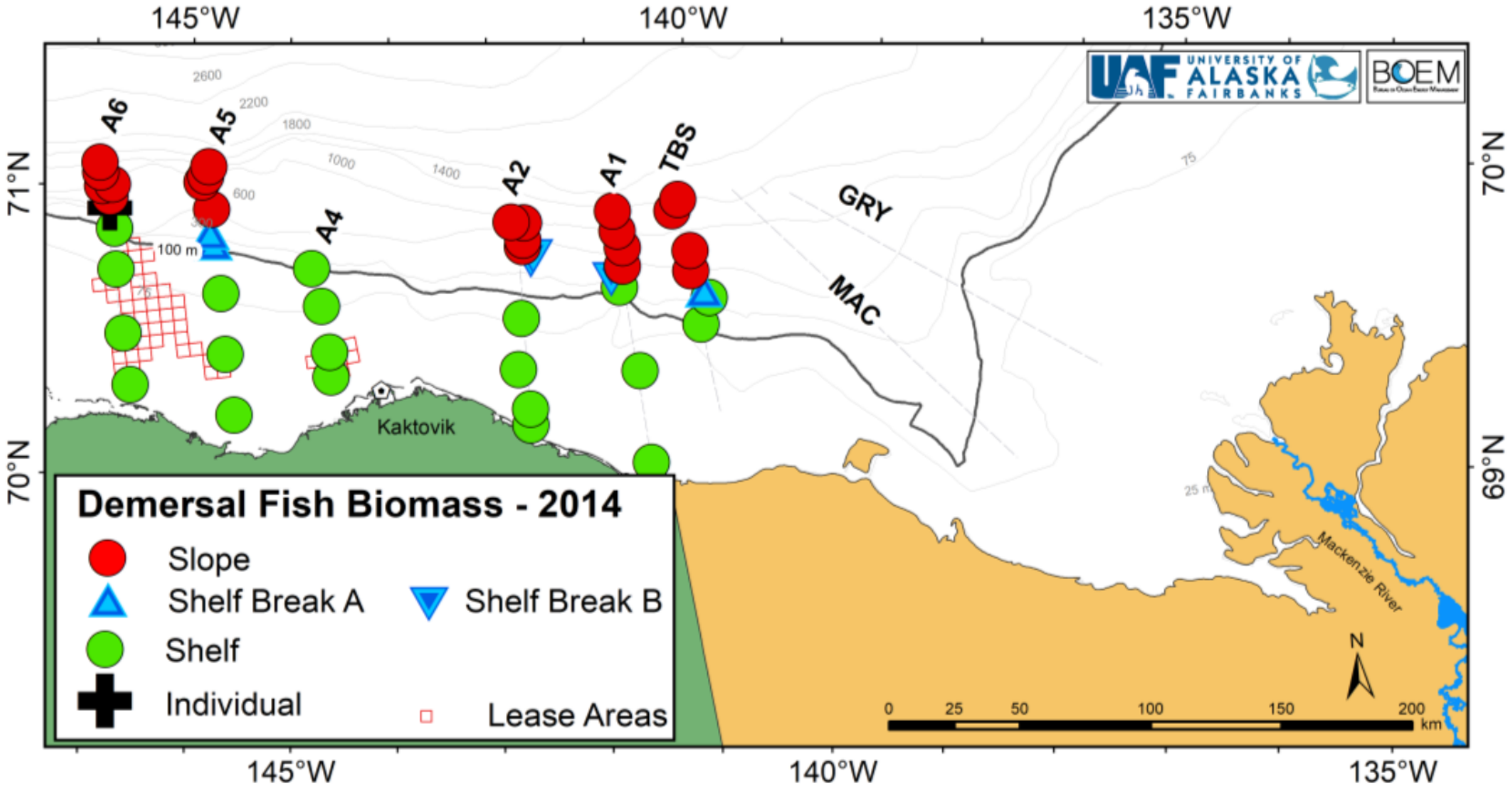

Figure 7.3.4.18. Map of demersal fish communities defined using fourth-root transformed (4RT) biomass of species collected by beam trawl in the Beaufort Sea during 2014.

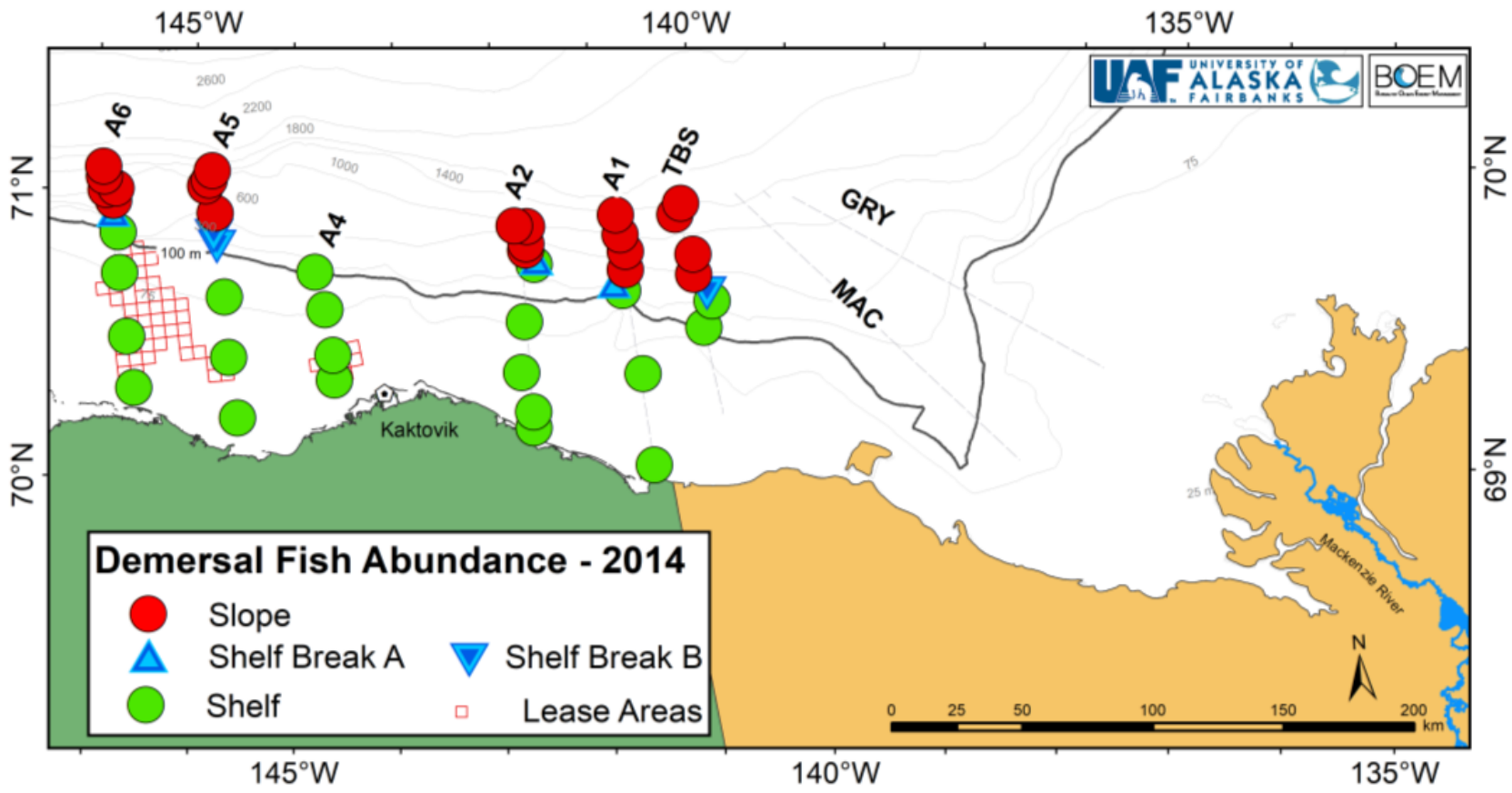

Figure 7.3.4.19. Map of demersal fish communities defined using fourth-root transformed (4RT) abundance of species collected by beam trawl in the Beaufort Sea during 2014.

Table 7.3.4.7. Demersal fish community composition as defined by biomass (fourth-root transformed) in 2014 beam trawl hauls.
Percent contribution of taxa density to each of five fish communities (p <0.01) and mean similarity of taxon density within community. Only taxa selected by SIMPER as descriptive of 90% of the community are included here. The distribution of communities is presented visually in Figure 7.3.4.18.

		2014 Fish Communities (Biomass)				
		Shelf	Shelf break A	Shelf break B	Slope	A6-200
Taxa	# Stations	20	3	3	21	1
Gadidae	*Boreogadus saida*	17.31	53.81	24.76	25.44	16.45
Cottidae	*Artediellus scaber*	3.84				
	Gymnocanthus tricuspis	15.91				
	Icelus spp. ≤40 mm	9.98				
	Icelus bicornis			23.00		15.31
	Icelus spatula	16.72				
	Triglops nybelini			33.95		22.55
	Triglops pingelii	12.80				
Agonidae	*Aspidophoroides olrikii*	7.33	46.19			
	Leptagonus decagonus					20.76
Liparidae	*Liparis fabricii*				9.20	
Zoarcidae	*Gymnelus* hemifasciatus	4.06				
	Lycodes adolfi				14.47	
	Lycodes mucosus					
	Lycodes polaris	3.57				
	Lycodes rossi			7.81		
	Lycodes sagittarius				22.46	
	Lycodes seminudus				20.98	
Stichaeidae	*Lumpenus fabricii*					
Total % Contributed		91.53	100.00	95.72	92.54	75.07
Within Community Similarity		42.89	43.28	47.67	38.78	100.00

Table 7.3.4.8. Demersal fish community composition as defined by abundance (fourth-root transformed) in 2014 beam trawl hauls.
Percent contribution of taxa density to each of four fish communities (p <0.01) and mean similarity of taxon density within community. Only taxa selected by SIMPER as descriptive of 90% of the community are included here. The distribution of communities is presented visually in Figure 7.3.4.19.

		2014 Fish Communities (Abundance)			
		Shelf	Shelf break A	Shelf break B	Slope
Taxa	# Stations	21	3	3	21
Gadidae	*Boreogadus saida*	16.34	50.00	15.53	30.57
Cottidae	*Artediellus scaber*	3.36			
	Gymnocanthus tricuspis	11.12			
	Icelus spp. ≤40 mm	14.02			
	Icelus bicornis			42.23	
	Icelus spatula	14.33			
	Triglops nybelini			15.36	
	Triglops pingelii	12.74			
Agonidae	*Aspidophoroides olrikii*	8.47	50.00		
	Leptagonus decagonus				
Liparidae	*Liparis fabricii*				6.72
Zoarcidae	*Gymnelus* hemifasciatus	4.84			
	Lycodes adolfi				17.38
	Lycodes mucosus			12.02	
	Lycodes polaris	5.19			
	Lycodes rossi				
	Lycodes sagittarius				17.49
	Lycodes seminudus				18.21
Stichaeidae	*Lumpenus fabricii*			14.86	
Total % Contributed		90.41	100.00	100.00	90.38
Within Community Similarity		42.24	52.91	36.74	45.03

To assess whether data from different years could be combined in a meaningful way (to maximize hypothetical data-poor and opportunistic future sampling), 2013 and 2014 data were combined. Shade plots helped visualize geographic concentrations and separation of species as well as species communities based on station and species affiliations (Figures 7.3.4.20–21) and made the shelf and slope communities highly visible. In 2014 there were two shelf break communities; all of the 200 m stations from both 2013 and 2014 (except A6-200 in 2014, which did not group with any other stations) were within one of the two shelf break communities, though they did not contain as many species as the shelf and slope communities. Six nearshore stations (10–20 m) from 2014 were grouped with the CPUE coastal community stations that separated out in 2013. *Boreogadus saida* was caught at almost every station in all communities. Measured by both BPUE (Table 7.3.4.9) and CPUE (Table 7.3.4.10), two stations continued to be individual in the nearshore (A6-20 in 2013) and at the shelf break (A6-200 in 2014). One

other station, A6-1000 in 2013, was composed of species that fit in the CPUE slope community, but was still unique in BPUE because there was only one small snailfish. Including all quantitative station data together from 2013 and 2014 increased the sample size and showed that there were still distinct shelf and slope communities (Figures 7.3.4.20–21). The increased sample size made the spatial patterns of BPUE (Figure 7.3.4.22) and CPUE (Figure 7.3.4.23) more discernable and resulted in communities that combined the spatial patterns of 2014 than 2013. Thus, we recommend combining years. This is a valuable finding as it is likely that sampling will continue to be data poor and opportunistic, such as collecting fish along the Distributed Biological Observatory (DBO) lines (DBO6 at 152° W and DBO7 at 143.6° W).

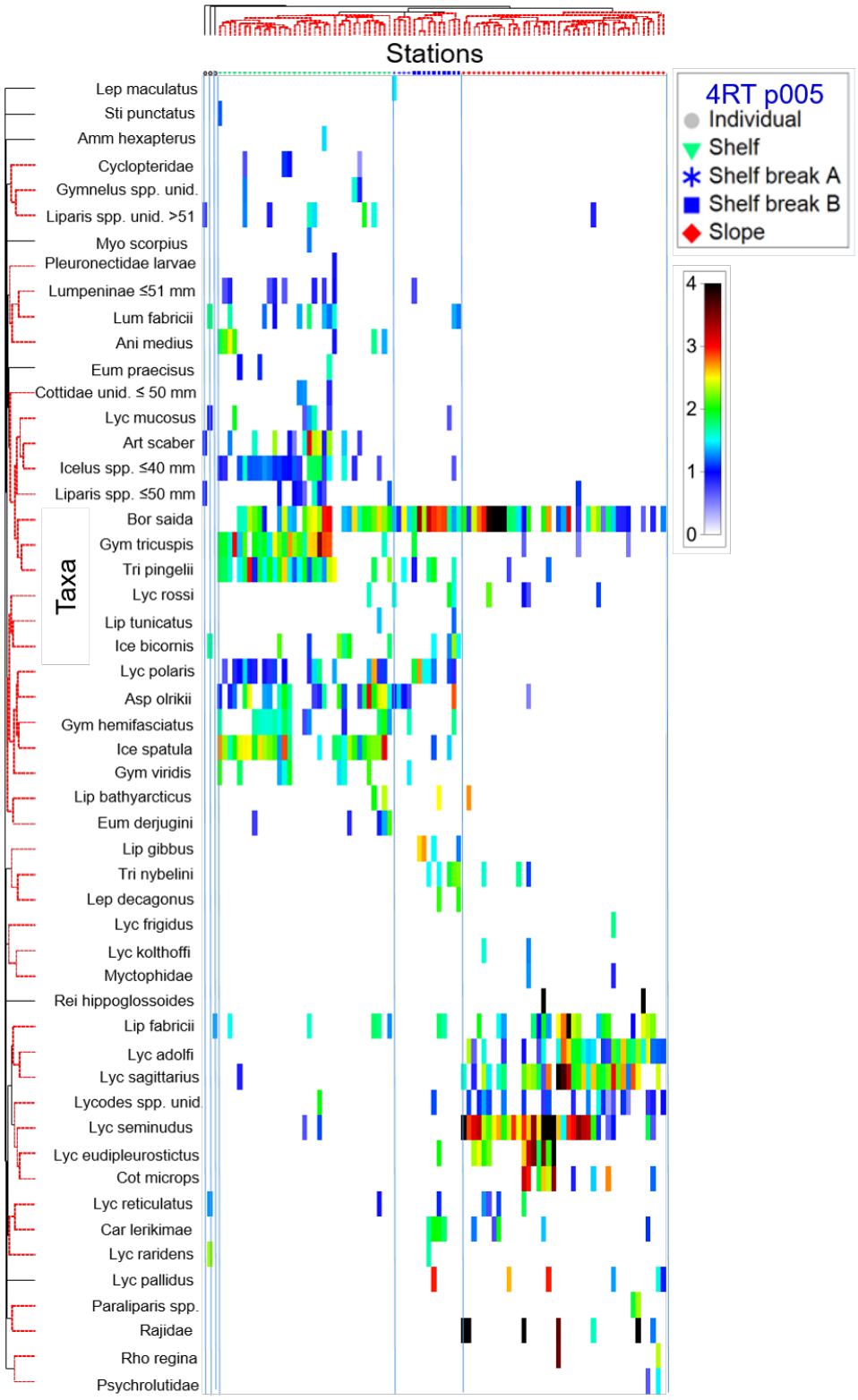

Figure 7.3.4.20. Matrix of community structure of demersal fishes in beam trawl hauls in 2013 and 2014 by biomass.

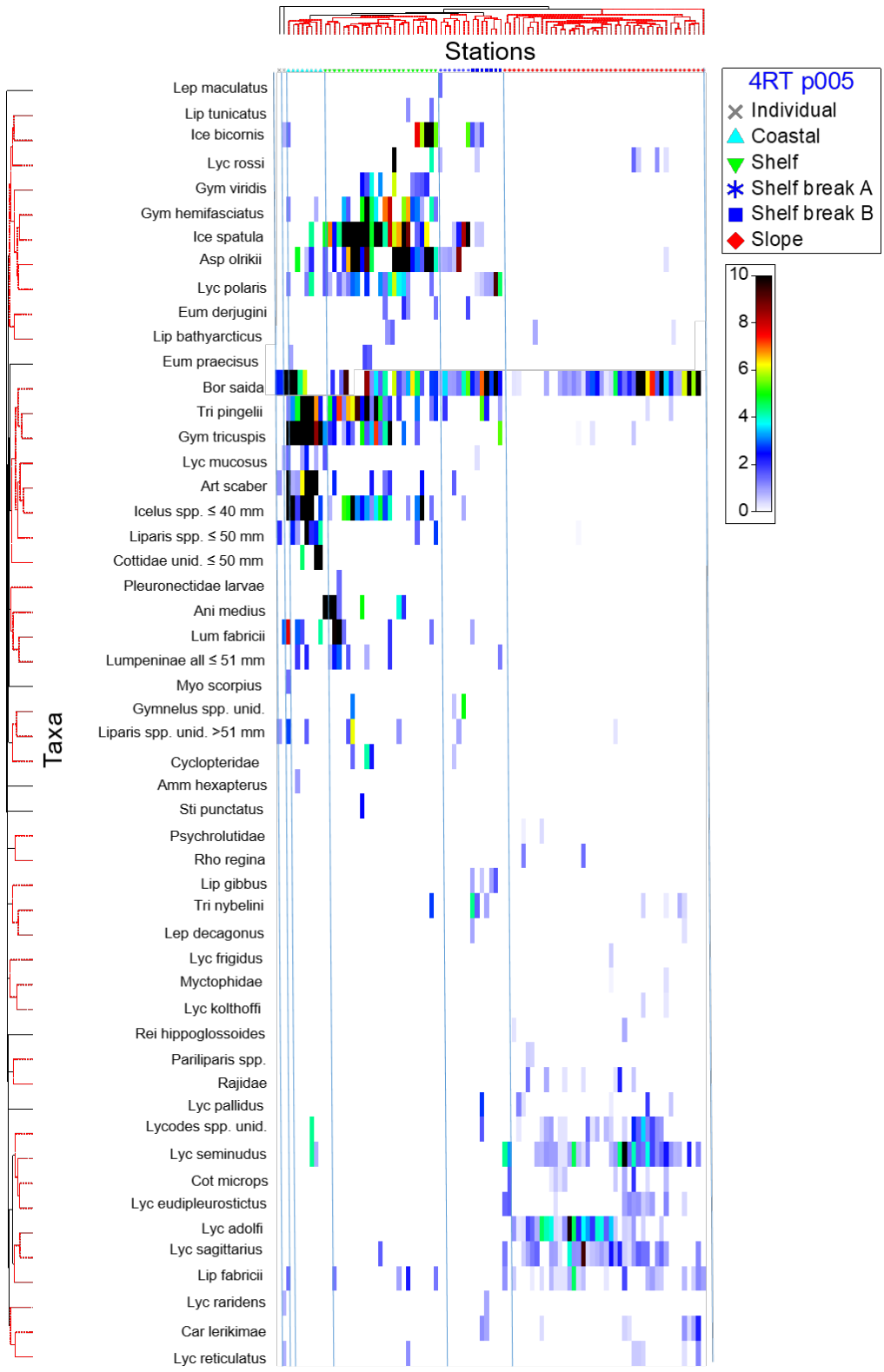

Figure 7.3.4.21. Matrix of Community structure of demersal fishes in beam trawl hauls in 2013 and 2014 by abundance. Red lines indicate non-significant differences among stations, and black lines indicate differences between clusters of p <0.05 for stations and p <0.005 for taxa. Abundance is # fish 1000 m^{-3} and intensity of the color ramp indicates proportionally higher abundance of the taxon at the station.

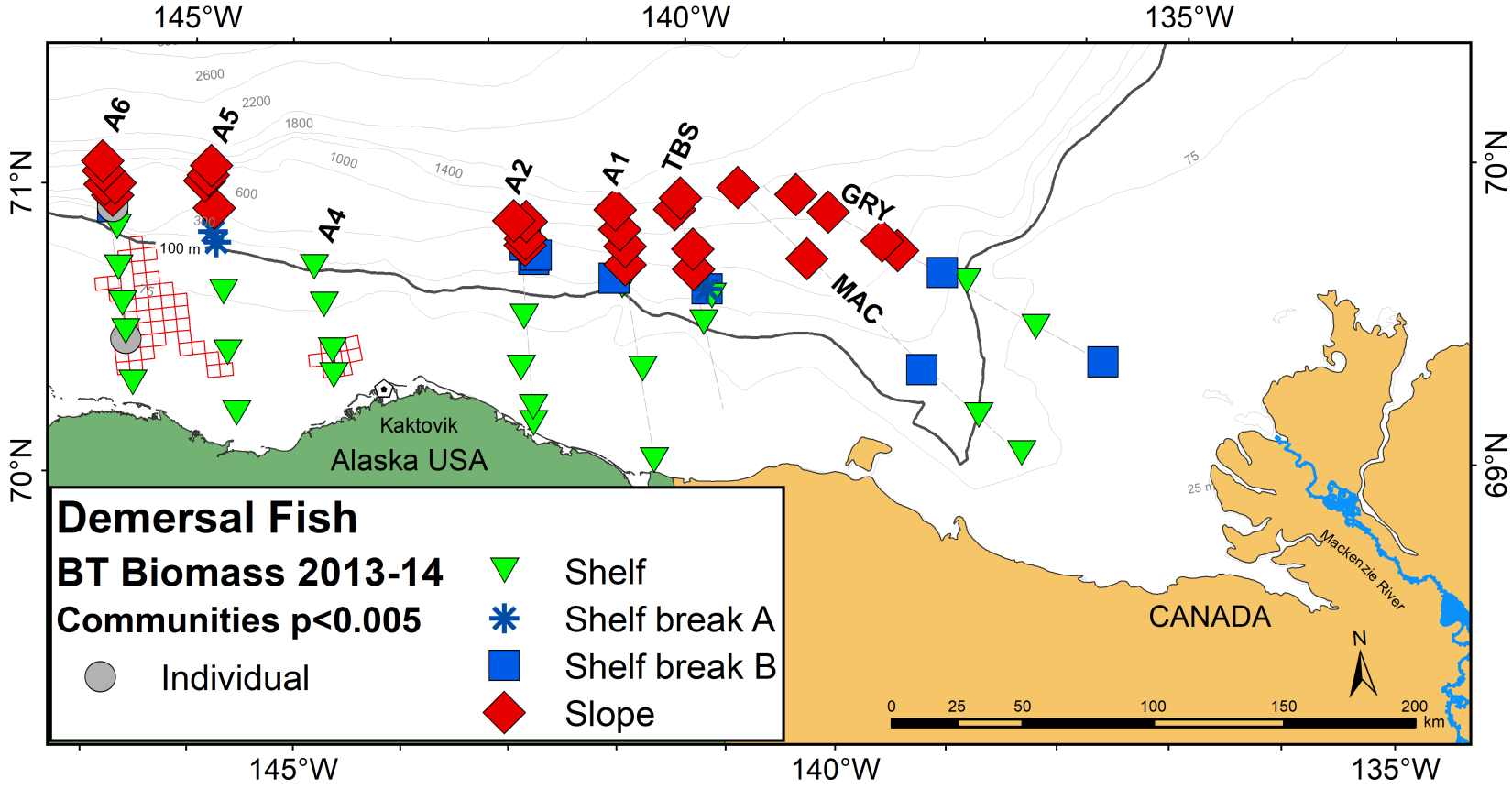

Figure 7.3.4.22. Demersal fish communities defined using fourth-root transformed (4RT) biomass of species collected by beam trawl in the Beaufort Sea during 2013 and 2014.

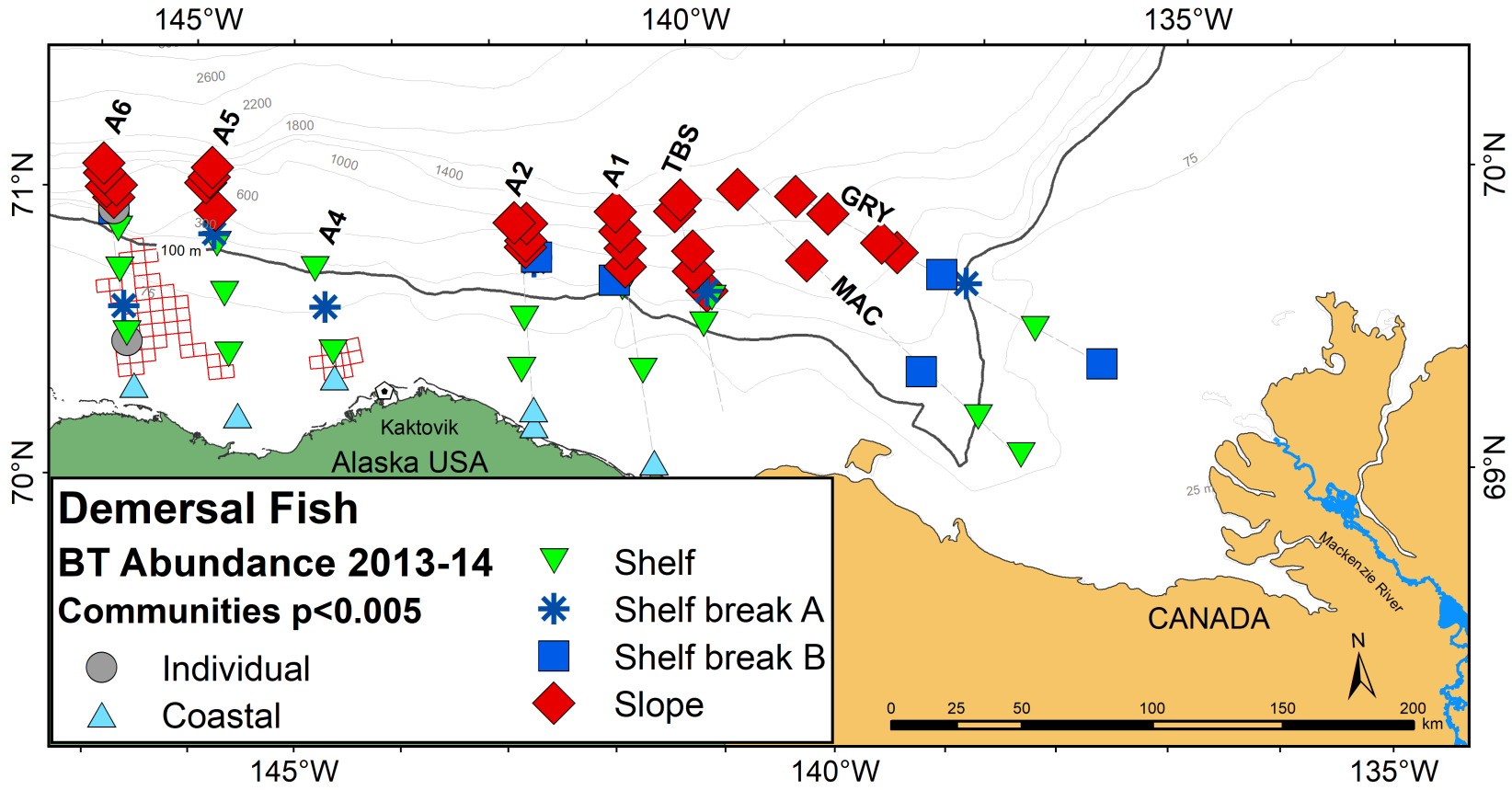

Figure 7.3.4.23. Demersal fish communities defined using fourth-root transformed (4RT) abundance of species collected by beam trawl in the Beaufort Sea during 2013 and 2014.

Table 7.3.4.9. Demersal fish community composition as defined by biomass (fourth-root transformed) in combined 2013 and 2014 beam trawl hauls.
Percent contribution of taxa biomass to each of four fish communities (p <0.005), three independent stations, and mean similarity of taxon density within community. Only taxa selected by SIMPER as descriptive of 90% of the community are included here. The distribution of communities is presented visually in Figure 7.3.4.22.

		Shelf	Shelf break A	Shelf break B	Slope	2013 A6-20	2013 A6-1000	2014 A6-200
		35	4	10	41	1	1	1
Gadidae	*Boreogadus saida*	16.96	55.28	53.62	18.71			
Cottidae	*Artediellus scaber*					34.70		
	Gymnocanthus tricuspis	13.85						
	Icelus bicornis			3.90				16.34
	Icelus spp. ≤40 mm	7.47						
	Icelus spatula	21.44						
	Triglops nybelini			8.11				
	Triglops pingelii	13.62						
Agonidae	*Aspidophoroides olrikii*	8.89	44.72					
Liparidae	*Careproctus lerikimae*			5.50				
	Liparis fabricii				7.46		100.0	
	Liparis gibbus			6.03				
	Liparis spp. ≤50 mm					34.36		
	Liparis spp. 51-110 mm					30.94		
Zoarcidae	*Gymnelus hemifasciatus*	3.86						
	Lycodes adolfi				14.54			
	Lycodes mucosus							1.06
	Lycodes polaris	3.96		15.50				
	Lycodes raridens							57.15
	Lycodes reticulatus							5.54
	Lycodes sagittarius				21.31			
	Lycodes seminudus				27.24			
	Lycodes spp. unid				3.98			
Stichaeidae	*Lumpenus fabricii*							19.91
Total % Contributed		90.05	100.0	92.65	93.24	100.0	100.0	100.0
With Community Similarity		41.31	44.43	35.70	38.77	100.0	100.0	100.0

Table 7.3.4.10. Demersal fish community composition as defined by abundance (fourth-root transformed) in combined 2013 and 2014 beam trawl hauls.
Percent contribution of taxa abundance to each of five fish communities (p <0.005), two independent stations, and mean similarity of taxon abundance within community. Only taxa selected by SIMPER as descriptive of 90% of the community are included here. The distribution of communities is presented visually in Figure 7.3.4.23.

		Coastal	Shelf	Shelf break A	Shelf break B	Slope	2013 A6-20	2014 A6-200
		8	25	7	7	44	1	1
Gadidae	*Boreogadus saida*	12.96	10.08	57.09	48.52	25.15		
Cottidae	*Artediellus scaber*	11.59					31.36	
	Gymnocanthus tricuspis	24.82	7.32					
	Icelus bicornis							12.50
	Icelus spp. ≤40 mm	14.23	8.40					
	Icelus spatula		22.07	13.85				
	Triglops nybelini				4.98			
	Triglops pingelii	16.60	11.30		4.46			
Agonidae	*Aspidophoroides olrikii*		15.30	27.28				
Liparidae	*Careproctus lerikimae*							
	Liparis fabricii					8.58		
	Liparis gibbus				10.40			
	Liparis spp. ≤50 mm	8.19					37.28	
	Liparis spp. 51-110 mm						31.36	
Zoarcidae	*Gymnelus hemifasciatus*		8.08					
	Lycodes adolfi					16.73		
	Lycodes mucosus							12.50
	Lycodes polaris		7.91		24.96			
	Lycodes raridens							12.50
	Lycodes reticulatus							12.50
	Lycodes sagittarius					17.21		
	Lycodes seminudus					20.64		
	Lycodes spp. unid					5.66		
Stichaeidae	*Lumpenus fabricii*	3.27						50.00
Total % Contributed		91.66	90.47	98.23	93.32	93.97	100.0	100.0
With Community Similarity		56.68	46.23	41.83	43.17	41.66	100.0	100.0

Environmental factors affected the community composition, biomass, and abundance of fishes on the Beaufort Sea shelf and slope in both 2013 and 2014. In an ANOSIM, depth had a significant effect (p <0.001) on fish communities in 2013 and 2014 in each year individually and in the two years combined (Table 7.3.4.11). In contrast, there was only a significant (p <0.05) effect of longitude on fish community in 2013 when sampling occurred across a wider range, i.e., eastward of the Mackenzie River in Canadian waters. Fish community composition was significantly different (p <0.001) between water masses (Polar Mixed Layer (PML), Arctic

Halocline Water (AHW), and Atlantic Water (AW)) in all comparisons within individual years (Table 7.3.4.12).

Depth and water mass were clearly delineated among fish catches at individual stations based on fish biomass and abundance in 2013 and 2014. Both BPUE and CPUE had a distinct break vertically between ≤200 and ≥350 m (Figure 7.3.4.24). The abundance shelf break groups (100–200 m; lower left in bottom figure) separated out from the more shallow group (≤50 m). The AW was clearly separated from the PML and the AHW in nMDS plots. PML was more definitively separated from AHW for CPUE than for BPUE (Figure 7.3.4.25). The AHW, which encompassed sample depths of 100 and 200 m, combined with PML in shallow shelf stations, especially for BPUE.

A quantifiable examination of the relationships between the combined 2013–2014 BPUE or CPUE and environmental variables was assessed using BEST (stepwise multivariate) analysis, which uses continuous variables and is more precise than ANOSIM. All environmental variables were not available at all stations. Variables included longitude, latitude, bottom depth, bottom temperature, bottom salinity, and bottom water density. Water mass is a categorical variable and, as such, cannot be directly assessed using BEST. Therefore, numerical proxies (depth ranges) were used so water mass could be included: depths 10–50 m for PML, 100–200 m for AHW, and ≥350 m for AW. Water mass was the variable with the most effect on biomass ($\rho = 0.65$). The relationship could be strengthened slightly ($\rho = 0.70$) by including bottom depth and bottom salinity (Table 7.3.4.13). The relationship for CPUE was dependent on water mass and was slightly stronger ($\rho = 0.68$) than for BPUE. Including salinity and depth ($\rho = 0.70$) resulted in the same relationship for 2013–14 CPUE as for 2013–14 BPUE. Though the results were confounded by including both depth and depth range proxies for the water masses, it is clear that the actual depth of the sample increases the strength relationship obtained by using depth ranges to represent water masses. On the US Beaufort Sea shelf and slope, salinity and bottom water density are associated with depth. Salinity increased with depth, and depth increased with distance from shore. Thus, statistically, the importance of environmental variables related to the BPUE and CPUE of demersal fishes in 2013 and 2014 combined could be separated, but it is critical to realize that each variable was related to depth.

CCA was performed as one more method to test the effect of environmental variables on demersal fish abundance. There was a significant relationship between demersal fish abundance and the variables tested over 89 stations (i.e., depth, longitude, bottom temperature, bottom salinity, and water mass). For 52 fish taxa ($F = 3.987$, $p < 0.001$) the ordination explained 22.6% of the total variance in demersal abundance. For the 22 taxa that described 90% of the communities ($F = 8.416$, $p < 0.001$) the ordination explained 38.1% of the total variance (Table 7.3.4.14). Depth, bottom temperature, bottom salinity, and water mass all had a significant effect on 23 taxa ($p = 0.001$); however, the influence of salinity was not as high ($p = 0.013$) for 52 taxa. Longitude was not a significant predictor of demersal fish abundance. Depth, bottom salinity, and bottom temperature had similar CCA1 values (i.e., the axis explaining the majority of the variance in demersal fish abundance). As depth increases, temperature and salinity increase; higher temperature and salinity values characterize the AW. The cross-correlation is verified by vectors pointing in a similar direction and because angles between vectors were small; smaller angles mean higher correlation (Figure 7.3.4.26, Appendix E5). For 54 stations, percent sediment classification (gravel, sand, mud) was available, none of which significantly contributed to explaining the variance of the demersal fish abundance, though depth, bottom salinity, and water mass were still significant (Table 7.3.4.15). Water masses are associated with shelf (PML), shelf

break (AHW), and slope (AW) fish communities. It should be noted that this is a generalization and that taxa closer to the center of the ordination (e.g., *Boreogadus saida*) are being influenced by a multitude of different processes, making it difficult to determine which variable most influences their abundance.

Table 7.3.4.11. Effects of depth and longitude on fish biomass and abundance (fourth root transformed) community composition in combined 2013 and 2014 beam trawl hauls in the Beaufort Sea.
2-way ANOSIM, R significance: ^{+}p <0.05, *p <0.001. All other environmental factors not significant.

		2-way crossed ANOSIM	
		R (Depth)	R (Longitude)
Biomass	2013	*0.655	$^{+}$-0.216
	2014	*0.759	-0.132
	2013-14	*0.705	$^{+}$0.206
Abundance	2013	*0.641	$^{+}$0.199
	2014	*0.779	-0.117
	2013-14	*0.708	0.096

Table 7.3.4.12. Effect of water mass on community composition as defined by fish biomass (upper half matrix) and abundance (lower half matrix, fourth-root transformed) in combined 2013 and 2014 beam trawl hauls in the Beaufort Sea.
1-way ANOSIM, R significance: ***p <0.005.

	Polar Marine Layer	Arctic Halocline	Atlantic Water
2013	Biomass R_{global} =***0. 669		
Polar Marine Layer		***0.298	***0.825
Arctic Halocline	***0.262		***0.700
Atlantic Water	***0.843	***0.711	
	Abundance R_{global} =***0.690		
2014	Biomass R_{global} =***0.756		
Polar Marine Layer		***0.528	***0.876
Arctic Halocline	***0.550		***0.784
Atlantic Water	***0.920	***0.795	
	Abundance R_{global} =***0.800		

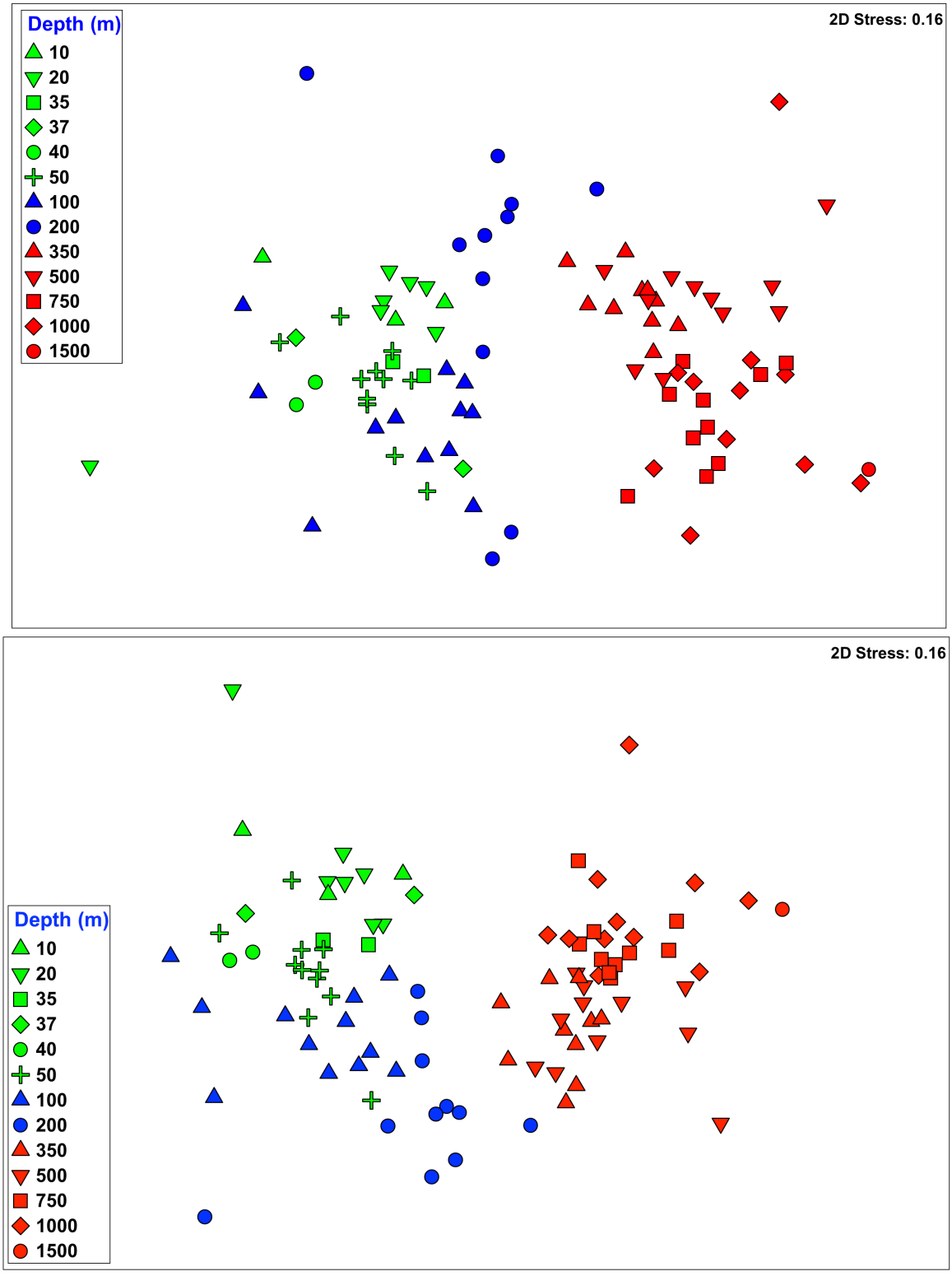

Figure 7.3.4.24. Demersal fish communities in beam trawls in the Beaufort Sea during 2013 and 2014 based on biomass (upper) and abundance (lower) coded at each station by depth.

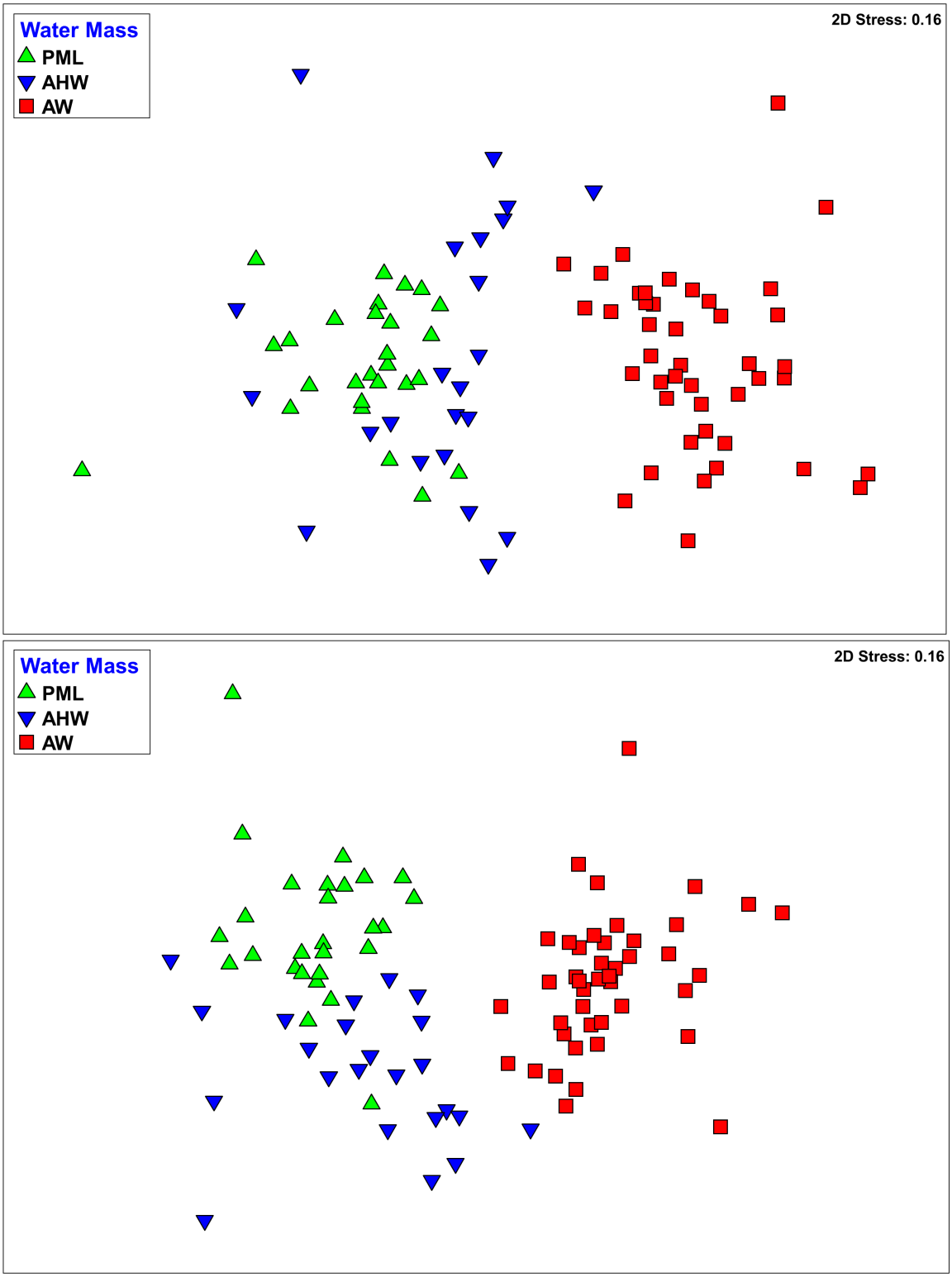

Figure 7.3.4.25. Demersal fish communities in beam trawls in the Beaufort Sea during 2013 and 2014 based on biomass (upper) and abundance (lower) coded at each station by water mass.
PML – Polar Mixed Layer, AHW – Arctic Halocline Water, AW – Atlantic Water.

Table 7.3.4.13. BEST (stepwise) relationship of demersal fishes captured by beam trawls and environmental variables in the Beaufort Sea in 2013 and 2014 combined.
Measures of effort for fish are biomass (BPUE) and abundance (CPUE). Variables considered include: year, longitude, latitude, bottom depth, water mass (proxy as range of depths), bottom temperature, bottom salinity, bottom density.

BPUE		
# variables	Rho	Variables
1	0.653	Water mass
2	0.680	Water mass, Depth,
3	0.701	Water mass. Depth, Salinity
4	0.695	Water mass, Depth, Salinity, Density
CPUE		
# variables	Rho	Variables
1	0.675	Water mass
2	0.681	Water mass, Salinity
3	0.701	Water mass, Salinity, Depth
4	0.700	Water mass, Salinity, Depth, Density

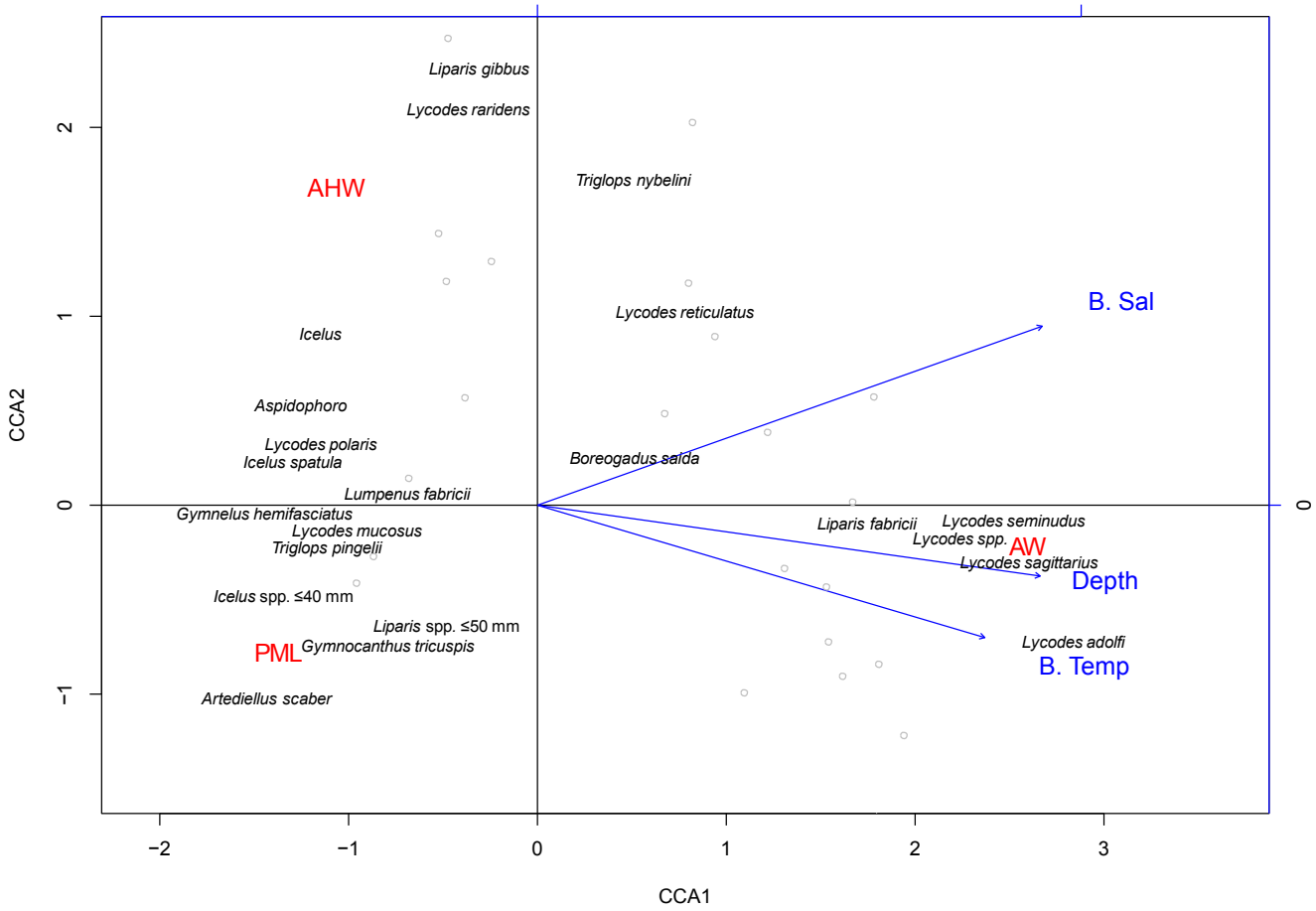

Figure 7.3.4.26. Canonical correspondence analysis (CCA) ordination relating demersal fish abundance in beam trawls during 2013 and 2014 to selected environmental variables at 89 stations.
Continuous environmental variables (blue) denoted by vectors are bottom depth (Depth), bottom salinity (B. Sal), bottom temperature (B. Temp), and longitude. Categorical variables (red) are water masses): PML – Polar Mixed Layer, AHW – Arctic Halocline Water, AW – Atlantic Water. Grey open circles are stations. Fish taxa (black) are those fishes that were selected by SIMPER analysis as descriptive of 90% of at least one of the five communities (Table 7.3.4.14). All taxa in each community are listed in Appendix E5.

Table 7.3.4.14. Canonical correspondence analysis abundance (4RT) of demersal fishes captured by beam trawls and environmental (normalized) variables in the Beaufort Sea at 89 stations in 2013 and 2014 combined.
Upper is for all 51 species and lower is for the 22 species that made up the upper 90% of abundance (Table 7.3.4.10). The F statistic, significance, and axis correlation (i.e., CCA1 and CCA2) of each continuous explanatory variable is listed. The cumulative percent variance explained by the first two CCA axes is listed underneath the CCA2 column in each figure. The categorical variable water mass does not have CCA axis values.

	F	*p*	CCA1	CCA2
Depth	2.955	0.001	0.905	-0.110
Longitude	1.015	0.395	0.126	0.158
Bottom Temp	2.518	0.001	0.806	-0.207
Bottom Salinity	1.802	0.013	0.909	0.280
Water Mass	1.997	0.001		
Cumulative %			11.42	4.20
Total %	3.987	0.001		22.58

	F	*p*	CCA1	CCA2
Depth	4.425	0.001	0.908	0.018
Longitude	1.395	0.108	0.109	-0.170
Bottom Temp	4.690	0.001	0.798	0.206
Bottom Salinity	2.937	0.001	0.880	-0.310
Water Mass	3.663	0.001		
Cumulative %			22.34	6.96
Total %	8.416	0.001		38.11

Table 7.3.4.15. Canonical correspondence analysis abundance (4RT) of demersal fishes captured by beam trawls and environmental (normalized) variables in the Beaufort Sea at 54 stations in 2013 and 2014 combined. The reduced dataset allowed percent mud to be included.
Upper is for all 43 species and lower is for the 22 species that made up the upper 90% of abundance (Table 7.3.4.10). The F statistic, significance, and axis correlation (i.e., CCA1 and CCA2) of each continuous explanatory variable is listed. The cumulative percent variance explained by the first two CCA axes is listed underneath the CCA2 column in each figure. The categorical variable water mass does not have CCA axis values.

	F	*p*	CCA1	CCA2
Depth	3.111	0.001	0.942	0.023
Longitude	0.997	0.309	0.079	0.213
Bottom Salinity	1.698	0.019	0.017	0.497
%Mud	1.235	0.089	0.702	0.545
Water Mass	1.992	0.001		
Cumulative %			10.92	6.27
Total %	2.750	0.001		25.98

	F	*p*	CCA1	CCA2
Depth	3.426	0.001	0.907	-0.129
Longitude	1.010	0.349	0.059	-0.198
Bottom Salinity	1.971	0.016	0.665	-0.517
%Mud	0.982	0.417	0.022	-0.383
%Gravel	1.007	0.371	-0.219	0.144
Water Mass	3.078	0.001		
Cumulative %			16.75	8.33
Total %	3.525	0.001		34.91

7.3.4.5 Demersal Assemblages – Presence/Absence 2012–2014

7.3.4.5.1 Small Net (Beam Trawl) Assemblages

Because of issues with sampling by beam trawl in 2012 (see Section 2.6), a comprehensive analysis of the three years (2012, 2013, and 2014) of beam trawl hauls was conducted on presence/absence of fish taxa. PA transformation gives equal weight to all taxa present; the effect is to down weight the most abundant taxa. When combined, six clusters and one station that did not cluster with anything else were separated at $p = 0.01$ (Figure 7.3.4.27). The two major communities were shelf and slope, as expected. The shelf (34 stations) was the most diverse community with 11 taxa composed of *Boreogadus saida*, five sculpins, one prickleback, very small snailfishes, and three eelpouts (Table 7.3.4.16). While the slope had more stations (48), there were fewer taxa (6). The slope had more abundant *B. saida*, four species of Zoarcid not found on the shelf, and one Liparid. By increasing the sample size and expanding the sample area into the central Beaufort Sea with the inclusion of 2012 data, more communities were differentiated than with 2013–2014 abundance data (Figure 7.3.4.28), including a coastal community and three shelf break communities, at depths of 100 and 200 m, with markedly different compositions but no discernible distribution pattern.

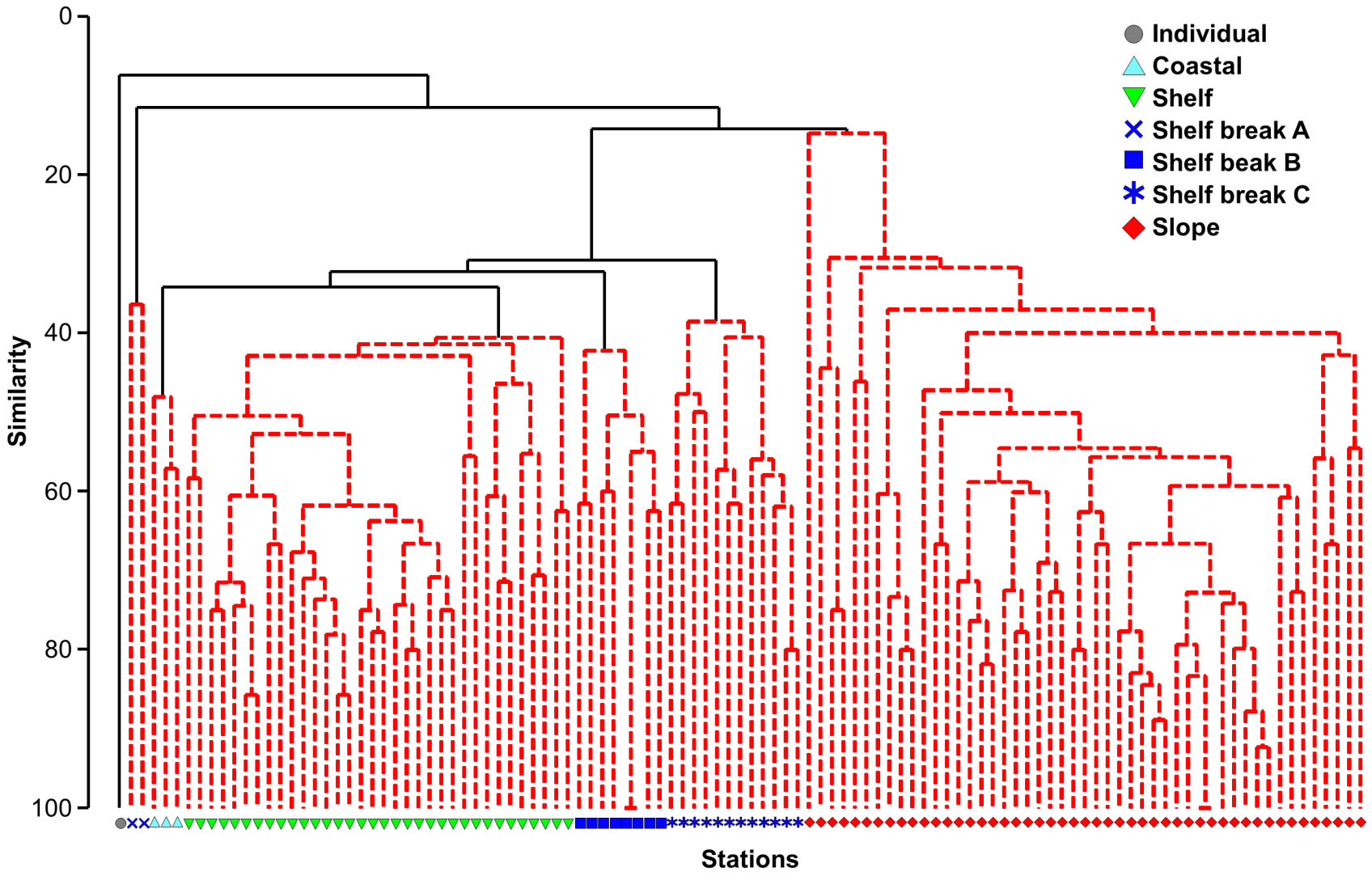

Figure 7.3.4.27. Community structure of demersal fishes in beam trawl hauls in 2012–2014 by presence/absence.
Red lines indicate non-significant differences among stations, and black lines indicate differences between station groups of p <0.01.

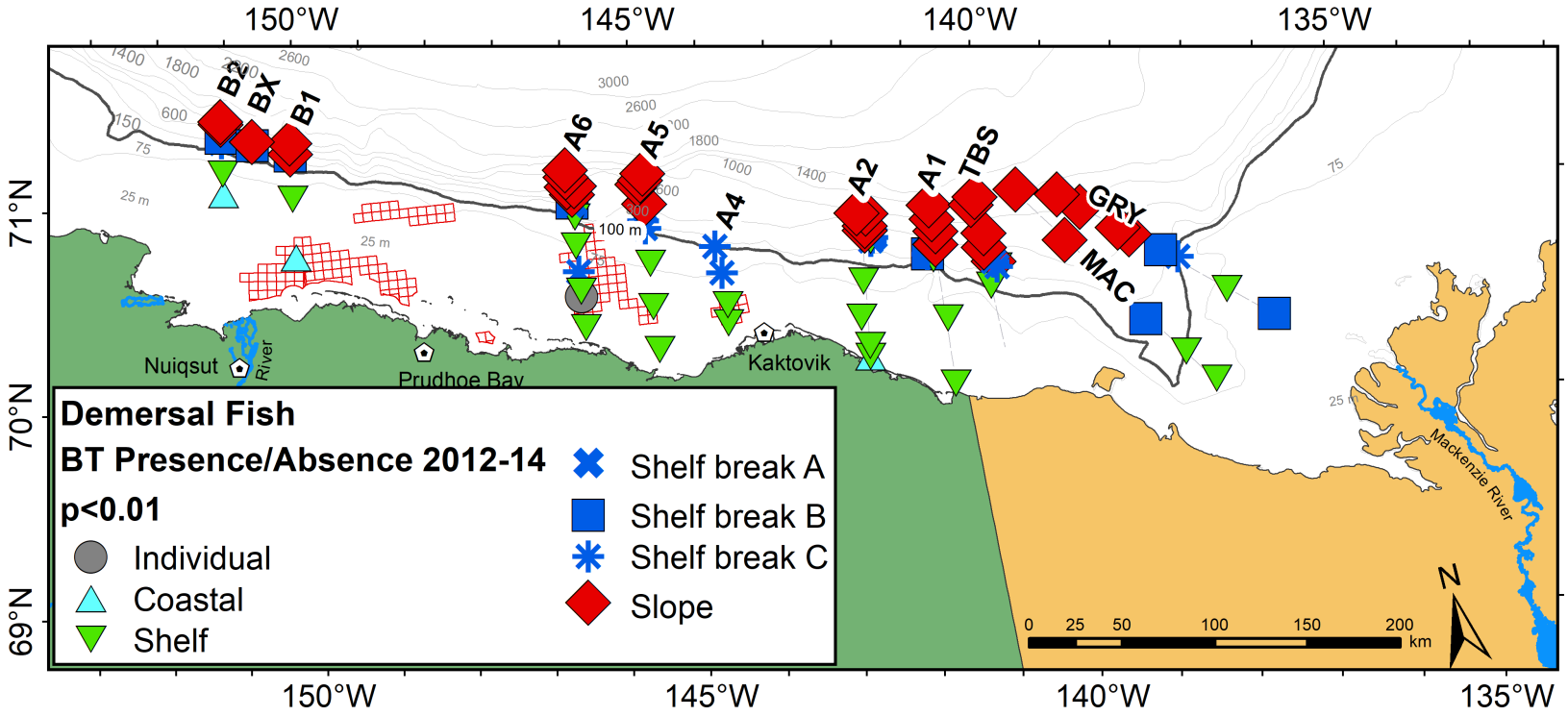

Figure 7.3.4.28. Map of demersal fish communities defined using presence/absence of species collected by beam trawl in the Beaufort Sea during 2012–2014.

Table 7.3.4.16. Presence/absence (PA) of demersal fishes 2012, 2013, and 2014 combined in the Beaufort Sea captured by beam trawl.
Percent contribution of taxa abundance to each of six fish communities (p <0.01) and mean similarity of taxon density within community. Only taxa selected by SIMPER as descriptive of 90% of the community are included here. The distribution of communities is presented visually in Figure 7.3.4.28.

		Fish Communities						
		Coastal	Shelf	Shelf break A	Shelf break B	Shelf break C	Slope	A6-20-13
Taxa	# Stations	3	34	2	8	12	48	1
Gadidae	*Boreogadus saida*	5.02	13.45		37.64	42.87	23.49	
	Cottidae unid. <50 mm	19.77						
Cottidae	Gymnocanthus tricuspis	19.77	12.53					
	Artediellus scaber	3.26	3.33					25.00
	Icelus spp. <40 mm	5.44	10.51					
	Icelus bicornis			50.00				
	Icelus spatula		11.10			18.75		
	Triglops pingelii	5.44	14.40		6.39			
Agonidae	*Aspidophoroides olrikii*		10.58			29.24		
Liparidae	*Liparis* spp. ≤50 mm	19.77	1.96					50.00
	Liparis spp. 51–110 mm							25.00
	Liparis fabricii						10.18	
	Liparis gibbus				8.43			
Zoarcidae	*Gymnelus hemifasciatus*	4.46	5.04					
	Lycodes spp. unid.		7.46				7.46	
	Lycodes adolfi						15.47	
	Lycodes polaris		8.69		37.64			
	Lycodes sagittarius						16.90	
	Lycodes seminudus						18.77	
Stichaeidae	*Lumpenus fabricii*	19.77		50.00				
Total % Contributed		94.98	91.58	100.00	90.09	90.86	90.86	100.00
Within-Community Similarity		51.10	50.09	36.36	50.50	44.28	44.28	100.00

7.3.4.5.2 Large Net (Otter Trawl) Assemblages

Otter trawls (OT) were successfully deployed at 21 stations in the central Beaufort (Colville River, 150º–151º W) in 2012 and at six stations in the eastern Beaufort (146º W) in 2013. A total of 33 unique fish taxa were captured in 2012–2013 at stations where OT gear was deployed. There were as many as 12 taxa captured at the shallow shelf station in the central Beaufort Sea west of 150° W (B transects) during 2012, with only a third as many taxa in 2013 (Figure 7.3.4.29). Because of issues with fishing capabilities (see Section 2.6), analysis was completed on presence/absence of taxa. The fishes clearly separated into shelf (≤100 m), and slope (≥200 m) communities (Figure 7.3.4.30). The pattern of fish presence was different on the shelf compared to the slope (Figure 7.3.4.31) as borne out by the significant difference in the ANOSIM comparison ($R = 0.429$, $p < 0.001$).

There were some differences in the taxa comprising the assemblages of fish captured with a larger net. *Boreogadus saida* was collected at all stations in both the shelf and slope communities (Table 7.3.4.17). Two other genera, *Liparis* spp. ≤50 mm (snailfishes) and *Lycodes* spp. (eelpouts) were captured at both shelf and slope stations, but the species may differ in each community. In addition to *B. saida*, the shelf community was composed mainly of sculpins, small *Liparis* spp., and *A. olrikii.* The slope community was dominated by *B. saida, L. fabricii,* three *Lycodes* species, and Greenland Halibut (*Reinhardtius hippoglossoides*).

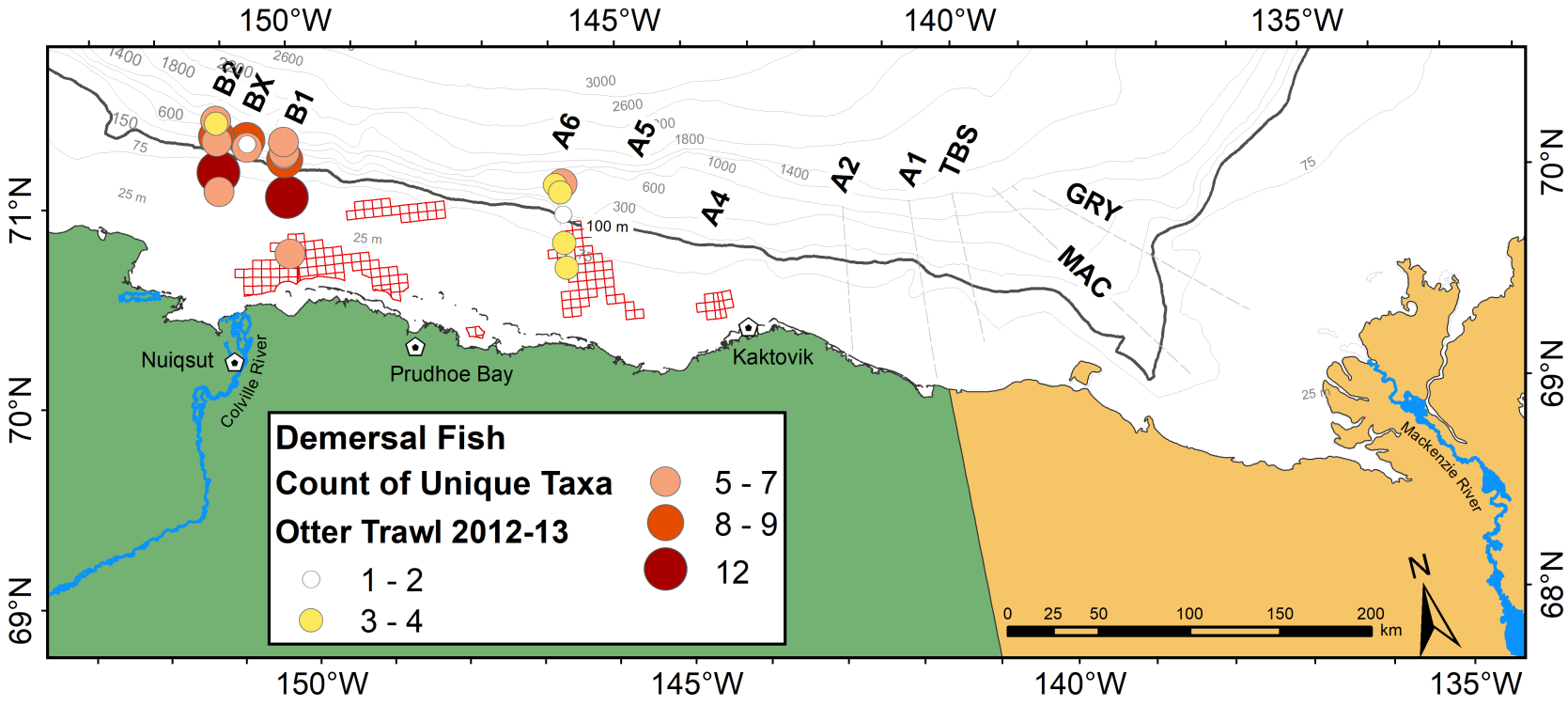

Figure 7.3.4.29. Number of unique demersal fish taxa captured by otter trawl at each station in the Beaufort Sea during 2012–2013.

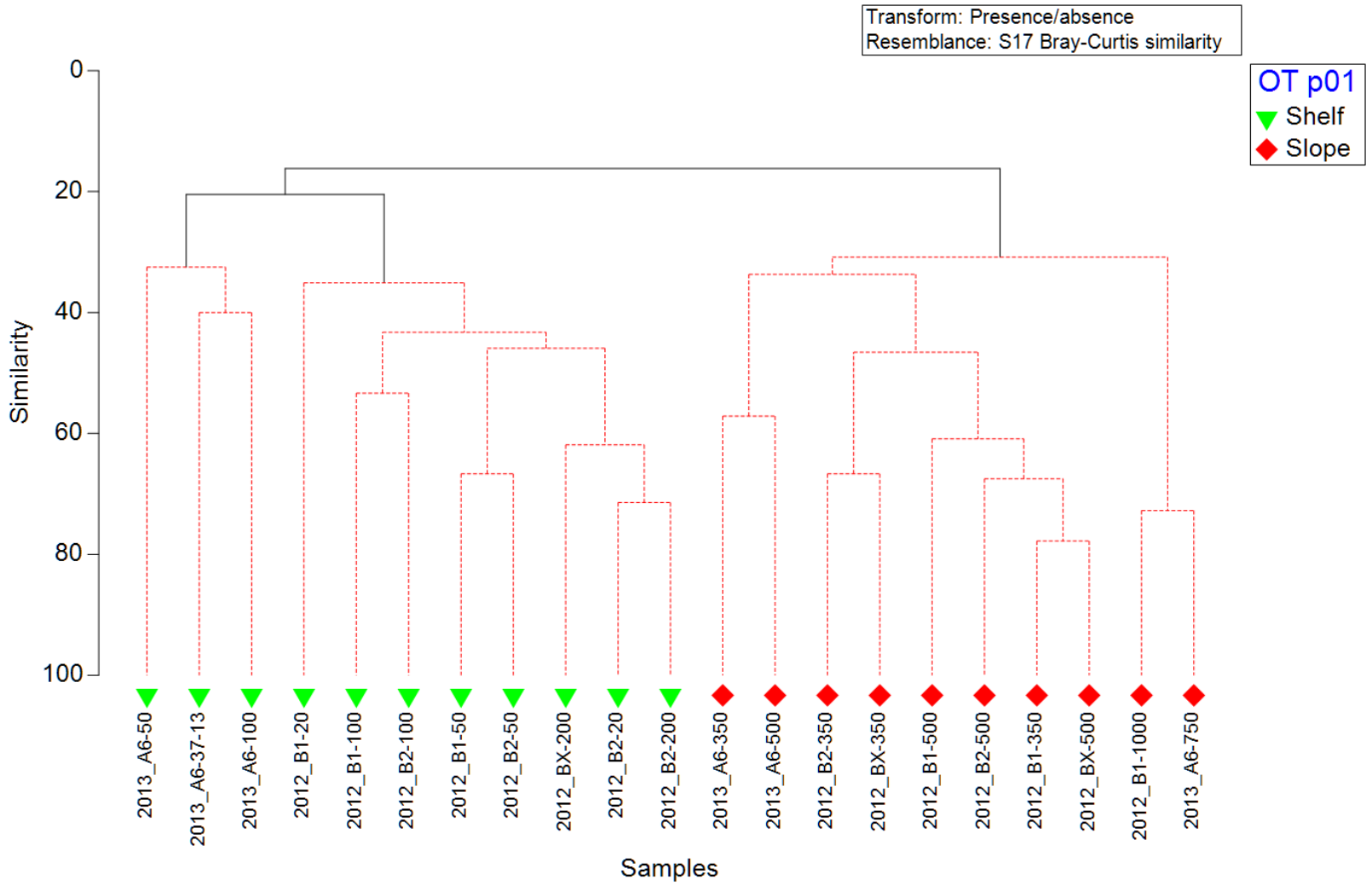

Figure 7.3.4.30. Community structure of demersal fishes in otter trawl hauls in 2012 and 2013 based by presence/absence. Cluster is based on Bray-Curtis similarity matrix. Red lines indicate non-significant differences among stations, and black lines indicate differences between station groups of p <0.01. Shelf ≤100 m, slope ≥200 m.

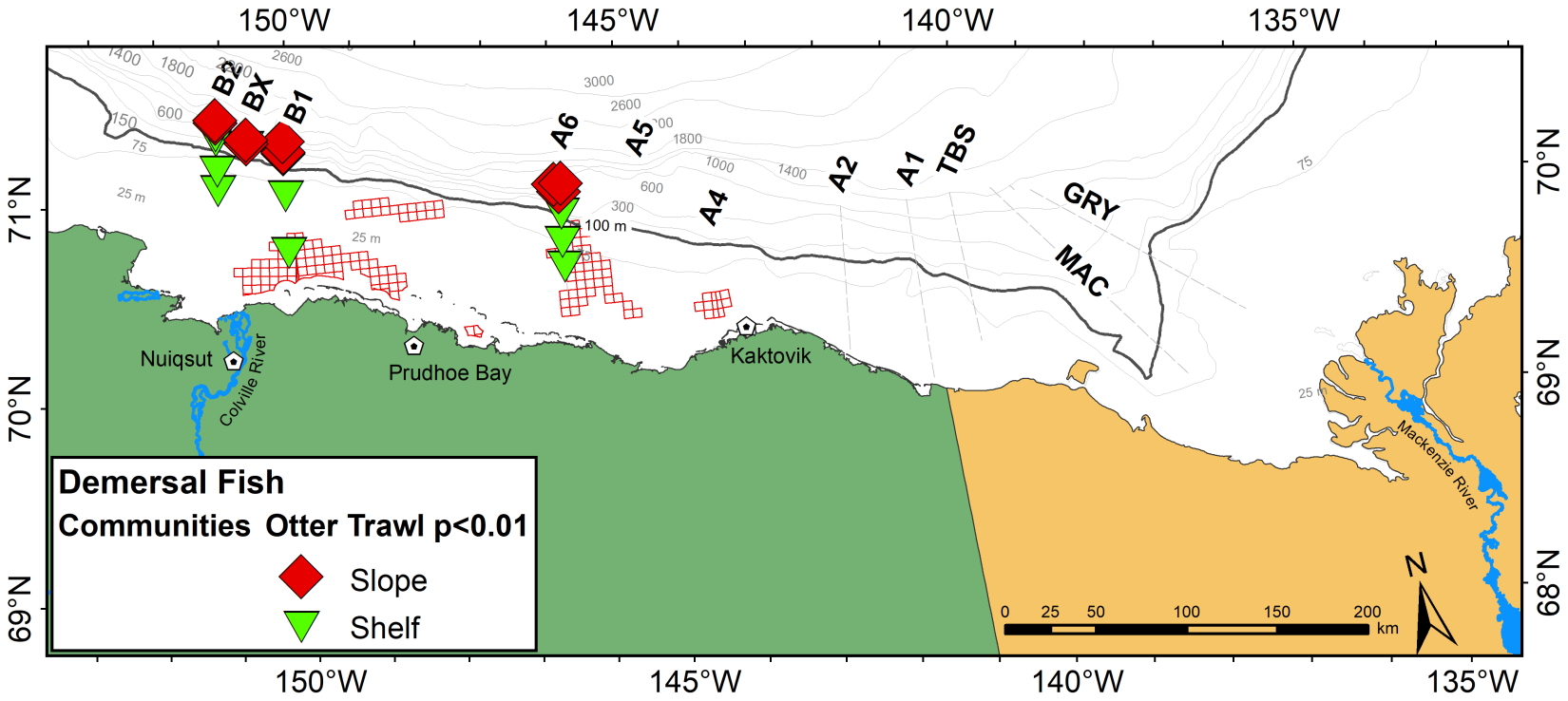

Figure 7.3.4.31. Demersal fish communities defined using presence/absence of species collected by otter trawl in the Beaufort Sea during 2012–2013.

Table 7.3.4.17. Demersal fish community composition as defined by presence/absence in 2012–2013 combined otter trawl hauls.
Percent contribution of taxa presence to each of two fish communities (p <0.01) and mean similarity of taxon density within community. Only taxa selected by SIMPER as descriptive of 90% of the community are included here. The distribution of communities is presented visually in Figure 7.3.4.31.

		Shelf	Slope
Taxa	# Stations	11	10
Gadidae	*Boreogadus saida*	24.90	28.60
Cottidae	*Artediellus scaber*	2.90	
	Gymnocanthus tricuspis	5.99	
	Icelus spatula	17.76	
	Triglops pingelii	9.94	
Liparidae	*Liparis* spp. ≤50 mm	12.74	4.20
	Liparis fabricii		25.32
Agonidae	*Aspidophoroides olrikii*	13.02	
Zoarcidae	*Lycodes reticulatus*	3.60	
	Lycodes sagittarius		7.13
	Lycodes seminudus		13.59
	Lycodes spp.		3.87
Pleuronectidae	*Reinhardtius hippoglossoides*		8.00
Total % Contributed		90.83	90.71
Within Community Similarity		33.90	41.38

7.3.4.5.3 Combined Bottom Assemblages

The two demersal trawl nets, beam and otter, had very different dimensions and configurations, and thus could not be quantitatively compared. As discussed in section 7.3.1, the two nets seemed to be fully selecting the species within the size of the gear capability and number of samples. The BT captured fishes as small as 14 mm and the larger-mesh OT caught fishes as small as 25 mm. The larger OT did not usually catch larger fish than the BT; the largest captured by OT was 638 mm compared to 790 mm by BT (Table 7.3.4.18). Therefore, presence/absence data collected from all bottom trawls could be combined and jointly analyzed. When the 129 samples were combined, seven clusters were produced at p = 0.01 (Figure 7.3.4.32). There was one independent station (A6-20 in 2013) that did not cluster with anything else in this or any other cluster analysis. Because presence/absence is a transformation that gives equal weight to all taxon without regard for biomass or abundance, the composition of the communities was not the same as for previously presented communities. As for all other analyses, shelf and slope communities were dominant; a coastal community and shelf break communities were present, though compositions of the latter were not the same as for the quantitative analysis of 2014–2014. This is the only analysis in which there were four shelf break communities formed; however, as in the previous analyses, there does not seem to be a pattern in the distribution of the shelf break communities (Figure 7.3.4.33). Within 90% of the taxa

describing the communities, only *Boreogadus saida* was a component of each of the seven (Table 7.3.4.19). *Liparis fabricii* was the only other species captured in both shallow (coastal) and deep (slope) water. Small (<50 mm) Cottidae were exclusively in the coastal community, small (40 mm) *Icelus* sculpins were unique to the shelf, and *Triglops nybelini* was only in the 3-station shelf break 4 community. One of two species of Agonidae was captured in the shelf and shelf break stations, though no Agonids were found in the coastal or slope communities. None of the five representative Liparid taxa were captured in the shelf or shelf break 3 communities. Across the four shelf break communities, there were six species and one generic taxon of eelpouts, but only *L. polaris* was found in more than one community. The most speciose communities, coastal and shelf, also had the highest within community similarities (>50%).

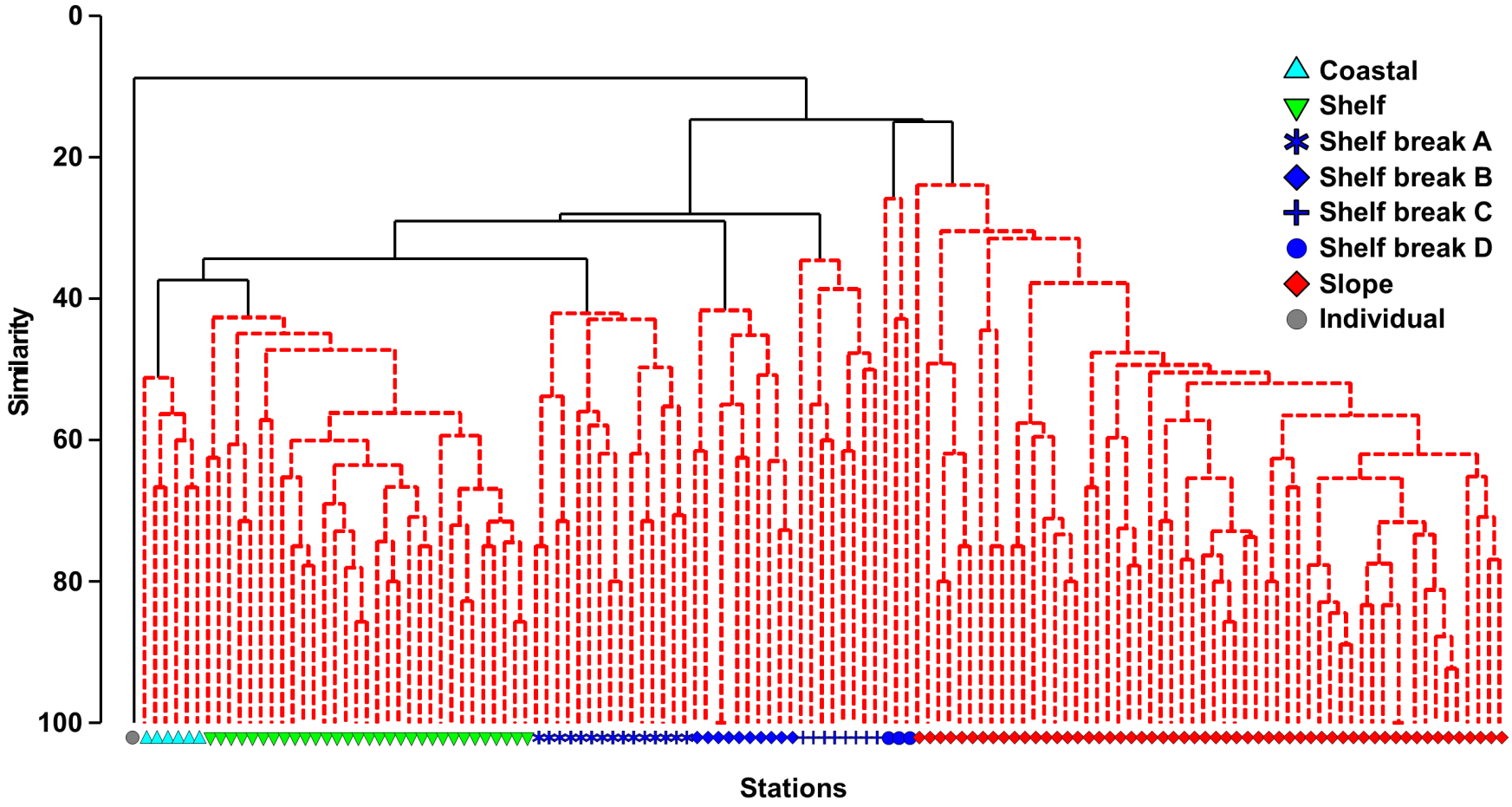

Figure 7.3.4.32. Presence/absence (PA) transformation for demersal fish catches from all stations sampled by beam and otter trawls in 2012, 2013, and 2014 in the Beaufort Sea.

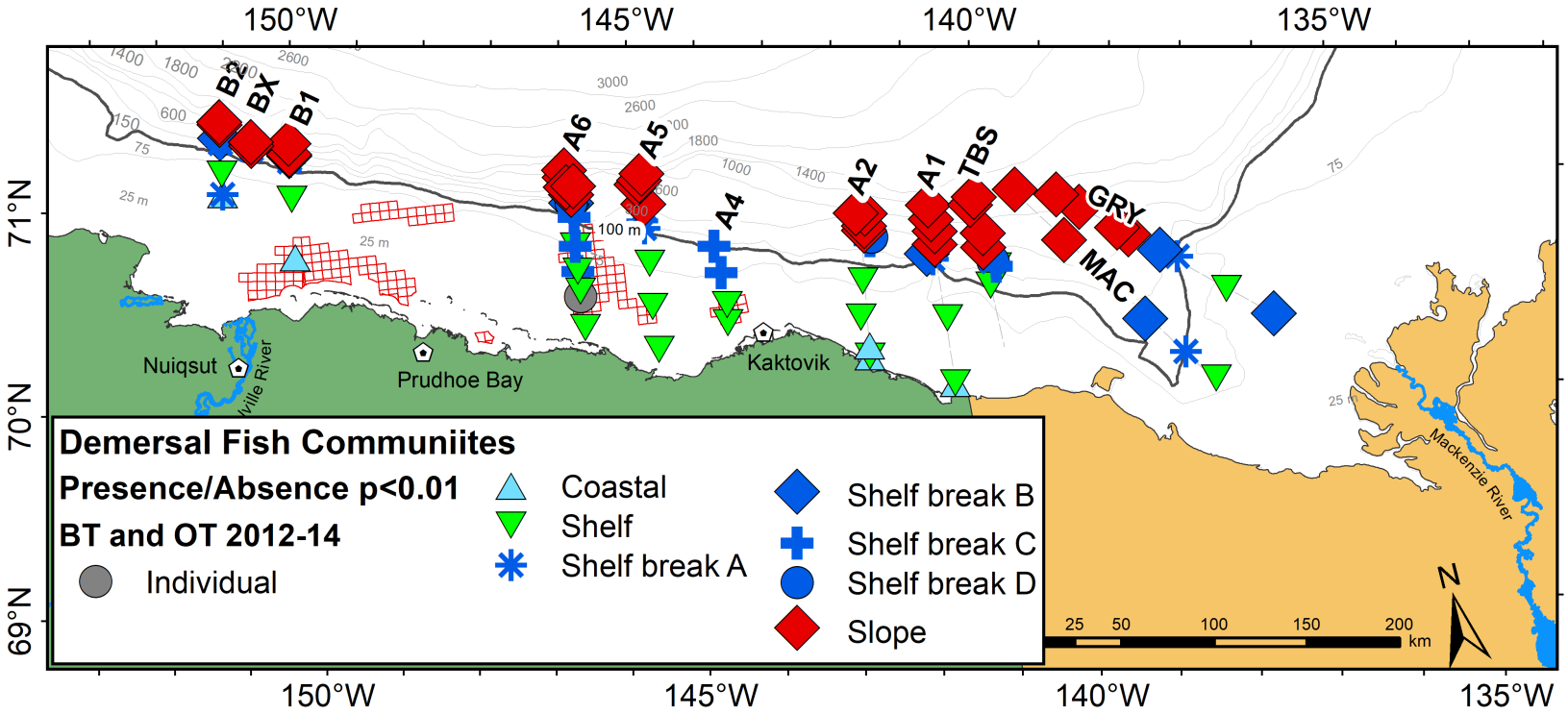

Figure 7.3.4.33. Demersal fish communities defined using presence/absence of species collected by beam and otter trawls in the Beaufort Sea during 2012–2014.

Table 7.3.4.18. Demersal fishes, by family and species, captured by two different bottom trawls. Beam trawls had 4-mm mesh in codend. Otter trawl had 19-mm mesh codend. N is total number caught. Size range minimum, maximum, mean and standard deviation of fishes by gear.

Species	Gear	n fish	Min–Max (mm)	Mean±SD
Rajidae				
Rajidae spp.				
	BT	8	156–485	313.1±111
	OT	1	147	147
Amblyraja hyperborea				
	BT	2	764–790	777±18.4
	OT	2	540–638	589±69.3
Osmeridae				
Mallotus catervarius				
	BT	5	90–135	113.2±17.9
Osmerus dentex				
	BT	1	110	110
	OT	1	94	94
Myctophidae				
Myctophidae sp.				
	BT	1	144	144
Benthosema glaciale				
	BT	2	81–84	82.5±2.1
Gadidae				
Boreogadus saida				
	BT	1408	15–230	79.8±38.4
	OT	800	25–240	91.1±37.8
Cottidae				
Cottidae spp.				
	BT	67	19–42	32.2±6.6
	OT	8	30–81	44.1±16.8
Artediellus scaber				
	BT	146	14–114	40.7±23.3
	OT	12	44–85	54.6±12.1
Gymnocanthus tricuspis				
	BT	714	19–147	42.7±14.9
	OT	88	28–110	47.0±17.1
Icelus bicornis				
	BT	103	27–87	45.2±12.1
Icelus spatula				
	BT	430	20–111	53.8±12.8
	OT	37	34–86	55.0±13.1
Icelus spp.				
	BT	133	20–38	27.3±3.1
	OT	1	87	87
Myoxocephalus scorpius				
	BT	6	45–89	71.2±19.4
	OT	1	44	44
Triglops nybelini				
	BT	15	81–126	98.4±13.3
Triglops pingelii				
	BT	204	26–120	62.1±20.9
	OT	65	38–137	75.9±20.5
Hemitripteridae				
Hemitripteridae sp.				
	BT	1	28	28
Psychrolutidae				
Psychrolutidae spp.				
	BT	2	37–120	78.5±58.7
Psychrolutidae cf. *Psychrolutes phrictus*				
	OT	1	100	100
Agonidae				
Aspidophoroides monopterygius				
	OT	1	95	95
Aspidophoroides olrikii				
	BT	303	27–80	56.0±8.1
	OT	67	37–74	57.7±8.1
Leptagonus decagonus				
	BT	4	54–161	108±60.1
Cyclopteridae				
Cyclopteridae spp.				
	BT	9	18–48	31.3±9.1
	OT	1	27	27
Eumicrotremus derjugini				
	BT	9	15–64	40.8±20.3
	OT	2	39–54	46.5±10.6
Psychrolutidae				
Cottunculus microps				
	BT	18	45–223	127.4±57.1
Liparidae				
Careproctus lerikimae				
	BT	22	46–142	97.2±26.5
	OT	29	52–145	91.3±23.3
Liparis bathyarcticus				
	BT	10	32–223	99.2±66.9
	OT	2	84–86	85.0±1.4
Liparis fabricii				
	BT	74	19–210	124.9±55.5
	OT	54	27–212	130.1±53.1
Liparis gibbus				
	BT	11	19–198	104.8±57.1
	OT	4	96–133	111.0±15.8
Liparis tunicatus				
	BT	4	48–75	61.3±13.7
	OT	1	147	147
Liparis spp.				
	BT	1196	17–133	36.1±7.5
	OT	141	18–126	37.1±11.4
Paraliparis bathybius				
	BT	3	150–181	165±15.5
Rhodichthys regina				
	BT	8	81–222	159.8±51.2

7.3.4.18. continued.

Species	Gear	n fish	Min–Max (mm)	Mean±SD
Zoarcidae				
Gymnelus hemifasciatus				
	BT	71	44–139	74.0±18.5
	OT	3	98–128	111.3±15.3
Gymnelus viridis				
	BT	11	69–117	92.5±13.5
	OT	3	96–115	104.3±9.7
Gymnelus spp.				
	BT	8	53–90	64.4±11.5
Lycenchelys kolthoffi				
	BT	1	183	183
Lycodes adolfi				
	BT	193	38–185	106.7±41.0
	OT	62	64–205	126.6±36.3
Lycodes eudipleurostictus				
	BT	27	55–396	203.5±88.5
	OT	2	135–330	232.5±137.9
Lycodes frigidus				
	BT	4	40–212	120.8±74.8
Lycodes jugoricus				
	BT	4	81–292	152.8±99.3
Lycodes mucosus				
	BT	11	36–126	60.5±30.7
	OT	4	77–102	83.8±12.2
Lycodes pallidus				
	BT	15	65–246	172.3±48.7
Lycodes polaris				
	BT	74	32–222	77.3±42
	OT	18	42–116	74.7±20.2
Lycodes raridens				
	BT	3	120–181	144.3±32.3
	OT	1	209	209
Lycodes reticulatus				
	BT	17	48–405	103.2±88.2
	OT	14	48–199	109.2±59
Lycodes rossi				
	BT	17	44–202	80.8±47.3
Lycodes sagittarius				
	BT	163	44–427	202.1±94.8
	OT	54	53–375	218.9±67.6
Lycodes seminudus				
	BT	155	41–444	181.6±108.2
	OT	49	67–465	160.3±111.8
Zoarcidae (continued)				
Lycodes squamiventer				
	BT	6	64–96	81.8±11.9
	OT	2	177–358	267.5±128
Lycodes spp.				
	BT	88	28–121	70.6±18.7
	OT	42	44–143	74.8±23.8
Stichaeidae				
Stichaeidae sp.				
	BT	1	49	49
Anisarchus medius				
	BT	78	49–134	79.6±20.4
	OT	3	79–90	84.0±5.6
Eumesogrammus praecisus				
	BT	5	31–101	60.4±30.7
	OT	1	78	78
Leptoclinus maculatus				
	BT	4	94–174	121.5±35.7
	OT	1	178	178
Lumpenus fabricii				
	BT	157	46–124	62.0±13.1
	OT	15	59–103	75.1±13.3
Stichaeus punctatus				
	BT	5	33–48	37.4±6.2
Lumpeninae				
Lumpeninae spp.				
	BT	61	26–67	48.0±10.7
Ammodytidae				
Ammodytes hexapterus				
	BT	2	95–114	104.5±13.4
Pleuronectidae				
Pleuronectidae (larva)				
	BT	2	43–45	44.0±1.4
Hippoglossoides robustus				
	BT	1	265	265
	OT	2	216–314	265±69.3
Reinhardtius hippoglossoides				
	BT	8	387–540	459±56.3
	OT	4	351–520	429±72.2

Table 7.3.4.19. Demersal fish community composition as defined by presence/absence in 2012–2014 beam and otter trawl hauls.
Percent contribution of taxa presence to each of seven fish communities (p <0.01), number of stations, and mean similarity of taxon density within community. Only taxa selected by SIMPER as descriptive of 90% of the community are included here. The distribution of communities is presented visually in Figure 7.3.4.33.

		Coastal	Shelf	Shelf break 1	Shelf break 2	Shelf break 3	Shelf break 4	Slope
Number of Stations		6	31	15	19	8	3	44
Gadidae	*Boreogadus saida*	12.22	10.35	35.93	36.96	25.21	15.10	24.00
Cottidae	Cottidae ≤50 mm	19.85						
	Artediellus scaber	6.96	3.43					
	Gymnocanthus tricuspis	19.85	14.05					
	Icelus bicornis					5.21	19.22	
	Icelus spp. ≤40 mm		13.63					
	Icelus spatula		13.52	3.73		57.07		
	Triglops nybelini						15.10	
	Triglops pingelii	7.19	13.76	5.89				
Agonidae	*Aspidophoroides olrikii*		9.47	35.93		4.81		
	Leptagonus decagonus						15.10	
Liparidae	*Careproctus lerikimae*				7.10			
	Liparis fabricii	13.23					19.22	12.22
	Liparis gibbus				5.46			
	Liparis spp. ≤50 mm	13.23		7.06	4.30			
	Liparis spp. 51–110 mm			4.11				
Zoarcidae	*Gymnelus hemifasciatus*		4.74					
	Lycodes adolfi							12.81
	Lycodes polaris		8.48		36.96			
	Lycodes reticulatus						16.26	
	Lycodes sagittarius							16.77
	Lycodes seminudus							19.96
	Lycodes spp. unid							7.11
Total % Contributed		92.53	91.42	92.64	90.78	92.30	100.0	92.87
With Community Similarity		56.47	54.49	46.90	48.53	42.07	31.54	45.30

nMDS revealed patterns and ANOSIM (non-parametric ANOVA) tested relationships among fish communities and physical factors associated with them. The four major groups of fishes (Figure 7.3.4.34) corresponded approximately to water mass and sample depth, i.e., coastal (10–20 m), shelf (20–50 m), shelf break (100–200 m), and slope (350–1500 m) (Figure 7.3.4.35). Depth significantly affected fish community (R = 0.533, p <0.001), and assemblages differed between all water masses (Table 7.3.4.20). Year and longitude were related to each other as sample locations in 2012 did not overlap with those in 2013 and 2014, and the easternmost stations in 2013 were not resampled in 2014. However, neither longitude (R = 0.001, p = 0.448) nor year of collection (Table 7.3.4.21, Figure 7.3.4.36) significantly affected fish community structure individually nor in relation to each other (Table 7.3.4.22). Furthermore, despite the difference in net sizes and codend mesh (i.e., BT 3 or 6 mm and OT 19 mm), there was no

statistical difference in fish assemblages between the nets (R = 0.02, p = 0.283), nor any pattern evident in the nMDS (Figure 7.3.4.36).

We examined the presence/absence of demersal fish in relation to environmental variables using BEST. Unfortunately, not all environmental variables could be assessed at all stations. Therefore, we developed the most robust sets of data possible to include the available environmental variables associated with beam trawl hauls. The largest data set had 124 collections of fish and environmental variables, including year, longitude, latitude, bottom depth, bottom temperature, bottom salinity, and bottom density (Table 7.3.4.23). When examining all 124 samples as a group, bottom salinity alone had a rho of 0.545. Adding depth increased the correlation to 0.599; however, adding more than two variables decreased the relationship. Consideration of only the 36 collections on the shelf (10–50 m) the best relationship included depth and bottom density, but the rho was only 0.412, much lower than for all depth samples combined. The correlation was the best, but not good (ρ = 0.185), when including only depth for the shelf break (100–200 m). With only slope samples (n = 56), the best achievable relationship included four variables: depth, latitude, bottom temperature, and bottom density, but the rho (ρ = 0.256) was much lower than for the whole data set or just the shelf. Using a subset of 70 stations increased the environmental variables available from seven to 12, and included year, bottom depth, longitude, latitude, bottom temperature, bottom salinity, bottom density, percent gravel, percent sand, percent mud, sediment chlorophyll-*a*, and sediment total organic carbon (TOC). The results were similar to the larger data set that tested fewer variables. A good correlation (ρ = 0.584) was produced including only depth (Table 7.3.4.24). The only sediment variable that was included was TOC, but only with three other variables and at a much reduced rho value (ρ = 0.524). Of the 70 stations, only 13 were ≥350 m, and those were all from 2012 when the box core was used to sample deep sites. These results bode well for being able to use the easiest to measure environmental variables for this analysis, i.e., depth, bottom temperature, and bottom salinity, with bottom density calculated from temperature and salinity.

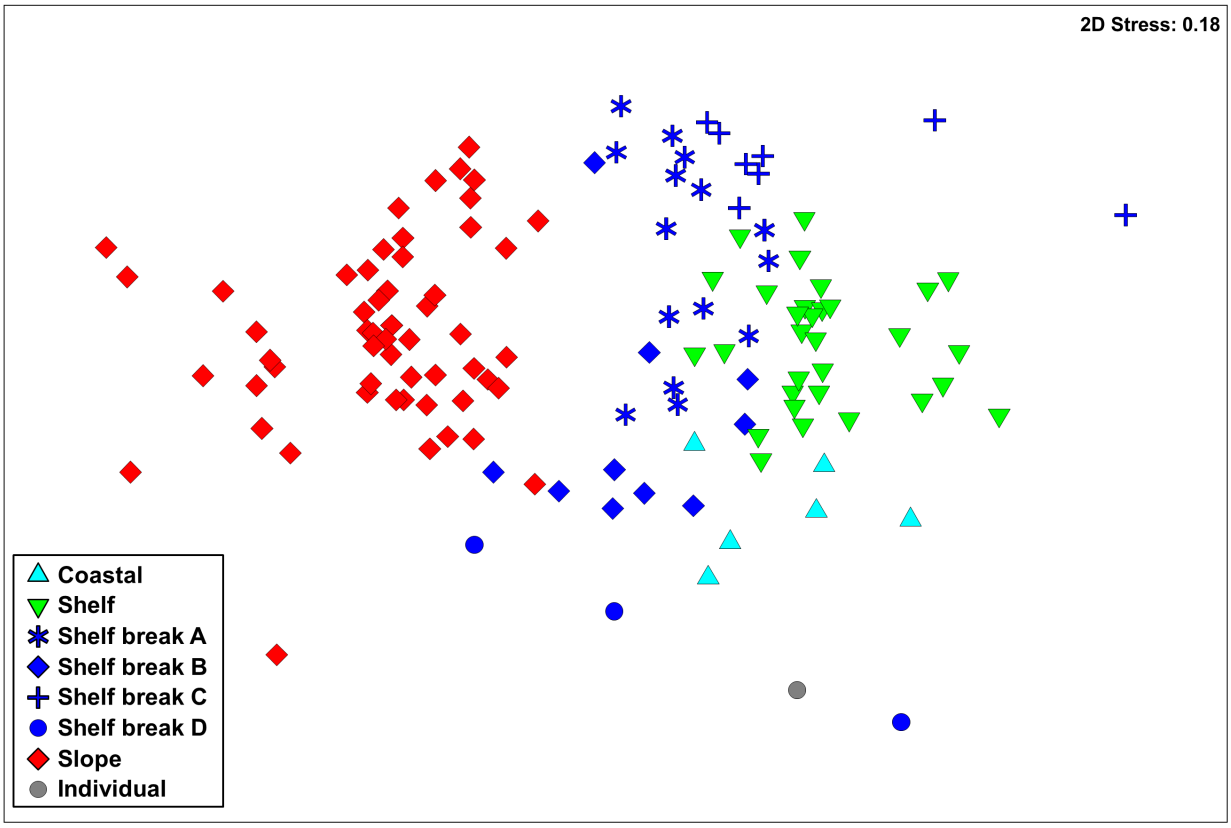

Figure 7.3.4.34. nMDS of demersal fish captured by beam and otter trawls in 2012, 2013, and 2014 in the Beaufort Sea based on presence/absence.

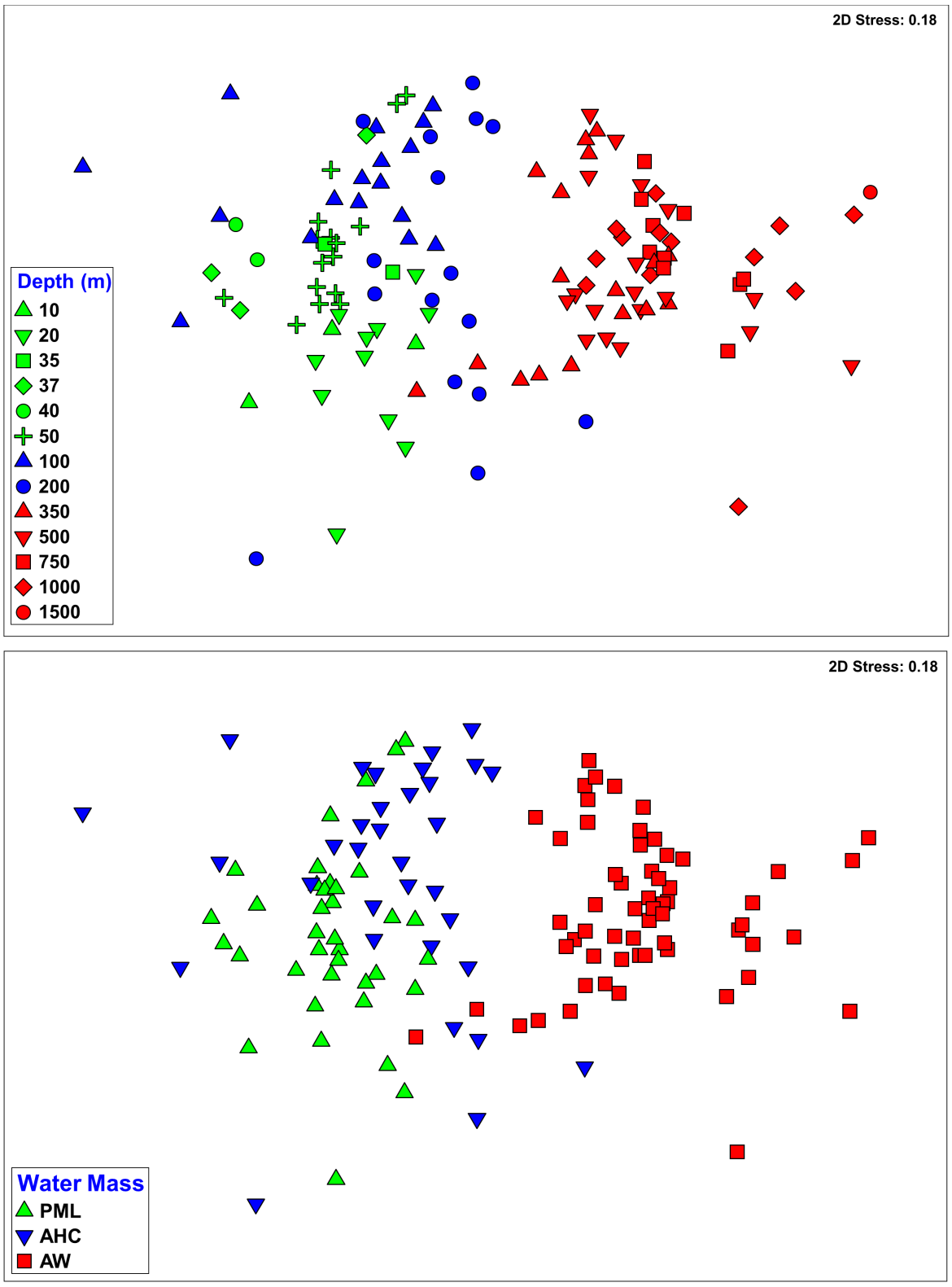

Figure 7.3.4.35. nMDS of demersal fish captured by beam and otter trawls in 2012, 2013, and 2014 based on presence/absence. PML – Polar Mixed Layer, AHW – Arctic Halocline Water, AW – Atlantic Water.

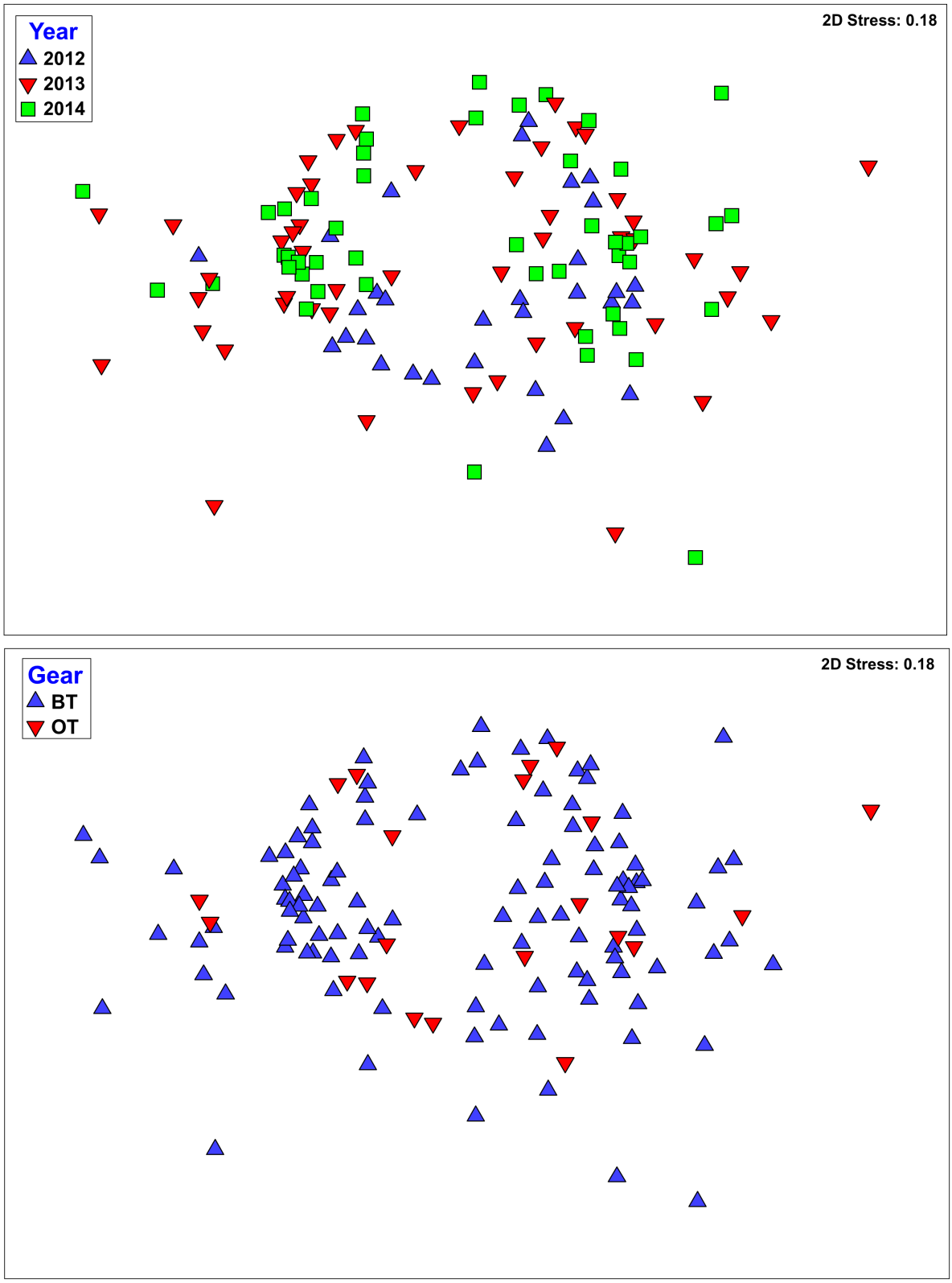

Figure 7.3.4.36. nMDS of demersal fish captured by beam and otter trawls in 2012, 2013, and 2014 based on presence/absence. BT – beam trawl, OT – otter trawl.

Table 7.3.4.20. Effects of water mass on community composition of demersal fish based on presence/absence in 2012–2014 beam and otter trawl stations in the Beaufort Sea.
PML – Polar Mixed Layer, AHW – Arctic Halocline Water, AW – Atlantic Water. One-way ANOSIM R is sample statistic rho, *p* is significance.

Water masses	R	*p*
PML vs. AHW	0.285	<0.001
PML vs. AW	0.820	<0.001
AHW vs. AW	0.688	<0.001

Table 7.3.4.21. Effects of year on community composition of demersal fish based on presence/absence at 2012–2014 beam and otter trawl stations in the Beaufort Sea.
One-way ANOSIM R is sample statistic rho, *p* is significance.

Years	R	*p*
2012 vs. 2013	0.047	0.04
2012 vs. 2014	0.071	0.14
2013 vs. 2014	0.005	0.287

Table 7.3.4.22. Effects of year and longitude on community composition of demersal fish based on presence/absence at 2012–2014 beam and otter trawl stations in the Beaufort Sea.
Two-way crossed ANOSIM R is sample statistic rho, *p* is significance.

	R	*p*
Year	-0.046	0.879
Longitude	-0.005	0.591

Table 7.3.4.23. BEST (stepwise) relationship of presence/absence of demersal fishes and environmental variables at 124 stations in the Beaufort Sea in 2012, 2013 and 2014.
Variables considered: year, bottom depth, longitude, latitude, bottom temperature, bottom salinity, and bottom density. N = 124 samples for which beam and otter trawl and environmental variables were available. In addition to the whole depth range, further analyses were conducted separately for samples on the shelf (10–50 m), shelf break (100–200 m), and slope (350–1000 m).

Shelf communities 10–50 m		n = 36
# variables	Rho	Variables
1	0.412	Bottom Density
2	0.422	Depth, Bottom Density
3	0.419	Depth, Bottom Salinity, Bottom Density
4	0.322	Depth, Bottom Temperature, Bottom Salinity, Bottom Density

Shelf Break communities 100–200 m		n = 32
# variables	Rho	Variables
1	0.185	Depth
2	0.151	Depth, Bottom Salinity
3	0.149	Depth, Bottom Salinity, Bottom Density
4	0.131	Year, Depth, Bottom Salinity, Bottom Density

Slope communities 350–1000 m		n = 56
# variables	Rho	Variables
1	0.197	Bottom Depth
2	0.256	Depth, Latitude
3	0.263	Depth, Latitude, Bottom Salinity
4	0.265	Depth, Latitude, Bottom Temperature, Bottom Density

All-depth communities 10–1000 m		n = 124
# variables	Rho	Variables
1	0.545	Bottom Salinity
2	0.599	Depth, Bottom Salinity
3	0.597	Depth, Bottom Salinity, Bottom Density
4	0.5325	Depth, Bottom Temperature, Bottom Salinity, Bottom Density

Table 7.3.4.24. BEST (stepwise) relationship of presence/absence of demersal fishes and environmental variables at 70 stations in the Beaufort Sea in 2012, 2013 and 2014.
Variables considered: year, bottom depth, longitude, latitude, bottom temperature, bottom salinity, bottom density, %gravel, %sand, %mud, sediment chlorophyll-*a*, and sediment total organic carbon (TOC). N = 70 samples for which beam and otter trawl and environmental variables were available.

10–1000 m		n = 70
# variables	Rho	Variables
1	0.584	Depth
2	0.574	Depth, Bottom Salinity
3	0.568	Depth, Bottom Salinity, Bottom Density
4	0.524	Depth, TOC, Bottom Salinity, Bottom Density

7.4 Discussion

This study is an important contribution to knowledge about the fishes that occupy the shelf and slope of the Beaufort Sea. This was the first systematic sampling using the same benthic (beam trawl) and pelagic (Isaacs-Kidd midwater trawl) fishing gears across the US Beaufort shelf and slope. Knowledge of the current status of fish populations in the Beaufort Sea is necessary to identify fish species life stages, essential fish habitat, and to inform the new emphasis on food web modeling and Arctic climate change issues. This research was designed to address the hypotheses that distribution, relative abundance, and species assemblages are equal across life stage, habitat, central and east US Beaufort Sea waters, east and west sides of the Mackenzie Canyon, and shelf (benthic and pelagic) and slope (benthic and pelagic) waters.

7.4.1 Beaufort Large Marine Ecosystem Patterns in Fish Richness, Biomass and Abundance

Our catch of least 51 unique taxa from 14 families is quite remarkable compared to the Arctic as a whole. According to Mecklenburg et al. (2011), there are 242 species of fish within 45 families in the greater Arctic region (sculpins and eelpouts make up more than half the species). Of these, 99 species are considered true arctic, predominantly arctic, and arctic-boreal fish. Thus, we captured over half the arctic species.

The two major fish families we found in the central and eastern US Beaufort Sea, Gadidae (cods) and Zoarcidae (eelpouts), are also among the most abundant across the whole Beaufort Sea. *Boreogadus saida* was the most abundant species between 7.5 m and 126 m depth in the western Canadian Beaufort Sea (Majewski et al. 2013). Using similar beam trawl gear as the present study, Norcross et al. (in review) also found *B. saida* to be the most abundant fish species captured on the shelf in the western and central US Beaufort Sea, with numbers equal to abundance of all Cottidae combined. In the western US Beaufort Sea, sampling with a NOAA 83-112 Eastern bottom trawl, Rand and Logerwell (2011) found the most abundant demersal fishes to be gadids (*B. saida*, and *Gadus chalcogrammus*), zoarcids (*Lycodes* spp.), and the pleuronectid (*Hippoglossoides robustus*). Eelpouts and snailfishes (Liparidae) were abundant but much less so than cods and sculpins. Similar families and species were the most abundant captured by Frost and Lowry in the 1970s (1983) including *B. saida*, *Lycodes polaris*), and *Icelus bicornis*. Other species that were abundant in the present study, including *Gymnocanthus*

tricuspis, *Icelus spatula*, *Lycodes polaris*, and *Aspidophoroides olrikii*, were also commonly caught in the Canadian Beaufort Sea (Majewski et al. 2013).

The present study is most comparable to its Canadian counterpart, Beaufort Regional Environmental Assessment (BREA), which also sampled 20–1000 m. Similar distributions of fish families and species were found across the whole Beaufort Sea (Majewski et al. 2016). *B. saida* was the most abundant species and was found across more areas and depths than other species (Figures 7.3.2.10–11). *G. tricuspis* (Appendix E3), I. *spatula* (Appendix E3), *and L. polaris* (Figure 7.3.4.36) were mainly on the shelf across the whole US–Canada Beaufort Sea area. While the agonid *A. olrikii* appeared on the broad shelf of the Canadian Beaufort Sea, in the US it was found mostly at 100–200 m (Appendix E2). As found in this study (Figure 7.3.4.36), BREA sampling in the Canadian Beaufort Sea showed that the distribution of particular zoarcids of Lycodes spp. changed with depth. Also, as in our study, they found that high biomass, low abundance species like *Reinhardtius hippoglossoides* (Pleuronectidae) and *Amblyraja hyperborea* (Rajidae) only occurred >350 m (Appendix E3).

In this study, communities of juvenile and larval midwater fishes demonstrated distribution patterns including west vs. east geographical concentrations, concentration on the slope, and spread along the coast. The number of juvenile and larval taxa captured pelagically was very small compared to that captured demersally. The abundance of midwater fishes was very low at the eastern transects, including in the Mackenzie River outflow. All Transboundary samples were collected in the late open-water season, which could bias the results. Additionally, the 2012 samples were collected later in the season than were 2013 samples. While there may be more or different small midwater fishes present at other times in the year, the ability to conduct benthic and pelagic trawls before August or after September in the Beaufort Sea is seldom possible without using a vessel with an ice-strengthened hull, which was not available to this project.

7.4.2 Life History Characteristics of US Beaufort Sea Fishes

This research added basic age and size life history information for several fishes. All but two of the species measured were shorter than sizes previously recorded. *Liparis fabricii* was in measurement error range (±2 mm), and the present study expanded the maximum known size of *Lycodes sagittarius* by 149 mm up to 429 mm (Table 7.4.1). Half of our measurements expand species' known maximum ages, including six species for which there were no previous records. *Lycodes polaris* age was extended by two years to age 7, and *Liparis fabricii*, previously without age record, now is documented as age 5. Three *Lycodes* species now have recorded ages including *L. adolfi,* age 12, and the two oldest species we aged, *L. sagittarius* (age 26) and *Lycodes seminudus* (age 24). The biggest surprises were the small species with double-digit ages: *Aspidophoroides olrikii* – 80 mm, age 15, and *Anisarchus medius* – 134 mm, age 19.

Despite having only six ages represented (0–5 yrs), the size at age structure of *Boreogadus saida* is very complex. Notable overlaps in size ranges of different ages make it difficult to estimate age based on length of fish. While all *B. saida* ≤64 mm are age-0 (Figure 7.3.2.1), another age-0 *B. saida* might be twice that length. A 125 mm fish could be age-0, age-1, age-2 or age-3. Because this confounding of size at age, the otoliths from *B. saida* were double or triple checked to confirm the ages assigned. The pattern of overlapping size at age held in each of the three years that *B. saida* was collected.

Because the pattern of broad size range at age for *B. saida* was observed in a large sample size and over all three years (n = 781; Figure 7.3.2.1), it is reasonable to assume that we observed a true size at age distribution. The average length at age for all ages of *B. saida* was greater in

2012 than in 2013 and 2014, possibly due to the later timing of the cruise in 2012. The cause of size differences in catches is not clear-cut; it could be because the 2012 fish came from a sampling area in the central Beaufort Sea or because they were captured in September, whereas the 2013 and 2014 came from the eastern Beaufort Sea in August and had less time to grow. Alternatively, environmental dissimilarities between the years could have caused the differences. Egg hatching events are highly variable both spatially and temporally (Bouchard and Fortier 2011). Hatch date of *B. saida* in the western and central US Beaufort Sea during 2011 ranged from early January to mid-June with a peak at the end of April (Norcross et al. in review). *B. saida* hatching between January and March favors larger juvenile growth and a greater chance of survival than those which hatch later from March through July (Craig et al. 1982, Bouchard and Fortier 2011). Earlier hatching is another possible explanation for the larger size of *B. saida* collected in 2012 compared to 2013 and 2014. Bouchard and Fortier (2011) hypothesize that *B. saida* in freshwater refuges experience warmer water, so they hatch earlier and have a longer growing season. While the outflow of the Colville River could make this a viable hypothesis for the larger lengths of *B. saida* in 2012, the concept fails because age-0 fish collected in the Mackenzie River plume in 2013 were not larger than those caught in 2014 when there was no sampling near the Mackenzie or Colville Rivers.

Based on our data, the fishes in the Beaufort Sea could be characterized as either "short-lived" (<age-10) or "long-lived" (>age-10) (Table 7.4.1). Little is known about ages of most of the species we captured. *B. saida* is clearly short lived with a maximum age-5 found in this study, in the Chukchi and Bering Seas (Helser et al. 2017), and in the Svalbard Archipelago (Nahrgang et al. 2014). Likewise, two sculpins we found up to age-7 are short lived: *Gymnocanthus tricuspis*, age-9 and 140 mm in the Chukchi Sea (Smith et al. 1997); *Icelus spatula*, age-7 and 210 mm off the Kuril Islands (Tokranov and Orlov 2005). We only aged *Liparis fabricii* to age-5, but considering it was at the maximum size range of Alaskan Arctic fish (Table 7.4.1), it seems to fall in the short-lived category. *Lycodes eudipleurostictus* were age-7 in our samples but can be age-9 in the Barents Sea (Wienerroither et al. 2013). *Lycodes polaris* maximum size in this collection was 222 m and age-7; however, in the Barents Sea they can be 550 mm (Wienerroither et al. 2013), indicating they are likely to achieve an older age. Though we only captured very young (age-2) and small (89 mm) *Myoxocephalus scorpius*, it can be age-15 in Newfoundland waters (Ennis 1970). All of the other fishes we captured were long-lived (age-≥10) (Table 7.4.1).

Life span is important to know because shorter-lived species have the potential to recover from negative environmental or other influences more quickly than longer-lived species. The median of the oldest age classes suggests the number of years required to turn over the population, i.e., to start over after a negative impact. Before the present study, there was no knowledge that US Arctic fishes were so long-lived, and this revelation should be considered when formulating Arctic policies. Long-lived species could be considered more stable because an event that negatively impacts a single year class would affect only a small percentage of the total population. However, if a negative effect lasts multiple years (e.g., warmer seawater, changes in oceanographic currents, anthropogenic forces, fishing), the impact could last longer and affect multiple year classes; it could take many years to rebuild the population structure (Birkeland and Dayton 2005). Reduction of older fish can result in strong evolutionary pressure that decreases body size and fecundity (Olsen et al. 2004). By removing older members of a fish population, genetic diversity can be lost, which might result in reduced adaptability (Hauser et al. 2002). Eelpouts sampled were very long-lived, up to 25 years (Figure 7.3.2.6–9), so this group

presents potential recovery issues. If the impact is prolonged, restoration of the population age structure may be impossible to achieve.

Table 7.4.1. Life history characteristic summary.
Based only on fishes caught in the Beaufort Sea 2012–2014 during the present research. Dashes indicate no data. Life stage - where captured in the water column. Life span - short <10 yrs, long ≥10 yrs. Maximum age in this study. Size range captured. T & L (Thorsteinson and Love 2016) records of maximum ages and sizes for comparison; question mark is no previous record. Grey cells are record extensions.

	Life stage	Life span	Max. age	Max. age T & L	Size range (mm)	Max. size (mm) T & L
Gadidae						
Boreogadus saida	pelagic, demersal	short	5	7-8	15–240	460
Cottidae						
Artediellus scaber	demersal	--	--	7	14–114	114
Gymnocanthus tricuspis	pelagic, demersal	short	7	9	19–147	299
Icelus bicornis	demersal	--	--	5	27–68	170
Icelus spatula	demersal	short	6	10	20–111	210
Myoxocephalus scorpius	pelagic, demersal	long	2	15	38–89	600
Triglops nybelini	demersal	--	--	?	81–126	170
Triglops pingelii	pelagic, demersal	--	--	9	26–130	233
Agonidae						
Aspidophoroides olrikii	pelagic, demersal	long	15	?	23–80	100
Psychrolutidae						
Cottunculus microps	demersal	--	--	--	45–223	--
Cyclopteridae						
Eumicrotremus derjugini	demersal	--	--	?	15–64	127
Liparidae						
Careproctus lerkimae	demersal	--	--	--	47–145	--
Liparis fabricii	demersal	short	5	?	18–212	210
Zoarcidae						
Lycodes adolfi	demersal	--	12	?	38–205	286
Lycodes eudipleurostictus	demersal	--	7	9	55–396	450
Lycodes polaris	demersal	--	7	5	32–222	333
Lycodes reticulatus	demersal	long	11	19	48–405	760
Lycodes sagittarius	demersal	long	26	?	44–427	278
Lycodes seminudus	demersal	long	24	?	41–465	560
Stichaeidae						
Anisarchus medius	pelagic, demersal	long	19	?	49–134	180
Lumpenus fabricii	pelagic, demersal	short	2	17	41–124	365
Stichaeus punctatus	pelagic, demersal	--	--	5	29–48	220
Pleuronectidae						
Hippoglossoides robustus	demersal	--	8	30	216–314	520
Reinhardtius hippoglossoides	demersal	--	--	36	351–525	1300

7.4.3 Pelagic and Demersal Distribution

Pelagic (young) and demersal (older) life stages of fishes in the Beaufort Sea did not have the same distributions. The distribution of the pelagic stage was not equal across the whole study area. The central Beaufort Sea abundance and assemblage of pelagic fishes was very different from that of the east US Beaufort Sea and the east and west sides of the Mackenzie Canyon (Table 7.3.3.2, Figure 7.3.3.6). In contrast, though the abundance of demersal fishes was greater in the central Beaufort Sea, the assemblages were not. Distribution of fishes by family in pelagic and demersal catches demonstrated life stage differences. The number of families and the biomass and abundance of fishes were greater in demersal than in pelagic catches. Seven families of fish were captured pelagically in the midwater trawls (Figure 7.3.1.5) and demersally in bottoms trawls (Figures 7.3.1.3 and 7.3.1.4): Osmeridae (smelts), Gadidae (cods), Cottidae (sculpins), Agonidae (poachers), Liparidae (snailfishes), Stichaeidae (pricklebacks) and Pleuronectidae (righteye flounders). Those seven families of fish were also captured demersally in the northeastern Chukchi Sea in 2009 and 2010 (Norcross et al. 2013). Of the seven families, all but Osmeridae were captured both pelagically and demersally in 2004 in the US and Russian portions of the Chukchi Sea; Osmeridae was captured in the pelagic zone but not in the demersal zone (Norcross et al. 2010). In the present study, there were seven additional families captured in the demersal zone than in the pelagic zone: Rajidae (skates), Myctophidae (lanternfishes), Hemitripteridae (sailfin sculpins), Psychrolutidae (fathead sculpins), Cyclopteridae (lumpfishes), Zoarcidae (eelpouts), and Ammodytidae (sand lances). Differences in families captured could be attributed to two factors: fishes without pelagic stages (Rajidae and Zoarcidae) and the size of mesh in fishing gear. The small mesh pelagic nets did not catch large individuals (e.g., Rajidae) and neither small nor large mesh demersal nets caught small individuals or taxa of small circumference (e.g., Ammodytidae). The BOEM-funded 2011 Central Beaufort Sea Fish Monitoring study (Norcross et al. in review) that only sampled the shelf from 14 to 184 m caught all but three of the 14 families captured by the present study; Rajidae, Myctophidae and Psychrolutidae were only captured on the slope in 2012–2014. This demonstrates the ubiquitous distribution of these Arctic fish families in the US Beaufort and Chukchi Seas.

Nearly all fishes caught by pelagic nets were larvae or small juveniles representing the first year of life. Of the at least 14 taxa that were captured in the pelagic region, only the flatfish *Limanda proboscidea* was caught as a larva but not in its demersal phase (Table 7.3.1.1). That is likely because this species is rare in the US Beaufort Sea and its depth range of 5–8 m (Thorsteinson and Love 2016) is shallower than we were able to sample. However, collecting even a single larva provides evidence that this species spawns locally.

Fewer taxa and lower abundance of larval and small juvenile life stages of fishes were collected in the eastern region during the summer season (12 August–2 September 2013) than in the central region fall season (20 September–1 October 2012). The location and season are confounded, meaning that either the central location, or the later season, or the interaction of the two is the most appropriate for collecting young-of-the-year of a limited set of taxa. *Boreogadus saida* hatch January to May in the Canadian Beaufort Sea (Bouchard and Fortier 2011). In fall 2012, an order of magnitude more *B. saida* were collected than in summer 2012, including some of the late cohorts as small as 15 mm (Figure 7.3.2.1 and 7.3.2.10)

However, fishes smaller than 30 mm included several taxa that were caught only by bottom trawl and four taxa that were caught both pelagically and demersally: *Boreogadus saida*, *Gymnocanthus tricuspis*, *Aspidophoroides olrikii*, and *Liparis fabricii*. Not much is known about the larval stages of the other fishes in the present study region, although recent publications exist

on ichthyoplankton in the Canadian Beaufort (Suzuki et al. 2015, Geoffroy et al. 2015). More could be learned about ichthyoplankton in the US Beaufort Sea through examination of larval fish samples collected in the 505-µm bongo net used to collect zooplankton in 2012–2014 for this Transboundary project (Chapter 4). Study of these fishes was not in the scope of the current project, but we saved the samples in the belief that they could inform us about larval fishes in the open-water season in the Beaufort Sea. These samples were all collected in the late open-water season, which presents some year-to-year comparison as well as seasonal limitation. There may be more or different small pelagic fishes present earlier or later in the year; however, being able to tow in the midwater before August or after September in the Beaufort Sea is unlikely without using a vessel with an ice-strengthened hull.

In this study, the vast majority of young *B. saida* were in shallow waters on the shelf (≤100 m; Figures 7.3.2.2 and 7.3.2.10), which seems to support the concept that once hatched, *B. saida* larvae are pelagic and remain in nearshore waters (Rass 1968). As in our study, Geoffroy et al. (2015) found that age-0 *B. saida* made up the vast majority (94%) of fish in the epipelagic scattering layer in the Canadian Beaufort Sea. Pelagic juveniles begin the descent to deeper, offshore waters where they inhabit demersal, pelagic, and cryopelagic zones in coastal and offshore marine habitats (Lowry and Frost 1981), thus explaining the greater abundance of older *B. saida* on the slope. We caught the largest biomass (i.e., older individuals) (Figure 7.3.2.2) of *B. saida* at 200–350 m depth (Figure 7.3.2.11). Acoustically, there appears to be a layer of *B. saida* at the bottom at 200–400 m and maintaining the same depth as depth drops rapidly on the slope (Geoffroy et al. 2015). Though we could not collect larger fish in conjunction with acoustics, the higher proportion of *B. saida* older than age-1 caught demersally on the slope (≥200 m) supports the concept of a deep layer of older *B. saida*.

7.4.4 Fish Species Assemblages – Shelf vs. Slope

There were clear differences between pelagic abundance in the central and east Beaufort Sea (Tables 7.3.3.2–3); abundance of pelagic fishes was greater in the central region. The central community was composed approximately equally of *B. saida*, *Liparis* spp. (snailfishes), and unidentified Lumpeninae. The eastern communities were even less diverse with 95% *B. saida* and 29% *Liparis* spp. on the slope, which was similar to communities found on the Mackenzie shelf (Suzuki et al. 2015). Longitude itself does not affect pelagic abundance, but serves as a proxy for along-shelf distance that freshwater flow onto the shelf changes with proximity to river mouths. In 2012, the surface water was intermediate (5 ºC, salinity of 25), perhaps indicating outflow from the Colville River. The effect of the outflow of the Mackenzie River could be seen in the temperature and salinity of the surface (≤10 m) water (Figures 3.17-8). The Mackenzie River plume was prominent in 2013 as evidenced by warm (7 ºC), low salinity (13) water. In 2014, the nearshore water was colder (2–5 ºC) and more saline (30). The increase in easterly winds that drives the Mackenzie River plume offshore and causes stratification of the shelf waters (Wood et al. 2013) does not immediately affect the bottom waters, so it does not directly affect demersal fishes.

The important habitat parameters affecting distribution of demersal fishes are depth, salinity, density, and water mass (Tables 7.3.4.11–12). All of these variables are cross-correlated, so it is not surprising that all of these environmental measures of habitat have an effect on fish distribution. These characteristics separate the nearshore, shallow shelf waters, which have a higher abundance of smaller fishes, from the offshore, deep slope habitat, which has fewer, but larger, individuals.

The slope below ~200 m is occupied by the warmer, more saline Atlantic Water (AW) with a distinct community consisting of >85% *Boreogadus saida*, *Lycodes adolfi, L. sagittarius,* and *L. seminudus* (Tables 7.3.4.4–9, 7.3.4.18). *B. saida* age 1+ are demersal on the slope from about 200–400 m; as depth increases, *B. saida* spread throughout the water column as deep as 600 m, but importantly, form a layer (visible acoustically) that remains at 200–400 m extending off the bottom (Geoffroy et al. 2015). As the bottom trawl passes through this layer of *B. saida* to and from the bottom, some *B. saida* could be captured. *Lycodes* eelpouts are demersal as evidenced by their diets; they increase in size and change in species composition with depth (Appendix H). The discovery of a slope community dominated by two genera has clear ecological implications. Disturbance of the slope community could have grave consequences, as it would restructure the paradigm of *B. saida – Lycodes* dominance. No other species are found on the slope that have all the characteristics displayed by these eelpouts: abundant, long lived and large. Thus, it is critical to acknowledge this community group and to avoid its disruption because there are no taxa evident that could substitute in this slope community (see Chapter 8, Appendix H).

The shelf community is more complex than the slope community is. The bottom salinity was lower on the shelf (Section 3.1) than on the slope due to freshwater runoff from Mackenzie River at the east of the study area and Colville River on the western edge of the study area. The shelf waters to about 50 m are well mixed and have a wide range of salinities and temperatures but are characteristically cold and fresh in the Polar Mixed Layer (PML) on the bottom. *B. saida* in our collections were usually <100 mm, but not always age-0 as they are assumed to be (based on acoustic sampling, not aging of otoliths) in the Canadian Beaufort Sea (Geoffroy et al. 2015). Unlike the slope community, there are more than two indicator taxa for the shelf community; at least three of four sculpin species (*Artediellus scaber, Gymnocanthus tricuspis, Icelus spatula, Triglops pingelii*) indicate the shelf community (Tables 7.3.4.8–11, 7.3.4.18–20). While there were differences in the combination of sculpins by biomass, abundance, location, and year, there was not a pattern that could narrow down the indicator species to a consistent specific location. Though *Lycodes polaris* is typically found on the shelf, it was not as abundant as the sculpins (Appendix H) and is not considered a reliable indicator species. *Aspidophoroides olrikii* is an additional shelf community indicator because it is not found in deep water; however, in our study it was very patchy with inconsistent occurrences of high abundance.

There is a mix of physical oceanography characteristics and fish compositions that exist between the two extremes of the AW and PML water masses and their associated fish communities. The AHW is usually on the bottom at depths of >50–200 m encompassing the shelf break; the salinity and temperature profiles that characterize this water mass vary with time and place. Strong easterly winds cause upwelling of AW onto the shelf (Pickart et al. 2011); this causes mixing of water masses that, at least temporarily, may affect fish distribution, resulting in patchy communities along the shelf break. These patchy communities are not distinct and might have no species in common with each other; like the water, they are a blend. Species found in the shelf break community, e.g., *B. saida, T. pingelii, A. olrikii,* or *L. polaris*, might also be found in shelf communities. Alternatively, the shelf break community might include a species unique to that community such as *Triglops nybelini, Icelus bicornis* and *Leptagonus decagonus* (Table 7.3.4.19).

The results of this study show similarities and differences in the fish communities that are important across the slope and shelf of the Beaufort Sea. The narrow continental shelf in US waters means that the shelf and slope are likely to influence each other frequently and relatively quickly. Prior to this study, there had been no demersal trawling for fish on the slope of the

Beaufort Sea. We knew the depth and temperature would be different on the slope (Pickart et al. 2011) from on the shelf, and we knew that Arctic fish communities previously had been linked to water masses (Norcross et al. 2010). The proximity of different shelf and slope fish communities to the shelf break raises the potential for circulation and upwelling in that area (Pickart 2004, Pickart et al. 2009) to, at least temporarily, change the makeup of community structure. Likewise, events on the shelf such as a wind shift that reverses the direction of the Mackenzie River outflow toward the west may affect both the shelf and slope.

7.4.5. Small-Scale Spatial Variability in Community Composition

Standard practice for sampling demersal fishes in logistically expensive locations like the Arctic is to conduct one trawl haul per station. In this study, similarity among hauls was excellent with the same composition at a station ranging from 43% to as high as 80%, indicating that one haul per station was sufficiently representative of fish communities at depths from 20 to 1000 m. There were very similar taxonomic structure patterns for both biomass and abundance. A depth pattern was also observed, with 20–100 m samples on the shelf grouped separately from 200–1000 m samples on the slope (Figure 7.3.4.8). It is possible that the similarity of catches among replicate hauls appeared to be so high because of the paucity of fish taxa (i.e., fewer combinations of catch composition were possible). In a more taxonomically rich environment, haul repeatability may not be as great, but additional sampling would be needed to prove that conclusively. For the eastern US Beaufort Sea, replicate hauls do not seem to be necessary.

7.4.6 Interannual Variability in Demersal Biomass and Abundance

Sampling four transects at the US-Canada border (146º–140º W) in both 2013 and 2014 revealed some difference in biomass and abundance of demersal fish catches, but also consistency. There was a shelf vs. the slope pattern in abundance as was found for community composition from 151°–138° W (Table 7.3.4.4). Biomass was 3–5 times greater at deep (slope) stations in 2013 than in 2014 (Figure 7.3.4.7); conversely, abundance of fishes at deep stations in 2013 was about half than in 2014 (Figure 7.3.4.8). However, except for differences at the 20 m stations, both abundance and biomass were proportionally similar at shallow (shelf) stations in both years. At 20 m stations biomass was more than five times higher and abundance was 2–3 times higher in 2014 than in 2013 (Figures 7.3.4.7–8). There was not a pattern of fish abundance at specific very shallow stations. Two years of sampling is not enough to make a judgement about interannual variability.

7.4.7 Fishing Gear and Fish Monitoring

In 2012–2014, we used a selection of nets to determine most efficient ways to collect fishes in the US Arctic. All nets we used were research size, not commercial size, and the vessel we used only had a single drum; therefore, we used single-warp nets. We examined distributional changes in fish by life stage (pelagic, demersal), physical habitat, and fish community composition. The objective of using multiple nets was to attempt to collect fish fully representative of the size distributions of the communities. The nets fished differently and provided a good representation of the availability of pelagic and demersal life stages of fishes in the Beaufort Sea in the open water season (Figure 7.3.1.6). Because the sizes, shapes, and fishing abilities of the pelagic and demersal nets were not the same, quantitative comparison of fish catches could not be made among the various nets. However, we were able to determine the most efficient net to use to fulfill the objectives for this and future studies.

To sample the pelagic region, the small IKMT is effective at collecting large larval and small juvenile pelagic fishes, but it is not effective at collecting eggs and small larval fishes. For pelagic fishes, a 3-mm mesh IKMT collects age-0 (larval and juvenile) fishes and is good to use late in the summer and in the early fall. Earlier in the season, it would be good to use a 1-mm mesh IKMT or a 505-µm bongo net to capture smaller fishes. If we had been able to sample in an ice-covered season with a Surface and Under Ice Trawl (SUIT; von Franeker et al. 2009), we might have seen a very different distribution of pelagic and demersal stages of *B. saida.* There have been observations that *B. saida* live in under-ice crevices and spawn under the ice (Gradinger and Bluhm 2004). We did not have a net that was effective at sampling under ice. However, the SUIT was used in Arctic waters in 2012 from the German icebreaker R/V *Polarstern* (David et al. 2015). At that time, a population of mostly age-1 (52–140 mm) *B. saida* was discovered under the ice and the authors David et al. (2015) speculated that under-ice may be a favorable environment that allows exchange of genetic material across the Arctic Ocean. Our collections indicate that abundance is not equal by life stage and that more larval and juvenile *B. saida* are in pelagic environments, whereas older *B. saida* occupy a demersal habitat.

Choice of bottom sampling nets is tied closely to study objectives because habitat sampled, vessel requirements and sampling selectivity differs among net types. Small beam trawls catch and accurately represent the small demersal fishes found on the shelf of the Beaufort Sea. They are also effective at catching larger demersal fishes on the Beaufort Sea slope to 1000 m depth. Despite the difference in mesh size, there was little difference between the nets in the size of fish caught. The BT could catch a 790 mm skate (*Amblyraja hyperborea*) and 14 mm sculpin (*Artediellus scaber*) while the OT caught a 638 mm skate and an 18 mm snailfish (*Liparis* spp.; Table 7.3.4.18). However, the much larger NOAA 83-112 Eastern bottom trawl, with a 34.1 m footrope (Logerwell et al. 2011) and swath at least two orders of magnitude greater, does catch larger fishes (Britt et al. 2013) expected to be found on the slope such as Arctic skate (*Amblyraja hyperborea*) and Greenland Halibut (*Reinhardtius hippoglossoides*). Large nets have a higher opening and we expected catches of fish from the water column (e.g., *Boreogadus saida*) to be much larger, especially based on the very large percentage of *B. saida* captured in the Chukchi Sea with a NOAA 83-112 (Barber et al. 1997) compared to numbers caught with a BT (Norcross et al. 2013). There did not seem to be an advantage to fishing with the OT as opposed to the BT. The disadvantages to using it were that it is larger and more awkward to use, and lack of historical record for fishing with a comparable OT in the Beaufort or Chukchi Seas for comparison purposes. All the nets we used, as well as the NOAA 83-112, have the potential to be used to monitor fishes in the Beaufort Sea. When the objective is to observe the composition of fish communities, we conclude that using a plumb staff beam trawl modified (Abookire and Rose 2005) to sample in mud is best for demersal fishes in the open water season.

Sampling with a BT yields information to differentiate between shelf and slope communities (Table 7.3.4.4). Cottidae (sculpins), Agonidae (poachers), Cyclopteridae (lumpfishes) and Stichaeidae (pricklebacks) are indicative of shelf communities. Rajidae (skates), Zoarcidae (eelpouts), and Pleuronectidae (righteye flounders) are indicative of the slope. While individuals of these families might be found in the alternate habitat, they are predominantly found in these defined habitats, thus higher levels of taxonomic identification could be used to separate slope and shelf communities. *B. saida* is morphologically distinct from the other indicator taxa and can more easily be identified to species. Though three *Lycodes* eelpout species, *L. adolfi, L. sagittarius,* and *L. seminudus* are on the slope, identification could be streamlined by only identifying them to genus. Likewise, the process of identifying shelf community fishes could be

streamlined by only identifying the sculpins to family (Cottidae). However, as *Gymnocanthus tricuspis* indicates the shallow water community in the western Canadian Beaufort Sea (Majewski et al. 2013), identification to at least genus is necessary as *Gymnocanthus, Icelus,* and *Triglops* are indicators of shelf and shelf break communities. The decision as to the precision of taxonomic identification of fish is dependent upon the question being asked. Higher levels of identification could be used to discern slope and shelf communities. In contrast, if the question is "has change occurred," a precise, species-level taxonomic identification (which may require morphometrics and genetics) would be needed to evaluate change.

7.5 Conclusions

The hypotheses tested for both pelagic and demersal, distribution, relative abundance, and species assemblages are equal across habitat, central and east US Beaufort Sea waters, east and west sides of the Mackenzie Canyon, and shelf and slope waters, were disproven for pelagic fishes. The species composition was not the same in the central Beaufort Sea, where more taxa and higher abundance were encountered, than in the eastern US Beaufort Sea and Mackenzie Canyon region. Though the central region did not have a very diverse pelagic composition (*B. saida*, *Liparis* spp. and Lumpeninae), it was rich in comparison to the eastern regions (*B. saida* and Lumpeninae). There were differences between the composition in fishes in the Mackenzie Canyon and those to the west in the eastern US Beaufort; the shelf community extended seaward over the slope, likely due to the outflow of the Mackenzie River. In contrast, to east of the Mackenzie trough, the shelf community was more similar to that of the central Beaufort Sea, which differed from the southeastern Beaufort Sea where *Arctogadus glacialis, Gymnocanthus tricuspis, Liparis gibbus,* and *Leptoclinis maculatus* characterized the Mackenzie shelf (Suzuki et al. 2015). Distribution, relative abundance and species assemblages differed across the whole sample area for pelagically-caught fishes.

Similarly, those measures were not equal across the area for demersally-captured fishes. The demersal fishes in the central and eastern parts of the US Beaufort Sea were distinctly separated as shelf and slope communities, with 100–200 m being a transition zone. The most clear-cut way to describe this area is as having three conspicuous groups of fish: cods, sculpins, and eelpouts. The entire area is characterized as occupied by *B saida*, though there is a size and age separation with smaller age-0 fish on the shelf compared to the slope. Fish communities on the shelf have several species of sculpins as members. Fish communities on the slope have several species of eelpouts. Depth, which is correlated to closely the environmental variables of temperature, salinity, and water mass, is the easiest factor to measure to estimate the distribution of these communities. Though abundance of fishes is greater in the western Beaufort Sea (Rand and Logerwell 2011, Logerwell et al. 2011, Norcross et al. in review), no east-west spatial gradient significantly defined the communities; therefore, the hypotheses were all disproved.

Though not an original hypothesis, we were able to test the age distribution of demersal fishes on the shelf vs. slope. Shelf fishes typically have shorter lifespans of about 5–7 years (e.g., Arctic Staghorn Sculpin). Slope species are mainly eelpouts with life spans of more than 12 years. Long-lived species, such as those found on the slope, should be more resilient to short-term perturbation. The environment on the slope is more stable below 300 m with little change in temperature, salinity, and water mass. Shorter-lived shallow shelf species would be less resilient in the short term and more subject to immediate effects of change in their environment (climate, anthropogenic, etc.). The median of the oldest age classes suggests the number of years required to turn over the population, i.e., to start over after a negative impact. However, the shorter life

span of shelf fishes would also mean that recovery time could be quicker than for species on the slope that live 2–4 times as long. Long-lived species could be considered more stable because an event that negatively impacts a single year class would affect only a small percentage of the total population. However, if a negative effect lasts multiple years (e.g., warmer seawater, changes in oceanographic currents, anthropogenic forces), the impact could last longer and affect multiple year classes; it could take many years to rebuild the population structure.

8.0 FEEDING ECOLOGY OF ABUNDANT FISHES

8.1 Introduction

The feeding ecology of Arctic fish populations is complex and requires examinations across several different disciplines to understand relationships across communities. The following reporting reflects a multitude of approaches by different scientific disciplines to elucidate the feeding ecology of abundant fishes. The Fish Diet section (8.2) uses the standard approach of examining gut contents of fishes captured, though there are also some stable isotope results reported for some species of fish. The Fish Fatty Acids section (8.3) uses yet another technique to identify key trophic linkages. The Benthic Food Web Structure section (8.4) explores the sources of nutrients by using stable isotopes as a tool.

8.2 Fish Diets

Ben Gray, Sarah Apsens, and Brenda Norcross

8.2.1 Introduction

Fishes are important links in Arctic marine food webs between lower trophic level prey (e.g., invertebrates) and upper trophic level predators (e.g., marine mammals, seabirds, and other fishes); however, little published information exists on the diets of Arctic species other than *Boreogadus saida* (Arctic Cod). The diets of the 12 most abundant species of fish are presented here in three groups. *B. saida*, family Gadidae, was the most numerous species captured and can be both benthic and pelagic so it was treated separately. *B. saida* is an abundant forage fish and a vital link between lower and upper trophic levels in Arctic marine food webs. While its diet has been the subject of studies throughout the Arctic, little is known about the factors that influence its diet in the western Beaufort Sea. To increase knowledge of lesser-known fish species in Arctic food webs, this research focuses on the diets of eleven primarily demersal fishes. Seven species from three families are of interest because of their relatively high abundance. In this study, family Cottidae (Sculpins) are represented by *Artediellus scaber* (Hamecon), *Gymnocanthus tricuspis* (Arctic Staghorn Sculpin), *Icelus spatula* (Spatulate Sculpin), and *Triglops pingelii* (Ribbed Sculpin); family Agonidae (Poachers) by *Aspidophoroides olrikii* (Arctic Alligatorfish); and family Stichaeidae (Pricklebacks) by *Anisarchus medius* (Stout Eelblenny) and *Lumpenus fabricii* (Slender Eelblenny). There are currently 16 recognized *Lycodes* species in the Alaskan Arctic, and 13 are believed to occupy the US Beaufort Sea (Thorsteinson and Love 2016). Though relatively numerous throughout the circumpolar Arctic, basic ecological information on members of the genus *Lycodes* is lacking. The four most abundant eelpout species in the Transboundary collections, Adolf's Eelpout (*Lycodes adolfi*), Polar (Canadian) Eelpout (*L. polaris*), Archer Eelpout (*L. sagittarius*), and Longear Eelpout (*L. seminudus*) are all demersal but occupy different depths of the shelf and slope. The objective of this component of the feeding ecology assessment was to analyze dietary patterns of the most abundant fish species.

8.2.2 Methods

8.2.2.1 Diet Analyses

Each fish was measured and stomachs of each species were dissected. Prey were identified to lowest possible taxa. Prey items were grouped into coarse taxonomic groups to aid in statistical analysis. Specific prey information was grouped taxonomically at the level of order or sub-order for Gadidae, Cottidae, Agonidae, and Stichaeidae. For Zoarcidae, non-crustacean prey were grouped by phyla or class and crustacean prey were grouped by subclass or order. The percent mean weight (%MW) or number (i.e., the amount of weight or number of individuals a particular prey group contributed to fish diets) was calculated for each prey group. The resulting %MW values for each prey group formed the basis of the between-species diet comparisons.

In all, 1,349 *Boreogadus saida* stomachs were examined. The different collection methods allowed for comparisons between demersal (i.e., seafloor) and pelagic (i.e., middle-to-upper water column) habitats. For brevity sake, we highlight the major differences found in *B. saida* diets between and within regions. Geographic locations, allowing for regional diet comparisons, included the central Beaufort Sea (transects B1-B2-BX), Camden Bay (transects A4-A5-A6), US-Canada transboundary (A1-A2-TBS), and Mackenzie River (MAC-GRY) (Figure 8.2.1). *B. saida* diets were further analyzed by their body sizes (10 mm length class increments) and depth groups (≤100 m and >100 m stations) that demark the Beaufort Sea shelf break.

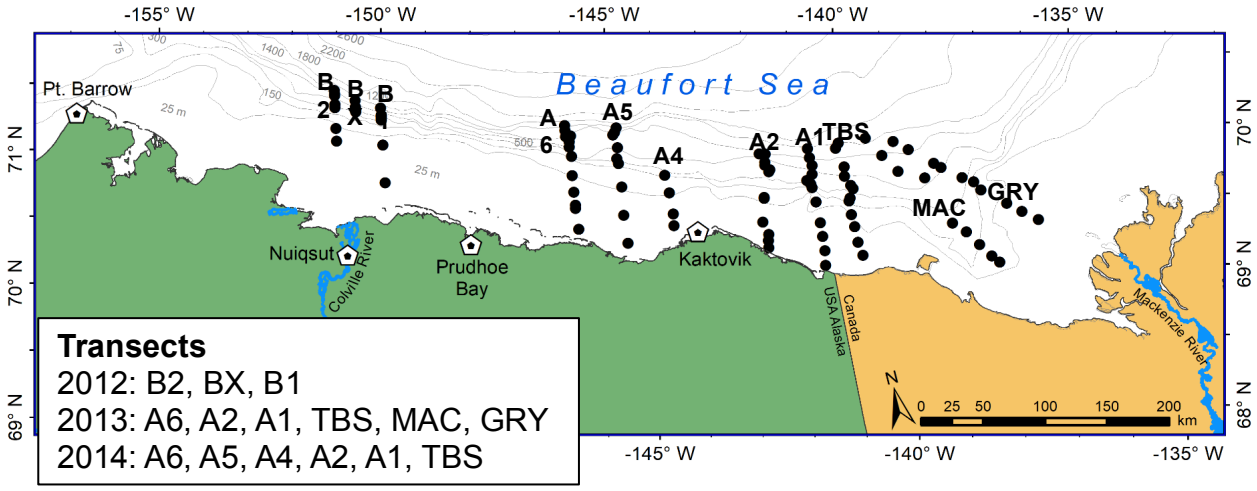

Figure 8.2.1. Transects and stations sampled in the Beaufort Sea.

A total of 928 fish stomachs were examined for family groups Agonidae, Cottidae and Stichaeidae. Of these, 757 contained identifiable prey and were used in the statistical analyses. Unidentifiable prey was included in the descriptive analysis but was excluded from the statistical analyses because its ecological relevance was unknown. Here, we present the major patterns detected between and within the seven species' diets based on the contribution of identifiable prey.

In total, 400 stomachs were collected from the four *Lycodes* species. *Lycodes* muscle tissue samples were processed for stable nitrogen and carbon isotopes. Nitrogen isotope signatures can be indicative of trophic level. Carbon isotope signatures can be indicative of the carbon sources

is a predator's diet. The results of the stable isotope analysis were summarized visually by plotting $\delta^{15}N$ and $\delta^{13}C$ in standard bi-plots.

Various multivariate statistical methods using percent weight (%W) were used to test for differences and look for patterns in diet composition. Not all analyses were used on each of the 12 species. Specific analyses depended on the number and distribution of fishes. A non-metric multidimensional scaling plot (nMDS) was used to visually assess the data. For *Lycodes* a permutational analysis of variance (PERMANOVA, PRIMER v.7) was used to test for interannual differences in diet composition and to test for overall differences in diet composition among the four species. Pairwise tests were used to test for differences in overall diet composition between *Lycodes* species. A similarity percentage analysis (SIMPER) was used to see which coarse prey groups contributed to observed differences and to quantify dissimilarity within a single *Lycodes* species and between *Lycodes* species. nMDS was also used to investigate variability patterns in diet composition among *Lycodes* species and among individual samples.

8.2.2.2 Size Class Analyses

Because the sample size for *Boreogadus saida* was so large (n = 1,439), we used a non-parametric multivariate analysis of variance (NP MANOVA) (conducted in R, version 3.2.2) to determine feeding size classes. Using all available data, we compared *B. saida* diet compositions between 10 mm increments (e.g., 20 mm vs. 30 mm). If there was a significant difference between a 10 mm increment, a size class was made at the break. If there was not a significant difference between two 10 mm increments, a NP MANOVA model that compared multiple 10 mm increments (e.g., 20 mm vs. 30 mm vs. 40 mm, etc.) was applied, with increments being added until a significant difference in diet compositions was identified. A size class was made from the first 10 mm bin in the comparison up to the bin previous to the increment that created the significant difference. This method was applied separately to demersal and pelagic-caught *B. saida* to determine differences in ontogenetic feeding patterns related to water column inhabitance.

Sample sizes of all other fish species were smaller and varied widely (n = 8–382 per species); therefore, we used either ordination (nMDS) or classification (cluster analysis) methods to approximate size classes. Both methods were conducted in PRIMER v7 and were used to find groupings in size intervals. These intervals (e.g., 21–30 or 91–150 mm) were defined to include a sample size of at least four individuals per interval. We used nMDS for comparisons among size intervals. Cluster analysis was used for fish species where only three size intervals were available. Therefore, nMDS was used to approximate size classes of *G. tricuspis*, *I. spatula*, *A. olrikii*, *L. adolfi*, *L. sagittarius*, and *L. seminudus,* and cluster analysis for *T. pingelii*, *A. medius*, and *L. fabricii*. Size classes were determined when discrete size intervals grouped at similarity percentages >40%. Due to small sample sizes, it was not possible to assign size classes for *A. scaber* or *L. polaris*.

8.2.3 Results

8.2.3.1 Diet Analyses

Throughout the transect groups (i.e., regions) *Boreogadus saida* diets proved to be more different than similar. However, one similarity was that *B. saida* relied heavily on calanoid copepods, which accounted for about 40–90% MW of pooled demersal and pelagic *B. saida* diet

compositions throughout the Transboundary study area (Appendix F). Regional differences in *B. saida* diets were most pronounced when considering prey groups other than calanoid copepods. Demersal *B. saida* in the Camden Bay region (transects A4-A5-A6) consumed the most diverse diets, with prey such as amphipods, cyclopoid copepods, isopods, mysids, and ostracods contributing more by %MW to diets within this region than all other regions. Ohter notable differences in prey groups included chaetognaths, which were consumed nearly exclusively by demersal and pelagic *B. saida* in the central region (B1-B2-BX), and marine cladocerans, which were only consumed by *B. saida* in the transboundary (A1-A2-TBS, pelagic fish only) and Mackenzie (GRY-MAC, demersal and pelagic fish) regions.

Within regions, diets differed more by *Boreogadus saida* body sizes and less among depths and years. With an increase in body size, fish shifted from consuming smaller to larger prey in both demersal (Figure 8.2.3.1) and pelagic (Figure 8.2.3.2) habitats. Prey size shifts drove the overall differences in prey groups consumed by smaller and larger fish, with the smallest *B. saida* (i.e., ≤59 mm fish) consuming the smallest prey (e.g., smaller species and stages of calanoid and cyclopoid copepods) and larger specimens consuming larger pelagic zooplankton (e.g., hyperiid amphipods and euphausiids), demersally-associated prey (e.g., isopods, mysids, and ostracods), and ultimately fish (Appendix F). The most detectable diet difference by depth was that larger, demersal *B. saida* consumed greater numbers of demersal prey (e.g., cumaceans and mysids) in ≤100 m depths. The only quantifiable, interannual difference was found for pelagic fish in the Transboundary (A1-A2-TBS) group between cruise years 2013 and 2014. Marine cladocerans were eaten in high amounts by *B. saida* in 2013, whereas, in 2014, cladocerans were replaced by copepod nauplii and cyclopoid copepods in diets. In the same year, marine cladocerans were eaten in high amounts by conspecifics in the GRY-MAC transect group.

Unidentified prey was found in high amounts in Agonidae, Cottidae, and Stichaeidae samples (Figure 8.2.3.3, Appendix G) but were not included in statistical analyses. At 60% diet similarity, nMDS found evidence of two feeding groups shared by multiple fish species: benthic (i.e., demersal) crustacean consumers (*A. medius* and *L. fabricii*) and benthic crustacean/ macroinvertebrate consumers (*A. scaber*, *I. spatula*, and *G. tricuspis*; Figure 8.2.3.4). Cumaceans, ostracods, and other copepods primarily composed the benthic crustaceans group and benthic amphipods, isopods, and polychaetes primarily composed the benthic crustaceans/macroinvertebrate group (Figure 8.2.3.4). *A. olrikii* (mostly amphipod consumers) and *T. pingelii* (mostly calanoid copepod, hyperiid amphipod, and fish consumers) showed different patterns in their diets thus were not included in either group (Figure 8.2.3.4).

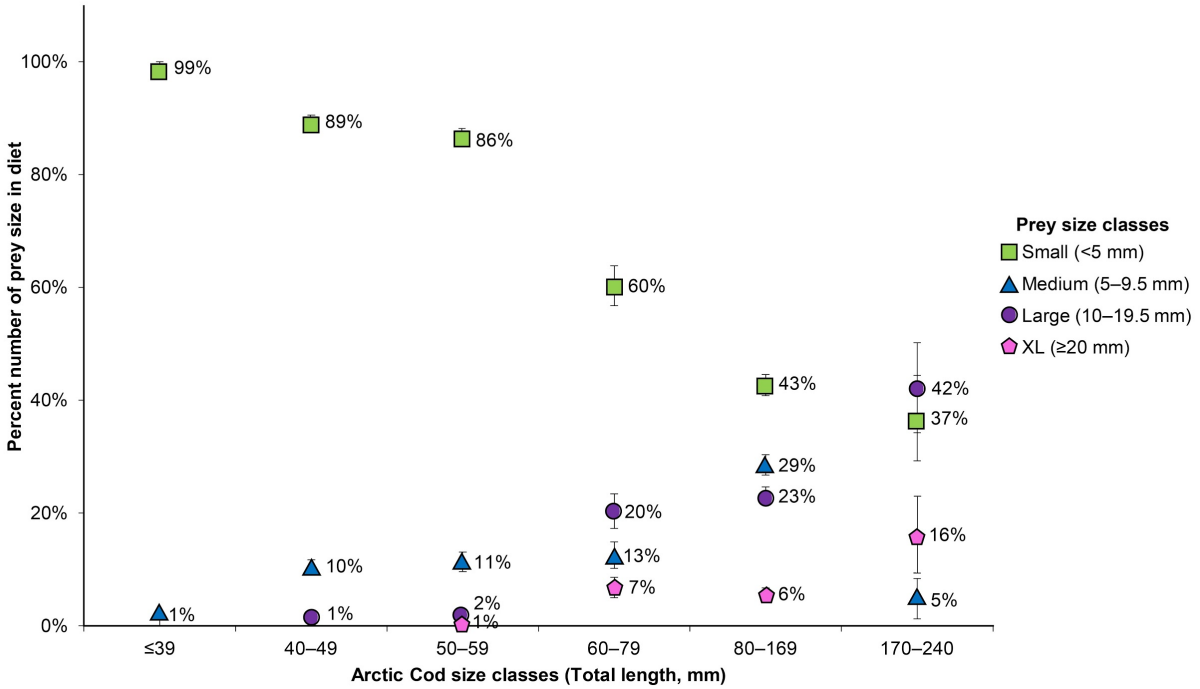

Figure 8.2.3.1. The percent contribution by number of small (<5 mm), medium (5–9.5 mm), large (10–19.5 mm) and extra-large (≥20 mm) prey eaten by demersal *Boreogadus saida,* summarized by six size classes of fish: (≤39 mm, 40–49 mm, 50–59 mm, 60–79 mm, 80–169 mm, and 170–240 mm).
Error bars signify the standard error of the mean percent number of prey sizes in demersal *B. saida* diet.

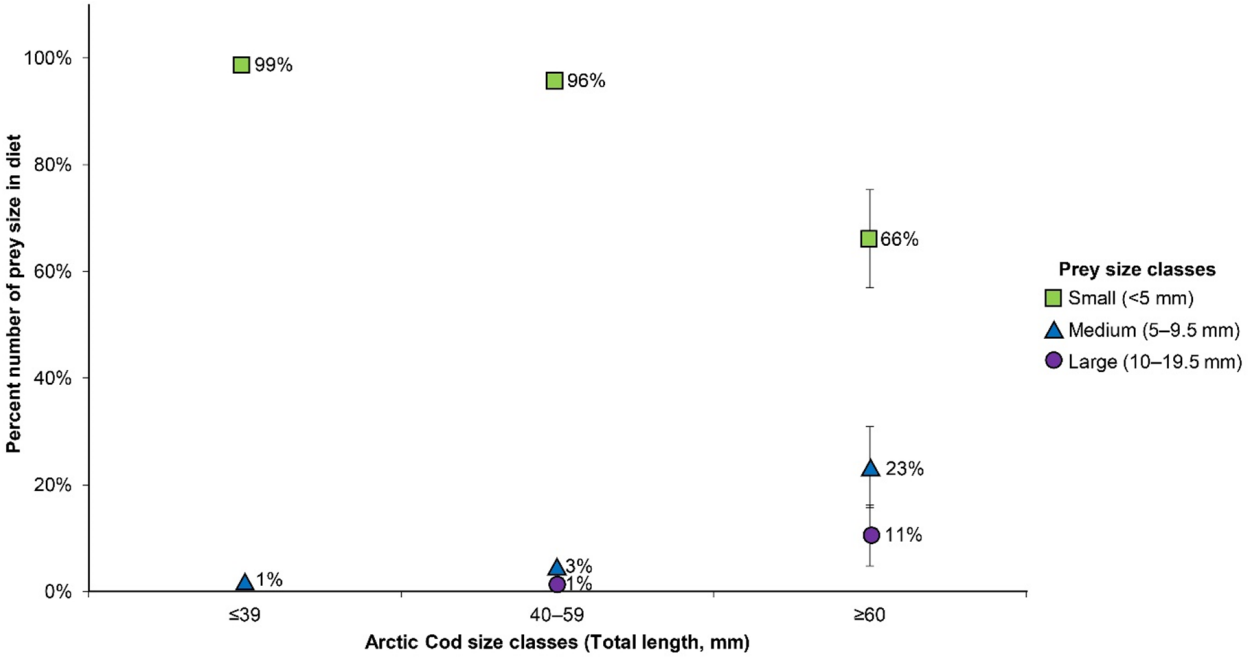

Figure 8.2.3.2. The percent contribution by number of small (<5 mm), medium (5–9.5 mm), and large (10–19.5 mm) prey summarized by three size classes of pelagic *Boreogadus saida*: (≤39 mm, 40–59 mm, ≥60 mm). Error bars signify the standard error of the mean percent number of prey sizes in pelagic *B. saida* diet.

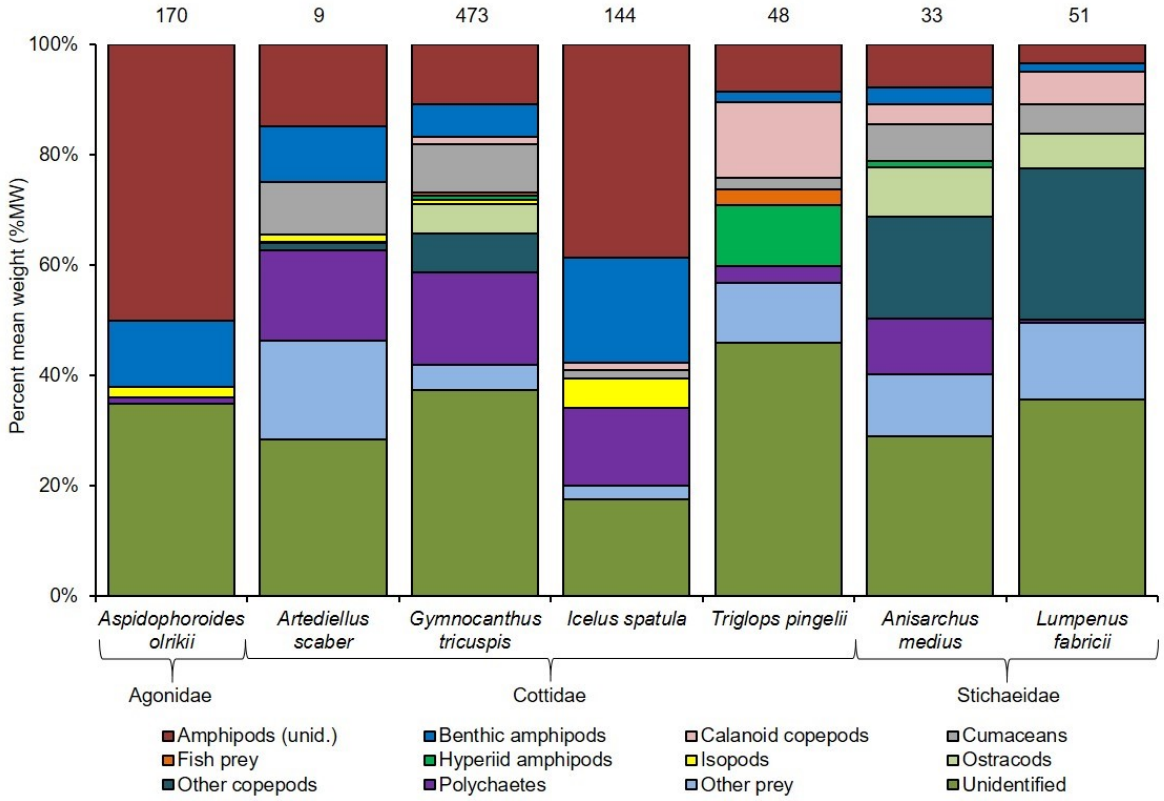

Figure 8.2.3.3. Pooled diet compositions of all *Aspidophoroides olrikii*, *Artediellus scaber*, *Gymnocanthus tricuspis*, *Icelus spatula*, *Triglops pingelii*, *Anisarchus medius*, and *Lumpenus fabricii*, based on mean weight of prey and including stomachs with unidentifiable prey. Stomach sample sizes are listed above each species column.

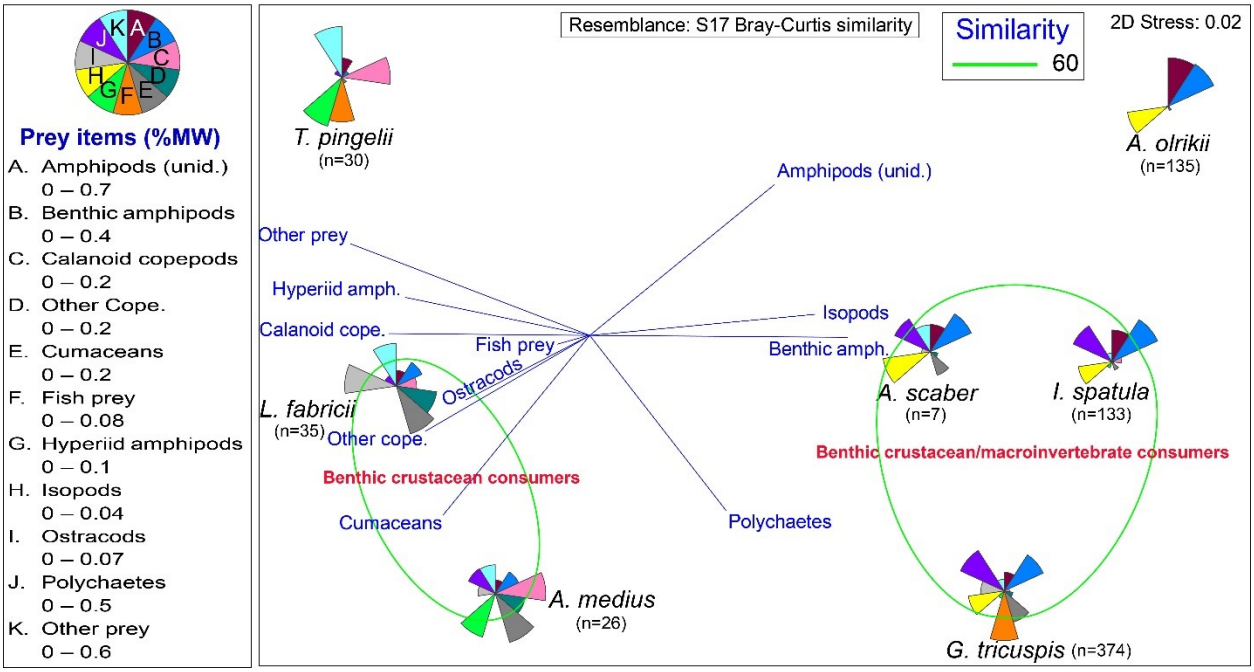

Figure 8.2.3.4. Non-metric multidimensional scaling (nMDS; 3D Stress: <0.01) of %MW of prey to determine diet similarities and differences among seven fish species.
Guilds, defined here as species that exhibited 60% similarity in prey use, are circled in green, with the respective guild names in red lettering.

There were significant relationships between some combination of fish lengths, station depths, latitudes, longitudes, and cruise years and the diet data for *A. olrikii*, *G. tricuspis*, *I. spatula*, and *L. fabricii*. Canonical correspondence analysis (CCA) determined that the majority of variance in these fishes' diets could be explained by fish length for *G. tricuspis* and *L. fabricii,* year for *A. olrikii*, and latitude for *I. spatula* (Appendix G). For *G. tricuspis*, an increase in fish length primarily highlighted an increase in the proportions of benthic amphipods, fish prey, and polychaetes in their diets and a decrease in hyperiid amphipods, isopods, ostracods, and other copepods. *L. fabricii* consumed larger proportions of amphipods, benthic amphipods, cumaceans and polychaetes with an increase in length. Year highlighted mostly rare prey use by *A. olrikii*, with polychaetes being consumed by a few fish in 2012. Benthic amphipod and ostracod proportions increased in *I. spatula* diet with an increase in latitude, while polychaete proportions were higher at more southerly stations. The was no relationship between fish lengths, station depths, latitudes, longitudes, and cruise years and the diet data for *A. scaber*, *T. pingelii*, and *A. medius*,

Overall, diet composition, defined as taxa composition and %MW of prey items, was significantly different among the four *Lycodes* species (Figure 8.2.3.5). Diet composition among the four eelpout species was low (11–15%). Within a single *Lycodes* species, similarity in diet composition among individual fish was also low (15–24%). In addition, eelpout species differed in the number of prey items consumed. *L. sagittarius* had the highest number of individual prey items (n = 1,448) and the highest number of coarse prey groups represented (n = 16). *L. polaris* had the fewest number of individual prey items (n = 134) and the fewest represented coarse prey groups (n = 11). *L. adolfi* and *L. seminudus* had similar numbers of individual prey items (n = 257 and n = 253 respectively), but *L. seminudus* had more coarse prey groups represented (n = 14) than *L. adolfi* (n = 12). CCA results also indicated that fish total length was significantly correlated with diet composition for all *Lycodes* species. Depth and longitude were significantly correlated with diet composition for *L. sagittarius*; however, depth and longitude were not significant for the other eelpout species. Increasing total fish length was associated with specific prey groups for each *Lycodes* species (Appendix H)

Differences were observed among eelpout species for stable nitrogen isotope signatures but not carbon isotope signatures (Appendix H). A bi-plot of $\delta^{15}N$ and $\delta^{13}C$ indicated differences in average nitrogen signature between *L. polaris* and the three other *Lycodes* species (Figure 8.2.3.6). Error bars for $\delta^{13}C$ overlapped, indicating no significant difference in carbon isotope signatures for all four eelpout species. Average $\delta^{13}C$ signatures ranged from -20.65 ± 0.8 (*L. adolfi*) to -20.22 ± 0.4 (*L. seminudus*). *L. seminudus* had the highest mean $\delta^{15}N$ signature (17.3 ± 0.9) and *L. polaris* had the lowest (15.0 ± 0.6).

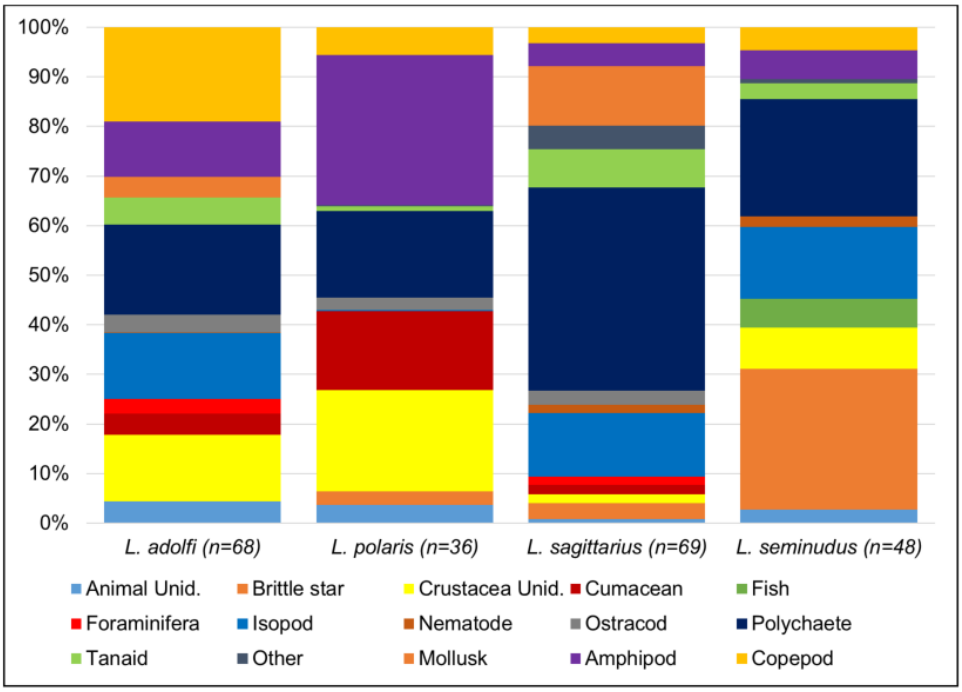

Figure 8.2.3.5. Percent mean weight (%MW) values for coarse prey groups found in stomachs of four eelpout species of the genus *Lycodes*.

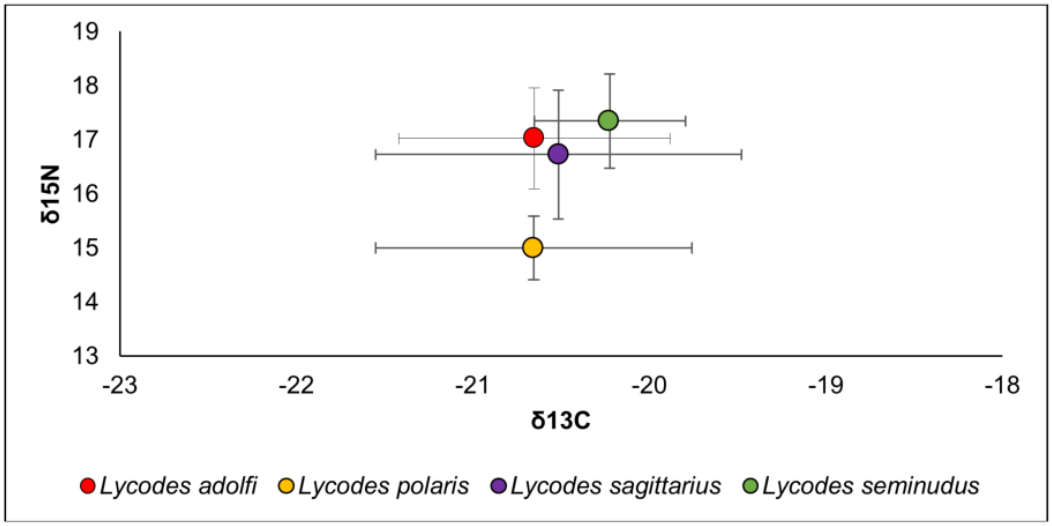

Figure 8.2.3.6. Average stable nitrogen and carbon isotope signatures for four eelpout species. Dots indicate mean values and error bars indicate standard deviations.

8.2.3.1 Size Class Analyses

Discrete ontogenetic shifts in diets were observable for members of the Gadidae, Cottidae, Agonidae, Zoarcidae and Stichaeidae families (Table 8.2.3.1, Appendix G, H). Size classes of *B. saida* diet differed slightly between demersally and pelagically caught fish. Based on their diet compositions, demersal *B. saida* separated into six discrete size classes: 39 mm, 40–49 mm, 50–59 mm, 60–79 mm, 80–169 mm, and 170–240 mm (Table 8.2.3.1). In contrast, pelagic *B. saida* separated into three discrete size classes: 39 mm, 40–59 mm, and ≥60 mm. At a 60% similarity level, there were three *G. tricuspis* size classes (≤70 mm, 71–90 mm, and 91–150 mm). Two size classes grouped for *I. spatula* at a 70% similarity level (≤50 mm and 51–80 mm). At a 60% similarity level, we determined two size classes for *T. pingelii* (≤50 mm and 51–114 mm). At an 80% similarity level, we determined two size classes for *A. olrikii* (≤60 mm and 61–80 mm). Diets of two of the zoarcids were too variable to determine any discrete shifts in prey use throughout ontogeny (Table 8.2.3.1). *Though L. adolfi partitioned into three cluster groups at 40% similarity, they did not break into discrete size classes (i.e., ≤50–100 mm and 60–190 mm) (Appendix H). At 40% similarity L. sagittarius grouped into three clusters that represented size classes ≤90–150 mm, 101–130 mm, and 151 to >300 mm. L. seminudus clustered into four size groups at 40% similarity; however*, they were mixed size groups (≤100 m, 101–250 mm, 251–300 mm, and a mixed group of 141–170 and >300 mm). Two size classes grouped at the 55% similarity level for *A. medius* (≤70 mm and 71–140 mm). Lastly, at the 55% similarity level, there were two size classes for *L. fabricii* (≤60 mm and 61–103 mm).

Table 8.2.3.1. Size class recommendations for fish families Gadidae, Cottidae, Agonidae, Zoarcidae, and Stichaeidae.
All analyses were based on the percent contribution by weight (%MW) of prey items to fish diet compositions. Size classes were indeterminable for *Artediellus scaber* and *Lycodes polaris* due to small sample sizes, and for *Lycodes adolfi*, *L. sagittarius*, and *L. seminudus* due to high variability in food habits. *B. saida* size classes are reported for both demersal (dem) and pelagic (pel) individuals.

Family	Species	n	Size class 1	Size class 2	Size class 3	Size class 4	Size class 5	Size class 6	Method
Gadidae	*B. saida* (dem)	1,023	≤ 39	40–49	50–59	60–79	80–169	170–240	NP MANOVA
	B. saida (pel)	416	≤ 39	40–59	≥ 60	–	–	–	NP MANOVA
	G. tricuspis	382	≤ 70	71–90	91–150	–	–	–	nMDS (60% Sim)
	I. spatula	134	≤ 50	51–80	–	–	–	–	nMDS (70% Sim)
	T. pingelii	34	≤ 50	51–114	–	–	–	–	Cluster (60% Sim)
Agonidae	*A. olrikii*	135	≤ 60	61–80	–	–	–	–	nMDS (80% Sim)
Zoarcidae	*L. adolfi*	107	Size classes indeterminable			–	–	–	nMDS (40–60% Sim)
	L. sagittarius	67	Size classes indeterminable			–	–	–	nMDS (40–60% Sim)
	L. seminudus	50	Size classes indeterminable			–	–	–	nMDS (40–60% Sim)
Stichaeidae	*A. medius*	27	≤ 70	71–140	–	–	–	–	Cluster (55% Sim)
	L. fabricii	37	≤ 60	61–103	–	–	–	–	Cluster (55% Sim)

8.2.4 Discussion

This study adresses information needs about the feeding ecology and diets of the most abundant fishes in the central and eastern Beaufort Sea: *Boreogadus saida*, *Artediellus scaber*, *Gymnocanthus tricuspis*, *Icelus spatula*, *Triglops pingelii*, *Aspidophoroides olrikii*, *Lycodes adolfi*, *L. polaris*, *L. sagittarius*, *L. seminudus, Anisarchus medius*, and *Lumpenus fabricii*. The information gained sets a benchmark for 2012–2014 for the use of prey by these 12 species over a large region of the US Beaufort Sea, and offers data that is important for food web models for this region.

Boreogadus saida are generalists (Renaud et al. 2012), meaning their diets generally reflect regional prey availability rather than selective feeding habits. Therefore, in theory, diet studies

should highlight the most regionally-abundant and important prey consumed by *B. saida*. Historically, there has been a lack of region-specific diet information available for *B. saida* in the western Arctic, making it necessary in the past to parameterize food web models using diet information from other regions (Whitehouse et al. 2014). Because prey availability and prey communities could vary widely throughout Arctic regions, this method could over- or under-estimate the importance of various prey. For prey like calanoid copepods, borrowing information from other regions would likely be acceptable given their similar importance throughout the northeastern Chukchi and western Beaufort Seas (Lowry and Frost 1981, Gray et al. 2015). However, the importance of prey such as chaetognaths and marine cladocerans would be unknown given that these prey types are relatively absent from the diets of *B. saida* outside of the Beaufort Sea. Because *B. saida* diet varies by year, habitat, region, and body size (Appendix F), studies should continue to document how particular prey groups vary in *B. saida* diets by these and other factors. Doing so would make it possible to implement and frequently refine a model that would greatly increase what is known about this species and its place in Arctic food webs.

Our research generally agrees with findings in the western Beaufort Sea regarding the diets of *G. tricuspis* (Atkinson and Percy 1992, Gray 2015), *A. olrikii*, *I. spatula*, *T. pingelii*, and *L. fabricii* (Atkinson and Percy 1992). *A. olrikii*, *G. tricuspis*, *I. spatula*, and *L. fabricii* each consume various taxa of demersal crustaceans and invertebrates (mostly combinations of benthic amphipods, copepods, cumaceans, and polychaetes) and *T. pingelii* consumes pelagic zooplankton (e.g., calanoid copepods and hyperiid amphipods). The major pattern that emerged from the between-species diet analysis was that fish diets were generally more similar within families than between them. For the within-species analysis, a combination of fish length, year, and latitude created most, but not all, of the variability in *A. olrikii*, *G. tricuspis*, *I. spatula*, and *L. fabricii* diets. While this study is informative, stronger conclusions could have been made were there less unidentifiable prey in each species' diet and were more stomachs available for *A. scaber*, *A. medius*, and *L. fabricii* (Appendix G)

L. adolfi, L. polaris, L. sagittarius, and *L. seminudus* have highly variable diets, both among individuals of the same species and among the four eelpout species. All four eelpout species have diets that are based heavily on demersal prey. Their high variability in diet and large number of unique prey items consumed suggests generalist feeding (Appendix H). *L. polaris* appears to be feeding on a lower trophic level than the other three *Lycodes* species. They may serve as potential competitors with other fish species for prey resources and space or as predators on other Arctic fish species. Larger *Lycodes* species may prey on other fish species in the region, at least opportunistically; however, the sample size was too small to draw solid conclusions on this front.

We recommend the size classes assigned here for representative species of families Gadidae, Cottidae, Agonidae, and Stichaeidae be viewed as a starting point for future diet studies. That said, we advise future researchers to periodically compare their results against ours, as differences in fish diets related to body size and spatial and temporal distributions, amongst other factors, will likely cause shifts from our recommended size classes. At this time, we cannot recommend size classes for the Arctic zoarcids examined here. We advise future researchers to examine the widest size range possible to highlight any ontogenetic shifts in prey use.

Knowledge of food web ecology of many Arctic fish species has been improved with this study, and could be further enhanced. Benchmark data on diet, distribution, and their ecological function is needed for these little understood fishes, as the Arctic ecosystem is rapidly changing

(IPCC 2014b). Additionally, ecological information on abundant but not necessarily culturally or commercially important fish groups is needed for long term monitoring of the Arctic ecosystem. Understanding interactions such as competition and predation among marine species is becoming more important as managers and major agencies are moving toward ecosystem-based management practices that require an in-depth knowledge of all abundant species, not just those with commercial or cultural importance. Lastly, characterizing the existing fish community is important for strengthening our understanding of how natural and anthropogenic changes may impact the ecosystem in the near future. This study produced one of the more comprehensive accounts of the diets of lesser-known fishes in the Arctic and offers a glimpse into their roles as predators in Arctic food webs.

8.3 Fish Fatty Acids

Sarah Hardy and Julia Dissen

8.3.1 Introduction

Boreogadus saida and Eelpout species are among the most widespread and abundant fishes throughout the Alaskan Arctic (Logerwell et al. 2011, Mecklenburg et al. 2011, Rand and Logerwell 2011). These forage fishes constitute a critical trophic step in the Arctic food web, linking primary and secondary production to higher trophic-level predators such as sea birds and marine mammals. In addition, forage fishes are subject to bottom-up controls by environmental conditions that affect primary production (Bouchard and Fortier 2011, Crawford et al. 2012). In the Arctic, changes in thickness and timing/extent of seasonal ice retreat are expected to alter patterns of primary production (Grebmeier 2012), which could affect the quality and quantity of available food sources for forage fishes (Chavez et al. 2011). This study examined inter- and intraspecific variation in lipid content and fatty acid profiles of *B. saida*, Canadian Eelpout (*Lycodes polaris*), and Longear Eelpout (*Lycodes seminudus*) across multiple years in the Beaufort and Chukchi Seas to explore how existing spatial and temporal differences in trophic conditions are manifested in forage fishes.

Fatty acids are components of dietary lipids and are essential for energy storage, structural components of cell walls, thermoregulation, and other important physiological processes (Parrish 2013). Inputs of fatty acids to the Arctic food web may vary in space and time due to environmental factors that impact phytoplankton species composition and their growth (Viso and Marty 1993, Reitan et al. 1994, Kelly and Scheibling 2012). These large-scale differences in fatty acid inputs to the food web are investigated here by comparing fatty acid profiles of fish from the Chukchi and Beaufort Seas, which differ in the magnitude of primary production as well as in a number of environmental controls on phytoplankton growth (Carmack and Wassmann 2006) that can, in turn, influence fatty acid composition of primary producers. Fatty acid profiles are like fingerprints that can be used to examine inter- or intraspecific differences in diet; their distinctive structures, and the apparent transfer of unaltered fatty acids from prey to predator, make them useful in identifying key trophic linkages (Dalsgaard et al. 2003, Budge et al. 2006, Parrish 2013).

In this study, fatty acids were quantified to characterize variability in fatty acid profiles across time and space in three Arctic forage fishes (*Boreogadus saida*, *Lycodes polaris*, and *Lycodes seminudus*) collected during multiple years in the Beaufort and Chukchi Seas. Stomach content analysis of *B. saida* and Eelpout has demonstrated that these forage fishes have distinct

but overlapping diets that include zooplankton (Walkusz et al. 2011, Gray et al. 2015). *B. saida* can be found feeding throughout the water column as well as near the seafloor. In contrast, Eelpout are primarily demersal species, and are normally found on soft muddy bottoms feeding on epibenthic prey (Aydin et al. 2007, Wienerroither et al. 2011). Comparing *B. saida* to Eelpout species can indicate how ecological differences (i.e., commonly feeding in pelagic versus demersal realms) affect fatty acid concentrations and nutritional value. Fatty acids were also compared between *Lycodes polaris* and *Lycodes seminudus* to investigate differences between two closely related species. Additionally, interannual and regional differences in fatty acid composition within species provide insights into variations in the food sources and nutritional quality of these taxa. Specific objectives were to (1) examine differences in fatty acid concentrations among species and determine if these species can be distinguished based on fatty acid profile regardless of within-species variations, (2) compare fatty acid profiles of *B. saida* from the Beaufort and Chukchi seas collected within the same years to examine spatial variability, and (3) analyze interannual variations in fatty acid composition of all three species in samples collected from 2010–2013.

8.3.2 Materials and Methods

Boreogadus saida, *Lycodes polaris*, and *Lycodes seminudus* were acquired from a series of expeditions in the Chukchi and Beaufort seas (Figure 8.3.2.1) between 2010 and 2013. Chukchi Sea samples were collected as part of the 2012 Russian-American Long-Term Census of the Arctic (RUSALCA) and 2010 and 2011 Alaska Monitoring and Assessment Program (AKMAP) cruises using plumb-staff beam and otter trawls (OT). Lipids were extracted from whole-body homogenates using a modified Folch extraction (Folch et al. 1957). Extracted lipids were converted to fatty acid methyl esters (FAME) as described by Budge et al. (2006). FAMEs were then analyzed for concentration of individual fatty acids using a gas chromatogram (GC) coupled to a flame ionization detector (FID) according to Bechtel and Oliveira (2006). Peaks were compared to retention times of commercial FAME standards. Concentrations of individual fatty acids were quantified as mg fatty acid/g lipids.

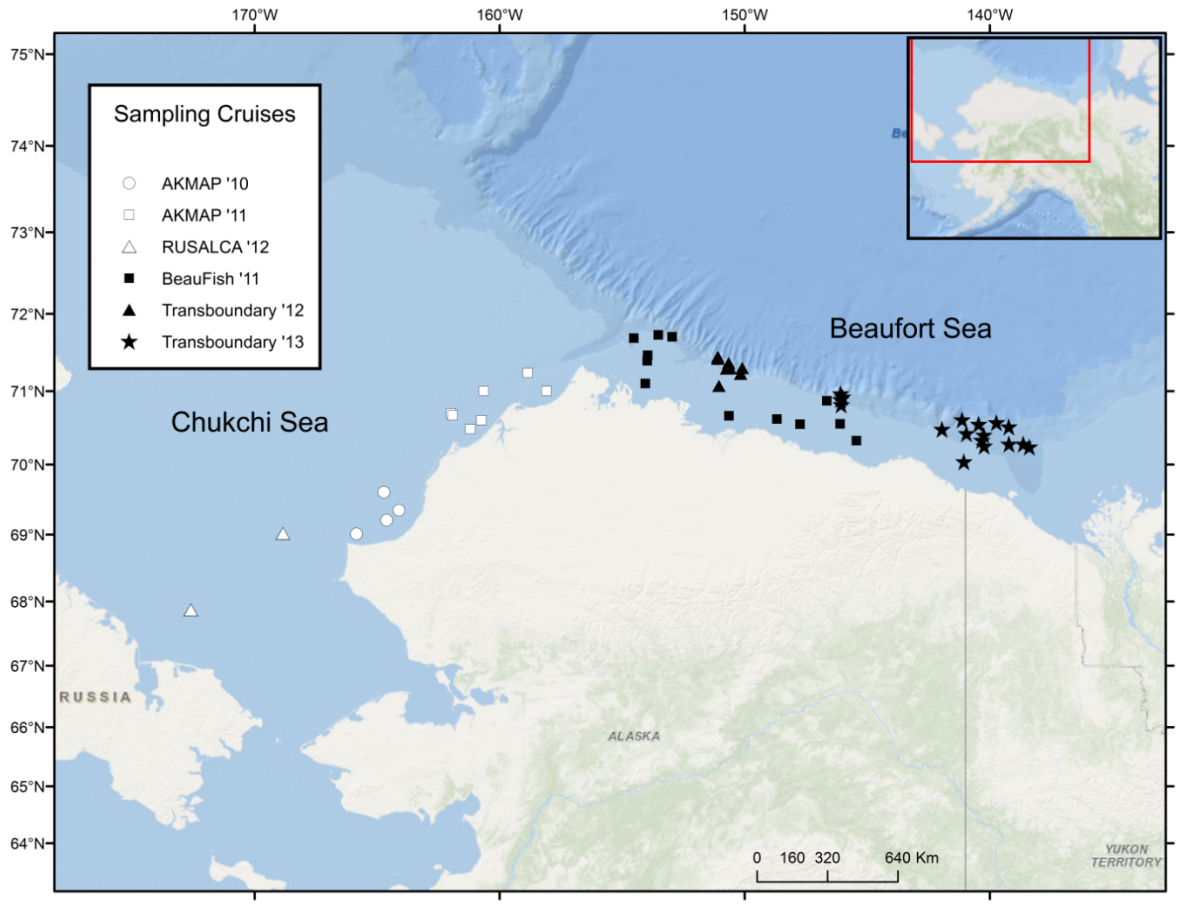

Figure 8.3.2.1. Stations in the Beaufort and Chukchi seas from which *Lycodes* spp. were collected for this report section.
Samples were taken during the Alaska Monitoring and Assessment Program 2010 (AKMAP '10) and 2011 (AKMAP '11), Central Beaufort Sea Fish Monitoring 2011 (BOEM-2011), Russian-American Long-Term Census of the Arctic 2012 (RUSALCA '12), and US Transboundary 2012 (Transboundary '12) and 2013 (Transboundary '13).

8.3.3 Results

Arctic Cod had a significantly different fatty acid profile than both Eelpout species, but the two Eelpout species did not differ significantly from each other (Figure 8.3.3.1a). With all sample years pooled, Arctic Cod had higher concentrations of total MUFAs (Figure 8.3.3.2). Arctic Cod and Longear Eelpout also differed significantly in total SFA, but all three species had similar amounts of total PUFA (Figure 8.3.3.2). Six fatty acids accounted for 64.5% of the dissimilarities in fatty acid profiles among Arctic Cod and Eelpout species, and all six fatty acids had higher mean concentrations in Arctic Cod than both Eelpout species. Mean concentrations of non-methylene-interrupted fatty acids (NMIs), indicators of benthic food sources, were highest in Longear Eelpout, followed by Canadian Eelpout, but were not identified in any Arctic Cod samples.

Within-species differences among regions were only examined for Arctic Cod as Eelpout were not collected in the Chukchi Sea. When data from all years were pooled, Arctic Cod had higher lipid content in the Chukchi Sea than in the Beaufort Sea. Fatty acid profiles of Arctic

Cod also differed between the Chukchi and Beaufort seas (Figure 8.3.3.1b). However, sample depth and fish weight were better predictors of within-species variation in fatty acid profile than region alone. All major classes of fatty acids (SFA, MUFA and PUFA) were higher in the Chukchi Sea than the Beaufort Sea (Figure 8.3.3.3), including the essential omega-3 fatty acids EPA and DHA.

Within the Beaufort Sea, mean lipid content as well as total SFA and MUFA of Arctic Cod were significantly higher in 2011 than 2012 and 2013 (Figure 8.3.3.4). In Chukchi Sea Arctic Cod, lipid content and total SFA, MUFA and PUFA showed the opposite trend, increasing from 2010 to 2012. When fatty acid profiles of Arctic Cod were examined within each region, they differed among years in almost all pairwise comparisons (Figure 8.3.3.1c–d). No significant difference was found in fatty acid profiles between years for either Eelpout species (Figure 8.3.3.1 e–f).

8.3.4 Discussion and Conclusions

This study demonstrated significant differences in fatty acid profiles between *Boreogadus saida* and the two Eelpout species, confirming niche separation in foraging habits of these fishes. Previous studies have found that fish and invertebrates with similar foraging ecologies have similar fatty acid profiles. However, the utility of fatty acid tracers in food web studies is limited without accurate data on how their composition varies between species, and across regional and temporal scales. In this study, differentiation of Eelpout species by fatty acid profile was dependent on sampling year. Subtle differences in diet may yield small differences in the composition and concentrations of fatty acids as a part of the total lipid pool in each species. Interestingly, profiles were more similar between species in some years than in others. Thus, inter-species differences observed when data are pooled across years could actually reflect interannual differences rather than real differences in foraging ecology between species.

Figure 8.3.3.1. Multivariate representation of fatty acid profiles of species, regions, and years. Non-metric multidimensional scaling (nMDS) plots of fatty acid profiles based on Bray-Curtis similarity matrices for (a) all samples, (b) 2011 and 2012 *Boreogadus saida,* from the Chukchi and Beaufort seas, (c) Beaufort Sea *B. saida*, (d) Chukchi Sea *B. saida*, (e) Beaufort Sea *Lycodes polaris*, and (f) Beaufort Sea *Lycodes seminudus*. Each data point represents the fatty acid profile of one individual fish.

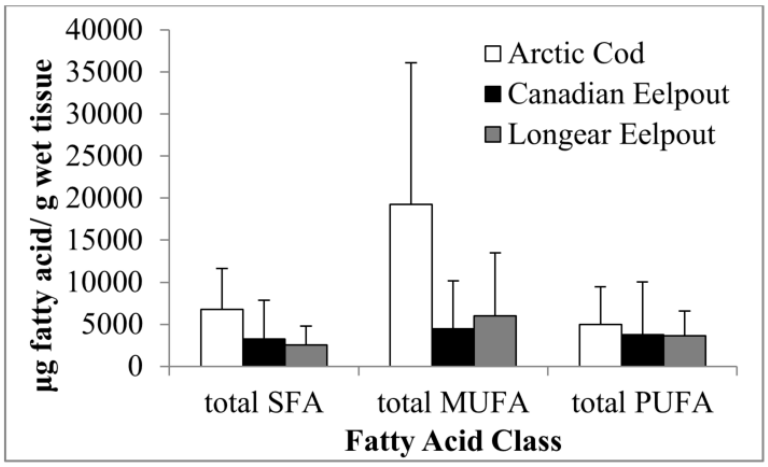

Figure 8.3.3.2. Variation in major fatty acid classes among *Boreogadus saida,* and Eelpout Species. Mean concentration of fatty acids by class for saturated fatty acids (SFA), monounsaturated fatty acids (MUFA), and polyunsaturated fatty acids (PUFA). Bars are shaded according to species. Error bars represent 1 standard deviation.

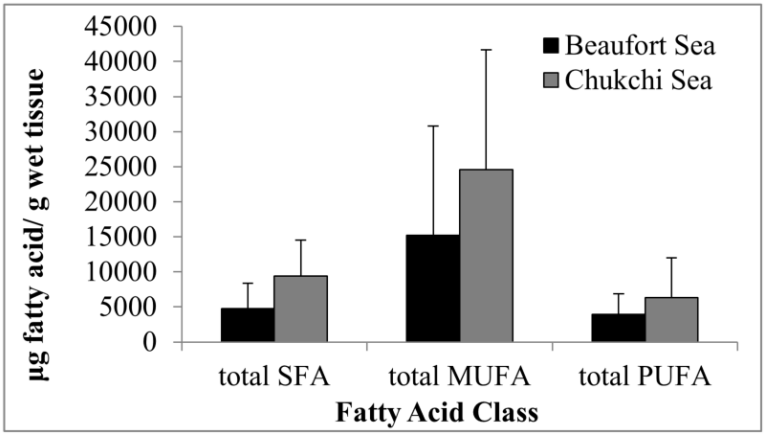

Figure 8.3.3.3. Regional variation in major fatty acid classes for *Boreogadus saida*.
Mean concentrations of total fatty acids in each class for saturated fatty acids (SFA), monounsaturated fatty acids (MUFA), and polyunsaturated fatty acids (PUFA) for Beaufort and Chukchi seas *B. saida*. Bars are colored according to region. Error bars represent 1 standard deviation.

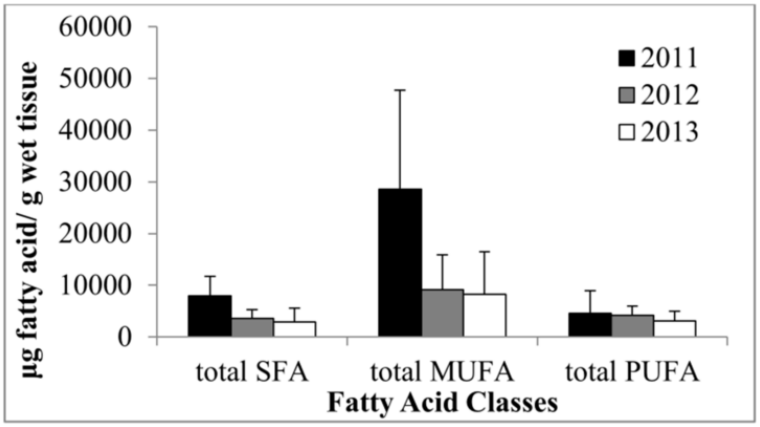

Figure 8.3.3.4. Temporal variation in major fatty acid classes for Beaufort Sea *Boreogadus saida*. Mean concentrations of total fatty acids in each class for saturated fatty acids (SFA), monounsaturated fatty acids (MUFA), and polyunsaturated fatty acids (PUFA) for Beaufort Sea *B. saida* from 2011–2013. Bars are colored according to year. Error bars represent 1 standard deviation.

The spatial variation observed in *Boreogadus saida* fatty acid profiles may be influenced by large-scale regional differences in primary production and environmental characteristics in the Beaufort and Chukchi Seas. Although *B. saida* have a broad distribution throughout diverse habitats in both regions, concentrations of certain fatty acids such as EPA were higher in the Chukchi Sea. When combined with higher total lipid, saturated fatty acids (SFA), and monounsaturated fatty acids (MUFA) content, high EPA concentration may also indicate a superior feeding environment of higher available lipid quality and/or quantity prey (Stowasser et al. 2012) in the Chukchi Sea relative to the Beaufort Sea. High concentrations of energy-dense MUFAs in Chukchi Sea fish tissues may represent an energetic advantage, and higher total lipid content in Chukchi Sea *B. saida* relative to the Beaufort Sea fish could make them better prey for higher trophic levels.

Regional differences in *Boreogadus saida* were most apparent in 2012, which was a low-ice year that resulted in high primary productivity across the Arctic, especially in the Chukchi Sea (Dolan et al. 2014). Variation in lipid content and fatty acids has been tied to year-to-year variations in primary and secondary production in other regions as well (Pethybridge et al. 2014). While average polyunsaturated fatty acids (PUFA) content was similar in both regions, Chukchi Sea *B. saida* did have elevated levels of PUFAs in 2012 over Beaufort *B. saida*, providing further evidence of better feeding conditions in that year. Interestingly, the essential fatty acids EPA and DHA, generally thought to be indicators of fish health and nutritional quality (Sargent et al. 1999), were also high in 2012 Chukchi Sea *B. saida*, although total lipid content was slightly lower. Although *B. saida* use sea ice for feeding and protection against predators, the high nutritional density of *B. saida* during a low ice year could suggest that this species encounters favorable feeding conditions under this environmental regime. Similar to trends in the Chukchi Sea, Beaufort Sea *B. saida* displayed an increase in the PUFAs EPA and DHA from 2011 to 2012. Alternatively, the significantly higher total SFA and MUFA in 2011 than 2012 in Beaufort Sea *B. saida* suggests that periods of favorable feeding conditions in the Beaufort and Chukchi Seas do not always coincide. These results support differences in *B. saida* fatty acid trends between the Chukchi and Beaufort Seas and encourage the use of fatty acids in monitoring regional variations in ecosystem dynamics. However, in this study, fish weight and collection depth were found to be significant covariates with fatty acid profile.

As the Arctic is a region especially vulnerable to climate change in the coming years, tools for annual monitoring of key species are needed to assess ecosystem change. Significant variation was observed in fatty acid profiles of fish collected from different years. This suggests that fatty acids could be a useful tool in interannual monitoring, such that the nutritional content of these fish can indicate the energy transfer and nutritional quality of the food chain they are feeding on and how these fish vary in quality for higher trophic level predators. In addition, despite significant within-species variation based on sampling year and region, fatty acid profiles of *Boreogadus saida* were significantly different than those of Eelpout. Conversely, the two Eelpout species were not reliably differentiated based on fatty acid profiles. Where prey species or groups such as forage fish and invertebrates in the Alaskan Arctic can be defined by fatty acid profile regardless of regional or temporal variations, fatty acid analysis could be reliably used to estimate predator diets.

8.4 Benthic Food Web Structure

Katrin Iken, Bodil Bluhm, and Lauren Bell

8.4.1 Introduction

Benthic food web structure is an important aspect of community functioning and varies with prominent water mass characteristics in the Arctic (Iken et al. 2010). Prior research suggests that benthic-pelagic coupling in the Alaskan Beaufort Sea is not as pronounced as in the Chukchi Sea (Dunton et al. 2005). Instead, it has become evident that the Beaufort Sea food webs may be considerably influenced by the strong terrestrial carbon influx from river drainage and coastal erosion (Dunton et al. 2006). In fact, Canada's Mackenzie River in the eastern Beaufort Sea delivers more terrestrially-derived particulate organic carbon (POC) to the Arctic Ocean (1.8×10^{12} g POC yr^{-1}; Telang et al. 1991) than all other Arctic rivers combined (Rachold et al. 2004). Across the Beaufort shelf and upper slope, terrestrial influence is particularly noticeable in the central shelf around the Colville River and is reflected in longer food webs with less trophic redundancy (i.e., a low degree of dietary overlap among taxa within a food web) than observed in the eastern Beaufort Sea region (Divine et al. 2015). Low trophic redundancy may mean high vulnerability to changes in environmental forcing or to loss of species as trophic niches may remain vacant. Distinct depth differences in food web structure of benthic communities have also been observed on the Canadian Beaufort shelf and slope, owing to the degradation of organic matter during sinking from surface waters to depth (Roy et al. 2015a).

Terrestrial organic matter (OM_{terr}) has traditionally been considered a poor food source for marine consumers (Cividanes et al. 2002), raising the question of whether benthic communities on the Beaufort Sea shelf and slope may be largely energy limited. Today, however, microbial metabolism is becoming increasingly understood as an efficient and quality-enhancing process than can make terrestrial carbon available for marine consumers (Rontani et al. 2014). While the trophic structure in the nearshore lagoons of the Beaufort Sea has been intensely studied (e.g., Dunton et al. 2006, 2012), food web structure is much less well known farther offshore on the shelf and especially on the slope. Identifying the availability of various food sources (e.g., marine versus terrestrial organic matter) and understanding their transfer through the food web to higher trophic levels is essential to assessing the structure of marine communities and their vulnerability to anthropogenic and climatic changes. Therefore, a particular focus in this study

was to examine the extent to which terrestrial carbon influences the offshore marine food webs of the Beaufort Sea, from shelf to slope.

Tracking of organic matter provenance and energy flow in aquatic food webs is commonly accomplished using the well-vetted technique of stable isotope analysis (Michener and Lajtha 2007). Carbon derived from different end members such as marine phytoplankton, ice algae, and terrestrial plant production have different isotopic signature ranges (Wooller et al. 2007); therefore, the carbon stable isotope ratio ($\delta^{13}C$) of an organic matter sample can indicate the relative composition of the endmember sources of that sample. Nitrogen stable isotope ratios ($\delta^{15}N$ values) show a stepwise enrichment of the heavier isotope (^{15}N) between food source and consumer due to trophic fractionation (Vander Zanden and Rasmussen 2001, Post 2002a), allowing for the creation of food webs based on the $\delta^{15}N$ values of consumers relative to their baseline food source. In addition to measuring the $\delta^{13}C$ and $\delta^{15}N$ values of organic matter, oxygen stable isotope ratios ($\delta^{18}O$ values) of surface waters can be used to trace the distribution and mixing of a freshwater source into the marine system. We used these isotopes to track freshwater from the Mackenzie River Plume (the largest river in the study area) in the surface waters over the Beaufort Sea shelf and slope, thereby providing a proxy of a potential pathway of OM_{terr} contained in this freshwater into the Arctic Ocean.

8.4.2 Objectives

The specific objectives for the food web component of the Transboundary project were to:

1. Characterize food source end members and freshwater presence using stable isotope analysis;
2. Describe lower trophic food web structure in the Beaufort Sea region using stable isotope analysis, including an interannual comparison.

These objectives were addressed with data collected in 2012, 2013 and 2014. 2012 and 2013 data were analyzed as part of the thesis work of Master of Science student, Lauren Bell. A version of the thesis has been published by the journal *Marine Ecology Progress Series* (Bell et al. 2016).

8.4.3 Methods

8.4.3.1 Sampling Area and Transect/Station Groupings

Samples for food web structure analysis were collected in 2012, 2013 and 2014 at all stations sampled during the cruises. The primary target regions were the central Beaufort Sea in 2012 and the eastern Beaufort Sea in 2013 and 2014. To best characterize the trophic structure in the central and eastern Beaufort Sea, the sampled transects were grouped (for some analyses) into regions based on distance to the Mackenzie River and its assumed relative OM_{terr} influence (Dunton et al. 2012). These included (from east to west): Inner Mackenzie Plume (IMP), Outer Mackenzie Plume (OMP), Camden Bay (CB), and Colville Plume (CP) (Figure 8.4.3.1.1). The 20, 37, 50, and 100 m depth stations were grouped as Beaufort ‘shelf’, while deeper stations were grouped as ‘slope’.

8.4.3.2 Water Sampling for Analysis of Freshwater Distribution

To trace the prevalence of freshwater across the study area during the time of sampling, surface and 10 m depth water samples were collected at each station only in 2013 for oxygen

($\delta^{18}O$) analysis. Water samples were collected from Niskin bottles attached to the CTD, pipetted into 2 mL glass vials (Agilent Technologies) with no headspace, crimped closed, and stored at room temperature until deuterium analysis.

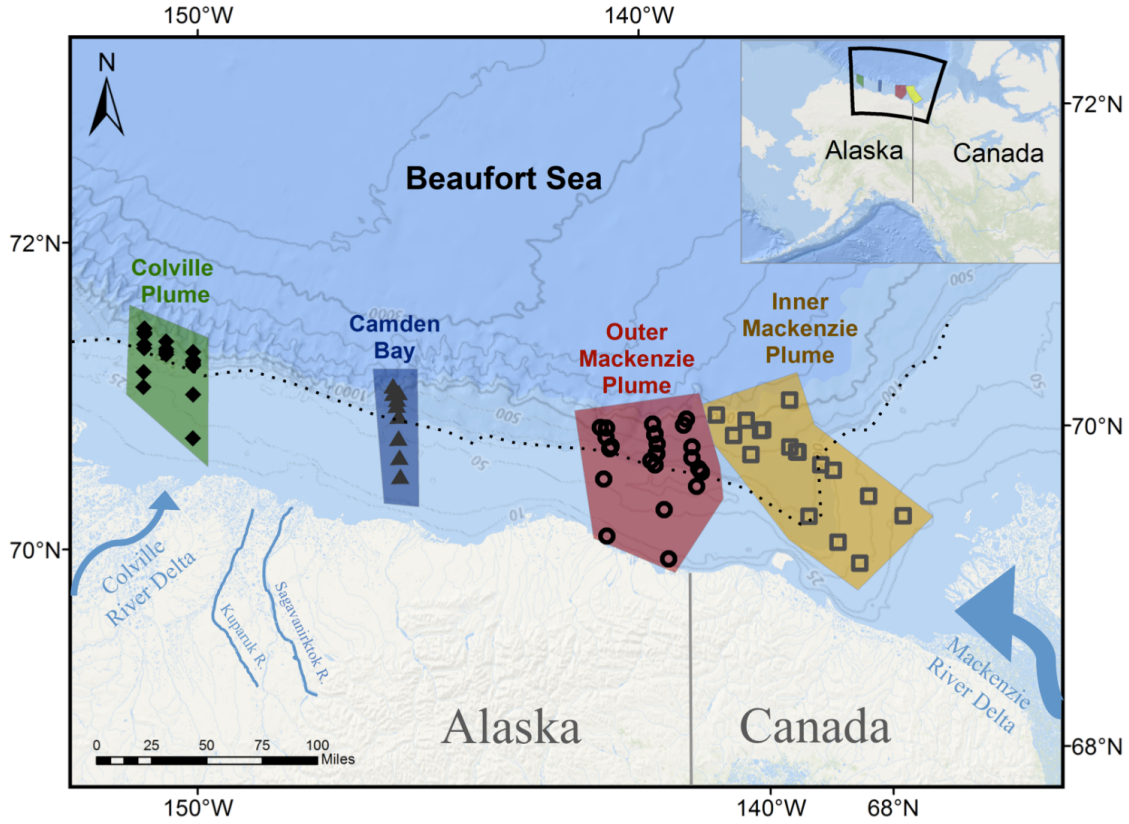

Figure 8.4.3.1.1. Map of sampling stations during 2012 and 2013 Transboundary cruises, grouped into four regions (from west to east: Colville Plume (CP, including transects B1, B2 and BX), Camden Bay (CB, including transect A1), Outer Mackenzie Plume (OMP, including transects A2, A1, and TBS), and Inner Mackenzie Plume (IMP, including transects MAC and GRY).

8.4.3.3 Particulate Organic Matter Sampling

In all years, particulate organic matter (POM) was collected from the water column (pPOM), and surface sediments (sPOM) provided baseline stable carbon and nitrogen isotope values for these potential food sources (Iken et al. 2005, Dunton et al. 2012). Water was sampled from the sub-surface chlorophyll-*a* maximum layer, or 20–30 m depth if no clear chlorophyll layer was present (n = 3 per station), using Niskin bottles. Approximately 1 L water for each pPOM replicate was filtered onto a pre-combusted Whatman GF/F filter and frozen at -20 °C until analysis. A single sample of sPOM was taken from the upper 1 cm of a box core (2012) or van Veen grab (2013) at each station, where available, and kept frozen until processing. The US-Canada Transboundary cruise was unable to sample surface sediments deeper than 200 m bottom depth in 2013. However, within three weeks of the Transboundary sampling, the Canadian Beaufort Regional Environmental Assessment (BREA) initiative took sediment samples near select 2013 slope stations (n = 5) using a box core. These samples were added to our sample set.

Sea ice algae can be an important food source in Arctic systems (Roy et al. 2015a); however, this study sampled during the ice-free summer period. To include a sea ice algal endmember reference value in the trophic mixing models, ice POM (iPOM) was collected off the northwest coast of Barrow, Alaska, (at 71.3815° N, 156.5243° W) on 8 April 2014. Bottom sections of sea ice (n = 2) were taken from ice cores, placed in Ziploc bags, and frozen in the field.

8.4.3.4 Faunal Sampling for Carbon and Nitrogen Stable Isotope Analysis

To investigate benthic food web structure across the Beaufort Sea, representative fauna at each station were collected for isotope analysis. Replicate (n = 3) samples of major benthic invertebrate taxa were collected from van Veen grabs, box cores, beam trawls (4-mm mesh), and otter trawls (19-mm mesh). Collections from trawls also included demersal fish species. We preferentially collected muscle tissue, but occasionally tissue was derived from tube feet (Asteroidea), oral discs (Ophiuroidea), body wall (Polychaeta, Echiura, Actinaria), or whole individuals (Amphipoda, Cumacea). Common fish species were sampled for muscle tissue. When possible, the guts of the whole animals were removed, and all tissues were rinsed with filtered seawater. Tissue samples were frozen onboard at -20 °C and then dried at 60 °C for 24 h. All taxon names were standardized to the World Register of Marine Species (www.marinespecies.org). Shelf and slope communities were then quantitatively assessed for the epibenthic invertebrate biomass distribution within trophic levels for 2013 samples, based on community biomass data from trawl samples (see Epifauna section 6.0).

8.4.3.5 Lab Processing of Stable Isotope Samples

At the University of Alaska Fairbanks (UAF), pPOM filters were fumed with HCl vapors for 24 h to remove carbonate. sPOM samples were repeatedly treated with 1 N HCl until all bubbling ceased to ensure removal of all carbonates (Iken et al. 2010, Goñi et al. 2013), rinsed until pH stabilized, and freeze-dried. Sea ice samples were thawed and centrifuged to concentrate iPOM (n = 3 replicates per ice piece) and then freeze dried. Benthic invertebrate tissue samples that contained carbonate were treated with 1 N HCl. Because lipids can be depleted in ^{13}C relative to protein or carbohydrate and significantly confound stable carbon isotope interpretation in animals with large lipid stores (Mintenbeck et al. 2008), all tissue samples were repeatedly treated with 2:1 chloroform:methanol to remove lipids. All pPOM and tissue samples were re-dried for 24 h at 60 °C prior to analysis.

8.4.3.6 Stable Isotope Analysis

Stable isotope data for all samples were obtained using continuous-flow isotope ratio mass spectrometry at the Alaska Stable Isotope Facility (ASIF) at UAF. Water samples from 2013 were measured for $\delta^{18}O$ values. All pPOM, sPOM, and iPOM samples and approximately 0.3 mg dry weight of each homogenized faunal tissue sample were analyzed for $\delta^{13}C$ and $\delta^{15}N$ values. $\delta^{18}O$ values were measured using a pyrolysis-elemental analyzer (ThermoScientific high temperature elemental analyzer-TC/EA) attached via a Conflo IV to an isotope ratio mass spectrometer (IRMS; Thermo Finnigan DeltaV^{Plus}). $\delta^{13}C$ and $\delta^{15}N$ values were measured using a Costech ESC 4010 elemental analyzer interfaced via a Conflo IV with an IRMS (Thermo Finnigan Delta V^{Plus}). Results are expressed as conventional δ notation in parts per thousand (‰) according to the following equation:

$$\delta\ (‰) = ([R_{sample}/R_{standard}] - 1) * 1000 \quad (1)$$

where R is the determined ratio of n(^{i}Element) / n(^{j}Element), abbreviated as ^{18}O: ^{16}O, ^{13}C: ^{12}C, or ^{15}N: ^{14}N. Standards were Vienna Standard Mean Ocean Water (VSMOW) for $\delta^{18}O$ values, Vienna Pee Dee Belemnite (VPDB) for $\delta^{13}C$ values, and atmospheric N_2 for $\delta^{15}N$ values. Instrument precision at ASIF was <0.5‰ for $\delta^{18}O$ values, and <0.2‰ for both $\delta^{13}C$ and $\delta^{15}N$ values.

8.4.4 Data Analysis

8.4.4.1 Stable Isotope Values of Water Samples (2013 Only)

Mackenzie River-derived freshwater is characterized by a flow-averaged $\delta^{18}O$ value of -19.2‰ (Cooper et al. 2008). Assuming near-surface (≤20 m) Beaufort Sea water is a mixture of sea ice melt and the Polar Mixed Layer (PML), the Beaufort Sea ocean-water $\delta^{18}O$ value has been specified as approximately -2.3‰ (Lansard et al. 2012). Trends in surface and 10 m depth water $\delta^{18}O$ values across the study area were visualized in Ocean Data View v.4.5.3 (Schlitzer 2011). For additional verification that water sample $\delta^{18}O$ values were related to freshwater influence, the correlation between water sample salinity and $\delta^{18}O$ values at surface and 10 m depth was tested using Spearman's rank correlation. Predictive relationships between water $\delta^{18}O$ values and longitude or log-transformed station bottom depth were tested using regression analyses ($\alpha = 0.05$).

8.4.4.2 Stable Isotope Values of End Members (POM)

Published references used for possible POM endmembers in mixing models included terrestrial POM ($\delta^{13}C$ = -28.8‰ ± 3.2‰, $\delta^{15}N$ = 0.8‰ ± 1.0‰; Schell et al. 1984, Goñi et al. 2000, Dunton et al. 2006), marine phytoplankton POM ($\delta^{13}C$ = -24.0‰ ± 0.4‰, $\delta^{15}N$ = 7.7‰ ± 0.3‰, McTigue and Dunton 2013), and ice POM ($\delta^{13}C$ = -21.6‰ ± 0.5‰, $\delta^{15}N$ = 8.1‰ ± 4.2‰, this study). Mixing models using Stable Isotope Analysis in R (SIAR) v.4 (Parnell et al. 2010) were used to assess endmember contributions to the pPOM and sPOM samples from this study. While both the Mackenzie River and coastal erosion are distinct vectors of OM_{terr} to marine consumers in the Beaufort Sea (Dunton et al. 2006, Casper et al. 2014), sufficient isotopic resolution to differentiate these two sources of OM_{terr} was not possible in this study. pPOM and sPOM $\delta^{13}C$ and $\delta^{15}N$ values were analyzed for significant differences among regions and between shelf or slope depth groups using two-way analysis of variance (ANOVA, $\alpha = 0.05$) followed by Tukey's post-hoc tests for differences among groups (R 3.0.3; R Development Core Team 2014).

Given the $\delta^{13}C$-enrichment in Arctic ice algal values over the growing season, the early growing season snapshot value we measured may be inadequately reflecting the contribution of iPOM to the food web. Therefore, we applied the mixing model analysis also with a $\delta^{13}C$ value of -15.5‰, which reflects a spring bloom situation at high ice algal biomass (Gradinger et al. 2009). This approach allowed us to evaluate how enriched ice algal $\delta^{13}C$ values would alter the estimate of relative contributions of the various organic matter sources to pPOM and sPOM samples.

To investigate how station bottom depth affected pPOM and sPOM composition, the total organic carbon (TOC) to total nitrogen (C:N) ratios and $\delta^{13}C$ and $\delta^{15}N$ values of 2012 and 2013 pPOM and sPOM samples were correlated with station bottom depth within regions. C:N ratios

can be an effective proxy for terrestrial organic matter influence because the atomic C:N ratios of terrestrial plants are typically >15, whereas phytoplankton atomic C:N ratios range between 4 and 10 (Macdonald et al. 2004). Lower C:N rations indicate higher food quality. Although $\delta^{15}N$ and C:N ratios of organic matter are much more susceptible to alteration during biogeochemical processing than $\delta^{13}C$ values (Thorton and McManus 1994), the simultaneous application of all three organic tracers can provide a stronger indication of the source and alteration history of POM samples than one tracer alone.

8.4.4.3 Relationship between Fauna and Food Sources in Relation to Depth

To discern regional differences in carbon source utilization, $\delta^{13}C$ values of consumers from 2012 and 2013 were grouped by feeding guild and analyzed for significant differences between the two fixed factors region and depth group (shelf or slope) using a two-way ANOVA (α = 0.05) and then tested for differences between factor groups using Tukey's post-hoc tests. Taxa were assigned to one of four feeding guilds: benthic sub-surface deposit feeders (n = 3), benthic surface deposit feeders (n = 9), benthic suspension feeders (n = 6), and benthic predators/ scavengers (n = 26). The impact of depth on trophic enrichment of $\delta^{15}N$ in benthic consumers was tested with linear regression analysis of the relationship between benthic consumer $\delta^{15}N$ value and bottom depth for the 2013–2014 study area. The majority of taxa did not occur across all depths; thus, only some of the most widespread benthic consumers from 2013 and 2014 samples were chosen for this analysis: the brittle star *Ophiocten sericeum,* the gastropod *Colus sabini,* the anemone *Allantactis parasitica*, polychaetes of the family Polynoidae, arthropods within the class Pycnogonida, and arthropods of the order Cumacea.

8.4.4.4 Food Web Structure

Community food web structure is based on the trophic position of the community members, which is calculated against a common baseline. pPOM has been frequently used as this trophic baseline in the analysis of Arctic marine food webs (see Søreide et al. 2006, Iken et al. 2010), and we used pPOM as one of our trophic baselines. We also used a primary consumer as an alternative baseline because near-surface pPOM changes during its vertical flux and does not sink entirely vertically to greater depth stations (Forest et al. 2013). Additionally, pPOM has high temporal variability that is not appropriately captured in a single sample taken during a cruise (Vander Zanden and Rasmussen 1999). Primary consumers provide a long-term integrated signal of basal food sources to the benthos (Vander Zanden and Rasmussen 1999, Iken et al. 2010). We used the surface deposit-feeding brittle star *Ophiocten sericeum* as a primary consumer based on its wide-spread distribution across longitudinal and depth ranges in the study area. The limited number and lack of replicate sediment POM samples prevented their use as a trophic baseline.

Food web length was determined by assuming an average 3.4‰ increase in $\delta^{15}N$ values per trophic level (TL) (Vander Zanden and Rasmussen 2001, Post 2002b), which were defined as discrete steps, such as TL 1, TL 2, TL 3, etc. In contrast, the individual trophic position (TP) of each consumer is a continuous variable calculated based on its isotopic distance to a chosen baseline, in this case pPOM as TL 1, or *Ophiocten sericeum* (Os) as TL 2. Trophic positions were calculated from the following equation:

$$TP_{POM\text{-}based} = ([\delta^{15}N_{consumer} - \delta^{15}N_{POM}]/3.4) + 1$$

$$TP_{Os\text{-}based} = ([\delta^{15}N_{consumer} - \delta^{15}N_{Os}]/3.4) + 2$$

Taxon TP was estimated such that the food web TL 1 category included consumers with TP 1.0 to 1.9, TL 2 contained all TP 2.0 to 2.9, etc., and any TP less than 1.0 was TP0. Appendix I contains tables with additional food web information. The Appendix I Table 1 lists sites where samples were collected for stable isotope analysis. For each taxon, Appendix I Table 2 reports trophic positions and average values of $\delta^{13}C$ and $\delta^{15}N$ values by region, shelf and slope.

The relative contribution of epifaunal biomass toward various trophic levels was calculated based on trawl samples in 2014 (see section 6.0). Because not all epifaunal invertebrates were also measured for stable isotope values, some of the community biomass remained unaccounted for and was labeled as "TL unknown." Across all transects and depth groups, the percentage of unknown was between 4 and 14% of the total biomass. Biomass contributions to trophic levels were assessed for shelf (10–100 m stations) and slope (200–1000 m stations) regions of transects A6 (146° W), A2 (142° W), A1 (141° W), and TBS (140° W) in 2014, the year where the most epibenthic invertebrate taxa were measured for stable isotope composition.

8.4.4.5 Interannual Comparison (2013, 2014)

Several transects were sampled for benthic food web structure in both 2013 and 2014 to assess interannual variability in food web structure. The repeat transects included A6 (146° W), A1 (141° W), and TBS (140° W). For both years and all three transects, we present the trophic positions of those taxa that were sampled in both years, grouped by shelf (10–100 m) and slope stations (200–1000 m) for each transect. We also present the relative contribution of these common taxa to each trophic level to depict persistence or differences in trophic structure between sampling years and transects. We used both POM and *Ophiocten sericeum* trophic baselines (described above) for the TL calculations.

8.4.5 Results

8.4.5.1 Freshwater Presence in Study Regions (Objective 1)

Surface water $\delta^{18}O$ values in 2013 were lowest (-12.2‰) near the Mackenzie River outflow, indicating highest riverine freshwater content. $\delta^{18}O$ values generally increased with distance from the Mackenzie River Delta (Figure 8.4.5.1.1a). By region, station bottom depth was a significant predictor of surface water $\delta^{18}O$ values ($p < 0.01$) in both the IMP and OMP regions. Shallower stations were associated with lower surface water $\delta^{18}O$ values between -12 to -10‰ in the IMP ($R^2 = 0.57$), indicating stronger freshwater presence. In contrast, shallow stations in the OMP region were associated with higher surface water $\delta^{18}O$ values (less freshwater) between -9 to -5‰ ($R^2 = 0.68$). Farther to the west, in the CB region, there was no relationship between

station bottom depth and surface water $\delta^{18}O$ values, which were around -6 to -5‰ throughout that region. At 10 m depth, the water $\delta^{18}O$ value isoscape was enriched in ^{18}O (indicting less influence of freshwater) relative to the surface. $\delta^{18}O$ values were nearly homogenous between -6 and -3‰ across the entire study area (Figure 8.4.5.1.1b), with no relationship between longitude or station bottom depth at a regional level.

8.4.5.2 Characterization of POM Food Sources (Objective 1)

We characterized the $\delta^{13}C$ and $\delta^{15}N$ values of pelagic POM (pPOM) and sediment POM (sPOM) to assess their composition from terrestrial, marine, and ice POM. pPOM and sPOM $\delta^{13}C$ and $\delta^{15}N$ values in 2012 and 2013 generally fell in between published isotopic values of terrestrial and marine organic matter endmembers, although several samples were outside of the standard deviations of these endmembers (Figure 8.4.5.2.1). Averaged across the entire study area, pPOM was composed of an estimated 58% marine-origin POM and 39% terrestrial-origin POM, with only 3% contribution by ice algal POM (based on the early season iPOM value we measured from our Barrow samples). In contrast, endmember contributions to sPOM samples were estimated to be more evenly distributed, with 33% from marine-origin POM, 31% from terrestrial-origin POM, and 36% from ice algal POM. When the more enriched ^{13}C value for iPOM (late season value from May 2003 in Barrow, Gradinger et al. 2009) was used in mixing model analysis, contributions from ice algal POM dropped significantly to 1% in pPOM and 10% in sPOM, while marine-origin POM contributions increased to 60% in both pPOM and sPOM.

The relationship between pPOM and sPOM isotope values and C:N ratios and station bottom depth was investigated for 2012 and 2013 to assess if these basal organic matter sources change with depth related to degradation processes. The C:N, $\delta^{13}C$, and $\delta^{15}N$ ratios of pPOM and sPOM grouped by region had no significant relationship ($p < 0.05$) with bottom depth (Figure 8.4.5.2.2), except for sPOM in the IMP region ($R^2 = 0.81$). $\delta^{13}C$ and C:N values were not significantly correlated in either pPOM or sPOM samples. When depth was grouped categorically into shelf versus slope, pPOM $\delta^{13}C$ values were significantly affected by both region and depth group (ANOVA, $p < 0.05$), although the interaction between fixed factors region and depth group was not significant. pPOM in the CP region was significantly enriched in ^{13}C compared with the CB, OMP, and IMP regions over both the shelf and the slope (Figure 8.4.5.2.2). In all regions except the IMP, mean pPOM $\delta^{13}C$ values were higher on the shelf relative to the slope; however, these differences were not significant because of high within-region variation. In sPOM, $\delta^{13}C$ values were significantly lower on the shelf versus slope in the CP and IMP regions but were not significantly different elsewhere (Figure 8.4.5.2.2). sPOM $\delta^{13}C$ values were not well correlated with pPOM $\delta^{13}C$ values when compared for the same stations ($R^2 = 0.16$). $\delta^{15}N$ values of pPOM and sPOM were not significantly different between shelf and slope stations across or within regions (data not shown).

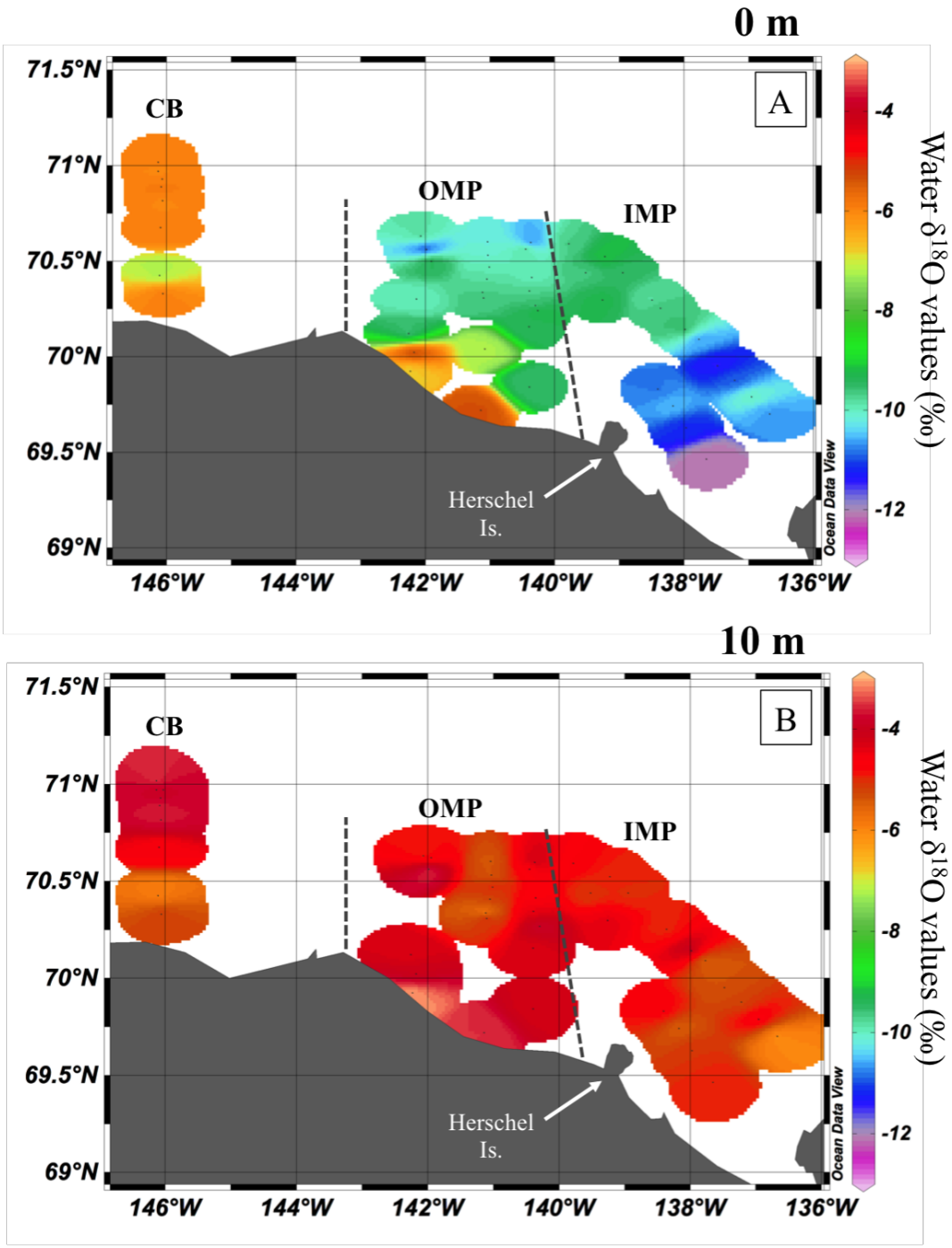

Figure 8.4.5.1.1. $\delta^{18}O$ values (‰) of water samples taken from the surface (A) and 10 m depth (B) in the 2013 sampling area (CB, OMP, and IMP regions).
The Mackenzie River Delta is to the bottom right (southwest) corner of the maps. A strong freshwater gradient from the Mackenzie River outflow was visible only in the surface layer.

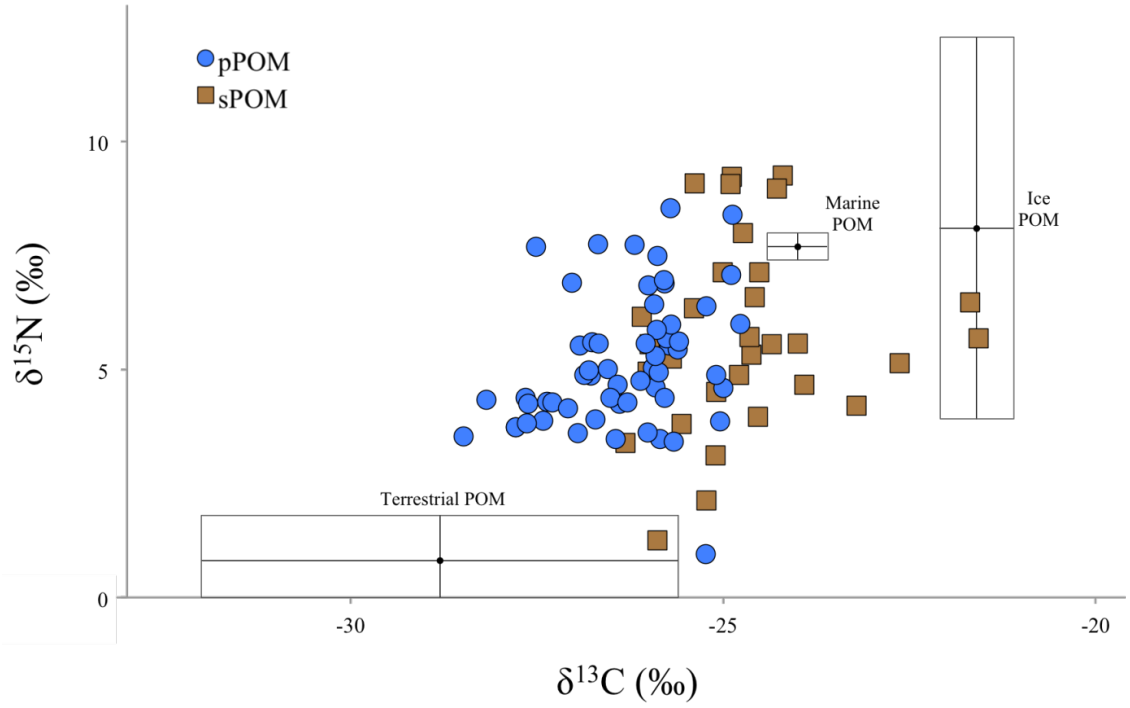

Figure 8.4.5.2.1. Biplot of $\delta^{13}C$ and $\delta^{15}N$ values for pelagic particulate organic matter (pPOM) and sediment POM (sPOM) compared alongside potential POM endmembers in the eastern Beaufort Sea. Each pPOM symbol represents a station average of three replicates, while sPOM symbols represent the single sample taken at each station. Boxes encompass standard deviations from the mean isotopic values of each POM endmember (ranges from literature sources, see text for details).

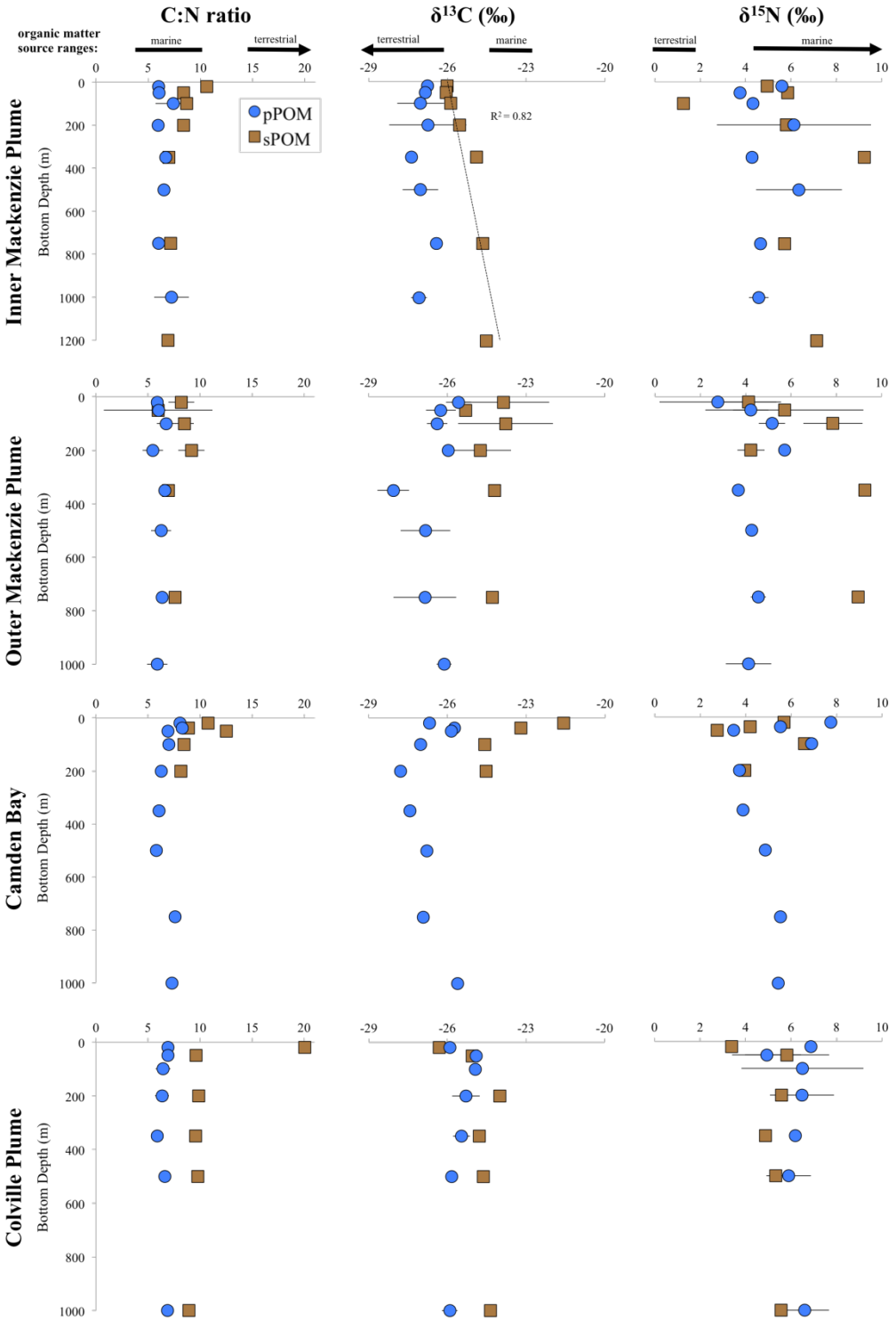

Figure 8.4.5.2.2. Carbon to nitrogen ratios, $\delta^{13}C$ and $\delta^{15}N$ values of pPOM and sPOM against station bottom depth, averaged by region.
Error bars indicate standard deviation between replicates across transects, and trend lines and R^2 values are only shown for significant relationships between organic matter tracer and station bottom depth. Arrows above the x-axis indicate typical value ranges for terrestrial and marine organic matter based on published literature.

8.4.5.3 Depth and Regional Trends in Benthic Consumers (Objective 2)

Benthic consumers from 2012 and 2013 collections were grouped by feeding guild and their $\delta^{13}C$ values plotted by region and shelf/slope group to compare patterns along the regional west to east extent of the regions. $\delta^{13}C$ values of feeding guilds generally decreased when moving eastward from the CP to the IMP region, although the statistical significance of these trends depended on feeding guild and region (Figure 8.4.5.3.1). Benthic predators in both the CP and CB regions were significantly (ANOVA, p <0.001) enriched in ^{13}C compared with predators on the IMP shelf and the OMP and IMP slope. The decreasing trends in $\delta^{13}C$ values from west to east regions for benthic sub-surface, surface deposit feeders, and suspension feeders were not significant. Within-region differences between the shelf and slope did not show a consistent pattern across feeding guilds (Figure 8.4.5.3.1).

The $\delta^{15}N$ values of a selection of the most widespread consumers from 2013 and 2014 collections (the brittle star *Ophiocten sericeum,* the gastropod *Colus sabini,* the anemone *Allantactis parasitica*, polychaetes of the family Polynoidae, arthropods within the class Pycnogonida, and arthropods of the order Cumacea) from across the study area were tested for depth-related patterns. Significant positive relationships of $\delta^{15}N$ values with bottom depth were found for all taxa, except *Ophiocten sericeum* (in 2014) and the Cumacea (Figure 8.4.5.3.2). The Cumacea was the only group in which $\delta^{15}N$ values actually decreased with increasing water depth (negative relationship), and this trend was significant in 2013.

8.4.5.4 Benthic Food Web Structure (Objective 2)

Trophic position of individual taxa, categorized by trophic level (TL), was calculated for all three collection years against two baselines: pPOM (TL 1) and the primary consumer *Ophiocten sericeum* (TL 2). Overall, most of the 1940 benthic taxa considered in this analysis for each region/depth group/year combination fell within TL 1–4 (Figure 8.4.5.4.1). Occasionally (and depending on baseline) a few taxa were in TL 0 (mostly cumaceans) or TL 5 (specifically the sea stars *Bathybiaster vexillifer*, *Crossaster papposus*, and *Icasterias panopla*).

Trophic structure, based on number of taxa within each trophic level, showed some broad similarities and differences among regions, between shelf and slope, and between the baselines used (Figure 8.4.5.4.1). Using the POM baseline, the western-most (CP) region had the largest number of taxa at higher TL, mostly TL 3–5 (Figure 8.4.5.4.1a). This pattern was very different when the primary consumer *Ophiocten sericeum* was used as trophic baseline. With *Ophiocten sericeum* as baseline, both shelf and slope communities in the CP region contained many more taxa in lower trophic levels (TL 0–2) than in any of the other regions, where more taxa were at TL 3 and 4 (Figure 8.4.5.4.1b). These differences of the CP food web structure compared with other regions were only partially driven, by different species being represented in that region. Many taxa were similar among regions but occupied different TL in different regions. In the regions other than CP, the taxon distribution among TL was more similar among the two baseline approaches, although there were slightly more taxa at lower TL with the POM baseline than the *Ophiocten sericeum* baseline (Figure 8.4.5.4.1).

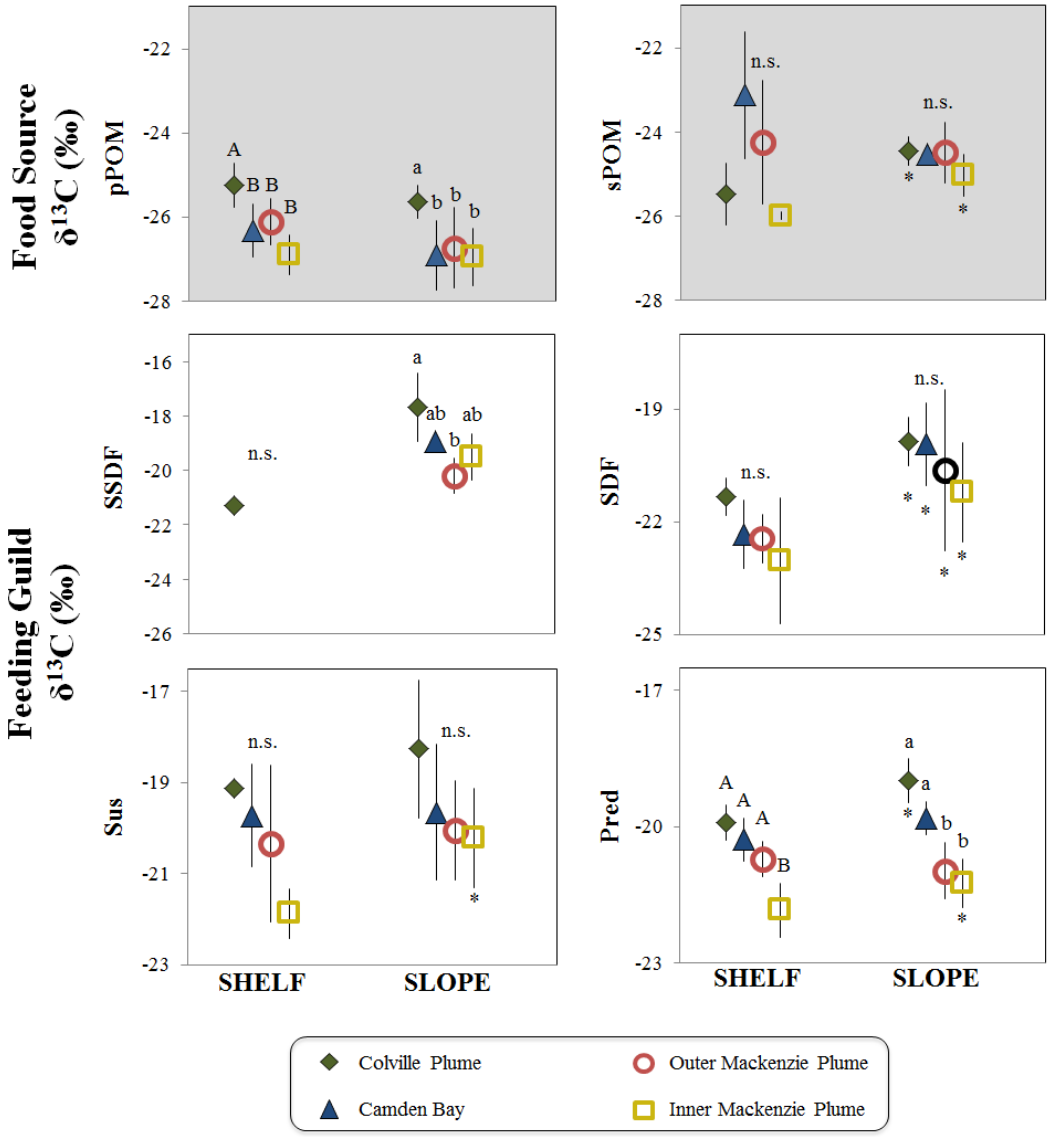

Figure 8.4.5.3.1. Mean (±SD) $\delta^{13}C$ values (‰) of possible food sources (pPOM and sPOM; shaded background) and consumer feeding guilds (white background), by region and depth group (shelf or slope) for 2012 and 2013.
Letters denote significantly different groupings among regions, comparing shelf (upper case) and slope (lower case) separately. Asterisks (*) denote significant differences between shelf versus slope depth groups within the same region. Note that $\delta^{13}C$ scale differs between rows. Pred – predators, SDF – surface deposit feeders, SSDF – sub-surface deposit feeders, Sus – suspension feeders.

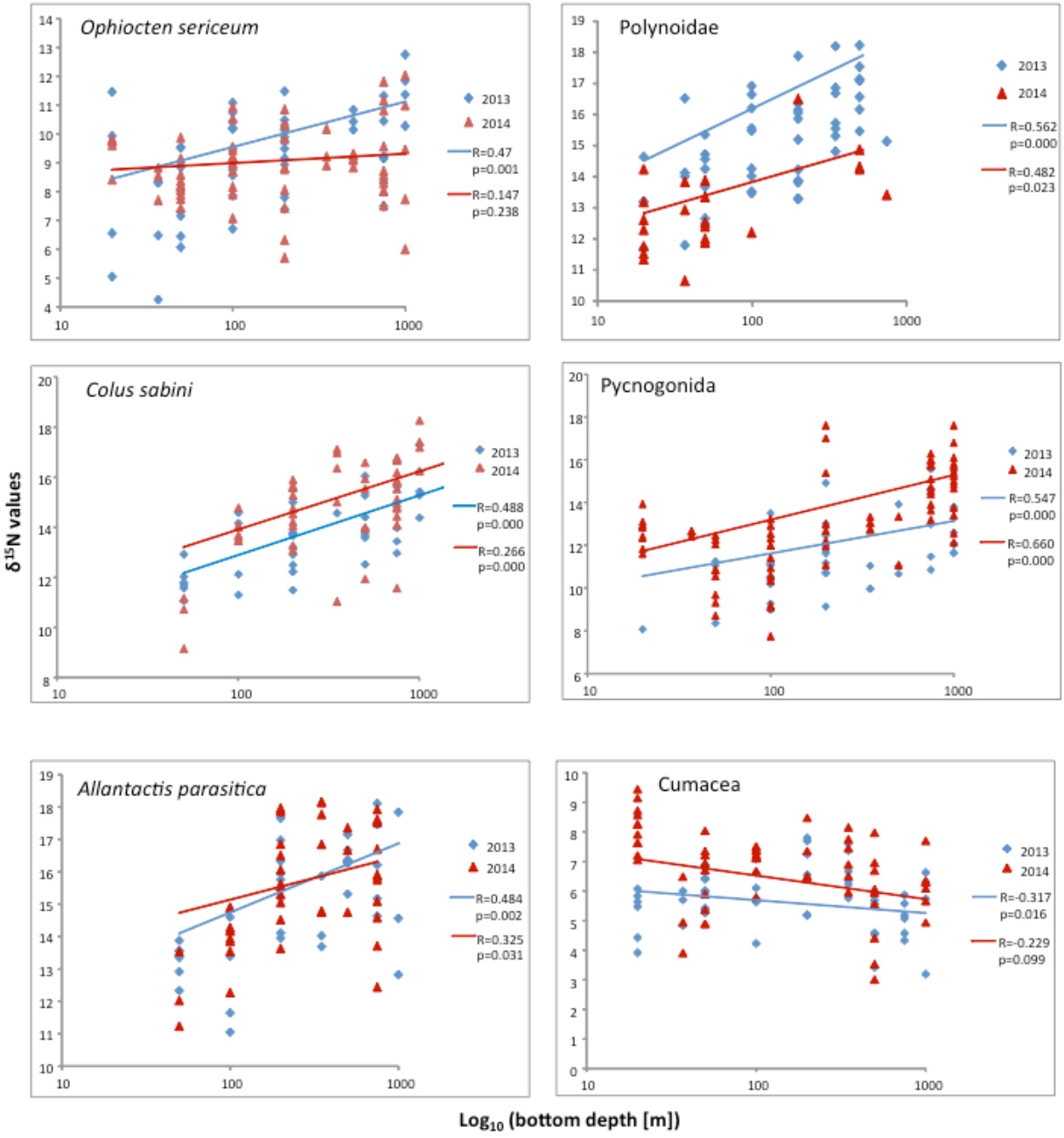

Figure 8.4.5.3.2. $\delta^{15}N$ values (‰) of select benthic consumer by bottom depth (on log-scale) across the 2013–2014 study area.
Each point represents the mean $\delta^{15}N$ value of a consumer at one station. Linear regression coefficients (R) and p-values are given in each plot, separately for the two collection years.

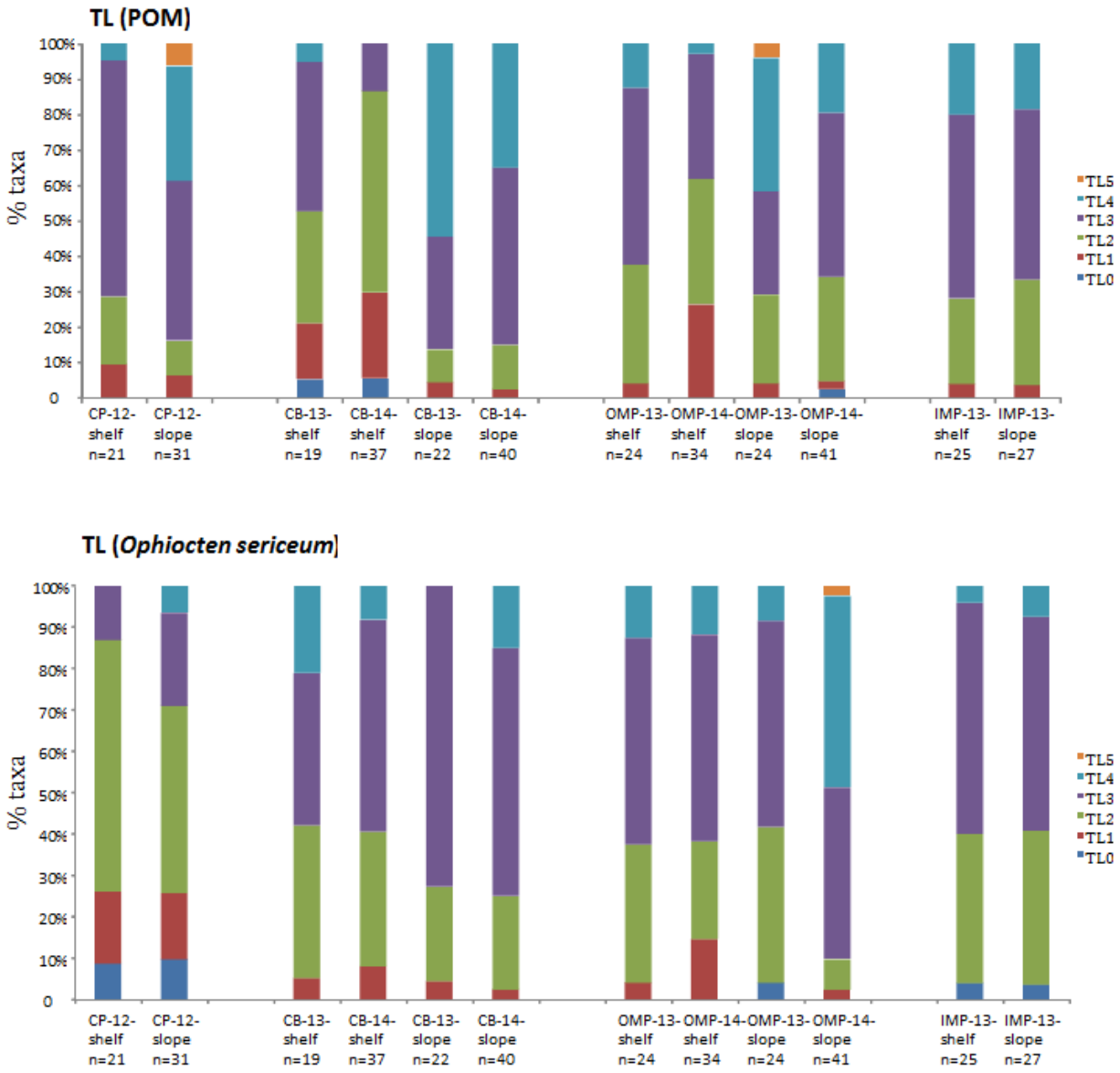

Figure 8.4.5.4.1. Contribution of benthic taxa (percent) to tropic levels (TL), calculated from three different baselines: pPOM (top panel) and the primary consumer *Ophiocten sericeum* (lower panel). Regions are presented as shelf and slope, with indication of the year of collection. Number of taxa (n) included are listed for each region/depth group/year.

There was no obvious longitudinal (among regions) trend in food web structure from CB to IMP (i.e., excluding the CP region). Depending on the baseline used, the slope communities occasionally had a higher percentage of taxa with higher TL (e.g., OMP region with *Ophiocten sericeum* and POM baselines, CB region with POM baseline) compared with shelf communities. In other cases, food web structure differed little between shelf and slopes. In some cases, food web structure at a certain region and shelf/slope region differed distinctly between the two years (e.g., OMP slope with *Ophiocten sericeum* as baseline), but there were no consistent trends (Figure 8.4.5.4.1).

Food web length differed slightly among regions and between the shelf and the slope when either pPOM or *Ophiocten sericeum* was used to determine the relative trophic positions of taxa. With pPOM as baseline (Figure 8.4.5.4.2a), food web lengths ranged from 4 to 6 TL. Food webs were longer on the slope compared with the shelf in (except for IMP region) (Figure 8.4.5.4.2a). In the OMP region, this difference was largely driven by a single predator occupying the highest TP, the sea star *Icasterias panopla*.

Food web structure and length standardized to the primary consumer *Ophiocten sericeum* as TP 2 (Figure 8.4.5.4.2b) differed considerably from pPOM-based estimates. CP region shelf and slope food webs based on this primary consumer were 1.1 and 1.3 TL shorter, respectively, than when using pPOM as a baseline. As a result, CP food webs changed from being relatively long, compared with all other regions, to being relatively short. This change occurred because many of the taxa that fell within TL 2 with a pPOM baseline fell within TL 1 in the CP region when using the *O. sericeum* baseline. Although the same consumer taxa were also present in the other regions, they occupied higher TPs there than the TL 2 represented by the primary consumer *O. sericeum*. Consequently, the longer food webs in the CB, OMP, and IMP regions were accompanied by an apparent "trophic gap" (Figure 8.4.5.4.2b) between pPOM and the lowest benthic consumer, excluding the cumaceans *Diastylis* spp., which always had extremely low TP. Food web structure across shelf and slope depth groups were similar to one another in the IMP and OMP regions regardless of whether POM or a primary consumer baseline was applied.

The relative distribution of epibenthic consumer biomass by trophic levels was calculated for 2014 collections for transects (from west to east) A6 (146° W), A2 (142° W), A1 (141° W), and TBS (140° W), for both shelf and slope communities (Figures 8.4.5.4.3–8.4.5.4.6). Although strong differences existed in relative biomass distribution within a single transect and depth group, depending on baseline used, some important underlying patterns emerged. Within the shelf communities, an increasing amount of biomass was attributed to higher TL from west (A6 transect, mostly within TL1 and 2) to east (TBS transect, mostly within TL 2 and 3) (Figures 8.4.5.4.3–8.4.5.4.6). Such a longitudinal gradient was less obvious for the slope communities. Slope communities always had a much higher proportion of biomass at higher TL compared with the shelf communities along the same transect.

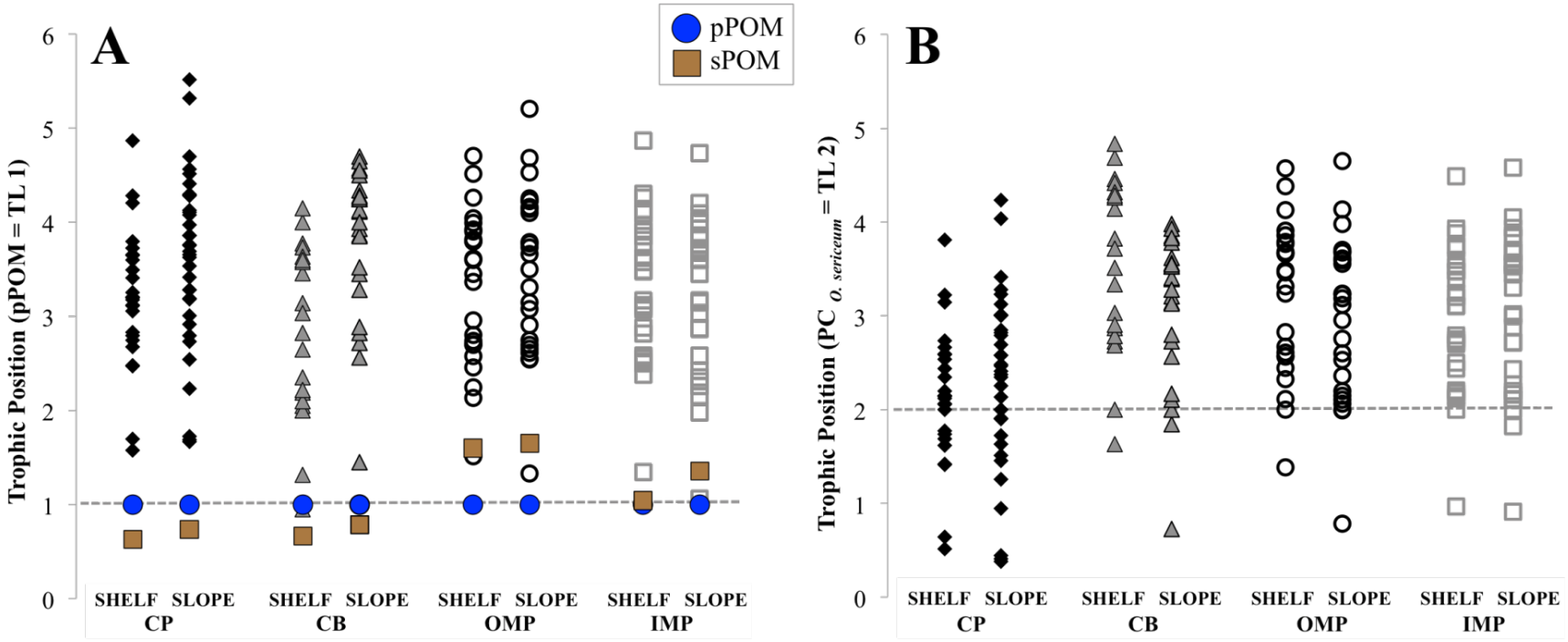

Figure 8.4.5.4.2. Trophic positions (TP) of individual consumers by shelf and slope regions in 2012 and 2013.
Food webs are based on (A) pPOM (TL 1, blue dashed line) or (B) the primary consumer *Ophiocten sericeum* (TL 2, gray dashed line).

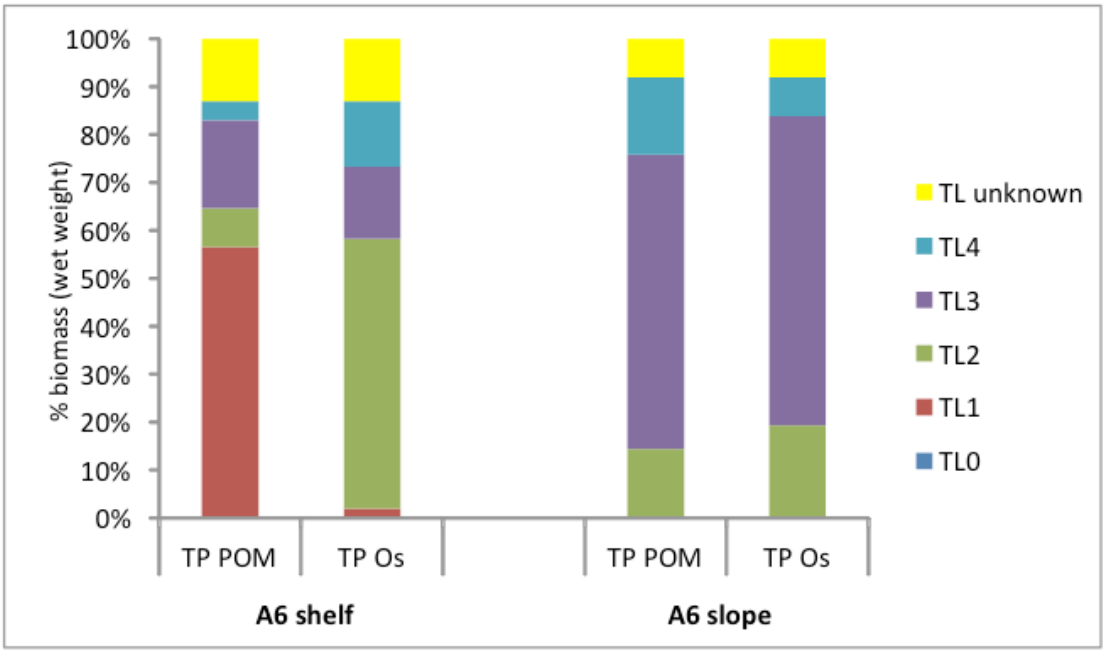

Figure 8.4.5.4.3. Relative distribution of epibenthic consumer biomass to trophic levels (TL) in shelf and slope communities at transect A6 (146° W) in 2014.
Trophic positions (TP) of taxa were calculated based on two different baselines: pelagic POM (TP POM) and the brittle star *Ophiocten sericeum* (TP Os). TL unknown indicates the relative biomass within the community from taxa that were not analyzed for their trophic position.

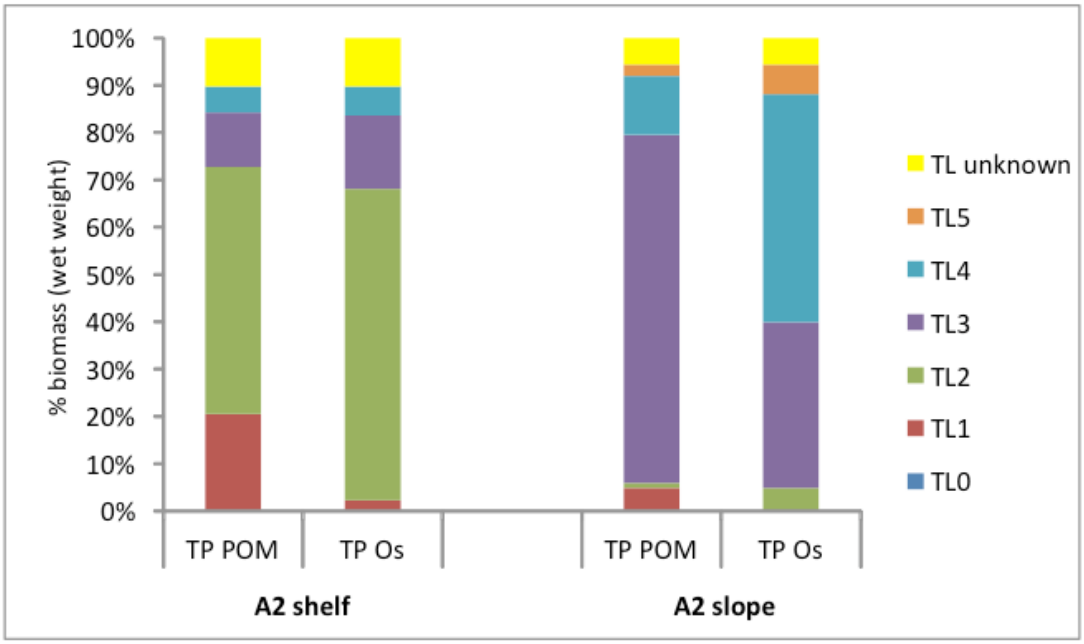

Figure 8.4.5.4.4. Relative distribution of epibenthic consumer biomass to trophic levels (TL) in shelf and slope communities at transect A2 (142° W) in 2014.
Trophic positions (TP) of taxa were calculated based on two different baselines: pelagic POM (TP POM) and the brittle star *Ophiocten sericeum* (TP Os). TL unknown indicates the relative biomass within the community from taxa that were not analyzed for their trophic position.

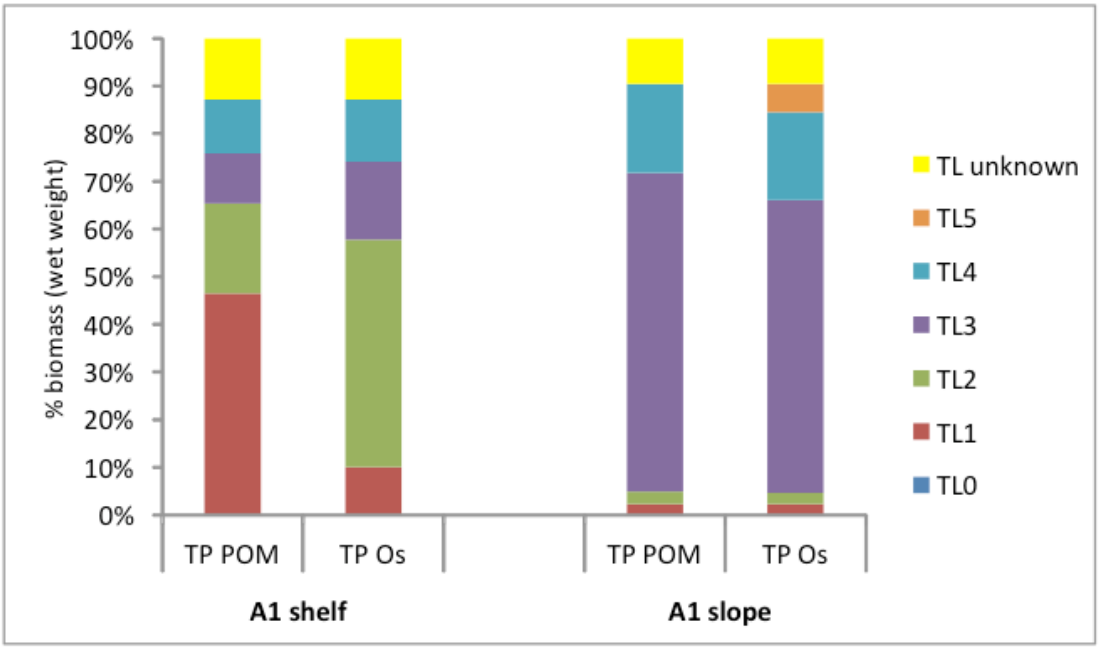

Figure 8.4.5.4.5. Relative distribution of epibenthic consumer biomass to trophic levels (TL) in shelf and slope communities at transect A1 (141° W) in 2014.
Trophic positions (TP) of taxa were calculated based on two different baselines: pelagic POM (TP POM) and the brittle star *Ophiocten sericeum* (TP Os). TL unknown indicates the relative biomass within the community from taxa that were not analyzed for their trophic position.

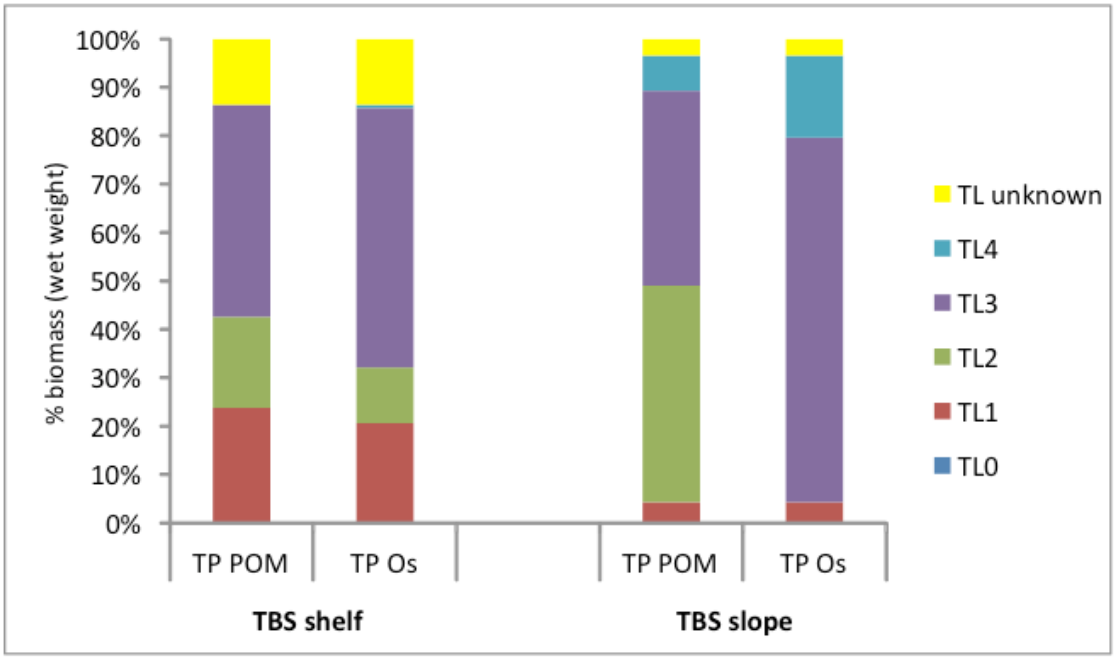

Figure 8.4.5.4.6. Relative distribution of epibenthic consumer biomass to trophic levels (TL) in shelf and slope communities at transect TBS (140° W) in 2014.
Trophic positions (TP) of taxa were calculated based on two different baselines: pelagic POM (TP POM) and the brittle star *Ophiocten sericeum* (TP Os). TL unknown indicates the relative biomass within the community from taxa that were not analyzed for their trophic position.

Differences between TL partitioning were evident between the two baselines used. For example, biomass of shelf communities at transects A6 and A1 was dominated by TL 1 with the POM baseline and TL 2 with the *Ophiocten sericeum* baseline (Figure 8.4.5.4.3, 8.4.5.4.5). Patterns in slope communities were more variable between the two baselines; slope communities at A2 had much larger biomass at higher TL (TL 3) with the POM baseline, while slope communities at TBS had higher biomass at lower TL compared with the *O. sericeum* baseline (Figures 8.4.5.4.4, 8.4.5.4.6). While these differences look striking, they were mostly driven by a single or few biomass-dominating taxa that fell just into one TL with one baseline but fell into the next higher or lower TL with another baseline. For example, in the transect A6 shelf community (Figure 8.4.5.4.3) the brittle star *O. sericeum*, the sea cucumber *Psolus peronii* and the scallop *Similipecten greenlandicus* constituted a total of 54% of community biomass. Each of these species had trophic positions (TP) between 2.0 and 2.2 (within TL 2) with the *O. sericeum* baseline but had TP between 1.8–1.9 (= within TL 1) with the POM baseline. This resulted in the distinct differences in shelf community proportional biomass in TL at transect A6 (Figure 8.4.5.4.3). Similarly for the slope communities, some biomass-dominant taxa that had TP within a lower TL with POM baseline compared with the *O. sericeum* baseline, resulting in higher proportions of lower TL biomass in POM-based food webs (e.g., A2 and TBS slope communities, Figures 8.4.5.4.4, 8.4.5.4.6). For example, the biomass-dominant sea star *Pontaster tenuispinus* and several predatory gastropods in the A2 slope community fell into TL 3 with the POM baseline but into TL 4 with the *O. sericeum* baseline (Figure 8.4.5.4.4). The brittle stars *Ophiopleura borealis* and *Ophiacantha bidentata*, and the feather star *Florometra* sp., were within TL 2 with the POM baseline but within TL 3 with the *O. sericeum* baseline, creating differences in the biomass distribution to TL in the TBS slope community (Figure 8.4.5.4.6). Because of this 'step effect' when using categorized TL, we chose to highlight trophic position of individual species in the interannual comparison of trophic structure in next section.

8.4.5.5 Interannual Comparison of Benthic Food Web Structure (Objective 2)

Interannual comparisons of benthic food web structure can show how variable or stable a system is; however, such comparisons can be sensitive to the specific taxa that were included in the analysis in each year. Therefore, we compared trophic structure, per transect and shelf/slope group, at transects A6 (146° W), A1 (141° W), and TBS (140° W), all sampled in 2013 and 2014, by including just those taxa that were analyzed in both years (per transect and shelf/slope group) (Figures 8.4.5.5.1–8.4.5.5.6, upper panels). These taxa represented the dominant species at each transect. We focused on the interannual patterns of trophic positions of individual taxa and their contribution to trophic level composition. While, again, individual taxa results differed by baseline used, the relative position of taxa within the food web was, in fact, very consistent between baselines. For example, *Diastylis* spp. (Cumacea) were always at the bottom of the food web at very low TP, regardless of baseline. Similarly, sea stars such as *Icasterias panopla*, *Crossaster papposus* and *Bathybiaster vexillifer* were always at high TP. Generally, the same taxa had very similar TP between 2013 and 2014, although a few taxa were an exception. For example, the amphipod Anonyx sp. on the slope of transect A1 had a TP within TL 2 for both baselines in 2013 and a TP within TL 4 in 2014; however, such drastic differences were rare. This indicates the individual TP of taxa were quite stable over the 2-year study period.

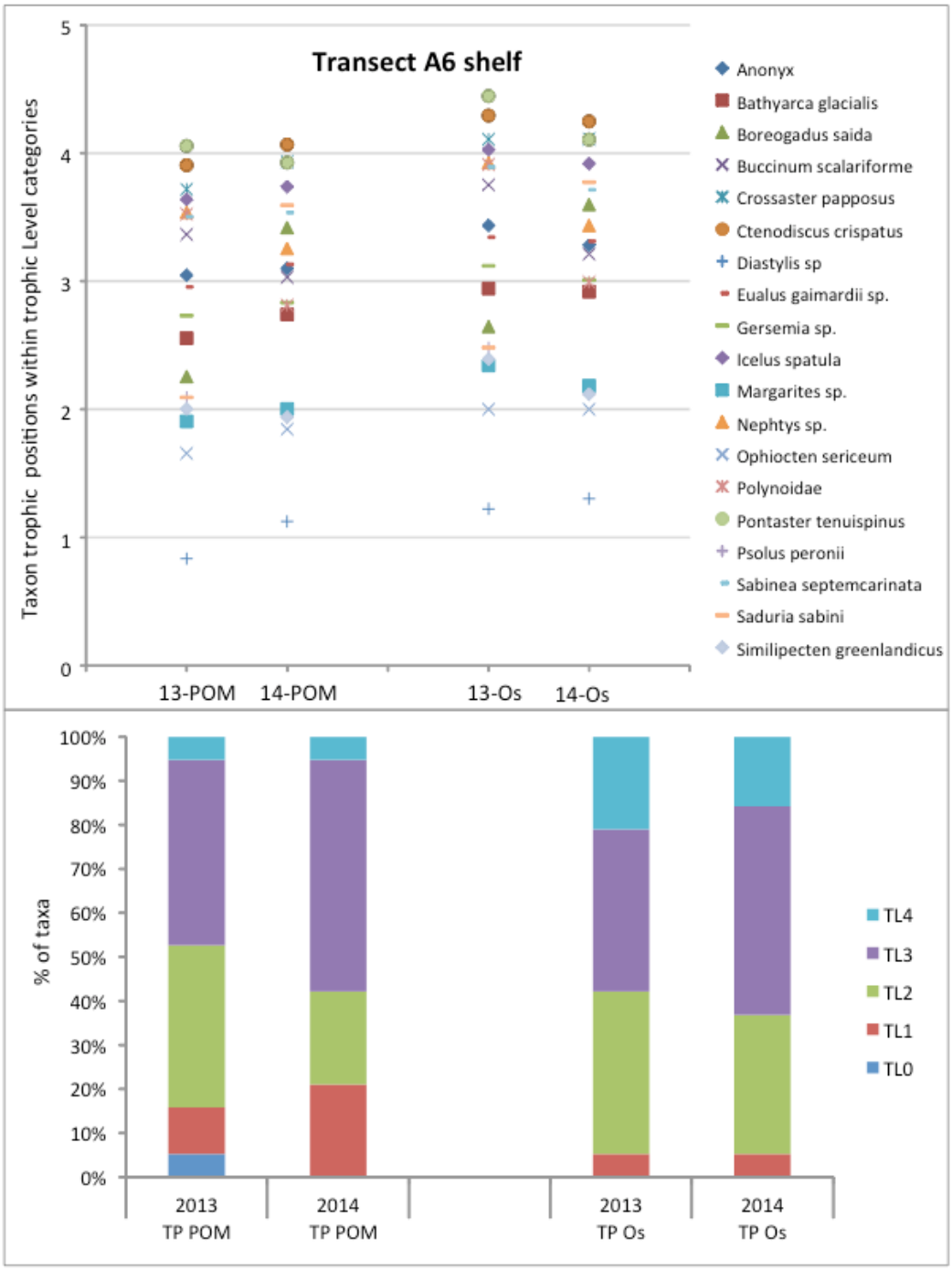

Figure 8.4.5.5.1. Trophic position of individual taxa sampled in both 2013 and 2014 on the transect A6 shelf, calculated from two different baselines: pelagic POM (TP POM) and the brittle star *Ophiocten sericeum* (TP Os) (upper panel). Proportional contribution of taxa to trophic levels (lower panel).

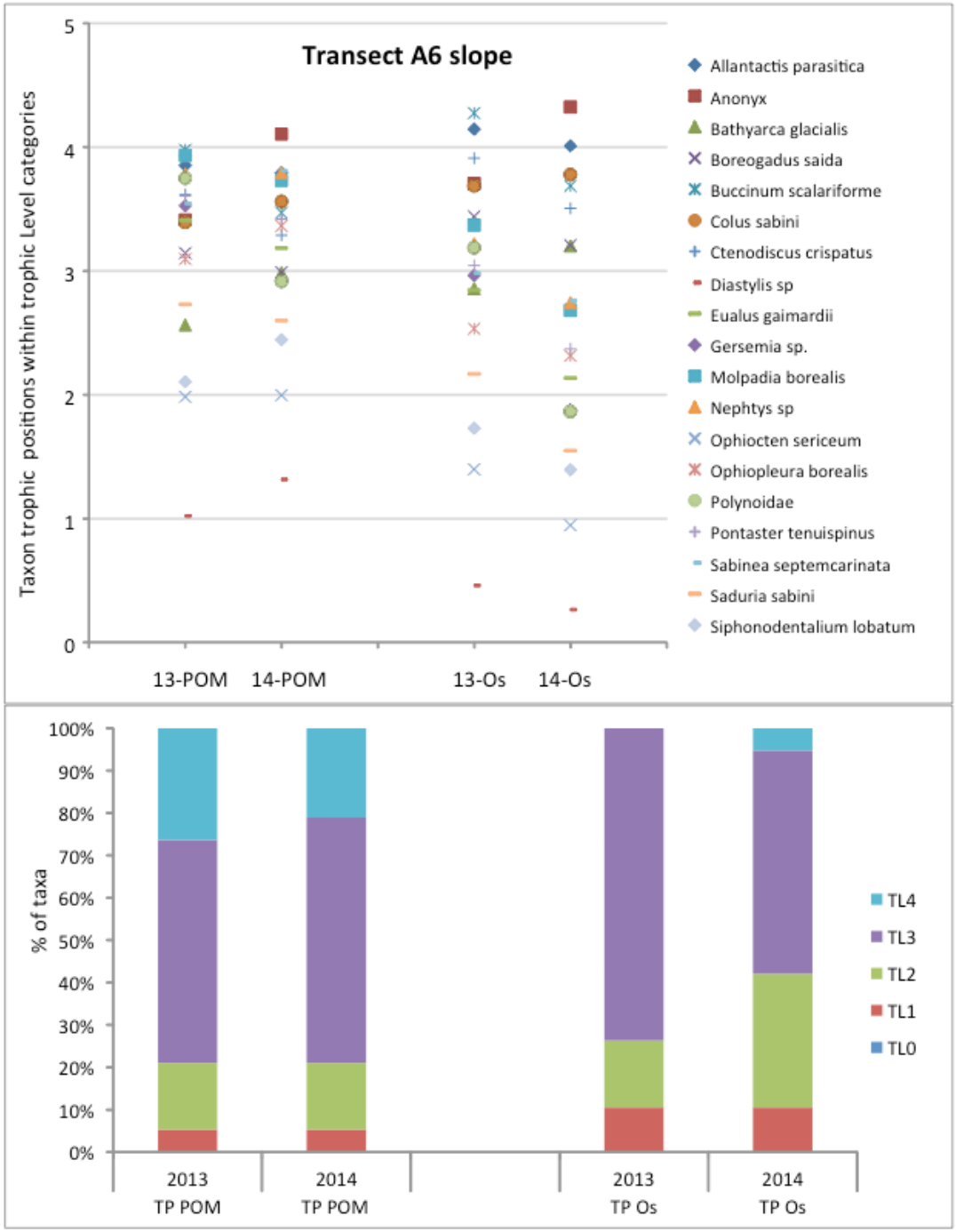

Figure 8.4.5.5.2. Trophic position of individual taxa sampled in both 2013 and 2014 on the transect A6 slope, calculated from two different baselines: pelagic POM (TP POM) and the brittle star *Ophiocten sericeum* (TP Os) (upper panel). Proportional contribution of taxa to trophic levels (lower panel).

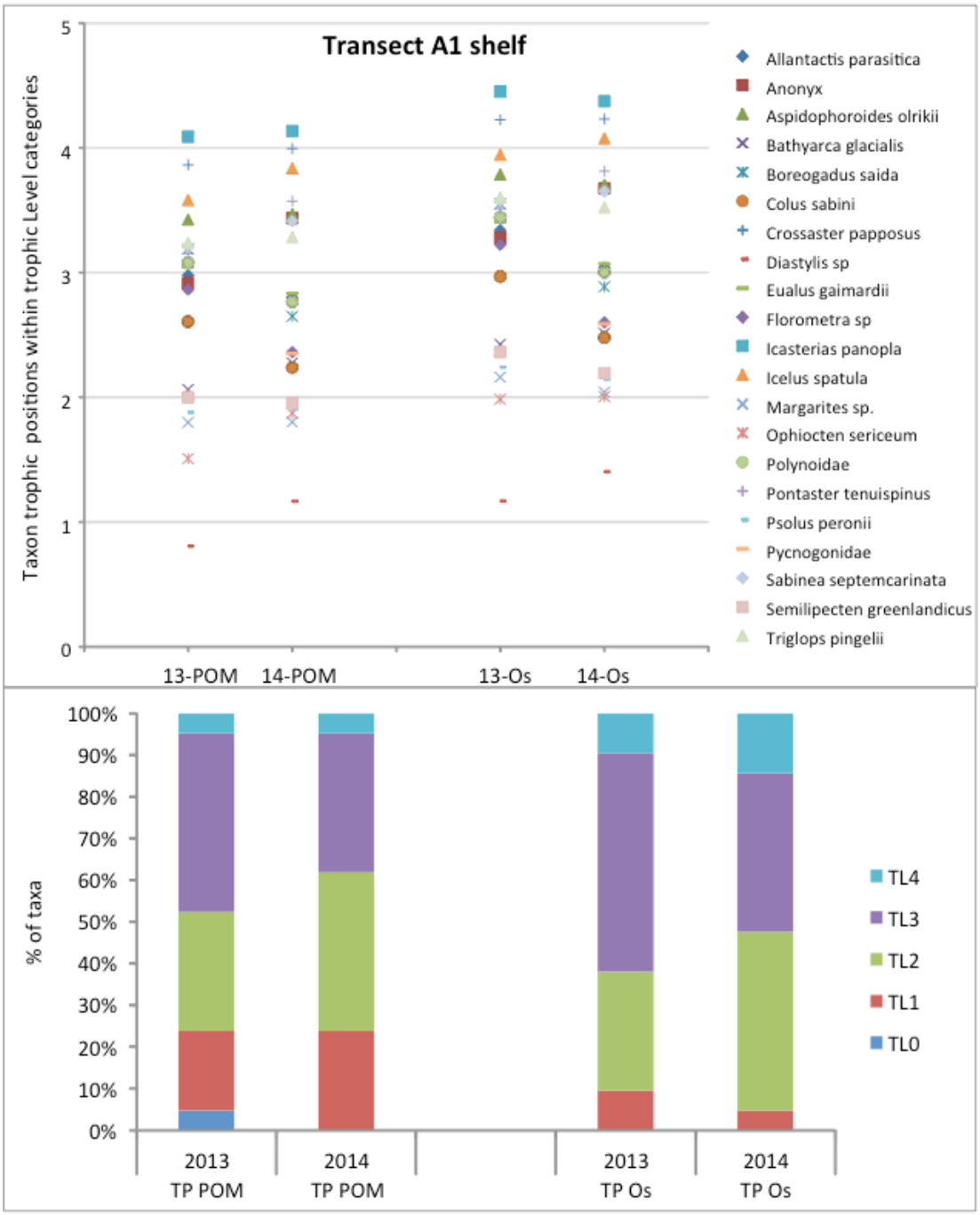

Figure 8.4.5.5.3. Trophic position of individual taxa sampled in both 2013 and 2014 on the transect A1 shelf, calculated from two different baselines: pelagic POM (TP POM) and the brittle star *Ophiocten sericeum* (TP Os) (upper panel). Proportional contribution of taxa to trophic levels (lower panel).

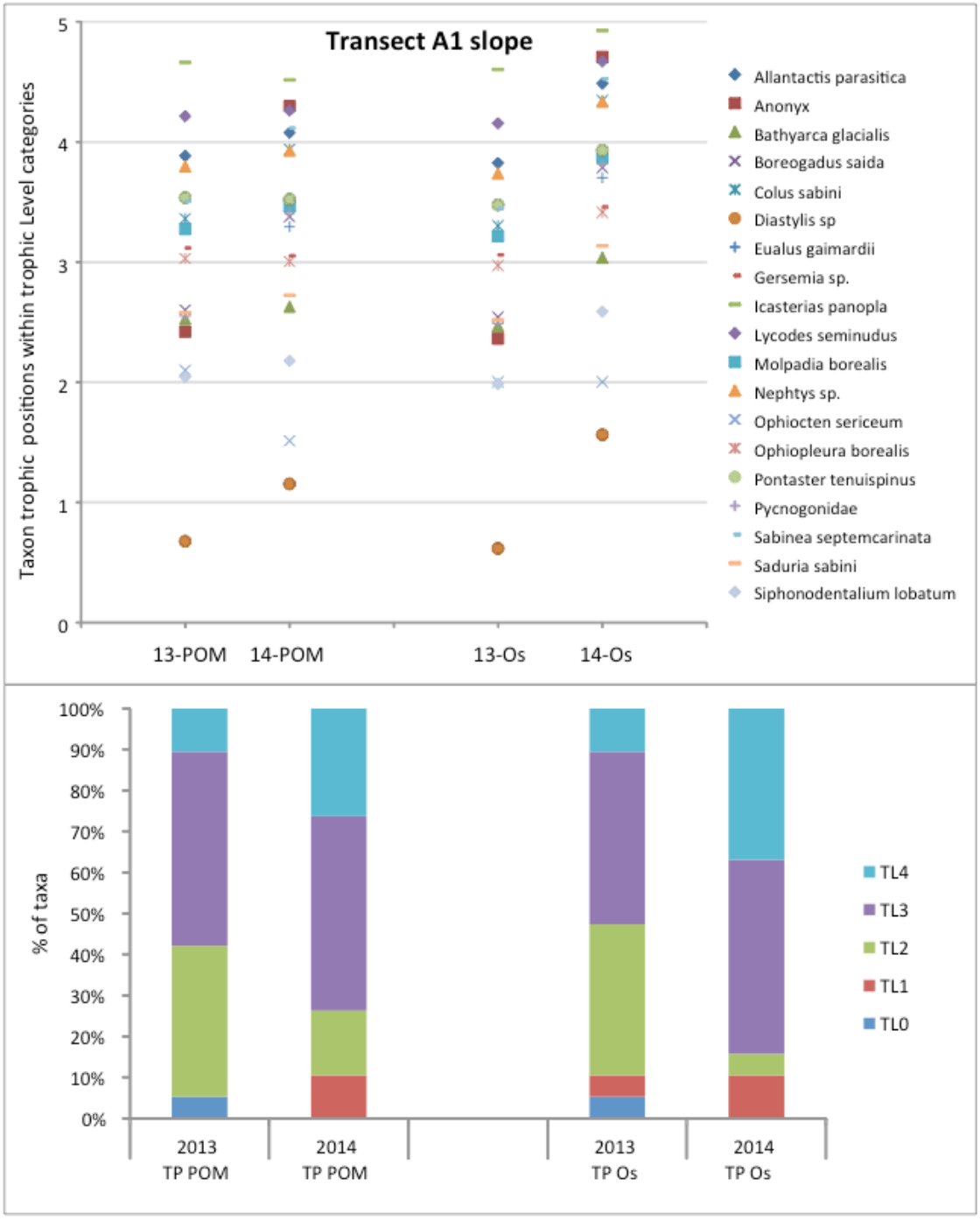

Figure 8.4.5.5.4. Trophic position of individual taxa sampled in both 2013 and 2014 on the transect A1 slope, calculated from two different baselines: pelagic POM (TP POM) and the brittle star *Ophiocten sericeum* (TP Os) (upper panel). Proportional contribution of taxa to trophic levels (lower panel).

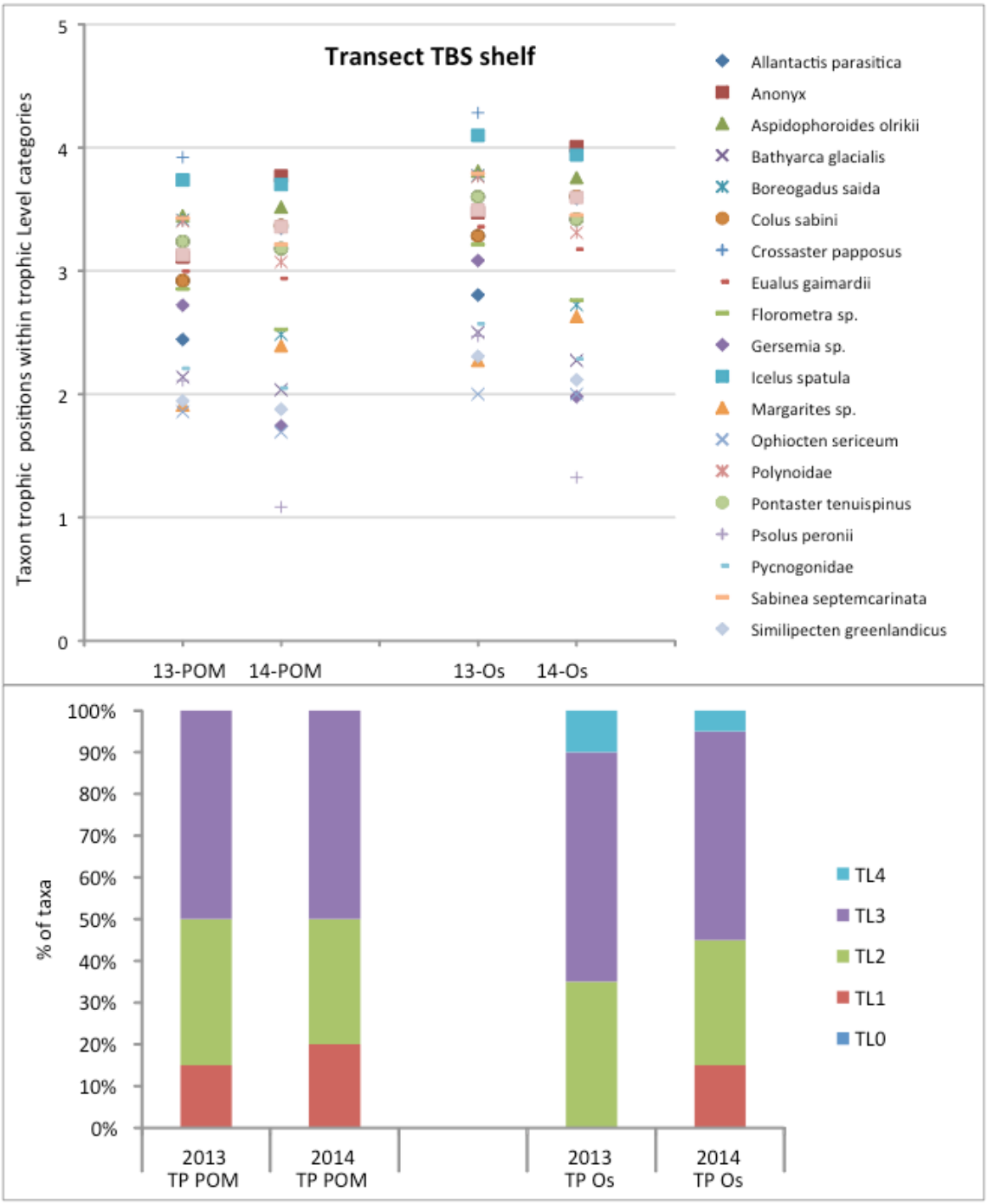

Figure 8.4.5.5.5. Trophic position of individual taxa sampled in both 2013 and 2014 on the transect TBS shelf, calculated from two different baselines: pelagic POM (TP POM) and the brittle star *Ophiocten sericeum* (TP Os) (upper panel). Proportional contribution of taxa to trophic levels (lower panel).

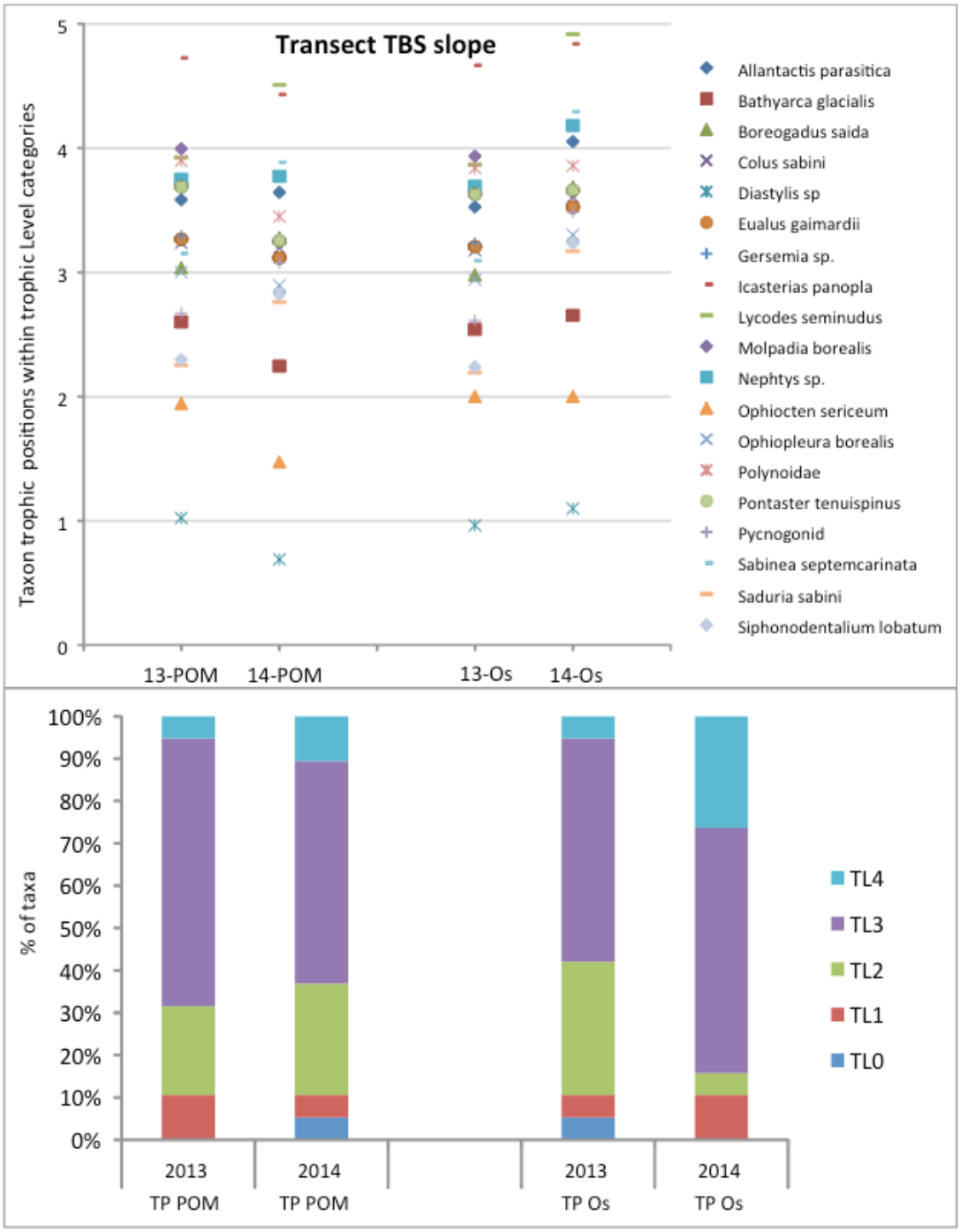

Figure 8.4.5.5.6. Trophic position of individual taxa sampled in both 2013 and 2014 on the transect TBS slope, calculated from two different baselines: pelagic POM (TP POM) and the brittle star *Ophiocten sericeum* (TP Os) (upper panel). Proportional contribution of taxa to trophic levels (lower panel).

In most cases, food web structure measured by the proportion of taxa contributing to the various TL was extremely stable between the two years (e.g., transect A6 slope–POM baseline; transect TBS shelf–POM baseline, Figures 8.4.5.5.1–8.4.5.5.6, lower panels). In some cases, interannual variation occurred (e.g., transect A1 slope–*Ophiocten sericeum* baseline, Figure 8.4.5.5.4, lower panel), and inspection of the individual taxa TP confirmed that these differences were likely due to the general shift of taxon TP into a higher TL in 2014 compared with 2013 (Figure 8.4.5.5.4, upper panel). The direct comparison of TP distribution of individual taxa and the more synthesized view of percent taxa contributing to distinct TL (Figures 8.4.5.5.1–8.4.5.5.6) presents evidence that the synthesis into discrete TL may oversimplify results; the presentation of distinct TL loses some of the important patterns, such as interannual consistency, that are obvious when displaying individual taxa.

8.4.6 Discussion

8.4.6.1 POM Food Sources in Relation to Freshwater (Objective 1)

Surface water $\delta^{18}O$ values in the upper 5 m (Figure 8.4.5.1.1) across the eastern Beaufort Sea suggested Mackenzie Plume influence westward of the Mackenzie Delta. The Coriolis force typically directs the Mackenzie Plume to the east of the river delta; however, the plume at the surface of an Ekman layer can react rapidly to easterly wind stress, which can drive the Mackenzie-derived waters offshore and to the west (Macdonald and Yu 2006, Mulligan et al. 2010). As would be expected, the freshwater signal indicated by $\delta^{18}O$ values was strongest near the immediate outflow of the river and became diluted farther offshore over the Beaufort Sea slope. In contrast, to the west of Herschel Island, the freshwater signal was inversed and was strongest offshore and weak nearshore. These trends may be explained by an easterly wind regime; easterly winds over 5 m s^{-1} at Tuktoyaktuk, Northwest Territory, Canada, were sustained for the 48 hrs immediately preceding our sampling in the Mackenzie region in August 2013 (OMP and IMP) (The Weather Underground, Inc.), which are favorable conditions for upwelling on the Beaufort shelf (Williams et al. 2006). Under such conditions, the associated Ekman transport of the Mackenzie surface plume would move northwards offshore and nearly parallel to IMP transects. In contrast, marine water, that was upwelled over the shelf break, forced by isobath divergence near Herschel Island, would reach the surface waters in the nearshore OMP (Macdonald and Yu 2006, Williams et al. 2006). There, Herschel Island diverts westward-flowing Mackenzie plume water away from the coast, allowing a pocket of upwelled water to remain close to shore. Our data support the presence of upwelling in this region at the time of sampling. The absence of any distinct freshwater signal at 10 m depth indicates that freshwater was confined to a thin surface layer.

Despite the Mackenzie River plume water, the relative proportion of OM_{terr} versus marine organic matter influence in pPOM samples did not differ between nearshore and offshore surface waters (Figure 8.4.5.2.2). Instead, $\delta^{13}C$ and $\delta^{15}N$ values of pPOM and sPOM indicated presence of OM_{terr} influence across shelf and slope over the entire study area. For the shelf, this confirms findings from our earlier work during the BOEM-2011 Central Beaufort study (Divine et al. 2015). This finding may indicate that the OM_{terr} initially entrained within the Mackenzie discharge is, at some point, disassociated from freshwater plume dynamics and is advected independently. Our data suggest the OM_{terr} reaches lateral distances and depths that the plume's freshwater does not, as earlier studies also suggest (Forest et al. 2007, 2013, Goñi et al. 2000). In addition, our data may be evidence that other vectors of OM_{terr} (e.g., coastal erosion, smaller

rivers) contributed significantly to the proportion of OM_{terr} present in pPOM and sPOM samples at Beaufort shelf and slope stations.

Interestingly, however, the POM C:N values were relatively low across the study area (i.e., lower than would be expected from terrestrial plants, <10 for 82% of POM samples, Figure 8.4.5.2.2). The C: N ratios in our study, therefore, did not match the isotopic evidence of OM_{terr} prevalence or the high surface sediment C:N values found in prior studies across the Beaufort Sea and characteristic of terrestrial plants (e.g., Goñi et al. 2000). C:N values are known to be more susceptible to biogeochemical alteration than $\delta^{13}C$ values (Thorton and McManus 1994), and the degree of microbial processing associated with both marine and terrestrial matter is high in the Beaufort Sea (Ortega-Retuerta et al. 2012, Kellogg and Deming 2014, Rontani et al. 2014). Therefore, we consider the $\delta^{13}C$ values to be a more conservative tracer of terrestrial versus marine organic matter in this study.

The regional distribution of pPOM and sPOM $\delta^{13}C$ values provided a spatial perspective of relative carbon source differences along and across the shelf and slope (Figure 8.4.5.3.1). While not always significant, we saw a west-to-east pattern of increasing OM_{terr} in the pPOM source, specifically with lower OM_{terr} in the western CP region (Figure 8.4.5.3.1). Relatively higher marine production in the CP region may derive both from local inputs as well as supplementary inputs of marine production advected into the CP region from the far-western Beaufort and Chukchi Seas (Ashjian et al. 2005, Bates et al. 2005, Okkonen et al. 2009). In contrast, no regional pattern was obvious for sPOM.

The following processes may work to obscure more distinct regional trends. First, microbial break-down of OM_{terr} can result in an increase in both $\delta^{13}C$ and $\delta^{15}N$ values of the OM_{terr} of more than 5‰ (Macko and Estep 1984). This increase consequently makes OM_{terr} less isotopically distinct from marine production and we need to assume some degree of isotopic transformation of pPOM during its transit to the seafloor (Macko and Estep 1984). Unfortunately, lacking precise knowledge of the ^{13}C and ^{15}N fractionation factors associated with microbial processing (Lehmann et al. 2002, and references therein), it is difficult to estimate the degree to which this activity may disguise the influence of OM_{terr} via isotope enrichment.

Second, the contributions of iPOM (isotopically enriched) could counteract OM_{terr} contribution (isotopically depleted). However, iPOM contributions to sPOM samples are challenging to approximate because iPOM isotopic signatures may vary strongly seasonally, related to the magnitude of the ice algal bloom (Gradinger et al. 2009). Using both our own (early spring) versus a later peak bloom iPOM signature resulted in large differences of iPOM contribution estimates to pPOM and sPOM. Given that we sampled weeks after break-up and that ice-associated production can be rapidly consumed at the seafloor after sinking (McMahon et al. 2006, Sun et al. 2007), we assume that the iPOM contribution is likely much lower than our high estimate.

Third, benthic consumers can rapidly utilize the fresh marine production (Morata et al. 2008, Renaud et al. 2008) so that little record of its presence remains in the marine sediments (Divine et al. 2015). That process would, in part, explain the lack of a distinct longitudinal pattern in the $\delta^{13}C$ values of sPOM across regions on both the shelf and slope. In addition, the relatively homogenous sPOM $\delta^{13}C$ values may be a consequence of vertical and horizontal POM flux (Forest et al. 2013) from upwelling events (Williams et al. 2006), bottom resuspension (Forest et al. 2007), and lateral advection (Hwang et al. 2008). These transport vectors can mix the terrestrial and marine composition of sPOM (Goñi et al. 2000, Divine et al. 2015), thus

concealing the pattern of increasing contributions of marine production in pPOM moving westward from the Mackenzie River outflow (Goñi et al. 2013).

8.4.6.2 Depth and Regional Trends in Benthic Consumers (Objective 2)

Above, we discussed the $\delta^{13}C$ patterns of the primary potential food sources, pPOM and sPOM, with respect to OM_{terr} contributions among regions and depth zones. We now assess how these food source patterns are reflected in benthic consumers. Although not statistically significant, suspension and surface deposit feeders also reflected the west-to-east decrease in $\delta^{13}C$ values seen in pPOM (Figure 8.4.5.3.1). This likely indicates their close association with the suspended and freshly settled material that they feed upon. In contrast, the increase in OM_{terr} inputs seen in pPOM toward the east was not present in sub-surface deposit feeders, likely due to the utilization of the more isotopically consistent sPOM food source. Benthic predator $\delta^{13}C$ patterns matched the west-to-east decrease in $\delta^{13}C$ values observed in pPOM. One explanation for this is that benthic predators reflect the isotopic composition of their diet, and it is possible that their diet is dominated by the more easily accessible suspension and surface-deposit feeders. Overall, these data support a transition in main food sources from more of the ^{13}C-enriched, marine production in the west to more of the ^{13}C-depleted, OM_{terr} in the east. Extensive literature provides evidence of this gradient (increasing OM_{terr} across the Beaufort shelf with proximity to the Mackenzie River) in nearshore benthic and shelf zooplankton communities and in sediments (e.g., Dunton et al. 1989, Goñi et al. 2000), corroborating the trend seen in this study through $\delta^{13}C$ values of pPOM and consumer tissues in shelf and slope benthos.

In addition to longitudinal (regional patterns), we assessed depth-related patterns of POM utilization in benthic consumers (Figure 8.4.5.3.2). pPOM undergoes bacterial degradation and remineralization processes that are a function of water depth (Robinson et al. 2012) or sinking time of the pPOM (Macko and Estep 1984). These processes result in a marked increase in $\delta^{15}N$ values in pPOM and the settled sPOM at depth (Altabet and Francois 2001). For $\delta^{15}N$ this increase may be >10‰ from 0 to 1000 m (Mintenbeck et al. 2007), indicative of increasingly degraded organic matter. Indeed, $\delta^{15}N$ values of most benthic consumers increased with increasing bottom depth (Figure 8.4.5.3.2), likely reflecting these depth-related degradation processes. One exception were the cumaceans, which are known from other food web studies to have extremely low TL (Iken et al. 2005, Bergmann et al. 2009, Renaud et al. 2011), suggesting they may be using different food sources not accounted for here, or that they isotopically fractionate their food differently, perhaps due to microbial gut flora. The otherwise consistent trend of consumer tissue ^{15}N enrichment with depth demonstrates the importance of using a depth-normalized approach to food web analysis (Roy et al. 2015a) to correct for variables related to station bottom depth and their effect on stable isotope values. We have implemented such an approach here by separating shelf from slope food web structures.

8.4.6.3 Benthic Food Web Structure (Objective 2)

The above-described patterns in benthic consumers were largely reflected in overall food web structure and length. Based on the *Ophiocten sericeum* baseline, food webs contained a larger number of lower TL taxa (Figure 8.4.5.4.1) and were shorter (Figure 8.4.5.4.2) in the western CP region compared with other regions. This pattern implies that trophic coupling between basal food sources and consumers was tighter in the west where pPOM $\delta^{13}C$ values also indicated marine production was present in higher proportion compared with more eastern Beaufort regions (see Figure 8.4.5.3.1 and above discussion). In the more eastern regions, we

observed a "trophic gap" between the food source(s) and consumers (Figure 8.4.5.4.2), suggesting missing consumers. We believe it is unlikely that unsampled benthic taxa occupy this gap because the food web was extensively sampled and the majority of taxa that occupied the gap region (TP <2) in the food webs of the CP region also occurred farther east but at higher trophic positions. Instead, we suggest that this gap is indicative of isotopic fractionation of the POM source by microbial processing. These microbial processes can account for additional trophic levels, thus transferring the benthic consumers feeding on this now microbially-modified POM source into higher TL (Sommer et al. 2002). The cumaceans, *Diastylis* spp., were the only sampled taxa falling consistently within this "trophic gap." Categorized as surface deposit feeders, their extremely low trophic positions in multiple food web studies suggest they may fractionate differently or feed on labile food sources not accounted for by these studies (Iken et al. 2005, Bergmann et al. 2009). We suggest that the presence of this "trophic gap" in the more eastern study region (CB, OMP, IMP regions), but not in the more western region (CP), is related to the increased presence of OM_{terr} (in the east) that requires additional microbial break-down before it can be used by benthic consumers.

OM_{terr} is largely composed of complex structural materials from vascular plants such as cellulose and xylan, thus it can be difficult for marine primary consumers to assimilate directly as they lack the necessary digestive enzymes (Tenore 1983, and references therein). Microbial decomposition of OM_{terr} can effectively break down these complex structures, making a higher proportion of the energy available in OM_{terr} to be utilized as a food source by other marine consumers (Garneau et al. 2009). The presence of this "trophic gap" in the terrestrially-influenced regional food webs of this study substantiates the critical role of the microbial loop in connecting OM_{terr} to marine consumers in the eastern Beaufort Sea (Vallières et al. 2008, Garneau et al. 2009, Rontani et al. 2014).

So far, we investigated food web length and structure based on the number of taxa contributing to distinct TL in the study area. However, the distribution of benthic biomass across trophic levels may be a better indicator of the actual energetic structure of food webs than simply looking at the distribution of taxa across trophic levels. More biomass was within lower TL in the shelf communities of transects A6, A2, and A1 in 2014 (60–70% of biomass in TL 1 and 2) compared with shelf biomass at transect TBS (~40% biomass in TL 1 and 2) (Figures 8.4.5.4.3–8.4.5.4.6). Although only about 1° longitude separate the TBS transect (140° W) and the next transect (A1, 141° W), this different biomass distribution within the food web could be related to the greater proximity of the TBS transect to the Mackenzie River outflow. This river discharge carries substantial amounts of OM_{terr} and there may be a higher level of microbial processing on the TBS shelf before material enters the benthic food web. The observed difference between the TBS transect and other transects is part of a gradient in OM_{terr} influence on the trophic structure in community biomass-based food webs. This is corroborated by other analyses that established that shelf biomass in the more western CP region was located to >90% in TL 1 and 2, while the shelf region even closer to the Mackenzie outflow only had about 20% of the benthic biomass in TL 1 and 2 (Bell et al. 2016). These data support the presence of the microbial loop at the lower trophic levels of these OM_{terr}-influenced food webs that leads to greater benthic consumer biomass at a higher TL. Differences in benthic consumer biomass among TL were not obvious in the slope communities (Figures 8.4.5.4.3–8.4.5.4.6). It is possible that the general depth-related microbial processing of all sinking material (Mintenbeck et al. 2007) mutes the specific effect of OM_{terr} degradation at these greater depths. This also is reflected in the fact that all slope food webs were fairly similar in the relatively high amount of biomass at higher TL (TL 3 and 4).

8.4.6.4 Interannual Comparison of Benthic Food Web Structure (Objective 2)

Arctic benthic communities are long-lived, allowing these communities to integrate short-term variability in environmental conditions (Bluhm et al. 2009, Grebmeier et al. 2015b). While we know that benthic community composition is relatively stable over time (see section 6.0), much less is known about temporal stability of food webs. Because surface production in Arctic waters is highly variable on seasonal and interannual scales, it is feasible to assume that this variability might translate into the trophic structure of benthic communities. When interannual food web structure was compared using the number of taxa within distinct TL, there were differences between years. However, trophic position of individual taxa over two of the study years was highly consistent overall, despite some outliers (Figures 8.4.5.5.1–8.4.5.5.6). This means that the naturally occurring variability in primary production is temporally well-integrated in these consumers across all trophic levels. The use of stable isotope analysis for this investigation probably contributes to the identification of this stability. Consumer tissues have stable isotope values that reflect their diet items (after trophic fractionation); however, it takes time for the stable isotope composition in these consumer tissues to turn over to a new isotope composition after a diet change. This turnover time is on the order of months for Arctic benthic invertebrates (Kaufman et al. 2008, Weems et al. 2012). Therefore, short-term changes in food sources or diet will not be sufficient to overcome this lag time in isotope composition and cause a change in the modeled trophic position based on stable isotope analysis, especially if trophic position is calculated against a baseline that in itself is less variable, such as a primary consumer (Vander Zanden and Rasmussen 1999). However, should food sources change over the long term, for example, though climate or human induced ecosystem changes, then food web structure should reflect these changing food baselines. Therefore, stable isotope analysis is an ideal tool to assess the long-term stability of marine food webs.

8.4.7 Conclusions

The interplay of high inputs of OM_{terr} from Alaska's and Canada's permafrost and rivers with both advected and *in situ* marine primary production drives variation in marine trophic structure across the shelf and slope in the Beaufort Sea. Stable isotope analyses of surface water, particulate organic matter, and benthic consumers at depth gradients from 20 to 1000 m revealed a strong isotopic imprint of OM_{terr} in the eastern Beaufort Sea in the Mackenzie River area, and this influence decreased westward from the Mackenzie River. Concurrent with high OM_{terr} influence, shelf and slope food webs in the eastern Beaufort Sea were characterized by comparatively longer food webs and a greater proportion of epibenthic consumer biomass at higher trophic levels compared with central Beaufort Sea food webs. We suggest that higher levels of microbial processing in the eastern (strongly river influenced) area is the underlying process explaining this pattern, although this aspect was not studied in this project. Other published work, however, found that well-developed microbial communities are associated with terrestrial matter in the Beaufort Sea and that they have high efficiency of metabolic OM_{terr} turnover (Ortega-Retuerta et al. 2012, Rontani et al. 2014). Our results, therefore, challenge the paradigm that OM_{terr} is an unusable or poor food source for marine consumers (Schell 1983, Berglund et al. 2007). While total primary production is lower in the central and eastern Beaufort Sea than in the western Beaufort and Chukchi Seas (Sakshaug 2004), microbially processed OM_{terr} may diminish the effect of low amounts of fresh algal food sources. Benthic food web structure over two study years was relatively stable, confirming that benthic consumers are good

integrators of short-term variability in surface production. It is likely that the microbial processing of the continuous OM_{terr} source also contributes to this food web stability.

With warming climate, the importance of OM_{terr} and its microbial processing may increase in the Arctic in the future. It has been shown that zooplankton biomass and biological processes, such as fish growth and total food web efficiency, can be positively correlated with terrestrially-associated microbial production when temperature is simultaneously increased (Lefébure et al. 2013). In addition, terrestrially-derived energy may have increasingly significant relevance for marine communities exposed to increased river runoff and coastal erosion inputs into the Arctic Ocean (Holmes et al. 2013, Doxaran et al. 2015).

9.0 CROSS-DISCIPLINARY TROPHIC LEVEL SYNTHESIS

Brenda Norcross, Russell Hopcroft, and Katrin Iken

The preceding sections were structured around discrete habitats and taxonomic assemblages (i.e., oceanography, zooplankton, benthos, and fish). Here, we take a cross-discipline approach to synthesize ecological results to fulfill the following program objectives (reworded for clarification):

Program Objective 2. Document and correlate baseline fish and invertebrate species presence, abundance, distribution, and habitat in the eastern Beaufort Sea OCS lease area during the open water season; and

Program Objective 6. Establish the physical and chemical characteristics that define ecoregions (i.e., oceanographic provinces) within the eastern US Beaufort Sea.

9.1 Summary of distribution patterns within the US-Canada Transboundary study area

The trophic levels included in this synthesis included zooplankton, epibenthos, pelagic fishes, and demersal fishes. These trophic levels occupy different parts of the water column and may react differently to ecosystem drivers and stressors even when in the same habitat. Here, we present brief summaries of the individual trophic levels before making comparisons.

At the base of the food chain, seawater chlorophyll-*a* concentration was generally low (<mg m^3) throughout the region in all surveys. As total chlorophyll concentration increased, the proportion of chlorophyll >20-µm and chlorophyll-*a* in the total pigments typically increased.

The concentration of chl-*a* (µg/g dry sediment) in surface sediments was highly variable across the study region (Figure 3.4.1.0), and grain size parameters were particularly important in separating sites by depth. The chl-*a* peak at 350 m suggests high food availability below the shelf break and merits further investigation. However, the source and lability of organic material deposited to sediments may be more important in separating locations from west to east. Shallow stations had a higher proportion of sand and gravel, and there was a transition toward finer-grained sediments and more degraded detritus at deep stations. There was evidence of disturbance and variability among locations at shallower sites suggesting that shelf locations may be much more variable in both food availability of fresh detritus and diversity of grain due to river runoff. Deeper sites had more persistent conditions characterized by muddier sediments as expected for slope habitats. Western sites appeared to be more gravelly locations with a higher C:N ratio, whereas the eastern sites showed the opposite trend, likely because of the influence of the Mackenzie River.

Zooplankton communities of the Beaufort Sea slope were similar in species composition, structure, and diversity to the communities known from the Arctic Ocean's interior basins (Kosobokova and Hopcroft 2010, Kosobokova et al. 2011), with the exception of higher contributions from euryhaline (wide range of salinities, 10–35; Section 3.1) and neritic taxa that become increasingly prominent over the shelf. Generally, depth-associated patterns of zooplankton abundance, biomass, and species diversity observed for the Transboundary study region agreed with other observations in the Arctic's interior basins (e.g., Kosobokova et al. 2011). However, average biomass in the depth intervals on the slope between 100 and 1000 m were higher than those reported from similar depth intervals in the Canadian Basin (Kosobokova and Hopcroft 2010), likely due to enhanced productivity along the continental shelf margin.

Expected increases in pelagic production on continental shelves due to reduced ice cover (Arrigo et al. 2008) should increase both zooplankton abundance and biomass on the shelf and likely result in increased export of production to the mesopelagic water layers of the Beaufort Sea when compared to historical values. This, in turn, should support higher mesopelagic zooplankton biomass in the slope region and has implications for trophic interactions, particle flux, and biogeochemical cycles.

Epibenthic communities in the central to eastern Beaufort Sea, including both shelf and slope, were diverse and had an overall phylum composition typical for Arctic benthic systems. Epibenthic communities had high interannual stability over the study years, especially in community composition, even though the abundance or biomass of some taxa varied greatly among years (Appendix D Table 1). Longitudinal changes in epibenthic communities were particularly noticeable between the central (≥150° W) and eastern (≤146° W) Beaufort Sea study regions but were less pronounced further east (146°–137° W). These longitudinal differences may represent a biogeographic break where the Pacific water influence from the Chukchi Sea diminishes, causing a change in the taxa present. Alternatively, they could reflect the influence of the Mackenzie River on the hydrographic environment, and thus species composition in the eastern study area. Either hypothesis could explain the observed importance of salinity and temperature as environmental variables driving variability in epibenthic communities.

Within the Transboundary area, there was a west–east pattern of pelagic but not of demersal fishes. Fish communities in the central to eastern Beaufort Sea area were dominated by five families: cods (Gadidae), sculpins (Cottidae), poachers (Agonidae) snailfishes (Liparidae) and eelpouts (Zoarcidae). There were more small pelagic fishes in the central area, and fewest demersal fishes in the Canadian Beaufort Sea near the Mackenzie River, though the numbers of taxa captured for both pelagic and demersal fish were greatest in the central region. Larval and small juvenile Arctic Cod, *Boreogadus saida*, were found pelagically across the whole area, mixed with snailfishes and pricklebacks (Stichaeidae) on the shelf and slope in the central region (151°–150° W, Colville River), mixed with snailfishes on the eastern shelf (146º–138º W), and comprising almost the entire catch of pelagic fishes in eastern slope communities. Not only was the ratio of dominant larval fish taxa different in the central Beaufort Sea, but their abundance was up to two orders of magnitude greater than in the eastern area (Figure 7.3.3.1). Demersal *B. saida* also occupied the entire Transboundary study area, from west to east and from shallow to deep. Snailfishes were of high proportion only in the central region but not abundant enough to form a separate community of demersal fishes. Demersal fish communities on the shelf could also be characterized as containing several species of sculpins, while fish communities on the slope had several species of eelpouts rather than sculpins.

Interior Arctic shelf systems such as the Beaufort Sea and the Laptev Sea in the Russian Arctic are typically less productive and support lower benthic biomass than inflow shelves such as the Chukchi Sea and the Barents Sea in the Atlantic Arctic (Carmack and Wassmann 2006). However, there is a strong push to detect biological "hotspots" in the Arctic (Grebmeier et al. 2015b). Hotspots are defined as regions of long-term high primary productivity and tight pelagic-benthic coupling that creates localized areas of persistent high benthic biomass over time scales of years to decades (Grebmeier et al. 2015a). While the Transboundary program design assessed broad-scale patterns, it lacked the spatial resolution and repeated sampling necessary to define hotspots. However, based on the epifauna and demersal fish data collected, there are clear differences in productivity in the eastern and central US Beaufort Sea, which would necessitate monitoring in both areas.

9.2 Depth-related patterns in taxon richness, biomass and abundance

Taxonomic focus for the Transboundary program was on the animal life from zooplankton to benthos and fish. When considering the ecosystem as a whole, it is important to determine similarities and differences between these taxonomic disciplines when they co-occur across the study areas and when they are exposed to the same physical attributes such as depth, temperature, and salinity, which are themselves highly confounded.

In the zooplankton, abundance and biomass were concentrated in the upper layer of the water column and decreased with water column depth, while species richness generally increased with depth as mesopelagic genera appeared. We observed a slight but non-significant increase in abundance and biomass in the transition zone from Arctic Halocline (AHW) to Atlantic waters (AW) (200–300 m), coinciding with an increased abundance of the large-bodied *Calanus* species and mesopelagic species such as *Spinocalanus longicornis.* The largest relative changes in both abundance and biomass between adjoining depth-strata occurred between the Polar Mixed Layer (PML) and AHW (i.e., at 50 m) and between the middle and bottom of the AW (i.e., at 500 m). Sampling of depth strata occurred at consistent depths: 0, 50, 100, 200, 300, 500, 1000 m across the survey. Boundaries of the vertically layered water masses in the Arctic are relatively stable (Macdonald et al. 1989, Codispoti et al. 2005) and boundaries observed in the Transboundary survey were consistent with these descriptions (Figures 3.1.1–3.1.3). Upwelling and other physical processes can temporarily shift these boundaries. For example, we observed possible upwelling in 2013; however, the duration and extent cannot be assessed with the data collected during the survey. These trends in abundance, biomass, and diversity are consistent with trends observed in still deeper waters within the Arctic basins (Kosobokova and Hopcroft 2010, Kosobokova et al. 2011). In contrast, species richness generally increased with depth, with a maximum in the 300–500 m layer (Table 4.9).

Total biomass and abundance of epibenthos also had distinct depth-related patterns, with biomass and abundance typically peaking on the outer shelf and upper slope at depth between 50–200 m (Figures 6.4.4 and 6.4.5). At shallower depths (20 m), biomass was often low, likely due to environmentally stressful conditions (low salinity, mobile substrates, ice scouring in winter). A noticeable increase occurred for abundance (less so for biomass) in the transition to 50 and 100 m shelf depths. This was mostly due to high abundances of some small-bodied taxa, primarily the brittle star *Ophiocten sericeum* (Figure 6.4.4). Biomass and abundance then decreased at depth >200 m, driven mostly by fewer individuals present not smaller body size. In fact, some of the most dominant taxa at depths >500 m were large-bodied sea stars (e.g., *Bathybiaster vexillifer*), holothurians (*Molpadia borealis*), and brittle stars (*Ophiopleura borealis*). This large body size of deeper slope species is contrary to previous observations that Arctic deep-sea fauna is small (Bluhm et al. 2011), but it may be that body size decreases closer to the actual deep-sea plain. The maximum depth stratum sampled in this project (1000 m) is located mid-slope and is likely exposed to a more dynamic food supply from downward shelf transport or upwelling (Bell et al. 2016) than the deep-sea plain proper, where limited food supply is thought to drive low abundance, biomass, and body size in the epibenthic communities and their food webs (Iken et al. 2005, Bluhm et al. 2011).

As with the other trophic levels, total biomass and abundance of fishes reflected depth-related patterns. Demersal fish showed an inverse relationship of biomass and abundance with few, very large fish in deep water and many, very small fishes in shallower water. In general, the species of fish in deep water were not the same as those in shallow water. Biomass was highest

at depths >350 m (Figure 7.3.4.16), primarily due to a few very large individual Greenland Halibut (*Reinhardtius hippoglossoides*) and Arctic Skate (*Amblyraja hyperborea*), which are known to occur on the slope throughout the Arctic region (Mecklenburg et al. 2011). Additionally, in the Canadian Beaufort Sea, *Boreogadus saida* biomass was highest in the water column at 350–500 m (Majewski et al. 2015). In the US waters, the demersal biomass of *B. saida* was in the same depth range (Appendix E3). The eelpout species we collected at depths ≥350 m were large, unlike the shallow water species (*Lycodes polaris*). Total abundance was moderately high ≤100 m, except in the Mackenzie River area (Figure 7.3.4.16), and highest abundances were found at the 20 m sites in Camden Bay. The pattern of fish species richness across the transboundary area differed from the shallow vs. deep pattern observed with biomass and abundance (Figure 7.3.4.5). Richness of demersal fish was both highest and lowest in Camden Bay, both in ≤100 m depth. Richness of larval and juvenile pelagic fishes was highest at the US-Canada border and lowest at the deep sites in Canadian waters off the Mackenzie River (Figure 7.3.3.3). While it is difficult to find historical data to compare depth-related distributions of Arctic fishes, it is known that all but the Pacific Arctic slope species *Lycodes raridens* also occur in the Atlantic Arctic (Mecklenburg and Steinke 2015).

Zooplankton, epifauna, and fish communities all have abundance and biomass patterns closely linked to depth, but the patterns are not the same across all levels. Demersal fish abundance was highest at depths <100 m, and especially at 20 m, despite that depth being the seaward landfast ice edge in the Beaufort Sea (Eiken, et al. 2005). Abundance of epibenthos was highest at slightly greater depths (50–200 m). Fish biomass was greatest at >350 m, much deeper than the epibenthos biomass peak at 50–200 m. On average, zooplankton abundances and biomass were greatest at stations <100 m in depth, although this was not true for all individual transects. In contrast, pelagic larval and juvenile fishes did not have a depth pattern; there were low abundances everywhere except in the central (150º W) Beaufort Sea. High abundance of small pelagic fishes found in the central area could be attributed to sampling there one month later than in the eastern area. There were also no links between increased zooplankton richness with depth (Table 4.9) and the richness patterns of pelagic or demersal fishes; however, fish biomass increased as depth increased.

9.3 Patterns in the Transboundary area compared with other Arctic regions

Previous chapters have compared results to other Arctic studies, and we summarize here to provide perspective across communities. As noted above, there was consistent separation at 200 m between the abundance values over the shelf and those of the slope for all trophic levels; hence, comparisons are made from that perspective. The taxonomic disciplines examined here are analogous to those reported in other Arctic areas in that the same broad-scale classifications (phylum through species) can be found with similar distributions.

The average zooplankton abundance and biomass on the shelf was comparable to, or lower than that reported from the Mackenzie delta (Walkusz et al. 2010) but higher than reported for the Canada Basin (Kosobokova and Hopcroft 2010, Hunt et al. 2014). The average biomass values for mesopelagic layers between 200 and 1000 meters on the continental slope of the Beaufort Sea were also higher than reported from the deep basins (e.g., Kosobokova and Hirche 2009, Table 4.11). The shelf was numerically dominated by *Pseudocalanus* species, as is typical of most arctic shelves (Hirche et al. 2006, Darnis et al. 2008, Kosobokova and Hirche 2009, Ershova et al. 2015b). However, the presence of euryhaline taxa, such as *Eurytemora* spp. and

rotifers in the PML in 2013 represents an important departure from similar species inventories of the Arctic's basins. These euryhaline taxa reflect the dynamic nature of the Beaufort Sea shelf environment, which can be profoundly influenced by seasonal freshwater inputs. The presence of rotifers within the PML is characteristic of major river outflows and is consistent with observations near the Mackenzie River (Walkusz et al. 2010) as well as the Laptev Sea, which is heavily influenced by numerous Siberian rivers (Abramova and Tuschling 2005). The influence of the Colville River was much less apparent than observed near the Mackenzie River, with only trace numbers of rotifers at two stations in 2012 sampling.

The low diversity guild of Arctic copepod taxa in the epipelagic realm gave way to increased contributions from mesopelagic taxa at depth on the Beaufort Sea slope, as observed in similar studies from the Canada Basin (e.g., Kosobokova and Hopcroft 2010). We did not encounter abyssopelagic deep-sea taxa, such as multiple *Lucicutia* and *Mimocalanus* species, which are largely restricted to depths below 1000 m (Kosobokova and Hopcroft 2010). Integration of the Transboundary dataset with previous studies in the Beaufort Sea during 2010 and 2011 improves spatial coverage and allows some broad general characterizations of gradients across the Beaufort shelf as a whole (see Smoot 2015). The Beaufort Sea around Barrow Canyon represents a transitional zone between the Pacific-affinity, benthic-rich Chukchi Sea and the Beaufort Sea, as reflected in its relatively high abundances of meroplanktonic larvae and Pacific expatriate taxa when compared to the rest of the Beaufort. In contrast, the central and eastern Beaufort are more traditionally Arctic in faunal character, with the influence of the Chukchi Sea and Pacific-derived waters increasingly weakened toward the Mackenzie River. The eastern Beaufort near the Mackenzie River is generally more estuarine than the rest of the Alaskan Beaufort (Walkusz et al. 2010), although conditions at specific locations likely vary seasonally and from year to year, depending on the intensity and extent of the river plume.

Major taxa contributing to the epibenthic community composition on the Beaufort Sea shelf and slope were very similar to what is known from other Arctic regions. Benthic communities in virtually every Arctic region are dominated by arthropods, mollusks, and polychaetes. Epibenthic taxon richness and composition on the US Beaufort shelf was also similar to the Chukchi Sea shelf, although the most numerically dominant ophiuroid on the eastern Beaufort shelf was *Ophiocten sericeum* rather than *Ophiura sarsii,* which is common on the Chukchi and western Beaufort shelves (Bluhm et al. 2009, Ravelo et al. 2014). One peculiarity of the Beaufort shelf and slope was the high abundance of pycnogonids, which are less common in other Arctic regions (Piepenburg et al. 2011). Very few brachyuran and anomuran crabs occurred in the Beaufort Sea, mostly restricted to the central Transboundary study region, which is different from the adjacent Chukchi Sea shelf where the snow crab *Chionoecetes opilio* and the lyre crab *Hyas coarctatus* can be community dominants (Bluhm et al. 2009, Ravelo et al. 2014). Maximum total epibenthic biomass on the Beaufort shelf was about an order of magnitude lower than previously reported for the adjacent Chukchi Sea shelf (Bluhm et al. 2009) and also lower than reported from the 2011 Beaufish project for the western Beaufort Sea shelf and upper slope. However, biomass reported for the central and western US Beaufort shelf (Konar 2013, Ravelo et al. 2015) was similar to results presented here in that the communities were correlated more strongly with depth than longitude. The findings of this study suggest that, as in other regions of the Arctic shelf and upper slope, high benthic biomass coincides with regions of persistently high food supply in the Transboundary area as in other regions of the Arctic shelf and upper slope.

It is difficult to find examples of depth-related patterns of fishes in other Arctic areas for comparison. Reist (1994) defined an Arctic guild as fish distributed wholly or primarily in

northern areas and adapted to relatively colder waters. By that definition, all the fish collected during the Transboundary cruises are in the Arctic guild. However, Mecklenburg and Steinke (2015) identified six zoogeographical categories of Arctic fish species: Arctic, spawning ≤0 ºC; Mainly Arctic but also in boreal waters; Arctic–Boreal, spawning below and above 0 ºC; Mainly Boreal but also at edges of Arctic; Boreal, spawning >0 ºC; and Widespread, in boreal and subtropical waters. We referred to the literature to determine zoogeographical categories for the fishes captured on Transboundary project. Many of the most abundant species that we collected are distributed in the circumpolar Arctic (Mecklenburg and Steinke 2015) including *Boreogadus saida*, Arctic Staghorn Sculpin (*Gymnocanthus tricuspis*), Bigeye Sculpin (*Triglops nybelini*), Gelatinous Seasnail (*Liparis fabricii*), Adolph's Eelpout (*Lycodes adolfi*), and Longear Eelpout (*Lycodes seminudus*). Others are categorized as Arctic–Boreal circumpolar (Mecklenburg and Steinke 2015) and included Spatulate Sculpin (*Icelus spatula*), Shorthorn Sculpin (*Myoxocephalus scorpius*), and Stout Eelblenny (*Anisarchus medius*). Collections most analogous to the Transboundary study were found in the Barents Sea at depths 167–495 m (Fossheim et al. 2006), which contains some of the same or Atlantic congeneric species. Comparable deep-water species we found in the Transboundary area included *B. saida*, Greenland Halibut, Arctic Skate, and Eelpouts. Other congenerics that we found in ≤100 m in temperatures <0 ºC were collected at deeper depths and temperatures 1 ºC warmer in the Barents Sea (Fossheim et al. 2015). Thus, there was some similarity between fish distributions at depth in the Barents and Beaufort Seas, but not for all species and not necessarily in relation to the same drivers (i.e., depth, temperature, salinity). Fish biomass density in the Barents Sea is an order of magnitude higher than in the Chukchi Sea (Hunt et al. 2013). Although we know the numbers of fish that we collected in the Beaufort Sea were low compared to the Chukchi Sea (Norcross et al. 2013), we cannot directly compare the biomass as we did not use commercial size nets and cannot estimate the abundance of fish in metric tons.

9.4 Interannual variability in biomass and abundance in the Transboundary region

This study afforded us the opportunity to examine variability of taxa sampled with the same gear in the same locations in both 2013 and 2014. Variability was evident for all taxonomic disciplines on small scales, as within a station, but not on the larger spatial scale of shelf vs. slope.

Zooplankton communities are noted for their high interannual variability in the Arctic (Day et al. 2013), diminishing usefulness of between-year comparisons. Nonetheless, the suite of species encountered at resampled stations share many similarities, including the presence of *Calanus glacialis*, *Pseudocalanus* spp., and *Oithona similis*. These similarities are particularly pronounced with exclusion of the estuarine species that were common in 2013, but not 2014. Similarities in community structure (see below) and for abundance and biomass were stronger for the smaller zooplankton (as collected by the 150-µm nets) than for larger zooplankton (as collected by the 505-µm nets). For the large zooplankton these high interannual differences were driven primarily by *Calanus glacialis*.

Though there was interannual variability of epibenthos, many patterns of biomass and abundance by depth were consistent over sampling years 2013 and 2014 (see Figure 6.4.6). For example, the 50-m depth stratum at transect A1 (141° W) and the 100-m stratum at transect TBS (140° W) always had the highest biomass at these transects, regardless of year sampled. This may be a potential hotspot and it would be worthwhile to monitor these locations in the future.

Despite the high variability in absolute biomass, the relative patterns of high or low biomass are quite persistent. This consistency across years was also evident when looking at the biomass of individual taxa along the shelf and slope station groups for 2013 and 2014 (Appendix D Table 1). This larger spatial view of "Beaufort shelf" and "Beaufort slope" integrates multiple stations across shelf depth and slope depth strata, and across the longitudinal transects, thus averaging over the variability of the individual stations results in the rather high variances associated with the averages (Appendix D Table 1). Despite high variances and absolute biomass values, the pattern of which species had high biomass (echinoderms: shelf–*Psolus peronei*, *Ophiocten sericeum;* slope–*Ophiopleura borealis*) was quite consistent over both years.

There were discernable, though non-significant, patterns in biomass and abundance for fish catches between the two years. Biomass was higher and abundance was lower at slope stations in 2013 than in 2014. Absolute abundance was higher on the shelf in 2014 but, proportionally, both biomass and abundance were equal in the two years. The patterns were consistent when comparing shelf ≤100 m and slope ≥200 m (Table 7.3.4.4). Biomass of fish was always greatest on the slope and abundance was always greatest on the shelf. Year was never a statistically significant factor affecting biomass, abundance, or community composition.

9.5 Community Structure

9.5.1 Analytical approach

Analytical considerations of appropriate community data transformations were assessed because communities are generally characterized by the highly unequal distribution of taxa. Our current questions targeted the overall community structure, not specific species. As such, we were interested in keeping the main dominance structure within the dataset while still accounting for species that occurred at lower abundance. We used a variety of transformations (i.e., square-root (2RT), fourth-root (4RT), $\log+1_{10}$, presence/absence) to assess the effect on community composition results. Overall patterns in community structure were relatively similar across all transformations, except for presence/absence transformation, which changed the results considerably and eliminated structure in community patterns seen with other transformations. We decided to employ a 4RT for all biological disciplines because it yielded the lowest stress level in two-dimensional ordination, and its intermediate severity best balanced the influence of common and rarer species.

9.5.2 Spatial and temporal variability in community composition

It is uncommon to replicate sampling at the scale of individual sites for epibenthos and fish. The main reason for lack of replicate trawl sampling is the expense associated with at-sea sampling. For most studies, more spatial coverage is chosen over replication. However, patchy distribution of epibenthic invertebrates and fish (Piepenburg and Schmid 1996, Mecklenburg and Steinke 2015) raises the question: how representative of the actual community is a single trawl haul for a given location? Here, we had the opportunity to take repeat trawl samples along one transect (A1, 141° W) in 2014. Our analysis showed that a single trawl was a good representation of the local community composition, which gives confidence to the information gleaned from the typical single-trawl hauls (Figures 6.4.9 and 7.3.4.8, Table 7.3.4.7). It is important to note that absolute abundance and biomass of both individual and whole taxa can be strongly variable (e.g., Anthozoa, *Chionoectes opilio*) between trawl hauls even if the overall community composition (i.e., the relative composition of taxa and overall structure) remains

quite stable. This was the case in this study when comparing two trawl gear types and true for repeat trawls completed on shallow shelf stations in the western Beaufort Sea in a previous study (Ravelo et al. 2015). In both cases, there were no significant differences in community composition and community structure among repeat trawls.

Though we could only directly compare two years, we found little evidence of variability in epibenthic invertebrate and fish communities in the eastern Beaufort Sea, indicating that these communities were likely stable over 2013 and 2014. Community composition at 2013 stations (transect A1, 141° W) that were resampled in 2014 was very similar among the two years. Separation in the non-metric multidimensional scaling (nMDS) ordination between repeat trawls within the same year was very similar to the separation between the two years (Figures 6.4.9, 7.3.4.12 and 7.3.4.13), indicating that intra- and inter-annual variability were similar. Further, comparing patterns in total biomass and abundance across several transects sampled in both 2013 and 2014 showed that overall patterns were similar (Figures 6.4.6, 7.3.4.10). These results support the idea that the longevity of most benthic invertebrates in the Arctic contributes to the long-term stability of the Arctic benthic communities (Bluhm et al. 1998, Philipp and Abele 2010, Grebmeier et al. 2015b) and that there was consistency of patterns in fish communities interannually (Fossheim et al. 2006). This longevity allows these communities to integrate short-term variability in the environment. However, stability in benthic community structure during the open water season may be temporally limited. If environmental conditions were to change over longer time scales, patterns in epibenthic (Grebmeier et al. 2015a) and fish (Fossheim et al. 2015) communities would likely also change, depending on the type, severity, and persistence of the environmental changes and the tolerance levels of the taxa involved.

9.6 Shelf–Slope, depth and water mass related patterns in community structure

Strong community segregation related to depth strata was prominent in all disciplines. Depth is a proxy for different environmental conditions in the Arctic system (Roy et al. 2014, 2015b) and, in the Beaufort Sea, it also coincides with the main water masses (Macdonald et al. 1989, Lansard et al. 2012), which are strongly correlated with community structure. Very shallow regions (<30 m) are heavily influenced by ice scour, sedimentation, and freshwater influence (Dunton et al. 2006, Mahoney et al. 2014). Shelf communities are stable but strongly influenced by changing food supply, both seasonally and through variations in water mass characteristics (e.g., nutrient regimes, upwelling; Iken et al. 2010). Generally, food availability decreases with increasing depth (Bluhm et al. 2011, Roy et al. 2014). The slope environment is dynamically impacted by water mass layers with different hydrographic properties. The strong influence of hydrographic conditions on community structure was reflected in our environmental analysis, which showed temperature and salinity were driving factors of community composition over the large depth range considered. As observed during the Transboundary project, vertical water mass layers over the Beaufort shelf and slope include a thin surface freshwater layer (0–10 m) from rivers and sea icemelt that overlays the Pacific-derived PML (≤50 m; Macdonald et al. 1989). The PML gives way to AHW between ~60–200 m. This AHW transitions into the warmer and more saline Atlantic-derived Water (AW) below 200 m, which layers over the cold Canada Basin deep water at approximately 800–1000 m depth (Lansard et al. 2012). Each water mass is distinct in temperature, salinity, nutrient concentration, and organic matter composition (Macdonald et al. 1989). Water masses are so distinctly defined by depth that it is impossible for us to distinguish between depth-driven community patterns, which might indicate community

turnover caused by depth-related physiological or food limitations, and patterns caused by the influence of other water mass properties (e.g., salinity, temperature, nutrients). Not only is depth a likely proxy for water masses and environmental conditions such as dynamic and stressful environmental conditions in very shallow waters, but also for abundant food supply on shelf depths, and increasing food limitations at greater depth.

The zooplankton communities observed during the Transboundary field surveys primarily separated along a shelf-slope axis (see Figures 4.1.13–4.1.16). In the Arctic, zooplankton communities are tied to the underlying hydrographic conditions (Darnis et al. 2008, Lane et al. 2008, Eisner et al. 2013, Questel et al. 2013, Ershova et al. 2015b). The community groupings observed during the Transboundary surveys reflect this phenomenon as well as traditional shelf-slope community differences. For example, the across-shelf transition from neritic to more oceanic taxa has long been recognized in the Arctic. In the Transboundary region and other Arctic waters (Grainger 1965, Darnis et al. 2008), *Pseudocalanus* species usually typify neritic shelf assemblages, while a suite of oceanic epipelagic and mesopelagic taxa are characteristic of offshore assemblages. The presence of Pacific expatriate species, including *Neocalanus* spp. and *Metridia pacifica*, demonstrate the hydrographic connectivity between the subarctic Pacific, the Chukchi Sea, and the Beaufort Sea.

Community structure of zooplankton was similar to other depth-stratified examinations in the Arctic, characterized by gross community separation according to stratified water masses (Kosobokova et al. 2011). The community in the PML is composed of a fairly low-diversity group of Arctic copepods. Carmack et al. (1989) note that exchange between the shelf environment and the offshore environment occurs primarily in waters above the halocline. Contributions from euryhaline taxa observed in the PML highlight this phenomenon. For example, abundance of euryhaline taxa, such as *Eurytemora* spp., varied across the upper layer of the survey area due to variations in the extent of the freshwater lens. Community differences associated with depth were more pronounced than differences associated with variation within a given water column depth interval, as seen on the basin-level scale (Auel and Hagen 2002). Depth ranges for species were largely consistent with these studies, with many species, such as *Calanus glacialis*, *C. hyperboreus*, *Spinocalanus longicornis*, and *Chiridius obtusifrons*, exhibiting vertical ranges that overlap multiple water masses (Figure 4.2.7). This is not surprising, given that water mass boundary depths are not absolute.

The primary shelf-slope zooplankton community gradient observed in the Beaufort Sea was modified by localized hydrographic conditions and processes. During 2013, the survey area was heavily influenced by a freshwater lens mixture of Mackenzie River water (as seen in Chapter 3 and Majewski et al. 2016) and meltwater contained a distinct faunal grouping of taxa such as *Limnocalanus macrurus*, marine cladocerans, and *Eurytemora* spp. in addition to the typical neritic assemblages. The 2014 survey area overlapped much of the same geographic range; however, prevailing oceanographic conditions in the upper water column were drastically different. Thus, it is not surprising that the zooplankton communities observed on the shelf in 2013 and 2014 were different. Across-shelf gradients associated with the Mackenzie River plume have also been recognized in the Canadian Beaufort. Walkusz et al. (2010) report ecological zones of zooplankton associated with intensity of the Mackenzie River plume, noting an “intense plume” assemblage, a “diffuse plume” assemblage, and an “offshore” assemblage (Section 4.1.4.1). Our findings mirror this description; stations from the 2013 survey year exhibited internal structure associated with location relative to the shelf break and the degree of freshwater influence. In both our work and that of Walkusz et al. (2010), the “intense plume”

assemblages were characterized by euryhaline and brackish water taxa, which is consistent with observations reported for other marginal Arctic seas influenced by major riverine input (e.g., Abramova and Tuschling 2005).

Depth, salinity, and temperature were the main variables influencing epibenthic community structure. Depth-related community structure changes coincided with dominance of characteristic taxa according to their typical depth ranges and possibly due to some resource partitioning, especially among the ophiuroid species, which may cause greater reliance on microbially-altered food sources. It is suggested that the stability of epibenthic communities is related to the longevity of most Arctic benthic species, which creates some resilience to changing conditions caused by climate changes or anthropogenic influences. However, this resilience is necessarily limited and likely depends on severity and persistence of the change and the tolerance levels of the taxa involved.

The continuous change in epibenthic community composition with depth (Table 6.4.5, Figure 6.4.8) was reflected in the distribution of some characteristic taxa. Shallow stations (20 m) were dominated by mobile species, such as decapod shrimp (*Eualus gaimardii*, *Sabinea septemcarinata*), *Ophiocten sericeum*, and amphipods (e.g., *Anonyx* sp.), which have large tolerance windows for environmental conditions such as low salinity. Most of these species also have omnivorous feeding habits, which allow them to capitalize on a large variety of food sources (Bell 2015). For example, the sea cucumber *Psolus peronii* had an extremely patchy distribution, restricted to around the 50-m depth stratum, which may indicate specific hydrographic features that favored this slow-moving, filter-feeding taxon (e.g., current regimes, minimal physical disturbance). There was a distinct depth zonation in brittle stars, and the dominant role each species plays within the communities at their specific depth ranges showcases the overall importance of brittle stars in Arctic benthic systems and may indicate resource partitioning among these species (Graeve et al. 1997). This zonation was observed in this study. The small brittle star *O. sericeum* is common in high densities in many Arctic shelf regions. It was highly abundant between 20–100 m depth in our surveys. The ophiuroid *Ophiacantha bidentata* was prominent at 100–200 m depth but was replaced in dominance by *Ophiopleura borealis* at depths >350 m. The sea star *Pontaster tenuispinus* started to occur at 200 m and dominated the community at 750 m, with another sea star, *O. borealis*, at the shallower end of its depth range. At 1000 m, the deep-sea scavenging/predatory sea star *Bathybiaster vexillifer* became co-dominant with the brittle star *O. borealis*. The sea star *B. vexillifer* is known to source carbon from both phyto-detrital and microbial sources (Howell et al. 2003), which supports our hypothesis that microbial processing of organic material is an essential component of the deep-slope food web of the Beaufort Sea (Bell 2015).

Shelf–slope processes had different effects on the pelagic and demersal fish communities. Pelagic fish community structure was less affected by shelf-slope processes than were demersal fish communities. In the central (150º W) region, there was no shelf-slope component to the pelagic community, which was represented, almost equally, by *Boreogadus saida*, snailfish, and prickleback larvae and juveniles (Table 7.3.3.1). In contrast, the eastern area was almost wholly *B. saida* on the slope and half as many pricklebacks as *B. saida* on the shelf. Demersal fish communities displayed distinct differences between shelf and slope habitats; shelf communities had a higher abundance of smaller fishes, and the slope communities had fewer, but larger, individuals of different species than those found on the shelf. All shelf communities examined had the common components of *B. saida*, *G. tricuspis*, and *I. spatula*. Depending on sampling year, and possibly spatial factors, a poacher, snailfish, or an eelpout was included in these shelf

communities. Slope communities were defined by *B. saida* and *Lycodes* spp. In the US Beaufort Sea, we found continental shelf communities were different from those on slopes as is typical (Mecklenburg and Steinke 2015) for all adjacent Arctic Seas.

In this study water mass was closely tied to depth, and in the Chukchi Sea it was a factor determining fish communities (Norcross et al. 2010). In the Beaufort Sea, shelf communities were clearly associated with Polar Mixed Layer (<50 m), and slope communities were clearly associated with Atlantic Water (AW) (>250 m deep; Figures 7.3.4.22, 7.3.4.24). However, the area of transition at 100–200 m is subject to change as the water masses move onshore/offshore and upslope/downslope. Because fish are more mobile than many epibenthic species, but not directly moved with the water masses like zooplankton, there can be a delayed response of species movement to changing water mass. The fishes in our analysis represent a point-in-time collection; therefore, the 100–200 m depths appear to have less distinct fish communities than the shallow and deeper areas. In particular, fishes collected at 200 m depth at times (locations) grouped with the shelf community and at times (locations) grouped with the slope community. Salinity and temperature (the components of water mass) were correlated with both biomass and abundance of demersal fishes, though not as strongly as was depth, and no a patterns were evident with factors of time and space. This demonstrates the transitional nature of the AHW between 50 and 200 m, which affects these fishes.

9.6.1 Indicator species in the Transboundary area

Similarity percentage analysis (SIMPER) can be used to help identify some taxa as indicator species for the shelf and the slope, and sub-habitats within them. Indicator species are defined by their frequency of occurrence as well as the biomass they contribute overall; this term does not necessarily relate to their ecological significance in the system or their resilience or vulnerability to disturbances in the system. However, given their prominence on shelf or slope, we can certainly assume that they are playing important roles in ecosystem functioning, and our knowledge helps us infer what those roles are.

For zooplankton, many species were shared across multiple habitats (e.g., the copepod *Oithona similis* was found at all stations), thus the challenge was to find those largely restricted to just one habitat. In all surveys, juveniles and adult *Pseudocalanus* species (Figure 4.2.3) usually typified neritic shelf assemblages, while the oceanic *Calanus hyperboreus* and *Microcalanus pygmaeus* were characteristic of offshore assemblages. The region around the Mackenzie River represents an extreme example of cross-shelf gradients, as indicated by a "plume" assemblage during 2013, characterized by euryhaline taxa that were largely absent in 2014 (e.g., *Eurytemora* spp., *Limnocalanus macrurus*, *Podon leuckartii*, *Evadne nordmanni*, and rotifers). As water depth increases near the slope, the mixtures of species shifted vertically (Figure 4.2.3), the *Pseudocalanus* species complex was identified as an indicator of the PML, *Paraeuchaeta glacialis* as an indicator for AHW, and *Spinocalanus longicornis* was identified as an indicator for the Atlantic layers. Several other taxa were found exclusively in the Atlantic layer including *Oncaea notopus*, *Chiridiella reductella*, and the cnidarian *Sminthea arctica*. In general, predatory biomass in AHW was dominated by the chaetognath *Parasagitta elegans*, while in AW it was the chaetognath *Eukrohnia hamata* and a variety of cnidarians.

Epibenthos communities were characterized by very different species on the shelf versus the slope. Some of the main indicator species on the shelf were the brittle star *Ophiocten sericeum*, the scallop *Similipecten greenlandicus*, the shrimp *Sabinea septemcarinata*, the amphipod *Anonyx* sp., and cumaceans *Diastylis* spp. (Appendix D Table 2). Some of these taxa are known

to be essential in mineralization processes of the organic matter on the Arctic shelf (Piepenburg and Schmid 1996, Blicher and Sejr 2011). Taxa such as cumaceans play specific but poorly understood roles in organic matter processing by feeding on particularly low trophic levels. Their status as indicator species on the Beaufort Sea shelf suggests that loss of these species from major disturbances of the system could have significant impacts on energy flow to higher trophic levels. For example, the brittle star *O. sericeum* was known to respond with increased metabolic rates and energy demands to disturbances of temperature increases and ocean acidification (Wood et al. 2011). It is reasonable to postulate that other disturbances, such as from oil and gas development, could affect this species.

Indicator epibenthic species of the slope environment were the sea stars *Pontaster tenuispinus* and *Bathybiaster vexillifer* and the brittle star *Ophiopleura borealis* (Appendix D Table 2). Again, while their specific ecosystem functions are not entirely known, their frequency and abundance indicate that they must play important roles in the system. The brittle star *O. borealis* is known to contain relatively high total lipid content and high levels of some essential fatty acids (Graeve et al. 1997, Gallagher et al. 1998), which could make them important sources of these lipids to higher trophic levels through predator-prey relationships. While brittle stars are typically not considered high-quality prey because of their high level of inorganic material, this particular species could be an important prey item and lipid/fatty acid source in the deeper slope environment, a system with overall low food availability. It was occasionally found in eelpout stomachs in this study. There is no information on the vulnerability of this and other slope species to disturbances; however, any disruption of such species with important ecosystem functions would likely have cascading effects through the remainder of the system.

For demersal fishes, the shelf communities were more diverse than the slope communities. *Boreogadus saida* was found at almost all stations and all depths and its presence cannot be used as an indicator of a unique community. However, size/age of *B. saida* can be used to employ it as an indicator species. As seen in the Transboundary region, demersal age-0 *B. saida* was more abundant on the shelf than were ages 1–5 (Figure 7.3.2.2). To the east of the Transboundary region in the Canadian Beaufort Sea, hydroacoustic analysis revealed age-0 juvenile *B. saida* were separated in the water column (at <100 m) from larger, older fish which are deeper (Geoffroy et al. 2015). The *B. saida* captured demersally in this study were similarly separated by bottom depth, with older, larger *B. saida* captured on the slope and younger, smaller *B. saida* captured on the shelf.

Presence/absence (PA) (Table 7.3.4.21) is the least specific and easiest measure of taxa characterizing communities. Indicators of the inner (20 m) demersal shelf community were small *Boreogadus saida*, Spatulate Sculpin (*Icelus spatula*) and Arctic Alligatorfish (*Aspidophoroides olrikii*). The outer (50–100 m) shelf community was more diverse; it included the three species from the inner shelf as well as more sculpin taxa: Arctic Staghorn Sculpin (*Gymnocanthus tricuspis*), Ribbed Sculpin (*Triglops pingelii*), and small (≤40 mm) *Icelus* that could not be identified to species. In sharp contrast, the slope community could easily be differentiated from the shelf communities. Indicators of the slope community were large *B. saida* and multiple species of large eelpouts of the genus *Lycodes*. As this was the first study to sample bottom fishes on the US Beaufort Sea slope, it is unknown what may cause changes in these communities. However, warming in the Barents Sea has caused northward expansion of boreal fish communities and simultaneous northward retraction of the Arctic shelf community (Fossheim et al. 2015). In the Barents Sea, community compositions are not as sharply

delineated by depth (i.e., shelf vs. slope), so direct extrapolations of changes expected in the western Arctic cannot be made.

9.7 Taxonomic level of monitoring in the Transboundary area

We explored the possibility of using higher-level taxonomic identifications as a viable tool for cost- and time-efficient monitoring of the Beaufort Sea shelf and slope systems. The premise of taxonomic sufficiency is that identification to a higher taxonomic level is more efficient and can be done by less-trained personnel, but care has to be taken to assure that critical information is not lost in the process. For example, closely related species may exhibit different ecological or biological responses and patterns that could be lost by grouping at higher taxonomic levels.

For the Arctic zooplankton, where ~350 different species exist (Gradinger et al. 2010b), the premise of lower taxonomic resolution being adequate to characterize communities is simply a fallacy. There are frequently substitutions of species within a genus that either alone, or in combination with other taxa, define community assemblages. For example, while *Calanus glacialis* is broadly distributed across the shelf in into oceanic waters, *Calanus hyperboreus* is primarily found in oceanic waters and, within this same family, *Neocalanus* copepods indicate entrainment of Pacific-origin waters. Similarly, the four species of *Paraeuchaeta* each define a different water mass layer, as do many other genera (see Kosobokova et al. 2011). The frequent failure to separate even "minor" taxa, such as the four species of chaetognaths (that exist in separate taxonomic orders) prevents one from using them as indicators of PML, AHW, and AW. Superficial but expedient sample analysis of virtually all the Outer Continental Shelf Environmental Assessment Program (OCSEAP) zooplankton collections from the 1970s and 1980s has rendered them nearly useless because the most abundant and diverse zooplankton group, the copepods, were only identified to order (Horner 1978, 1979, 1980, 1981). Regrettably, after being stored for two decades, these OCSEAP samples were disposed of because the perception was no additional information could be extracted from them (Horner pers. comm.).

In epifauna analysis, we found that the distinct depth-related gradient in community composition was considerably weakened when analyzing epibenthic communities at the higher taxonomic level of mostly class or order level (Figure 6.4.8). Considering that depth-related trends were most important in both visual community ordinations (Figure 6.4.8) and in BioENV analysis of community structure in relation to environmental variables (Table 6.4.5), higher taxonomic grouping could cause loss of this significant information. Using higher taxonomic level identifications would also impact the level of individual taxa that we identified as ecologically important or as indicator taxa. For example, the abundance of the brittle star species *Ophiura sarsii* in the more central region (B-transects, 151–150° W) compared with the dominance of *Ophiocten sericeum* in the more eastern study region (146–138° W sampled in 2013 and 2014) was detected based on identification to species level. By grouping on the class level Ophiuroidea, this separation would not be evident. This may be an important consideration for monitoring efforts that focus on changes in community structure over time. Different ophiuroid taxa also were indicator species of the shelf community (*O. sericeum*) versus the slope community (*Ophiopleura borealis*), which could not be distinguished at the class level. Other examples are within the order Isopoda, where we found some taxa (*Saduria* spp.) to be broadly distributed across all depth strata while others were restricted to the shelf (*Synidotea bicuspida*), a distinction only possible with species-level identifications (Appendix D Table 1). Therefore, the value of being able to assess species-specific responses within the benthic community is

undeniable. Here it was necessary that some groups of epifauna were kept at higher levels because of difficulty of field identifications or a global lack of taxonomic experts for verification. This is challenging for some of the taxonomically more difficult groups such as bryozoans, hydroids, sponges, and etc.

For Arctic fishes, it is rare to use classifications above the species level. In some cases, when a species-level identification cannot be made, identification and analysis is conducted at the genus level. This generally occurs with very small fishes such as small sculpins and snailfishes that are notoriously difficult to identify to species. Analytical complications arise when specimens are not identified to the lowest possible taxonomic category. For example, if 90 fish can be identified to 10 individual *Icelus* species and 10 specimens cannot be identified to species, meaning they are not necessarily the same 10 *Icelus* species, it is necessary to perform analysis of all 100 fish at the generic level. To analyze as 10 species plus one genus could potentially bias the results as we would not know if there were actually 11 or more species, if the 10 generic-level identifications actually represented one of each of the 10 species, or if the 10 generic-level identifications actually were all one of the 10 species, or some combination of these options. Obviously the statistical tests using any of these combinations would yield very different results, but it would be impossible to know what was accurate. By grouping all identified and unidentified specimens at a higher taxonomic level, the results would be accurate, but less precise. An example of this application is that indicators of the fish coastal community include *Liparis* spp. ≤50 mm and *Icelus* spp. ≤40 mm (Table 7.3.49). We are certain of the identification of Spatulate Sculpin (*Icelus spatula*) that are >40 mm, but we do not know how many of the small *Icelus* spp. are Spatulate Sculpin or Twohorn Sculpin (*Icelus bicornis*; Appendix E2). However, it is critical to have been able to identify Spatulate Sculpin to species as it is that species, not the genus *Icelus*, that is an indicator of the shelf community.

Boreogadus saida and sculpins are indicators of the shelf community. *B. saida* is found on the shelf as well as on the slope; however, on the shelf *B. saida* are <100 m (Figure 7.3.2.1) at ages 0–1 (Figure 7.3.2.2). Some combination of sculpins (*Artediellus scaber, Gymnocanthus tricuspis, Icelus spatula, Triglops pingelii*) is an indicator of the shelf community (Tables 7.3.4.3, 7.4.3.9). Not all sculpin species are at every station, but at least three of these four sculpin species indicate a Beaufort Sea shelf community. Arctic Alligatorfish (*Aspidophoroides olrikii*) indicates a shelf community because it is not found in deep water; however, its distribution is very patchy with inconsistent occurrences of high abundance. If this species is caught, it indicates a shelf community. Though Canadian Eelpout (*Lycodes polaris*) is typically found on the shelf, it is not considered a reliable indicator species because its distribution is to 200 m and it is not as abundant as the sculpins.

Boreogadus saida and three eelpout species (*Lycodes adolfi, L. sagittarius,* and *L. seminudus*) are good indicators of slope communities (Tables 7.3.4.3, 7.4.3.9). *B. saida* age 1+ are demersal on the slope from about 200–400 m; as depth increases, *B. saida* spread throughout the water column as deep as 600 m, but importantly, form an acoustically visible layer that remains at 200–400 m extending off the bottom (Geoffroy et al. 2015). The eelpouts *L. adolfi, L. sagittarius*, and *L. seminudus* are species for which there are no substitutes to indicate the slope community.

If fishes were only identified to family, some differentiations could be made between shelf and slope communities (Table 7.3.4.4). Cottidae (sculpins), Agonidae (poachers), Cyclopteridae (lumpfishes) and Stichaeidae (pricklebacks) are indicative of shelf communities and Rajidae (skates), Zoarcidae (eelpouts), and Pleuronectidae (righteye flounders) are indicative of the

slope. While some individuals of these families may be found in the alternate habitat, they are predominantly found in these areas. Gadidae, in the Beaufort Sea that means *Boreogadus saida*, could not be used to differentiate shelf and slope communities unless they were measured (see Section 9.6.1).

Use of lower or higher taxonomic identifications depends on the scientific questions being asked or the purpose of the monitoring program to be initiated. If zooplankton, benthic epifauna, or fish are being used as indicators of change from climate or oil and gas exploration, then species-level information is likely critical, especially for the taxa we identified as indicator species. A much lower taxonomic identification level is sufficient for purposes of total biomass and abundance. If biodiversity observations are being used as metrics that inform managers about ecosystem health and services (Palumbi et al. 2008, Duffy et al. 2013), then an even lower, more precise taxonomic level identification than we have done here may need to be implemented.

9.8 Interdisciplinary comparisons

It is valuable to visualize related spatial patterns for an ecosystem perspective. With few exceptions, station depth ranked as the strongest structuring variable for zooplankton, epifauna and demersal fish communities, in terms of both biomass (Figures 9.1–9.3) and abundance (Figures 9.4–9.6). The 100–200 m contour, which generally corresponds to the shelf break (Brugler et al. 2014), formed a consistent breakpoint across assemblages. Subsequent subdivisions often occurred for the shallowest stations within all three trophic levels; however, cross-discipline locations of on-shelf subdivisions were not consistent. Subdivisions were also apparent for the epifauna along the slope. The higher sub-structure within the epibenthic community is likely due to the low mobility and high number of species that alternate in dominating relative community biomass and abundance. The shelf break subdivisions in the fish community coincided with the outer shelf and upper slope epibenthic communities in 2014 (Figures 9.3, 9.6). During 2013, additional structuring in the zooplankton and epifauna communities, but not in fish communities, was noticeable in the Mackenzie River Plume in the eastern study region (Figures 9.2, 9.5).

Acknowledging the similarities among zooplankton, epibenthic, and demersal fish communities that can be seen in the temporal and spatial scales (Figures 9.1–9.6), we also explored the relationships statistically to test the hypothesis that distribution of marine fish species is independent of observed abundance of zooplankton and benthic invertebrates, and that zooplankton and benthic invertebrates are independent of each other. The RELATE test (PRIMER v.7) is a non-parametric permutation form of Pearson's coefficient based on the principal of matrix correlations using a Spearman coefficient (Clarke et al. 2014a). The RELATE test provides a useful means of testing and quantifying the extent of similarities in community organization among different ecosystem components. Within the two years (2013 and 2014) for which quantitative abundance data were available for zooplankton, epibenthos and fish, comparisons were made using 10,000 permutations (Table 9.1). In both years demersal fish CPUE (# 1000 m^{-2}) was highly correlated (p <0.0001) to both 150-µm and 505-µm zooplankton (# m^{-3}). Similar high correlations (p <0.0001) were found in 2013 and 2014 between fish and epibenthos abundance (# 1000 m^{-2}). In addition to direct correlations with fish, epibenthos (# 1000 m^{-2}) and 150-µm and 505-µm zooplankton (# m^{-3}) were highly correlated (p <0.0001) to each other in both 2013 and 2014. Similarly, relationships using community biomass were highly significant.

Across-shelf structure is well recognized for many Arctic communities, and has been noted previously in this chapter. Globally, zooplankton communities are known to be structured on the shelf, as noted in several previous Arctic studies (e.g., Grainger 1965, Lane et al. 2008, Darnis et al. 2008). Similarly, cross-shelf patterns have been found for benthos (Bluhm et al. 2009, Pisareva et al. 2015) and demersal fish (Majewski et al. 2013, 2016). For zooplankton, these patterns are driven by gradients in primary productivity from the nearshore environment to offshore environment and by depth (Yamaguchi 2008, Schnack-Scheil et al. 2008, Kosobokova et al. 2011). Cross-shelf epibenthic community patterns can also be driven by productivity regimes, disturbance regimes, and substrate differences such as coarser sediment structure in coastal and higher flow portions of the shelf than depositional regions (Bluhm et al. 2009, Blanchard et al. 2013, Pisareva et al. 2015). Depth only becomes a driver for epifaunal communities on the slope. On the shelf of the Chukchi Sea, large-scale differences relate to water mass (Norcross et al. 2010) and small-scale differences of richness and density of fish on the shelf are explained by temperature and the erosional or depositional nature of sediment characteristics (Norcross et al. 2013). In the Beaufort Sea, water mass, temperature, and salinity explained differences in demersal fish communities; at times total organic carbon (TOC), percent gravel, percent sand, or percent mud may also partially affect community composition. There was a surprising coherence of taxonomic clustering break points across trophic levels at the shelf break depths. The confounded nature of depth, temperature, salinity, and habitat variability makes it hard to determine which of these variables is most influential, and it is possible that the most significant factors differ among zooplankton, epibenthos, and fish community types. It is notable that the warmer water found in the AW layer, at depths >~250 m (Section 3.1, this document), provides a potential refuge for warmer-affinity expatriated zooplankton species that might otherwise experience lethal winter temperatures on the shelves or, in the case of epibenthos, species of Atlantic biogeography (Bluhm et al. 2011). Perhaps the warm Atlantic layer is associated with the circumpolar distribution of *Boreogadus saida*, *Artediellus scaber*, *Myoxocephalus scorpius*, *Anisarchus medius*, and *Hippoglossoides robustus* (Mecklenburg et al. 2011), species we collected on the shelf and shelf break of the Beaufort Sea.

Distinct patterns were seen within and among years. It is notable that, despite a similar clustering structure, the zooplankton collections were most like each other within a year, although larger interannual differences occurred. In contrast, the epifauna and fish community clusters formed at a much lower level of similarity, but their community composition tended to be more similar across years. Similar patterns have recently been noted for the northeastern Chukchi Sea (Blanchard et al. 2017) and attributed to the shorter life spans and highly modulated seasonality of zooplankton communities in comparison to benthos and fishes. This suggests that planktonic habitat is generally smoother and less variable than the benthic and demersal habitats. Accordingly, it should be easier to link plankton to environmental gradients on an annual basis. In contrast, the benthic and demersal habitats tended to be more heterogeneous at the scale of sampling, which ranged from 10s of meters to ~5 km and the epibenthic and fish communities still responded to larger scale environmental gradients. It has been suggested that fish distributions [and likely epibenthos] are not directly controlled by a single abiotic factor but rather by large-scale processes and changes in interdependent physical, chemical, and geological factors that, in aggregate, affect the biotic factors (Majewski et al. 2013). Therefore, these ecosystem components are likely excellent indicators of longer-term, persistent changes in environmental conditions.

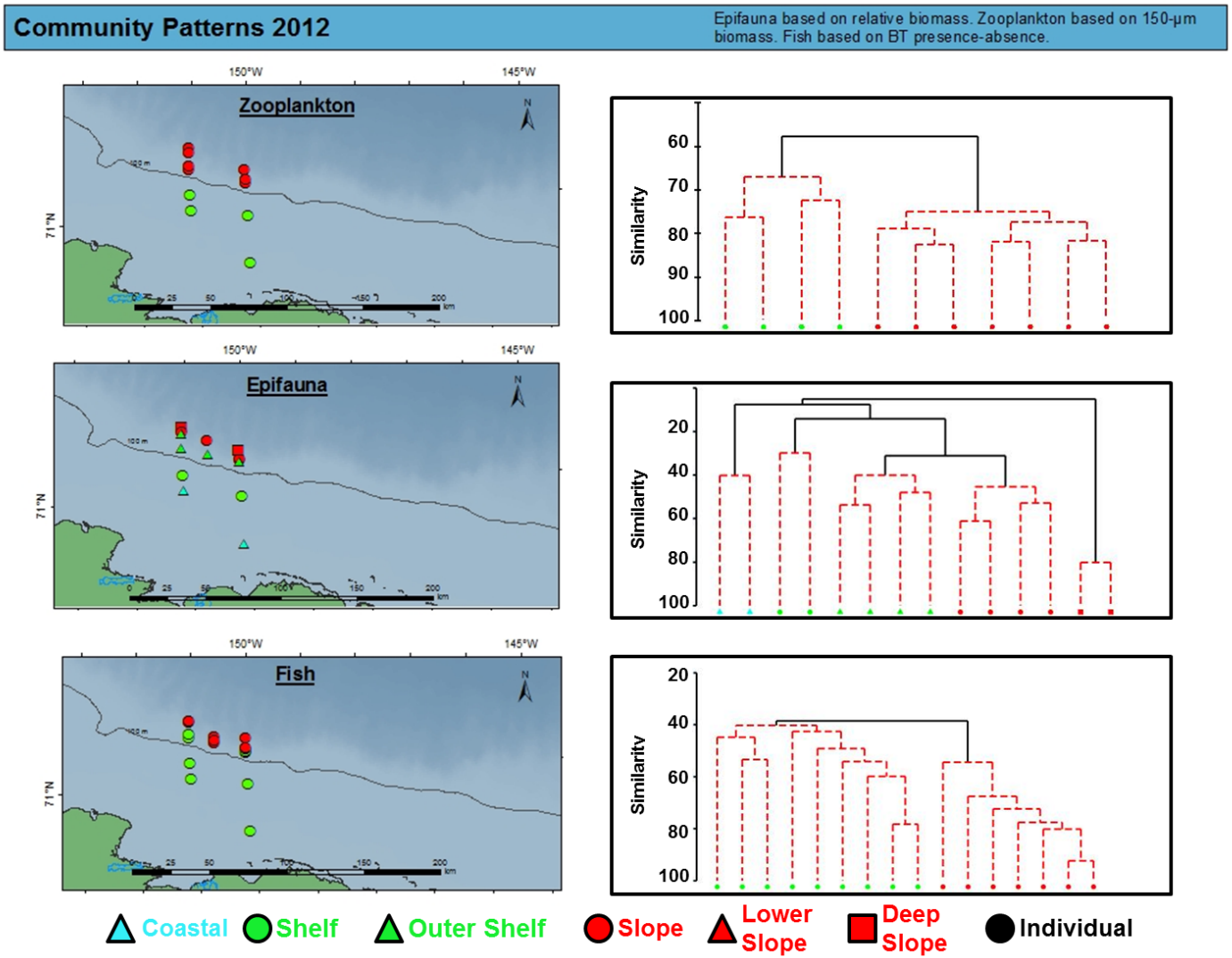

Figure 9.1. Community patterns for zooplankton and epifauna based on biomass, and fish presence/absence (PA) for B transects (150°–151° W, Colville Region) in the Beaufort Sea in 2012.
Spatial distribution of communities (left panels) shows very similar shelf and slope groupings. Cluster analysis (right panels) shows station groupings at each trophic level.

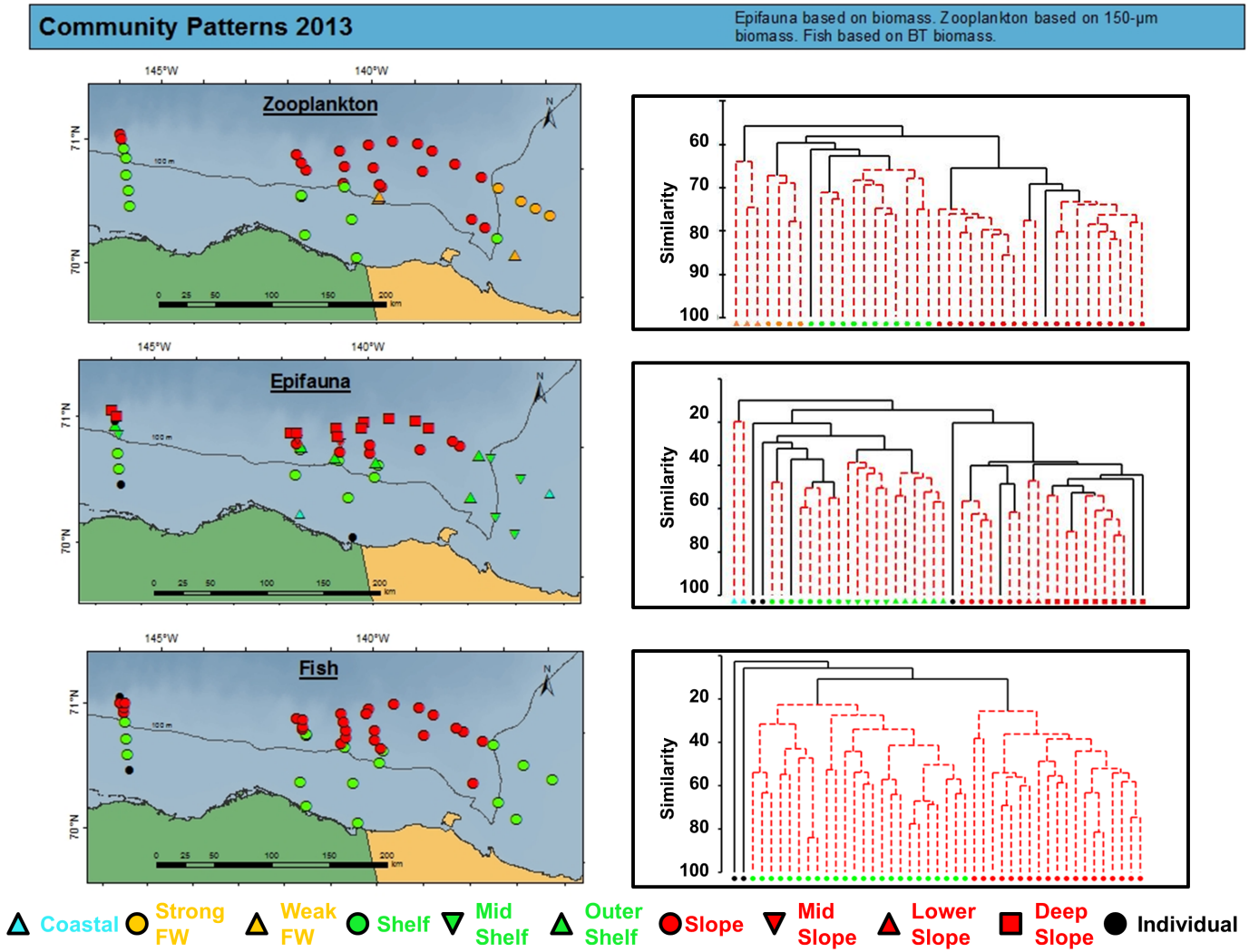

Figure 9.2. Community patterns for zooplankton, epifauna, and fish based on biomass for A and Canadian transects (146°–136° W, Camden Bay, US–Canada border, and Mackenzie regions) in the Beaufort Sea in 2013.
Spatial distribution of communities (left panels) shows very similar shelf and slope groupings. Cluster analysis (right panels) shows station groupings at each trophic level.

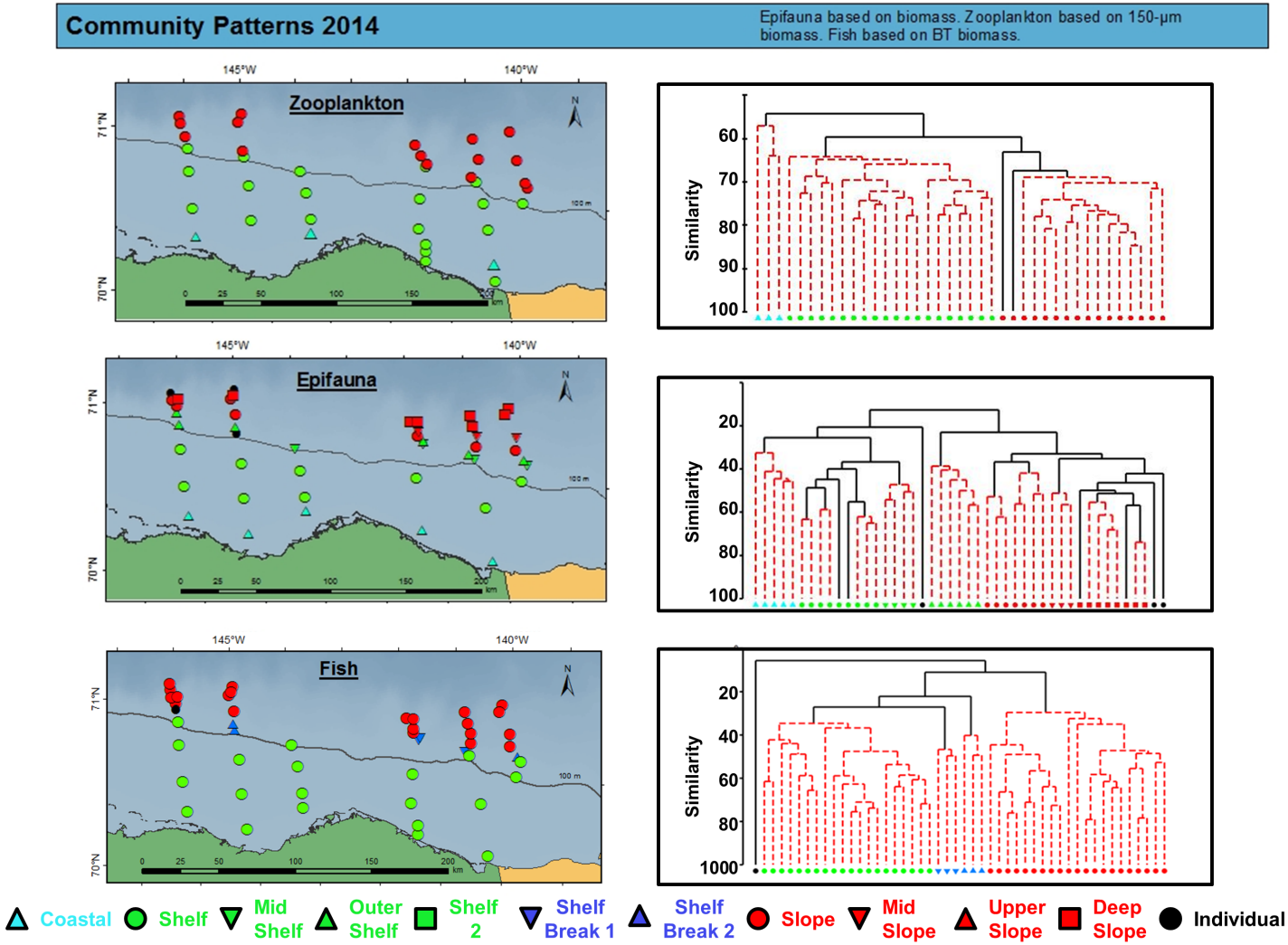

Figure 9.3. Community patterns for zooplankton, epifauna, and fish based on biomass for A and TBS transects (146°–140° W, Camden Bay and US–Canada border regions) in the Beaufort Sea in 2014.
Spatial distribution of communities (left panels) shows very similar shelf and slope groupings. Cluster analysis (right panels) shows station groupings at each trophic level.

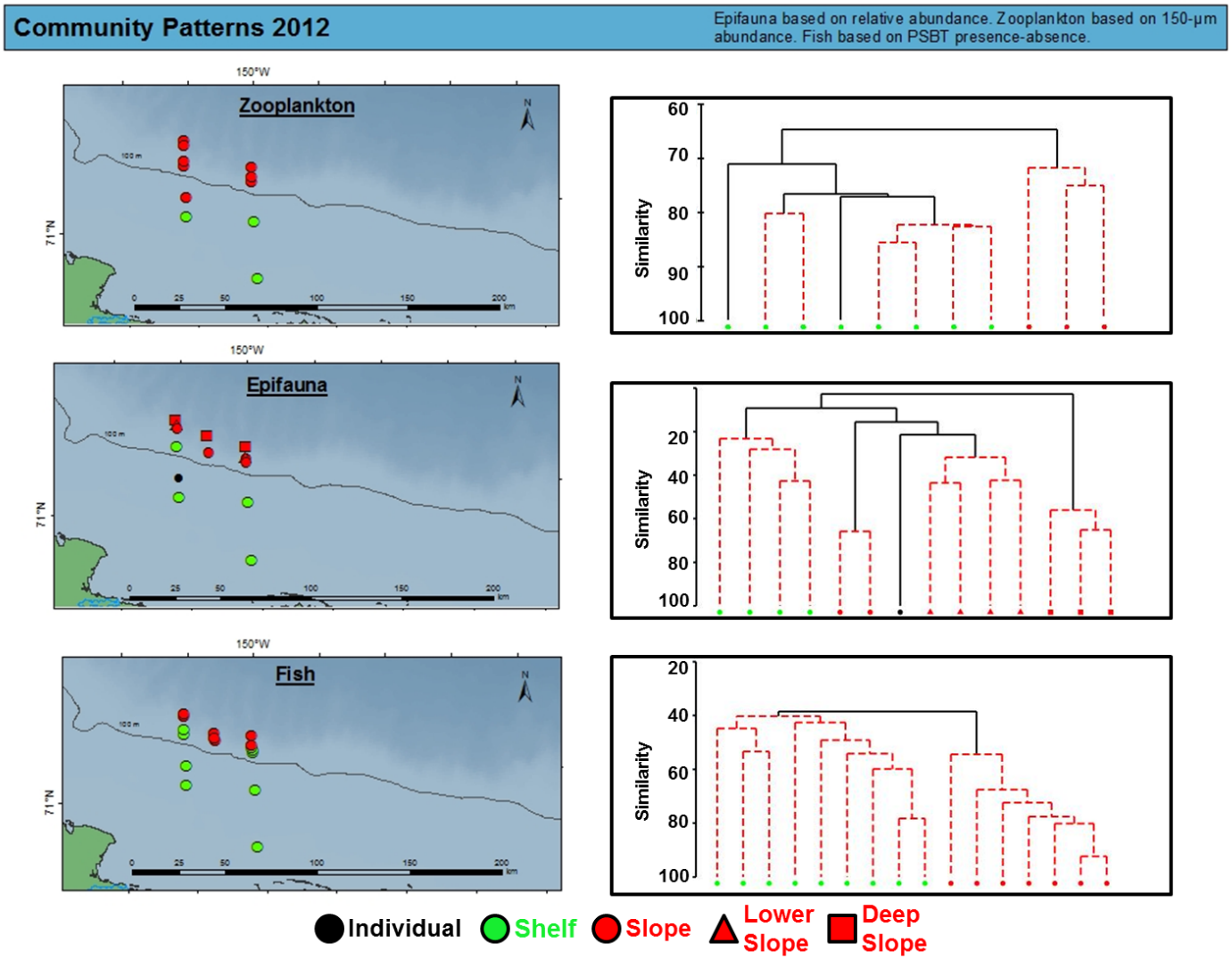

Figure 9.4. Community patterns for zooplankton and epifauna based on abundance, and fish presence/absence for B transects (150°–151° W, Colville region) in the Beaufort Sea in 2012.
Spatial distribution of communities (left panels) shows very similar shelf and slope groupings. Cluster analysis (right panels) shows station groupings at each trophic level.

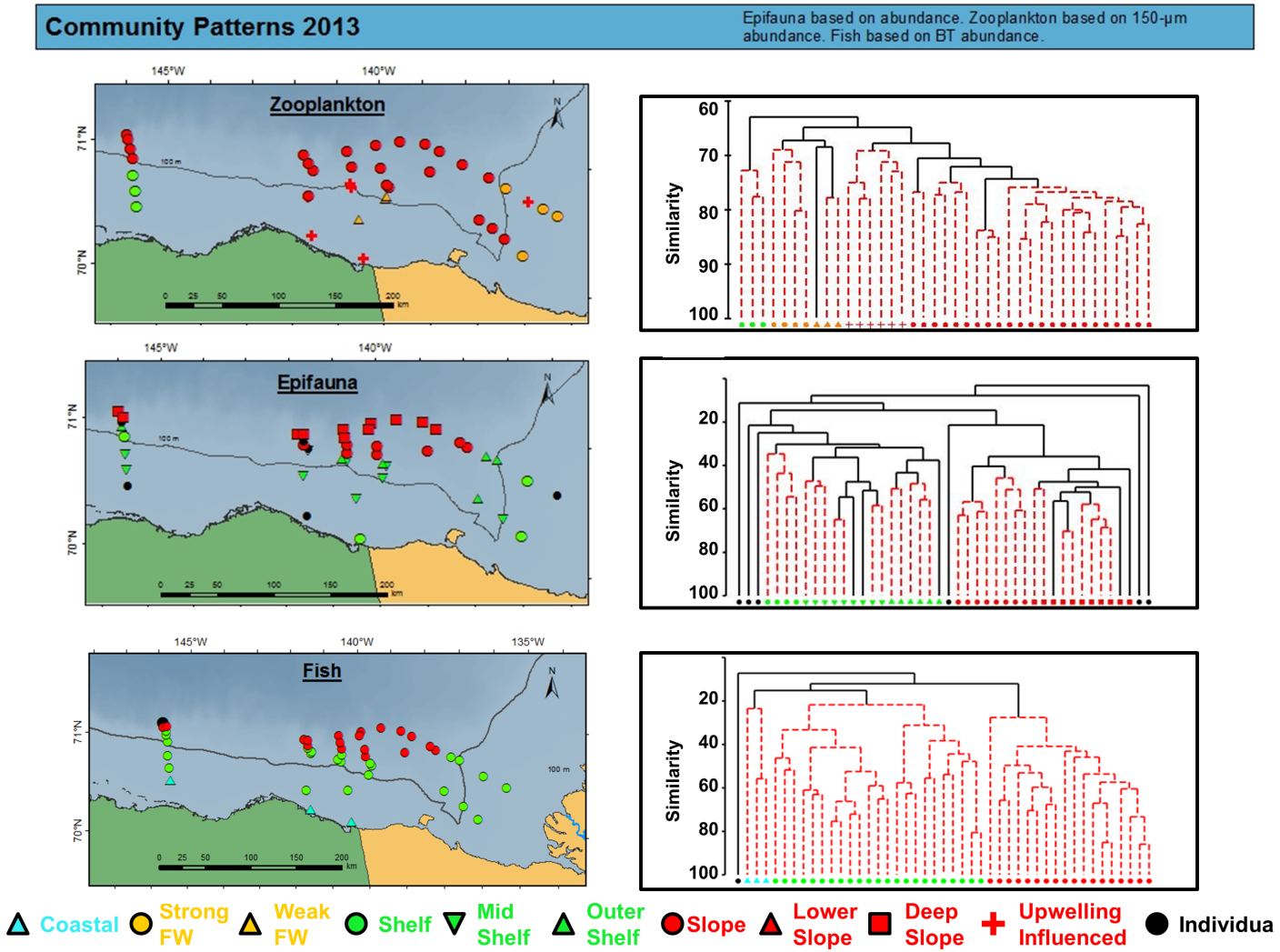

Figure 9.5. Community patterns for zooplankton, epifauna, and fish based on abundance for A and Canadian transects (146°–136° W, Camden Bay US–Canada border, and Mackenzie regions) in the Beaufort Sea in 2013.
Spatial distribution of communities (left panels) shows very similar shelf and slope groupings. Cluster analysis (right panels) shows station groupings at each trophic level.

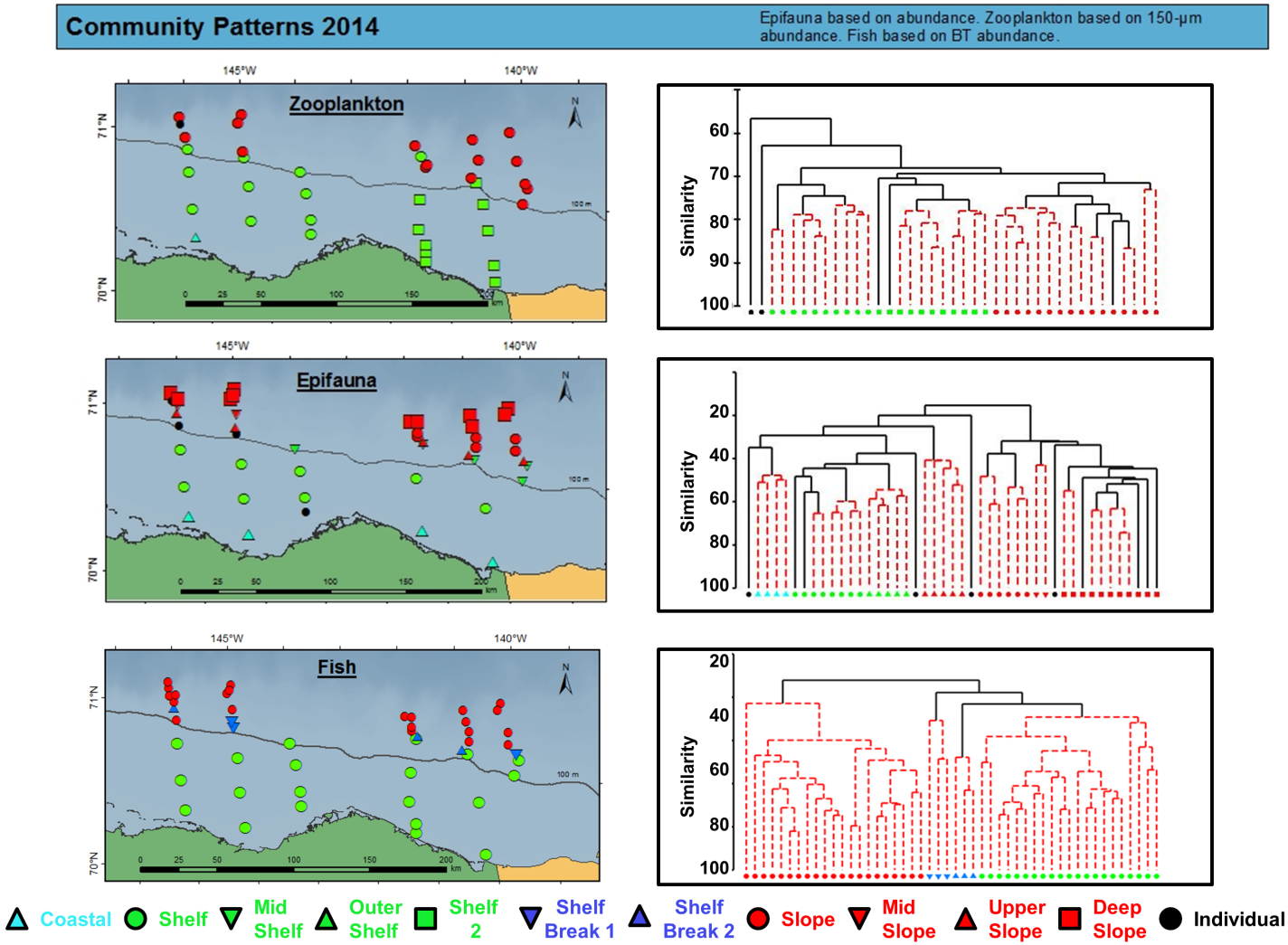

Figure 9.6. Community patterns for zooplankton, epifauna, and fish based on abundance for A and TBS transects (146°–140° W, Camden Bay and US–Canada border regions) in the Beaufort Sea in 2014.
Spatial distribution of communities (left panels) shows very similar shelf and slope groupings. Cluster analysis (right panels) shows station groupings at each trophic level.

Table 9.1. Similarity in distribution of communities of demersal fishes and zooplankton, and demersal fishes and epibenthos in 2013–2014 in the Beaufort Sea. Communities are based on abundance. Demersal fishes and epibenthos were collected by beam trawl, and zooplankton with a 150-µm or 505-µm net. n is the number of samples, rho is the Pearson coefficient and *p* is the significance level. The smaller the value of p, the better the significance and the more closely related the community patterns. All trophic levels have a significant spatial relationship to each other.

		2013			2014		
		n	Rho	*p*	n	Rho	*p*
Demersal Fishes	Zooplankton (150-µm)	32	0.333	<0.0001	36	0.298	<0.0001
	Zooplankton (505-µm)	33	0.412	<0.0001	36	0.443	<0.0001
	Epibenthos	45	0.475	<0.0001	48	0.640	<0.0001
Epibenthos	Zooplankton (150-µm)	33	0.436	<0.0001	37	0.299	<0.0001
	Zooplankton (505-µm)	33	0.447	<0.0001	36	0.509	<0.0001

10.0 UNDER ICE

Katrin Iken, Eric Wood, Brenda Norcross, and Lorena Edenfield

10.1 Introduction

Under-ice surveys were conducted as part of the US-Canada Transboundary project in order to assess the distribution of some critical fish and invertebrate species during the ice-covered winter season. Two surveys are reported here, including nearshore under-ice surveys in the Beaufort Sea during 2014 and an opportunistic vessel-based survey near and within the ice-covered areas of the Bering and southern Chukchi Seas during 2015. The 2014 under-ice survey was restricted to nearshore waters due to logistical constraints of accessing offshore locations in the Beaufort Sea during winter and because some taxa, such as Arctic Cod, *Boreogadus saida*, are reported to utilize the nearshore environment as juveniles in winter. Nearshore surveys were conducted using self-contained underwater breathing apparatus (SCUBA) diving in an attempt to provide habitat characterizations for organism distributions.

BOEM requested the following five objectives for the under-ice component of this project:

Objective 1. Establish a small-scale baseline of fishes under coastal sea ice in the nearshore Beaufort Sea, specifically around Kaktovik, in late winter (March) and spring (May). Because of logistical constraints in getting access to locals with expertise working on ice in Kaktovik sampling could not occur before April 2014. A second sample trip could not occur in May because of the bowhead whale hunt. As no fish were captured in 2014, a baseline of fish could not be established.

Objective 2. Describe sea ice habitat use of *Boreogadus saida* in terms of distribution along specific under-ice structures such as ridges. Too few *B. saida* were observed to adequately describe their habitat.

Objective 3. Measure local hydrographic conditions under coastal sea ice, which was accomplished.

Objective 4. Assess distribution and abundance of lower trophic plankton, ice-associated macrofauna and benthic macrofauna under coastal sea ice.

Objective 5. Establish food-web relations between lower-trophic organisms and fishes under the coastal sea ice using stable isotope analysis and fish gut content analysis. As fishes were not collected, it was not possible to accomplish this objective. However, lessons learned from the exploratory under-ice expeditions are discussed because they may assist in designing further studies.

10.2 Methods

10.2.1 2014 Season

Sampling took place from 13 to 21 April 2014 off the coast of Kaktovik, Alaska, near Barter Island. The objectives of this season included surveying for fish and other macrofauna with SCUBA, deploying gill nets to estimate fish presence and abundance, and characterizing ice structures macrofauna were associated with. Ancillary data collection was also a part of the project and included water column chlorophyll content, vertical temperature and salinity profiles, ice bottom layer chlorophyll content, sediment bottom community, and zooplankton community.

Sites were selected based on several criteria including proximity to pressure ridges, ice depth, water depth, and ease of access via snow machine. The sites were selected utilizing knowledge from local guides (Figure 10.1) and were at least a kilometer apart. Site 1 was 4.5 m, Site 2 was 6.5 m and Site 3 was 7.6 m deep.

Gear was staged in Kaktovik and, along with the guides and researchers, was transported by sled and snow machine to the research site each morning. Suitable locations were found by testing ice thickness with pilot holes at sites that matched the other criteria. The access holes were placed within 5 m of the pilot holes and were prepared and cut as equilateral triangles with 1.5 m to 2 m sides (Figure 10.2).

The access holes were cut using a variety of tools, including chainsaws with differing bar lengths, pole saws, ice picks, manual and gas powered ice augers, and shovels. Each hole was cut and removed in layers by cutting a grid of blocks with the chainsaws and breaking the blocks free with the heavy ice pick. Blocks were removed with ice tongs and the ice debris was shoveled out. This process was repeated until the hole was between 20 cm and 25 cm to the bottom of the sea ice. At this point, a manual ice auger was used to punch through one corner of the hole and seawater would fill the hole. Once filled, holes would be drilled in the other two corners and manual pole saws would be used to cut the remaining ice free. Once the hole was cleared of ice and debris, sampling began.

Under-ice surveys were conducted after the underwater environment was scouted for potential safety hazards. Swath transects were used for the under-ice and benthic environments surveys. The associated ice structure was noted when fish or other macrofauna were encountered in the under-ice. Gill nets (variable mesh size) were centered under the access holes at each site and allowed to soak for 12–24 hours. The ancillary data listed above were also collected at each site.

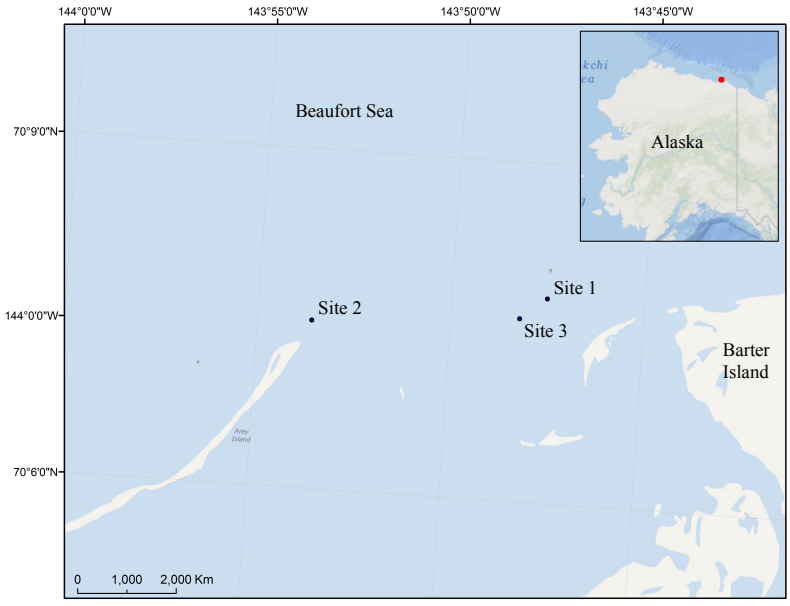

Figure 10.1. Under-Ice study location in the vicinity of Barter Island, eastern Beaufort Sea, 2014.

Figure 10.2. Photographic summary of ice removal procedure to create holes for dive access.
A triangular shape is outlined on the ice and then blocks cut with chain saws are removed layer by layer (a–e). Once the hole fills with water and the bottom later is cut free with hand saws, the floating block is cut apart and removed (f).

10.2.2.1 SCUBA Under-Ice Surveys and Sampling

Three SCUBA divers were active at all times during under-ice sampling. Of the two tethered divers in the water, one diver was tethered to the surface while the other was tethered to the first diver to remove the possibility of two surface tethers crossing and tangling. One rescue diver was in dive gear and ready at the surface in case of emergency. The fourth member of the sampling team was responsible for surface-tending the tether line and communicating with below-surface divers via tether signals.

Divers conducted two to four visual transects radially extending from each access hole for 30 to 40 m. Under-ice sampling included surveys for ice-associated macrofauna, collection of ice samples for chlorophyll-*a* analysis, benthic surveys and gill nets for macrofauna, and diver-assisted oblique zooplankton tows. Ice-associated macrofauna (e.g., amphipods) were sparsely distributed, so swath surveys rather than quadrat counts were conducted. Ice structure (flat, ridged) was noted at locations where macrofauna were found. Some amphipod individuals were opportunistically hand-collected for later detailed identification. Fist-sized pieces of ice (n = 3 for each site) were chiseled off of the overhead ice environment and collected in separate sampling bags (zippered plastic freezer bags) to measure ice chlorophyll content. These ice samples were melted, filtered onto pre-combusted GF/F filters, and frozen for later analysis at the University of Alaska Fairbanks (UAF). Swath surveys were conducted of the benthic transects to assess the epibenthic community under the sea ice.

Divers assisted in other gear deployments. Zooplankton were collected with a 150-µm mesh ring net, hauled obliquely through the water column with a diver assisting in deploying the net approximately 5 m from the access hole close to the bottom. Zooplankton samples were immediately preserved in EtOH for later identification and relative abundance estimates. A gill net (variable mesh size) was also deployed at each site by divers under the ice. The net was marked in the middle and one side brought out first with one diver stretching the floating line and one diver stretching the leaded line. Divers then returned to the hole to receive the lines for the second side, stretching it out from the opposite side of the access hole. Nets were left in the water for 12–24 hours and pulled up by hand. Any macrofauna (e.g., amphipods) were collected and frozen for later identification.

10.2.2.2 Hydrographic and Benthic Grab Sampling

Vertical profiles of the water column under-ice were taken by lowering an Aqua TROLL 200 CTD (In-Situ Inc.) through the access hole to measure temperature and salinity at 1 m vertical increments. Surface water samples (n = 3 for each site) were collected in dark 1 L bottles for measurement of pelagic chlorophyll-*a* concentrations. Water samples were later filtered onto pre-combusted GF/F filters and frozen until later analysis at UAF. Benthic macrofauna were collected using a small Ponar grab (231 cm^2 surface area, n = 2 for each site) lowered through the access hole. Faunal contents of the grab were sieved over 500-µm and frozen for analysis at UAF.

10.2.3 2015 Season

To test methods that could be used to sample under-ice in the Beaufort Sea in the future, we tested methods in the Bering Sea because it was more accessible. The RV *Sikuliaq* ice trials took place in the Bering Sea and southern Chukchi Sea from 19 March 2015 to 9 April 2015 (Figure 10.3). The cruise was an opportunity to sample fish in and around ice-covered, pelagic environments using larger scale gear than the previous two projects. Two different midwater trawl nets were utilized. The Isaacs-Kidd midwater trawl (IKMT) was fished six times and the Aluette midwater trawl (AMT) was fished four times.

Each net was fished once in an "open water" environment on our transit to the ice edge. These deployments will not be included in the discussion because they do not relate to the topic, but they were successful in fishing and proved the RV *Sikuliaq's* ability to effectively fish the IKMT and AMT. The other deployments were divided into two fishing environments: "middle of lead", and "near ice edge" (Figure 10.4).

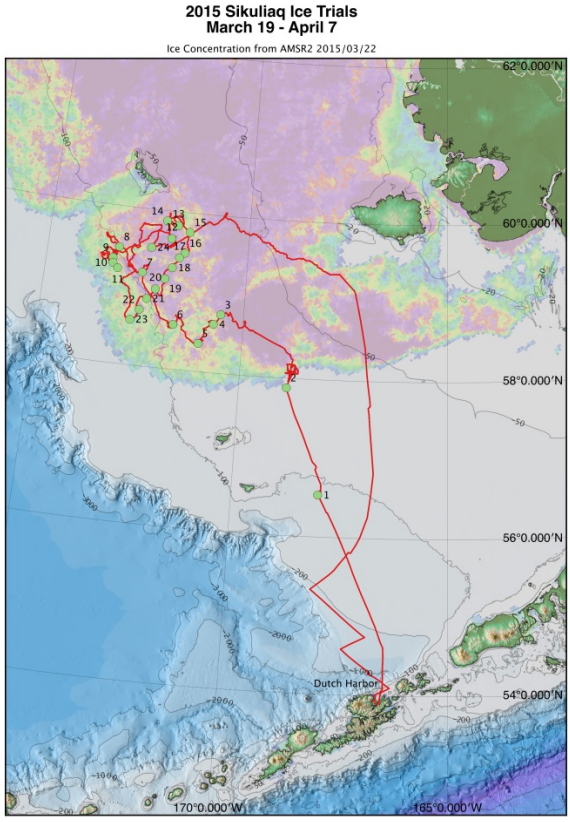

Figure 10.3. Map of stations sampled during 2015 RV *Sikuliaq* ice trials. Ice concentration from AMSR2 (Advanced Microwave Scanning Radiometer 2) satellite for 22 March 2015, where purple in complete ice cover. (Map courtesy of Steve Roberts)

Fishing the "middle of lead" environment was effectively the same as a standard open water deployment in terms of fishing technique. The IKMT was deployed and fished at a speed of 3.5–4.0 kts and the AMT was deployed at 1.5–2.0 kts and fished at 1.5 kts. The A-frame remained at an upright position while deploying both nets. The IKMT was fished in a double oblique pattern and the AMT was fished at a target depth of 50 m for 20 minutes in ideal conditions, but fishing in the "middle of lead" environment caused issues. The length and size of a lead varied greatly, and determined when the net would need to be retrieved to avoid fishing in jumbled ice; fishing time was often truncated to less than 20 minutes with the AMT or only a single oblique with the IKMT.

Fishing the "near ice edge" environment required modifications to the fishing technique. The "near ice edge" was still in the leads, but was deployed, fished, and retrieved in a band of frazzle ice (approximately 10–30 cm thick). This young ice often formed adjacent to the much thicker (approximately 45–100 cm) first-year ice flows. An attempt to fish the IKMT with the previously described methods caused the net to fill with ice at the surface and the tow was deemed non-quantitative. Because of this, we altered the technique by slowing the boat to 1.0 kt during deployment and using the vessel's thrusters to clear the deployment channel of ice. Once the net was in the water, we lowered the A-frame about even with the vessel deck to get the mouth underwater quickly and to keep the net close to the boat in the ice-free area created by the boats thrusters. The vessel operator would then speed up to the fishing speed of 3.5–4.0 kts. It was

important to keep a straight path, or make shallow corrections to the course, as sudden changes in course would cause the net to swing into the jumbled ice surrounding the cleared path. Once the tow was ready to retrieve, the boat would again slow to 1.0 kt and the net would be pulled in through the ice-free area created by the thrusters. This method was successful at fishing the "near ice edge" environment, as evident by the water-column associated invertebrates present in the hauls, and from videos taken from a camera attached to the IKMT mouth during the tow. Unfortunately, the design of the AMT net with doors to spread the mouth requires a higher vessel speed at deployment than this approach allows. The AMT doors and bridle have a tendency to tangle at low speeds. Because of this, it was determined that the AMT could not be fished with the modified fishing methods used for the IKMT in the "near ice edge" environment.

Figure 10.4. Midwater trawl stations were divided into two different fishing environments during ice-associated trawling, 2015.

10.3 Results–*2014 Season*

10.3.1 Fish and Amphipod Dive Surveys, Gill Net

We observed a total of three *Boreogadus saida* during under-ice surveys, one at each dive location (Table 10.1). *B. saida* were approximately 30–40 mm in length. They were located directly under the ice along pressure ridges, typically within crevices. Survey transects included various ice structures: flat areas, structured pressure ridges, and grounded pressure ridges. *B. saida* were observed in the structured pressure ridge areas with open water underneath, but never in the flat areas or at or close to the grounded areas of a pressure ridge. Cod did not react to dive lights but did retreat from diver movement.

We observed several species of amphipods including all species considered ice endemic: *Gammarus wilkitzkii*, *Apherusa glacialis* and *Onisimus* sp. In addition, we observed *Atylus carinatus* several times on the ice, which is typically a common benthic species on the Beaufort Sea shelf. Similar to *B. saida*, all amphipods were located along pressure ridges instead of the open, flat areas, but only in one occasion close to a grounded pressure ridge region (large accumulation at site 3). *G. wilkitzkii* was also found immediately at the ice hole (bottom edge), presumably attracted by the light. At one location (site 1) we found a large cluster (approx. 50

individuals) of *G. wilkitzkii* along the bottom of a grounded pressure ridge. We were unable to see what may have attracted the animals to this location (e.g., a food source) but it shows that amphipod distribution can be highly clumped.

A gill net was brought out at each site and soaked for 12–24 h. With the exception of the amphipod *Gammarus wilkitzkii* at site 1, nothing was caught by gill net. The gill net was diver deployed and we followed techniques developed by the ice diving team from 2013; these techniques were efficient and successful from the RV *Sikuliaq* platform in 2015 as they were during the 2013 expedition (Norcross et al. in review). However, since the hole is typically made in a flat ice area (because making ice holes on a ridge is impossible), the net was also deployed in flat areas. This could be one reason why no other macrofauna was caught by the net. Positioning the net directly along a ridge, away from the hole, would be difficult and possibly dangerous for the divers. Because of the limited light conditions, the danger of a diver being entangled in the fine mesh of the net is too great to move the net away from the light provided by the hole. We suggest that gill nets are not an effective means to capture large ice-associated macrofauna in the highly structured coastal sea ice.

Table 10.1. Observations of under-ice fauna during dive transects and from gill nets.

Date	Site	transect length	net soak time	observation
4/15/2014	site 1	20 m	—	1 *Boreogadus saida* (~40 mm), 9 *Atylus carinatus*
4/19/2014	site 2	35 m	—	5 *Apherusa glacialis* (gravid)
4/19/2014	site 2	25 m	—	no observations
4/19/2014	site 2	40 m	—	1 *Boreogadus saida* (~30 mm), 1 *Gammarus wilkitzkii*, 1 *Atylus carinatus*
4/19/2014	site 3	30 m	—	1 *Boreogadus saida* (~40 mm), 3 *Gammarus wilkitzkii*, 1 *Onisimus* sp.
4/20/2014	site 1	35 m	—	no observations
4/20/2014	site 1	30 m	—	~50 *Gammarus wilkitzkii* (large accumulation)
4/16/2014	site 1	—	14 h	6 *Gammarus wilkitzkii*
4/19/2014	site 2	—	24 h	no catch
4/20/2014	site 3	—	19 h	no catch

10.3.2 Bottom Surveys, Grab Samples

The most common organism observed during bottom transect surveys was the isopod *Saduria entomon*. They were observed at each site in numerous individuals. At site 2 we also observed lysianassid amphipods that were scavenging on a decaying, unidentifiable food source. Swarms of suprabenthic shrimp or mysids were observed at site 1 but could not be collected. At site 2 we observed several individuals of the kelp *Saccharina latissima* growing on shell pieces or small pebbles. It is known that small rocky patches with kelp growth occur in the greater vicinity of Camden Bay but it was not known that kelp occurs outside these protected rock patches in exposed areas such as those investigated during this project.

Bottom grab samples differed in composition based on site location (Figure 10.5). Site 1 had the highest diversity overall, although the benthic fauna was dominated to more than 50% by

polychaetes. Site 2 had the lowest diversity with just two taxa, mostly small individuals of the isopod *Saduria entomon*. Site 3 was also dominated by polychaetes, similar to site 1, but mostly be sabellids. Bottom substrate at site 1 was fine sand, gravel/pebbles at site 2, and clay with a thin mud layer at site 3. These substrate differences are created by different flow regimes at the sites and are likely responsible for the differences in benthic community structure.

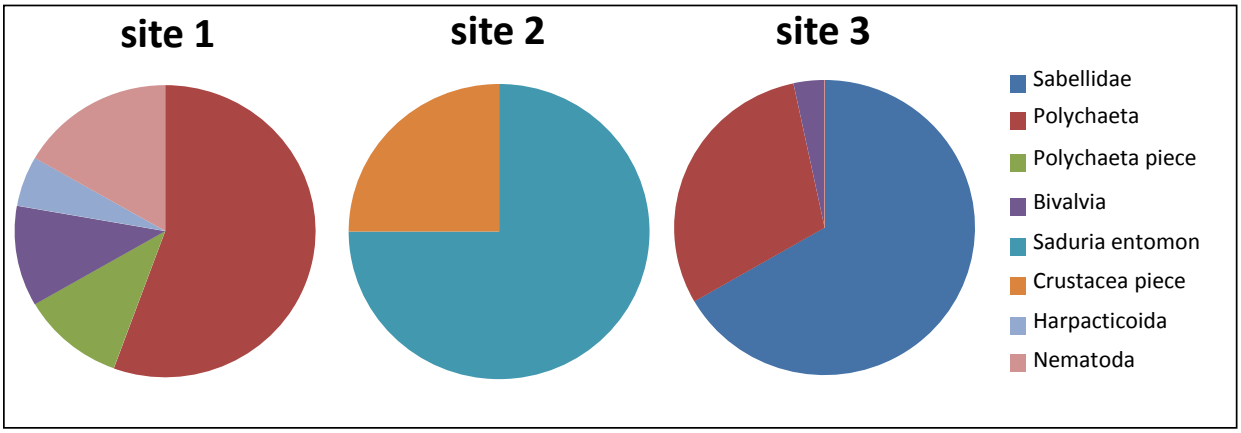

Figure 10.5. Relative abundance of benthic taxa in grab samples at the three study sites in 2014.

10.3.3 Zooplankton Communities

A total of 18 taxonomic units were identified in zooplankton samples at the three study sites (Table 10.2, identifications provided by Caitlin Smoot, UAF). At all sites, copepods contributed most to the overall abundance, especially the three taxa *Acartia longiremis*, *Eurytemora* spp., and *Pseudocalanus* spp. The copepod *Oithona similis* also was regularly represented. All taxa encountered are fairly typical for the region and comparable to what is present during open water seasons. However, the high abundances of *Eurytemora* spp. were unusual as this group typically does not dominate the zooplankton community. This may be related to the fact that some *Eurytemora* species are known to be sympagic (Werner and Arbizu 1999, Kramer 2010), or to the extreme nearshore location of the under-ice sampling. Similar to *Eurytemora*, several other copepod species found here (*A. longiremis*, *O. similis*, *Triconia borealis*, *Pseudocalanus* spp.) have been reported as Arctic sea-ice-associated (Werner and Arbizu 1999).

10.3.4 Hydrography and Water and Sea Ice Chlorophyll

Temperature and salinity were measured in 1 m increments from surface to bottom at each site. The overall patterns are similar among sites, with warmer temperatures and lower salinity at the surface but a well-mixed water column underneath (Figure 10.6).

Water column chlorophyll was very low at all three sites (<0.5 µg/L), and similar phaeophytin concentrations (Figure 10.7a). Chlorophyll concentrations in sea ice were about an order of magnitude higher than in water (3–12 µg/L), but much higher in phaeophytin concentrations (Figure 10.7b), indicating the presence of degraded primary production in the sea ice, a potential food source for sympagic detrital consumers.

Table 10.2. Relative abundance (%) of various taxa found in zooplankton net samples at the three study sites.

Taxonomic unit	Higher tax. level	site 1	site 2	site 3
Acartia longiremis	Copepoda	11.8	30.0	18.5
Barnacle cyprid	Cirripedia	0.1	0.0	0.0
Calanoid nauplii	Copepoda	0.0	0.2	0.4
Calanus glacialis	Copepoda	0.1	1.1	0.0
Cnidaria	Cnidaria	0.0	0.0	0.2
Ctenophore	Ctenophora	0.1	0.0	0.0
Cyclopoid	Copepoda	0.8	0.3	0.0
Euphausiid (juvenile)	Euphausiacea	0.0	0.0	0.2
Eurytemora spp.	Copepoda	72.0	19.5	41.7
Fritillaria borealis	Larvacea	0.0	0.5	0.2
Gammarus wilkitzkii	Amphipoda	0.3	0.0	0.0
Harpacticoid	Copepoda	0.8	0.9	0.4
Microsetella norvegica	Copepoda	0.0	0.3	0.0
Oikopleura spp.	Larvacea	0.0	0.2	0.0
Oithona similis	Copepoda	4.1	5.0	1.9
Triconia borealis	Copepoda	1.0	0.3	0.2
Pseudocalanus male	Copepoda	0.1	0.0	0.0
Pseudocalanus spp.	Copepoda	8.6	41.8	36.3

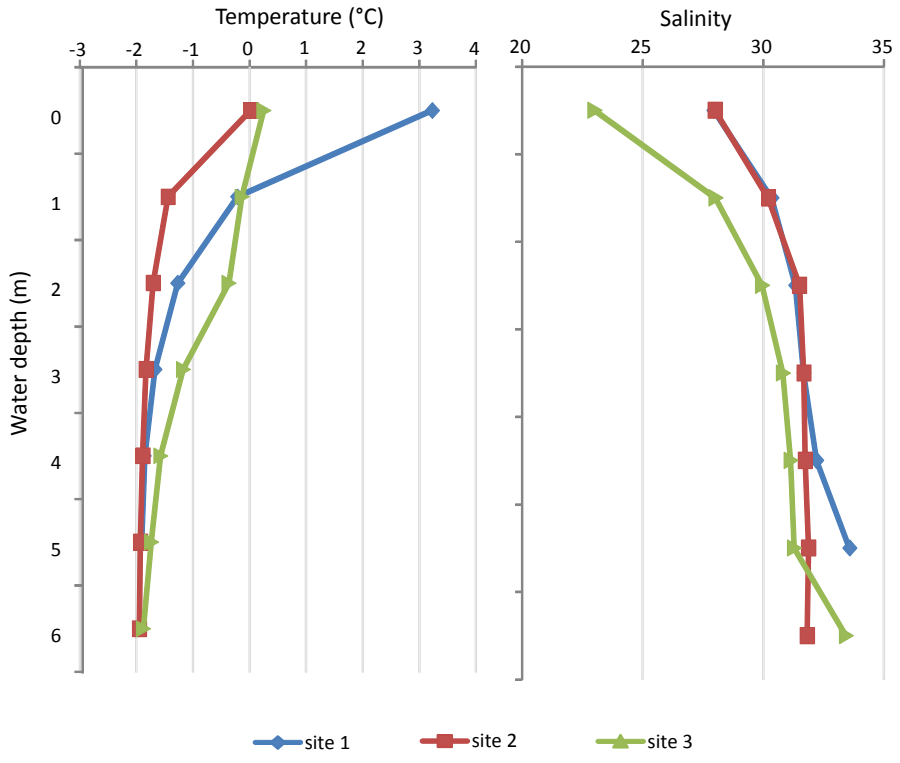

Figure 10.6. Temperature (left) and salinity (right) vertical profiles at the three study sites.

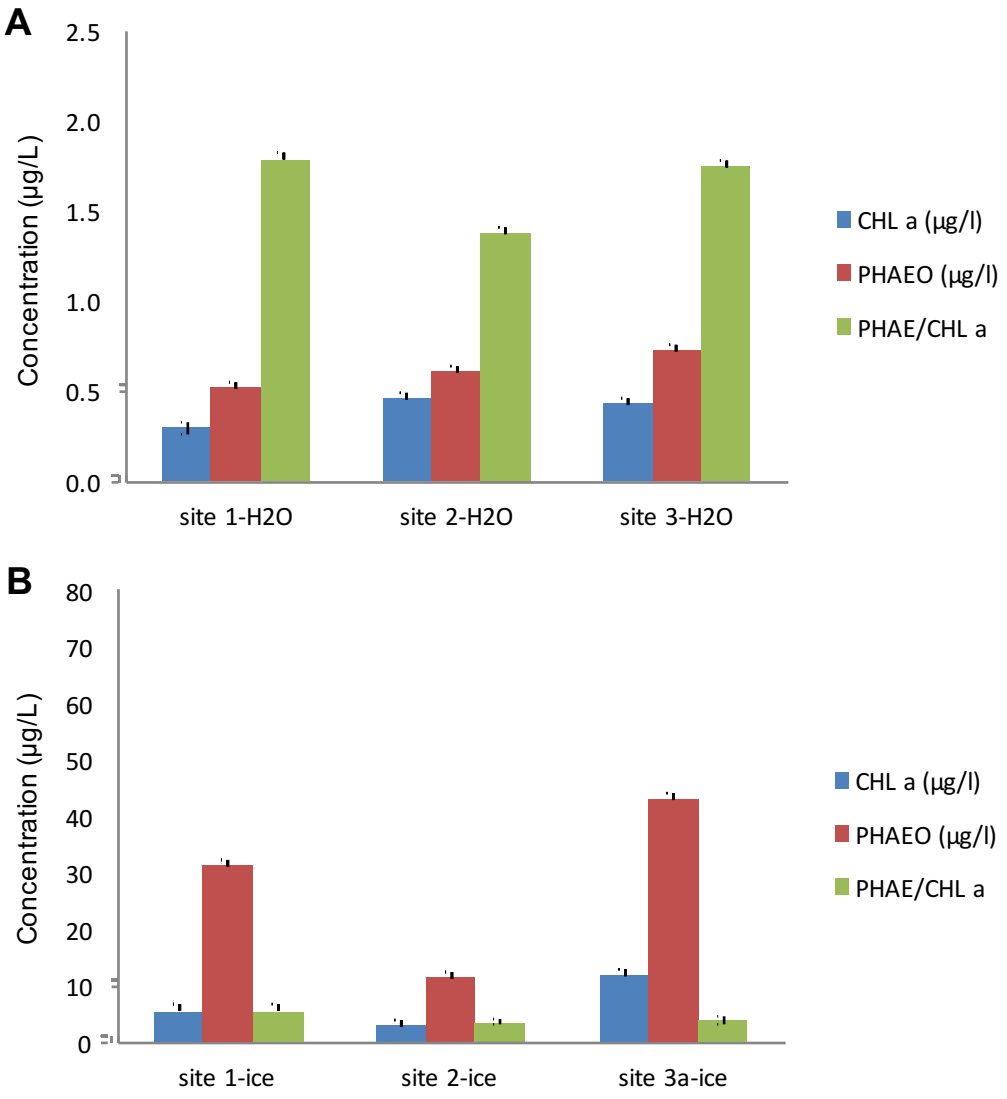

Figure 10.7. Water column (a) and sea ice (b) chlorophyll and phaeophytin concentrations and their respective ratio at the three dive sites.

10.4 Assessment of Survey Strategies

10.4.1 Ice Conditions

Coastal sea ice around Kaktovik was very thick (on average 1.5–2 m, thicker in vicinity of ridges and overfrozen floes) making dive access difficult. The surface of the coastal sea ice is strongly jumbled, making it impossible for snow machines and sleds to access the smoother ice farther from shore. The ice thickness can limit the amount of open water column underneath, especially in the vicinity of grounded pressure ridges. We found that careful ice scouting and even making several pilot holes to assess ice thickness is imperative. Distance to a pressure ridge has to be great enough to provide some flat ice but close enough that ridge structure can be

reached during tethered dives (max. distance 35–40 m). It is recommended to test more than one pilot hole to ensure ice thickness. Pilot holes require a hand-held or gas powered ice auger, but given the ice thickness, sufficient extensions are needed. Because of the heavy sediment load in the ice, all cutting edges dull easily and replacement edges are useful.

Carving out ice holes is extremely labor intensive. Cutting though the ice with chain saws is physically demanding and sufficient people knowledgeable in and able to perform this work should be part of the field team. Cutting through ice is also demanding on the chain saws and sufficient chain saws with a generous number of replacement chains and bars should be provided. Ice tongs and a long-handled ice pick are invaluable to remove ice blocks. Hand-held, long-handled ice saws are needed to cut the bottom ice layer once the hole has flooded. A hand net or colander-type sieve is useful to remove slush from the ice hole after it has filled with water.

10.4.2 Under-Ice Surveys

Abundances of macrofauna (fish and amphipods) in this area are too sparse to use quadrant sampling techniques, which have been proven useful in other locations with dense under-ice fauna (e.g., Gradinger et al. 2010a). Instead, we used line transects to enumerate under-ice fauna, although straight transects lines were hindered by the irregular shape of the under-ice surface and the need to swim around ice keels or avoiding grounded ridges. Therefore, any abundance estimates are rough approximations only.

Coastal sea ice in Kaktovik is covered by snow and contains very large amounts of sediment, effectively attenuating all light from above. Very strong dive lights are needed to illuminate the under-ice surface to see any macrofauna. While we had dive lights, some failed and were not bright enough to illuminate a large area. We recommend extra bright dive lights for such operations.

Ice sampling was accomplished with chisel and hammer, used to cut off fist-sized pieces of ice from the underside around the pressure ridge structures. It is extremely difficult to take actual ice cores from underneath the ice (tested during a NOAA Ocean Exploration-funded research cruise in 2009 and found to be unsuitable), so we instead took irregular-sized ice pieces for which the volume was determined after melting. While this does not provide a standardized surface area, it still is a suitable method for determining chlorophyll content in the bottom ice layer. Taking ice cores from the ice surface was impossible due to the thickness of the ice.

A gill net was brought out at each site and soaked for 12–24 h. Except for some *G. wilkitzkii* at site 1, we did not catch anything with the gill net. The gill net was diver deployed and we followed techniques developed by the ice diving team from 2013, which was efficient and successful in deploying the net. However, since the hole is typically made in a flat ice area (because making ice holes on a ridge is impossible), the net was also deployed in flat areas. This could be one reason why no other macrofauna was caught by the net. Positioning the net directly along a ridge, away from the hole, would be difficult and possibly dangerous for the divers. Because of the limited light conditions, the danger of getting entangled in the fine mesh of the net is too great to move the net away from the light provided by the hole. We suggest that gill nets are not an effective means to capture larger ice-associated macrofauna in the highly structured, coastal sea ice.

10.4.3 Zooplankton Surveys

We used a 150-µm ring net for zooplankton tows through the ice hole. Because of the limited depth of the water column underneath the ice (on average, with total depth of ~6 m, 2 m of ice leaves only 4 m of water column), vertical tows were considerably space-restricted. We experimented with diver-assisted plankton tows where a diver drags the net underneath the ice approximately 6 m away from the hole and holds it close to the bottom, then signals to the surface net tender to pull the net up. This way the net is taken obliquely and pulled though a slightly larger water column. This worked well although care must be taken to avoid that the net rises and scrapes under the ice.

10.4.4 Bottom Sampling

We used a hand-deployed Ponar grab (231 cm^2 surface area) to collect bottom sediments through the ice holes. This worked well, except that a bottom of very hard clay at two sites (sites 1 and 3), prevented sediment collection beyond shallow surface scrapes. We still believe that this is a suitable method to collect bottom sediments.

Bottom surveys conducted by divers were useful for assessing the presence of mobile epifauna, such as isopods. We typically conducted these benthic surveys on the return from a survey of ice-associated fauna, which made efficient use of the dive time.

10.5 Results–*2015 Season*

We were able to fish the IKMT a total of six times and the AMT a total of four times (Table 10.3). A total of eight fishes were collected during this cruise. Six fishes were captured with the IKMT and none were captured with the AMT. Fish personnel were allowed to retain a fish found in the sea chest (part of the engine cooling water intake system) of the vessel during a maintenance inspection, and another fish that was captured in the Van Veen benthic grab (Table 10.4).

Table 10.3. Summary of fishing effort and fish collection during SKQ201505S. A lead is an open water trawling area surrounded by ice, which is large enough to trawl without having to break ice during towing.

Station	Haul	Date	Start Latitude	Start Longitude	End Latitude	End Longitude	Site description	Issues with trawl?
Isaacs-Kidd Midwater Trawl (IKMT)								
1	1	3/20/2015	56.5372	-167.9985	56.5564	-167.9833	Open water	
4	2	3/24/2015	58.6416	-170.8229	58.6230	-170.7750	Middle of Lead	
6	3	3/26/2015	58.5444	-171.7947	58.5768	-171.7944	Middle of Lead	
13	4	3/31/2015	59.8350	-171.7987	N/A	N/A	Near Ice Edge	Lost the net, which was full of ice
13	5	3/31/2015	59.8295	-171.9229	59.8358	-171.9290	Near Ice Edge	
16	6	4/1/2015	59.5131	-171.5406	59.5037	-171.6236	Near Ice Edge	
Aluette Midwater Trawl (AMT)								
1	1	3/20/2015	56.5841	-167.9399	56.5825	-167.9337	Open water	
4	2	3/24/2015	58.6448	-170.7922	58.6479	-170.7830	Middle of Lead	
6	3	3/26/2015	58.5778	-171.8017	58.5694	-171.8009	Middle of Lead	
8	4	3/28/2014	59.4188	-173.3245	59.4260	-173.3326	Near Ice Edge	Net full of ice

Table 10.4. List of fishes captured during this cruise. Standard length (SL) was measured of larval fishes because caudal fins were not fully developed, and total length (TL) was measured of older fishes.

Station	Gear-Haul	Species	Length (mm)	Notes
1	IKMT-1	Scorpaenidae (rockfish family)	10.0, SL	flexion larva
1	IKMT-1	Scorpaenidae (rockfish family)	11.0, SL	flexion larva
1	IKMT-1	Scorpaenidae (rockfish family)	11.1, SL	flexion larva
1	IKMT-1	Scorpaenidae (rockfish family)	11.1, SL	flexion larva
1	IKMT-1	Scorpaenidae (rockfish family)	>8, SL	flexion larva, damaged fish
16	IKMT-6	Lumpeninae (prickleback subfamily)	56, TL	
13	Van Veen-3	*Icelus spatula* (Spatulate Sculpin)	43, TL	
N/A	vessel sea chest	*Icelinus borealis* (Northern Sculpin)	153, TL	found during maintenance check

10.6 Discussion

From the two years of sampling (2014, 2015) a total of nine fish were collected or observed during scuba sampling. Three *Boreogadus saida* were observed in 2014, and a juvenile Lumpeninae fish was caught during ice tows in 2015. In 2015, five Scorpaenidae flexion larvae were caught during an "open water" tow, but the tow was a practice tow for the crew to get familiar with the equipment and was in an environment that can't be considered for a near or under-ice comparison.

In 2013 (Norcross et al. in review), sites were selected by contractors and were selected on flat ice, away from pressure ridges. The rugosity measurements showed both sites featured no brash ice, and the under-ice environment was completely flat. The remotely operated vehicle (ROV) deployment at site 2 did note a pressure ridge, but at a distance too far from the hole for divers to survey. That pressure ridge appeared to have macrofauna around it but the ROV could not get close enough to identify anything. The lack of under-ice structure was believed to be the reason for the lack of fish observations. Because of this, it was recommended that the science crew be involved in the site selection process in the future so that proximity to pressure ridges could be considered.

The sites for the 2014 expedition were selected by the science crew, and proximity to pressure ridges was a priority in the selection process. More fish were observed during the 2014 project, but their relative abundance was still very small, with only one fish noted at each site. All of the fish noted were associated with under-ice structure, and nothing was seen associated with flat ice. The gill net deployments were successful and captured amphipods, but no fish were caught at any of the sites. The deployed gill nets were centered under the diver access hole, which meant that they were deployed in a flat ice environment. Moving the nets to the nearby pressure ridge was discussed, but the danger of divers being entangled in the net was too great. Because of this, using gill nets to sample for ice-associated fish like *Boreogadus saida* is not recommended.

Surveys in 2014 (Kaktovik) specifically targeted areas that contained a variety of ice structures, such as flat under-ice surfaces, small to large pressure ridges, and grounded pressure ridges. In contrast, most areas in the 2013 survey were flat ice surfaces. All fauna observed in 2014 were at pressure ridge structured ice, similar to what has been observed previously in more offshore regions (Gradinger and Bluhm 2004, Gradinger et al. 2010a). Conversely, no fauna

were observed in 2013. This confirms that *Boreogadus saida* and amphipod macrofauna prefer structured ice and are unlikely to be observed in flat ice areas. While flat ice may be thinner and easier to work for the creation of ice holes, it is unsuitable to accomplish the objectives of this project, which is to assess distribution of under-ice macrofauna along ice structures.

We suggest that having scientists experienced with coastal sea ice on site during site selection is imperative to choose locations that have a high probability in harboring ice-associated macrofauna such as *Boreogadus saida* and amphipods. Sites selection during the 2013 survey in Barrow was done by the logistics support, while in 2014 the scientists were on site and selected sites as well as excavated the ice. Large equipment that can effectively melt ice holes are unable to traverse jumbled nearshore ice and are restricted to flat areas that can easily be accessed from land. Hence, there is a trade-off between logistically-easier site preparation that does not yield any fauna because of the lack of under-ice structure, and appropriate site selection by on-site scientists that demands labor intensive hand formation of ice holes.

We believe that an ROV would likely not be a suitable tool for the heavily structured coastal ice around Kaktovik. Ice keels protrude several meters off the ice into the water column and the chances that the ROV tether will tangle around the ice is very high. ROV is an excellent tool under flat ice (as was surveyed in Barrow) or even under structured ice where divers can assist with untangling the tether should it get caught. This would be difficult given the extremely poor light conditions under the coastal ice in Kaktovik.

In 2015, gear deployment was successful, and the presence of pelagic invertebrates in the nets showed that the gear was fishing correctly, but very few fish were caught. There are a few contributing factors that likely led to the lack of fish being caught. First, the lack of a winch that could handle 9/16" towing cable meant that we could not sample with bottom trawls. Second, the AMT is designed to be fished paired with hydroacoustics, which the RV *Sikuliaq* was not equipped with at the time of the ice trials. Third, the length of the leads limited the distance and time that the trawls could fish, leading to shorter trawls than are typically fished with the IKMT and AMT. The IKMT and AMT are also nets not specifically designed to fish under ice, which led to the nets filling with ice in the "near ice edge" environment. Without hydroacoustics or nets designed to fish under undisturbed ice, where fish like *Boreogadus saida* are known to associate, it is very unlikely fish will be caught using the methods described above.

Lessons learned across all three years can be applied to future under-ice studies. Proper site selection proved to be vital. In 2013 the lack of scientist supported site selection meant that sites were selected for ease of access, not proximity to ice structure with which under-ice fauna are known to associate. Because of this, scientists and local guides selected sites together in 2014. The 2014 sites were adjacent to pressure ridges and observations of under-ice fauna improved. Every fauna observation was associated with the pressure ridge structure, which is similar to what other studies have observed in sea ice further offshore (Gradinger and Bluhm 2004, Gradinger et al. 2010a).

However, 2014 was not without its site selection issues. Pilot holes were drilled to assess ice depth before the diver access holes were cut, but they were not always effective. Site 2 had a pilot hole drilled and the ice depth was no greater than 2 m, but at the access hole, which was within 5 meters of the pilot hole, the ice was closer to 4 m thick. The average ice removed from each diver access hole was an estimated 5000 kg, so the extra effort of properly scouting an area to assess ice depth is much less than the effort required to cut a diver access hole deeper than expected. It is recommended that several pilot holes be drilled before choosing a site for a diver access hole.

Sampling in the sea ice in 2015 was a much different approach, but similar site selection issues were encountered. The “middle of lead” environment was easier to fish than the “near ice edge” but it was likely too far from the under-ice environment to reliably encounter fish associated with the ice. The “middle of lead” tows were an effective way to test the vessels ability to fish, but they were less than ideal for sampling the under-ice fauna.

Just like site selection, choosing the proper gear for the job is vital in the remote arctic, especially for under-ice sampling. Getting through the ice is a difficult job that can be made easier with heavy equipment. The 2013 under-ice diving in Barrow used heavier equipment to get through the ice more quickly, but the overall logistical costs were 3–5 times higher than in Kaktovik. Hauling heavier gear also limited where an access hole could be cut because of the logistical challenge of moving across the ice. In 2014, the team used hand held tools to cut the access holes. This enabled site selection closer to pressure ridges, at a reduced relative cost, but the time and effort required increased substantially.

Many of the 2015 RV *Sikuliaq* ice trials’ gear issues were already covered above, including the lack of hydroacoustics, and a winch that was too small for bottom trawls. The two midwater trawls used during the ice trails also lacked the ability to fish on the surface, or under undisturbed ice, where fish are known to associate. Other studies (David et al. 2015) have found success using nets such as a Surface and Under Ice Trawl (SUIT) and its use aboard the RV *Sikuliaq* would have likely improved our ability to catch ice associated fish such as *Boreogadus saida*.

11.0 INTERANNUAL VARIATION ASSESSMENT PLAN FOR FISH

Brenda Norcross and Russ Hopcroft

In fulfillment of Objective 2: "Based on survey results, recommend a nested sampling design and refinements of survey methods for future monitoring studies", we present a plan to standardize assessment of interannual variability of fish in the Beaufort Sea.

11.1 Monitoring Recommendations

When designing a fisheries monitoring survey, the objectives must be clear. To get a complete picture of the ecosystem in which the fishes live, the physical environment (salinity, temperature, nutrients, sediment) and other trophic levels (epibenthos, benthic infauna, and zooplankton) should be investigated simultaneously. Monitoring designs should accommodate multiple scales of variation of these indicators (Smale et al. 2011).

To meet these needs, we recommend a comprehensive interannual monitoring plan in the US Beaufort Sea that extends from Pt. Barrow to the US-Canada border, with priority given to areas that have been sampled previously. Further cooperation with Canada for continued collections from the Mackenzie River delta to the border is desirable. This is a very large area, the distance from Pt. Barrow to the US-Canada border is ~600 km (~320 nmi); this distance extended into Canada to the Mackenzie River is ~700 km (378 nmi). Based on transects sampled (Table 11.1) and catch of fish, we recommend transects every 1° longitude between 155.1° W and 141.1° W, for a total of 15 transects (Figure 11.1). Transects are offset by 0.1° to ensure even spacing while allowing sampling west of the Alaska Eskimo Whaling Commission Conflict Avoidance Agreement (CAA) restriction of 150° W starting on 25 August each year.

In any study plan, there is a tradeoff between sampling a large area without immense detail and sampling a smaller area in extreme detail. Sampling across the entire US Beaufort Sea coast on a broad scale from 155.1°–141.1° W would provide a within-year perspective of the ecosystem (Table 11.2). To cover such a broad area, transects should be spaced every four degrees of longitude (i.e., 154.1°, 150.1°, 146.1°, 142.1° W), with closely spaced stations covering a range of depths, e.g., eight stations per transect, across the shelf. Because of the amount of transit time that would be required, four transects is probably all that could be achieved from an optimal 3-week cruise. Alternatively, more transects could be sampled, e.g., every 2–3 degrees longitude, but with only 3–5 stations per transect. A smaller, refined scale could be sampled by focusing all sampling efforts in the limited area in which oil exploration is to take place, e.g., Camden Bay (146.1°–143.1° W). Four transects would be sampled as in the broad-scale approach, but less transit time would mean that more time could be allotted for sampling each transect and stations could be closely spaced (Table 11.2).

Table 11.1. Sample collections in the Beaufort Sea by year and longitude.

Year Sampled:		2010	2011	2012	2013	2014
Max depth sampled (m):		100	223	1000	1000	1000
Area **Longitude**	**Transect**					(1x1500 m)
Western Beaufort			X			
Central Beaufort			X			
151.1	B2		X	X		
150.6	BX		X	X		
150.1	B1		X	X		
Camden Bay/Eastern Beaufort		X	X			
146.1	A6	X	X		X	X
145.1	A5	X	X			X
US-Canada Transboundary Area						
144.1	A4					X
142.1	A2				X	X
141.1	A1				X	X
140.1	TBS				X	X
~139.1	MAC				X	
~138.1	GRY				X	

We suggest a combination of these approaches. Four evenly-spaced transects that have a history of previous collections are proposed as a core set that broadly covers the US Beaufort Sea: 154.1° W, 150.1° W, 146.1° W, and 142.1° W (Figure 11.1). In the western Beaufort Sea, trawling was conducted at 154.1° W in 2008 and 2011. In the central Beaufort Sea 150.1° W (B1) was sampled in 2011 and 2012 (Table 11.1). In the central/eastern Beaufort Sea 146.1° W (A6) was sampled in 2010, 2011, 2013, and 2014. In the eastern Beaufort Sea 142.1° W (A2) was sampled in 2013 and 2014. Ideally some stations on each of these four transects would be visited on each cruise. Comprehensive surveys, analogous to TB-2013, should be conducted over a different area of the Beaufort Sea on a rotating basis, taking into consideration BOEM's need for updated information. For example, if the western Beaufort Sea is not a current area of interest, a whole cruise would not be devoted to that area, but 154.1° W should be sampled every two to three years to maintain the time series. Within this range of longitude are two lines of Distributed Biological Observatory (DBO) sampling framework established to detect changes in the ecosystem through repeat sampling along designated longitudinal transects (https://www.pmel.noaa.gov/dbo/). The DBO lines were established at locations of high productivity, biodiversity, and rates of biological change for lower trophic levels. Those locations have not been established as areas of productivity for fish, however, altering the monitoring plan to sample along these lines would not only provide more data for the DBO program, but also would enhance a monitoring program by potentially providing additional data at times outside of a directed monitoring effort.

Both along-shelf breadth and across-shelf distance must be considered in planning. As was learned from the deepest stations near the shelf break (~200 m) in 2011 (Norcross et al. in review) and the slope (≥200–1000 m) stations in 2012 and 2013, the water masses and the fishes that occupy the deep areas are different than those on the shelf (≤100 m). However, the warmer Atlantic Water (AW) can upwell onto the shelf, as was evident in 2011. The action of upwelling

can also affect the distribution of fishes such that fish normally found on the slope are captured on the shelf. With insights gained from sampling slope stations in 2012, 2013, and 2014, it is easier to retrospectively assess which species captured in 2011 are deep water species, e.g., *Lycodes seminudus*. Thus physical and biological properties of slope water can affect shelf habitats. Sampling both the shelf and slope is necessary to determine not only the extent to which slope characteristics may be exhibited in shelf waters, but also with reverse of flow, the extent to which physical and biological characteristics of the shelf region may be evident on the slope.

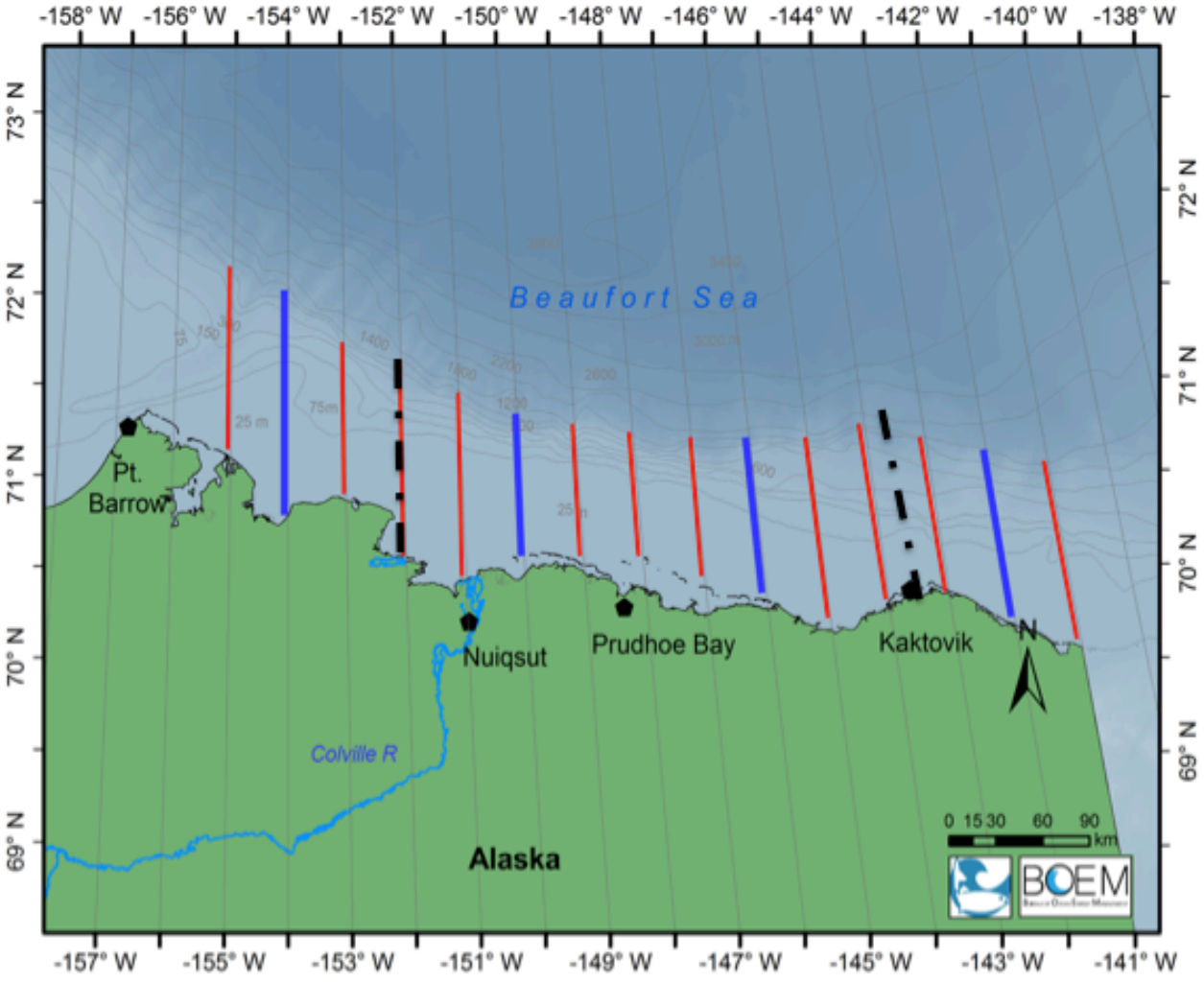

Figure 11.1. Recommended transect design for a Beaufort Sea interannual assessment plan. Every fourth transect (wide blue lines) is recommended as a core transect to be routinely sampled. Transects are placed 0.1° W of each degree of longitude and from 20 to 1000 m depth. The dashed lines are DBO6 (152° W) and DBO7 (143.6° W).

Closely spaced stations within the cross-shelf transects, covering depths as in 2013 and 2014 (i.e., 20, 50, 100, 200, 350, 500, 750, 1000 m), provides in-depth knowledge about distribution of fishes in relation to depth and water mass. This is the preferred scale when sampling on the limited along-shelf extent recommended above. Sampling five to six transects on one cruise

would likely only allow time to sample these eight depths per transect. However, the actual number of transects that could be completed will be highly dependent upon weather. If a broad-scale along-shelf survey is planned, we recommend sampling 20 and 100 m on the shelf and 200, 350 and 750 m on the slope.

The scientific scope must be accommodated within the desired geographic scope of the monitoring. A thorough examination of the physical and biological entities is needed to understand the ecosystem. While including more tropic levels would produce a comprehensive study, the tradeoff is either a longer cruise or less time (called wire time) for each tropic level to sample (Table 11.2). As learned from various tropic level compromises on cruises from 2011 through 2014 (Appendix J), it is not possible to give all tropic levels equal weight within a limited amount of ship time and space. Because the objective here was to design a demersal and pelagic fish monitoring plan, the value of each scientific discipline was based on its overall contribution to assessing fish distribution, abundance, and shared resources. To evaluate fish habitat, measurements of salinity and temperature (CTD) throughout the water column are critical, as they affect not only distribution of individual species, but also community composition. For fishes that spend time on, not just near, the bottom, sediment grain size is important. As the benthic biota of the Beaufort Sea shelf is predominantly epifauna, fish communities and epibenthic communities are intertwined (Bluhm et al. 2014) and both need to be examined in considering the region's food web. Epibenthos must be examined as both potential prey and competition for. Infauna and zooplankton are the lower trophic food sources for benthic and pelagic fishes. Sampling the base of the food web does not require any additional wire time because a CTD can have a fluorometer for chlorophyll and Niskin bottles for water samples. Stable isotopes are an excellent, expedient method to examine multiple trophic levels in a food web. Similarly, chemical water mass tracer techniques could be added (at additional cost) and, in conjunction with standard hydrographical analysis, enhance assessment of shelf break upwelling processes (Hopcroft et al. 2005).

There is usefulness to inclusion of all these disciplines, but compromises were made to accommodate them (Table 11.2). On the TB-2014 cruise that meant less wire time for fishing multiple gear types. Epibenthos is captured in the same trawl hauls as fish so the capture does not require any additional wire time, though taxonomic expertise is needed onboard ship to identify the specimens. Infauna, as food for benthic-feeding fishes such as sculpins, can be collected with the same grab or core used to collect sediment. If the objective is to determine relative abundance of infauna species in relation to what is consumed by food, 3–5 replicate samples are not necessary. The level of precision may be necessary to characterize the infauna community, but that is a different objective. Likewise, if pelagic fishes are not being sampled at discreet depths in the water column, then information about vertical distribution of zooplankton cannot inform the feeding habits of the fishes.

The precision of fish identification needed must also be considered. The discovery of a multitude of eelpout species in the Beaufort Sea is surprising and added ecological complexity to interpretation of the fish communities and potential impacts. The resolution of the identification of species within the genus *Lycodes* using DNA revealed ecological differences among eelpouts species, i.e., depth and size differences appear to be spatial (shelf vs. slope distributions) by species. For this project, and future projects in the US Arctic, we now know that identifying *Lycodes* solely on morphological features (Mecklenburg et al. 2002, Thorsteinson and Love 2016) is not always reliable for even the most abundant *Lycodes* species (Appendix H). Accurate species identifications are needed for calculating species-specific CPUE and BPUE values,

plotting species distribution, determining length–weight and length–age relationships, and diet studies. Because *L. adolfi, L. sagittarius*, and *L. seminudus* are such important components of the slope fish community, as well as *L. polaris* in the shelf break community (Table 7.3.4.10), identification of *Lycodes* to species for these numerous ones is a worthwhile endeavor for future studies. However, generalized depth distribution, i.e., *L. polaris* <200 m, *L. seminudus* mostly 350–500 m, *L. sagittarius* 350–1000 m, and *L. adolfi* 750–1000 m (Appendix H), could be acceptable for broad scale monitoring of the Beaufort Sea shelf and slope and precise DNA-based identification would not be necessary. DNA was not used to confirm identifications of other species because the issue with the *Lycodes* was at all life stages, including adults; whereas only very small (young) life stages of other species could not be identified, e.g., *Liparis*.

A separate purpose of a monitoring program could be established to evaluate the persistence of indicator species, as opposed to the health of the ecosystem generally. As described in sections 7.4.5 and 9.7, for multiple trophic levels, i.e., fish, epibenthos and zooplankton taxa, this project has identified key indicators of shelf vs. slope communities. Using that knowledge a simplified field study could be conducted to examine the abundance and biomass of only those designated taxa; measuring only presence or absence can indicate latitudinal or depth range extensions or contractions (Perry et al. 2005, Smale et al. 2011). As well as indicator species, assemblage characteristics, including species composition and individual measures of length and weight, should also be monitored (Smale et al. 2011).

11.2 Lessons Learned

- Sample both the shelf and the slope to understand the whole ecosystem of the US Beaufort Sea.
- Keep local communities informed of planned and completed sampling; defer to their wishes.
- Continue to sample into Canada area to assess the influence of the Mackenzie River on US Beaufort Sea shelf fishes and lower trophic levels.
- Decide specific goals of each sampling cruise in advance so tradeoffs can be evaluated.
- Choose which gear and which stations to sample to meet the specific objectives.
- Weigh tradeoffs between what accomplishments are desirable and what are possible, e.g., repeat stations for interannual variability vs. sample new locations for breadth, replicate samples vs. additional gear.
- Start sampling earlier in season, i.e., July instead of August to work around whaling dates.
- Allocate time to test new gear and to compare with that previously used.
- Use a larger CTD with more bottles to ensure adequate samples for better resolution of deep nutrient pools.
- Collect size fractionated chlorophyll-a on all cruises
- Perform a five-minute 150-µm tow zooplankton tow in the freshwater upper mixed layer to resolve community differences between the freshwater lens and the rest of the Polar Mixed Layer.
- Use a real-time Multinet control/data coupled with SIMRAD altimeter on zooplankton Multinet to monitor the distance to the seafloor.
- Use a hydroacoustic system to efficiently sample with an Aluette or other midwater net.

- Use a PSBT-A with Spectra® bridles, a real-time SIMRAD depth sounder, and a time-depth recorder (TDR) that is downloaded after the tow for fish/epibenthic trawling.
- Verify fish species identification; preliminary field identifications should only be used with caution.
- Plan for processing samples in the laboratory to take longer than expected.

Table 11.2. Sampling alternatives for Beaufort Sea fish and lower trophic level monitoring.

	Issue	Pros	Cons
Scale of Sampling	Broad scale: 155°–141° W	Gain ecological perspective large area	Must interpolate between stations
	Refined scale: 150°–146° W	In-depth information	Limited area sampled
	Shelf ≤200 m	Area of potential oil development	Smaller area to sample
	Slope >200–1000 m	Physical and biological influences on shelf	Cost more to sample larger area
	Closely spaced stations	More depths per transect	Time consuming
	Widely spaced stations	Less time consuming	Fewer depths, less information per transect
Disciplines to sample	High # disciplines	More comprehensive ecological base	Less wire time per discipline, more scientists
	Fewer # disciplines	More wire time per discipline, few scientists	Less comprehensive ecological base
	Fish	Requested by BOEM	Time consuming to process
	Epibenthos	Captured in fish trawls	Time consuming to process
	Physical (CTD)	Needed by all disciplines	Need access to CTD
	Zooplankton	Important in food web	Time consuming to process
	Infauna	Important in food web	Time consuming to process
	Sediment	Relatively inexpensive and quick results	Wire time to deploy sediment grab
	Water chemistry (nutrients)	Important in food web, shares CTD wire time	Money to process
	Chlorophyll	Flow through is quick measure of productivity	Is instantaneous value, not a rate
Vessel	Arctic vessel	Required for safety and convenience in Arctic	Few vessels available
	Vessel availability	Trusted vessels exist	Cannot reserve exact dates desired for work
		R/V *Sikuliaq*	Reserve months to years ahead
	Vessel cost	Small costs less	Large costs more
	# hrs/da	Get more done working 24 hr/da	Accomplish less working 12 hr/da
	work 24 hrs/da	Requires larger vessel for more people	Few vessels can hold enough people
Timing	Whaling closure begins 25 Aug	Observe CAA to respect natives	Restricts where and when can sample
	Timing of cruise	1–21 August, after ice out, before CAA	Actual ice-out time, availability of vessel
	Build in 30% days lost to weather	Ensure all stations are sampled	Costs more money

LITERATURE CITED

Aagaard, K., C. H. Pease, A. T. Roach, and S. A. Salo. 1989. Beaufort Sea Mesoscale Circulation Study – Final Report, p. 114. NOAA Tech Mem, ERL PMEL-90.

Abookire, A.A. and C.S. Rose. 2005. Modifications to a plumb staff beam trawl for sampling uneven, complex habitats. Fisheries Research 71(2):247–254.

Abramova, E. and K. Tuschling. 2005. A 12-year study of the seasonal and interannual dynamics of mesozooplankton in the Laptev Sea: significance of salinity regime and life cycle patterns. Global and Planetary Change 48(1):141–164.

Albrecht, G.T., A.E. Valentin, K.J. Hundertmark, and S.M. Hardy. 2014. Panmixia in Alaskan populations of the snow crab *Chionoecetes opilio* (Malacostraca: Decapoda) in the Bering, Chukchi, and Beaufort Seas. Journal of Crustacean Biology 34(1):31–39.

Altabet, M.A. and R. Francois. 2001. Nitrogen isotope biogeochemistry of the Antarctic Polar Frontal Zone at 170°W. Deep-Sea Research Part II: Topical Studies in Oceanography 48(19–20):4247–4273.

Ambrose, W., L. Clough, P. Tilney, and L. Beer. 2001. Role of echinoderms in benthic remineralization in the Chukchi Sea. Marine Biology 139(5):937–949.

Anderson, M.J. and D.C.I. Walsh. 2013. PERMANOVA, ANOSIM, and the Mantel test in the face of heterogeneous dispersions: what null hypothesis are you testing? Ecological Monographs 83(4):557–574.

Andreu-Soler A., F. J. Oliva-Paterna, and M. Torralva. 2005. A review of length-weight relationships of fish from the Segura River basin (Siberian Peninsula). Journal of Applied Ichthyology 22:295–296.

Arashkevich, E., P. Wassmann, A. Pasternak, and C.W. Riser. 2002. Seasonal and spatial changes in biomass, structure, and development progress of the zooplankton community in the Barents Sea. Journal of Marine Systems 38:125–145.

Arrigo, K.R., G. Van Dijken, and S. Pabi. 2008. Impact of a shrinking Arctic ice cover on marine primary production. Geophysical Research Letters 35(19):L19603.

Arrigo, K. R. and others 2012. Massive Phytoplankton Blooms Under Arctic Sea Ice. Science 336:1408.

Ashjian, C. J., R.G. Campbell, H.E. Welch, M. Butler, and D. Van Keuren. 2003. Annual cycle in abundance, distribution, and size in relation to hydrography of important copepod species in the western Arctic Ocean. Deep-Sea Research Part I: Oceanographic Research Papers 50(10–11):1235–1261.

Ashjian, C.J., S.M. Gallager, and S. Plourde. 2005. Transport of plankton and particles between the Chukchi and Beaufort Seas during summer 2002, described using a Video Plankton Recorder. Deep Sea Research Part II:Topical Studies in Oceanography 52(24–26):3259–3280.

Ashjian, C.J., S.R. Braund, R.G. Campbell, J.C George, J. Kruse, W. Maslowski, S.E. Moore, C.R. Nicolson, S.R. Okkonen, B.F Sherr, E.B. Sherr, and Y.H. Spitz. 2010. Climate variability, oceanography, bowhead whale distribution, and Inupiat subsistence whaling near Barrow, Alaska. Arctic 63:179–194.

Atkinson, E.G. and J.W. Wacasey. 1989. Benthic invertebrates collected from the western Canadian Arctic, 1951 to 1985. Canadian Data Report of Fisheries and Aquatic Sciences. pp 138.

Atkinson, E.G. and J.A. Percy. 1992. Diet comparison among demersal marine fish from the Canadian Arctic. Polar Biology 11(8):567–573.

Audubon Alaska. 2015. A synthesis of important areas in the U.S. Chukchi and Beaufort Seas: The best available data to inform management decisions. pp 25 + Appendices. Access date 1-May-2016. Report: http://docs.audubon.org/sites/default/files/documents/important_areas_chukchi_beaufort_science_synthesis_8apr2015_lr.pdf, Map: http://docs.audubon.org/sites/default/files/documents/6._sea_floor_substrate.pdf

Auel, H. 1999. The ecology of Arctic deep-sea copepods (Euchaetidae and Aetideidae). Aspects of their distribution, trophodynamics and effect on the carbon flux. Berichte zur Polarforschung. Vol. 319. Bremerhaven, Germany: Alfred Wegener Institute. pp 97.

Auel, H. and W. Hagen. 2002. Mesozooplankton community structure, abundance and biomass in the central Arctic Ocean. Marine Biology 140(5):1013–1021.

Aydin, K.S., S. Gaichas, I. Ortiz, D. Kinzey, and N. Friday. 2007. A comparison of the Bering Sea, Gulf of Alaska, and Aleutian Islands large marine ecosystems through food web modeling. US Department of Commerce, NOAA Tech Memo NMFS-AFSC-178, p 1–298.

Barber, W.E., R.L. Smith, M. Vallarino, and R.M. Meyer. 1997. Demersal fish assemblages of the northeastern Chukchi Sea, Alaska. Fish B-NOAA 95:195–209.

Barnes, P. W., D. M. Schell, and E. Reimnitz [eds.]. 1984. The Alaskan Beaufort Sea: Ecosystems and Environment. Academic Press.

Bates, N.R., M.H.P. Best, and D.A. Hansell. 2005. Spatio-temporal distribution of dissolved inorganic carbon and net community production in the Chukchi and Beaufort Seas. Deep Sea Research Part II: Topical Studies in Oceanography 52(24–26):3303–3323.

Bates, N.R., J.T. Mathis, and L.W. Cooper. 2009. Ocean acidification and biologically induced seasonality of carbonate mineral saturation states in the western Arctic Ocean. Journal of Geophysical Research-Oceans 114:C11007.

Bates, N.R., M.I. Orchowska, R. Garley, and J.T. Mathis. 2013. Summertime calcium carbonate undersaturation in shelf waters of the western Arctic Ocean - how biological processes exacerbate the impact of ocean acidification. Biogeosciences 10:5281–5309.

Bechtel, P.J. and A.C.M. Oliveira. 2006. Chemical characterization of liver lipid and protein from cold-water fish species. Journal of Food Science 71(6):S480–S485.

Bell, L. 2015. The influence of terrestial matter in marine food webs of the Beaufort Sea shelf and slope. Fairbanks, AK: M.S. thesis, Univeristy of Alaska Fairbanks. 79 p.

Bell, L.E., B.A. Bluhm, and K. Iken. 2016. Influence of terrestrial organic matter in marine food webs of the Beaufort Sea shelf and slope. Marine Ecology Progress Series 550:1–24.

Berglund, J., U. Müren, U. Båmstedt, and A. Andersson. 2007. Efficiency of a phytoplankton-based and a bacteria-based food web in a pelagic marine system. Limnology and Oceanography 52(1):121–131.

Bergmann, M., J. Dannheim, E. Bauerfeind, and M. Klages. 2009. Trophic relationships along a bathymetric gradient at the deep-sea observatory HAUSGARTEN. Deep-Sea Research Part I: Oceanographic Research Papers 56(3):408–424.

Birkeland, C. and P.K. Dayton. 2005. The importance in fishery management of leaving the big ones.Trends in Ecology and Evolution 20(7):356-358.

Blachowiak-Samolyk, K., S. Kwasniewski, K. Dmoch, H. Hop, and S. Falk-Petersen. 2007. Trophic structure of zooplankton in the Fram Strait in spring and autumn 2003. Deep-Sea Research Part II 54:2716-2728.

Blanchard, A.L., R.H. Day, A.E. Gall, L.A.M. Aerts, J. Delarue, E.L. Dobbins, R.R. Hopcroft, J.M. Questel, T.J. Weingartner, and S.S. Wisdom. 2017. Ecosystem in the offshore northeastern Chukchi Sea. Progress in Oceanography 159:130–153.

Blanchard, A.L. and H.M. Feder. 2014. Interactions of habitat complexity and environmental characteristics with macrobenthic community structure at multiple spatial scales in the northeastern Chukchi Sea. Deep-Sea Research Part II: Topical Studies in Oceanography 102:132–143.

Blanchard, A.L., C.L. Parris, A.L. Knowlton, and N.R. Wade. 2013. Benthic ecology of the northeastern Chukchi Sea. Part II. Spatial variation of megafaunal community structure, 2009–2010. Continental Shelf Research 67:67–76.

Blicher, M.E. and M.K. Sejr. 2011. Abundance, oxygen consumption and carbon demand of brittle stars in Young Sound and the NE Greenland shelf. Marine Ecology Progress Series 422:139–144.

Blott, S.J. and K. Pye. 2001. GRADISTAT: a grain size distribution and statistics package for the analysis of unconsolidated sediments. Earth Surface Processes and Landforms 26(11):1237–1248.

Bluhm, B.A., W.G. Ambrose Jr., M. Bergmann, L.M. Clough, A.V. Gebruk, C. Hasemann, K. Iken, M. Klages, I.R. MacDonald, P.E. Renaud, I. Schewe, T. Soltwedel, and M. Wlodarska-Kowalczuk. 2011. Diversity of the arctic deep-sea benthos. Marine Biodiversity 41(1):87–107.

Bluhm, B.A., F. Huettmann, and B.L. Norcross. 2014. Ecological analysis of Western Beaufort Sea data. OCS Study BOEM 2014-014, Anchorage, AK: USDOI, MMS, Alaska OCS Region, 46 pp.

Bluhm, B.A., K. Iken, and L.B. Divine. 2015. Population assessment of snow crab, *Chionoecetes opilio*, in the Chukchi and Beaufort Seas including oil and gas lease areas. Final Report, Coastal Marine Institute; Award M11AC00003.

Bluhm, B.A., K. Iken, S.M. Hardy, B.I. Sirenko, and B.A. Holladay. 2009. Community structure of epibenthic megafauna in the Chukchi Sea. Aquatic Biology 7:269–293.

Bluhm, B.A., D. Piepenburg, and K. von Juterzenka. 1998. Distribution, standing stock, growth, mortality and production of *Strongylocentrotus pallidus* (Echinodermata: Echinoidea) in the northern Barents Sea. Polar Biology 20(5):325–334.

Bouchard, C. and L. Fortier. 2011. Circum-arctic comparison of the hatching season of polar cod (*Boreogadus saida*): A test of the freshwater winter refuge hypothesis. Progress in Oceanography 90(1–4):105–116.

Boxshall, G.A. 1985. The comparative anatomy of two copepods, a predatory calanoid and a particle-feeding mormonilloid. Philosophical Transactions of the Royal Society of London Series B-Biological Sciences 311(1150):303–307.

Bray, J.R. and J.T. Curtis. 1957. An ordination of the upland forest communities of southern Wisconsin. Ecological Monographs 27(4):325–349.

Britt, L.L., R.R. Lauth, and B.L. Norcross. 2013. Paired catch comparisons from two standard bottom trawls used in arctic surveys. In: Distribution of fish, crab and lower trophic communities in the Chukchi Sea AK-11-08. Draft report to Department of the Interior Bureau of Ocean Energy Management. Interagency agreement # M12PG00018.

Brugler, E.T., R.S. Pickart, G.W.K. Moore, S. Roberts, T.J. Weingartner, and H. Statscewich. 2014. Seasonal to interannual variability of the Pacific water boundary current in the Beaufort Sea. Progress in Oceanography 127:1–20.

Budge, S.M., S.J. Iverson, and H.N. Koopman. 2006. Studying trophic ecology in marine ecosystems using fatty acids: A primer on analysis and interpretation. Marine Mammal Science 22(4):759–801.

CAFF. 2017. State of the Arctic Marine Biodiversity Report. Conservation of Arctic Flora and Fauna International Secretariat, Akureyri, Iceland. 978-9935-431-63-9.

Carey Jr., A.G., P.H. Scott, and K.R. Walters. 1984. Distributional ecology of shallow southwestern Beaufort Sea (Arctic Ocean) bivalve Mollusca. Marine Ecology Progress Series 17:125–134.

Carmack, E.C., R.W. MacDonald, and J.E. Papadakis. 1989. Water mass structure and boundaries in the Mackenzie Shelf Estuary. Journal of Geophysical Research - Oceans 94(C12):18043–18055.

Carmack, E. and P. Wassmann. 2006. Food webs and physical–biological coupling on pan-Arctic shelves: unifying concepts and comprehensive perspectives. Progress in Oceanography 71(2–4):446–477.

Casper, A.F., M. Rautio, C. Martineau, and W.F. Vincent. 2014. Variation and assimilation of Arctic riverine seston in the pelagic food web of the Mackenzie River Delta and Beaufort Sea transition zone. Estuaries and Coasts 38:1656–1663.

Chavez, F.P., M. Messie, and J.T. Pennington. 2011. Marine primary production in relation to climate variability and change. Annual Review of Marine Science 3:227–260.

Chisholm, S. W. 1992. Phytoplankton size, p. 213-237. *In* P. G. Falkowski and A. D. Woodhead [eds.], Primary productivity and biogeochemical cycles in the sea. Plenum.

Cividanes, S., M. Incera, and J. López. 2002. Temporal variability in the biochemical composition of sedimentary organic matter in an intertidal flat of the Galician coast (NW Spain). Oceanologica Acta 25(1):1–12.

Clarke, K.R. and R.N. Gorley. 2015. PRIMER v7: User Manual/Tutorial. PRIMER-E Ltd., Plymouth. pp 296.

Clarke, K.R., R.N. Gorley, P.J. Somerfield, and R.M. Warwick. 2014a. Change in marine communities: an approach to statistical analysis and interpretation, 3rd edition. PRIMER-E, Plymouth.

Clarke, K.R., P.J. Somerfield, and R.N. Gorley. 2008. Testing of null hypotheses in exploratory community analyses: similarity profiles and biota-environment linkage. Journal of Experimental Marine Biology and Ecology 366(1–2):56–69.

Clarke, K.R., J.R. Tweedley, and F.J. Valesini. 2014b. Simple shade plots aid better long-term choices of data pre-treatment in multivariate assemblage studies. Journal of the Marine Biological Association of the United Kingdom 94(1):1–16.

Clarke, K. R. and R.M. Warwick. 2010. Change in Marine Communities: An Approach to Statistical Analysis and Interpretation. PRIMER-E Ltd., Plymouth. pp 172.

Cochrane, S.K.J., S.G. Denisenko, P.E. Renaud, C.S. Emblow, W.G. Ambrose, Jr., I.H. Ellingsen, and J. Skardhamar. 2009. Benthic macrofauna and productivity regimes in the Barents Sea - Ecological implications in a changing Arctic. Journal of Sea Research 61(4):222–233.

Codispoti, L. A. and others. 2013. Synthesis of primary production in the Arctic Ocean: III. Nitrate and phosphate based estimates of net community production. Progress in Oceanography 110:126–150.

Codispoti, L., C. Flagg, V. Kelly, and J.H. Swift. 2005. Hydrographic conditions during the 2002 SBI process experiments, Deep Sea Research Part II 52(24–26):3199–3226. doi:10.1016/j.dsr2.2005.10.007

Comiso, J.C. 2002. A rapidly declining perennial sea ice cover in the Arctic. Geophysical Research Letters 29(20):17-1–17-4.

Conlan, K., A. Aitken, E. Hendrycks, C. McClelland, and H. Melling. 2008. Distribution patterns of Canadian Beaufort Shelf macrobenthos. Journal of Marine Systems 74(3–4):864–886.

Cooper, L.W., J.W. McClelland, R.M. Holmes, P.A. Raymond, J. Gibson, C.K. Guay, and B.J. Peterson. 2008. Flow-weighted values of runoff tracers ($\delta^{18}O$, DOC, Ba, alkalinity) from the six largest Arctic rivers. Geophysical Research Letters 35(18):L18606.

Cottier, F.R., G.A. Tarling, A. Wold, and S. Falk-Petersen. 2006. Unsynchronized and synchronized vertical migration of zooplankton in a high arctic fjord. Limnology and Oceanography 51(6):2586–2599.

Coyle, K.O., J.A. Gillispie, R.L. Smith, and W.E. Barber. 1997. Food habits of four demersal Chukchi Sea fishes. American Fisheries Society Symposium: Fish Ecology in Arctic North America 19:310–318.

Craig, P.C., W.B. Griffiths, L. Haldorson, and H. McElderry. 1982. Ecological studies of *Arctic cod* (*Boreogadus saida*) in Beaufort Sea coastal waters, Alaska. Canadian Journal of Fisheries and Aquatic Sciences 39(3):395–406.

Craig, P.C., W.B. Griffiths, L. Haldorson, and H. McElderry. 1985. Distributional patterns of fishes in an Alaskan Arctic lagoon. Polar Biology 4(1):9–18.

Crawford, R., S. Vagle, and E. Carmack. 2012. Water mass and bathymetric characteristics of polar cod habitat along the continental shelf and slope of the Beaufort and Chukchi seas. Polar Biology 35(2):179–190.

Daase, M., S. Falk-Petersen, O. Varpe, G. Darnis, J.E. Søreide, A. Wold, E. Leu, J. Berge, B. Philippe, and L. Fortier. 2013. Timing of reproductive events in the marine copepod *Calanus glacialis*: a pan-Arctic perspective. Canadian Journal of Fisheries and Aquatic Sciences 70(6):871–884.

Dalsgaard, J., M.S. John, G. Kattner, D. Muller Navarra, and W. Hagen. 2003. Fatty acid trophic markers in the pelagic marine environment. Advances in Marine Biology 46:225–340.

Darnis, G. and L. Fortier. 2014. Temperature, food and the seasonal vertical migration of key Arctic copepods in the thermally stratified Amundsen Gulf (Beaufort Sea, Arctic Ocean). Journal of Plankton Research 36:1092–1108.

Darnis, G., D.G. Barber, and L. Fortier. 2008. Sea ice and the onshore-offshore gradient in pre-winter zooplankton assemblages in southeastern Beaufort Sea. Journal of Marine Systems 74(3–4):994–1011.

Daufresne, M., K. Lengfellner, and U. Sommer. 2009. Global warming benefits the small in aquatic ecosystems. Proceedings of the National Academy of Sciences of the United States of America 106(31):12788–12793.

David, C., B. Lange, T. Krumpen, F. Schaafsma, J.A. van Franeker, and H. Flores. 2015. Under-ice distribution of polar cod *Boreogadus saida* in the central Arctic Ocean and their association with sea-ice habitat properties. Polar Biology pp 1–14.

Day, R.H., T.J. Weingartner, R.R. Hopcroft, L.A.M. Aerts, A.L. Blanchard, A.E. Gall, B.J. Gallaway, D.E. Hannay, B.A. Holladay, J.T. Mathis, B.L. Norcross, J.M. Questel, and S.S. Wisdom. 2013. The offshore northeastern Chukchi Sea: a complex high-latitude system. Continental Shelf Research 67:147–165.

Dilling, L., J. Wilson, D. Steinberg, and A. Alldredge. 1998. Feeding by the euphausiid *Euphausia pacifica* and the copepod *Calanus pacificus* on marine snow. Marine Ecology Progress Series 170:189–201.

Divine, L.M., K. Iken, and B.A. Bluhm. 2015. Regional benthic food web structure on the Alaska Beaufort shelf. Marine Ecology Progress Series 531:15–32.

Dolan, J.R., E.J. Yang, T.W. Kim, and S.H. Kang. 2014. Microzooplankton in a warming Arctic: a comparison of tintinnids and radiolarians from summer 2011 and 2012 in the Chukchi Sea. Acta Protozoologica 53(1):101–113.

Dorgelo, J. and P.E.G. Leonards. 2001. Relationship between C/N ratio of food types and growth rate in the snail *Potamopyrgus jenkinsi* (E.A. Smith). Journal of the North American Benthological Society 20(1):60–67.

Doxaran, D., E. Devred, and M. Babin. 2015. A 50% increase in the amount of terrestrial particles delivered by the Mackenzie River into the Beaufort Sea (Canadian Arctic Ocean) over the last 10 years. Biogeosciences Discussions 12(11):305–344.

Doyle, M.J., K.L. Mier, M.S. Busby, and R.D. Brodeur. 2002. Regional variation of springtime ichthyoplankton assemblages in the northeast Pacific Ocean. Progress in Oceanography 53(2):247–281.

Duffy, J.E., L.A. Amaral-Zettler, D.G. Fautin, G. Paulay, T.A. Rynearson, H.M. Sosik, and J.J. Stachowicz. 2013. Envisioning a marine biodiversity observation network. BioScience 63(5):350–361.

Dufrene, M. and P. Legendre. 1997. Species assemblages and indicator species: the need for a flexible asymmetrical approach. Ecological Monographs 67(3):345–366.

Dunton, K.H., J.L. Goodall, S.V. Schonberg, J.M. Grebmeier, and D.R. Maidment. 2005. Multi-decadal synthesis of benthic–pelagic coupling in the western Arctic: role of cross-shelf advective processes. Deep-Sea Research Part II: Topical Studies in Oceanography 52(24–26):3462–3477.

Dunton, K.H., S.M. Saupe, A.N. Golikov, D.M. Schell, and S.V. Schonberg. 1989. Trophic relationships and isotope gradients among Arctic marine fauna. Marine Ecology Progress Series 56:89–97.

Dunton, K.H., S.V. Schonberg, and L.W. Cooper. 2012. Food web structure of the Alaskan nearshore shelf and estuarine lagoons of the Beaufort Sea. Estuaries and Coasts 35(2):416–435.

Dunton, K.H., T. Weingartner, and E.C. Carmack. 2006. The nearshore western Beaufort Sea ecosystem: Circulation and importance of terrestrial carbon in arctic coastal food webs. Progress in Oceanography 71(2–4):362–378.

Eilertsen, H.C., K.S. Tande, and J.P. Taasen. 1989. Vertical distributions of primary production and grazing by *Calanus glacialis* Jaschnov and *Calanus hyperboreus* Kroyer in Arctic waters (Barents Sea). Polar Biology 9:253–260.

Eisner, L., N. Hillgruber, E. Martinson, and J. Maselko. 2013. Pelagic fish and zooplankton species assemblages in relation to water mass characteristics in the northern Bering and southeast Chukchi seas. Polar Biology 36(1):87–113.

Emmerton, C.A., L.F.W. Lesack, and W.F. Vincent. 2008. Nutrient and organic matter patterns across the Mackenzie River, estuary and shelf during the seasonal recession of sea-ice. Journal of Marine Systems 74:741–755.

Ennis, G.P. 1970. Age, growth, and sexual maturity of the shorthorn sculpin, *Myoxocephalus scorpius*, in Newfoundland Waters. Journal of the Fisheries Research Board of Canada 27(12):2155–2158.

Ershova, E.A., R.R. Hopcroft, K.N. Kosobokova, K. Matsuno, R.J. Nelson, A. Yamaguchi, and L.B. Eisner. 2015a. Long-term changes in summer zooplankton communities of the western Chukchi Sea, 1945–2012. Oceanography 28:100–115.

Ershova, E.H., R.R. Hopcroft, and K.N. Kosobokova. 2015b. Inter-annual variability of summer mesozooplankton communities of the western Chukchi Sea: 2004–2012. Polar Biology 38(9):1461–1481.

Etter, R.J. and J.F. Grassle.1992. Patterns of species diversity in the deep sea as a function of sediment particle size diversity. Nature 360(6404):576–578.

Fabiano, M. and R. Danovaro. 1998. Enzymatic activity, bacterial distribution, and organic matter composition in sediments of the Ross Sea (Antarctica). Applied and Environmental Microbiology 64(10):3838–3845.

Falardeau, M., D. Robert, and L. Fortier. 2014. Could the planktonic stages of polar cod and Pacific sand lance compete for food in the warming Beaufort Sea? ICES Journal of Marine Science 71:1956–1965.

Falk-Petersen, S., S. Timofeev, V. Pavlov, and J.R. Sargent. 2006. Climate variability and the effect on arctic food chains. The role of *Calanus*. In: Orbaek T., R. Tombre, E. Kallenborn, E. Hegseth, S. Falk-Petersen, and A. H. Hoel [eds.]. Arctic-Alpine Ecosystems and People in a Changing Environment. Berlin: Springer. pp 147–166.

Fechhelm, R.G., C.M. Merrill, N.D. Jahans, and M.R. Link. 2010. Year 28 of the long-term monitoring of nearshore Beaufort Sea fishes in the Prudhoe Bay region: 2010 annual report. Report for BP Exploration (Alaska) Inc. by LGL Alaska Research Associates, Inc., Anchorage, Alaska, pp 84.

Feder, H.M., S.C. Jewett, and A. Blanchard. 2005. Southeastern Chukchi Sea (Alaska) epibenthos. Polar Biology 28(5):402–421.

Ferraro, S.P. and F.A. Cole. 1990. Taxonomic level and sample size sufficient for assessing pollution impacts on the Southern California Bight macrobenthos. Marine Ecology Progress Series 67(3):251–262.

Folch, J., M. Lees, and G.H. Sloane Stanley. 1957. A simple method for the isolation and purification of total lipids from animal tissues. Journal of Biological Chemistry 226(1):497–509.

Forest, A., M. Babin, L. Stemmann, M. Picheral, M. Sampei, L. Fortier, Y. Gratton, S. Bélanger, E. Devred, and J. Sahlin. 2013. Ecosystem function and particle flux dynamics across the Mackenzie Shelf (Beaufort Sea, Arctic Ocean): an integrative analysis of spatial variability and biophysical forcings. Biogeosciences Discussions 10(5):2833–2866.

Forest, A., M. Sampei, H. Hattori, R. Makabe, H. Sasaki, M. Fukuchi, P. Wassmann, and L. Fortier. 2007. Particulate organic carbon fluxes on the slope of the Mackenzie Shelf (Beaufort Sea): physical and biological forcing of shelf-basin exchanges. Journal of Marine Systems 68(1–2):39–54.

Fossheim, M., E.M. Nilssen, and M. Aschan. 2006. Fish assemblages in the Barents Sea. Marine Biology Research 2:260–269.

Fossheim, M., R. Primicerio, E. Johannesen, R.B. Ingvaldsen, M.M. Aschan, and A.V. Dolgov. 2015. Recent warming leads to rapid borealization of fish communities in the Arctic. Nature Climate Change 5:673–678.

Froese, R. 2006. Cube law, condition factor and weight-length relationships: history, meta-analysis and recommendations. Journal of Applied Ichthyology 22(4):241–253.

Frost, K.J. and L.F. Lowry. 1983. Demersal fishes and invertebrates trawled in the northeastern Chukchi and western Beaufort seas, 1976–77. NOAA Technical Report NMFS SSRF 764. pp 22.

Gallagher, M.L., W.G. Ambrose Jr, and P.E. Renaud. 1998. Comparative studies in biochemical composition of benthic invertebrates (bivalves, ophiuroids) from the Northeast Water (NEW) Polynya. Polar Biology 19(3):167–171.

Garneau, M.È., W.F. Vincent, R. Terrado, and C. Lovejoy. 2009. Importance of particle-associated bacterial heterotrophy in a coastal Arctic ecosystem. Journal of Marine Systems 75(1–2):185–197.

Geoffroy, M., A. Majewski, M. LeBlanc, S. Gauthier, W. Walkusz, J.D. Reist, and L. Fortier. 2015. Vertical segregation of age-0 and age-1+ polar cod (*Boreogadus saida*) over the annual cycle in the Canadian Beaufort Sea. Polar Biology 1–15. doi: 10.1007/s00300-015-1811-z

Giacalone, V.M., G. D'Anna, F. Badalamenti, and C. Pipitone. 2010. Weight-length relationships and condition factors for thirty-eight fish species in trawled and untrawled areas off the coast of northern Sicily (central Mediterranean Sea). Journal of Applied Ichthyology 26(6):954–957.

Goñi, M.A., A.E. O'Connor, Z.Z. Kuzyk, M.B. Yunker, C. Gobeil, and R.W. Macdonald. 2013. Distribution and sources of organic matter in surface marine sediments across the North American Arctic margin. Journal of Geophysical Research - Oceans 118(9):4017–4035.

Goñi, M.A., M.B. Yunker, R.W. Macdonald, and T.I. Eglinton. 2000. Distribution and sources of organic biomarkers in Arctic sediments from the Mackenzie River and Beaufort Shelf. Marine Chemistry 71(1–2):23–51.

Gordon, L. I., J.C. Jennings, A.A. Ross, and J.M. Krest. 1993. A suggested protocol for continuous flow automated analysis of seawater nutrients (phosphate, nitrate, nitrite and silicic acid) in the WOCE Hydrographic Program and the Joint Global Ocean Fluxes Study. Corvallis: Oregon State University. pp 51.

Gosselin, M., M. Levasseur, P. E. Wheeler, R. A. Horner, and B. C. Booth. 1997. New measurements of phytoplankton and ice algal production in the Arctic Ocean. Deep Sea Research Part II 44:1623–1644.

Gradinger, R. 2009. Sea-ice algae: Major contributors to primary production and algal biomass in the Chukchi and Beaufort Seas during May/June 2002. Deep-Sea Research Part II 56:1201–1212.

Gradinger, R. and B. Bluhm. 2004. In-situ observations on the distribution and behavior of amphipods and Arctic cod (*Boreogadus saida*) under the sea ice of the High Arctic Canada Basin. Polar Biology 27(10):595–603.

Gradinger, R., B. Bluhm, and K. Iken. 2010a. Arctic sea-ice ridges – safe havens for sea-ice fauna during periods of extreme ice melt? Deep-Sea Research Part II: Topical Studies in Oceanography 57:86–95.

Gradinger, R., B.A. Bluhm, R.R Hopcroft, A. Gebruk, K.N. Kosobokova, B. Sirenko, and J.M. Wesławski. 2010b. Marine Life in the Arctic, in: McIntyre, A.D. (ed.), Life in the World's Oceans. Blackwell Publishing Ltd, New York, pp. 183-202.

Gradinger, R, M.R. Kaufman, and B.A. Bluhm. 2009. Pivotal role of sea ice sediments in the seasonal development of near-shore Arctic fast ice biota. Marine Ecology Progress Series 394:49–63.

Graeve, M., G. Kattner, and D. Piepenburg. 1997. Lipids in Arctic benthos: does the fatty acid and alcohol composition reflect feeding and trophic interactions? Polar Biology 18(1):53–61.

Grainger, E.H. 1965. Zooplankton from the Arctic Ocean and adjacent Canadian waters. Journal of the Fisheries Research Board of Canada 22:543–564.

Grainger, E.H. and C. Grohe. 1975. Zooplankton data from the Beaufort Sea, 1951 to 1975. Canada Fisheries and Marine Service Technical Report. Quebec: Environment Canada, Fisheries and Marine Services. pp 62.

Gray, B.P. 2015. Comparisons of Arctic Cod (*Boreogadus saida*), Arctic Staghorn Sculpin (*Gymnocanthus tricuspis*), and Shorthorn Sculpin (*Myoxocephalus scorpius*) diets across the northeastern Chukchi and western Beaufort Seas. MS Thesis, School of Fisheries and Ocean Sciences, University of Alaska Fairbanks.

Gray, B.P., B.L. Norcross, A.L. Blanchard, A.H. Beaudreau, and A.C. Seitz. 2015. Variability in the summer diets of juvenile polar cod (*Boreogadus saida*) in the northeastern Chukchi and western Beaufort Seas. Polar Biology: 1–12.

Grebmeier, J.M. 2012. Shifting patterns of life in the Pacific Arctic and Sub-Arctic seas. Annual Review of Marine Science 4:63–78.

Grebmeier, J.M. and J.P. Barry. 1991. The influence of oceanographic processes on pelagic-benthic coupling in polar regions: a benthic perspective. Journal of Marine Systems 2(3):495–518.

Grebmeier, J. M., and W. Maslowski. 2014. The Pacific Arctic Sector: status and trends. Springer.

Grebmeier, J.M., B.A. Bluhm, L.W. Cooper, S.L. Danielson, K.R. Arrigo, A.L. Blanchard, J.T. Clarke, R.H. Day, K.E. Frey, R.R. Gradinger, M.Kędra, B. Konar, K.J. Kuletz, S.H. Lee, J.R. Lovvorn, B.L. Norcross, and S.R. Okkonen. 2015a. Ecosystem characteristics and processes facilitating persistent macrobenthic biomass hotspots and associated benthivory in the Pacific Arctic. Progress in Oceanography 136:92–114.

Grebmeier, J.M., B.A. Bluhm, L.W. Cooper, S.G. Denisenko, K. Iken, M. Kędra, and C. Serratos. 2015b. Time-series benthic community composition and biomass and associated environmental characteristics in the Chukchi Sea during the RUSALCA 2004–2012 Program. Oceanography 28(3):116–133.

Grebmeier, J.M., L.W. Cooper, H.M. Feder, and B.I. Sirenko. 2006. Ecosystem dynamics of the Pacific-influenced Northern Bering and Chukchi Seas in the Amerasian Arctic. Progress in Oceanography 71(2–4):331–361.

Gunderson, D.R. and I.E. Ellis. 1986. Development of a plumb staff beam trawl for sampling demersal fauna. Fisheries Research 4(1):35–41.

Haro-Garay, M. J. 2003. Diet and functional morphology of the mandible of two planktonic amphipods from the Strait of Georgia, British Columbia, *Parathemisto pacifica* (Stebbing, 1888) and *Cyphocaris challengeri* (Stebbing, 1888). Crustaceana 76(11):1291–1312.

Hauser, L., G.J. Adcock, P.J. Smith, J.H.B. Ramirez, and G.R Carvalho. Loss of microsatellite diversity and low effective population size in an overexploited population of New Zealand snapper (*Pagrus auratus*). Proceedings of the National Academy of Sciences U.S.A. 99:11742–11747.

Hays, G.C., A.J. Richardson, and C. Robinson. 2005. Climate change and marine plankton. Trends in Ecology and Evolution 20:337–344.

Helser, T.E., J.R. Colman, D.M. Ander, and C.R. Kastelle. 2017. Growth dynamics of saffron cod (*Eleginus gracilis*) and Arctic cod (*Boreogadus saida*) in the Northern Bering and Chukchi Seas. Deep Sea Research Part II: Topical Studies in Oceanography 135:66–77.

Henrichs, S.M. 1993. Early diagenesis of organic matter: The dynamics (rates) of cycling of organic compounds. Organic Geochemistry: Principles and Applications. Engel M.H. and S.A. Macko. New York, NY, Plenum Press. pp 101–117.

Hill, V., M. Ardyna, S. H. Lee, and D. E. Varela. 2017. Decadal trends in phytoplankton production in the Pacific Arctic Region from 1950 to 2012. Deep Sea Res. II.

Hill, V., G. Cota, and D. Stockwell. 2005. Spring and summer phytoplankton communities in the Chukchi and Eastern Beaufort Seas. Deep-Sea Res. II. 52:3369–3385.

Hill, V.J., P.A. Matrai, E. Olson, S. Suttles, M. Steele, L.A. Codispoi, and R.C. Zimmerman. 2013. Synthesis of integrated primary production in the Arctic Ocean: II. *In situ* and remotely sensed estimates. Progress in Oceanography 110:107–125.

Hirche, H.-J., K.N. Kosobokova, B. Gaye-Haake, I. Harms, B. Meon, and E.-M. Nothig. 2006. Structure and function of contemporary food webs on Arctic shelves: A panarctic comparison. The pelagic system of the Kara Sea – Communities and components of carbon flow. Progress in Oceanography 71:288–313.

Holme, N.A. and A.D. McIntyre. 1984. Methods for the study of marine benthos. 2nd edition. Blackwell Scientific Publishers, Oxford, London. pp 387.

Holmes, R.M., M.T. Coe, G.J. Fiske, T. Gurtovaya, J.W. McClelland, A.I. Shiklomanov, R.G.M. Spencer, S.E. Tank, and A.V. Zhulidov. 2013. Climate change impacts on the hydrology and biogeochemistry of Arctic rivers. In: Goldman C.R., M. Kumagai, and R.D. Robarts [eds.]. Climatic change and global warming of inland waters: impacts and mitigation for ecosystems and societies. John Wiley & Sons, Ltd: Oxford, UK. pp 3–26.

Homma, T. and A. Yamaguchi. 2010. Vertical changes in abundance, biomass and community structure of copepods down to 3000 m in the southern Bering Sea. Deep-Sea Research Part I: Oceanographic Research Papers 57(8):965–977.

Hopcroft, R.R. 2005. Diversity in larvaceans: How many species? In: Gorsky G., M.J. Youngbluth, and D. Deibel [eds.]. Response of Marine Ecosystems to Global Change: Ecological Impact of Appendicularians. Paris: Contemporary Publishing International. pp 45–57.

Hopcroft, R.R., B. Bluhm, and R. Gradinger. 2008. Arctic Ocean synthesis: analysis of climate change impacts in the Chukchi and Beaufort Seas with strategies for future research. Final Report to the North Pacific Research Board. Anchorage. pp 182.

Hopcroft, R.R., C. Clarke, R.J. Nelson, and K.A. Raskoff. 2005. Zooplankton communities of the Arctic's Canada Basin: the contribution by smaller taxa. Polar Biology 28(3):198–206.

Hopcroft, R.R., K.N. Kosobokova, and A.I. Pinchuk. 2010. Zooplankton community patterns in the Chukchi Sea during summer 2004. Deep-Sea Research Part II: Topical Studies in Oceanography 57(1–2):27–39.

Hopcroft, R. R., C. Stark, and C. Clarke. 2012. WEBSEC-72: Rescue of historical Beaufort Sea zooplankton communities. North Pacific Research Board Final Report 929. Anchorage, pp. 19.

Hopkins, T.L. 1969. Zooplankton standing crop in the Arctic basin. Limnology and Oceanography 14(1):80–85.

Hopky, G.E., M.J. Lawrence, and D.B. Chiperzak. 1994a. NOGAP B2; Zooplankton data from the Canadian Beaufort Sea shelf 1984 and 1985. Canadian Data Report of Fisheries and Aquatic Sciences. Vol. 922. Winnipeg: Canada Department of Fisheries and Oceans. pp 164.

Hopky, G.E., M.J. Lawrence, and D.B. Chiperzak. 1994b. NOGAP B2; Zooplankton data from the Canadian Beaufort Sea shelf, 1986.Canadian Data Report of Fisheries and Aquatic Sciences. Vol. 923. Winnipeg: Canada Department of Fisheries and Oceans. pp 225.

Hopky, G.E., M.J. Lawrence, and D.B. Chiperzak. 1994c. NOGAP B2; Zooplankton data from the Canadian Beaufort Sea shelf, 1987 and 1988.Canadian Data Report of Fisheries and Aquatic Sciences. Vol. 912. Winnipeg: Canada Department of Fisheries and Oceans. pp 219.

Horner, R.A. 1978. Beaufort Sea Plankton Studies, NOAA OCSEP Annual Report of Principal Investigators for the Year Ending March 1978. Volume V. Receptors - Fish, Littoral, Benthos, pp. 85–142.

Horner, R.A. 1979. Beaufort Sea Plankton Studies. NOAA OCSEP Annual Report of Principal Investigators for the Year Ending March 1979. Volume III. Receptors - Fish, Littoral, Benthos, pp. 54–639.

Horner, R. 1980. Beaufort Sea plankton studies. NOAA OCSEP Final Report 13, pp. 65–314.

Horner, R.A. 1981. Beaufort Sea Plankton Studies, NOAA OCSEP Annual Report of Principal Investigators for the Year Ending March 1981, pp. 239–385.

Howell, K.L., D.S.M. Billett, and P.A. Tyler. 2002. Depth-related distribution and abundance of sea stars (Echinodermata: Asteroidea) in the Porcupine Seabight and Porcupine Abyssal plain, N.E. Atlantic. Deep-Sea Research Part I: Oceanographic Research Papers 49:1901–1920.

Howell, K.L., D.W. Pond, D.S.M. Billett, and P.A. Tyler. 2003. Feeding ecology of deep-sea seastars (Echinodermata: Asteroidea): a fatty-acid biomarker approach. Marine Ecology Progress Series 255:193–206.

Hufford, G.L., S.H. Fortier, D.E. Wolfe, J.F. Doster, D.L. Noble, P.W. Barnes, H.V. Weiss, H, K. Chew, M. Guttman, A. Host, A.S. Naidu, and T.C. Mowatt. 1974. An ecological survey in the Beaufort Sea August-September 1971-1972. Oceanographic Report. United States Coast Guard Oceanographic Unit, Washington, D.C., pp. 268.

Hunt, B.P.V., J.R. Nelson, B. Williams, F.A. McLaughlin, K.V. Young, K.A. Brown, S. Vagle, and E.C. Carmack. 2014. Zooplankton community structure and dynamics in the Arctic Canada Basin during a period of intense environmental change (2004–2009). Journal of Geophysical Research - Oceans 119(4):2518–2538.

Hunt, G.L., A.L. Blanchard, P. Boveng, P. Dalpadado, K. Drinkwater, L Eisner, R. Hopcroft, K.M. Kovacs, B.L. Norcross, P. Renaud, M. Reigstad, M. Renner, H.R. Skjoldal, A. Whitehouse, R.A. Woodgate. 2013. The Barents and Chukchi Seas: comparison of two Arctic shelf ecosystems. Journal of Marine Systems 109–110:43–68.

Hwang, J., T.I. Eglinton, R.A. Krishfield, S.J. Manganini, and S. Honjo. 2008. Lateral organic carbon supply to the deep Canada Basin. Geophysical Research Letters 35(11):L11607.

Ikeda, T., Y. Kanno, K. Ozaki, and A. Shinada. 2001. Metabolic rates of epipelagic marine copepods as a function of body mass and temperature. Marine Biology 139(3):587–596.

Iken, K., B.A. Bluhm, and K. Dunton. 2010. Benthic food-web structure under differing water mass properties in the southern Chukchi Sea. Deep-Sea Research Part II: Topical Studies in Oceanography 57(1–2):71–85.

Iken, K., B.A. Bluhm, and R. Gradinger. 2005. Food web structure in the high Arctic Canada Basin: evidence from $\delta^{13}C$ and $\delta^{15}N$ analysis. Polar Biology 28(3):238–249.

IPCC. 2014a. Climate Change 2014: Synthesis Report. Contribution of Working Groups I, II, and III to the Fifth Assessment Report of the Intergovernmental Panel on Climate Change [Core Writing Team, Pachauri R.K. and L.A. Meyer (eds.)]. Geneva: IPCC. pp 151.

IPCC. 2014b. Summary for policymakers. In: Climate change 2014: Impacts, adaptation, and vulnerability. Part A: Global and sectorial aspects. Contribution of working group II to the Fifth Assessment Report of the Intergovernmental Panel on Climate Change [Field, C.B, V.R. Barros, D.J., Dokken, K.J. Mach, M.D. Mastrandrea, T.E. Bilir, B.M. Chatterjee, K.L. Ebi, Y.O. Estrada, R.C. Genova, B. Girma, E.S. Kissel, A.N. Levy, S. MacCracken, P. R. Mastrandrea, and L.L. White (eds.)]. Cambridge University Press, Cambridge, United Kingdom and New York, NY, USA. pp 1–32.

Johnson, M.W. 1956. The plankton of the Beaufort and Chukchi Sea areas of the Arctic and its relation to the hydrography. Montreal: Arctic Institute of North America. pp 32.

Kaufman, M.R., R.R. Gradinger, B.A. Bluhm, and D.M. O'Brien. 2008. Using stable isotopes to assess carbon and nitrogen turnover in the Arctic sympagic amphipod *Onisimus litoralis*. Oecologia 158(1):11–22.

Kellogg, C.T.E. and J.W. Deming. 2014. Particle-associated extracellular enzyme activity and bacterial community composition across the Canadian Arctic Ocean. FEMS Microbiology Ecology 89(2):360–375.

Kelly, J.R. and R.E. Scheibling. 2012. Fatty acids as dietary tracers in benthic food webs. Marine Ecology Progress Series 446:1–22.

Kenny, A.J. and I. Sotheran. 2013. Characterising the physical properties of seabed habitats. In: A. Eleftheriou (Ed.), Methods for the Study of Marine Benthos, John Wiley & Sons, Ltd. West Sussex, UK. pp 47–95.

Konar, B. 2013. Epibenthic community variability on the Alaskan Beaufort Sea continental shelf. Finl Report, OCS Study BOEM 2013-01148. University of Alaska Fairbanks and USDOI, BOEM Alaska OCS Region. pp 43.

Konar, B., A. Ravelo, J. Grebmeier, and J.H. Trefry. 2014. Size frequency distributions of key epibenthic organisms in the eastern Chukchi Sea and their correlations with environmental parameters. Deep-Sea Research part II: Topical Studies in Oceanography 102:107–118.

Kosobokova, K. 2012. Zooplankton of the Arctic Ocean. Community structure, ecology, spatial distribution. GEOS, Moscow, pp. 272.

Kosobokova, K. and H.J. Hirche. 2000. Zooplankton distribution across the Lomonosov Ridge, Arctic Ocean: species inventory, biomass and vertical structure. Deep-Sea Research Part I: Oceanographic Research Papers 47(11):2029–2060.

Kosobokova, K. and H.J. Hirche. 2009. Biomass of zooplankton in the eastern Arctic Ocean - a base line study. Progress in Oceanography 82(4):265–280.

Kosobokova, K. and R.R. Hopcroft. 2010. Diversity and vertical distribution of mesozooplankton in the Arctic's Canada Basin. Deep-Sea Research Part II: Topical Studies in Oceanography 57(1–2):96–110.

Kosobokova, K., R.R. Hopcroft, and H.J. Hirche. 2011. Patterns of zooplankton diversity through the depths of the Arctic's central basins. Marine Biodiversity 41(1):29–50.

Kosobokova, K.N., H. Hanssen, H.J. Hirche, and K. Knickmeier. 1998. Composition and distribution of zooplankton in the Laptev Sea and adjacent Nansen Basin during summer, 1993. Polar Biology 19:63–76.

Kramer, M. 2010. The role of sympagic meiofauna in Arctic and Antarctic sea-ice food webs. PhD dissertation at the Institute for Polar Ecology, Christian Albrechts University Kiel. pp 215.

Kwok, R. and D.A. Rothrock. 2009. Decline in Arctic sea ice thickness from submarine and ICES at records: 1958–2008. Geophysical Research Letters 36(15): L15501.

Laakmann, S., M. Kochzius, and H. Auel. 2009. Ecological niches of Arctic deep-sea copepods: vertical partitioning, dietary preferences and different trophic levels minimize inter-specific competition. Deep-Sea Research Part I: Oceanographic Research Papers 56(5):741–756.

Lane, P.V.Z., L. Llinas, S.L. Smith, and D. Pilz. 2008. Zooplankton distribution in the western Arctic during summer 2002: hydrographic habitats and implications for food chain dynamics. Journal of Marine Systems 70(1–2):97–133.

Lansard, B., A. Mucci, L.A. Miller, R.W. Macdonald, and Y. Gratton. 2012. Seasonal variability of water mass distribution in the southeastern Beaufort Sea determined by total alkalinity and $\delta^{18}O$. Journal of Geophysical Research - Oceans 117(C3):C03003.

Lavoie, D., K.L. Denman, and R.W. Macdonald. 2010. Effects of future climate change on primary productivity and export fluxes in the Beaufort Sea. Journal of Geophysical Research - Oceans 115(C4):C04018.

Lefébure, R., R. Degerman, A. Andersson, S. Larsson, L.O. Eriksson, U. Båmstedt, and P. Byström. 2013. Impacts of elevated terrestrial nutrient loads and temperature on pelagic food-web efficiency and fish production. Global Change Biology 19(5):1358–1372.

Lehmann, M.F., S.M. Bernasconi, A. Barbieri, and J.A. McKenzie. 2002. Preservation of organic matter and alteration of its carbon and nitrogen isotope composition during simulated and in situ early sedimentary diagenesis. Geochimica et Cosmochimica Acta 66(20):3573–3584.

Leu, E., J.E. Søreide, D.O. Hessen, S. Falk-Petersen, and J. Berge. 2011. Consequences of changing sea-ice cover for primary and secondary producers in the European Arctic shelf seas: timing, quantity, and quality. Progress in Oceanography 90(1–4):18–32.

Levin, L.A., R.J. Etter, M.A. Rex, A.J. Gooday, C.R. Smith, J. Pineda, C.T. Stuart, R.R. Hessler, and D.L. Pawson. 2001. Environmental influences on regional deep-sea species diversity. Annual Review of Ecology and Systematics 32:51–93.

LGL Alaska Research Associates, Inc. 1999. The 1998 Endicott Development Fish Monitoring Program. Vol. I: Fish and hydrography data report. Report for BP Exploration (Alaska) Inc. and North Slope Borough. pp 21 + Appendices.

Link, H., D. Piepenburg, and P. Archambault. 2013. Are hotspots always hotspots? The relationship between diversity, resource and ecosystem functions in the Arctic. PLoS One 8(9):e74077.

Logerwell, E., K. Rand, S. Parker-Stetter, J. Horne, T. Weingartner, and B. Bluhm. 2010. Beaufort Sea marine fish monitoring 2008: pilot survey and test of hypotheses. Final Report of OCS study M07PG13152, BOEMRE 2010-048. pp 262.

Logerwell, E., K. Rand, and T.J. Weingartner. 2011. Oceanographic characteristics of the habitat of benthic fish and invertebrates in the Beaufort Sea. Polar Biology 34:1783–1796.

Lovvorn, J.R., S.E. Richman, J.M. Grebmeier, and L.W. Cooper. 2003. Diet and body condition of spectacled eiders wintering in pack ice of the Bering Sea. Polar Biology 26(4):259–267.

Lowry, L.F., G. Sheffield, and J.C. George. 2004. Bowhead whale feeding in the Alaskan Beaufort Sea, based on stomach contents analyses. Journal of Cetacean Research and Management 6:215–223.

Lowry, L.F. and K.J. Frost. 1981. Distribution, growth, and foods of Arctic cod (*Boreogadus saida*) in the Bering, Chukchi, and Beaufort seas. The Canadian Field-Naturalist 95(2):186–191.

MacDonald, I.R., B.A. Bluhm, K. Iken, S. Gagaev, and S. Strong. 2010. Benthic macrofauna and megafauna assemblages in the Arctic deep-sea Canada Basin. Deep Sea Research Part II: Topical Studies in Oceanography 57(1):136–152.

Macdonald, R.W. and Y. Yu. 2006. The Mackenzie estuary of the Arctic Ocean. Handbook of Environmental Chemistry 5:91–120.

Macdonald, R.W., A.S. Naidu, M.B. Yunker, and C. Gobeil. 2004. The Beaufort Sea: distribution, sources, fluxes, and burial rates of organic carbon. In: Stein R. and R.W. Macdonald [eds.]. The organic carbon cycle in the Arctic Ocean. Springer: Heidelberg. pp 177–192.

Macdonald, R.W., E.C. Carmack, F.A. McLaughlin, K. Iseki, D.M. Macdonald, and M.C. O'Brien. 1989. Composition and modification of water masses in the Mackenzie Shelf estuary. Journal of Geophysical Research - Oceans 94(C12):18057–18070.

Macdonald, R. W., C. S. Wong, and P. E. Erickson. 1987. The distribution of nutrients in the southeastern Beaufort Sea: Implications for water circulation and primary production. J. Geophys. Res. **92:** 2939-2952.

Macko, S.A. and M.L.F. Estep. 1984. Microbial alteration of stable nitrogen and carbon isotopic compositions of organic matter. Organic Geochemistry 6:787–790.

Mahoney, A.R., H. Eicken, A.G. Gaylord, and R. Gens. 2014. Landfast sea ice extent in the Chukchi and Beaufort Seas: the annual cycle and decadal variability. Cold Regions Science and Technology 103:41–56.

Majewski, A.R., B.R. Lynn, M.K. Lowdon, W.J. Williams, and J.D. Reist. 2013. Community composition of demersal marine fishes on the Canadian Beaufort Shelf and at Herschel Island, Yukon Territory. Journal of Marine Systems 127:55–64.

Majewski, A.R., K.D. Suchy, S.P. Atchison, J. Henry, S.A. MacPhee, W. Walkusz, J. Eert, M. Dempsey, A. Niemi, L. de Montety, M. Geoffroy, C. Giraldo, C. Michel, P. Archambault, W.J. Williams, L. Fortier, and J.D. Reist. 2016. Uniqueness of fishes and habitat utilization in oil and gas lease blocks relative to non-lease areas in the Canadian Beaufort Sea. 2016. Environmental Studies Revolving Funds Report Series, No. 2012-04N, Report Series 203. February 2016. Ottawa. xi + 90 p. DOI: 10.13140/RG.2.1.1757.2726.

Majewski, A.R., W. Walkusz, B.R. Lynn, S. Atchison, J. Eert, and J.D. Reist. 2015. Distribution and diet of demersal Arctic Cod, *Boreogadus saida*, in relation to habitat characteristics in the Canadian Beaufort Sea. Polar Biology 1-12. DOI: 10.1007/s00300-015-1857-y.

Mantoura, R.F.C., S.W. Wright, S.W. Jeffrey, R.G. Barlow, and D.E. Cummings. 1997. Filtration and storage of pigments from microalgae. Phytoplankton pigments in oceanography. Jeffrey S.W., R.F.C. Mantoura, and S.W. Wright. Paris, UNESCO Publishing**.** pp 283–305.

Matarese, A.C., A.W. Kendall Jr., D.M. Blood, and B.M. Vinter. 1989. Laboratory guide to early life history stages of Northeast Pacific fishes. NOAA Technical Report NMFS 80. pp 652.

Mathis, J.T., R.S. Pickart, R.H. Byrne, C.L. McNeil, G.W.K. Moore, L.W. Juranek, X.W. Liu, J. Ma, R.A. Easley, M.M. Elliot, J.N. Cross, S.C. Reisdorph, F. Bahr, J. Morison, T. Lichendorf, and R.A. Feely. 2012. Storm-induced upwelling of high pCO(2) waters onto the continental shelf of the western Arctic Ocean and implications for carbonate mineral saturation states. Geophysical Research Letters 39(7):L07606.

Matrai, P.A., E. Olson, S. Suttles, V. Hill, L.A. Codispoti, B. Light, and M. Steele. 2013. Synthesis of primary production in the Arctic Ocean: I. Surface waters, 1954–2007. Progress in Oceanography 110:93–106.

Matsuura, H. and S. Nishida. 2000. Fine structure of the "button setae" in the deep-sea pelagic copepods of the genus *Euaugaptilus* (Calanoida:Augaptilidae). Marine Biology 137(2):339–345.

Matta, M.E. and D.K. Kimura [eds.]. 2012. Age determination manual of the Alaska Fisheries Science Center Age and Growth Program. NOAA Professional Paper NMFS 13. pp 97.

Mauchline, J., J.H.S. Blaxter, A.J. Southward, and P.A. Tyler. 1998. The biology of calanoid copepods. San Diego: Academic Press. pp 710.

McClain, C.R. and J.P. Barry. 2010. Habitat heterogeneity, disturbance, and productivity work in concert to regulate biodiversity in deep submarine canyons. Ecology 91(4):964–976.

McConnell, M. 1977. An analysis of the zooplankton community structure of the western Beaufort Sea (WEBSEC 1971). MS Thesis. Naragansett: University of Rhode Island. pp 218.

Mclaughlin, F., K. Shimada, E. Carmack, M. Itoh, and S. Nishino. 2005. The hydrography of the southern Canada Basin, 2002. Polar Biology 28:182-189.

McMahon, K.W., W.G. Ambrose Jr., B.J. Johnson, M.Y. Sun , G.R. Lopez, L.M. Clough, and M.L. Carroll. 2006. Benthic community response to ice algae and phytoplankton in Ny Ålesund, Svalbard. Marine Ecology Progress Series 310:1–14.

McTigue, N.D. and K.H. Dunton. 2013. Trophodynamics and organic matter assimilation pathways in the northeast Chukchi Sea, Alaska. Deep-Sea Research Part II: Topical Studies in Oceanography 102:84–96.

Mecklenburg, C., P. Møller, and D. Steinke. 2011. Biodiversity of arctic marine fishes: taxonomy and zoogeography. Marine Biodiversity 41(1):109–140.

Mecklenburg, C.W., T.A. Mecklenburg, and L.K. Thorsteinson. 2002. Fishes of Alaska. American Fisheries Society, Bethesda, MD. pp 1037.

Mecklenburg, C. and D. Steinke. 2015. Ichthyofaunal baselines in the Pacific Arctic region and RUSALCA study area. Oceanography 28(3):158–189. http://dx.doi.org/10.5670/oceanogr.2015.64.

Michener, R. and K. Lajtha [eds.]. 2007. Stable isotopes in ecology and environmental science. Blackwell Publishing: Oxford. pp 565.

Mincks, S.L., C.R. Smith, and D.J. DeMaster. 2005. Persistence of labile organic matter and microbial biomass in Antarctic shelf sediments: Evidence of a sediment "food bank." Marine Ecology Progress Series 300:3–19.

Mintenbeck, K., T. Brey, U. Jacob, R. Knust, and U. Struck. 2008. How to account for the lipid effect on carbon stable-isotope ratio (δ^{13} C): sample treatment effects and model bias. Journal of Fish Biology 72(4):815–830.

Mintenbeck, K., U. Jacob, R. Knust, W.E. Arntz, and T. Brey. 2007. Depth-dependence in stable isotope ratio δ^{15}N of benthic POM consumers: the role of particle dynamics and organism trophic guild. Deep-Sea Research Part I:Oceanographic Research Papers 54(6):1015–1023.

Mohammed, A.A. and E.H. Grainger. 1974. Zooplankton data from the Canadian Arctic Archipelago, 1962. Canada Fisheries and Marine Service Technical Report. Environment Canada, Fisheries and Marine Services, Ste. Anne de Bellevue, Que, pp. 140.

Morata, N., P.E. Renaud, S. Brugel, K.A. Hobson, and B.J. Johnson. 2008. Spatial and seasonal variations in the pelagic-benthic coupling of the southeastern Beaufort Sea revealed by sedimentary biomarkers. Marine Ecology Progress Series 371:47–63.

Mulligan, R.P., W. Perrie, and S. Solomon. 2010. Dynamics of the Mackenzie River plume on the inner Beaufort shelf during an open water period in summer. Estuarine, Coastal and Shelf Science 89(3):214–220.

Mumm, N. 1991. On the summerly distribution of mesozooplankton in the Nansen Basin, Arctic Ocean. Alfred Wegener Institute for Polar and Marine Research, Bremerhaven, Germany, pp. 174.

Mumm, N., H. Auel, H. Hanssen, W. Hagen, C. Richter, and H.J. Hirche. 1998. Breaking the ice: large-scale distribution of mesozooplankton after a decade of Arctic and transpolar cruises. Polar Biology 20(3):189–197.

Nishida, S. and S. Ohtsuka. 1996. Specialized feeding mechanism in the pelagic copepod genus *Heterorhabdus* (Calanoida: Heterorhabdidae), with special reference to the mandibular tooth and labral glands. Marine Biology 126(4):619–632.

Nijssen, B., G.M O'Donnell, A.F. Hamlet, and D.P. Lettenmaier. 2001. Hydrologic sensitivity of global rivers to climate change. Climatic Change 50:143–175.

Nohara, D., A. Kitoh, M. Hosaka, and T. Oki. 2006. Impact of climate change on river discharge projected by multimodel ensemble. Journal of Hydrometeorology 7:1076–1089.

Norcross, B.L., B.A. Holladay, S.J. Apsens, L.E. Edenfield, B.P. Gray, and K.L. Walker. In review. Central Beaufort Sea Marine Fish Monitoring, Final Report. OCS Study BOEM 2017-033, Anchorage, AK: USDOI, BOEM, Alaska OCS Region.

Norcross, B.L., B.A. Holladay, M.S. Busby, and K.L. Mier. 2010. Demersal and larval fish assemblages in the Chukchi Sea. Deep-Sea Research II: Topical Studies in Oceanography 57(1–2):57–70.

Norcross, B.L., S.W. Raborn, B.A. Holladay, B.J. Gallaway, S.T. Crawford, J.T. Priest, L.E. Edenfield, and R. Meyer. 2013. Northeastern Chukchi Sea demersal fishes and associated environmental characteristics, 2009–2010. Continental Shelf Research 67:77−95.

NPFMC. 2009. Fisheries Management Plan for Fish Resources of the Arctic Management Area. North Pacific Fishery Management Council. 605 West 4th Ave, Suite 306, Anchorage, AK.

Okkonen, S.R., C.J. Ashjian, R.G. Campbell, W. Maslowski, J.L. Clement-Kinney, and R. Potter. 2009. Intrustion of warm Bering/Chukchi waters onto the shelf in the western Beaufort Sea. Journal of Geophysical Research - Oceans 114(C1):C00A11.

Olsen, E.M., M. Heino, G.R Lilly, M.J. Morgan, J. Brattey, B. Ernande, and U. Dieckmann. 2004. Maturation trends indicative of rapid evolution preceded the collapse of northern cod. Nature 428:932–935.

Orlov, A. and C. Binohlan. 2009. Length-weight relationships of deep-sea fishes from the western Bering Sea. Journal of Applied Ichthyology 25:223-227.

Orr, J.W., Y. Kai, and T. Nakabo. 2015. Snailfishes of the *Careproctus rastrinus* complex (Liparidae): redescriptions of seven species in the North Pacific Ocean region, with the description of a new species from the Beaufort Sea. Zootaxa 4018(3): 301–348. doi: 10.11646/zootaxa.4018.3.1

Ortega-Retuerta, E., W. Jeffrey, M. Babin, S. Bélanger, R. Benner, D. Marie, A. Matsuoka, P. Raimbault , and F. Joux. 2012. Carbon fluxes in the Canadian Arctic: patterns and drivers of bacterial abundance, production and respiration on the Beaufort Sea margin. Biogeosciences Discussions 9(5):6015–6050.

Page, L.M., H. Espinosa-Pérez, L.T. Findley, C.R. Gilbert, R.N. Lea, N.E. Mandrak, R.L. Mayden, and J.S. Nelson. 2013. Common and scientific names of fishes from the United States, Canada, and Mexico, 7th edition. American Fisheries Society, Special Publication 34, Bethesda MD. 384 pp.

Palumbi, S.R., P.A. Sandifer, J.D. Allan, M.W. Beck, D.G. Fautin, M.J. Fogarty, B.S. Halpern, L.S. Incze, J.A. Leong, E. Norse, and J.J. Stachowicz. 2008. Managing for ocean biodiversity to sustain marine ecosystem services. Frontiers in Ecology and the Environment 7(4):204–211.

Parnell, A.C., R. Inger, S. Bearhop, and A.L. Jackson. 2010. Source partitioning using stable isotopes: coping with too much variation. PLoS ONE 5(3):e9672.

Parrish, C.C. 2013. Lipids in marine ecosystems. ISRN Oceanography 2013:16.

Parsons, T.R., Y. Maite, and C.M. Lalli. 1984. A Manual for chemical and biological methods in seawater analysis. Toronto: Pergamon Press. pp 173.

Patrício, J., H. Adão, J.M. Neto, A.S. Alves, W. Traunspurger, and J.C. Marques. 2012. Do nematode and macrofauna assemblages provide similar ecological assessment information? Ecological Indicators 14(1):124–137.

Pearson, T.H. and R. Rosenberg. 1978. Macrobenthic succession in relation to organic enrichment and pollution in the marine environment. Oceanography and Marine Biology Annual Review 16:229–311.

Perry A.L., P.J. Low, J.R. Ellis and J.D. Reynolds. 2005. Climate change and distribution shifts in marine fishes. Science 308:1912–1915

Pethybridge, H., N. Bodin, E.J. Arsenault-Pernet, J.H. Bourdeix, B. Brisset, J. L. Bigot, D. Roos, and M. Peter. 2014. Temporal and inter-specific variations in forage fish feeding conditions in the NW Mediterranean: lipid content and fatty acid compositional changes. Marine Ecology Progress Series 512:39–54.

Philipp, E. and D. Abele. 2010. Masters of longevity: Lessons from long lived bivalves. Gerontology 56(1):55–65.

Pickart, R.S. 2004. Shelfbreak circulation in the Alaskan Beaufort Sea: Mean structure and variability. Journal of Geophysical Research - Oceans 109(C4):C04024.

Pickart, R.S., G.W.K. Moore, D.J. Torres, P.S. Fratantoni, R.A. Goldsmith, and J. Yang. 2009. Upwelling on the continental slope of the Alaskan Beaufort Sea: storms, ice, and oceanographic response. Journal of Geophysical Research - Oceans 114(C1): C00A13.

Pickart, R.S., L.M. Schulze, G.W.K. Moore, M.A. Charette, K.R. Arrigo, G. Van Dijken, and S.L. Danielson. 2013. Long-term trends of upwelling and impacts on primary productivity in the Alaskan Beaufort Sea. Deep-Sea Research Part I: Oceanographic Research Papers. 79:106–121.

Pickart, R.S., M.A. Spall, G.W.K. Moore, T.J. Weingartner, R.A. Woodgate, K. Aagaard, and K. Shimada. 2011. Upwelling in the Alaskan Beaufort Sea: Atmospheric forcing and local versus non-local response. Progress in Oceanography 88(1–4):78–100.

Piepenburg, D. 2005. Recent research on Arctic benthos: common notions need to be revised. Polar Biology 28(10):733–755.

Piepenburg, D., P. Archambault, W. Ambrose, A. Blanchard, B. Bluhm, M. Carroll, K. Conlan, M. Cusson, H. Feder, J. Grebmeier, and others. 2011. Towards a pan-Arctic inventory of the species diversity of the macro- and megabenthic fauna of the Arctic shelf seas. Marine Biodiversity 41:57–70.

Piepenburg, D., T.H. Blackburn, C.F. von Dorrien, J. Gutt, P.O.J. Hall, S. Hulth, M.A. Kendall, K.W. Opalinski, E. Rachor, and M.K. Schmid. 1995. Partitioning of benthic community respiration in the Arctic (northwest Barents Sea). Marine Ecology Progress Series 118:119–213.

Piepenburg, D. and M.K. Schmid. 1996. Brittle star fauna (Echinodermata: Ophiuroidea) of the Arctic northwestern Barents Sea: composition, abundance, biomass and spatial distribution. Polar Biology 16(6):383–392.

Piepenburg, D., J. Voss, and J. Gutt. 1997. Assemblages of sea stars (Echinodermata: Asteroidea) and brittle stars (Echinodermata: Ophiuroidea) in the Weddell Sea (Antarctica) and off Northeast Greenland (Arctic): a comparison of diversity and abundance. Polar Biology 17(4):305–322.

Pisareva, M.N., R.S. Pickart, M.A. Spall, C. Nobre, D.J. Torres, G.W.K. Moore, and T.E. Whitledge. 2015. Flow of Pacific water in the western Chukchi Sea: Results from the 2009 RUSALCA expedition. Deep-Sea Research I: Oceanographic Research Papers 105:53–73.

Post, D.M. 2002a. The long and short of food-chain length. Trends in Ecology and Evolution 17(6):269–277.

Post, D.M. 2002b. Using stable isotopes to estimate trophic position: models, methods and assumptions. Ecology 83(3):703–718.

Questel, J.M., C. Clarke, and R.R. Hopcroft. 2013. Seasonal and interannual variation in the planktonic communities of the northeastern Chukchi Sea during the summer and early fall. Continental Shelf Research 67:23–41.

Quinn, G.P. and M.J. Keough. 2002. Experimental design and data analysis for biologists. Cambridge University Press, Cambridge. pp 467–469.

R Development Core Team. 2014. R: A language and environment for statistical computing. R Foundation for Statistical Computing, Vienna, Austria. Retrieved from http://www.R-project.org/.

Rachold, V., H. Eicken, V.V. Gordeev, M.N. Grigoriev, H.W. Hubberten, A.P. Lisitzin, V.P. Shevchenko, and L. Schirrmeister. 2004. Modern terrigenous organic carbon input to the Arctic Ocean. In: Stein R. and R.W. Macdonald [eds.]. The organic carbon cycle in the Arctic Ocean. Springer: Heidelberg. pp 33–55.

Rand, K.M. and E.A. Logerwell. 2011. The first demersal trawl survey of benthic fish and invertebrates in the Beaufort Sea since the late 1970s. Polar Biology 34(4):475–488.

Rass, T.S. 1968. Spawning and development of polar cod. Rapports et Proces-verbaux des Réunions. Conseil International pour l'Éxploration de la Mer 158:135–137.

Ravelo, A.M., B. Konar, and B.A. Bluhm. 2015. Spatial variability of epibenthic communities on the Alaska Beaufort Shelf. Polar Biology 38(1):1783–1804.

Ravelo, A.M., B. Konar, J.H. Trefry, and J.M. Grebmeier. 2014. Epibenthic community variability in the northeastern Chukchi Sea. Deep-Sea Research II: Topical Studies in Oceanography 102:119–131.

Reist, J.D. 1994. An overview of the possible effects of climate change on northern freshwater and anadromous fishes. In: Cohen S.J. (Ed.), Mackenzie Basin Impact Study (MBIS), Interim Report 2, Environment Canada, Ottawa. pp 377–385.

Reitan, K.I., J.R. Rainuzzo, and Y. Olsen. 1994. Effect of nutrient limitation on fatty acid and lipid content of marine microalgae. Journal of Phycology 30(6):972–979.

Renaud, P.E., J. Berge, Ø. Varpe, O. Lønne, J. Nahrgang, C. Ottesen, and I. Hallanger. 2012. Is the poleward expansion by Atlantic cod and haddock threatening native polar cod, *Boreogadus saida*? Polar Biology 35(3):401–412.

Renaud, P.E., N. Morata, M.L. Carroll, S.G. Denisenko, and M. Reigstad. 2008. Pelagic-benthic coupling in the western Barents Sea: processes and time scales. Deep Sea Research Part II: Topical Studies in Oceanography 55(20–21):2372–2380.

Renaud, P.E., M. Tessmann, A. Evenset, and G.N. Christensen. 2011. Benthic food-web structure of an Arctic fjord (Kongsfjorden, Svalbard). Marine Biology Research 7(1):13–26.

Richardson, A. J. 2008. In hot water: zooplankton and climate change. ICES Journal of Marine Science 65:279-295.

Ricker, W.E. 1975. Computation and interpretation of biological statistics of fish populations. Bulletin of the Fisheries Research Board of Canada. pp 400.

Ringuette, M., L. Fortier, M. Fortier, J.A. Runge, S. Belanger, P. Larouche, J.M. Weslawski, and S. Kwasniewski. 2002. Advanced recruitment and accelerated population development in Arctic calanoid copepods of the north water. Deep-Sea Research Part II: Topical Studies in Oceanography 49(22–23):5081–5099.

Roberts, D., A. Gebruk, V. Levin, and B.A.D. Manship. 2000. Feeding and digestive strategies in deposit-feeding holothurians. Oceanography and Marine Biology. An Annual Review 38:257–310.

Robinson, C., D.K. Steinberg, T.R Anderson, J. Aristegui, C.A. Carlson, J.R. Frost, J.F. Ghiglione, S. Hernandez-Leon, G.A. Jackson, R. Koppelmann, B. Queguiner, O. Ragueneau, F. Rassoulzadegan, B.H. Robison, C. Tamburini, T. Tanaka, K.F Wishner, and J. Zhang. 2010. Mesopelagic zone ecology and biogeochemistry - a synthesis. Deep-Sea Research Part II 57:1504-1518.

Robinson, R.S., M. Kinast, A.L. Albuquerque, M. Altabet, S. Contreras, R. De Pol Holz, N. Dubois, R. Francois, E. Galbraith, T-C. Hsu, T. Ivanochko, S. Jaccard, S-J. Kao, T. Keifer, S. Kienast, M. Lehmann, P. Martinez, M. McCarthy, J. Möbius, T. Pedersen, T.M. Quan, E. Ryabenko, A. Schmittner, R. Schneider, A. Schneider-Mor, M. Shigemitsu, D. Sinclair, C. Somes, A. Studer, R. Thunell, and J-Y. Yang. 2012. A review of nitrogen isotopic alteration in marine sediments. Paleoceanography 27(4):PA4203.

Roff, J. C. and R.R. Hopcroft. 1986. High-precision microcomputer based measuring system for ecological research. Canadian Journal of Fisheries and Aquatic Sciences. 43(10):2044–2048.

Román, E. and X. Paz. 1997. Length/Weight relationships for Greenland halibut, *Reinhardtius hippoglossoides*, from Northwest Atlantic (NAFO Regulatory Area: Divisions 3L, 3M and 3NO). Northwest Atlantic Fisheries Organization Serial No. N2845, NAFO SCR Doc. 97/16, 18 p.

Rontani, J-F., B. Charrière, R. Sempéré, D. Doxaran, F. Vaultier, J.E. Vonk, and J.K. Volkman. 2014. Degradation of sterols and terrigenous organic matter in waters of the Mackenzie Shelf, Canadian Arctic. Organic Geochemistry 75:61–73.

Roy, V., K. Iken, and P. Archambault. 2014. Environmental drivers of the Canadian Arctic mega-epibenthic communities. PLoS ONE 9(7):e100900.

Roy, V., K. Iken, and P. Archambault. 2015b. Regional variability of megabenthic community structure across the Canadian Arctic. Arctic 68(2):180–192.

Roy, V., K.I. Iken, M. Gosselin, J-E. Tremblay, S. Belanger, and P. Archambault. 2015a. Benthic faunal assimilation pathways and depth-related changes in food-web structure across the Canadian Arctic. Deep-Sea Research Part I: Oceanographic Research Papers 102:55–71.

Rudels, B., A. Larsson, and P.-I. Sehlstedt. 1991. Stratification and water mass formation in the Arctic Ocean: some implications for the nutrient distribution. Polar Res. **10:** 19-31.

Sakshaug, E. 2004. Primary and secondary production in the Arctic seas. In: R. Stein and R.W. Macdonald [eds.]. The organic carbon cycle in the Arctic Ocean. Springer: Heidelberg. pp 57–81.

Sargent, J., G. Bell, L. McEvoy, D. Tocher, and A. Estevez. 1999. Recent developments in the essential fatty acid nutrition of fish. Aquaculture 177(1–4):191–199.

Schell, D.M. 1983. Carbon-13 and carbon-14 abundances in Alaskan aquatic organisms: delayed production from peat in Arctic food webs. Science 219(4588):1068–1071.

Schell, D.M., P.J. Ziemann, D.M. Parrish, K.H. Dunton, and E.J. Brown. 1984. Foodweb and nutrient dynamics in nearshore Alaska Beaufort Sea waters. US Dep. Commerce, NOAA, OCSEAP Final Rep. 25. pp 327–499.

Schlitzer, R. 2011. "Ocean data view version 4.5.3" Alfred Wegener Institute for Polar and Marine Research, Bremerhaven, Germany.

Schnack-Schiel, S.B., J. Michels, E. Mizdalski, M.P. Schodlok, and M. Schröder. 2008. Composition and community structure of zooplankton in the sea ice-covered western Weddell Sea in spring 2004 - with emphasis on calanoid copepods. Deep-Sea Research II. 55:1040–1055.

Serreze, M.C., M.M. Holland, and J. Stroeve. 2007. Perspectives on the Arctic's shrinking sea ice cover. Science 315(5818):1533–1536.

Simpson, K. G., J.-É. Tremblay, Y. Gratton, and N. M. Price. 2008. An annual study of inorganic and organic nitrogen and phosphorus and silicic acid in the southeastern Beaufort Sea. Journal Geophysical Research 113:C07016.

Smale, D.A., T.J. Langlois, G.A. Kendrick, J.J. Meeuwig, and E.S. Harvey. 2011. From fronds to fish: the use of indicators for ecological monitoring in marine benthic ecosystems, with case studies from temperate Western Australia. Review of Fish Biology and Fisheries 21:311–337

Smirnov, A.V. 1994. Arctic echinoderms: Composition distribution and history of the fauna. In: David B., A. Guille, J.P. Feral, and M. Roux [eds.]. Echinoderms through Time. Balkema, Rotterdam. pp 135–143.

Smith, R.L., W.E. Barber, M. Vallarino, J.G. Gillispie, and A. Ritchie. 1997. Population biology of the Arctic staghorn sculpin in the northeastern Chukchi Sea. In: Reynolds JB [eds.]. Fish ecology in arctic North America. American Fisheries Society Symp 19, Bethesda, Maryland, pp 133-139.

Smith, C.R., S. Mincks, and D.J. DeMaster. 2006. A synthesis of bentho-pelagic coupling on the Antarctic shelf: Food banks, ecosystem inertia and global climate change. Deep-Sea Research Part II: Topical Studies in Oceanography 53(8–10):875–894.

Smoot, C.A. 2015. Contemporary mesozooplankton communities of the Beaufort Sea. M.S. Thesis. Fairbanks: University of Alaska Fairbanks. pp 110.

Smoot, C.A and R.R. Hopcroft. 2017. Depth-stratified community structure of Beaufort Sea slope zooplankton and its relations to water masses. Journal of Plankton Research 39(1):79–91. https://doi.org/10.1093/plankt/fbw087

Sommer, U., H. Stibor, A. Katechakis, F. Sommer, and T. Hansen. 2002. Pelagic food web configurations at different levels of nutrient richness and their implications for the ratio fish production: primary production. In: Sustainable Increase of Marine Harvesting: Fundamental Mechanisms and New Concepts Springer, Netherlands. pp 11–20.

Søreide, J.E., H. Hop, M.L. Carroll, S. Falk-Petersen, and E.N. Hegseth. 2006. Seasonal food web structures and sympagic–pelagic coupling in the European Arctic revealed by stable isotopes and a two-source food web model. Progress in Oceanography 71(1):59–87.

Søreide, J.E., E. Leu, J. Berge, M. Graeve, and S. Falk-Petersen. 2010. Timing of blooms, algal food quality and *Calanus glacialis* reproduction and growth in a changing Arctic. Global Change Biology 16(11):3154–3163.

Stephens, M.P., D.C. Kadko, C.R. Smith, and M. Latasa. 1997. Chlorophyll-*a* and phaeopigments as tracers of labile organic carbon at the central equatorial Pacific seafloor. Geochimica et Cosmochimica Acta 61(21):4605–4619.

Stowasser, G., D.W. Pond, and M.A. Collins. 2012. Fatty acid trophic markers elucidate resource partitioning within the demersal fish community of South Georgia and Shag Rocks (Southern Ocean). Marine Biology 159(10):2299–2310.

Stroeve, J.C., M.C. Serreze, M.M. Holland, J.E. Kay, J. Malanik, and A.P. Barrett. 2012. The Arctic's rapidly shrinking sea ice cover: a research synthesis. Climatic Change 110:1005–1027.

Sun, M-Y., M.L. Carroll, W.G. Ambrose Jr., L.M. Clough, L. Zou, and G.R. Lopez. 2007. Rapid consumption of phytoplankton and ice algae by Arctic soft-sediment benthic communities: evidence using natural and ^{13}C-labeled food materials. Journal of Marine Research 65(4):561–588.

Suzuki, K.W., C. Bouchard, D. Robert, and L. Fortier. 2015. Spatiotemporal occurrence of summer ichthyoplankton in the southeast Beaufort Sea. Polar Biology 38(9):1379–1389.

Telang, S.A., R. Pocklington, A.S. Naidu, E.A. Romankevich, I.I. Gitelson, and M.I. Gladyshev. 1991. Carbon and mineral transport in major North American, Russian Arctic, and Siberian rivers: the St. Lawrence, the Mackenzie, the Yukon, the Arctic Alaskan rivers, the Arctic Basin rivers in the Soviet Unon, and the Yenisei. In: Degens E.T., S. Kempe, and J.E. Richey [eds.]. Biogeochemistry of major world rivers. Wiley: Chichester. pp 75–104.

Tenore, K.R. 1983. What controls the availability to animals of detritus derived from vascular plants: organic nitrogen enrichment or caloric availability? Marine Ecology Progress Series 10:307–309.

Ter Braak, C.J.F. 1986. Canonical correspondence analysis: a new eigenvector technique for multivariate direct gradient analysis. Ecology 67:1167–1179.

Thibault, D., E.J.H. Head, and P.A. Wheeler. 1999. Mesozooplankton in the Arctic Ocean in summer. Deep-Sea Research Part I: Oceanographic Research Papers. 46(8):1391–1415.

Thorsteinson, L.K., L.E. Jarvala, and D.A. Hale. 1992. Arctic fish habitat use habitat investigations: nearshore studies in the Alaskan Beaufort Sea, Summer 1990. Annual Report OCS Study MMS 92-0011. pp 78.

Thorsteinson, L.K., and M.S. Love [eds.]. 2016. Alaska Arctic marine fish ecology catalog: US Geological Survey Investigations Report 2016-5038 (OCS Study, BOEM 2016-048), 768 p., http://dx.doi.org?10.3133/sir20165038.

Thorton, S.F. and J. McManus. 1994. Application of organic carbon and nitrogen stable isotope and C/N ratios as source indicators of organic matter provenance in estuarine systems: evidence from the Tay Estuary, Scotland. Estuarine, Coastal and Shelf Science 38(3):219–233.

Tokranov, A.M. and A. M. Orlov. 2005. Some features of the biology of *Icelus spatula* (Cottidae) in Pacific waters off the Northern Kuril Islands. Journal of Ichthyology 45(3):229–236.

Tremblay, J. and others. 2008. Vertical stability and the annual dynamics of nutrients and chlorophyll fluorescence in the coastal, southeast Beaufort Sea. Journal Geophysical Research (C Oceans) 113:C07S90. doi:10.1029/2007JC004547

Tucker, W.B., W.F. Weeks, and F.M. 1979. Sea Ice ridging over the Alaskan continental shelf. Journal Geophysical Research 84:4885–4897.

Turner, J.T., H. Levinsen, T.G. Nielsen, and B.W. Hansen. 2001. Zooplankton feeding ecology: grazing on phytoplankton and predation on protozoans by copepod and barnacle nauplii in Disko Bay, West Greenland. Marine Ecology Progress Series 221:209–219.

US EPA Office of Water. 2010. National Coastal Condition Assessment Laboratory Methods Manual, Washington DC, EPA No. 841-R-09-002. pp 192–198.

Vallières, C., L. Retamal, P. Ramlal, C.L. Osburn, and W.F. Vincent. 2008. Bacterial production and microbial food web structure in a large Arctic river and the coastal Arctic Ocean. Journal of Marine Systems 74(3–4):756–773.

Vander Zanden, M.J. and J.B. Rasmussen. 1999. Primary consumer $\delta^{13}C$ and $\delta^{15}N$ and the trophic postion of aquatic consumers. Ecology 80(4):1395–1404.

Vander Zanden, M.J. and J.B. Rasmussen. 2001. Variation in $\delta^{15}N$ and $\delta^{13}C$ trophic fractionation: implications for aquatic food web studies. Limnology and Oceanography 46(8):2061–2066.

Viso, A.-C. and J.-C. Marty. 1993. Fatty acids from 28 marine microalgae. Phytochemistry 34(6):1521–1533.

Walkusz, W., A. Majewski, and J.D. Reist. 2013. Distribution and diet of the bottom dwelling Arctic cod in the Canadian Beaufort Sea. Journal of Marine Systems 127:65–75.

Walkusz, W., J.E. Paulić, S. Kwaśniewski, W.J. Williams, S. Wong, and M.H. Papst. 2010. Distribution, diversity and biomass of summer zooplankton from the coastal Canadian Beaufort Sea. Polar Biology 33(3):321–335.

Walkusz, W., J.E. Paulic, W.J. Williams, S. Kwaśniewski, and M.H. Papst. 2011. Distribution and diet of larval and juvenile Arctic cod (*Boreogadus saida*) in the shallow Canadian Beaufort Sea. Journal of Marine Systems 84(3–4):78–84.

Walkusz, W., W.J. Williams, L.A. Harwood, S.E. Moore, B.E. Stewart, and S. Kwasniewski. 2012. Composition, biomass and energetic content of biota in the vicinity of feeding bowhead whales (*Balaena mysticetus*) in the Cape Bathurst upwelling region (south eastern Beaufort Sea). Deep-Sea Research Part I 69:25–35.

Wallace, M.I., F.R. Cottier, J. Berge, G.A.Tarling, C. Griffiths, and A.S. Brierley. 2010. Comparison of zooplankton vertical migration in an ice-free and a seasonally ice-covered Arctic fjord: an insight into the influence of sea ice cover on zooplankton behavior. Limnology and Oceanography 55:831–845.

Ward, J.E. and S.E. Shumway. 2004. Separating the grain from the chaff: particle selection in suspension- and deposit-feeding bivalves. Journal of Experimental Marine Biology and Ecology 300(1–2):83–130.

Wassmann, P., C.M. Duarte, S. Agusti, and M.K. Sejr. 2011. Footprints of climate change in the Arctic marine ecosystem. Global Change Biology 17:1235–1249.

Weems, J., K. Iken, R. Gradinger, and M.J. Wooller. 2012. Carbon and nitrogen assimilation in the Bering Sea clams *Nuculana radiata* and *Macoma moesta*. Journal of Experimental Marine Biology and Ecology 430–431:32–42.

Weingartner, T. J., D. J. Cavalieri, K. Aagaard, and Y. Sasaki. 1998. Circulation, dense water formation, and outflow on the northeast Chukchi shelf. Journal Geophysical Research 103:7647–7661.

Weingartner, T. J., S. R. Okkonen, and S. L. Danielson. 2005. Circulation and Water Property Variations in the Nearshore Alaskan Beaufort Sea, p. 103. Final Report. OCS Study MMS 2005-028.

Werner, I. and P.M. Arbizu. 1999. The sub-ice fauna of the Laptev Sea and the adjacent Arctic Ocean in summer 1995. Polar Biology 21(2):71–79.

Whitehouse, G.A., K. Aydin, T. Essington, and G. Hunt Jr. 2014. A trophic mass balance model of the eastern Chukchi Sea with comparisons to other high-latitude systems. Polar Biology 37(7):911–939.

Wienerroither R., E. Johannesen, A. Dolgov, I. Byrkjedal, A Aglen, O. Bjelland, K. Drevetnyak, K.B. Eriksen, Å. Høines, G. Langhelle, H. Langøy, P. Murashko, T. Prokhorova, D. Prozorkevich, O. Smirnov, and T. Wenneck. 2013. Atlas of the Barents Sea Fishes based on the winter survey. IMR-PINRO Joint Report Series 2-2013. ISSN 1502-8828, 220 pp.

Wienerroither, R., E. Johannesen, A. Dolgov, I. Byrkjedal, O. Bjelland, K. Drevetnyak, K.B. Eriksen, Å. Høines, G. Langhelle, H. Langøy, T. Prokhorova, D. Prozorkevich, and T. Wenneck. 2011. Atlas of the Barents Sea Fishes. IMR/PINRO Joint Report Series 1-2011.

Williams, W.J., E.C. Carmack, K. Shimada, H. Melling, K. Aagaard, R.W. Macdonald, and R.G. Ingram. 2006. Joint effects of wind and ice motion in forcing upwelling in Mackenzie Trough, Beaufort Sea. Continental Shelf Research 26(19):2352–2366.

Wilson, S.E., D.K. Steinberg, F.L.E. Chu, and J.K.B. Bishop. 2010. Feeding ecology of mesopelagic zooplankton of the subtropical and subarctic North Pacific Ocean determined with fatty acid biomarkers. Deep-Sea Research Part I 57:1278–1294.

Wood, H.L., J.I. Spicer, M.A. Kendall, D.M. Lowe, and S. Widdicombe. 2011. Ocean warming and acidification; implications for the Arctic brittlestar Ophiocten sericeum. Polar Biology 34(7):1033–1044.

Wood, K.R., J.E. Overland, S.A. Salo, N.A. Bond, W.J. Williams, and X. Dong. 2013. Is there a ‘‘new normal’’ climate in the Beaufort Sea? Polar Research 32:19552.

Woodgate, R., T.J. Weingartner, and R. Lindsay. 2012. Observed increases in Bering Strait oceanic fluxes from the Pacific to the Arctic from 2001 to 2011 and their impacts on the Arctic Ocean water column. Geophysical Research Letters 39:L24603.

Wooller, M.J., G.D. Zazula, M. Edwards, D.G. Froese, R.D. Boone, C. Parker, and B. Bennett. 2007. Stable carbon isotope compositions of Eastern Beringian grasses and sedges: investigating their potential as paleoenvironmental indicators. Arctic, Antarctic, and Alpine Research 39(2):318–331.

Yamaguchi, A. 2008. Comparison of mesozooplankton biomass down to the greater depths (0-3000 m) between 165˚E and 165˚W in the North Pacific Ocean: the contribution of large copepod *Neocalanus cristatus*. In: Tewles, KB (ed.) The Pacific and Arctic Oceans: new Oceanographic Res. Nova Science Publishers, Inc. 17 p.

Yamaguchi, A., Y. Watanabe, H. Ishida, T. Harimoto, K. Furusawa, S. Suzuki, J. Ishizaka, T. Ikeda, and M.T. Masayuki. 2002. Community and trophic structures of pelagic copepods down to greater depths in the western subarctic Pacific (WEST-COSMIC). Deep-Sea Research Part I 49:1007–1025.

Yen, J. 1983. Effects of prey concentration, prey size, predator life stage, predator starvation, and season on predation rates of the carnivorous copepod *Euchaeta elongata*. Marine Biology 75:69–77.

Yen, J. 1987. Predation by carnivorous marine copepod, *Euchaeta norvegica*, on eggs and larvae of the North Atlantic cod *Gadus morhua*. Journal of Experimental Marine Biology and Ecology 112:283–296.

TECHNICAL SUMMARY

ACCESS NUMBER: 2017-034

STUDY TITLE: US-Canada Transboundary Fish and Lower Trophic Communities: Abundance, Distribution, Habitat and Community Analysis

REPORT TITLE: US-Canada Transboundary Fish and Lower Trophic Communities: Abundance, Distribution, Habitat and Community Analysis

CONTRACT NUMBER: M12AC00011

SPONSORING OCS REGION: Alaska

APPLICABLE PLANNING AREA: Beaufort Sea

FISCAL YEARS OF PROJECT FUNDING: 2011–2018

COMPLETION DATE OF REPORT: December 2017

CUMULATIVE PROJECT COST: 4,731,465

PROJECT MANAGER(S): Brenda L. Norcross

AFFILIATION (OF PROJECT MANAGER): University of Alaska Fairbanks

ADDRESS: PO Box 757220, Fairbanks, AK 99775-7220

PRINCIPAL INVESTIGATOR(S)*: Brenda L. Norcross, Bodil Bluhm, Sarah Hardy, Russel Hopcroft, Katrin Iken

KEY WORDS: Beaufort Sea, oceanography, temperature, salinity, sediment, chlorophyll, zooplankton, infauna, epibenthos, fish, assemblages, food web, under ice, monitoring

BACKGROUND: Historical data were limited, especially in the eastern Beaufort Sea, where information about marine fish and lower trophic communities has been extrapolated from data in the western Beaufort Sea, Chukchi Sea or Bering Sea. There was no knowledge about the effect of the Mackenzie River on the US eastern Beaufort Sea ecology.

OBJECTIVES:

1. Collaborate with Fisheries and Oceans Canada (DFO) Central Arctic Region to coordinate cruise times and sample.
2. Document and correlate baseline fish and invertebrate species (zooplankton, infauna, epibenthos) presence, abundance, distribution, and habitat in the eastern Beaufort Sea during the open water season.

3. Test under-ice methods to provide baseline information for the ice-covered season.
4. Based on survey results, recommend a nested sampling design and refinements of survey methods for future monitoring studies.
5. Document the physical and chemical water characteristics that will contribute to a collaborative effort to establish oceanographic boundary conditions in the eastern US Beaufort Sea.

DESCRIPTION: Open water shipboard surveys were conducted during September 2012 and August 2013 and 2014 from the central US Beaufort Sea north of Harrison Bay (151° W) into the eastern Canadian Beaufort Sea just east of the Mackenzie Canyon (137° W). Sampling included physical and chemical oceanography, chlorophyll, benthic environment, zooplankton, infauna, epifauna, demersal fish and midwater fish. This project was the first time that US Beaufort Sea continental slope at 200–1000 m was extensively sampled by bottom trawl.

SIGNIFICANT CONCLUSIONS: Distinct community patterns for all trophic levels were seen within and among years. Zooplankton communities were most similar to each other within a year, although larger interannual differences occurred. In contrast, the epifauna and fish communities formed at a much lower level of similarity, but their community composition tended to be more similar across years. Patterns may be due to the shorter life spans and highly modulated seasonality of zooplankton communities in comparison to benthos and fishes. This suggests that planktonic habitat is generally smoother and less variable than the benthic and demersal habitats. Thus, it should be easier to link plankton to environmental gradients on an annual basis. In contrast, the benthic and demersal habitats tended to be more heterogeneous at the scale of sampling, which ranged from 10s of meters to ~5 km and the epibenthic and fish communities still responded to larger scale environmental gradients. Fish and epibenthos distributions are likely not directly controlled by a single abiotic factor but rather by large-scale processes and interdependent physical, chemical, and geological factors. Therefore, these ecosystem components are likely excellent indicators of longer-term, persistent changes in environmental conditions. Depth, which is correlated to closely the environmental variables of temperature, salinity, density and water mass, is the easiest factor to measure to estimate the distribution of these communities.

Shelf fishes typically have shorter lifespans of about 5–7 years and slope species are mainly eelpouts with life spans of more than 12 years. The median of the oldest age classes suggests the number of years required to turn over the population, i.e., to start over after a negative impact. Shorter-lived shallow shelf species would be less resilient in the short term and more subject to immediate effects of change in their environment. Long-lived species on the slope should be more resilient to short-term perturbation; the environment on the slope is more stable below 300 m with little change in temperature, salinity, and water mass. Long-lived species could be considered more stable because an event that negatively impacts a single year class would affect only a small percentage of the total population. However, if a negative effect lasts multiple years (e.g., warmer seawater, changes in oceanographic currents, anthropogenic forces), the impact could last longer and affect multiple year classes; it could take many years to rebuild the population structure.

The interplay of high inputs of terrestial organic matter (OM_{terr}) from Alaska's and Canada's permafrost and rivers with both advected and *in situ* marine primary production drives variation

in marine trophic structure across the shelf and slope in the Beaufort Sea. Our results challenge the paradigm that OM_{terr} is an unusable or poor food source for marine consumers.

STUDY RESULTS: This research identified fish species inhabiting the eastern Beaufort Sea study area and provided baseline information about abundance, distribution, habitat, and variability of zooplankton, infauna, epifauna, and fishes. Strong community segregation was related to depth strata and prominent in all trophic levels; water mass was closely tied to depth. The 100–200 m contour, which generally corresponds to the shelf break, formed a consistent breakpoint across assemblages. Zooplankton, epifauna, and fish communities all had abundance and biomass patterns closely linked to depth, but the patterns did not coincide.

Zooplankton abundance and biomass was greatest at stations <100 m. The primary shelf-slope zooplankton community gradient was modified by localized hydrographic conditions and processes. Juvenile and adult *Pseudocalanus* species usually typified neritic shelf assemblages, while the oceanic *Calanus hyperboreus* and *Microcalanus pygmaeus* were characteristic of offshore assemblages. As water depth increased near the slope, the mixtures of zooplankton species shifted vertically and indicated water masses. The *Pseudocalanus* species complex indicated the Polar Mixed Layer (PML), *Paraeuchaeta glacialis* indicated Arctic Halocline Water (AHW), and *Spinocalanus longicornis* indicated Atlantic Water (AW).

Abundance and biomass of epibenthos was highest at 50–200 m depths. In contrast, the peak macro-infauna abundance was at 350 m, mainly Cossuridae polychaetes. Depth, salinity, and temperature were the main variables influencing epibenthic community structure. The small-bodied brittle star, *Ophiocten sericeum*, indicated the shelf at 50–100 m; whereas depths >500 m were characterized by large-bodied sea stars (e.g., *Bathybiaster vexillifer*), holothurians (*Molpadia borealis*), and brittle stars (*Ophiopleura borealis*). The distinct depth zonation in brittle stars and the dominant role each species plays within the communities at their specific depth ranges showcases the overall importance of brittle stars in Arctic benthic systems and may indicate resource partitioning among these species.

Demersal fish showed an inverse relationship of biomass and abundance with few, very large fish in deep water (biomass greatest at >350 m) and many, very small fishes in shallower water (abundance highest at depths <100, especially at 20 m). In general, the species of fish in deep water were not the same as those in shallow water. Shelf communities were clearly associated with PML (≤50 m) and characterized by small *Boreogadus saida* (<100 mm) and at least three of four sculpin species (*Artediellus scaber, Gymnocanthus tricuspis, Icelus spatula, Triglops pingelii*). Slope communities were linked with AW (>250 m) and typified by *B. saida* (>100 mm), *Lycodes adolfi, L. sagittarius,* and *L. seminudus*. There were less distinct, patchy fish communities at 100–200 m, the depth of the AHW, often with no species in common. Species found in the shelf break community may or may not be found in shelf communities. Salinity and temperature (the components of water mass) were correlated with both biomass and abundance of demersal fishes, though not as strongly as was depth.

In contrast, pelagic larval and juvenile fishes did not have a depth pattern; there were low abundances everywhere except in the central (150º W) Beaufort Sea. The central community was composed approximately equally of *B. saida*, *Liparis* spp. (snailfishes), and unidentified Lumpeninae. The eastern communities were even less diverse with many *B. saida* on the slope and *B. saida*, Cottidae ≤50 mm, and *Liparis* spp. on the shelf.

Feeding ecology examined at multiple levels. Fish species' diets were generally more similar within families than between them except for *Lycodes adolfi, L. polaris, L. sagittarius,* and *L.*

seminudus which had highly variable diets, both among individuals of the same species and among all Zoarcidae. Significant differences in fatty acid profiles between *B.* and *Lycodes* species confirmed separation in foraging habits of these fishes. Food web structure showed a strong isotopic imprint of OM_{terr} in the eastern Beaufort Sea in the Mackenzie River area that decreased westward from the Mackenzie River. Concurrent with high OM_{terr} influence, shelf and slope food webs in the eastern Beaufort Sea were characterized by comparatively longer food webs and a greater proportion of epibenthic consumer biomass at higher trophic levels compared with central Beaufort Sea food webs. Benthic food web structure over two study years was relatively stable, confirming that benthic consumers are good integrators of short-term variability in surface production.

A comprehensive monitoring plan was developed to be flexible based in any of multiple possible objectives. The objectives could range from health of the ecosystem to persistence of indicator species.

STUDY PRODUCT(S):

Apsens, S.J. 2017. Characterization of the diets of four *Lycodes* species in the U.S. Beaufort Sea. Fairbanks, AK: M.S. thesis, Univeristy of Alaska Fairbanks. xx p.

Bell, L. 2015. The influence of terrestial matter in marine food webs of the Beaufort Sea shelf and slope. Fairbanks, AK: M.S. thesis, Univeristy of Alaska Fairbanks. 79 p.

Bell, L.E., B.A. Bluhm, and K. Iken. 2016. Influence of terrestrial organic matter in marine food webs of the Beaufort Sea shelf and slope. Marine Ecology Progress Series 550:1–24.

Dissen, J. 2015. Fatty acid profiles of Alaskan Arctic forage fishes: evidence of regional and temporal variation. Fairbanks, AK: M.S. thesis, Univeristy of Alaska Fairbanks. 104 p.

Smoot, C.A. 2015. Contemporary mesozooplankton communities of the Beaufort Sea. Fairbanks, AK: M.S. thesis, Univeristy of Alaska Fairbanks. 110 p.

Smoot, C.A. and R.R. Hopcroft. 2017. Cross-shelf gradients of epipelagic zooplankton communities of the Beaufort Sea and the influence of localized hydrographic features. Journal of Plankton Research 39(1):65–78. https://doi.org/10.1093/plankt/fbw080

Smoot, C.A and R.R. Hopcroft. 2017. Depth-stratified community structure of Beaufort Sea slope zooplankton and its relations to water masses. Journal of Plankton Research 39(1):79–91. https://doi.org/10.1093/plankt/fbw087

Walker, K. 2017. Estimating sizes of fish consumed by ice seal diets using otolith length – fish length relationships. Fairbanks, AK: M.S. thesis, Univeristy of Alaska Fairbanks.

MAP SHOWING AREA OF STUDY:

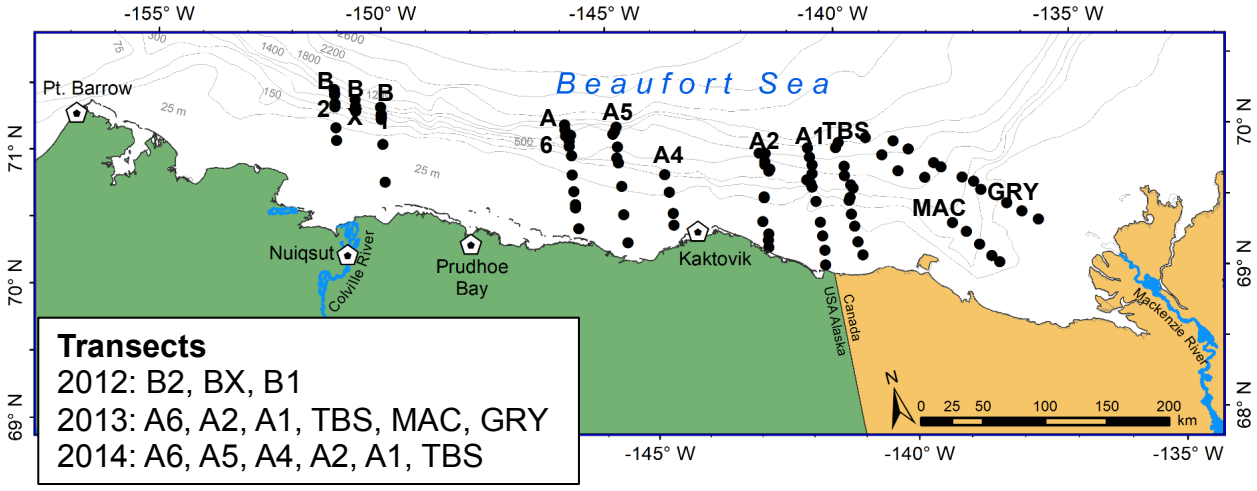

Transects and stations sampled in the Beaufort Sea 2012–2014.

2012: B2, BX, B1
2013: A6, A2, A1, TBS, MAC, GRY
2014: A6, A5, A4, A2, A1, TBS